Symmetric Functionalization of Polyhedral Phenylsilsesquioxanes as a Route to Nano-Building Blocks

by

Mark Francis Roll

A dissertation submitted in partial fulfillment
Of the requirements for the degree of
Doctor of Philosophy
(Macromolecular Science and Engineering)
in the University of Michigan
2010

Doctoral Committee:

Professor Richard M. Laine, Chair
Associate Professor Mark M. Banaszak Holl
Associate Professor Jinsang Kim
Associate Professor Adam J. Matzger

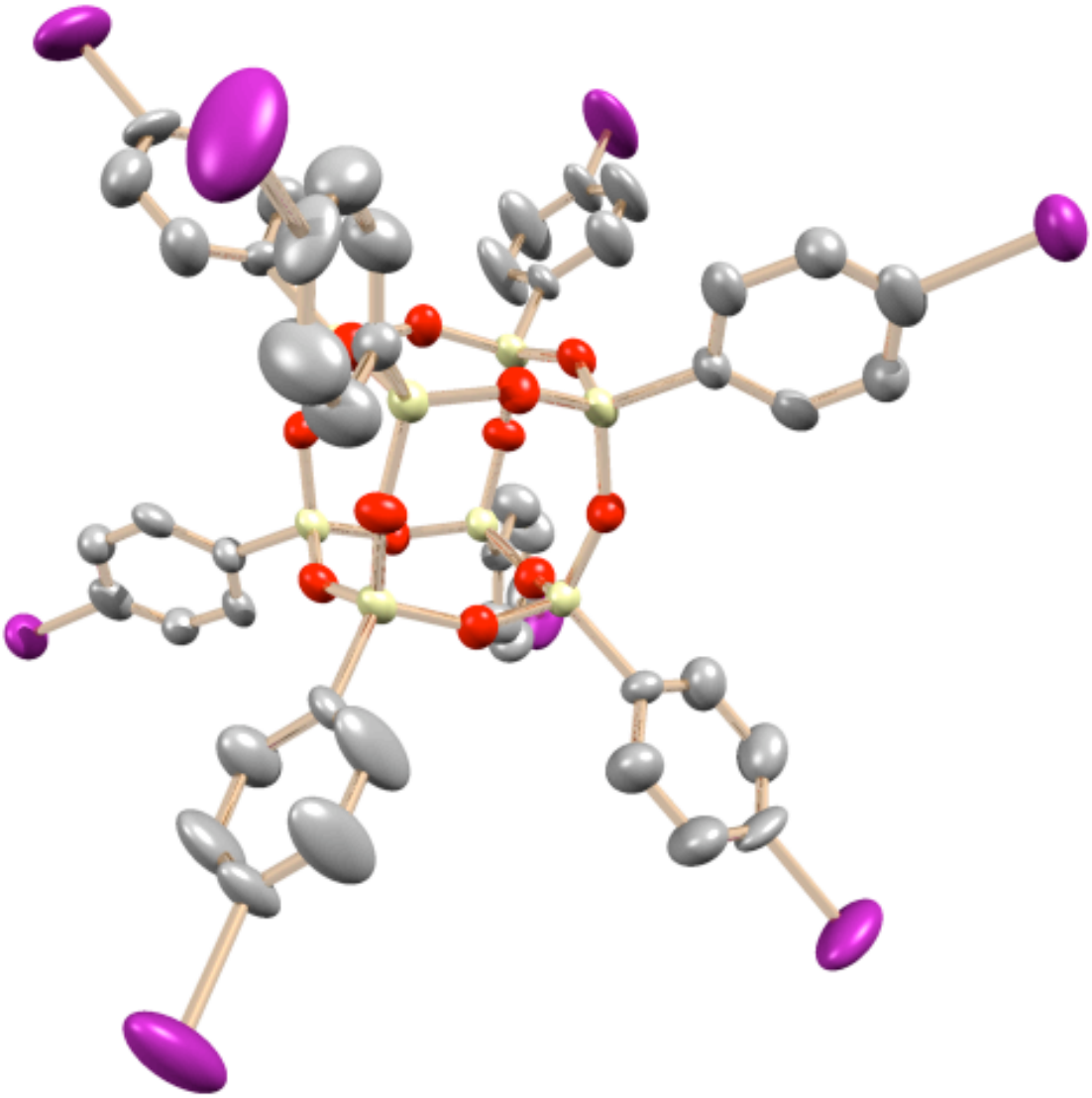

To My Family

(Genetic and Otherwise)

Acknowledgements

This would not have been possible without the generosity and assistance of many:

My wife Katherine and daughter Josephine,
My Parents, Sister and Brothers,
My In-laws and Relations

My advisor, Professor R. M. Laine
And the entire Laine Research Group

My committee:
Professor Mark M. Banaszak Holl
Professor Jinsang Kim
Professor Adam J. Matzger

Special Thanks to:
Professor John L. Gland (emeritus)
Professor Brian Coppola
Professor Robert M. MacCrone (emeritus, Renesselear Polytechnic Institute)
Professor Alan Wolf (The Cooper Union)
Professor Wallace Chinitz (emeritus, The Cooper Union)
Professor George Sidebotham (The Cooper Union)
Dr. Nancy Kerner
Dr. Jeffrey W. Kampf
Mr. James A. Windak
Ms. Aiko Nakatani

For support and assistance in moments of great duress:
Dr. Chad M. Brick
Dr. Michael H. Stewart
Dr. José Azurdia
Mr. Nicholas D. James
Ms. Priyanka Mathur
Ms. Santy Sulaiman

For the essentials:
Comet Coffee
Zingerman's Deli and Roadhouse

Finally, I am forever indebted to Ms. E. B. Heuser for her endless hospitality.

Preface

This dissertation describes steps taken towards advancing Macromolecular Science and Engineering through the development of silsesquioxane chemistry for the synthesis nano-building blocks on an engineering scale. It is an attempt to realize a set of tools for the production of tailored materials on a meaningful scale, starting from inexpensive precursors. At each synthetic step, this work attempts to simplify processing to make the products feasible for larger scale production. It is hoped that the tools described herein will be disseminated as widely as they are found to be useful.

Table of Contents

Dedication.....ii

Acknowledgements..... iii

Preface.....iv

List of Figures.....vii

List of Tables.....xiii

List of Schemes.....xiv

List of Appendices.....xv

Abstract.....xvi

Chapter

I Nano-Building Blocks.....1

i Hybrid Materials.....5

ii Review of Potential Nano-Building Blocks.....6

iii Polyhedral Phenylsilsesquioxanes as Nano-Building Blocks..15

iv Phenylsilsesquioxane Nano-Building Blocks for Tailored Materials.....18

v Supermolecular Structures from Nano-Building Blocks.....23

II Nano-Building Blocks via Iodination of OPS, dPS and DPS.....35

i Introduction.....35

ii Polyhedral Phenylsilsesquioxanes as Nano-Building Blocks..36

iii Iodination of Polyhedral Phenylsilsesquioxanes.....37
iv Results and Discussion.....39
v Conclusions.....62
III Nano-Building Blocks via Bromination of OPS.....68
i Introduction.....68
ii Results and Discussion.....69
iii Conclusions.....89
IV Hexaarylbenzene and Graphene Nano-Building Blocks.....94
i Introduction.....94
ii Results and Discussion.....98
iii Conclusions.....125
V Supermolecular Coordination of Halogenated OPS Derivatives..132
i Introduction.....132
ii Results and Discussion.....137
iii Conclusions.....162
VI Future Work.....166
VII Experimental.....174

Appendices.....197

List of Figures

Figure 1.1 Hypothetical cubane material proposed by Eaton.....2
Figure 1.2 Model of D4R silica cage $(Si_8O_{12})^{8-}$.....3
Figure 1.3 Hypothetical D4R-based structure.....4
Figure 1.4 Selected prismanes (*hydrogens omitted for clarity*) from the Cambridge Crystallographic Data Centre (CCDC).....7
Figure 1.5 Structures of tetraphenyladamantane complexes (CCDC).....9
Figure 1.6 Crystal structures of adamantane derivatives (CCDC) 10
Figure 1.7 Schematic diagram and crystal structure of dodecahedral borane compounds under discussion (CCDC).....11
Figure 1.8 Silaprismane crystal structures via CCDC.....12
Figure 1.9 Possible silsesquioxane (SQ) topologies.....13
Figure 1.10 Q_8 silsesquioxane (SQ) crystal structures (CCDC).....15
Figure 1.11 T_8 SQ crystal structures (CCDC).....15
Figure 1.12 Resonance structures of *ortho* electrophilic attack on a halobenzene.....22
Figure 1.13 Resonance structures of *para* electrophilic attack on a halobenzene.....22
Figure 2.1 The symmetrically iodinated tetraphenyladamantane, **a**.; and hexaphenylbenzene, **b.**.....38
Figure 2.2 ^1H NMR spectrum of decaphenylsilsesquioxane in $CDCl_3$.....41
Figure 2.3 ^{13}C NMR spectrum of decaphenylsilsesquioxane in $CDCl_3$.....41
Figure 2.4 MALDI-TOF spectrum of decaphenylsilsesquioxane (Dithranol/Ag^+).....42
Figure 2.5 50 % thermal ellipsoid plots of decaphenylsilsesquioxane • toluene. Hydrogen atoms and toluene solvents are omitted for clarity. Full XRD data can be found in Appendix 1.....42
Figure 2.6 ^1H NMR spectrum of I_8OPS in $CS_2/CDCl_3$.....46

Figure 2.7 ^{1}H NMR spectrum of $I_{10}dPS$ in $CDCl_3$.....47
Figure 2.8 Different chemical environments in DPS. "Equatorial" phenyls in purple, "polar" phenyls in blue.....48
Figure 2.9 ^{1}H NMR spectrum of $I_{12}DPS$ in $CS_2/CDCl_3$.....49
Figure 2.10 ^{13}C NMR spectrum of I_8OPS in $CS_2/CDCl_3$.....50
Figure 2.11 ^{13}C NMR spectrum of $I_{10}dPS$ in $CDCl_3$.....50
Figure 2.12 ^{13}C NMR spectra of $I_{12}DPS$ in $CS_2/CDCl_3$.....51
Figure 2.13 MALDI-TOF spectrum of recrystallized I_8OPS (Dithranol/$AgNO_3$).....51
Figure 2.14 MALDI-TOF spectrum of $I_{10}DPS$ (Dithranol/$AgNO_3$).....52
Figure 2.15 MALDI-TOF spectrum of $I_{12}DPS$ (Dithranol/$AgNO_3$).....52
Figure 2.16 FTIR homologous iodophenylsilsesquioxanes 3200-450 cm^{-1}.....53
Figure 2.17 FTIR homologous iodophenylsilsesquioxanes 2000-450 cm^{-1}.....53
Figure 2.18 TGA of octa(iodophenyl)silsesquioxane under air and nitrogen.....54
Figure 2.19 TGA of the homologous iodophenylsilsesquioxanes.....55
Figure 2.20 50 % thermal ellipsoid plots of octa(*p*-iodophenyl)silsesquioxane. Hydrogen atoms are omitted for clarity. Full XRD data can be found in Appendix 2.....56
Figure 2.21 50 % thermal ellipsoid plots of deca(*p*-iodophenyl)silsesquioxane. Hydrogen atoms are omitted for clarity. Full XRD data can be found in Appendix 3.....57
Figure 2.22 50 % thermal ellipsoid plots of dodeca(*p*-iodophenyl)silsesquioxane. Hydrogen atoms and *m*-xylene solvents are omitted for clarity. Full XRD data can be found in Appendix 4.....58
Figure 2.23 Ball-and-stick figures generated via single-crystal X-ray diffraction.....62
Figure 3.1 MALDI-TOF MS of octa(bromophenyl)silsesquioxane (Ag^+/Dithranol).....71
Figure 3.2 Proposed complexation of bromide ion with silsesquioxane cage face.....73
Figure 3.3 ^{1}H NMR spectrum of octa(*o*-bromophenyl)silsesquioxane in $CS_2/CDCl_3$.....74
Figure 3.4 ^{13}C NMR spectrum of octa(*o*-bromophenyl)silsesquioxane in $CS_2/CDCl_3$.....75
Figure 3.5 MALDI-TOF spectrum of octa(*o*-bromophenyl)silsesquioxane (Dithranol/$AgNO_3$) 75

Figure 3.6 50 % thermal ellipsoid plots of octa(*o*-bromophenyl)silsesquioxane • 2.5 *m*-xylene. Hydrogen atoms and *m*-xylene solvates are omitted for clarity. Full XRD data can be found in Appendix 5.....76
Figure 3.7 ^{1}H NMR spectrum of octa(2,5-dibromobromophenyl)silsesquioxane in $CS_2/CDCl_3$.....79
Figure 3.8 MALDI-TOF MS of octa(2,5-dibromophenyl)silsesquioxane. (Dithranol/$AgNO_3$).....79
Figure 3.9 50 % thermal ellipsoid plots of octa(2,5-dibromophenyl)silsesquioxane carbon disulfide solvate. Hydrogen atoms and carbon disulfide solvates are omitted for clarity. Full XRD data can be found in Appendix 6.....80
Figure 3.10 MALDI-TOF MS showing corner cleavage during bromination. (Ag^+/Dithranol).....82
Figure 3.11 MALDI-TOF MS of tetraicosabrominated OPS (Ag^+/Dithranol).....83
Figure 3.12 ^{1}H NMR spectrum of tetraicosabrominated OPS in $CS_2/CDCl_3$.....84
Figure 3.13 50 % thermal ellipsoid plots of tetraicosabrominated OPS • 5 *o*-dichlorobenzene (R-factor of 6.3 %). Hydrogen atoms and *o*-dichlorobenzene solvates are omitted for clarity. Dashed bonds indicate partially occupied bromines. Full XRD data can be found in Appendix 7.....84
Figure 3.14 TGA traces of brominated OPS derivatives in air, ceramic yields in Table **3.1**.....86
Figure 3.15 DSC traces of brominated OPS derivatives under nitrogen.....87
Figure 3.16 FTIR spectra of brominated OPS derivatives, 3200-400 cm^{-1}.....88
Figure 3.17 FTIR spectra of brominated OPS derivatives 1600-400 cm^{-1}.....88
Figure 4.1 Conjugated polymers A. poly(*p*-phenyleneethynylene), B. poly(*p*-phenylene), C. poly(*p*-phenylenevinylene).....95
Figure 4.2 ^{1}H NMR spectrum of the phenylacetylene derivative, **1a** in $CDCl_3$.....99
Figure 4.3. ^{13}C NMR spectrum of the phenylacetylene derivative, **1a** in $CDCl_3$.....100
Figure 4.4. MALDI-TOF spectrum of the phenylacetylene derivative, **1a** (Ag^+/Dithranol) 101

Figure 4.5 50 % thermal ellipsoid plots of **1a** • 5 *m*-xylene solvate. Hydrogen atoms and toluene solvates are omitted for clarity. Full XRD data can be found in Appendix 8 102
Figure 4.6 ^{1}H NMR spectrum of the tolylacetylene derivative, **1b** in $CDCl_3$.....103
Figure 4.7 ^{13}C NMR spectrum of the tolylacetylene derivative, **1b** in $CDCl_3$.....104
Figure 4.8. MALDI-TOF spectrum of the tolylacetylene derivative, **1b** (Ag^+/Dithranol) 105
Figure 4.9. ^{1}H NMR spectrum of the trimethylsilylacetylene derivative, **1c** in $CS_2/CDCl_3$.....105
Figure 4.10. ^{13}C NMR spectrum of the trimethylsilylacetylene derivative, **1c** in $CS_2/CDCl_3$.....106
Figure 4.11. MALDI-TOF spectrum of the trimethylsilylacetylene derivative, **1c** (Ag^+/Dithranol).....106
Figure 4.12 ^{1}H NMR of di(*p*-tolyl)acetone in $CDCl_3$.....108
Figure 4.13 ^{1}H NMR of tetra(*p*-tolylcyclopentadienone in $CDCl_3$.....109
Figure 4.14 ^{1}H spectrum of 56 Aryl in $CDCl_3$.....110
Figure 4.15 ^{13}C spectrum of the 56 Aryl in $CDCl_3$.....111
Figure 4.16 MALDI-TOF spectrum of the 56 Aryl (Ag^+/Dithranol).....111
Figure 4.17 FTIR spectrum of the 56 Aryl.....112
Figure 4.18 50 % thermal ellipsoid plots of 56 Aryl • 18 toluene. Labels, hydrogen atoms and toluene solvates are omitted for clarity. Full XRD data can be found in Appendix 9.....113
Figure 4.19 ^{1}H spectrum of the permethylated 56 Aryl in $CDCl_3$.....114
Figure 4.20 Depiction of methyl group environments in permethylated 56 Aryl.....115
Figure 4.21 MALDI-TOF spectrum of the permethylated 56 Aryl (Ag^+/Dithranol).....115
Figure 4.22 ^{1}H spectrum of the t-butylated 56 Aryl in $CDCl_3$.....117
Figure 4.23 MALDI-TOF spectrum of the *t*-butylated 56 Aryl (Ag^+/Dithranol).....117
Figure 4.24 ^{1}H spectrum of the cyclized, *t*-butylated 56 Aryl in $CDCl_3$.....119
Figure 4.25 MALDI-TOF spectrum of the cyclized 56 Aryl.....120
Figure 4.26 FTIR spectra of the 56 Aryl and its cyclization product, 3200-400 cm^{-1}...121
Figure 4.27 FTIR spectra of the 56 Aryl and its cyclization product, 1700-400 cm^{-1}...121

Figure 4.28 FTIR spectra of the permethyl 56 Aryl and its cyclization product, 3200-400 cm^{-1}.....122
Figure 4.29 FTIR spectra of the permethyl 56 Aryl and its cyclization product, 1700-500 cm^{-1}.....123
Figure 4.30 Powder XRD pattern of the cyclized permethylated 56 Aryl.....124
Figure 4.31 Diagram of possible *d*-spacings.....123
Figure 5.1 Type I (A.), Type II (B.), and X_3 (C.) halogen···halogen short contacts.....133
Figure 5.2 A. Calculated electrostatic potentials for iodobenzene. B General schematic model of halobenzene molecule.....134
Figure 5.3 Four coplanar I_8OPS molecules coordinated via I···I Type II short contacts (distances in Å).....139
Figure 5.4 I···I Type II short contacts (Å) in cis-1,3,5-tris(Iodomethyl)-1,3,5-triphenylcyclotriphosphazene.....139
Figure 5.5 ArC···I interactions found in (4-iodophenyl)triphenylmethane (Å).....140
Figure 5.6 ArC···I interactions found in octa(*p*-iodophenyl)silsesquioxane (Å).....141
Figure 5.7 Square C···I coordination motif as seen in I_8OPS.....142
Figure 5.8 Square C···I coordination motif as seen in diiodoacetylene.....142
Figure 5.9 I···O and C···H interactions found in I_{10}dPS (Å).....144
Figure 5.10 Edge-to-face coordination in benzene (Phase I).....145
Figure 5.11 H···I and H···H short contacts found in I_{10}dPS (Å).....146
Figure 5.12 C···I and C···C short contacts found in I_{10}dPS (Å).....146
Figure 5.13 ArC···I interactions found in I_{10}dPS (Å).....147
Figure 5.14 I_{12}DPS molecules coordinated via C···H, I···I, and Si···I short contacts.....149
Figure 5.15 I_{12}DPS molecules coordinated via C···I and C···H short contacts.....150
Figure 5.16 I_{12}DPS molecules coordinated via C···I short contacts.....150
Figure 5.17 Intramolecular bromine short contacts in *o*-Br_8OPS.....152
Figure 5.18 Tetrahedral bromine coordination in *o*-Br_8OPS.....153
Figure 5.19 Tetrahedral coordination motif in tetrabromophenylmethane.....154
Figure 5.20 Cage and C-H Short Contacts along the *a* and *b*-axis in *o*-Br_8OPS.....154
Figure 5.21 Si···Br short contact pair in Br_{16}OPS.....156
Figure 5.22 Br···Br short contact pairs in Br_{16}OPS.....157

Figure 5.23 Si···Br short contact pairs in Br_{16}OPS.....157
Figure 5.24 Si···Br short contacts along the *c* axis in Br_{24}OPS.....159
Figure 5.25 Br_{24}OPS Br···Br Type II short contacts in Br_{24}OPS.....160

List of Tables

Table 2.1 Crystal Structure Data for Decaphenylsilsesquioxane • toluene.....43
Table 2.2 Characterization of the homologous iodophenylsilsesquioxanes.....45
Table 2.3 NMR Characterization of the homologous iodophenylsilsesquioxanes.....46
Table 2.4 Crystal structure data for the iodophenylsilsesquioxanes.....56
Table 2.5 Product yields, Conversions, GPC, and MALDI-TOF Data for Scheme **2.1** compounds.....59
Table 2.6 Unit cell volume, Z and solvent void calculations for selected Heck derivatives.....62
Table 3.1 Crystal Structure Data for octa(*o*-bromophenyl)silsesquioxane • 2.5 *m*-xylene.....77
Table 3.2 Crystal Structure Data for octa(2,5-dibromophenyl)silsesquioxane • carbon disulfide.....80
Table 3.3 Crystal Structure Data for tetraicosabrominated OPS • 5 *o*-dichlorobenzene..85
Table 3.4 Characterization data for the brominated OPS derivatives.....85
Table 4.1 Characterization of ethynyl derivatives.....98
Table 4.2 Crystal Structure Refinement Data for **1a** • 5 *m*-xylene.....101
Table 4.3 Crystal Structure Refinement Data for 56 Aryl • 18 toluene.....113
Table 5.1 Details of short contacts to be discussed in this chapter. 135
Table 5.2 Listing of short contacts found in the crystal structure of octa(*p*-iodophenyl)-silsesquioxane.....143
Table 5.3 Listing of short contacts found in the crystal structure of deca(*p*-iodophenyl)-silsesquioxane.....147
Table 5.4 Listing of short contacts found in the crystal structure of dodeca(*p*-iodophenyl)silsesquioxane.....151
Table 5.5 Listing of short contacts found in the crystal structure of *o*-Br_8OPS.....155
Table 5.6 Listing of short contacts found in the crystal structure of Br_{16}OPS.....158
Table 5.7 Listing of short contacts found in the crystal structure of tetraicosabrominated OPS.....161

List of Schemes

Scheme 1.1 Synthesis of tetraphenyladamantane....8
Scheme 1.2 Aramid synthetic route used by Reichert and Matthias....8
Scheme 1.3 Condensation and rearrangement of polymeric and oligomeric silsesquioxane 16
Scheme 1.4 Si-C cleavage reactions using fluoride....23
Scheme 2.1 Functionalization of I_8OPS using traditional coupling chemistries (see Experimental)....39
Scheme 2.2 Iodination of phenylsilsesquioxane....44
Scheme 3.1 Bromination of octa(phenyl)silsesquioxane (OPS)....71
Scheme 3.2 Synthesis of octa(dibromophenyl)silsesquioxane....78
Scheme 3.3 Synthesis of tetraicosabrominated OPS....82
Scheme 4.1 Scholl cyclization of hexaphenylbenzene (HPB) to form hexa-*peri*-benzocoronene (HBC)....96
Scheme 4.2 Proposed synthesis for Octagraphene....97
Scheme 4.3 Sonogashira coupling of terminal acetylene and iodophenylsilsesquioxane....98
Scheme 4.4 Synthesis of di-*p*-tolylacetone....107
Scheme 4.5 Synthesis of tetra-*p*-tolylcyclopentadienone....108
Scheme 4.6 *t*-Butylation of 56 Aryl....116
Scheme 4.7 Scholl-type dehydrogenative cyclization....118
Scheme 6.1 Proposed cyclotrimerization octa(diphenylacetylene)silsesquioxane....168
Scheme 6.2 Proposed synthesis of tetra(4-R-phenyl)tetracyclopentadieone....169
Scheme 6.3 Proposed Diels-Alder condensation of octa(diphenylacetylene)-silsesquioxane with tetra(*p*-bromophenyl)tetracyclopentadienone....169

List of Appendices

Appendix 1 Crystallographic data for Decaphenylsilsesquioxane.....197

Appendix 2 Crystallographic data for I_8OPS.....240

Appendix 3 Crystallographic data for I_{10}dPS.....249

Appendix 4 Crystallographic data for I_{12}DPS.....263

Appendix 5 Crystallographic data for *o*-Br_8OPS.....279

Appendix 6 Crystallographic data for Br_{16}OPS.....293

Appendix 7 Crystallographic data for Br_{24}OPS.....304

Appendix 8 Crystallographic data for Octa(diphenylacetylene)silsesquioxane.....323

Appendix 9 Crystallographic data for Octa(hexaphenylbenzene)silsesquioxane.....339

ABSTRACT

The design and synthesis of nanometer scale structures is of intense current interest. Herein we report on the ability to use symmetric, robust, mutable silsesquioxane ($[RSiO_{3/2}]_n$) nano-building blocks to produce well-defined 3-D structures for electronic or adsorption applications. We are able to show the systematic effects of supermolecular coordination to modulate the density of the molecular packing.

This dissertation first describes the synthesis of the elusive decaphenylsilsesquioxane, and the exploration of the substitutionally specific *para* iodination of the octa-, deca- and dodeca-(*p*-iodophenyl)-silsesquioxanes, whose single-crystal X-ray diffraction structures are reported. Octa(*p*-iodophenyl)-silsesquioxane shows supermolecular coordination via Desiraju's halogen-halogen short-contact synthon, forming an open structure with a solvent accessible cavity comprising 40% of the unit cell.

The application of palladium, nickel and copper catalyzed cross-coupling techniques using the carbon-iodine bond is explored in order to divergently synthesize crystalline derivatives. These derivatives include the octa(diphenylacetylene)-silsesquioxane and the octa(hexaphenylbenzene)silsesquioxane (56 Aryl), whose single-crystal X-ray diffraction structures are reported. We show that 56 Aryl, which contains

more carbon atoms than any other discrete molecule in the Cambridge Structural Database, crystallizes into an extremely open structure with a solvent accessible cavity comprising 55% of the total volume. The supermolecular ordering driven by the bulky hexaphenylbenzene moieties gives nanometer-scale channels along the *ab* plane.

Substitutional specificity is explored in the bromination of octaphenylsilsesquioxane (OPS), and single-crystal X-ray diffraction structures are reported for the octa-, hexadeca- and tetraicosa-brominated derivatives. Precise synthetic control is demonstrated by the unique catalyst-free bromination of OPS, providing the octa(*o*-bromophenyl)-silsesquioxane in low yield. An iron tribromide catalyzed hexadeca-bromination gives the crystalline octa(2,5-dibromophenyl)-silsesquioxane in good yield, with a high density of 2.3 g/cc. Finally, the iron tribromide-catalyzed tetraicosa-bromination of OPS is described, producing a low yield of crystals with a solid solution of substitution patterns coordinated by bromine-bromine short contacts.

Lastly, the Scholl-type, dehydrogenative cyclization of the octa(hexaarylbenzene)silsesquioxane systems is explored by the addition of iron trichloride/nitromethane to a refluxing solution of the silsesquioxane in stannic chloride/dichloromethane. The products are analyzed by Proton Nuclear Magnetic Resonance Spectroscopy, Matrix Assisted Laser Desorption and Ionization – Time of Flight Mass Spectroscopy and Diffuse Reflectance Fourier Transform Infra Red Spectroscopy.

Chapter I

Nano-Building Blocks

The assembly of 2- and 3-D structures from molecular components or nano-building blocks is of immense current interest because of the potential to realize novel properties in nano-sized materials and/or to tailor global properties perfectly by manipulation of component organization at the finest length scales.[1,2] The ordering in such well-ordered materials with molecular continuity fulfills the mathematical relationships found for Bravais lattices. The higher the component symmetry, the lower the energy requirements to reorient and align adjacent components during the assembly of 2- and 3-D structures.[1]

In this light, there is great need for highly symmetrical nano-building blocks, offering diverse and easily modified functionality. A properly chosen macromolecular building block of nanometer scale should allow the design of materials on a nm by nm basis, a "bottom-up" approach.[3] One hypothetical model of such a nano-structured material was proposed by Eaton, using an ethynyl functionalized cubane, shown in Figure **1.1**.[4]

In principle, this type of selective assembly would allow the tailoring global properties through the manipulation of nanometer length scale features. In addition, altering the chemical reactivity of these nano-building blocks through synthetic means would presumably allow modulation of the interaction and coupling between the blocks, in order to exactly tailor properties.[2] A flexible, modular approach should allow for the production of materials with a wide variety and range physical properties and the capability to tune these properties with a high degree of precision.[2]

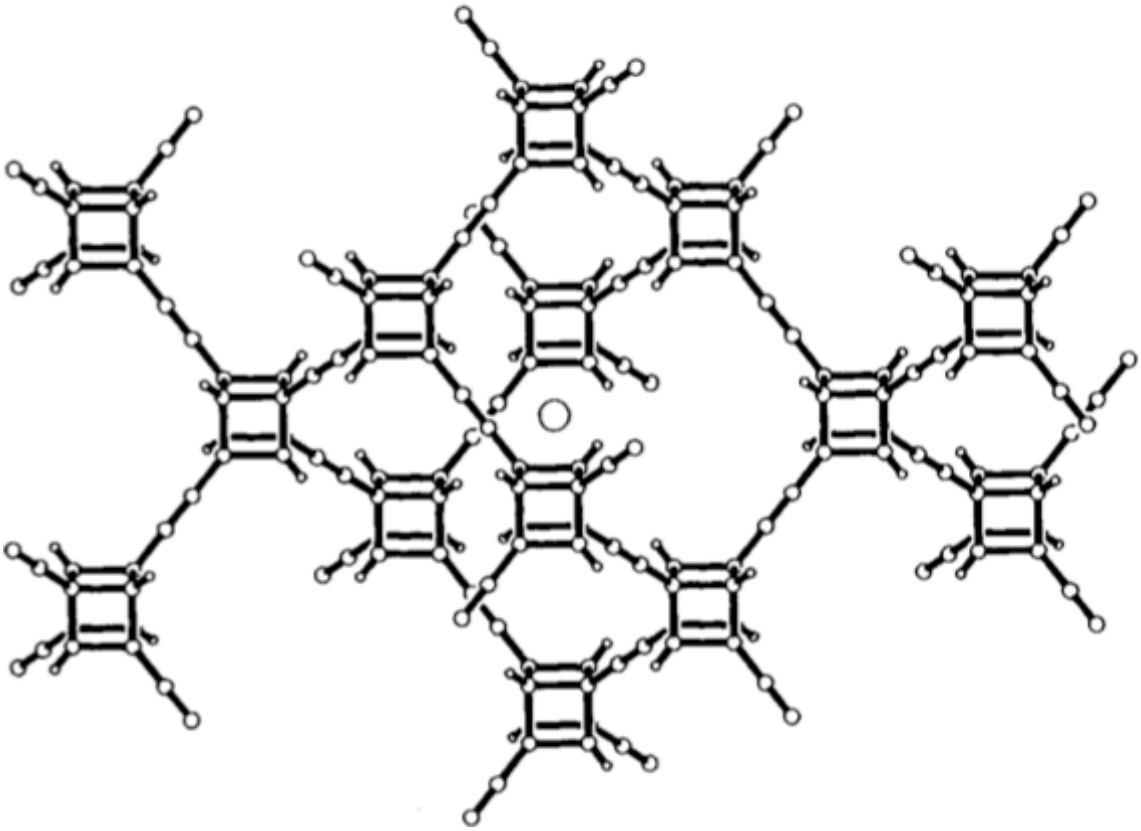

Figure 1.1 Hypothetical cubane material proposed by Eaton.[4]

There are numerous literature examples of molecules possessing high degrees of 2-D symmetry, however, there exist only a smaller number of molecular classes possessing structure and functionality with high 3-D symmetry. Perfect (cubic) symmetry

in 3-D and octa-functionality, such that each octant in Cartesian space contains one functional group, offers the potential to assemble macroscopic structures nm by nm in 2- or 3-dimensions, shown elegantly by Eaton in Figure **1.1**.[4]

Figure **1.2** shows a model "Double Four Ringed" member or D4R unit, a well-known structural motif from the study of zeolites.[5,6] A silica D4R unit consists of eight silicon atoms in a cubic configuration, with twelve bridging oxygen atoms.[5,6] The fourth silicon substitution position is occupied by a linking oxygen, providing connectivity, functionality, or both.

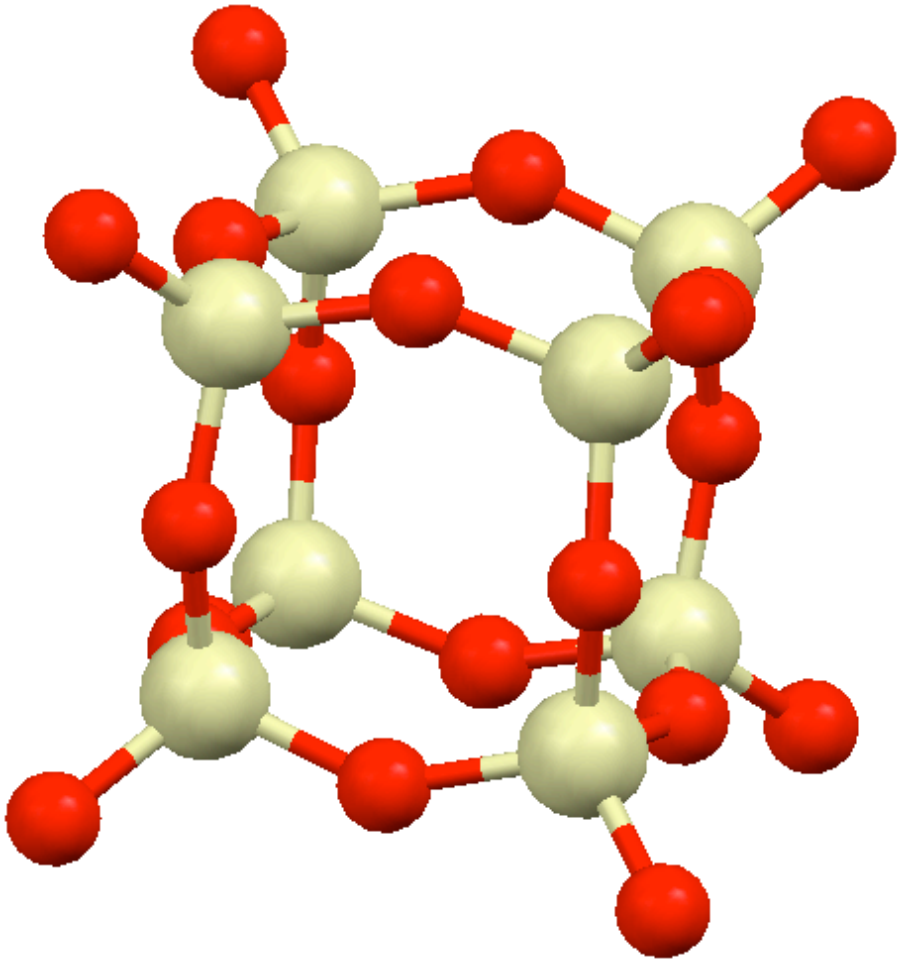

Figure 1.2 Model of D4R silica cage $(Si_8O_{12})^{8-}$.
(beige:silicon; red:oxygen)

This cubic D4R configuration, without linking oxygens, is shown on the left of Figure **1.3**. The right portion of the figure demonstrates one cross-linking motif possible with cubic building blocks.[6] Mellot-Draznieks et al described ten D4R-based structures found through computational modeling, demonstrating the geometric flexibility of cubic nano-building blocks.[5]

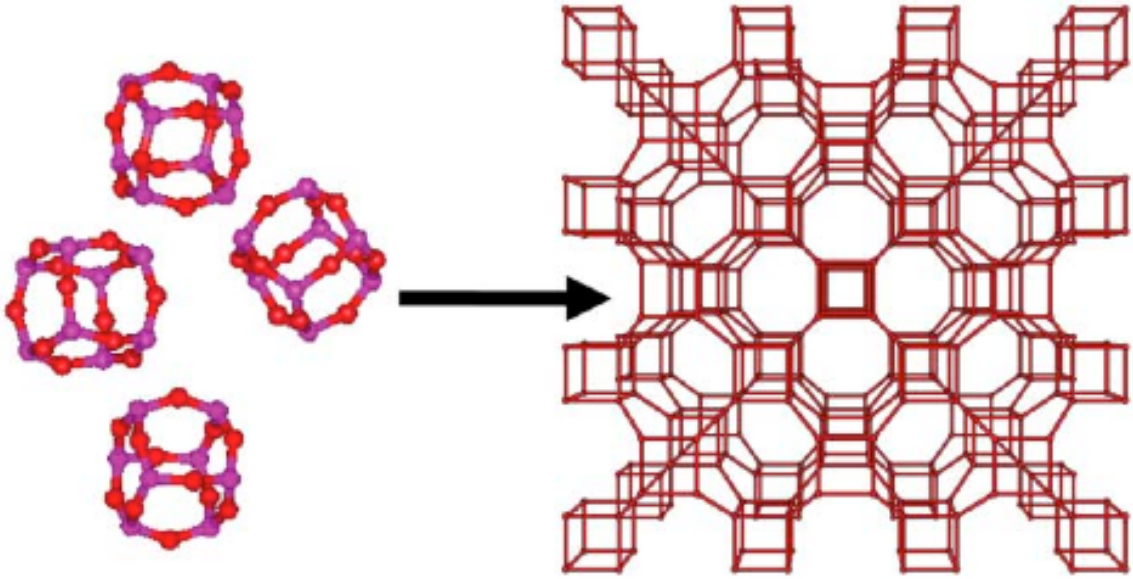

Figure 1.3 Hypothetical D4R-based structure.[6]

Cubanes,[7-13] dodecahedranes,[14] tetrahedranes,[15,16] and diamondoids (adamantanes)[17-21] are examples of organic molecules with high 3-D symmetry. Their pure hydrocarbon composition limits their thermal stability and the available synthetic routes for functionalization. Fortunately, their short-comings are addressed by certain *hybrid* compounds.[22,23] By incorporating both organic and inorganic components, functionality may now be modified by organic or inorganic synthetic methods to incorporate novel bonding modes (e.g. metal organic frameworks[24,25]) and enhanced thermal stability.[22,23]

Hybrid Materials

There are many motivations to explore hybrid materials in the context of nano-building blocks.[6,23] One motivation is to incorporate different bonding patterns and geometries. Boranes can exhibit icosahedral geometry,[26-31] while silaprismanes[32-37] and silsesquioxanes[38-69] offer synthetic access to variety of prismatic species via condensation of trifunctional silane monomers. The incorporation of species with different atomic weights alters the vibrational characteristics of the resulting compound, increasing heat capacities and thermal conductivities.[70]

Finally, bond energies may be increased beyond range of hydrocarbons, providing greater thermal stability. For instance, the standard, single Si-O bond energy is roughly 450 kJ/mol, significantly higher than the 350 kJ/mol for carbon-carbon single bonds.[71] One practical example of this greater stability is the use of silicone oil in heating baths. The higher stability of the Si-O backbone allows for the use of higher temperatures with a longer service life.

Though all hybrid materials incorporate organic and inorganic components, the nature of the interaction between these components naturally leads to two classifications. Sanchez et al define Type I hybrid materials as consisting of inorganic and organic molecular components that interact weakly with each other (van der Waals forces, hydrogen bonding, etc.).[22] In Type II hybrids, inorganic and organic atomic species are linked by covalent or iono-covalent bonds,[22] incorporating the advantages of the organic and inorganic components with molecular homogeneity.

Type II hybrid materials include, for example: polycarbosilanes,[72-75] organoboranes,[26-31,76] and phosphazenes.[77] In contrast to these families, the previously mentioned dodecahedral boranes,[26-31] silaprismanes[32-37] and silsesquioxanes[38-69] and offer nano-building block characteristics: e.g. 3-D symmetry, allowing for the possible assembly of highly ordered structures with continuity on the atomic level, and access to a wide range of chemical functionality. Our investigations center on the silsesquioxane family of organosilicon[72,73] compounds. These molecules feature D4R-like core structures and are discussed in more detail in the following review of potential nano-building blocks.

Review of Potential Nano-Building Blocks

Prismanes

Cubanes are the most synthetically accessible of the prismane hydrocarbons. Eaton explored their synthesis and developed a variety of methods to modify their functionality through organic and organometallic synthetic approaches.[4,7-13] Their high symmetry and chemical simplicity are remarkable, and part of the motivation for this work was the potential of cubanes to serve as molecular nano-building blocks (Figure **1.1**).[4] Figure **1.4** shows three examples of prismane compounds.

However, as Eaton notes in his 1992 review of cubane chemistry, "Fortunately, any good student, having gone through the procedure once to become familiar with its details, can easily make 10 grams of (cubane) in a month or so."[7] Unfortunately, to date the availability and cost of these materials has not improved, and ten gram batches are not sufficient for engineering applications.

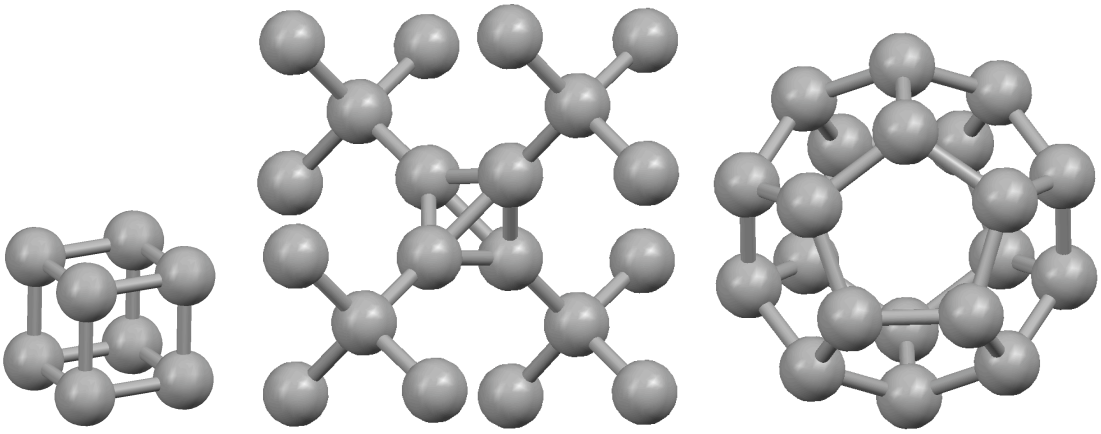

Cubane (C_8H_8)[9] Tetra-*t*-butyl-tetrahedrane ($C_{16}H_{36}$)[15] Dodecahedrane ($C_{20}H_{20}$)[15]

Figure 1.4 Selected prismanes (*hydrogens omitted for clarity*) from the Cambridge Crystallographic Data Centre (CCDC). (grey:carbon)

Adamantanes

The diamondoids, hydrocarbons with the adamantyl skeleton (see 1-bromoadamantane, Scheme **1.1**), offer some intriguing routes to nano building-blocks via functionalization of the four symmetrical bridgehead carbons. One route is the Friedel-Crafts alkylation of 1-bromoadamantane with benzene.[17] Tetraphenyladamantane (TPA) has tetrahedral symmetry, aromatic functionality and a melting point of ~400°C.[17] Though this compound is practically insoluble,[17] Mathias and Reichert recognized that electrophilic aromatic substitution could provide a synthetic route to soluble, functional compounds.[18-20]

After the researchers successfully synthesized the all *para* iodinated TPA, the resulting tetraiodo-aromatic compounds were functionalized by palladium and organolithium chemistries to yield the tetraethynyl[19] and tetracarboxylate[20] compounds, respectively. Mathias and Reichert thermally cross-linked the ethynyl modified TPA[19]

and synthesized branched and hyperbranched aramid polymers using Pd catalyzed carbonylation of *para*-iodinated TPA in the presence of haloanilines (see Scheme **1.2**).[20]

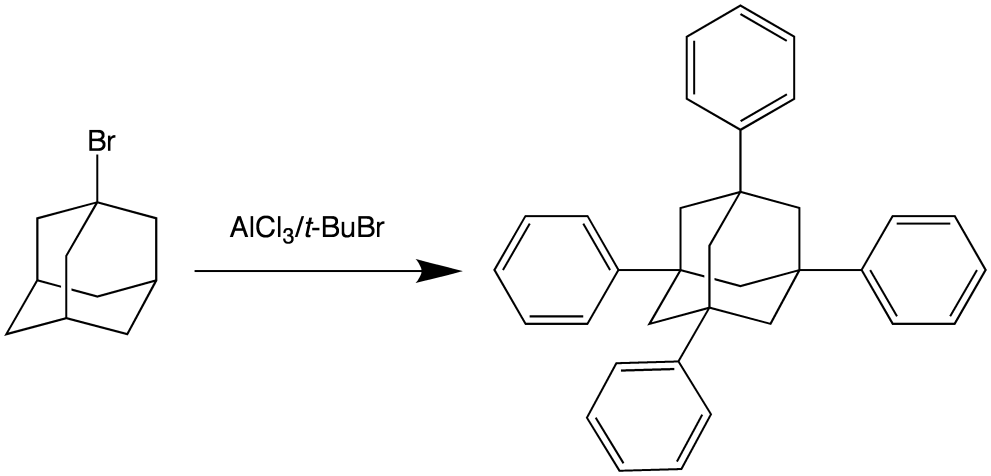

Scheme 1.1 Synthesis of tetraphenyladamantane.[17]

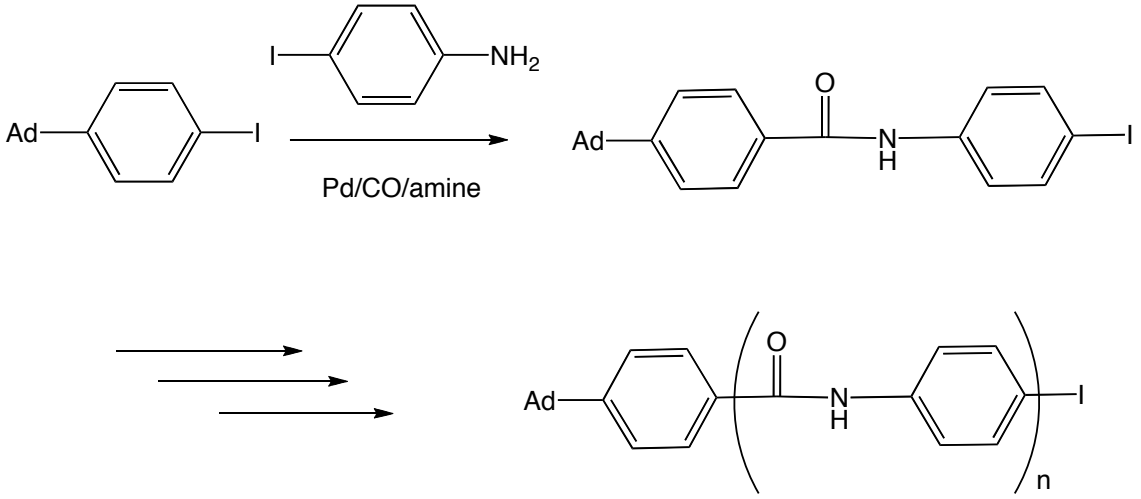

Scheme 1.2 Aramid synthetic route used by Reichert and Matthias.[20]

Mathias and Reichert note that the incorporation of the rigid adamantane core improved the solubility of the branched aramids relative to their linear analogs at equivalent molecular weights.[20] Unfortunately, they did not characterize either the ethynyl or aramid precursors or products by X-ray analysis, or other related method, to characterize the molecular structures and their ordering.[18-20]

With the current interest in nano-building blocks for the development of new materials, investigations of the solid-state structures in TPA materials have begun. The solid-state arrangement of TPA and its derivatives including their intermolecular coordination via hydrogen bonding and aromatic C···H short-contacts has only been recently discussed.[21-22] Metal ion coordination to carboxylate and phosphonate groups for the formation of metal organic frameworks (MOFs) have also been recently explored.[25,78,79]

Reichart et al synthesized the tetracarboxylic acid derivative via carboxylation of the tetralithiated tetra(*p*-iodophenyl)adamantane.[20] This compound was subsequently used by Yaghi et al to form a zinc metal organic framework (MOF) material, shown in Figure **1.5**.[25] The tetraphosphonic acid derivative was prepared by phosphonation of the tetra(*p*-iodophenyl)adamantane and subsequent hydrolysis.[78] Its crystal structure (Figure **1.5**) is ordered by strongly hydrogen bonded network.[78] A separate research group used the tetraphosphonic acid to synthesize microcrystalline vanadium phosphonate catalysts.[79]

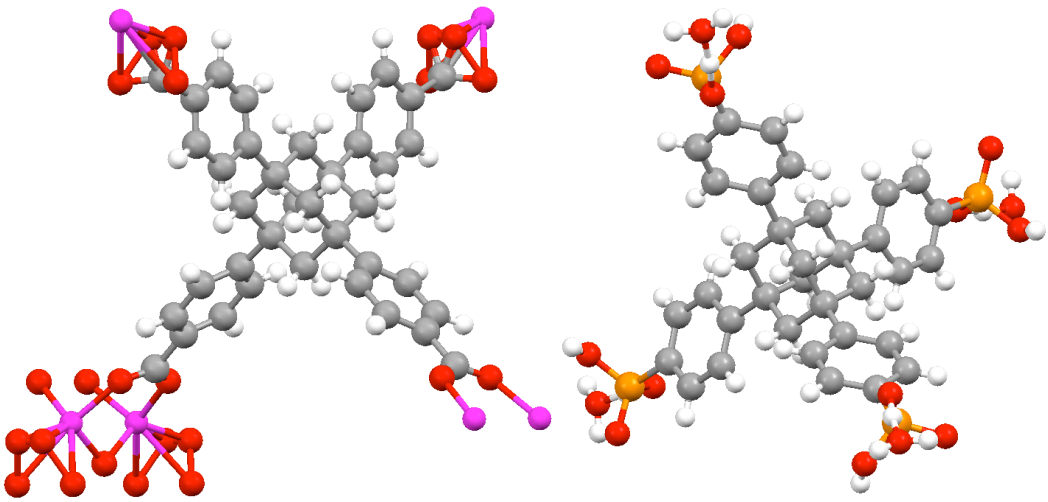

TPA tetracarboxylate zinc complex[25] TPA tetraphosphonic acid[78]

Figure 1.5 Structures of tetraphenyladamantane complexes (CCDC).
(oxygen: red; zinc: pink; carbon: grey; hydrogen: white; phosphorus: orange)

More recently, Bazan et al synthesized stilbenoid oligomers as simple model of the conjugated polymer poly(phenylenevinylene) (PPV), and additionally, their tetrahedral equivalents using carbon, silicon and adamantane as cores.[22] After synthesizing the tetra(stilbene)adamantane compound, the authors characterized it by NMR, differential scanning calorimetry, mass spectrometry and X-ray diffraction.[22] In other words, the authors designed and produced a photo-physically active, rigid, 3-D symmetric nano-building block and determined its organization via intermolecular coordination in solid state, akin to our goals for cubic silsesquioxanes (Figure **1.6**).[22]

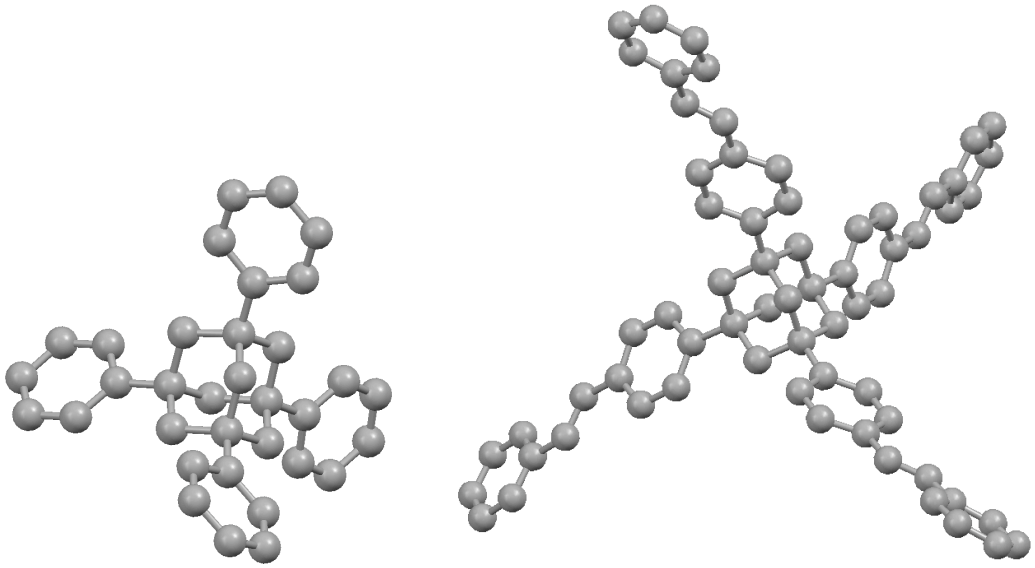

Tetraphenyladamantane[21] Tetra(stilbene)adamantane[22]

Figure 1.6 Crystal structures of adamantane derivatives (CCDC).

Dodecahedral boranes

An enormous number of boron containing hybrid compounds have been synthesized due to the accessibility of boron precursor compounds and their flexible chemistry.[26-31,76,80,81] Some examples include the dodecahedral boranes,[26-31] boronate oligomers and polymers,[80,81] organoboron conjugated oligomers and polymers.[76] Boronate

(boronic acid ester) polymers have been explored by Lavigne[80] and used by El-Kaderi et al as the basis for 3-D covalent organic frameworks.[81] The dodecahedral boranes are potential nano-building blocks that demonstrate unique aromatic bonding structure[26,30,31,82] and can serve as weakly coordinating anions.[83]

Hawthorne et al, recently demonstrated the synthesis and modification of dodecafunctional carborane derivatives (Figure **1.7**).[26-31] These compounds offer the multi-functionality and 3-D symmetry desired in a nano-building block. Most recently, stable and reversible two-electron redox characteristics were reported for these compounds,[26] suggesting their possible incorporation into functional microelectronic devices.[82]

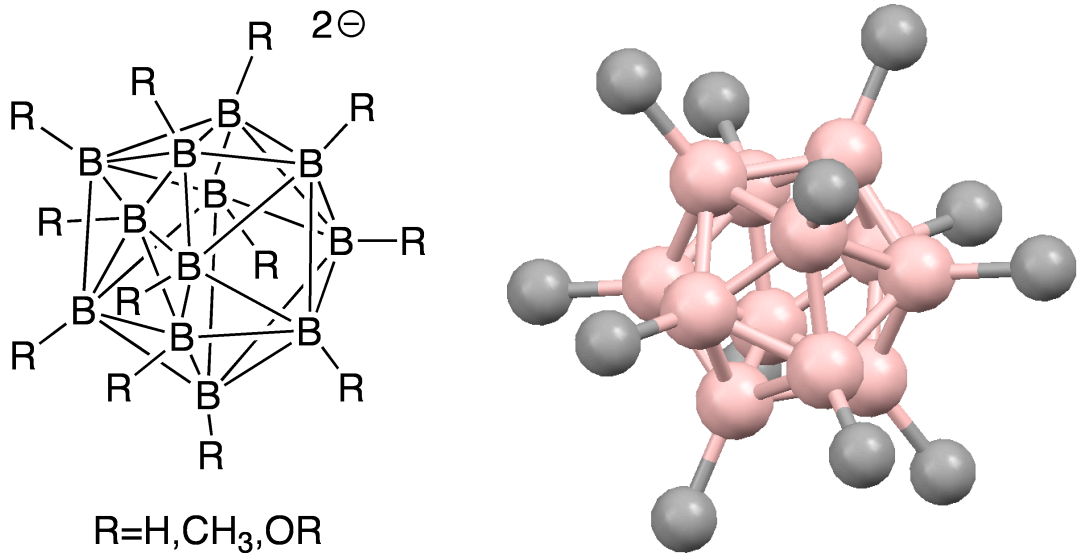

Dodecahedral borane ($B_{12}R_{12}^{2-}$) Dodecamethyldodecaborane ($B_{12}C_{12}H_{36}^{2-,1-}$)[30,31]

Figure 1.7 Schematic diagram and crystal structure of dodecahedral borane compounds under discussion (CCDC).

The aromatic delocalization of the boron core is under current study,[82] in part due to the remarkable stability of dodecahedral borane radical anions.[30] Compounds with such electronic character are of interest for the precise manipulation of electron spin in

microelectronic devices for information processing, a field known as spintronics.[84] Unfortunately, the price of the precursors (alkali dodecahydrododecaborates),[27] is also high, limiting the possibilities for scaling and application.

Silaprismanes

Polysilane compounds, incorporating an organic periphery on an Si-Si backbone may be synthesized by the condensation of Si-H monomers with the subsequent generation of hydrogen (dehydrocoupling).[72] Another route is the reductive coupling of chlorosilanes by alkali metals with the concurrent production of a metal chloride salt (dehalocoupling or Wurtz-type coupling),[32-37,72,73] and this chemistry has allowed for the isolation of 3-D symmetrical compounds with silaprismane cores (Figure **1.8**).[32,33,36]

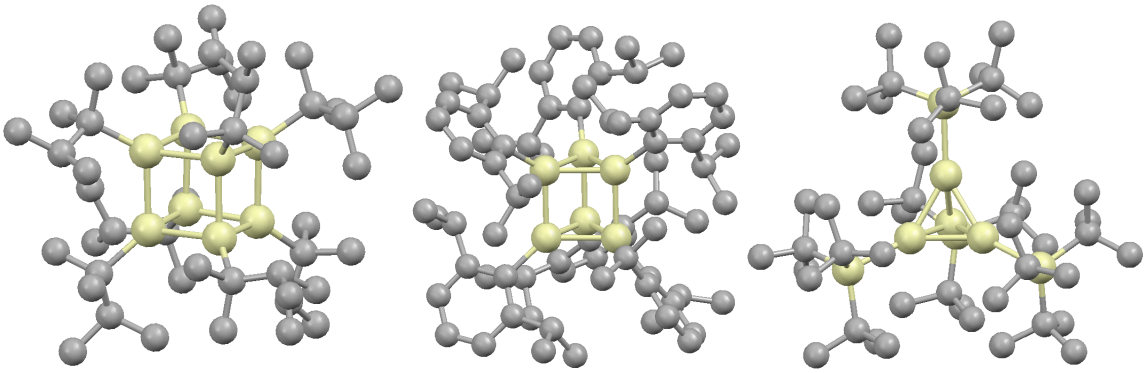

Octasilacubane[36] ($Si_8C_8H_8$) | Hexasilaprismane[33] ($Si_6C_{72}H_{102}$) | Tetrasilahedrane[32] ($Si_8C_{48}H_{108}$)

Figure 1.8 Silaprismane crystal structures via CCDC.

Silaprismanes, including the tetrasilahedrane,[32] hexasilaprismane,[33] and octasilacubane,[34-37] have been synthesized through Wurtz-type couplings.[72,73] They may be relatively stable in the presence of water, presumably due the great steric bulk of the organic groups surrounding the core.[32-37] These compounds have a wide range of colors, (colorless,[32] yellow,[33] orange-red,[36] or purple[34]), suggesting unique bandgap

characteristics related to the sigma conjugation found in polysilanes.[72,73] Unfortunately, these syntheses require extensive use of air-sensitive organometallic compounds, limiting scalability. Subsequent functionalization has not been reported, however, cubic silsesquioxanes may be prepared by the oxidation of the Si-Si bonds in octasilacubanes.[73] Fortunately, there are more efficient synthetic routes to the cubic silsesquioxanes.

Silsesquioxanes

Silsesquioxanes (SQs) are related to silicones and siloxanes, as they all possess organic functionality and Si-O-Si bonds. Siloxanes consist of a linear Si-O-Si backbone, with two R groups per repeat unit (R=organic functional group). In contrast, silsesquioxanes have a characteristic -[$RSiO_{3/2}$]- repeat unit.[39] This trifunctional monomer provides access to linear, closed or network structures, as schematically suggested in Figure **1.9**.[39] Silicone resins combine linear and network components allowing for the production of highly cross-linked, thermally robust materials, though with poor mechanical properties.[39] The strong silicon-oxygen bond (~450 kJ/mol)[71] gives this family of compounds their high thermal and oxidative stability, leading to their extensive use as oils, coatings, sealants and gaskets.[39]

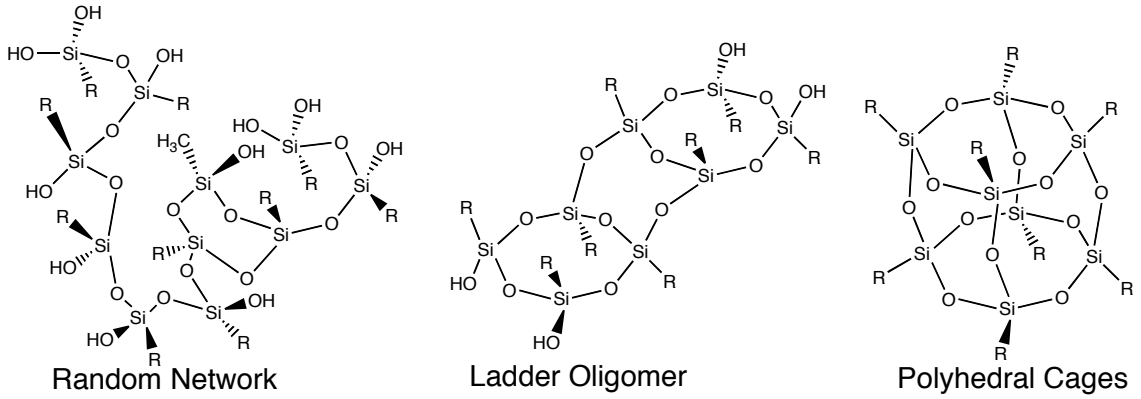

Figure 1.9 Possible silsesquioxane (SQ) topologies.

Cubic silsesquioxanes, Q_8 $[RMe_2SiOSiO_{1.5}]_8$ and T_8 $[RC_6H_4SiO_{1.5}]_8$ SQs or POSS materials,[38,40] with a D4R-like silica core structure (Figure **1.2**, **1.9**), are easily prepared in comparison to the previously discussed prismane (Figure **1.5**) family of compounds.[7-16] These compounds have high thermal stability, (~500˚C in air for octaphenylsilsesquioxane (OPS)[45]), octa-functionality (with a possibility of forty possible positions for functional groups with OPS[45]), and a wide variety of possible chemical consituents.[38,40]

In an effort to develop robust octa-functional nano-building blocks, we and others are exploring the utility of SQs as novel materials in their own right and for nm by nm assembly of high-performance materials. Thus, SQs based on $[RMe_2SiOSiO_{1.5}]_8$, where R = H, alkenyl (Figure **1.10**), or epoxy groups, permit nanometer tailoring in nanocomposities.[46,49,51,52,56] Sellinger et al reported the synthesis of a photo- or thermally curable silsesquioxanes with low viscosity and high silica loadings, up to 65%.[48,49] Zhang et al used SQ systems to produce porous, thermally stable compounds with surface areas up to 580 m^2/g.[59] Epoxy composites with tunable mechanical properties (e.g. elastic moduli and fracture toughness) were reported by Choi et al, by varying amine linking chemistry and stoichiometry.[51,52,53,56,58]

Several groups have also explored the use of $[vinylSiO_{1.5}]_8$ (Figure **1.11**) as a starting point for highly symmetrical molecules;[41-43] but with only a few examples directed towards materials synthesis.[44,46] We have continued our development of octa-functional nano-building blocks with the related $(RPhenylSiO_{1.5})_8$ T_8 (Figure **1.11**)

systems where R = NH_2 (from R = NO_2), Br and I via the electrophilic substitution of OPS $(HPhenylSiO_{1.5})_8$.[45,47,50,53,58,60-65]

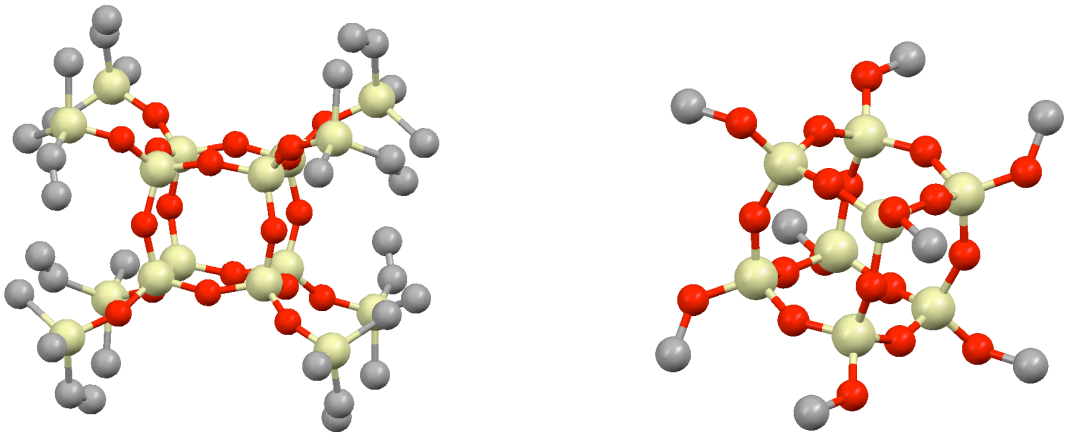

Octa(vinyldimethylsiloxy)SQ ($Si_{16}O_{20}C_{32}H_{72}$) OctamethoxySQ ($Si_8O_{20}C_8H_{24}$)

Figure 1.10 Q_8 silsesquioxane (SQ) crystal structures (CCDC).

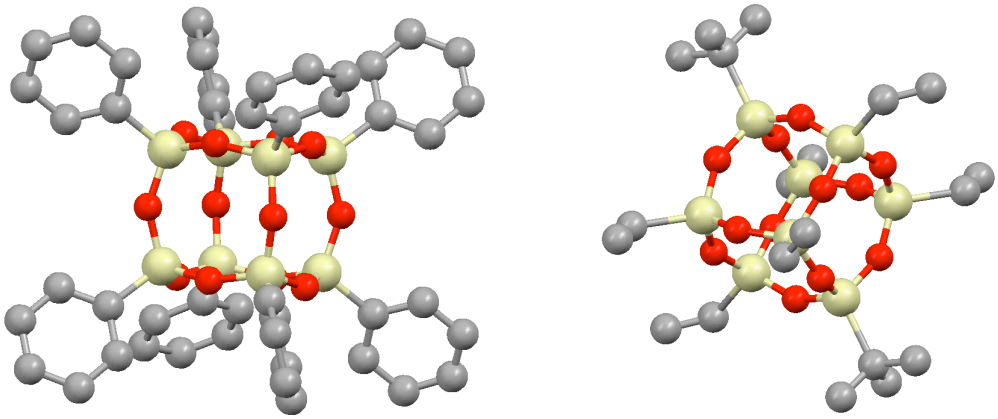

Octaphenylsilsesquixoane ($C_{48}H_{40}Si_8O_{12}$) Octavinylsilsesquioxane ($C_{16}H_{24}Si_8O_{12}$)

Figure 1.11 T_8 SQ crystal structures (CCDC).

Polyhedral Phenylsilsesquioxanes as Nano-Building Blocks

The following section will discuss the polyhedral silsesquioxanes, including their synthesis and characteristics. In particular, octa-, deca-, and dodeca-phenylsilsesquioxanes (OPS, dPS, and DPS) will be introduced and discussed.[45]

Industrial scale production of siloxanes and silicones[27] provides many silane precursors in commercial quantities, at low cost. In particular, phenyltrichlorosilane may

hydrolyzed and condensed to form oligomeric phenylsilsesquioxanes, as suggested in Scheme **1.3**, not meant to be complete. The hydrolysis of the trichlorosilane monomer produces silanols, which subsequently undergo intermolecular condensation to form Si-O-Si linkages. As this intermolecular condensation and rearrangement continues, a variety of oligomer topologies are generated, as documented by several groups.[45,66,67,86,87]

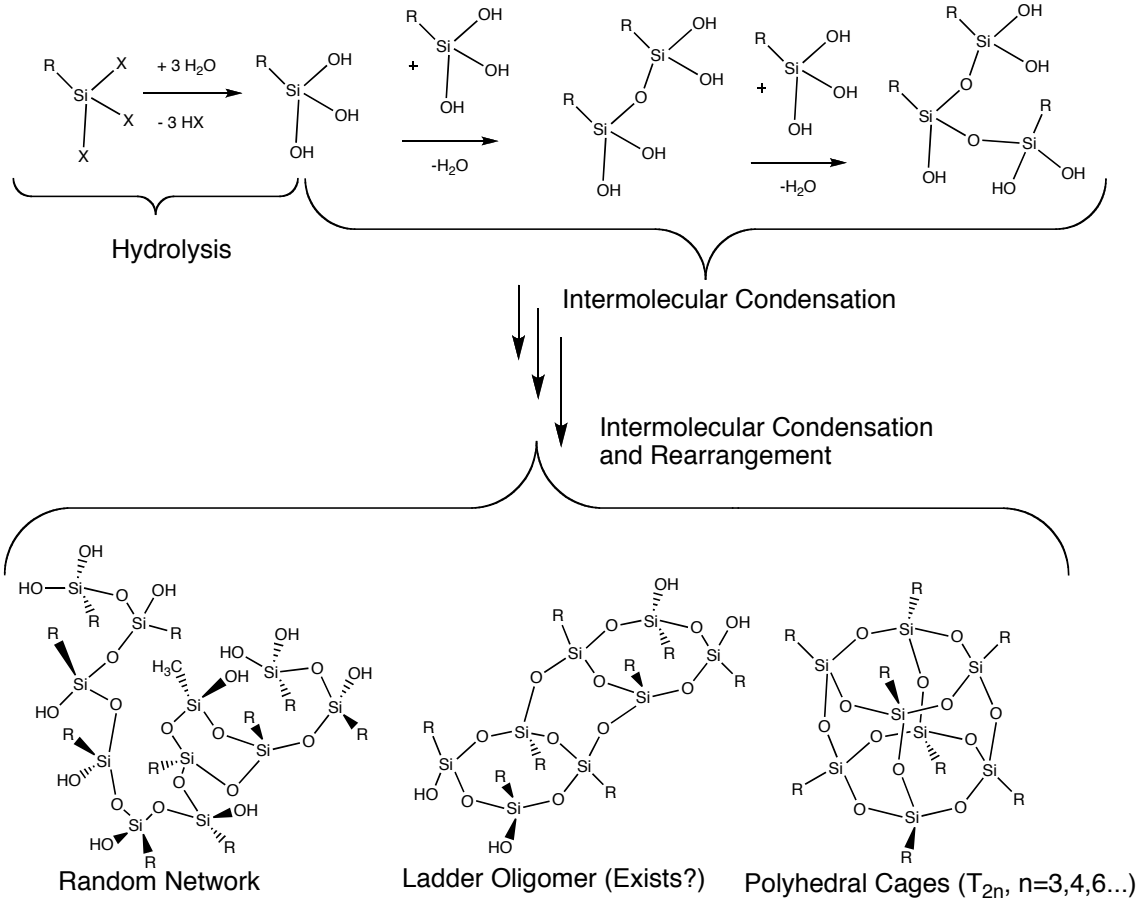

Scheme 1.3 Condensation and rearrangement of polymeric and oligomeric silsesquioxane.[86]

These hydrolysis, condensation and rearrangement reactions are catalyzed by strong inorganic bases.[45,66,67,86,87] These catalysts rapidly cleave and equilibrate the Si-O bonds in polyphenylsilsesquioxane (PPS),[45,66,67,86,87] leading to the formation of every possible oligomer configuration, if only in infinitesimal percentages. Kawakami et al

found that this catalytic rearrangement favors the formation of cyclic oligomers of six to nine monomer units.[86,87]

Octaphenylsilsesquioxane

At early stages in the synthesis of OPS, toluene, potassium hydoxide, water, and PPS form a homogenous solution, and equilibration of the oligomers occurs rapidly.[66] Although there is only a small probability for the formation of OPS, the symmetric octamer, it precipitates from the solution once formed due to its insolubility.[45] The reaction continuously precipitates octaphenylsilsesquioxane until the end of the desired reaction period, when the product is isolated by filtration.[66]

Kawakami finds that rearrangement of phenyltrimethoxysilane in refluxing benzene with catalytic benzyltrimethylammonium hydroxide gives OPS in 84 % yield after 4 h.[86,87] Brown reports 95+% conversion of PPS to OPS using catalytic KOH in refluxing benzene after 48 h.[45]

OPS is synthesized in our lab at kilogram scales from phenyltrichlorosilane, available at $36/kg from Gelest, Inc.[66] Phenyltrichlorosilane is first converted to the triethoxy equivalent by direct reaction with ethanol. After removal of excess ethanol and acid, toluene, KOH and trace water are introduced, and the solution is heated to reflux to effect condensation and rearrangement. After 2 d at reflux, this reaction gives OPS in 95% yield by simple filtration.[66]

Decaphenylsilsesquioxane

The pentagonal decaphenylsilsesquioxane (dPS) has only been isolated by Brown et al as the most soluble crystalline product of the KOH equilibrated PPS in toluene or benzene.[45] Five-fold symmetry is rare among reported macromolecules, but the

exploration of pentagonal symmetry and quasicrystals in small molecule tiling patterns,[88,89] polymers,[90] polyoxometalates,[91] and metals,[92,93] has been a topic of many recent reports. Two T_{10} decasilsesquioxane crystal structures are found in the Cambridge Crystallographic Database, the decamethylsilsesquioxane[95] and the monophenyl-nonahydrido-decasilsesquioxane.[96] The decahydridosilsesquioxane crystal structure was reported by Bürgi et al.[97]

Brown et al recovered decaphenylsilsesquioxane from the 9:1 methanol:toluene soluble fraction of the PPS/KOH equilibration in an unreported yield.[45] In contrast to OPS and DPS (see below), where isolation is accomplished by the precipitation of the desired product, the high solubility of dPS greatly hinders its isolation. Since the rearrangement equilibria are composed of a number of polyhedral species, the isolation of a single species from the solution equilibrium is difficult. In Chapter 2, we describe the isolation of dPS and its characterization of by NMR, X-ray diffraction and MALDI-TOF.

Dodecaphenylsilsesquioxane

Dodecaphenylsilsesquioxane (DPS) was isolated by Brown et al in ~60% yield from the equilibration of $(PhSiO_{1.5})_n$/KOH in refluxing THF, at 0.9 M concentration of PPS.[4] As with the synthesis of OPS, the insoluble product precipitates continuously from the reaction solution and is isolated by filtration at the end of the reaction.[4] In this case, the product is determined to be a clathrate (1:2 DPS:THF) that is less soluble than OPS in THF.[4]

Phenylsilsesquioxane Nano-Building Blocks for Tailored Materials

The Laine Group has pursued the use of phenylsilsesquioxane compounds as the basis for new, high performance (thermal stability, modulus, fracture toughness,[51-56]

thermal expansion,[60] electronic properties) materials.[42,97] Octaamino or OAPS $(NH_2PhenylSiO_{1.5})_8$ has served as a platform for the production of imide nanocomposite materials with high cross-link densities, thermal stabilities and high compressive strengths.[54,58] The production of epoxy nanocomposites with octaamino has allowed for the systematic study of mechanical property variation (T_g, rubbery modulus, and coefficient of thermal expansion) with respect to cross-link density and chemical composition.[53,60]

The work presented in this dissertation investigates routes to well-defined, nano-building blocks with different degrees of functionality and symmetry through octa-, deca- and dodeca- phenylsilsesquioxanes (OPS, dPS, and DPS).[45] The following two chapters will discuss the electrophilic aromatic substitution of these phenylsilsesquioxanes: Iodination in Chapter 2 and Bromination in Chapter 3. Chapter 4 discusses the synthesis of hexaarylbenzene and graphene systems from ethynyl functionalized phenylsilsesquioxanes, and Chapter 5 discusses aspects of the supermolecular coordination found in these systems.

Electrophilic Substitution of Phenylsilsesquioxanes

The aromatic functionality on the periphery of these cages suggests the use of electrophilic aromatic substitution as a primary route for functionalization.[67,98] Previous studies have shown that the inorganic silica core and the linking C-Si bond of OPS are remarkably stable in the presence of strong electrophiles.[61,67] In electrophilic aromatic substitution, an electrophile attacks the π-electrons of the aromatic ring, forming a carbonium ion which loses a proton, providing the substituted aromatic.[98] Morrison and Boyd list ten prototypical substitutions, five of which are generally applicable to aromatic

systems, including: nitration, sulfonation, halogenation, and Friedel-Crafts alkylation and acylation.[98]

Olsson and Gronwall first demonstrated the electrophilic nitration of OPS using fuming nitric acid.[67] Since this early report, electrophilic aromatic substitution has proven to be a very useful technique for the synthesis of OPS derivatives. The reduction of the nitro group to provide amino functionality was subsequently demonstrated by Tamaki et al.[47] Bromination of OPS was explored by several groups, including He, et al,[68] Brick, et al,[61] and Erben, et al[69] with variations in catalyst, temperature, and heating technique. Brick et al were the first to alkylate OPS, producing low-melting solids.[63]

Though the synthesis of functionalized derivatives of OPS is readily accomplished by aromatic electrophilic substitution, the subsequent analysis has been hindered by the range of substitution patterns.[61,63,64,67-69] Electrophilic aromatic substitutions typically occur probabilistically, leading to an *ortho:para:meta (o:p:m)* ratios of substitution.[98] The presence of substituents on the aromatic ring alters the distribution of π-electron density, influencing the substitution pattern.[98]

Four characteristics used to describe these effects, *deactivating*, *activating*, *ortho/para directing*, and *meta directing*.[98] In general, activating groups that donate electron density to the aromatic ring, including alkyl, amine, alkoxy and hydroxyl groups, raise the reactivity towards substitution.[98] Deactivating groups, that pull electron density from the aromatic ring, including nitro, halogen, ammonium, trihalomethyl and carboxylate groups, lead to a lower reactivity towards substitution.[98]

The mechanisms of activation and direction are found to be intimately related to the substituent's inductive and resonant effects.[98] Activating groups are generally

ortho/*para* directors, but so are deactivating halogen substituents, due to the release of p-orbital electrons of the halogen into the π-orbital electrons of the aromatic ring.[98,99] Deactivating groups strongly reduce the reactivity for substitution at the *ortho* and *para* positions, and therefore effectively act as *meta* directors.[98,99,100] These observations are of interest in this context due to the observations and conclusions of Feher et al.[101]

Feher et al suggest that the silsesquioxane cage acts as an electron withdrawing substituent, roughly equivalent to a trifluoromethyl (CF_3) group, on the basis of ^{13}C chemical shift correlation to Hammet substituent constants.[101] CF_3 groups are found to be extremely strong *meta* directors, quantitatively in the case of nitration;[99] so it might be expected that the nitration of OPS would yield the *meta* substituted derivative in good yield. However, Tamaki et al report that nitration of OPS occurs in a roughly equivalent manner at the *meta* and *para* positions on the basis of ^{13}C NMR data.[47]

Nelson's review of the literature showed that these *o:p:m* directing effects differ from reaction to reaction.[99] For example, previous nitration studies found that electron withdrawing halogens uniformly direct *para* 60-70%, with the remainder predominantly *ortho*, and only traces *meta* substitution.[99] With respect to bromination, Ferguson et al studied $AlBr_3$ catalyzed bromination of halobenzenes and found a 90 % preference for *para* substitution.[100] Therefore, even if a given substituent shows one directing effect for nitration, it might show a different effect for iodination or bromination.

Morrison and Boyd discuss one variation of this empirical effect with consideration of the resonance structures the halobenzene under *ortho* or *para* attack.[98] Since the halogen is capable of stabilizing a positive charge, these additional resonance contributions lead to a greater likelihood of electrophilic substitution at these positions.

This *resonance* effect, seen schematically in Figures **1.12** and **1.13**, counteracts the *inductive* effect due to the electronegativity of the halogen.

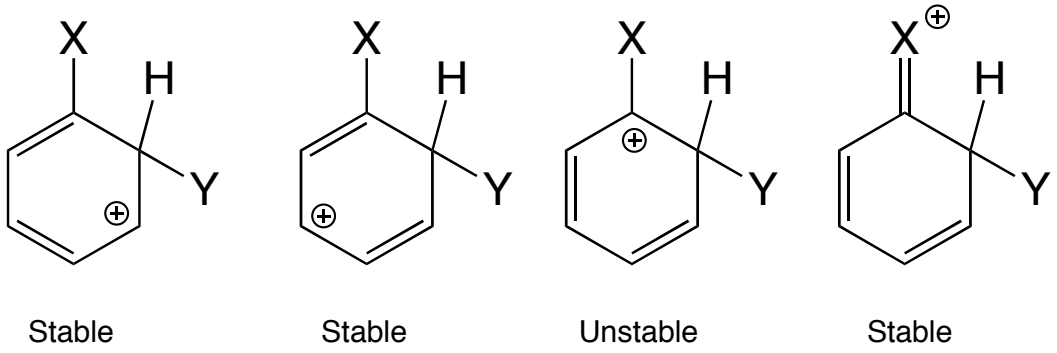

Figure 1.12 Resonance structures of *ortho* electrophilic attack on a halobenzene.[98]

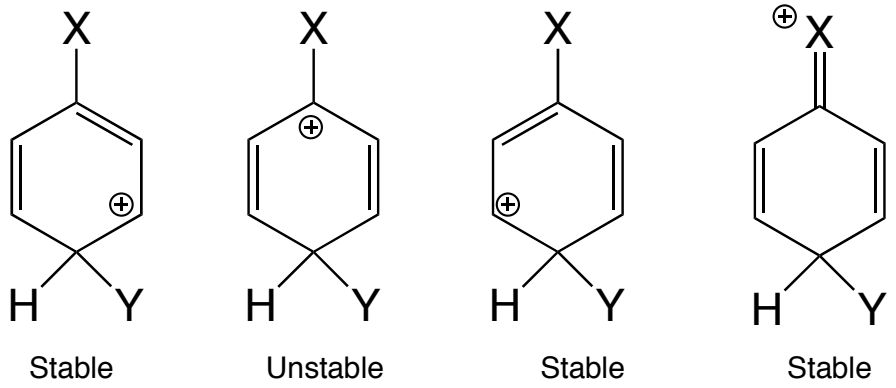

Figure 1.13 Resonance structures of *para* electrophilic attack on a halobenzene.[98]

Considering these *o:p:m* ratios, we see the chances of forming a fully symmetric, octa-functional molecule is low, namely the *highest substitution probability raised to the eighth power*. A substitution reaction with a positional selectivity of 90% has maximum theoretical yield of 43% of the perfectly symmetric octamer. Brick et al reported a *para* bromination preference of 60%, giving a theoretical yield of the symmetrically *para* brominated octamer < 2 %.[61] The equivalent probability of *para* or *meta* for OPS nitration by Tamaki et al gives < 0.5 % theoretical yield of the symmetric octamer.[47]

These theoretical yields additionally presume that the symmetrical material can be separated efficiently from large number of almost identical compounds. From these data,

it appears that a new synthetic route is necessary to reach the required selectivity. Even through it is possible to successfully tailor global properties at nanometer length scales using asymmetric nano-building blocks careful choice of the assembly chemistries;[53,54,58,60] it is still highly desirable to avoid introducing defects at the earliest stage of functionalization.

A low yield of a symmetrical eight-fold substitution reaction practically precludes recrystallization for purification or the analytical use of single-crystal X-ray diffraction. Interpretation of ^{1}H NMR spectra is hindered by multiple overlapping resonances from each different substitution pattern. With NMR analysis functionally impractical, cleavage of the organic group by fluoride provides a good method of analyzing the substitution pattern, as shown in Scheme **1.4**.[61]

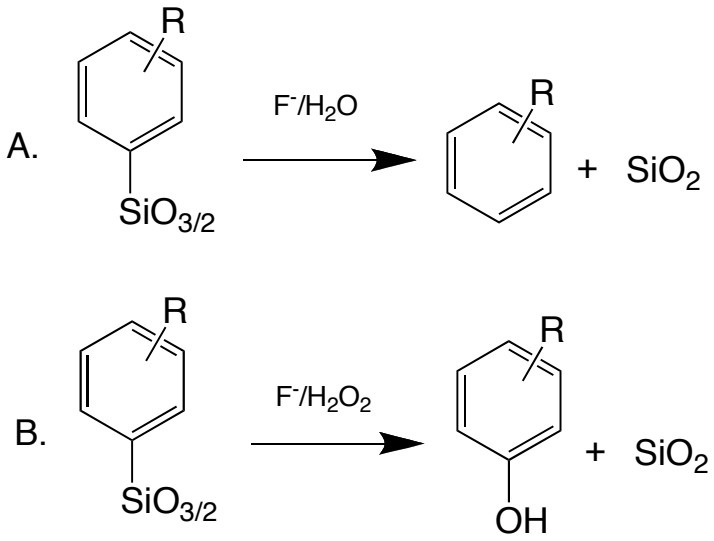

Scheme 1.4 Si-C cleavage reactions using fluoride.[61]

Supermolecular Structures from Nano-Building Blocks

Our goal is to develop nano-building blocks from polyhedral phenylsilsesquioxanes as tools to produce nano-structured materials or nanocomposites.

To achieve this goal, precise knowledge of the chemical constitution of the building block must be known, in order to develop structure-property relationships and successfully tailor or tune material properties. Therefore, synthetic control over the chemical substitution of the nano-building block and the ability to analyze its derivatives are paramount. We have discussed the synthetic flexibility of OPS, providing the potential to alter a wide variety of material properties. Additionally, some portion of the functionality must direct the assembly of these building blocks over macroscopic length scales through chemical bonding or supermolecular coordination.

Supermolecular chemistry is a promising route for molecular assembly and an area of great current interest.[102,103] The fundamental character of this field is defined by Desiraju as the interaction of molecules through coordination motifs, or synthons, to generate macroscopic, crystalline solids.[102] The degree of molecular order allows for X-ray analysis to be used in the refinement of crystal structures, which may be used to determine the nature of the supermolecular coordination. However, achieving this degree of order requires a crystalline molecular- or nano-building block.[102,103]

This area of chemistry encompasses the rapidly growing study of metal-organic-frameworks (MOFs)[25,79,105] and covalent-organic-frameworks (COFs).[80,81,104] Both MOFs and COFs have utilized the symmetry of the constituent organic building blocks to drive the development of new coordination motifs and porosity characteristics. With respect to 3-D molecular scaffolds, tetra-functional methanes,[80] silanes,[80] and adamantanes[25] have been used to introduce tetrahedral geometry to coordination structure, in addition to the previously discussed tetraphenyladamantane (TPA) derivatives.

The previously discussed examples of TPA coordination compounds[21,22,25,78,79] (Figure **10**) suggest the potential to conduct supermolecular assembly using OPS derivatives, if the synthetic hurdle to substitutional selectivity can be overcome. Such nano-building blocks could be used to produce materials with tunable mechanical, optical and electronic properties. This dissertation documents progress towards these goals.

Chapter 2 describes the successful iodination of octa-, deca- and dodeca-phenylsilsesquioxane[45] using iodine monochloride in methylene chloride ca. -40°C.[64] In the case of the octamer we have successfully isolated the > 95% *para*- isomer. Thereafter, we began efforts to modify these compounds using palladium carbon-carbon coupling chemistry, secondary derivatives of these compounds were synthesized via Heck, Sonogashira, and Suzuki couplings.[64]

In Chapter 3 we will discuss how we have extended our previous examinations of OPS bromination with respect to both the degree and the specificity of the substitution. We have discovered a route to the octa(*ortho*-bromophenyl)silsesquioxane, in addition to the symmetric octa(2,5-dibromphenyl)silsesquioxane, and the disordered tetraicosabrominated OPS.

Chapter 4 will discuss the Diels-Alder cyclization of tetraarylcyclopentadienones with the ethynyl-functionalized derivatives[106] to synthesize and octa(hexaphenylbenzene)silsesquioxane. This 4 kilo-dalton macromolecule crystallizes into a 1 cubic nanometer unit cell with Z=1 and contains the more carbons than any other discrete compound in the Cambridge Structural Database.

Finally, we have explored the Scholl-type cyclization of these octa-(hexaarylbenzene)-silsesquioxanes to form the octa-(hexa-*peri*-benzocoronene)-

silsesquioxanes.[107] Planar, poly-aromatic hydrocarbons (PAHs), such as hexa-*peri*-benzocoronene, show a high degree of π-delocalization. Their structural similarity to graphite has led to the use of the term graphene.[107] The potential for the use of PAH materials in advanced electronic devices has led to theoretical, synthetic and analytical work documenting their properties.[108,109] Müllen has systematically investigated the synthesis of such graphenes from small molecule and oligomer precursors, as well as their use in microelectronic devices such as Field Effect Transistors.[109]

The extension of PAH chemistry onto the cubic silsesquioxanes would allow for the exploration of electronic and photophysical effects by rigidly orienting the graphene moieties with respect to one another. To date, soluble graphenes utilize pendant alkyl groups on the periphery of the aromatic core to block π···π stacking and subsequent precipitation.[107-109] We presume that attaching these graphenes onto a rigid core would prevent complexation, limiting the solubility of unfunctionalized graphenes.

This degree of synthetic control over the substituent position on such a silsesquioxane nano-building block will allow ease of purification and design of a wide variety of materials with nm by nm control. These materials maintain the same high temperature stability while introducing great structural control, unique photo-physical properties, and possible electronic delocalization. This dissertation describes work towards these materials.

References Cited:

1. Detken, A.; Zimmermann, H.; Haeberlen, U.; Poupko, R.; Luz, Z. "Molecular Reorientation and Self-Diffusion in Solid Cubane by Deuterium and Proton NMR." *Journal of Physical Chemistry* **100**, 9598–604 (1996).
2. Hawker, C.J.; Wooley, K.L. "The Convergence of Synthetic Organic and Polymer Chemistry," *Science* **309**, 1200-5.
3. Feynman, R. "There's Plenty of Room at the Bottom." *Journal of Microelectromechanical Systems* **1**, 60-6 (1992).
4. Eaton, P.E.; Galoppini, E.; Gilardi, R. "Alkynylcubanes as Precursors of Rigid-Rod Molecules and Alkynylcyclooctatetraenes." *Journal of the American Chemical Society*, **116**, 7588-96 (1994).
5. Mellot-Draznieks, C.; Girard, S.; Ferey, G. "Novel Inorganic Frameworks Constructed from Double-Four-Ring (D4R) Units: Computational Design, Structures, and Lattice Energies of Silicate, Aluminophosphate, and Gallophosphate Candidates." *Journal of the American Chemical Society* **124**, 15326-35 (2002).
6. Morris, R.E. "Modular materials from zeolite-like building blocks." *Journal of Materials Chemistry* **15**, 931-8 (2005).
7. Eaton, P. E. Cubane: Starting Materials for the Chemistry of the 1990s and the New Century. *Angewandte Chemie, International Edition in English* **31**, 1421–36 (1992).
8. Yildrim, T.; Gehring, P. M.; Neumann, D. A.; Eaton, P. E.; Emrick, T. "Solid Cubane: A Brief Review." *Carbon* **36**, 809–15 (1998).
9. Fleischer, E.B. "X-Ray Structure Determination of Cubane." *Journal of the American Chemical Society* **86**, 3889-90 (1964).
10. Eaton, P.E.; Pramod, K.; Emrick, T.; Gilardi, R."Building with Cubane-1,4-diyl. Synthesis of Aryl-Substituted Cubanes, p-[n]Cubyls, and Cubane-Separated Bis(arenes)." *Journal of the American Chemical Society* **121**, 4111-23 (1999).
11. Eaton, P.E.; Gilardi, R.L.; Zhang, M.-X. "Polynitrocubanes: Advanced High-Density, High-Energy Materials." *Advanced Materials* **12**, 1143-8 (2000).
12. Zhang, M.-X.; Eaton, P.E.; Gilardi, R. "Hepta- and Octanitrocubanes." *Angewandte Chemie, International Edition in English* **39**, 401-4 (2000).
13. Eaton, P.E.; Zhang, M.-X.; Gilardi, R.; Gelber, N.; Iyer, S.; Surapaneni, R. "Octanitrocubane: A New Nitrocarbon." *Propellants, Explosives, Pyrotechnics* **27**, 1-6 (2002).
14. Bertau, M.; Wahl, F.; Weiler, A.; Scheumann, K.; Worth, J.; Keller, M.; Prinzbach, H. "From Pagodanes to Dodecahedranes - Search for a Serviceable Access to the Parent ($C_{20}H_{20}$) Hydrocarbon." *Tetrahedron* **53**, 10029-40, (1997).

15. Irngartinge, H.; Goldmann, A.; Jahn, R.; Nixdorf, M.; Rodewald, H.; Maier, G.; Malsch, K.-D.; Emrich, R."Tetra-tert-butyltetrahedrane - Crystal and Molecular Structure." *Angewandte Chemie, International Edition in English* **23**, 993-4 (1984).

16. Maier, G.; Neudert, J.; Wolf, O.; Pappusch, D.; Sekiguchi, A.; Tanaka, M.; Matsuo, T. "Tetrakis(trimethylsilyl)tetrahedrane." *Journal of the American Chemical Society* **124**, 13819-26 (2002).

17. Newman, H. "Facile Syntheses of 1,3-Diphenyl, 1,3,5-Triphenyl-, and 1,3,5,7-Tetraphenyladamantane from 1-Bromoadamantane." *Synthesis* **1972**, 692-3.

18. Reichert, V.R.; Mathias, L.J. "Expanded Tetrahedral Molecules from 1,3,5,7-Tetraphenyladamantane." *Macromolecules* **27**, 7015-23 (1994).

19. Reichert, V.R.; Mathias, L.J. "Highly Cross-Linked Polymers Based on Acetylene Derivatives of Tetraphenyladamantane." *Macromolecules* **27**, 7030-4 (1994).

20. Reichert, V.R.; Mathias L.J. "Tetrahedrally-Oriented Four-Armed Star and Branched Aramids." *Macromolecules,* **27**, 7024-9 (1994).

21. Boldog, I.; Lysenko, A.B. Rusanov, E.B.; Chernegab, A.N.; Domasevitcha, K.V. "1,3,5-Triphenyladamantane and 1,3,5,7-tetraphenyladamantane" *Acta Crystallographica* **C65**, o248–o252 (2009).

22. Wang, S.; Oldham W.J.Jr.; Hudack, R.A. Jr.; Bazan, G.C. "Synthesis, Morphology, and Optical Properties of Tetrahedral Oligo(phenylenevinylene) Materials." *Journal of the American Chemical Society* **122**, 5695-709 (2000).

23. Sanchez, C.; de A.A. Soler-Illia, G.J.; Ribot, F.; Lalot, T.; Mayer, C.R.; Cabuil, V. "Designed Hybrid Organic-Inorganic Nanocomposites from Functional Nanobuilding Blocks." *Chemistry of Materials* **13**, 3061-8 (2001).

24. Sanchez, C.; Julia, B.; Belleville, P.; Popall, M. "Applications of hybrid organic–inorganic nanocomposites." *Journal of Materials Chemistry* **15**, 3559–92 (2005).

25. Kim, J.; Chen, B.; Reineke, T.M.; Li, H.; Eddaoudi, M.; Moler, D.B.; O′Keeffe, M.; Yaghi, O.M. "Assembly of Metal-Organic Frameworks from Large Organic and Inorganic Secondary Building Units: New Examples and Simplifying Principles for Complex Structures." *Journal of the American Chemical Society* **123**, 8239-47 (2001).

26. Lee, M.W.; Farha, O.K. Hawthorne, M.F.; Hansch, C.H. "Alkoxy Derivatives of Dodecaborate : Discrete Nanomolecular Ions with Tunable Pseudometallic Properties." *Angewandte Chemie, International Edition in English* **46**, 3018 –22 (2007).

27. Farha, O. K.; Julius, R. L.; Lee, M. W.; Huertas, R. E.; Knobler, C. B.; Hawthorne, M. F. Synthesis of Stable Dodecaalkoxy Derivatives of hypercloso-$B_{12}H_{12}$. *Journal of the American Chemical Society* **127**, 18243–51 (2005).

28. Bayer, M.J.; Frederick Hawthorne, M.F. "An Improved Method for the Synthesis of [closo-$B_{12}(OH)_{12}]^{2-}$." *Inorganic Chemistry* **43**, 2018–20 (2004).

29. Peymann, T.; Knobler, C. B.; Khan, S. I.; Hawthorne, M. F. Dodecahydroxy-closo-dodecaborate^{2-}. *Journal of the American Chemical Society* **123**, 2182–5 (2001).

30. Peymann, T.; Knobler, C.B.; Hawthorne, M.F. "An unpaired electron incarcerated within an icosahedral borane cage: synthesis and crystal structure of the blue, air-stable {[closo-B12(CH3)12]·}2 radical." *Chemical Communications* **1999**, 2039–40.

31. Peymann, T.; Knobler, C.B.; Hawthorne, M.F. "An Icosahedral Array of Methyl Groups Supported by an Aromatic Borane Scaffold: The [closo-$B_{12}(CH_3)_{12}$]$^{2-}$ Ion." *Journal of the American Chemical Society* **121**, 5601-2 (1999).

32. Wiberg, N.; Finger, C.M.M.; Polborn, K. "Tetrakis(tri-tert-butylsilyl)-tetuahedro-tetrasilane (tBu,Si),Si, : The First Molecular Silicon Compound with a Si, Tetrahedron." *Angewandte Chemie, International Edition in English* **32**, 1054-6 (1993).

33. Sekiguchi, A.; Yatabe, T.; Kabuto, C.; Sakurai, H."The "Missing" Hexasilaprismane: Synthesis, X-ray Analysis, and Photochemical Reactions." *Journal of the American Chemical Society* **115**, 5853-4 (1993).

34. Kazuaki Furukawa, K.; Fujino, M.; Matsumoto, N. "Cubic silicon cluster." *Applied Physics Letters* **60**, 2744-5 (1992).

35. Sekiguchi, A.; Yatabe, T.; Kamatani, H.; Kabuto, C.; Sakurai, H. "Preparation, Characterization, and Crystal Structures of Octasilacubanes and Octagermacubanes." *Journal of the American Chemical Society* **114**, 6260-2 (1992).

36. Matsumoto, H.; Higuchi, K.; Kyushin, S.; Goto, M. "Octakis(1,1,2-trimethylpropyl)octasilacubane: Synthesis, Molecular Structure, and Unusual Properties." *Angewandte Chemie, International Edition in English* **31**, 1354-6 (1992).

37. Matsumoto, H.; Higuchi, K.; Hoshino, Y.; Koike, H.; Naoi, Y.; Nagai, Y. "The First Octasilacubane System: Synthesis of Octakis-(t - butyldimethylsilyl) pentacyclo [4.2.0.02,5.03,8.04,7] octasilacubane." *Journal of the Chemical Society, Chemical Communications* **1988,** 1083-4.

38. Laine, R. M. "Nanobuilding blocks based on the [$OSiO_{1.5}$]$_x$ (x = 6, 8, 10) silsesquioxanes." *Journal of Materials Chemistry* **15**, 3725–44 (2005).

39. Baney, R. H.; Itoh, M.; Sakakibara, A.; Suzuki, T. "Silsesquioxanes." *Chemical Reviews* **95**, 1409–30 (1995).

40. Voronkov, M. G.; Lavrent'yev, V. I. "Polyhedral Oligosilsesquioxanes and Their Homo Derivatives." *Topics in Current Chemistry* **102**, 199–236 (1982).

41. Vautravers, N.R.; Pascal Andre, P.; Slawina, A.M.Z.; Cole-Hamilton, D.J. "Synthesis and characterization of photoluminescent vinylbiphenyl decorated polyhedral oligomeric silsesquioxanes."*Organic and Biomolecular Chemistry* **7**, 717–24 (2009).

42. Sulaiman, S.; Bhaskar, A.; Zhang, J.; Guda, R.; Goodson T, III; Laine, R.M. "Molecules with Perfect Cubic Symmetry as Nanobuilding Blocks for 3-D Assemblies. Elaboration of Octavinylsilsesquioxane. Unusual Luminescence Shifts May Indicate Extended Conjugation Involving the Silsesquioxane Core." *Chemistry of Materials* **20**, 5563-73 (2008).

43. Itami, Y.;Marciniec, B.; Kubicki, M. "Functionalization of Octavinylsilsesquioxane by Ruthenium-Catalyzed Silylative Coupling versus Cross-Metathesis." *Chemistry: A European Journal* **10**, 1239-48 (2004).

44. Babin, S.; and Koops, H. W. P. "Three-dimensional electron-beam lithography using an all-dry resist process." *Journal of Vacuum Science and Technology B* **14**, 3860-3 (1996).

45. Brown, J.F. Jr.; Vogt, L.H.; Prescott, P.I. "Preparation and Characterization of the Lower Equilibrated Phenylsilsesquioxanes." *Journal of the American Chemical Society* **86**, 1120-5 (1964).

46. Xu, H.; Yang, B.; Gao, X.; Li, C.; Guang, S. "Synthesis and Characterization of Organic–Inorganic Hybrid Polymers with a Well-Defined Structure from Diamines and Epoxy-Functionalized Polyhedral Oligomeric Silsesquioxanes." *Journal of Applied Polymer Science* **101**, 3730-5 (2006).

47. Tamaki, R., Tanaka, Y.; Asuncion, M.Z.; Choi, J.; Laine, R.M. "Octa(aminophenyl)silsesquioxane as a Nanoconstruction Site." *Journal of the American Chemical Society* **123**, 12416-7 (2001).

48. Sellinger, A.; Laine, R.M. "Silsesquioxanes as Synthetic Platforms. 3. Photocurable, Liquid Epoxides as Inorganic/Organic Hybrid Precursors." *Chemistry of Materials* **8**, 1592-3 (1996).

49. Sellinger, A.; Laine, R.M. "Silsesquioxanes as Synthetic Platforms. Thermally Curable and Photocurable Inorganic/Organic Hybrids." *Macromolecules* **29**, 2327-30 (1996).

50. Asuncion, M.Z.; Laine, R.M. "Silsesquioxane Barrier Materials." *Macromolecules* **40**, 555-62 (2007).

51. Choi, J.; Yee, A.F.; Laine, R.M. "Organic/Inorganic Hybrid Composites from Cubic Silsesquioxanes. Epoxy Resins of Octa(dimethylsiloxyethylcyclohexylepoxide) Silsesquioxane." *Macromolecules* **36**, 5666-82 (2003).

52. Choi, J.; Yee, A.F.; Laine, R.M. "Toughening of Cubic Silsesquioxane Epoxy Nanocomposites Using Core-Shell Rubber Particles: A Three-Component Hybrid System." *Macromolecules* **37**, 3267-76 (2004).

53. Choi, J.; Kim, S.G.; Laine, R.M. "Organic/Inorganic Hybrid Epoxy Nanocomposites from Aminophenylsilsesquioxanes." *Macromolecules* **37**, 99-109 (2004).

54. Tamaki, R.; Choi, J.; Laine, R.M. "A Polyimide Nanocomposite from Octa(aminophenyl)silsesquioxane." *Chemistry of Materials* **15**, 793-797 (2003).

55. Zhang, C.; Bunning, T.J.; Laine, R.M. "Synthesis and Characterization of Liquid Crystalline Silsesquioxanes." *Chemistry of Materials* **13**, 3653-62 (2001).

56. Choi, J.; Harcup, J.; Yee, A.F.; Zhu, Q.; Laine, R.M. "Organic/Inorganic Hybrid Composites from Cubic Silsesquioxanes." *Journal of the American Chemical Society* **123**, 11420-30 (2001).

57. Costa, R.O.R.; Vasconcelos, W.L.; Tamaki, R.; Laine, R.M. "Organic/Inorganic Nanocomposite Star Polymers via Atom Transfer Radical Polymerization of Methyl Methacrylate Using Octafunctional Silsesquioxane Cores." *Macromolecules* **34**, 5398-407 (2001).

58. Choi, J.; Tamaki, R.; Kim, S.G.; Laine, R.M. "Organic/Inorganic Imide Nanocomposites from Aminophenylsilsesquioxanes." *Chemistry of Materials* **15**, 3365-75 (2003).

59. Zhang, C.; Babonneau, F.; Bonhomme, C.; Laine, R.M.; Soles, C.L.; Hristov, H.A.; Yee, A.F. "Highly Porous Polyhedral Silsesquioxane Polymers. Synthesis and Characterization." *Journal of the American Chemical Society* **120**, 8380-8391 (1998).

60. Sulaiman, S.; Brick, C.M. De Sana, C.M.; Katzenstein, J.M.; Laine, R.M.; Basheer, R.A. "Tailoring the Global Properties of Nanocomposites. Epoxy Resins with Very Low Coefficients of Thermal Expansion." *Macromolecules* **39**, 5167-9 (2006).

61. Brick, C.M. Tamaki, R.; Kim, S.-G.; Asuncion, M.Z.; Roll, M.; Nemoto, T.; Ouchi, Y.; Chujo Y.; Laine, R.M. "Spherical, Polyfunctional Molecules Using Poly(bromophenylsilsesquioxane)s as Nanoconstruction Sites." *Macromolecules* **38**, 4655-60 (2005).

62. Brick, C. M.; Ouchi, Y.; Chujo, Y.; Laine, R. M. "Robust Polyaromatic Octasilsesquioxanes from Polybromophenylsilsesquioxanes, Br_xOPS, via Suzuki Coupling." *Macromolecules* **38**, 4661–5 (2005).

63. Brick, C. M.; Chan, E. R.; Glotzer, S. C.; Martin, D. C.; Marchal, J. C.; Laine, R. M. "Self-lubricating nano ball bearings." *Advanced Materials* **19**, 82–9 (2007).

64. Roll, M.F.; Asuncion, M.Z.; Kampf, J.; Laine, R.M. "*para*-Octaiodophenylsilsesquioxane, $[p\text{-}IC_6H_4SiO_{1.5}]_8$, a Nearly Perfect Nano-Building Block." *ACS Nano* **2**, 320-6 (2008).

65. Asuncion M.Z.; Roll M.F.; Laine, R.M. "Octaalkynylsilsesquioxanes, Nano Sea Urchin Molecular Building Blocks for 3-D-Nanostructures." *Macromolecules* **41**, 8047-52 (2008).

66. Sulaiman, S. unpublished results.

67. Olsson, K.; Gronwall, C. "Octa(arylsilsesquioxanes), $(ArSi)_8O_{12}$ I. Phenyl, 4-tolyl, and 1-naphthyl compounds." *Arkiv foer Kemi* **17**, 529-40 (1961).

68. He, C.B.; Xiao, Y.; Huang, J.C.; Lin, T.T.; Mya, K.Y.; Zhang, X.H. "Highly efficient luminescent organic clusters with quantum dot-like properties." *Journal of the American Chemical Society* **126**, 7792-3 (2004).

69. Erben, C.; Grade, H.; Goddard, G.D. "Bromination of octaphenylsilsesquioxane." *Silicon Chemistry* (2006). DOI: 10.1007/s11201-005-9000-5.

70. Berry, R.S.; Rice, S.A.; Ross, J. Matter in Equilibrium: Statistical Mechanics and Thermodynamics. 2nd edition. Oxford University Press: New York (2002).

71. Kotz, J.C.; Treichel, P. Jr. Chemistry and Chemical Reactivity. 4th edition. Saunders College Publishing: New York (2009).

72. Richter, R.; Roewer, G.; Böhme, U.; Busch, K.; Babonneau, F.; Martin, H.P.; Müller, E."Organosilicon Polymers—Synthesis, Architecture, Reactivity and Applications."*Applied Organometallic Chemistry* **11**, 71–106 (1997).

73. Matsumoto, H.; Kyushin, S.; Unno, M.; Tanaka, R. "Syntheses, structures, and properties of ladder oligosilanes and ladder oligogermanes." *Journal of Organometallic Chemistry* **611**, 52 – 63 (2000).

74. Corriu, R.J.P. "Ceramics and Nanostructures from Molecular Precursors." *Angewandte Chemie, International Edition in English* **39**, 1376-98 (2000).

75. Rathore, J.S; Interrante, L.V. "A Photocurable, Photoluminescent, Polycarbosilane Obtained by Acyclic Diene Metathesis (ADMET) Polymerization." *Macromolecules* **42**, 4614–21 (2009).

76. Matsumi, N.; Chujo, Y. "π-Congjugated Organoboron, Polymers via the Vacant p-orbital of the Boron Atom." *Polymer Journal* **40**, 77-89 (2008).

77. Allcock, H.R. "Recent developments in polyphosphazene materials science." *Current Opinion in Solid State and Materials Science* **10**, 231–240 (2006).

78. Jones, K.M.E.; Mahmoudkhani, A.H.; Chandler, B.D.; Shimizu, G.K.H. "An adamantane-based tetraphosphonic acid that forms an open diamondoid net via a hydrogen-bonded phosphonic acid–water cluster." *CrystEngComm* **8**, 303–5 (2006).

79. Vasylyev, M.; Neumann, R. "Preparation, Characterizaton, and Catalytic Aerobic Oxidation by a Vanadium Phosphonate Mesoporous Material Constructed from a Dendritic Tetraphosphonate." *Chemistry of Materials* **18**, 2781-3 (2006).

80. Niu, W.; Caroline O'Sullivan, C.; Rambo, B.M.; Smith, M.D.; Lavigne, J.J. "Self-repairing polymers: poly(dioxaborolane)s containing trigonal planar boron." *Chemical Communications* **2005**, 4342–44.

81. El-Kaderi, H.M.; Hunt, J.R.; Mendoza-Cortés, J.L.; Côté, A.P.; Taylor, R.E.; O'Keeffe, M.; Yaghi, O.M. "Designed Synthesis of 3D Covalent Organic Frameworks." *Science* **316**, 268-72 (2007).

82. Wolfgang Kaim, W.; Hosmane, N.S.; Zulis, S.; Maguire, J.A.; Lipscomb, W. N. "Boron Atoms as Spin Carriers in Two- and Three- Dimensional Systems." *Angewandte Chemie, International Edition in English* **48**, 5082–91 (2009).

83. Reed, C.A. "Carboranes: A New Class of Weakly Coordinating Anions for Strong Electrophiles, Oxidants, and Superacids." *Accounts of Chemical Research* **31**, 133-139 (1998).

84. Felser, C.; Fecher, G.H.; Balke, B. “Spintronics : A Challenge for Materials Science and Solid-State Chemistry.” *Angewandte Chemie, International Edition in English* **46**, 668-99 (2007).

85. Watanabe, A.; Nagai, Y.; Matsuda, M.; Suezawa, M.; Sumino, K. “Amorphous silicon structure of heat-treated poly (n-propylsilyne) studied by far-infrared spectroscopy.” *Chemical Physics Letters* **207**, 132-6 (1993).

86. Pakgamsai, C.; Kawakami, Y “Tendency of Loop Formation of Oligosilsesquioxanes Obtained from (4-Substituted phenyl)trimethoxysilane Catalyzed by Benzyltrimethylammonium Hydroxide in Benzene.” *Polymer Journal* **36**, 455-64 (2004).

87. Pakgamsai, C.; Kobayashi, N.; Koyano, M.; Sasaki, S.; Kawakami, Y. “Characterization of the Benzene-Insoluble Fraction of the Hydrolyzate of Phenyltrimethoxysilanes in the Presence of Benzyltrimethylammonium Hydroxide.” *Journal of Polymer Science: Part A: Polymer Chemistry* **42**, 4587-97 (2004).

88. Zhou, Z.; Harris, K.D.M.”Optimizing the Number of Components in a Molecular Quasicrystal: A Three-Component Material Based on the Penrose Tiling.” *Journal of Physical Chemistry C* **112**, 16186–8 (2008).

89. Guillermet, O.; Niemi, E.; Nagarajan, S.; Bouju, X.; Martrou, D.; Gourdon, A.; Gauthier, S.”Self-Assembly of Fivefold-Symmetric Molecules on a Threefold-Symmetric Surface.” *Angewandte Chemie, International Edition in English* **48**, 1970–3 (2009).

90. Hayashida, K.; Dotera, T.; Takano, A.; Matsushita, Y. “Polymeric Quasicrystal: Mesoscopic Quasicrystalline Tiling in ABC Star Polymers.” *Physical Review Letters* **98**, 195502 (2007).

91. Schäffer, C.; Merca, A.; Bögge, H.; Todea, A.M.; Kistler, M.L.; Liu, T.; Thouvenot, R.; Gouzerh, P.; Müller, A. “Unprecedented and Differently Applicable Pentagonal Units in a Dynamic Library : A Keplerate of the Type $\{(W)W_5\}_{12}\{Mo_2\}_{30}$.” *Angewandte Chemie, International Edition in English* **48**, 149 –53 (2009).

92. Shechtman, D.; Blech, I.; Gratias, D.; Cahn, J.W. “Metallic phase with long-range orientational order and No Translational Symmetry.” *Physical Review Letters* **53**, 1951-3 (1984).

93. Levin, D. Steinhardt, P.J. “Quasicrystals: A New class of Ordered Structures.” *Physical Review Letters* **53**, 2477-80 (1984).

94. Baidina, I.A.; Podberezskaya, N.V.; Borisov, S.V.; Alekseev, V.I.; Martynova, T.N.; Kabnev, A.N. “X-ray Structural Study of the Silasesquioxanes. II Crystal Structure of the Decamethylsilasesquioxane” *Zhurnal Strukturnoi Khimii* **21**, 125-9 (1980).

95. Calzaferri, G.; Claudia Marcolli, C.; Imhof, R.; Tornroos, K.W. "The monophenylhydrosilasesquioxanes $PhH_{n-1}Si_nO_{1.5n}$ where n = 8 or 10." *Journal of the Chemical Society, Dalton Transactions* **1996**, 3313-22.

96. Burgi, H.-B.; Tornroos, K.W. Calzaferri, G.; Burgy, H. "X-ray Diffraction Study of the Molecular Structure of a Spherohydridosilasesquioxane, $H_{10}Si_{10}O_{15}$, a Flexible Assembly of Rigid Tetrahedra." *Inorganic Chemistry* **32**, 4914-9 (1993).

97. Sellinger, A.; Tamaki, R.; Laine, R.M.; Ueno, K.; Tanabe H.; Williams, E.; Jabbour, G.E. "Heck coupling of haloaromatics with octavinylsilsesquioxane: solution processable nanocomposites for application in electroluminescent devices." *Chemical Communications* **2005**, 3700–2.

98. Morrison, R.T.; Boyd, R.N. Organic Chemistry. 2nd edition. Allyn and Bacon, Inc.: Boston (1966).

99. Nelson, K.L. "Directive Effects in Electrophilic Aromatic Substitution." *Journal of Organic Chemistry* **21**, 145-55 (1956).

100. Ferguson, L.N.; Garner, A.Y.; Mack, J.L. "Bromination of Halobenzenes." *Journal of the American Chemical Society* **76**, 1250-1 (1953).

101. Feher, F.J.; Budzichowski, T.A. "Syntheses of highly-functionalized polyhedral oligosilsesquioxanes." *Journal of Organometallic Chemistry*, **379**, 33-40 (1989).

102. Desiraju, G.R. "Supramolecular Synthons in Crystal Engineering-A New Organic Synthesis," *Angewandte Chemie: International Edition in English* **34**, 2311-27 (1995).

103. Desiraju, G.R. "Crystal Engineering: A Holistic View." *Angewandte Chemie: International Edition in English* **46**, 8342-56 (2007).

104. Maly, K.E. "Assembly of nanoporous organic materials from molecular building blocks." *Journal of Materials Chemistry* **19**, 1781–1787 (2009).

105. Tranchemontagne, D.J.; Mendoza-Cortes, J.L.; O'Keeffe, M.; Yaghi, O.M. "Secondary building units, nets and bonding in the chemistry of metal–organic frameworks." *Chemical Society Reviews* **38**, 1257–83 (2009).

106. Williamson, K.L. Macroscale and Microscale Organic Experiments, 2nd ed, D.C. Heath and company, Toronto, 1994.

107. Wu, J.; Pisula,W.; Mullen, K. "Graphenes as Potential Material for Electronics." *Chemical Reviews* **107**, 718–47 (2007).

108. Zhi, L.; Mullen, K. "A bottom-up approach from molecular nanographenes to unconventional carbon materials." *Journal of Materials Chemistry* **18**, 1472–1484 (2008).

109. Tsao, H.N.; Räder, H.J.; Pisula, W.; Rouhanipour, A.; Müllen, K. "Novel organic semiconductors and processing techniques for organic field-effect transistors." *phys. stat. sol. (a)* **205**, 421–9 (2008).

Chapter II

Nano-Building Blocks via Iodination of OPS, dPS, and DPS

Introduction

As discussed in Chapter 1, the assembly of 2- and 3-D structures from molecular components or nano-building blocks is of great interest.[1-9] Altering the chemical reactivity of these nano-building blocks through synthetic means would presumably allow modulation of the coupling and interaction between the blocks, in order to exactly tailor properties.[10]

Although there are numerous literature examples of molecules possessing high degrees of 2-D symmetry, only a smaller number of molecular classes possessing structure and functionality with high 3-D symmetry are known. Cubic symmetry in 3-D and octa-functionality, such that each octant in Cartesian space contains one functional group, is particularly desirable.

Cubic silsesquioxanes, Q_8 $[RMe_2SiOSiO_{1.5}]_8$ and T_8 $[RC_6H_4SiO_{1.5}]_8$ SQs or POSS compounds,[11-13] with a D4R-like silica core structure, are easily prepared in comparison to the previously discussed cubane and prismane (Chapter 1, Figure **5**) families of compounds.[1,4,5] These compounds have high thermal stability, (~500°C in air for OPS); octa-functionality (with a possibility of forty possible functional groups for OPS), and a wide variety of possible chemical consituents.[13,14]

Polyhedral Phenylsilsesquioxanes as Nano-Building Blocks

As discussed in Chapter 1, phenyltrichlorosilane ($PhSiCl_3$) may hydrolyzed and condensed to form polyphenylsilsesquioxane ($(PhSiO_{1.5})_n$, PPS), as shown in Scheme **2** (Chapter 1). By controlling solution chemistry in the synthesis of OPS; toluene, catalytic potassium hydoxide, trace water, and polyphenylsilsesquioxane (PPS) form a homogenous solution that continuously precipitates octaphenylsilsesquioxane. This crystalline, insoluble product may be isolated by filtration of the reaction solution at the end of the desired reaction period.[14-16] The filtrate may be fractionated to yield deca- and dodecameric species.[14]

The pentagonal decaphenylsilsesquioxane (dPS) has only been reported by Brown et al without a yield.[14] Brown et al fractionally crystallized the soluble products from $(PhSiO_{1.5})_n$/KOH equilibration. The equilibrium fraction soluble in 9:1 methanol:toluene was recrystallized using toluene to give decaphenylsilsesquioxane.[14] In contrast to OPS, where isolation is accomplished by the precipitation of the desired product; the high solubility of dPS greatly hinders its separation from PPS, which is also highly soluble. Since the reaction solution during base catalyzed equilibration is populated by a large number of open and closed cage polyhedral species, the isolation of a single, soluble, closed species from the equilibrium is unlikely.[14,16]

Dodecaphenylsilsesquioxane (DPS) was isolated by Brown et al in ~60% yield from the equilibration of $(PhSiO_{1.5})_n$/KOH in refluxing THF at 0.9 M concentration of $(PhSiO_{1.5})_n$.[14] The insoluble product isolated at the end of the reaction was a clathrate (1:2 DPS:THF), less soluble than OPS in THF.[14] OPS and DPS are available in commercial quantities, and offer the multi-functionality and 3-D symmetry necessary for a nano-

building block. dPS, while not commercially available currently, will be useful for comparison of physical properties and chemical reactivity.

The aromatic corners of OPS suggest the application of electrophilic aromatic substitution as a primary route to functionalize OPS.[17] Previous studies show that the inorganic core and the linking C-Si bond of OPS are remarkably stable in the presence of strong electrophiles.[17-19] In electrophilic aromatic substitution, an electrophile attacks the π-electrons of the aromatic ring, forming a carbonium ion which loses a proton, providing the substituted aromatic (Chapter 1, Figures **1.12** and **1.13**).[20] Morrison and Boyd list ten prototypical substitutions, five of which are generally applicable to aromatic systems, including: nitration, sulfonation, halogenation, and Friedel-Crafts alkylation and acylation.[20]

Iodination of Polyhedral Phenylsilsesquioxanes

Halogenation reactions typically use a Lewis Acid to polarize a diatomic halogen, X_2.[18,20] This induced polarization generates an electrophilic halogen "X^+," which attacks the aromatic ring.[20] An oxidizing agent is typically used in iodination to generate I^+ *in situ*.[20,21]

Vogel suggests the use of fuming nitric acid as an oxidant in the iodination of benzene.[22] The expensive hypervalent iodine reagent bis-(trifluoroacetoxy)iodobenzene (BFIB) has been used as an oxidant in the synthesis of tetra(*p*-iodophenyl)adamantane[23] and hexa(*p*-iodophenyl)benzene[24] (See Figure **2.1a**,**b**). In contrast, the less expensive iodine monochloride (ICl) is permanently polarized due to the higher electronegativity of chlorine, acting effectively as a stable I^+ source.[21] ICl is commercially available in

methylene chloride solution, the best solvent for OPS, which reduces the heterogeneity of the reaction.

Iodinated aromatics, such as the tetra(p-iodophenyl)adamantane[23] and the hexa(p-iodophenyl)benzene,[24] are useful precursors for the synthesis of complex molecular systems, like our targeted nano-building blocks. One reason is the extensive development of catalytic C-C and C-heteroatom bond forming reactions via cross-coupling over the past few decades which has multiplied the types of functionality which may be incorporated.[25-34]

Some examples of C-C bond formation based on C-halogen functionalization include the Heck,[27] Stille,[33] Suzuki[26] and Sonogashira[25] reactions. The incorporation of heteroatoms, multiplying the accessible functionality, can be accomplished through amination,[29,34] phosphonation,[31] etherfication[30] and thioetherification.[32] Examples of such reactions are shown below in Scheme **2.1**, and discussed below in "Synthesis and Physical Characterization of Cross-coupling Derivatives."

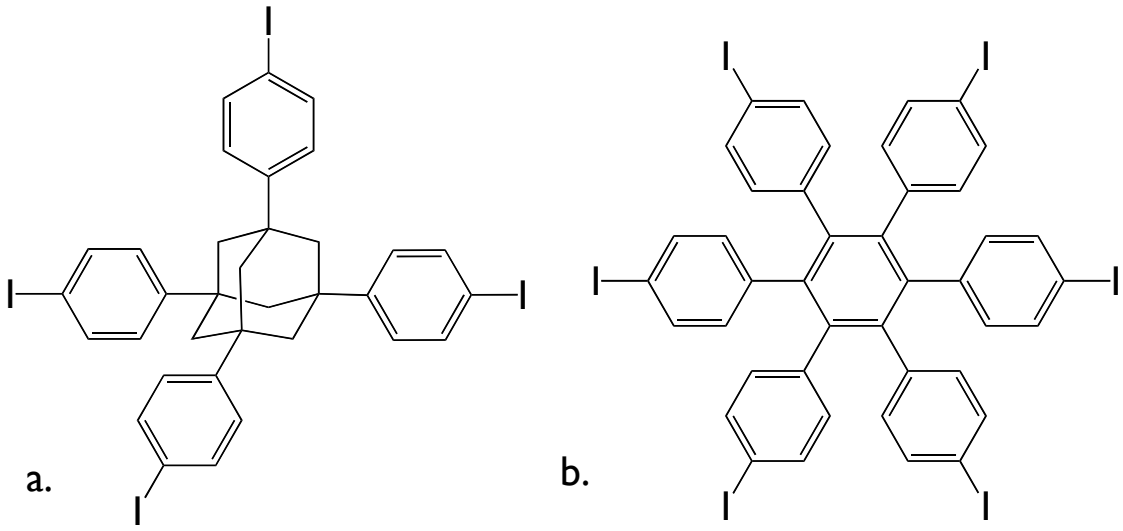

Figure 2.1 The symmetrically iodinated tetraphenyladamantane, **a**.; and hexaphenylbenzene, **b**.

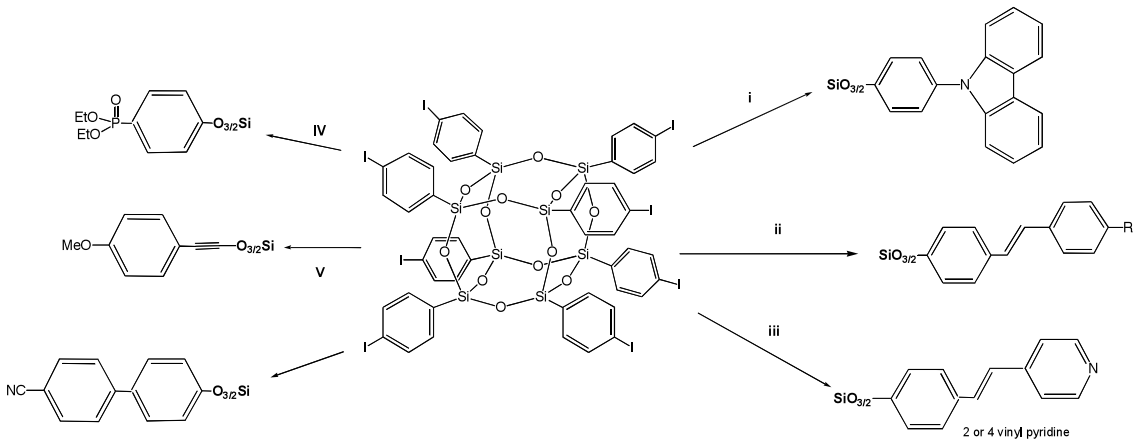

Scheme 2.1 Functionalization of I_8OPS using traditional coupling chemistries (see Experimental).[41,42]

In addition, the low energy of the C-I bond has allowed extensive studies into thermolysis[35-38] and photolysis[38-40] of aryl iodides to generate aryl radicals.[41-43] These radicals could be used to initiate other reactions or create new bonds via radical recombination.[44-45] A nano-building block bearing multiple radicals could be used to create highly cross-linked materials in photolithography, or as UV curing agents.

As discussed in Chapter 1, while previous electrophilic substitutions of OPS have produced material without symmetric functionality, they do not preclude the discovery of reactions that substitute with greater specificity. Therefore, the foregoing provide the impetus to investigate the iodination of the polyhedral phenylsilsesquioxanes.

Results and Discussion

Synthesis and Physical Characterization of Decaphenylsilsesquioxane

Because OPS and DPS have been well characterized,[14-16] the following discussion will begin with the synthesis and characterization of decaphenylsilsesquioxane (dPS). Though KOH is often used as the base catalyst to rearrange silsesquioxane cages, alkali metal picrates have been shown to complex with silsesquioxane cages.[46] To separate the

effects of complexation and rearrangement, it was desirable to use a catalyst with minimal interaction with the cage.

Previous work showed that $Ba(OH)_2$ does not react with OPS derivatives in toluene or xylenes, even under reflux.[47] However, the combination of $Ba(OH)_2$ and *catalytic* 18-crown-6 gives an active catalyst for rearrangement. If BaO is substituted for $Ba(OH)_2$, any adventitious water is removed by the dessicating action of BaO.[48]

Combining these insights, we have found that the anhydrous base-catalyzed rearrangement of dodecaphenylsilsesquioxane in *m*-xylene under high dilution (3 g DPS/ 100 ml *m*-xylene) allows for the isolation of decaphenylsilsesquioxane. Specifically, the rearrangement of DPS by BaO/18-crown-6 equilibration in *m*-xylene is conducted at reflux for 1 d, and dPS is isolated by repeated recrystallization from toluene in 15% yield.

Since the ^{1}H and ^{13}C NMR spectra have not been reported previously, they are included here in Figures **2.2** and **2.3** with assignments. ^{1}H NMR shows three distinct multiplets, one of which overlaps the chloroform solvent resonance. Peak assignments are made by comparison with the ^{1}H NMR spectra of OPS, as well as peak integration and multiplicity. ^{13}C NMR shows two sharp signals at 134.116 and 127.658 ppm with two smaller peaks at 130.545 and 130.484 ppm. Assignments in this case are based on peak intensities as well as ^{13}C NMR spectra of OPS.

MALDI-TOF spectrum of the decaphenylsilsesquioxane is shown below in Figure **2.4**. One of the three independent molecules in the decaphenylsilsesquioxane•toluene crystal structure is shown in Figure **2.5**.

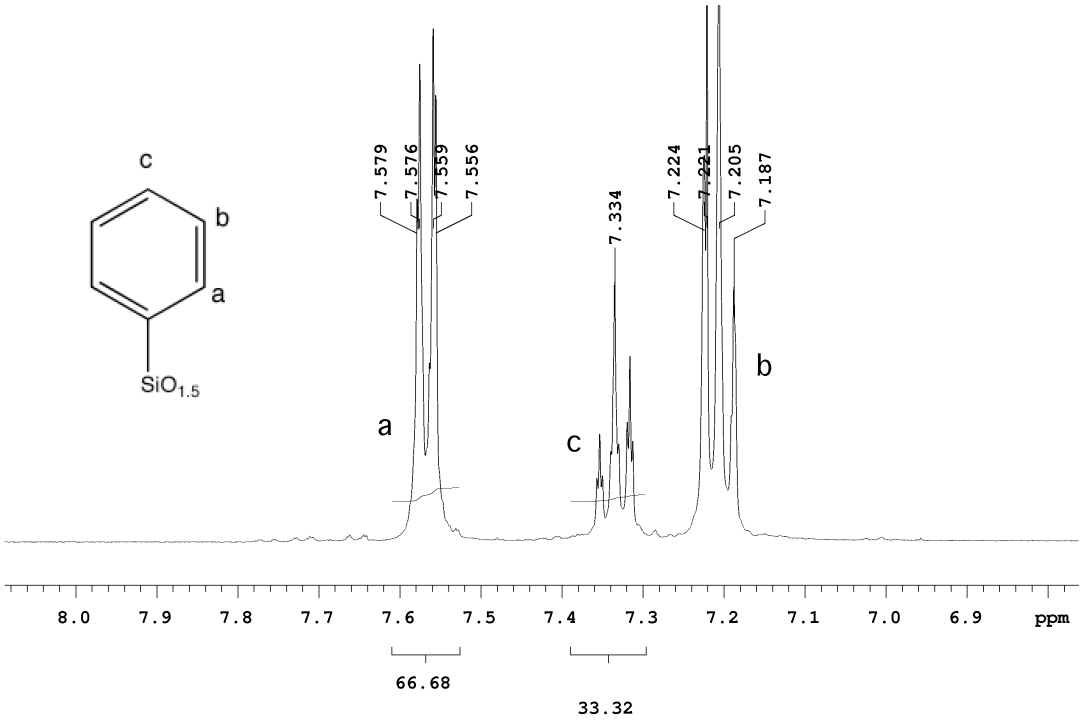

Figure 2.2 ^{1}H NMR spectrum of decaphenylsilsesquioxane in $CDCl_3$.

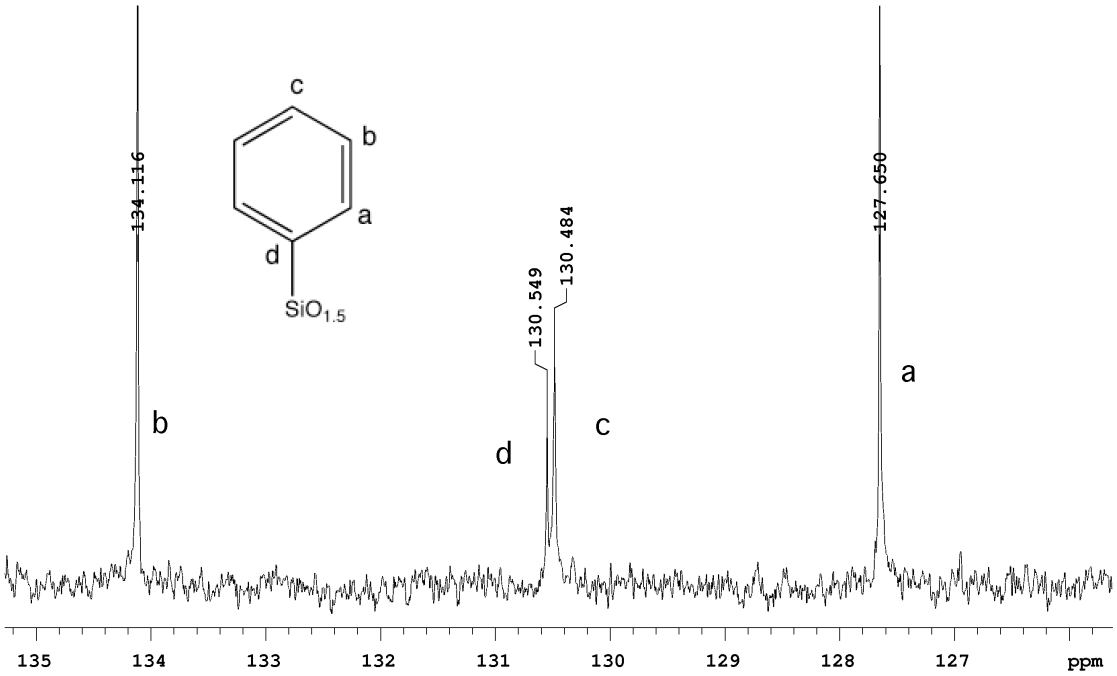

Figure 2.3 ^{13}C NMR spectrum of decaphenylsilsesquioxane in $CDCl_3$

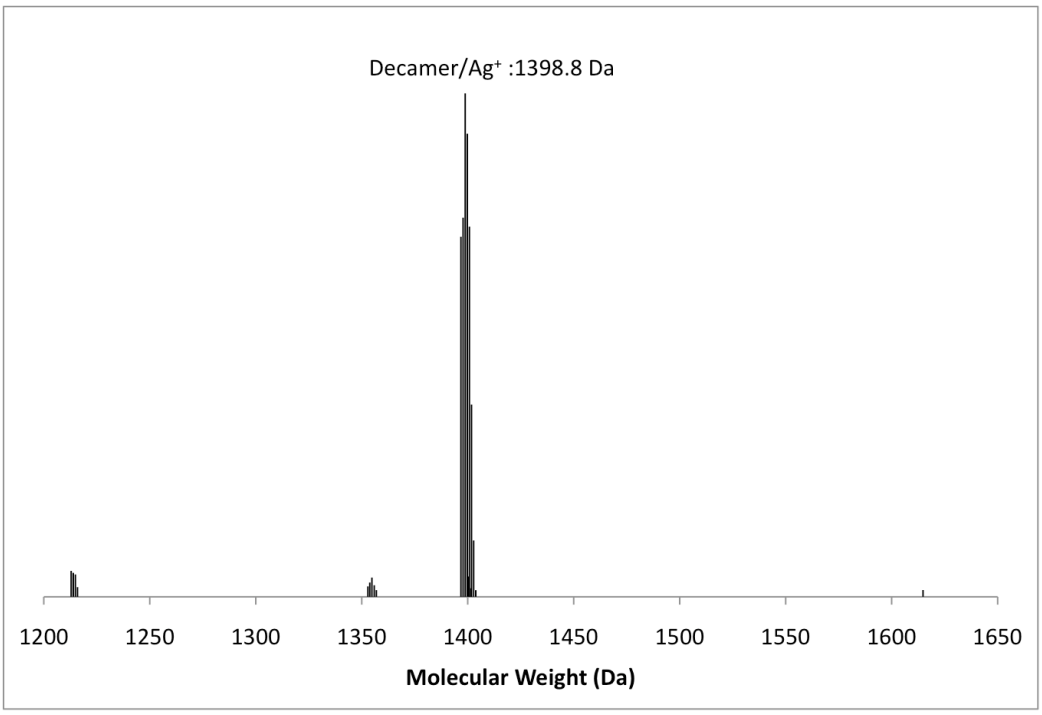

Figure 2.4 MALDI-TOF spectrum of decaphenylsilsesquioxane (Dithranol/Ag^+).

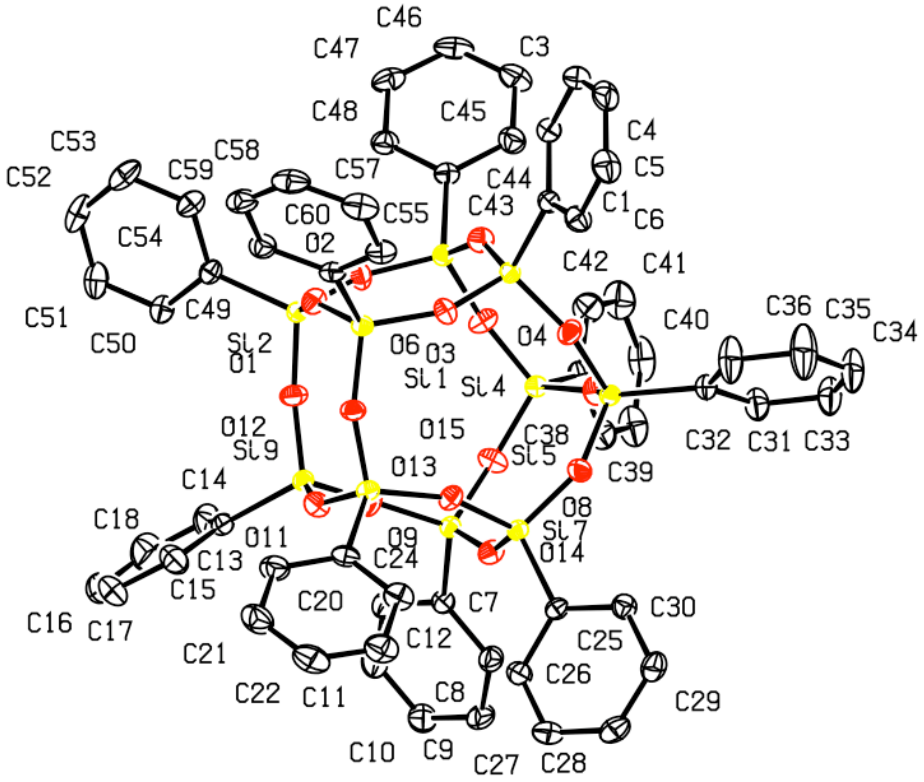

Figure 2.5 50 % thermal ellipsoid plots of decaphenylsilsesquioxane • toluene. Hydrogen atoms and toluene solvents are omitted for clarity.
Full XRD data can be found in Appendix 1.

Table 2.1 Crystal Structure Data for decaphenylsilsesquioxane • toluene

	dPS • toluene
Space Group	P-1, triclinic
Unit Cell Dimensions	a= 12.5377(9) Å b= 24.6836(17) Å c= 35.061(2) Å
	α = 72.7060(1)° β= 80.4340(1)° γ= 81.3950(1)°
Unit Cell Volume	10157.8(12) $Å^3$
Z, Density	6, 1.358 Mg/m^3
R-factor	4.1 %

Decaphenylsilsesquioxane is a uniquely soluble member of the family of polyhedral phenylsilsesquioxanes. Its isolation in this case is accomplished by reducing the number of open-cage species present. Since the formation of each dangling silanol from an open cage silsesquioxane requires the addition half of one water molecule, we use anhydrous conditions. By minimizing the open-cage species, we maximize the population of closed cage species, predominantly OPS, dPS and DPS. The separation of these three species is readily accomplished by recrystallization.

We now discuss the iodination of the OPS, dPS and DPS systems as a route to provide symmetrically functionalized nano-building blocks with a variety of geometries.

Synthesis and Physical Characterization of Iodinated OPS, dPS, and DPS

For operational simplicity, initial reactions of OPS with ICl in methylene chloride (see Scheme **2.2**) were conducted at room temperature. Complete octa-substitution was readily achieved, and recrystallization from ethyl acetate afforded < 20 % of the theoretical yield as colorless crystals of I_7OPS and I_8OPS by filtration. The filtrate was

reduced to an oil and precipitated into methanol and recovered as a white powder comprised of I_7OPS, I_8OPS, and I_9OPS in ~65-70 % theoretical yield, based on octa-substitution. We were pleasantly surprised to discover that iodination of OPS with ICl at -40°C followed by recrystallization from ethyl acetate provided 30-40 % colorless crystals of I_7OPS and I_8OPS by filtration, based on octa-substitution. As before, the remaining material was reduced to an oil, precipitated into methanol, and recovered as a white powder comprised of I_7OPS, I_8OPS, and I_9OPS. The next concern was the quantifying the differences in substitution pattern for each fraction.

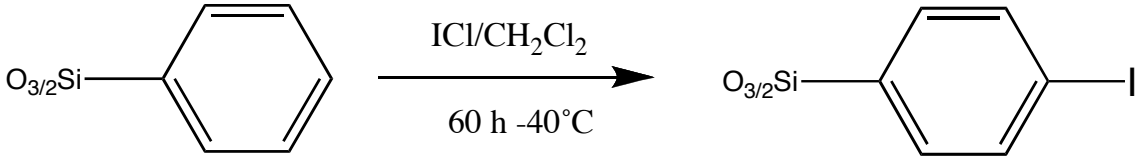

Scheme 2.2 Iodination of phenylsilsesquioxane.

Though initial NMR data suggested *para* substitution, oxidative cleavage using fluoride (Chapter 1, Scheme **1.3**, B.) was used to produce the iodophenols, allowing the substitution patterns of the crystalline and oil fractions to be quantified. Recrystallization, giving 30-40 % of the theoretical yield by mass, is found to remove the I_9 isomer and GC/MS analysis of the resulting iodophenols shows *para*-iodophenol and only traces of phenol or other iodophenols.[19]

^{1}H NMR of the phenolic cleavage products reveals a few percent of additional iodophenol isomers. The identities of these isomers were confirmed by spiking the cleavage products with 2-iodophenol and 3-iodophenol in separate experiments (see Experimental, Chapter 7). Only traces of phenol were detected in these experiments, indicating essentially complete octa-iodination. In this way, the product that is shown to

be ≥ 99 % octa-substituted and ≥ 95% para- substituted, see Figure **2.6** and Table **2.2**. The amorphous oil fraction, 45-50 % of the theoretical yield by mass, consists of a mixture with I_7-I_9 isomers, with 80-85 % *para*- substitution.

Fortunately, iodination of dPS and DPS is readily accomplished using the same low temperature iodination method. In fact, as suggested in Scheme **2.2**, the stoichiometry is exactly the same. For the decamer, its high solubility hinders the isolation of the product by reducing the solubility difference between the symmetrically and non-symmetrically substituted isomers. Due to the high solubility of the decamer in toluene/methanol solutions, precipitation of the I_{10}dPS into methanol leads to significantly lower yields. Careful recrystallization from ethyl acetate gives a few percent of deca(*p*-iodophenyl)silsesquioxane as single crystals suitable for X-ray diffraction.

Table 2.2 Characterization of the homologous iodophenylsilsesquioxanes

Compound	Yield (%)	GPC Mn (Da)	GPC PDI	CY Calc	CY* Found	MALDI Calc. (Da)	MALDI Found (Da)
I_8OPS	90 %	1159	1.01	23.5	22	2148.6 (Ag+)	2148
I_{12}DPS	90 %			23.5	24	3168.9	3167.3
I_{10}dPS	80 %			23.5	23	2658.72	2657

*CY = Ceramic yield in air/10°C/min.

For the DPS, the dodeca-iodinated product is recovered in 90 % yield and the symmetrically substituted material is readily recrystallized from *m*-xylene in 20 % yield. Since the probability of symmetric substitution is now the probability of *para* substitution raised to the 12th power, this is reasonably lower than the yield of the crystalline octamer. The remaining ~70 % of the reaction product is isolated after precipitation into methanol as white powder, shown by MALDI-TOF to be a mixture of I_{10}-I_{13} isomers.

NMR spectroscopy is extremely valuable for characterizing of the octa-, deca- and dodeca-(*p*-iodophenyl)silsesquioxanes. Octa- and deca-(*p*-iodophenyl)silsesquioxane offer relatively simple ^{1}H NMR spectra (Figures **2.6** and **2.7**, next page), two multiplet resonances consistent with *para-* substitution. One notable feature is the ca. 0.15 ppm upfield shift seen in the decamer. This indicates a slight difference in the electronic nature of the T_8 and T_{10} cages (Table **2.3**).

Table 2.3 NMR Characterization of the homologous iodophenylsilsesquioxanes

Compound	^{1}H NMR Peaks	^{13}C NMR Peaks
I_8OPS	7.728-7.707, 7.365-7.345	137.377, 135.199, 128.069, 99.655
I_{10}dPS	7.635-7.615, 7.203-7.183	137.430, 135.527, 128.909, 98.942
I_{12}DPS	7.629-7.609, 7.532-7.512, 7.180-7.160, 7.049-7.024	137.386, 137.258, 135.395, 135.294, 129.041, 98.967

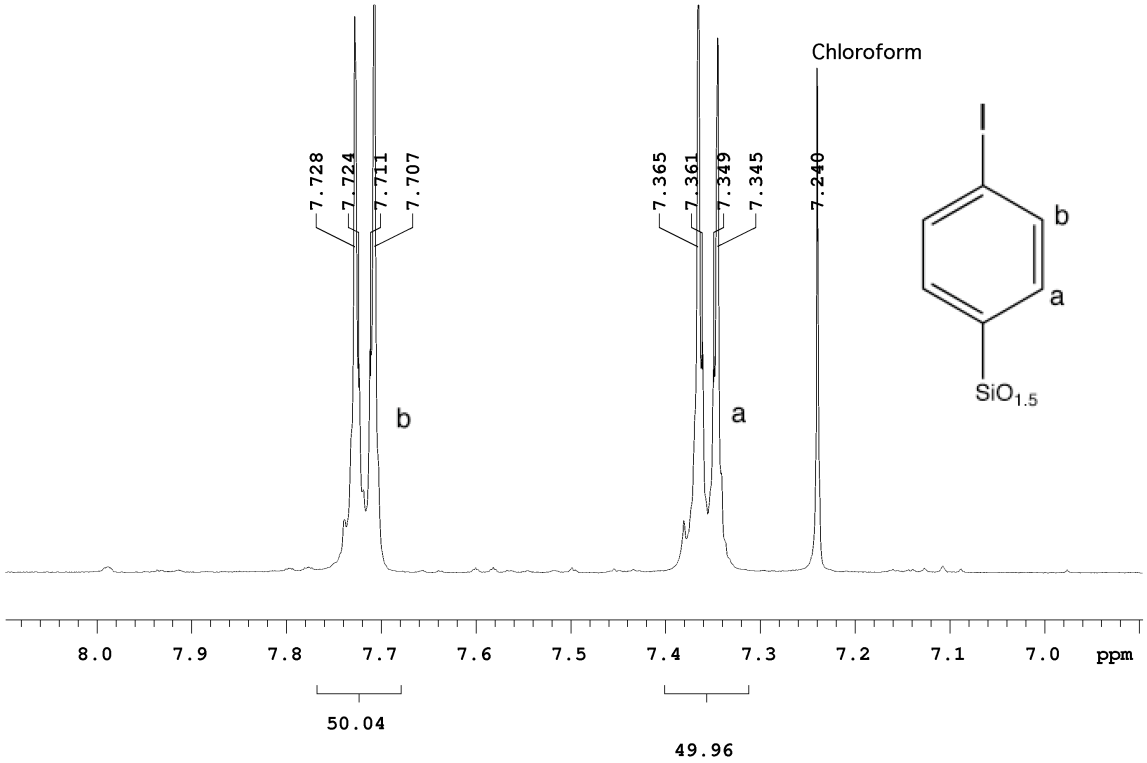

Figure 2.6 ^{1}H NMR spectrum of I_8OPS in $CS_2/CDCl_3$.

As discussed by Marsmann et al, each vertex silicon in the octamer belongs to three eight-membered rings. However, in the decamer, each vertex silicon belongs to two eight-membered rings and one ten-membered ring. In the dodecamer, the situation is more complex.

Consideration of the DPS single crystal structure from the Cambridge Crystallographic Data Centre in Figure **2.8** reveals the presence of eight "equatorial" phenyl groups, where each vertex silicon belongs to one eight-membered ring and two ten-membered rings. There are four "polar" phenyl groups, where each vertex silicon belongs to two eight-membered rings and one ten-membered ring. Marsmann et al find that the higher strain of the four-membered ring is manifested as a *upfield* shift in the ^{29}Si spectrum of the silsesquioxane compound of ~2 ppm from ~65 ppm between the octamer and decamer, depending on the R group.[49]

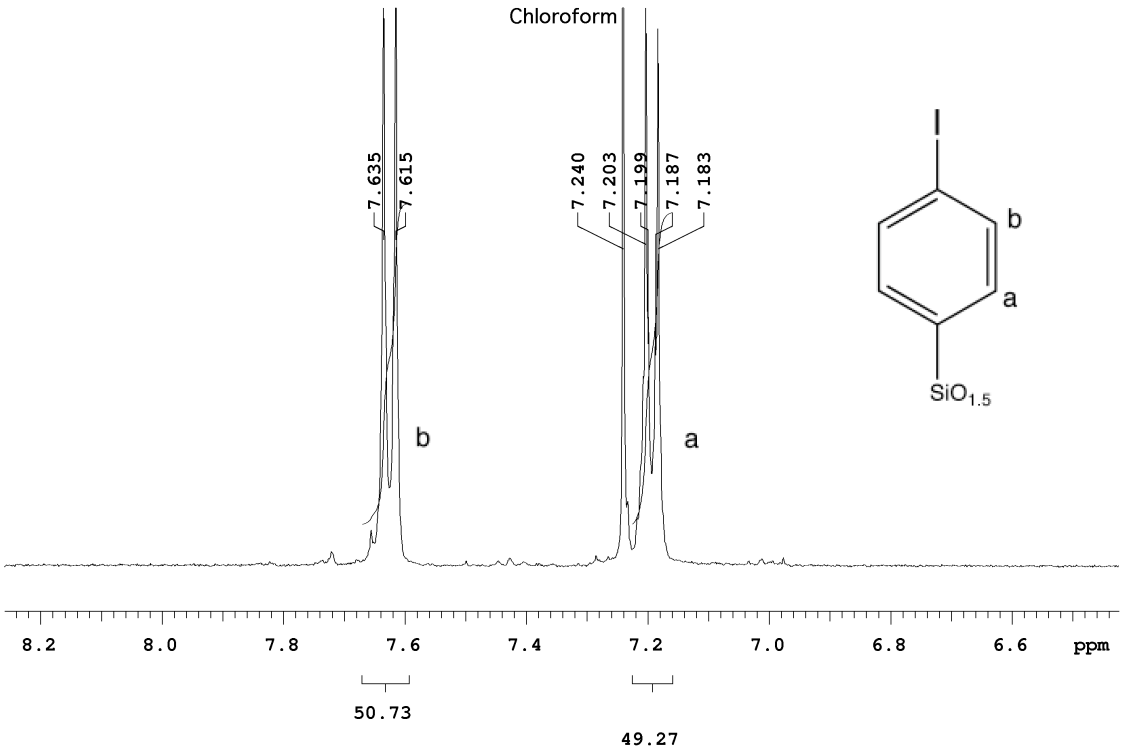

Figure 2.7 ^{1}H NMR spectrum of $I_{10}dPS$ in $CDCl_3$.

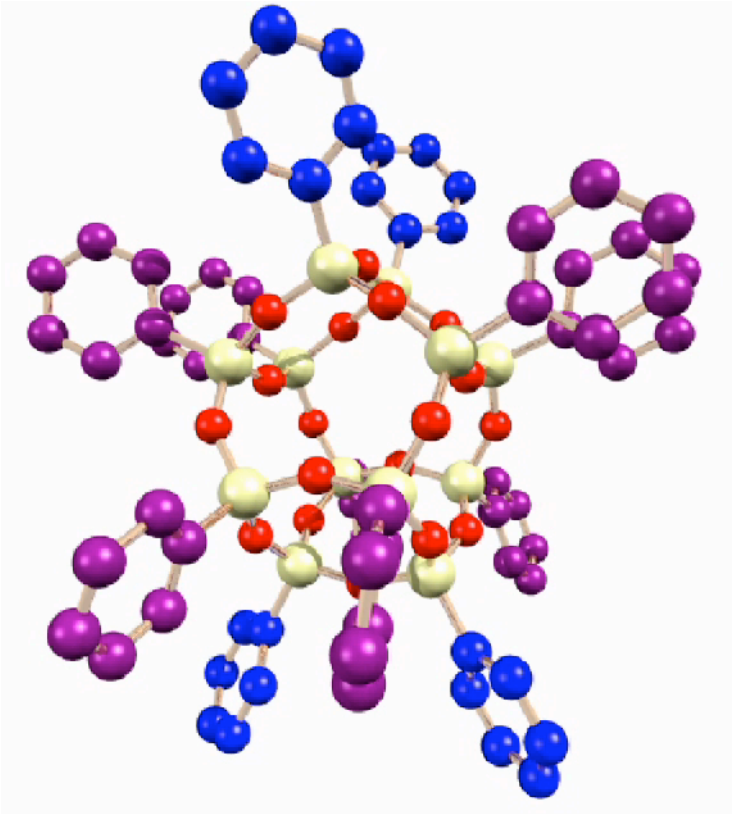

Figure 2.8 Different chemical environments in DPS.
"Equatorial" phenyls in purple, "polar" phenyls in blue.

This same effect is found in the ^{1}H NMR spectra of the octa-, deca- and dodeca-(*p*-iodophenyl)silsesquioxanes. As seen in Table **2.3**, Figures **2.6** and **2.7**, each multiplet is shifted ca. 0.1-0.2 ppm upfield with the as each vertex is incorporated into a five-membered ring.

In the case of the of the dodeca(*p*-iodophenyl)silsesquioxane, the ^{1}H NMR spectrum in Figure **2.9** shows two pairs of multiplets. Since four and eight aromatic rings are bonded to two types of silicon vertices, respectively, a 1:2 integration is expected and found experimentally in the spectrum (Figure **2.9**). Additionally, the peaks corresponding to the four aromatic rings bonded to equivalent silicon vertices to those in the decamer (the "polar" positions, where each vertex silicon belonging to two eight-membered rings and one ten-membered ring), are very close to 7.6 and 7.2 ppm (Table **2.3**).

The eight aromatic rings bonded to vertex silicon in the "equatorial" positions (belonging to one eight- membered ring and two ten-membered rings) show the largest upfield shifts, ca. 0.3 ppm from I_8OPS (Table **2.3**). The small additional peaks in the spectrum likely belong to traces of *meta* or *ortho* iodinated aromatic rings.

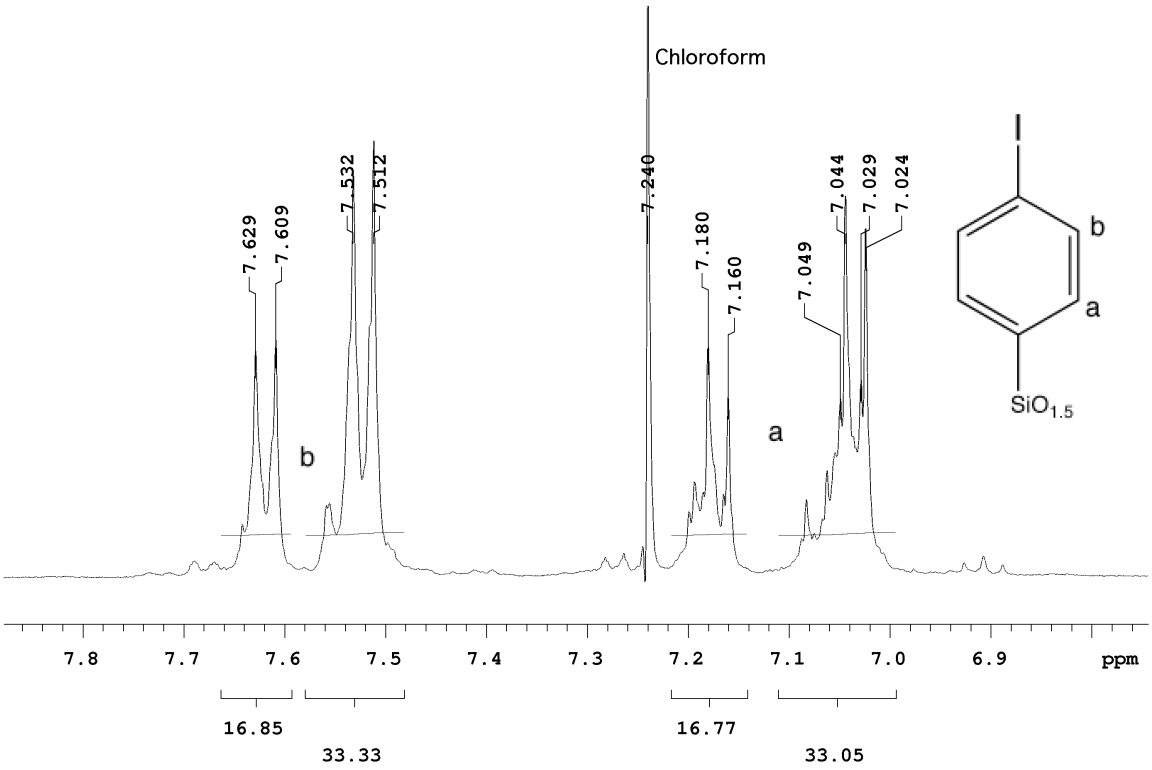

Figure 2.9 ^{1}H NMR spectrum of $I_{12}DPS$ in $CS_2/CDCl_3$.

Octa- and deca-(*p*-iodophenyl)silsesquioxane are also characterized by relatively simple ^{13}C NMR spectra (Figures **2.10** and **2.11**). Proton-decoupling (see Experimental) strengthens NMR signals arising from carbons bonded to hydrogen. In this case, again, the peaks in the decamer are shifted upfield 0.3-1 ppm relative to those in the octamer (Table **2.3**).

The proton decoupled ^{13}C spectrum of the dodecamer in Figure **2.12** shows the presence of two distinct pairs of resonances, as expected from the ^{1}H NMR spectrum.

The larger resonances from the "equatorial" phenyl groups, where each vertex silicon belonging to one eight-membered ring and two ten-membered rings, are shifted upfield relative to the "polar" phenyl groups by 0.15 ppm.

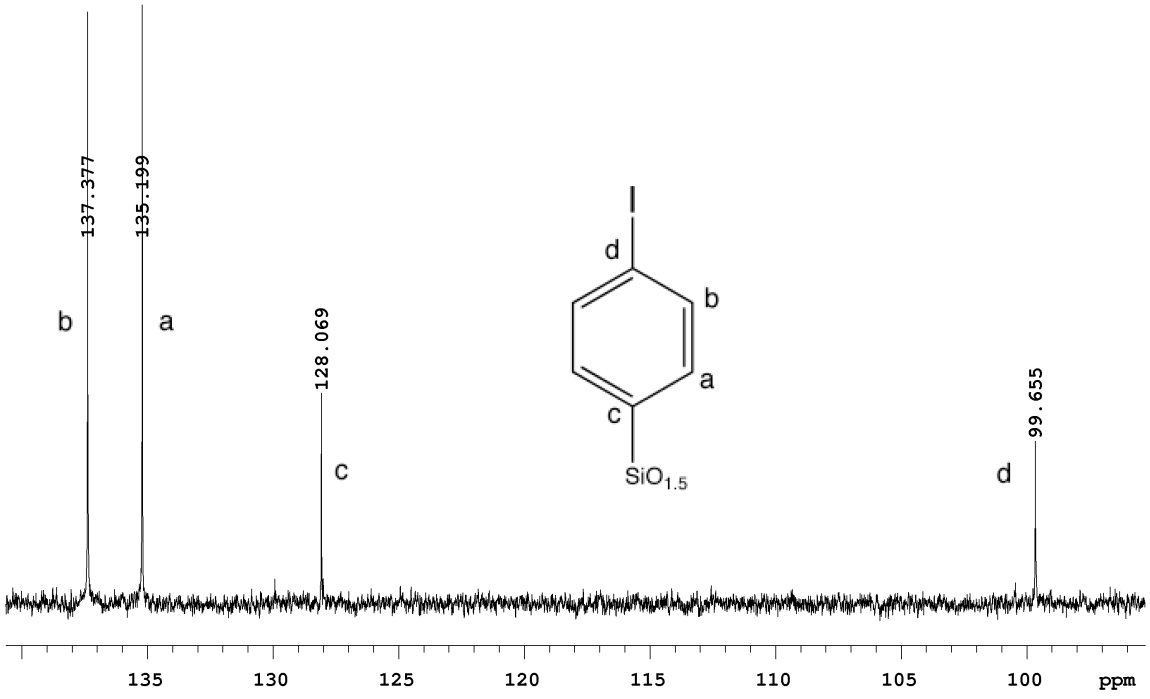

Figure 2.10 ^{13}C NMR spectrum of I_8OPS in $CS_2/CDCl_3$.

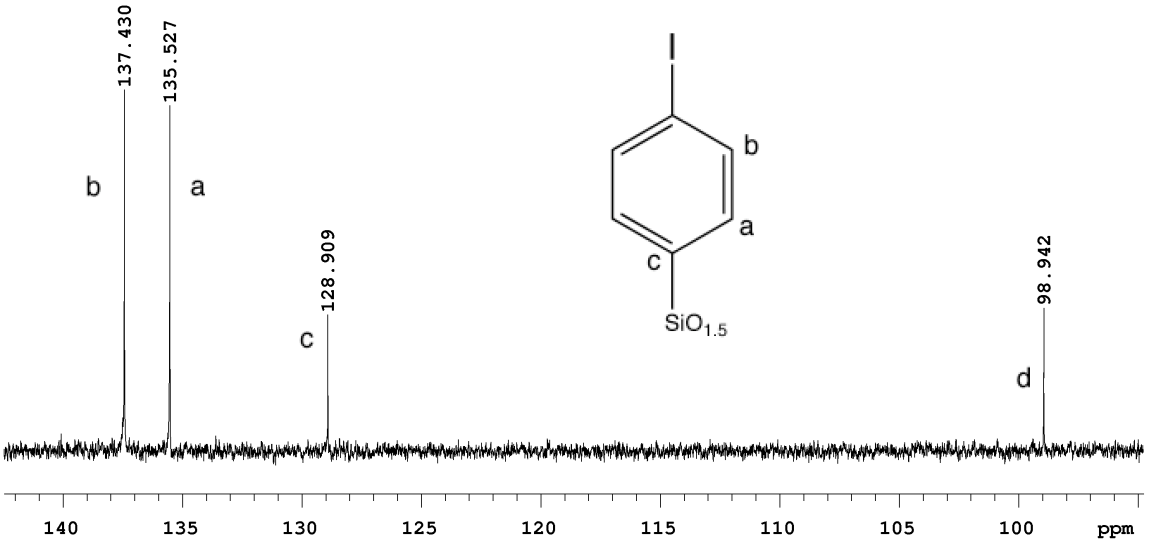

Figure 2.11 ^{13}C NMR spectrum of $I_{10}dPS$ in $CDCl_3$.

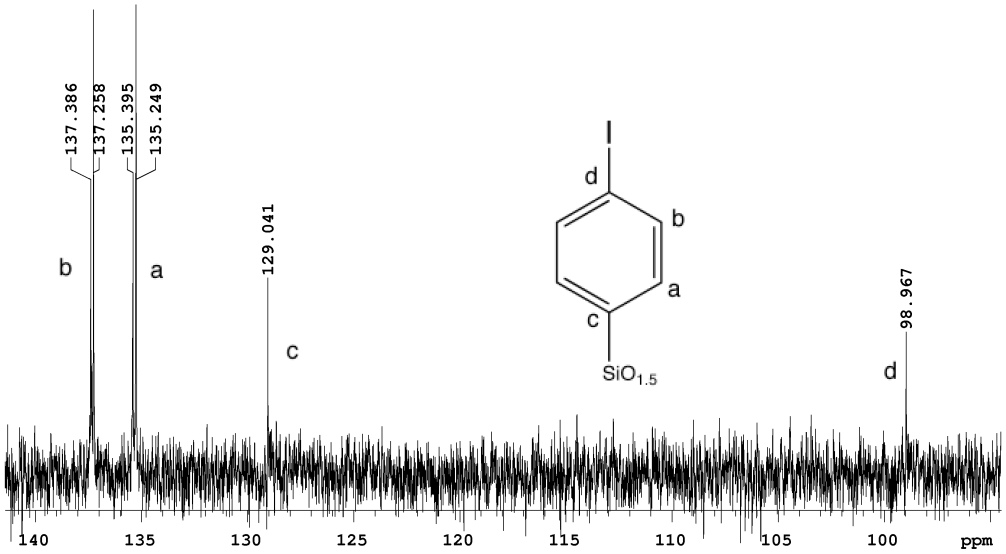

Figure 2.12 ^{13}C NMR spectra of $I_{12}DPS$ in $CS_2/CDCl_3$.

MALDI-TOF analysis indicates that these compounds have relatively narrow mass distributions (Figures **2.13**, **2.14**, and **2.15**). The breadth of the distribution increases from two peaks for the octamer to three peaks for the decamer and dodecamer. The relatively higher insolubility and larger size of the dodecamer may lead it to crystallize more rapidly from *m*-xylene, incorporating molecules with unsubstituted phenyl groups.

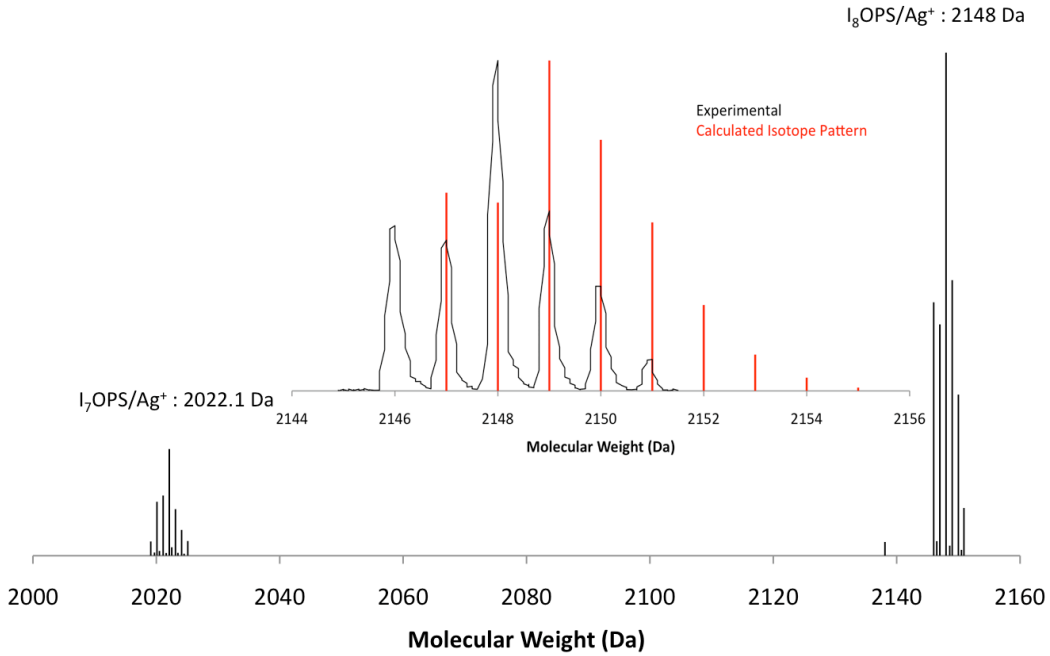

Figure 2.13 MALDI-TOF spectrum of recrystallized I_8OPS (Dithranol/$AgNO_3$).

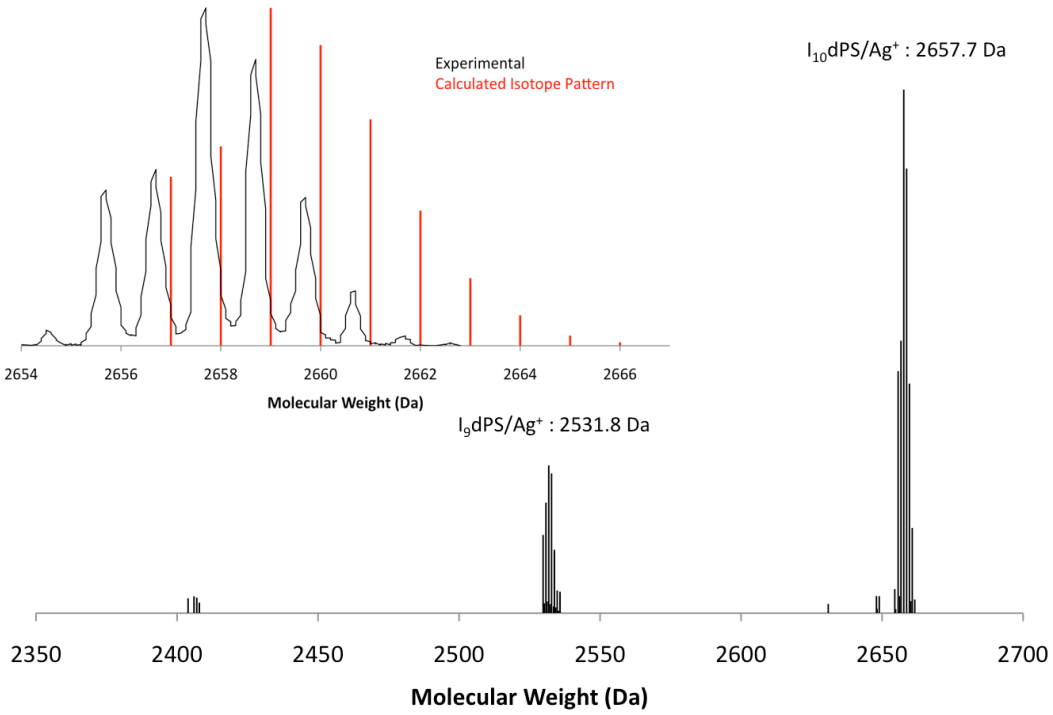

Figure 2.14. MALDI-TOF spectrum of I_{10}dPS (Dithranol/$AgNO_3$).

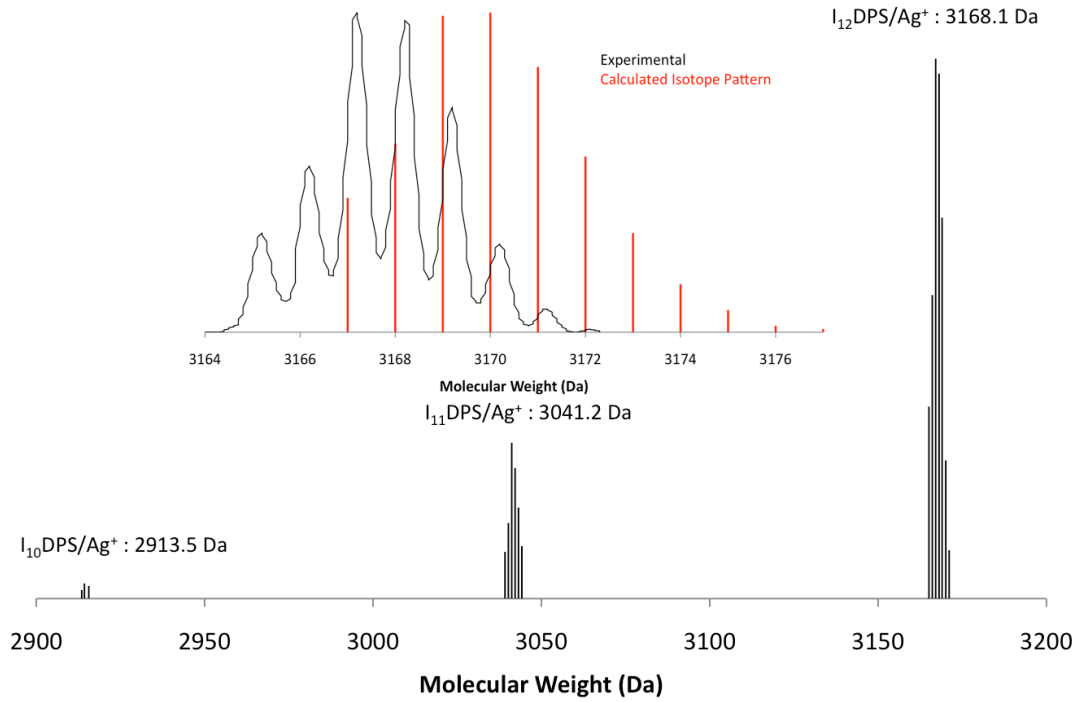

Figure 2.15 MALDI-TOF spectrum of I_{12}DPS (Dithranol/$AgNO_3$).

FTIR spectra of these compounds are shown in Figures **2.16** and **2.17**, which perfectly overlap one another. The presence of the ν Si-O-Si bands of the silsesquioxane

core are seen from 1200-1000 cm^{-1}, and the vibrational contributions of the aromatic rings are seen from 3100-3000(ν C-H), 1575-1500 (ν/δ C-C), and 800-750 (δ C-H) cm^{-1}.

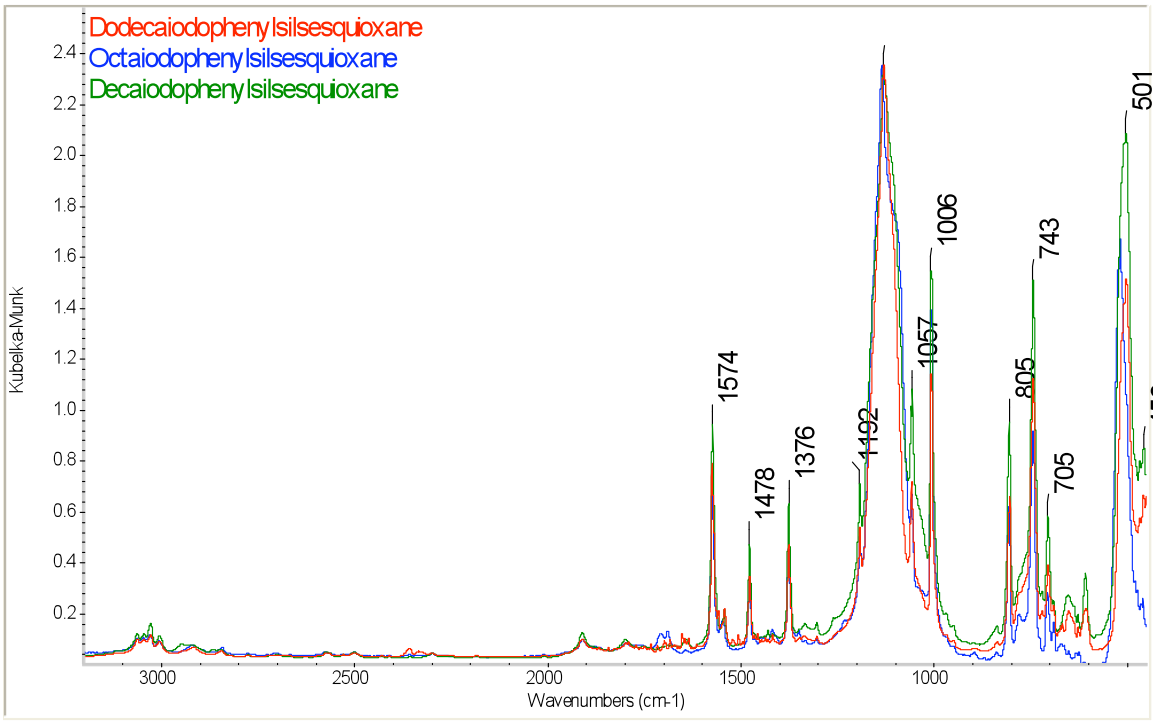

Figure 2.16 FTIR homologous iodophenylsilsesquioxanes 3200-450 cm^{-1}.

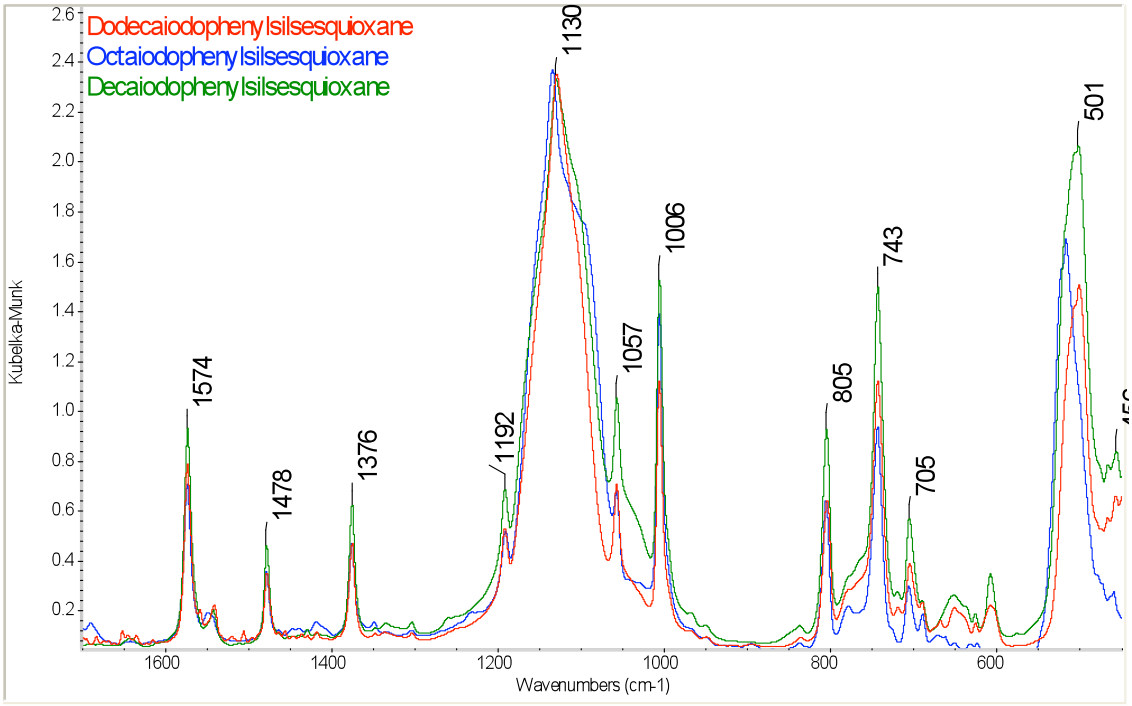

Figure 2.17 FTIR homologous iodophenylsilsesquioxanes 2000-450 cm^{-1}.

Thermal gravimetric analyses (TGAs) of I_8OPS (ethyl acetate removed under vacuum) were conducted under air and nitrogen (Figure **2.18**). The data collected in air are consistent with the proposed composition, giving a ceramic yield of 22% in comparison to the theoretical yield of 23.5% with complete decomposition to silica. The onset of mass loss ca. 425˚C indicates the possibility of the C-I bond thermolysis.[35-38]

The reaction was repeated under nitrogen, and the same behavior was found. I_8OPS is 49 wt % iodine, and 50 wt % mass loss at ca. 425˚C is indicated in Figure **2.18**. The aryl radicals produced in the thermolysis may recombine to form C-C bonds, producing a covalently cross-linked solid.[37] Figure **2.19** shows TGA analyses of all three (*p*-iodophenylsilsesquioxanes, and the ceramic yields are nearly identical. The same ~50 % mass-loss at ca. 425˚C is seen, consistent with the 49 wt% of iodine in these compounds. Again, each compound co-crystallizes with solvent, however these solvent molecules are readily removed under vacuum and are not seen in these data.

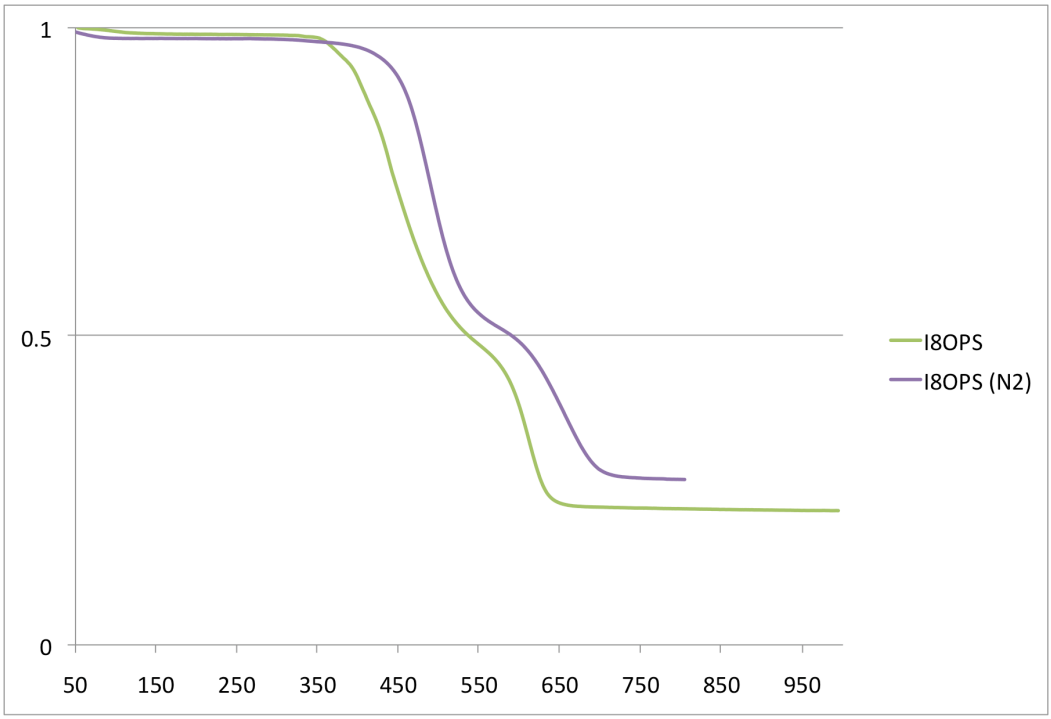

Figure 2.18 TGA of octa(iodophenyl)silsesquioxane under air and nitrogen.

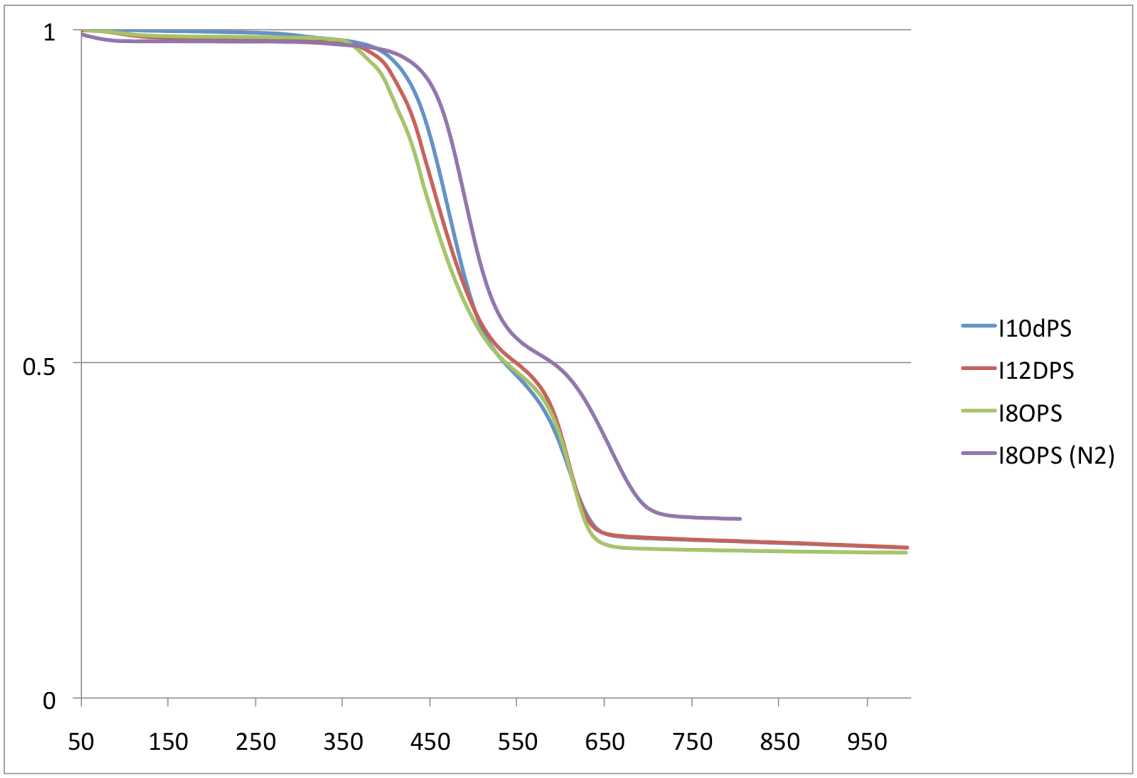

Figure 2.19 TGA of the homologous iodophenylsilsesquioxanes.

Crystal Structure Analyses of I_8OPS, I_{10}dPS, I_{12}DPS

In the following section, the crystal structures of the homologous iodophenylsilsesquioxanes are discussed. Table **2.4** contains basic data for each refined crystal structure.

X-ray quality crystals of I_8OPS were grown from hot ethyl acetate. Single crystal X-ray diffraction analysis reveals that I_8OPS crystallizes in the tetragonal space group I4/m. The unit cell contains 4 molecules with a total volume of 8618.9 $Å^3$. The SQUEEZE subroutine of the PLATON suite was used to account for the scattering a disordered ethyl acetate solvent molecule. Figure **2.20** shows the final refinement of the structure.

Table 2.4 Crystal structure data for the iodophenylsilsesquioxanes

	I_8OPS	I_{10}dPS	I_{12}DPS
Space Group	I4/, tetragonal	C2/c, monoclinic	C2/c, monoclinic
Unit Cell Dimensions	a= 20.0403(11)Å b= 20.0403(11) Å c= 21.4606(12) Å	a= 28.054(2) Å b= 15.6168(11) Å c = 22.3246(16) Å	a= 32.082(9) Å b= 14.704(4) Å c= 28.755(8) Å
	α, β, γ=90°	α, γ=90; β= 108.859(1)°	α, γ=90; β= 118.438(4)°
Unit Cell Volume	8618.9 Å^3	9255.7 Å^3	11927.9 Å^3
Z	4, 1.641 Mg/m^3	4, 1.831 Mg/m^3	4, 1.941 Mg/m^3
R-factor	7.4 % (9.7 %)*	4.6 % (6.6 %)*	9.2

* Before use of SQUEEZE to account for disordered solvent

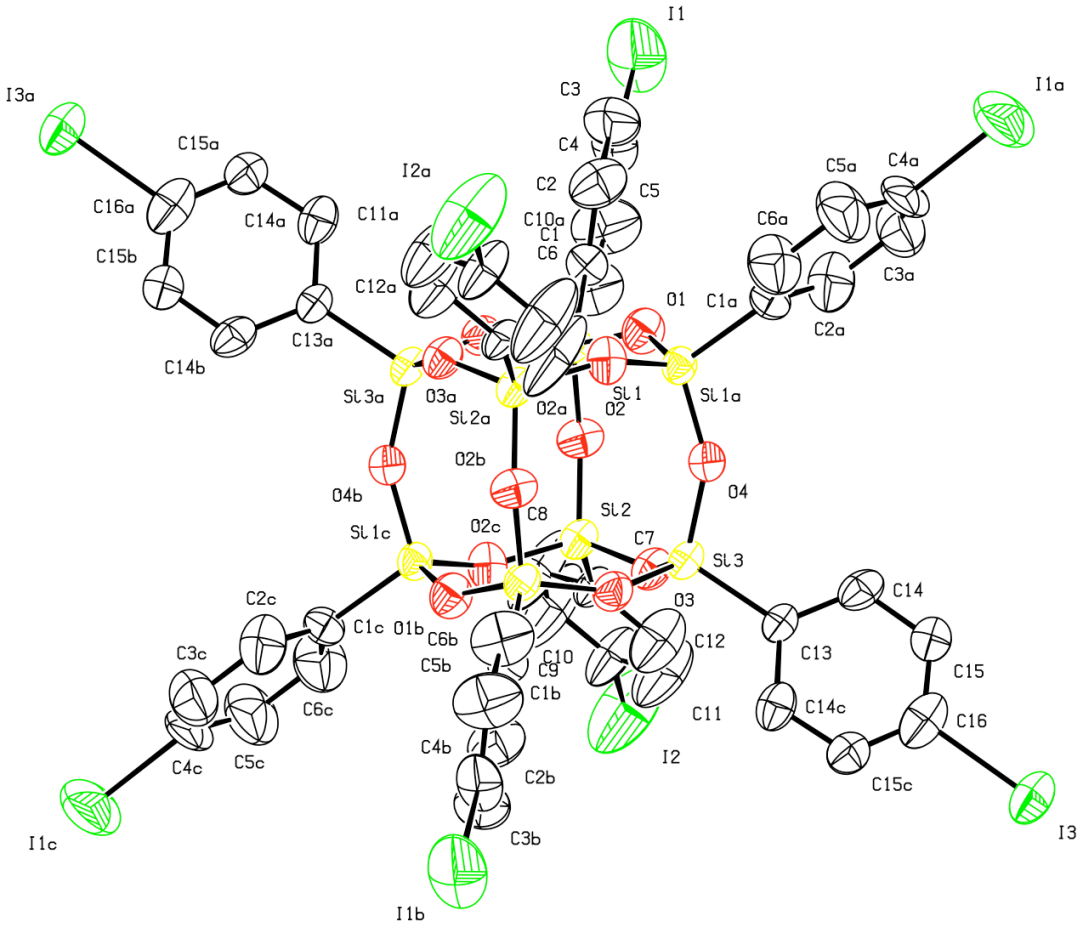

Figure 2.20 50 % thermal ellipsoid plots of octa(*p*-iodophenyl)silsesquioxane. Hydrogen atoms are omitted for clarity. Full XRD data can be found in Appendix 2.

X-ray quality crystals of $I_{10}OPS$ were grown from hot ethyl acetate. Single crystal X-ray diffraction analysis reveals that $I_{10}OPS$ crystallizes in the tetragonal space group I4/m. The unit cell contains 4 molecules with a total volume of 9255.7 $Å^3$. The SQUEEZE subroutine of the PLATON suite was used to account for the scattering disordered ethyl acetate solvent molecules. Figure **2.21** shows the final refinement of the structure.

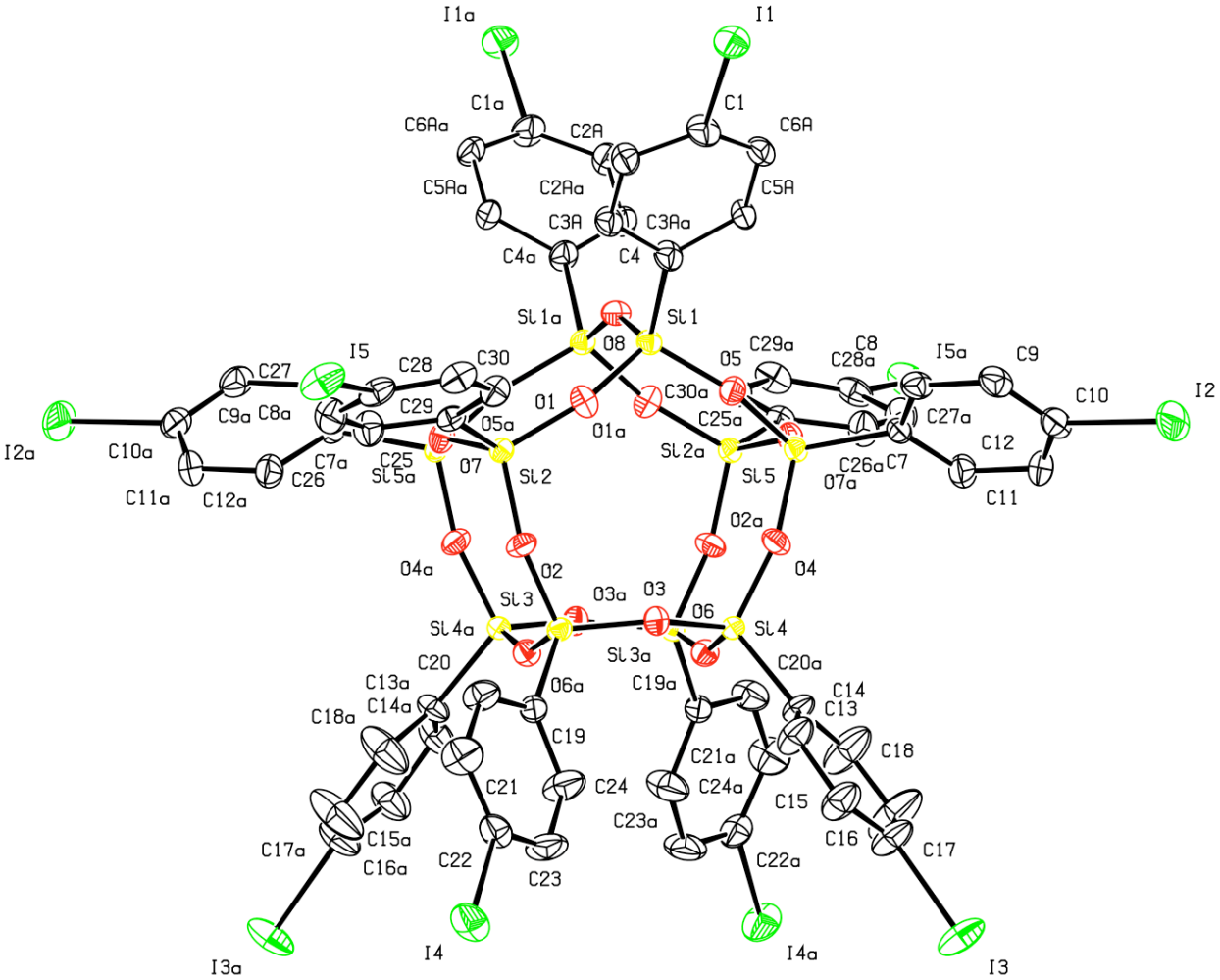

Figure 2.21 50 % thermal ellipsoid plots of deca(*p*-iodophenyl)silsesquioxane. Hydrogen atoms are omitted for clarity. Full XRD data can be found in Appendix 3.

X-ray quality crystals of I_{12}DPS were grown from hot m-xylene with 5% tetradecane. Single crystal X-ray diffraction analysis shows that I_{12}DPS crystallizes in the monoclinic space group C2/c. The unit cell contains 4 molecules with a total volume of 11928 Å^3. Figure **2.22** shows the structural refinement. Two ordered *m*-xylene molecules co-crystallize with I_{12}DPS, and are not shown.

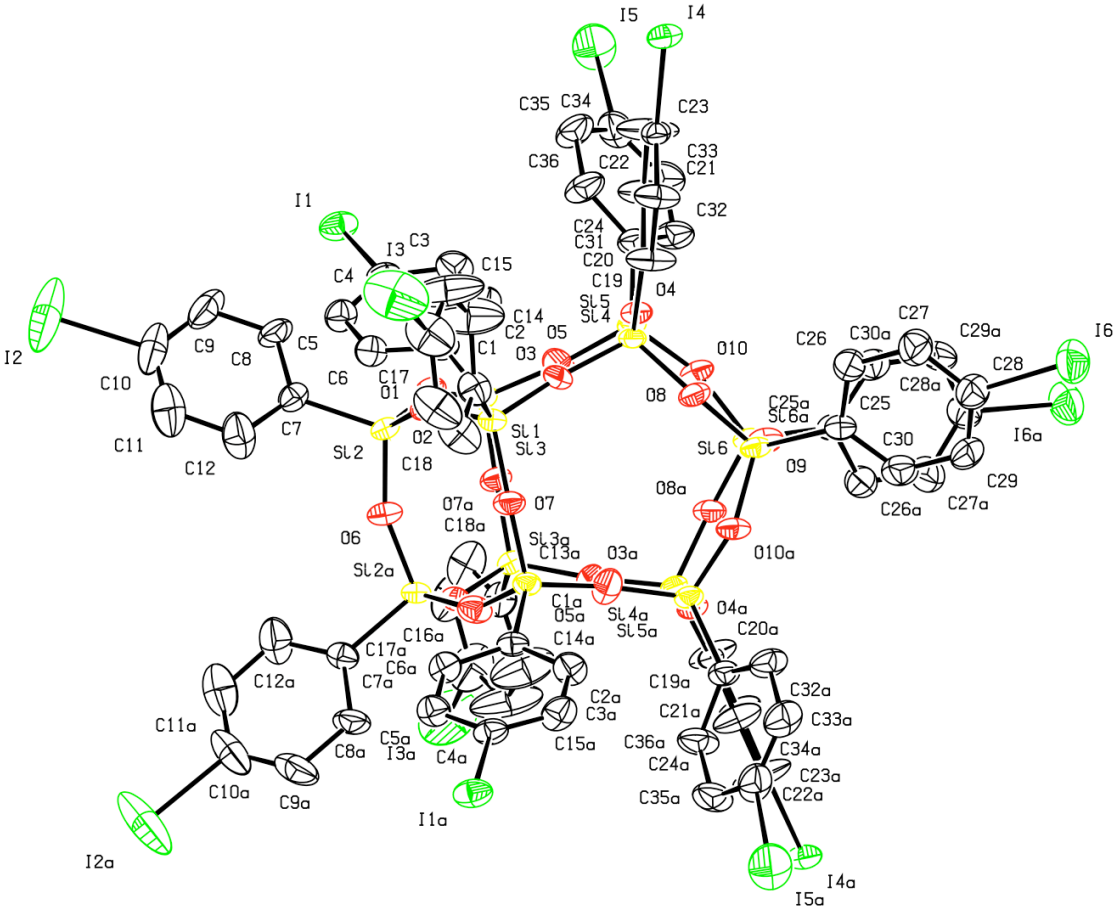

Figure 2.22 50 % thermal ellipsoid plots of dodeca(*p*-iodophenyl)silsesquioxane. Hydrogen atoms and *m*-xylene solvents are omitted for clarity. Full XRD data can be found in Appendix 4.

Synthesis and Physical Characterization of Cross-coupling Derivatives

After completing the analysis of the substitution pattern, we began initial efforts to develop diverse functionality (tools) for eventual use in producing stars, core-shell

materials, novel dendrimers and low defect density nanocomposites (subject to the effects of TΔS). Given the forgoing comments regarding the functionalization of haloaromatics, significant efforts were made to modify I_8OPS using these traditional Heck, Sonogashira, Stille and Suzuki coupling methods. [14] Scheme **2.1** illustrates a basic set of reactions undertaken to demonstrate the versatility of I_8OPS as a 3-D nano-building block. The resulting compounds were characterized using a variety of techniques with the results summarized in Table **2.5**.

Table 2.5 Product yields, Conversions, GPC, and MALDI-TOF Data for Scheme **2.1** compounds

Compound	Yield† (%)	% conv. H_2O_2/F-	GPC M_n (Da)	GPC PDI	CY Calc*	CY Found	MALDI Calc. (Da)	MALDI Found (Da)
I_8OPS	90	99††	1159	1.01	23.5	22	2148.6 (Ag+)	2148 (100%)
Biphenyl	83	93	1052	1.01	25.4	24	1750.2 (Ag+)	1749 (100%)
4-Cyanobiphenyl	64	88	1556	1.08	26.0	26	--	--
4-MeOPhethyne	85	99%	1327	1.01	22.6	23.8	--	--
Stilbene	91	99+	1609	1.02	26.0	22	1958.5 (Ag+)	1958 (100%)
Methylstilbene	87	99	1620	1.04	24.4	22	2070.7 (Ag+)	2071 (100%)
4-N-Carbazole	76	92	2516	1.2	20.4	23	--	--
4-vinylpyridine	48	90	1454	1.02	25.9	22	1858.5(+)	1858 (100%)
2-vinylpyridine	50	91	1513	1.02	25.9	20	1858.5(+)	1858 (100%)
Diethylphosphonate	81	--	1086	1.01	49.4**	56	2128.2 (Li+)	2128 (100%)

†Isolated yield calculated relative to complete conversion of aryl iodide. ††Conversion calculated relative to unreacted aryl iodide. *CY = Ceramic yield in air/10°C/min. **Conversion assumes product is $SiO_2{\cdot}0.5P_2O_5$ silicophosphate glass.

Although the yields and conversions are quite high there is still room for improvement. The ability to effect 100% conversion of all eight aryl iodides to the functional groups shown is necessary to develop minimal defect 3-D nanostructures either by covalent, electrostatic or dative bonding. The incorporation of ethynyl groups gives access to Diels-Alder cyclization, which will be discussed in much more detail in

Chapter 4. Incorporating pyridyl groups allows for the possibility to construct framework materials using the coordination of these groups to metal atoms. The phosphonate group opens the possibility hydrolysis to the acid and subsequent hydrogen bonding or metal complexation.

Only the alkynes and stilbenes are obtained easily with 100 % conversion, we believe it will also be possible to get 100 % conversion other compounds shown in Scheme **2.1** with further refinement of synthetic procedures given that only unreacted iodide remains.[19] Even with complete conversion, assembly in 3-D will generate defect structures when the substitution patterns are not perfect, so a concerted effort was made to understand and utilize recrystallization to purify I_8OPS and the subsequent products.

Though the distribution in substitution patterns in I_8OPS has been quantified, we also report H_2O_2/F^- cleavage of the octastilbene derivative provides a material that is > 95 % 4-hydroxystilbene, 2-3% 3-hydroxystilbene and < 1% 2-hydroxystilbene as determined by GC-MS. Given that the crystallization process is well-known to self-select for purity,[22] we believe that assembly of low-defect density 3-D structures is possible through the use I_8OPS as a starting material. Thus, these materials and related analogs may still serve as nano-building blocks.

Brief comments about the ceramic yields (CY) of Table **2.5** are warranted. First, the CY (to SiO_2) for I_8OPS in air is expected to be 23.5%, and the found ceramic yield is 22 %, a little low. Three exceptions are the alkyne, phosphonate and carbazole compounds. As seen in the tetraalkyne adamantane systems, the alkyne substituted octasilsesquioxanes polymerize to give 3-D carbon networks stable to temperatures > 550°C and may not completely oxidize in the time frame of the TGA, as evidenced by

dark residues after the TGA runs rather than white SiO_2.[50] The phosphonate system can be expected to decompose to give phosphosilicate glasses,[51] encapsulating residual carbon. Finally, the carbazole system, which has the poorest conversion, retains the highest content of residual aryl iodide, and the decomposition process may lead to more char from carbonization, thus limiting the oxidation at the heating rates used for our standard TGA runs.

All of these compounds are highly soluble and offer oxidative stabilities > 400°C (TGA). The alkyne systems polymerize on heating, as mentioned above, to provide materials air stable to > 550°C.[50] Of particular interest are the cyano and 4-vinyl-pyridine moieties, which offer the potential for 3-D dative bonding. The 2-vinyl-pyridine system may provide access to octa-iridium systems of potential use in light emitting diodes, light harvesting, and novel photovoltaics.[52] Finally, while the UV-Vis absorptions of the stilbenes are essentially the same as the parent organic molecules, their emission characteristics are very different, being red-shifted up to 80 nm (≈ 0.75 eV) as will be discussed elsewhere.[53]

Crystal Structure Analyses of Stilbene and 2-Vinylpyridine Derivatives

The synthesis of the crystalline I_8OPS has allowed for the synthesis of crystalline Heck derivatives. Well-formed crystals of the stilbene and the 2-vinyl pyridine compounds can be isolated but diffract poorly. There appears to be significant disorder in the positions of the organic substituents. This is consistent with previous work by Feher who writes, “Like many polyhedral silsesquioxanes, (the trisilanol silsesquioxane

compound) crystallizes from many solvent systems as well formed but poorly diffracting (even at 158 K) crystals."[54]

The refinements are shown in Figure **2.23**, and the R-factors for the each are 13%. While the positions of the organic substituents are not well refined, the silica cages, are well refined. This allows for the determination of Z (molecules per unit cell) and the unit cell volume, as detailed in Table **5**.

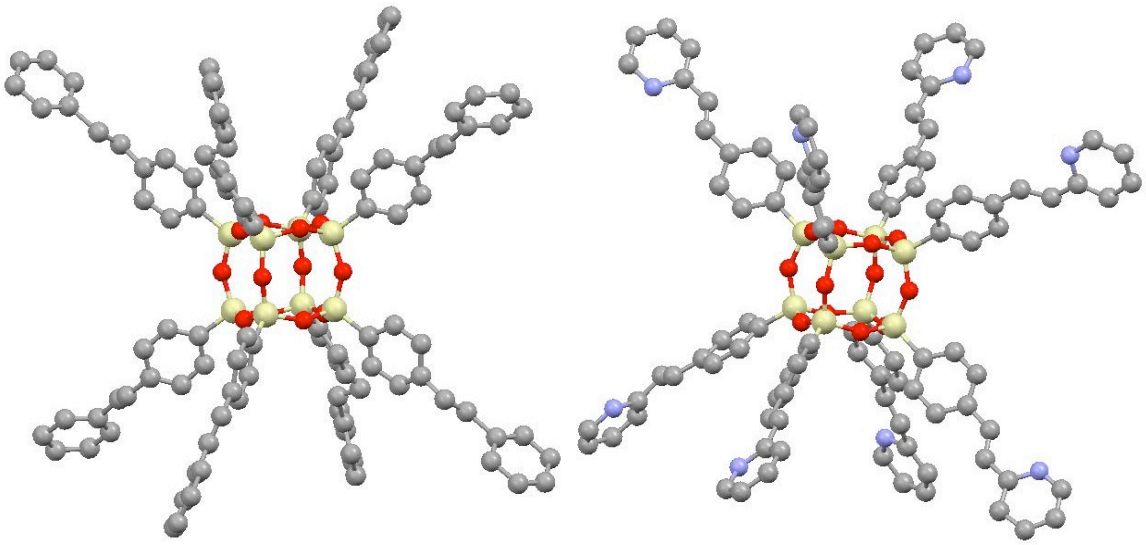

Octa(stilbene)silsesquioxane Octa(2-stilbazole)silsesquioxane

Figure 2.23 Ball-and-stick figures generated via single-crystal X-ray diffraction.

Table 2.6 Unit cell volume, Z and solvent void calculations for selected Heck derivatives

Compound	Unit Cell Volume	Z	Space Group
Stilbene	11050 Å^3	4	C2/c, monoclinic
2-Vinylpyridine	6778 Å^3	2	P-1, triclinic

Conclusions

This chapter has described the symmetric iodination of the T_8, T_{10}, and T_{12} phenylsilsesquioxanes. A synthetic route to the T_{10} decaphenylsilsesquioxane has been described to complement the commercially available T_8 and T_{12} compounds. I_8OPS can

be synthesized in 100 g quantities with > 90% yields and following careful recrystallization to ≥ 95 % selectivity for para-substitution. I_{10}dPS has been isolated in minimal quantities and I_{12}DPS has been isolated at the 25 g scale. Each of these compounds offers nearly equivalent chemical reactivity with very different geometries.

The crystal structures of these three compounds have been determined, an analysis of the differing motifs in supermolecular coordination will be undertaken in Chapter 5. These compound offer a variety of symmetries and allow the addition of diverse functional groups. This functionalization is explored for the I_8OPS system. The high degree of symmetry, coupled with the ability to tailor the functionality of the periphery, suggest that these molecules will also offer potential to create 3-D network structures with minimum numbers of defects.

Viewed from one perspective, their assembly offers the potential to create organic/inorganic nanocomposites with completely tailored properties, from the nanometer length scale up. From another vantage point, these molecules might be used for the surface modification of other structures, with similar goals in mind. Future publications will address these possibilities. This accomplishment has allowed for the systematic extension of these nano-building blocks, and these will be discussed in greater detail in Chapter 4.

References Cited:

1. Detken, A.; Zimmermann, H.; Haeberlen, U.; Poupko, R.; Luz, Z. "Molecular Reorientation and Self-Diffusion in Solid Cubane by Deuterium and Proton NMR." J. Phys. Chem. 1996, 100, 9598–9604.
2. Hawker, C.J.; Wooley, K.L. "The Convergence of Synthetic Organic and Polymer Chemistry," *Science* **309**, 1200-5.
3. Feynman, R. "There's Plenty of Room at the Bottom." *Journal of Microelectromechanical Systems* **1**, 60-6 (1992).
4. Eaton, P.E.; Galoppini, E.; Gilardi, R. "Alkynylcubanes as Precursors of Rigid-Rod Molecules and Alkynylcyclooctatetraenes." *Journal of the American Chemical Society*, **116**, 7588-96 (1994).
5. Eaton, P.E.; Pramod, K.; Emrick, T.; Gilardi, R. "Building with Cubane-1,4-diyl. Synthesis of Aryl-Substituted Cubanes, p-[n]Cubyls, and Cubane-Separated Bis(arenes)." *Journal of the American Chemical Society* **121**, 4111-23 (1999).
6. Reichert, V.R.; Mathias, L.J. "Expanded Tetrahedral Molecules from 1,3,5,7-Tetraphenyladamantane." *Macromolecules,* **27**, 7015-23 (1994).
7. Reichert, V.R.; Mathias, L.J. "Highly Cross-Linked Polymers Based on Acetylene Derivatives of Tetraphenyladamantane." *Macromolecules,* **27**, 7030-4 (1994).
8. Lee, M.W.; Farha, O.K. Hawthorne, M.F.; Hansch, C.H. "Alkoxy Derivatives of Dodecaborate : Discrete Nanomolecular Ions with Tunable Pseudometallic Properties." *Angewandte Chemie, International Edition in English* **46**, 3018 –3022 (2007).
9. Farha, O. K.; Julius, R. L.; Lee, M. W.; Huertas, R. E.; Knobler, C. B.; Hawthorne, M. F. "Synthesis of Stable Dodecaalkoxy Derivatives of hypercloso-$B_{12}H_{12}$." *Journal of the American Chemical Society* **127**, 18243–51 (2005).
10. Sanchez, C.; de A.A. Soler-Illia, G.J.; Ribot, F.; Lalot, T.; Mayer, C.R.; Cabuil, V. "Designed Hybrid Organic-Inorganic Nanocomposites from Functional Nanobuilding Blocks," *Chemistry of Materials*, **13**, 3061-8 (2001).
11. Laine, R. M. "Nanobuilding blocks based on the $[OSiO_{1.5}]_x$ (x = 6, 8, 10) silsesquioxanes." *Journal of Materials Chemistry* **15**, 3725–44 (2005).
12. Baney, R. H.; Itoh, M.; Sakakibara, A.; Suzuki, T. "Silsesquioxanes." *Chemical Reviews* **95**, 1409–30 (1995).
13. Voronkov, M. G.; Lavrent'yev, V. I. Polyhedral Oligosilsesquioxanes and Their Homo Derivatives. *Topics in Current Chemistry* **102**, 199–236 (1982).
14. Brown, J.F. Jr.; Vogt, L.H.; Prescott, P.I. "Preparation and Characterization of the Lower Equilibrated Phenylsilsesquioxanes." *Journal of the American Chemical Society* **86**, 1120-5 (1964).
15. Sulaiman, Santy. Unpublished results.

16. Pakgamsai, C.; Kobayashi, N.; Koyano, M.; Sasaki, S.; Kawakami, Y."Characterization of the Benzene-Insoluble Fraction of the Hydrolyzate of Phenyltrimethoxysilanes in the Presence of Benzyltrimethylammonium Hydroxide." *Journal of Polymer Science: Part A: Polymer Chemistry*, **42**, 4587-97 (2004).

17. Olsson, K.; Gronwall, C. "Octa(arylsilsesquioxanes), $(ArSi)_8O_{12}$ I. Phenyl, 4-tolyl, and 1-naphthyl compounds." *Arkiv foer Kemi* **17**, 529-40 (1961).

18. Brick, C.M. Tamaki, R.; Kim, S.-G.; Asuncion, M.Z.; Roll, M.; Nemoto, T.; Ouchi, Y.; Chujo Y.; Laine, R.M. "Spherical, Polyfunctional Molecules Using Poly(bromophenylsilsesquioxane)s as Nanoconstruction Sites." *Macromolecules* **38**, 4655-60 (2005).

19. Roll, M.F.; Asuncion, M.Z.; Kampf, J.; Laine, R.M. "para-Octaiodophenylsilsesquioxane, $[p\text{-}IC_6H_4SiO_{1.5}]_8$, a Nearly Perfect Nano-Building Block." *ACS Nano* **2**, 320-6 (2008).

20. Morrison, R.T.; Boyd, R.N. *Organic Chemistry, 1966, 2nd ed*.

21. Galli, C. "Aromatic Iodination: Evidence of reaction Intermediate and of the *sigma*-Complex Character of the Transition State." *Journal of Organic Chemistry*, **56**,3238-45 (1991).

22. Vogel, A. Practical Organic Chemistry. John Wiley and Sons: New York (1966).

23. Reichert, V.R.; Mathias, L.J. "Expanded Tetrahedral Molecules from 1,3,5,7-Tetraphenyladamantane." *Macromolecules,* **27**, 7015-23 (1994).

24. Kobayashi, K.; Kobayashi, N.; Ikuta, M.; Therrien, B.; Sakamoto, S.; Yamaguchi, K. "Syntheses of Hexakis(4-functionalized-phenyl)benzenes and Hexakis[4-(4′-functionalized-phenylethynyl)phenyl]benzenes Directed to Host Molecules for Guest-Inclusion Networks." Journal of Organic Chemistry 70, 749-52 (2005).

25. Negishi, E.; Anastasia, L. "Palladium-Catalyzed Alkynylation." *Chemical Reviews* **103**, 1979–2017 (2003).

26. Miyaura, N.; Suzuki, A."Palladium-Catalyzed Cross-Coupling Reactions of Organoboron Compounds." *Chemical Reviews* **95**, 2457-83 (1995).

27. Nicolaou, K.C.; Bulger, P.G.; Sarlah, D. "Palladium-Catalyzed Cross-Coupling Reactions in Total Synthesis." *Angewandte Chemie, International Edition in English* **44**, 4442-89 (2005).

28. Barrios-Landeros, F.; Carrow, B.P.; Hartwig, J.F. "Effect of Ligand Steric Properties and Halide Identity on the Mechanism for Oxidative Addition of Haloarenes to Trialkylphosphine Pd(0) Complexes." *Journal of the American Chemical Society* 131, 8141–54 (2009).

29. Hartwig, J.F.; Kawatsura, M.; Hauck, S. I.; Shaughnessy, K.H.; Alcazar-Roman, L.M. "Room-Temperature Palladium-Catalyzed Amination of Aryl Bromides and Chlorides and Extended Scope of Aromatic C-N Bond Formation with a Commercial Ligand." *Journal of Organic Chemistry* **64**, 5575-80 (1999).

30. Vorogushin, A.V; Huang, X.; Buchwald, S.L. "Use of Tunable Ligands Allows for Intermolecular Pd-Catalyzed C-O Bond Formation." *Journal of the American Chemical Society* **127**, 8146-9 (2005).

31. Balthazor, T.M.; Grabiak, R.C. "Nickel-Catalyzed Arbuzov Reaction: Mechanistic Observations." *Journal of Organic Chemistry* **45**, 5425-6 (1980).

32. Fernandez-Rodriguez, M.A.; Hartwig, J.F. "A General, Efficient, and Functional-Group-Tolerant Catalyst System for the Palladium-Catalyzed Thioetherification of Aryl Bromides and Iodides." *Journal of Organic Chemistry* **74**, 1663-72 (2009).

33. Babudri, F.; Farinola, G.M.; Naso, F. "Synthesis of conjugated oligomers and polymers: the organometallic way." *Journal of Materials Chemistry* **14**, 11–34 (2004).

34. Wolfe, J.P.; Buchwald, S.L. "Room Temperature Catalytic Amination of Aryl Iodides." *Journal of Organic Chemistry* **62**, 6066-8 (1997).

35. Robaugh, D.; Tsang, W. "Thermal Decomposition of Phenyl Iodide, and *o*-Iodotoluene." *Journal of Physical Chemistry* **90**, 5363-7 (1986).

36. Kumaran, S.S; Su, M.-C.; Michael, J.V. "Thermal decomposition of iodobenzene using I-atom absorption." *Chemical Physics Letters* **269**, 99-106 (1997).

37. Cho, H.-Y.; Ajaz, A.; Himali, D.; Waske, P.A.; Johnson, R.P. "Microwave Flash Pyrolysis." *Journal of Organic Chemistry* **74**, 4137–42 (2009).

38. Szulczewski, G.J.; White, J.M. "Thermal and photon-stimulated reactions of iodobenzene on Ag(111)." *Surface Science* **399**, 305-15 (1998).

39. Ajitha, D.; Fedorov, D.G.; Finley, J.P.; Hirao, K. "Photodissociation of alkyl and aryl iodides and effect of fluorination: Analysis of proposed mechanisms and vertical excitations by spin – orbit ab initio study." *Journal of Chemical Physics* **117**, 7068-76 (2002).

40. Sharma, R.K.; Kharasch, N. "The Photolysis of Iodoaromatic Compounds." *Angewandte Chemie, International Edition in English* **7**, 36-44 (1968).

41. Zhang, X.; Friderichsen, A.V.; Nandi, S.; Ellison, G.B.; David, D.E.; McKinnon, J.T.; Lindeman, T.G.; Dayton, D.C; Nimlos, M.R."Intense, hyperthermal source of organic radicals for matrix-isolation spectroscopy." *Review of Scientific Instruments* **74**, 3077-86 (2003).

42. Friderichsen, A.V.; Radziszewski, J.G.; Nimlos, M.R.; Winter, P.R.; Dayton, D.C.; David, D.E; Ellison, G.B. "The Infrared Spectrum of the Matrix-Isolated Phenyl Radical." *Journal of the American Chemical Society* **123**, 1977-88 (2001).

43. Bunnett, J.F; Wamser, C.C. "Radical Abstraction of Iodine from Aryl Iodides." *Journal of the American Chemical Society* **88**, 5534-37 (1966).

44. Smith, D.W. Jr.; Shah, H.V.; Perera, K.P.U.; Perpall, M.W.; Babb, D.A.; Martin, S.J. "Polyarylene Networks via Bergman Cyclopolymerization of Bis-ortho-diynyl Arenes." *Advanced Functional Materials* **17**, 1237–46 (2007).

45. Johnson, J.P.; Bringley, D.A.; Wilson, E.E.; Lewis, K.D.; Beck, L.W.; Matzger, A.J. "Comparison of "Polynaphthalenes" Prepared by Two Mechanistically Distinct Routes." *Journal of the American Chemical Society* **125**, 14708-9 (2003).

46. Dittmar, U.; Marsmann, H.C.; Rikowski, E. "Silsesquioxanes as Crown Ether Analogs." *Organosilicon Chemistry III: from molecules to materials*. 395-9 (1998).

47. James, N.D. Unpublished results.

48. Booth, H.S.; McIntyre, L.H. "Barium Oxide as Dessicant." *Industrial And Engineering Chemistry* **2**, 12-15 (1930).

49. Rikowski, E.; Marsmann, H.C. "Cage-rearrangement of silsesquioxanes." *Polyhedron* **16**, 3357-61 (1997).

50. Asuncion M.Z.; Roll M.F.; Laine, R.M. "Octaalkynylsilsesquioxanes, Nano Sea Urchin Molecular Building Blocks for 3-D-Nanostructures." *Macromolecules* **41**, 8047-52 (2008).

51. Croswell, R.T.; Reisman, A.; Simpson, D.L.; Temple, D.; Williams, C.K. "Differential Thermal Analysis of Glass Mixtures Containing SiO_2,GeO_2, B_2O_3, and P_2O_5." *Journal of The Electrochemical Society*, **146** (12) 4569-79 (1999).

52. Lamansky, S.; Djurovich, P.; Murphy, D.; Abdel-Razzaq, F.; Kwong, R.; Tsyba, I.; Bortz, M.; Mui, B.; Bau, R.; Thompson, M.E. "Synthesis and Characterization of Phosphorescent Cyclometalated Iridium Complexes." *Inorganic Chemistry* **40**, 1704-11 (2001).

53. Laine, R.M.; Santy Sulaiman, S.; Brick, C.; Roll, M.; Tamaki, R.; Asuncion, M.Z.; Neurock, M.; Filhol, J.-S.; Lee, C.-Y.; Zhang, J.; Goodson III, T.; Curtis, J.; Ronchi, M.; Pizzoti, M. "Synthesis, and photophysical properties of Stilbeneoctasilsesquioxanes. Emission behavior coupled with theoretical modeling studies suggest a 3-D excited state involving the silica core." Manuscript in preparation.

54. Feher, F.J.; Terroba, R.; Ziller, J.W. "A new route to incompletely-condensed silsesquioxanes: base-mediated cleavage of polyhedral oligosilsesquioxanes." *Chemical Communications*, **1999** 2309-10 (2009).

Chapter III

Nano-Building Blocks via Bromination of OPS

Introduction

As discussed in Chapter 1, The assembly of 2- and 3-D structures from molecular components or nano-building blocks is of immense current interest.[1-9] A properly chosen macromolecular building block of nanometer scale should allow the design of materials on a nm by nm basis, and the chemical reactivity of these nano-building blocks would be modified by synthetic means to modulate the coupling and interaction between the blocks.[10]

While many molecules possess high degrees of 2-D symmetry, a much smaller set of compounds possess three-dimensionally symmetric structures and functionalities. Perfect (cubic) symmetry in 3-D and octa-functionality, as found in the cubane and cubic D4R-based silsesquioxane compounds, offer the potential to assemble macroscopic structures nm by nm in 2- or 3-dimensions.[10,11,12] Ten distinct D4R-based networks have been described through computational modeling, demonstrating the geometric flexibility of cubic nano-building blocks.[11]

Cubic silsesquioxanes, Q_8 $[RMe_2SiOSiO_{1.5}]_8$ and T_8 $[RC_6H_4SiO_{1.5}]_8$ SQs or POSS compounds,[12,13] with D4R-like silica core structure, are easily prepared in comparison to the hydrocarbon or other hybrid alternatives.[4,5] High thermal stability (~500°C in air for OPS), octa-functionality (with a possibility of forty possible functional groups for OPS)

and a wide variety of possible chemical modifications make OPS a good nano-building block precursor.[14]

As discussed in Scheme **3.2**, Chapter 1, the commercially available phenyltrichlorosilane ($PhSiCl_3$) is easily hydrolyzed and condensed to form polyphenylsilsesquioxane (PPS).[14,15] Strong inorganic bases (KOH, e.g.) can be used to equilibrate PPS in refluxing toluene by rapid rearrangement of the three Si-O linkages, driving the formation of the highly insoluble, cubic octamer $(PhSiO_{1.5})_8$, OPS.[14,15] As a result, octaphenylsilsesquioxane continuously precipitates from the reaction solution, and may be isolated by filtration of the reaction solution at the end of the desired reaction period.[15] In this chapter we discuss the bromination of OPS to give symmetrically substituted nano-building blocks.

Results and Discussion

Octabromination of Octaphenylsilsesquioxane

Brominated aromatics, such as the tetra(p-bromophenyl)adamantane[10] and the hexa(p-bromophenyl)benzene,[11] have been used as precursors for the synthesis of complex supermolecular systems, like our proposed Br_xOPS nano-building blocks. As with iodinated aromatics (Chapter 2), the development of catalytic C-C and C-heteroatom bond forming reactions via cross-coupling over the past few decades has multiplied the types of functionality which may be incorporated.[36-46] Examples of such reactions are shown in Chapter 2, Scheme **2.1**.

We now turn our attention to the selective bromination of OPS. In bromination, Lewis acids, often iron compounds, are used to complex with Br_2. This complexation

generates species that behave like cationic Br^+ and readily substitute aromatic groups.[30,31] Iron, or iron trichloride, is often used in this role.[30] Iron catalyzed bromination of OPS was explored by Brick et al[32] and He et al.[33] The bromination of OPS by IBr was reported by Erben et al.[34]

These studies gave products that were relatively disordered with respect to substitution pattern and number. However, following our success with iodination (Chapter 2), we concluded it might be possible to more selectively brominate OPS. Serendipitously, Takahashi, in this research group, found a significant preference for *ortho*-bromination upon exploring OPS bromination by bromine alone in dilute methylene chloride solution at room temperature.[35]

Benzene does not react with bromine in the absence of a Lewis Acid catalyst.[30] In contrast to published methods, we find that the addition of OPS to neat bromine leads to rapid bromination of the aromatic rings. While it is known that bromination of phenols and other activated aromatic systems occurs without a catalyst present,[30] the silsesquioxane cage should be *deactivating*.[36] Feher et al have proposed that the cage has electron withdrawing character similar to a CF_3 group based on analysis of Hammett constant correlations.[36] This should substantially reduce the rate of electrophilic substitution by reducing the electron density in the aromatic ring.[30]

We now report that the careful addition of bromine to a suspension of OPS in methylene chloride (1g OPS/ 5 ml CH_2Cl_2) at a bromine to phenyl molar ratio of 1.65:1, followed by heating to reflux, provides octa-brominated OPS with a narrow distribution in substitution number (Scheme **3.1**). Figure **3.1** shows a MALDI-TOF spectrum of the as-prepared material.

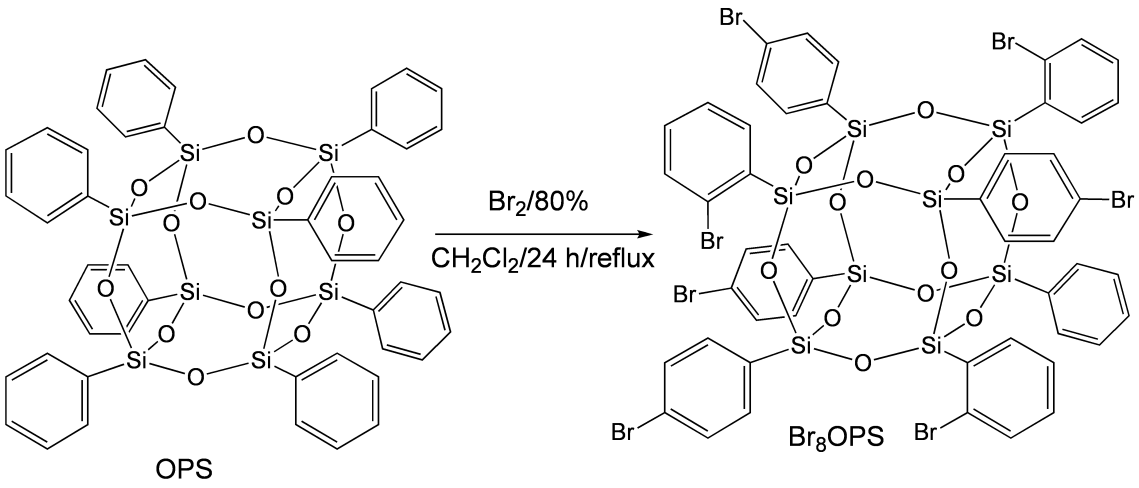

Scheme 3.1 Bromination of octa(phenyl)silsesquioxane (OPS).

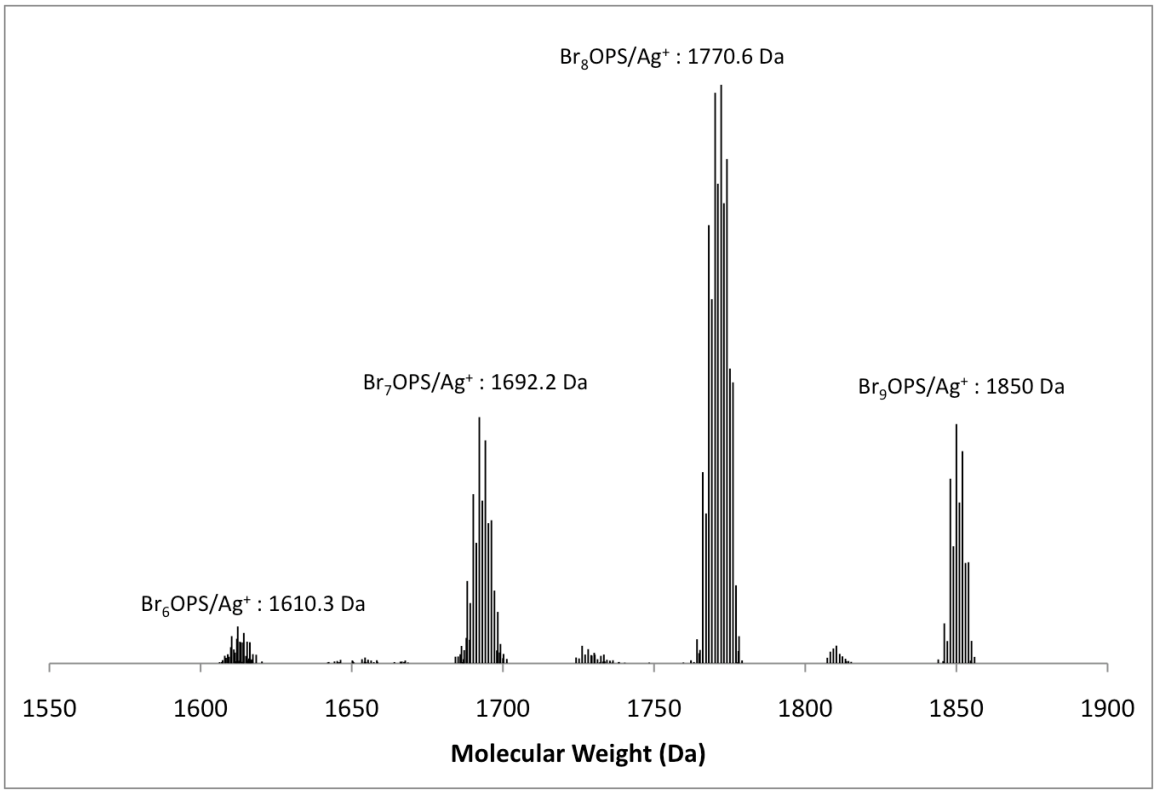

Figure 3.1 MALDI-TOF MS of octa(bromophenyl)silsesquioxane(Ag^+/Dithranol).

Once it was determined that octa-bromination with a narrow distribution in substitution number could be achieved, the substitution pattern of the aromatic bromides was determined. The previously described[32] F^-/H_2O_2 technique was used to oxidatively cleave the aromatic rings from each corner of the octasilsesquioxane cage and the resulting mixture of phenols was isolated (Chapter 1, Scheme **1.3**, B).[32] GC-MS was used to determine the ratio of *ortho* to *para* isomers by integrating the responses from each.

If the silsesquioxane cage is an electron withdrawing substituent, as proposed by Feher et al, significant *meta* substitution should occur due to deactivation of the *ortho* and *para* positions. However in this case, oxidative Si-C cleavage of the octa(bromophenyl)silsesquioxane shows no *meta* substituted phenols. More surprisingly, the *ortho* substitution is preferred to substitution at the more sterically available *para*-position 85 % to 15 %, in line with the observations of Takahashi.[35]

This unexpected result may be rationalized by considering recent calculations by Park et al, who found that halide anion complexation on the cubic faces of octasilsesquioxanes is energetically favorable by 10-60 Kcal/mole.[37] Separate experiments in our laboratory suggest that tetrabutylammonium bromide, chloride and iodide may interact with OPS in methylene chloride solution and possibly co-crystallize, as discussed in Chapter 6 regarding Future Work.

Thus in solution at room temperature, we can speculate that diatomic bromine spontaneous polarization occurs at the cage face, leading to a relatively higher concentrations of Br^+ close to the *ortho* position, as depicted in Figure **3.2**. In other words, it could be that the silsesquioxane cage itself drives the bromination of OPS.

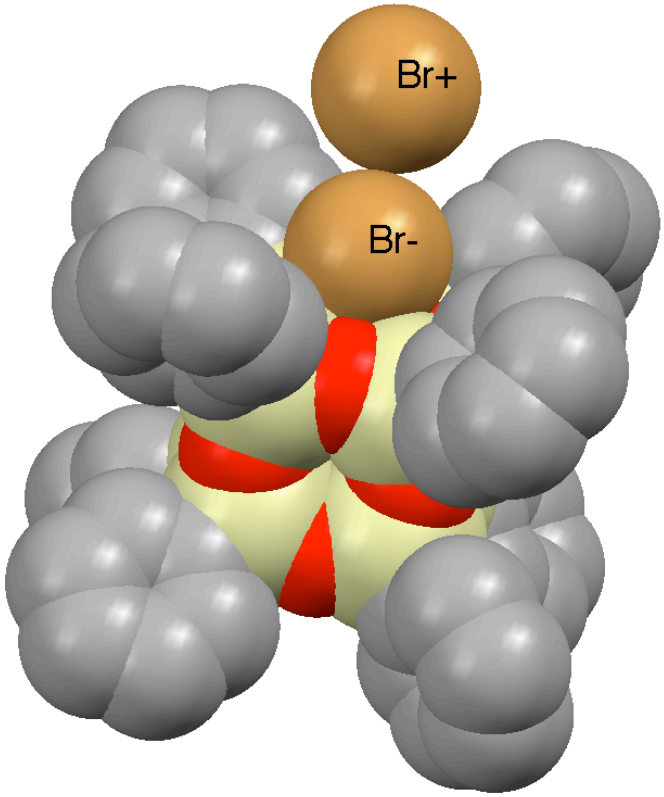

Figure 3.2 Proposed complexation of bromide ion with silsesquioxane cage face.

During the work-up of octa(bromophenyl)silsesquioxane (Scheme **1**), trituration of the crude product in ethyl acetate at room temperature and filtration gave a microcrystalline fraction (~10 % of the total yield by mass). The filtrate is reduced and precipitated into 5 volumes of cold methanol. If the bromination reaction (Scheme **1**) volume is quadrupled (~1 g OPS/ 20 ml CH_2Cl_2) and the length of the reaction is increased to one week, the ethyl acetate insoluble material comprises roughly 40% by mass of the total. This microcrystalline material is recrystallized from hot *o*-dichlorobenzene, and large colorless crystals suitable for single crystal X-ray diffraction are obtained in very low yield, <5 % by mass of the total. The remaining *o*-dichlorobenzene soluble material (~85 %) is precipitated into cold methanol and isolated as a fine white powder, and is determined to be average Br_8OPS, as shown in Figure **3.1**.

The ^{1}H NMR shown in Figure **3.3** indicates four primary multiplets, centered at 7.77, 7.47, 7.25 and 7.23 ppm. Based on the conclusion of Feher et al, that the cage acts as an electron withdrawing substituent equivalent to a CF_3 group, peak assignments from *o*-bromobenzotrifluoride (via the Spectral Database for Organic Compounds or SDBS), correspond to: a=7.68 ppm, b=7.67 ppm, c=7.41 ppm, and d=7.38 ppm.[38] In contrast, for *o*-bromonitrobenzene, a=7.74 ppm, b=7.47 ppm, c=7.45 ppm, d=7.84 ppm. These assignments appear to be a better qualitative fit, and are used below.[38] The shift of c indicates the silsesquioxane cage may possess electron withdrawing character intermediate between a CF_3 and a NO_2 group.

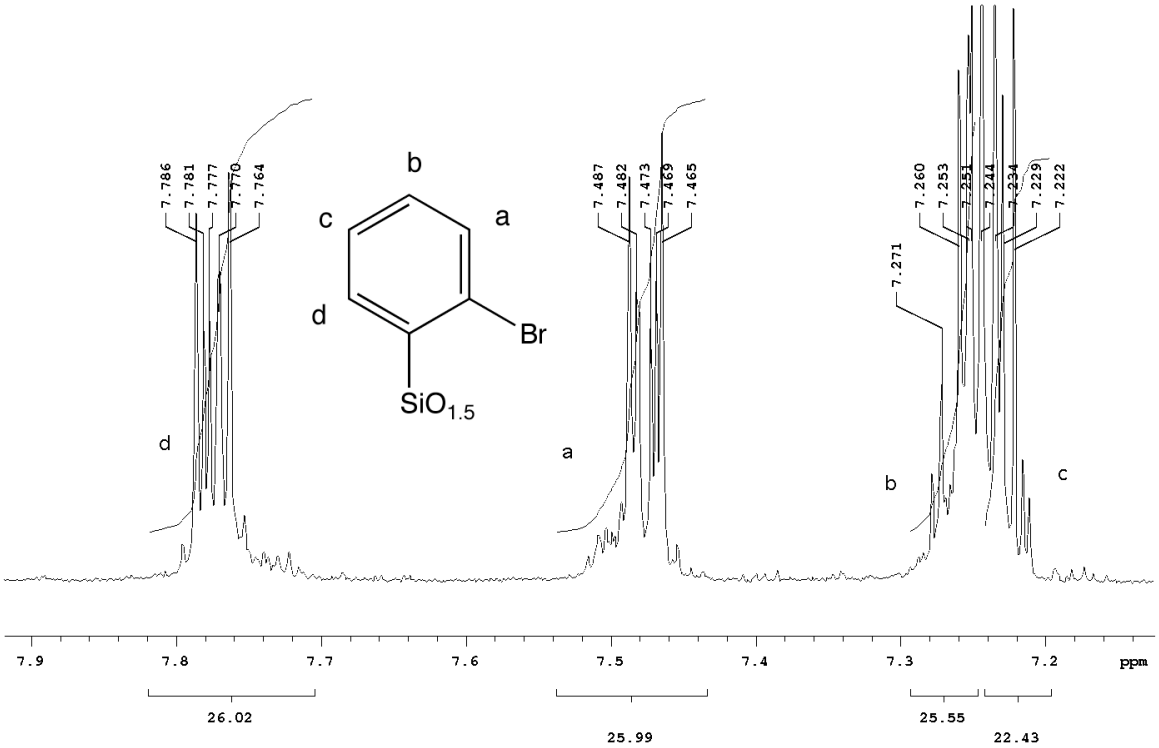

Figure 3.3 ^{1}H NMR spectrum of octa(*o*-bromophenyl)silsesquioxane in $CS_2/CDCl_3$

The ^{13}C NMR spectrum is shown in Figure **3.4**, assignments are made based on the consideration of the assignments of *o*-bromonitrobenzene from SDBS and

consideration of peak integrations.[38] The MALDI-TOF spectrum of crystalline octa(*o*-bromophenyl)silsesquioxane is shown below in Figure **3.5**.

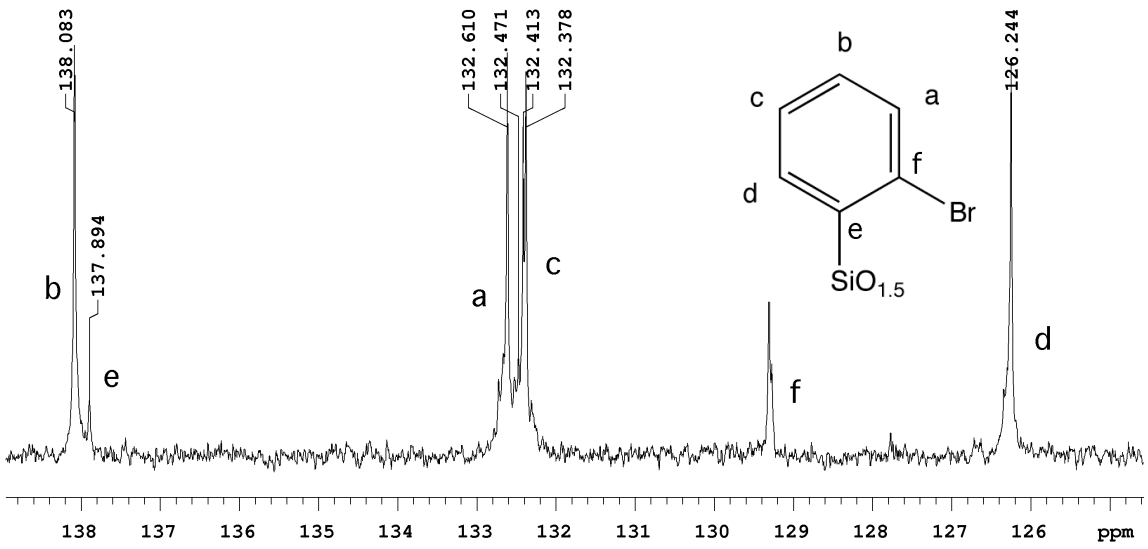

Figure 3.4 ^{13}C NMR spectrum of octa(*o*-bromophenyl)silsesquioxane in $CS_2/CDCl_3$.

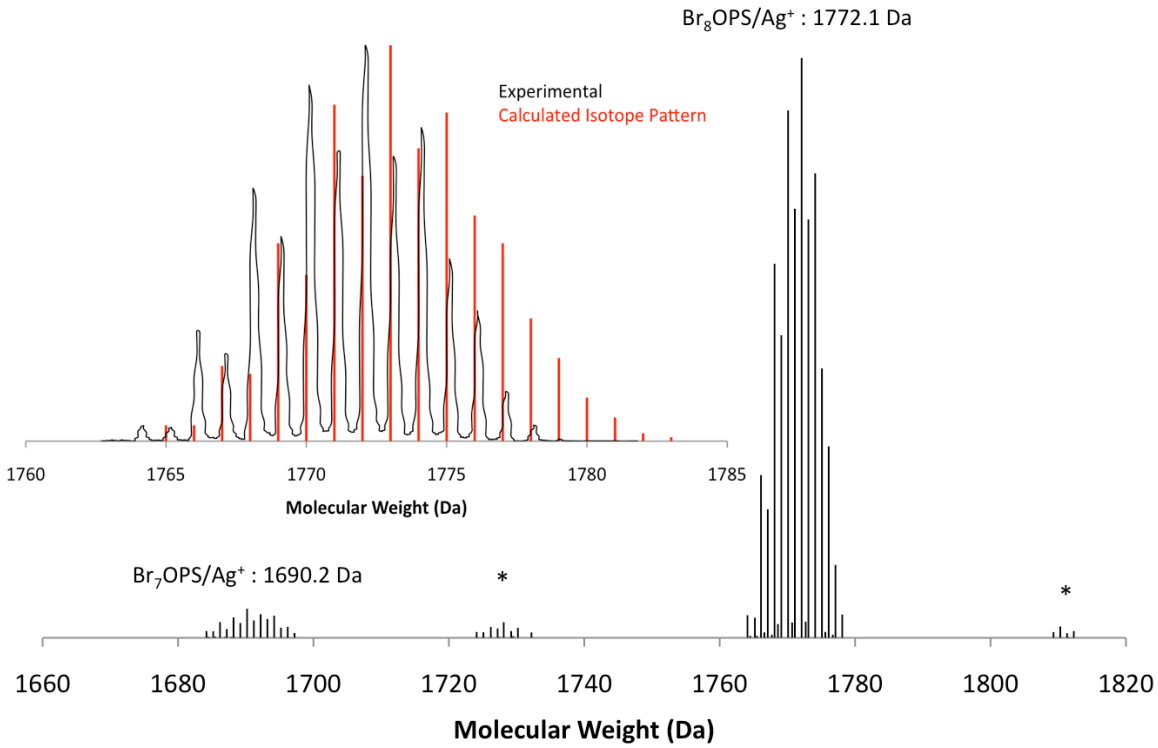

Figure 3.5 MALDI-TOF spectrum of octa(*o*-bromophenyl)silsesquioxane (Dithranol/$AgNO_3$).

X-ray quality crystals of *o*-Br_8OPS were grown by slow cooling of hot, saturated *m*-xylene solutions, as described in the Experimental (Chapter 7). Single crystal X-ray diffraction analysis revealed that *o*-Br_8OPS crystallizes in the tetragonal space group I4(1)/a (Figure **3.6**). The unit cell contains eight molecules with a total volume of 15348.5 $Å^3$. The 2.5 *m*-xylene solvents are disordered. Two of the solvents were modeled by partial occupancy, while one half of one *m*-xylene per unit cell was modeled using the SQUEEZE sub-routine of the PLATON program suite.[31]

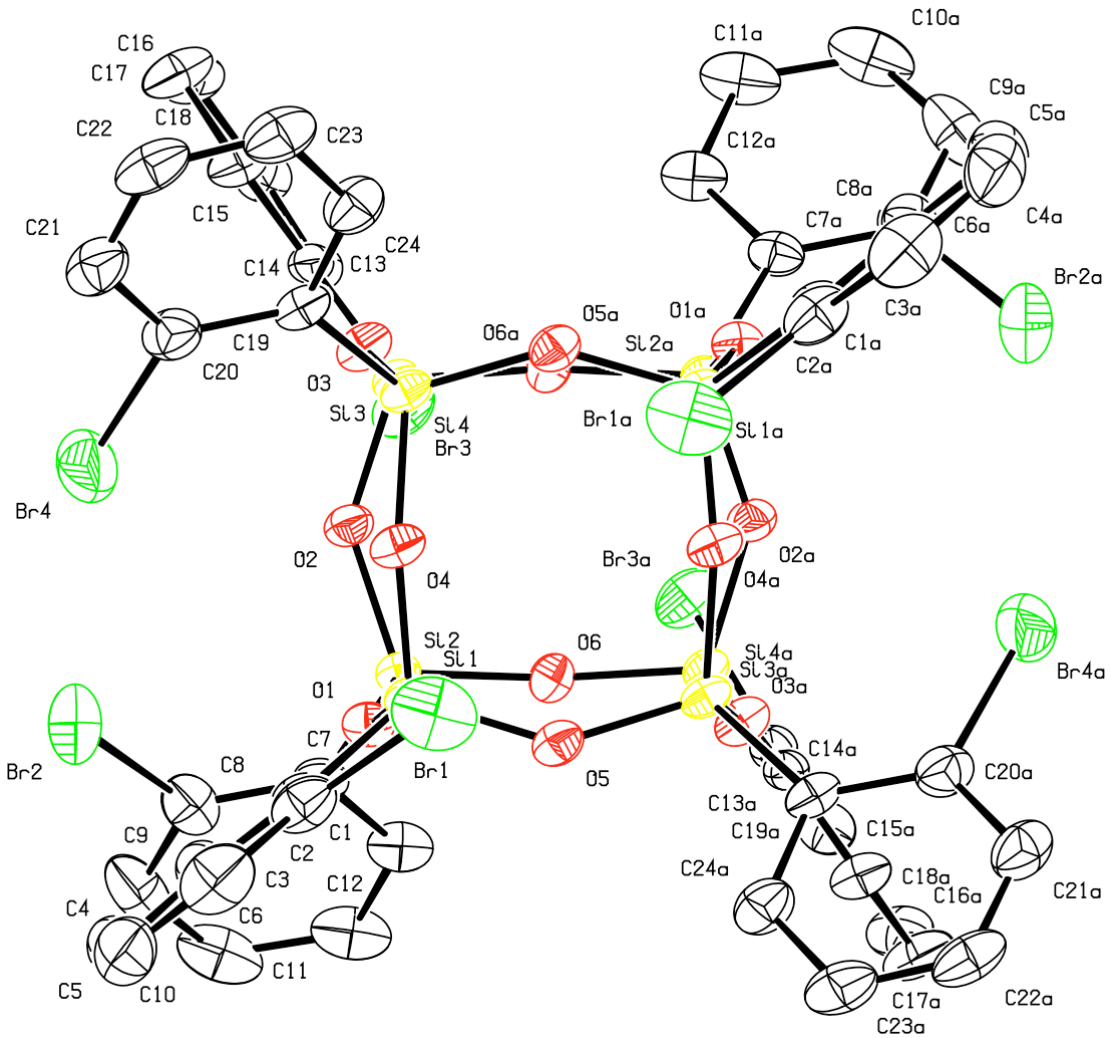

Figure 3.6 50 % thermal ellipsoid plots of octa(*o*-bromophenyl)silsesquioxane • 2.5 *m*-xylene. Hydrogen atoms and *m*-xylene solvates are omitted for clarity. Full XRD data can be found in Appendix 5.

Table 3.1 Crystal Structure Data for octa(*o*-bromophenyl)silsesquioxane • 2.5 *m*-xylene

	o-Br_8OPS
Space Group	I4(1)/a, tetragonal
Unit Cell Dimensions	a= 20.5738(10)Å b= 20.5738(10) Å c= 36.261(4) Å
	a = 90° b= 90° g= 90°
Unit Cell Volume	15348.5(19) $Å^3$
Z	8
R-factor	5.3 % (5.3 %)*

* Before use of SQUEEZE to account for disordered solvent

Hexadecabromination of Octaphenylsilsesquioxane

While the degree of substitution of this uncatalyzed bromination may be increased by adding more bromine, it is found experimentally that the average degree of bromination does not exceed fourteen. Previously, we reported that iron powder used as a catalyst dramatically accelerates the reaction and allows for substitution up to an average of sixteen.[33] It was also observed that as the substitution number reached sixteen, insoluble products precipitated from the reaction solution.[33] Unfortunately, once isolated, it was found to be insoluble in all traditional laboratory solvents, including ethyl acetate, toluene, tetrahydrofuran and acetone.

However, Olson and Gronwall reported bromination of the thiophenylsilsesquioxane systems some forty years earlier, and noted its remarkable solubility in carbon disulfide.[32] We find that the insoluble Br_{16}OPS material is also soluble in carbon disulfide.

We wished to maximize the production of this microcrystalline isomer, and found the slow addition of bromine to a stirring suspension of OPS and $FeBr_3$ in methylene chloride at 0°C leads to an instantaneous, vigorous reaction. $FeBr_3$ was used as a

homogenous catalyst, to reduce the heterogeneity of the previous Fe^0 bromination system (Scheme **3.2**).[32] After the suspended OPS reacts and dissolves, a new precipitate forms as the reaction continues. After 24 h, the residual bromine is quenched. The recovered insoluble material is dissolved by the addition of carbon disulfide, and the organic layer is washed twice with brine.

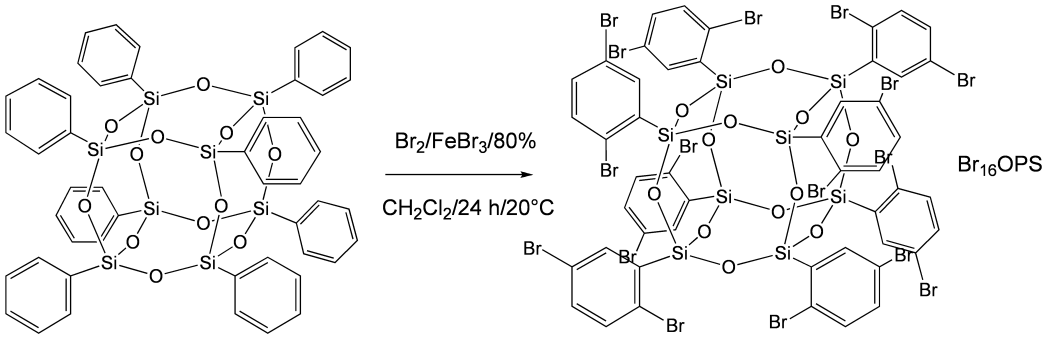

Scheme 3.2 Synthesis of octa(dibromophenyl)silsesquioxane

The ^1H NMR spectrum of the material in $CDCl_3/CS_2$ shows two multiplets (Figure **3.7**). Starting with the conclusion of Feher et al, peak assignments are made by comparison to 2,5-dichlorobenzotrifluoride, where a=7.43 ppm, b=7.44 ppm, and c=7.67 ppm.[38] In comparison to 2,5-dibromonitrobenzene, where a=7.62 ppm, b=7.55 ppm, and c=7.98 ppm.[38] In Figure **3.7**, assignments for $Br_{16}OPS$ are a,b=7.4 ppm and c=7.85 ppm. Again, the shift of c indicates the silsesquioxane cage may possess electron withdrawing character intermediate between a CF_3 and a NO_2 group. Figure **3.8** shows MALDI-TOF MS analysis of the crystalline material, indicating the desired hexadecabrominated isomer. Oxidative cleavage indicates essentially the single 2,5- isomer of dibromophenol (>95%).

X-ray quality crystals of 2,5-$Br_{16}OPS$ carbon disulfide solvate were grown by slow evaporation of a 1:1:1 carbon disulfide/dichloromethane/dodecane solution. Single

crystal X-ray diffraction analysis revealed that 2,5-Br_{16}OPS crystallizes in the triclinic space group P-1 (Figure **3.9**). The unit cell contains one molecule with a total volume of 1699.3 $Å^3$ and a density of 2.318 g/cc. The single carbon disulfide solvent is disordered.

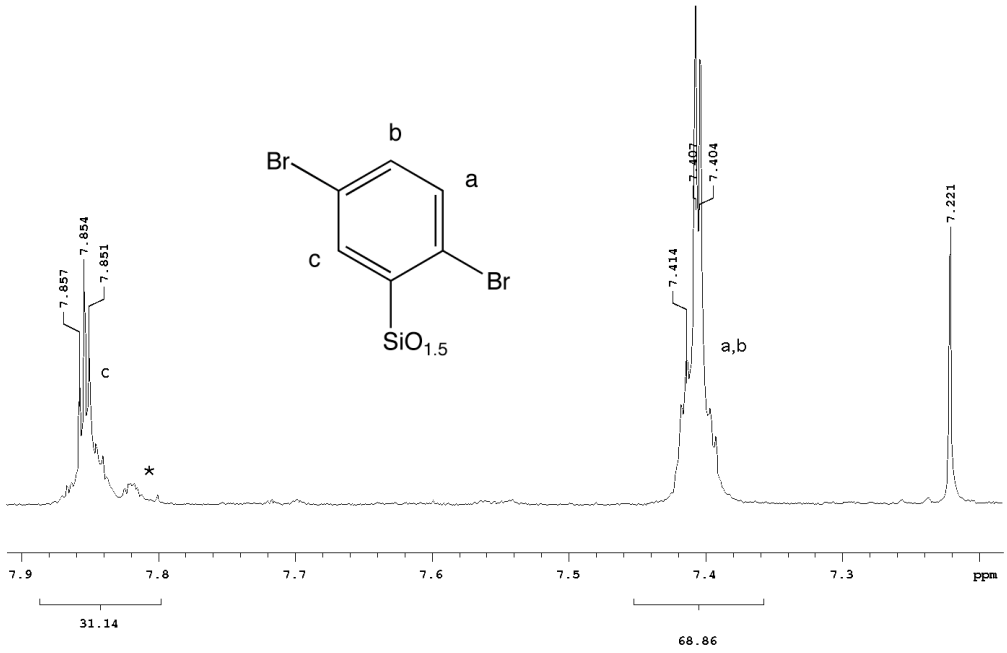

Figure 3.7 ^{1}H NMR spectrum of octa(2,5-dibromobromophenyl)silsesquioxane in $CS_2/CDCl_3$.

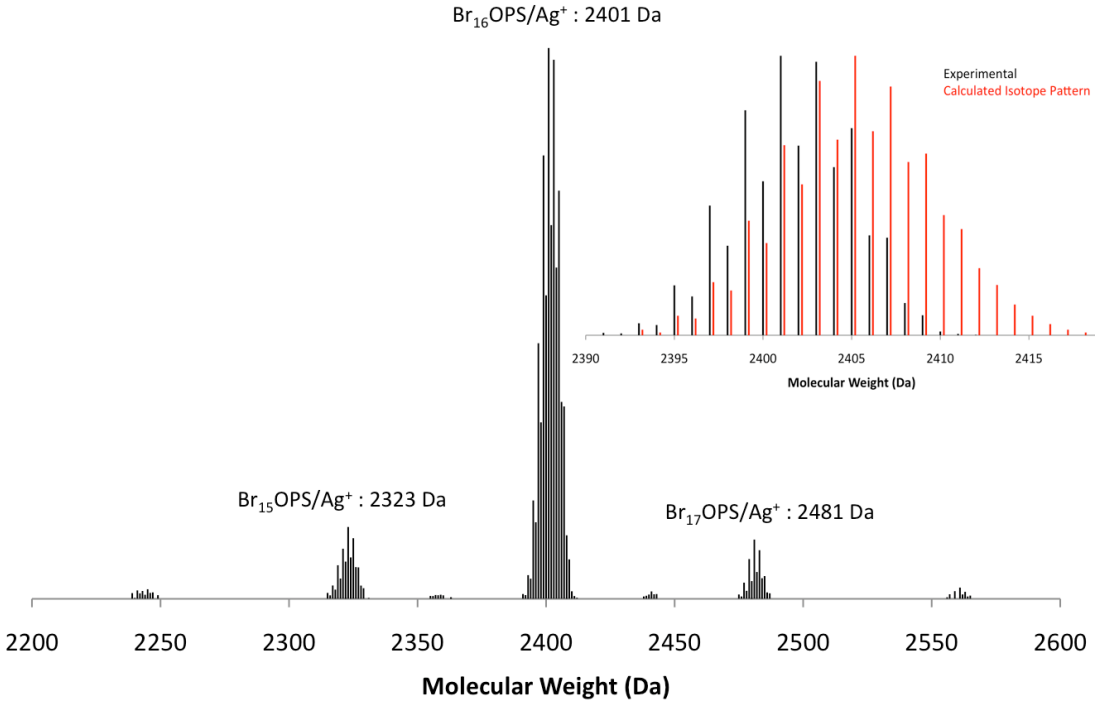

Figure 3.8 MALDI-TOF MS of octa(2,5-dibromophenyl)silsesquioxane. (Dithranol/$AgNO_3$).

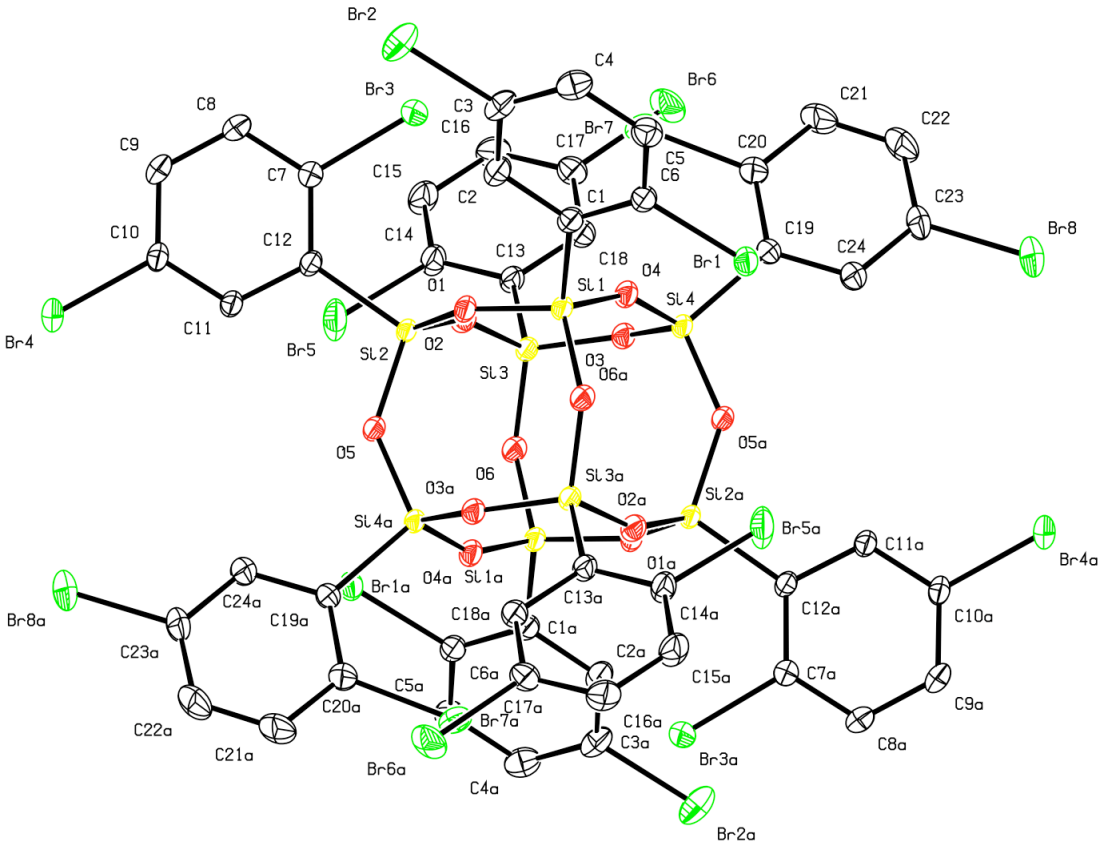

Figure 3.9 50 % thermal ellipsoid plots of octa(2,5-dibromophenyl)silsesquioxane carbon disulfide solvate. Hydrogen atoms and carbon disulfide solvates are omitted for clarity. Full XRD data can be found in Appendix 6.

Table 3.2 Crystal Structure Data for octa(2,5-dibromophenyl)silsesquioxane • carbon disulfide

	$Br_{16}OPS$
Space Group	P-1, triclinic
Unit Cell Dimensions	a= 12.7172(9) Å b= 12.7392(9) Å c= 13.0890(9) Å
	a = 97.592(1)° b= 109.075(1)° g= 116.231(1)°
Unit Cell Volume	1699.3(2) $Å^3$
Z	1
R-factor	2.7 %

It was previously assumed that the iron catalyst promotes a dynamic rearrangement of the substitution pattern, allowing for the insolubility driven

precipitation of the crystalline 2,5- isomer.[33,34] As a test of this hypothesis, the same number of equivalents of bromine were added to a stirring suspension of OPS in methylene chloride at 0˚C, and allowed to react without the iron catalyst until the evolution of HBr slowed.

At this point the reaction mixture was cooled and stirring was stopped as $FeBr_3$ catalyst was added. Once the vent and nitrogen were reinstalled, the ice-bath is removed the reaction was allowed to continue. The reaction continues vigorously, and after 24 h the reaction is quenched and a soluble product is isolated.

The obtained product is completely soluble in methylene chloride, ~1 g/ml at RT, in addition to CS_2. The F^-/H_2O_2 cleavage of the material indicates a 2:1 ratio of two isomers of dibromophenol, and these are assigned to 2,5-dibromophenol and 3,4-dibromophenol, respectively, by ^1H NMR.[39] Presumably this decrease in symmetry prevents any significant crystallization from occurring. The MALDI-TOF spectrum shows a narrow distribution in substitution number, as seen with the crystalline product.

Tetraicosabromination of OPS

The addition of the $FeBr_3$ catalyst after an initial stage of bromination without catalyst increases the degree of bromination beyond sixteen (Scheme **3.3**, Figure **3.10, 3.11**), providing highly insoluble white powders. Attempts to increase the degree of bromination to twenty-four led to significant Si-C cleavage as a side-reaction, leaving a silanol functionalized corner, as detected in the crude reaction products by MALDI-TOF (Figure **3.10**). It appears that the tri-brominated corners are readily cleaved under the highly acidic (due to HBr produced), oxidizing (due to excess Br_2) conditions. Repeated

recrystallization of the reaction product from hot *o*-dichlorobenzene removes the cleaved products and allows isolation of crystalline material in low yields, <10 %.

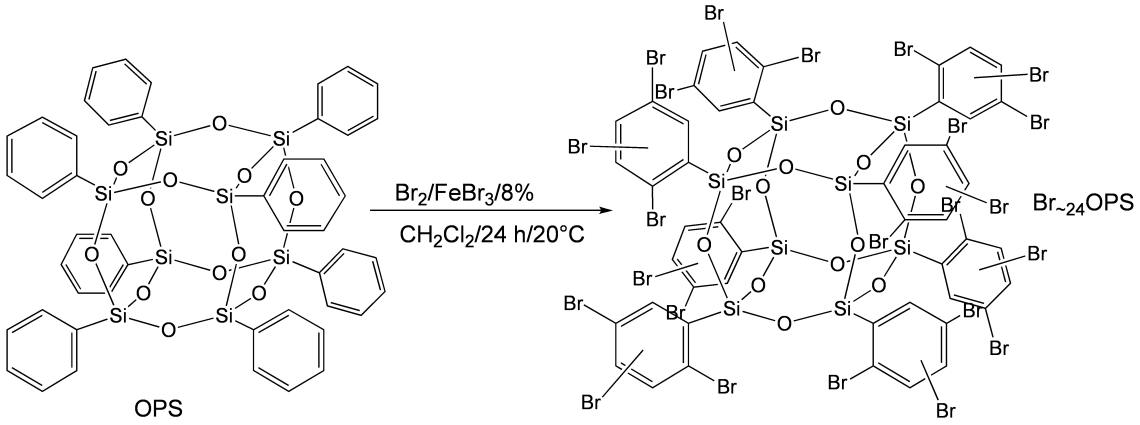

Scheme 3.3 Synthesis of tetraicosabrominated OPS.

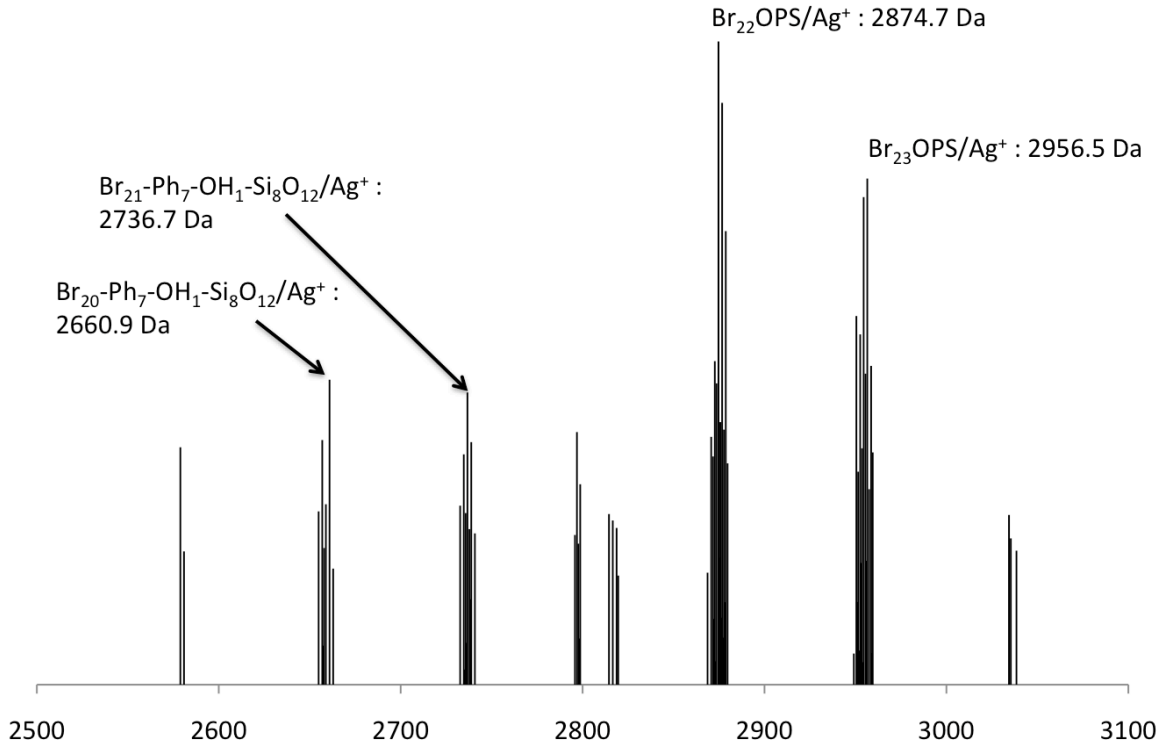

Figure 3.10 MALDI-TOF MS showing corner cleavage during bromination. (Ag^+/Dithranol).

GC/MS analysis of the oxidative cleavage products indicate two primary tribromophenols and a tetrabromobenzene isomer. MALDI-TOF analysis indicates a broader distribution in the degree of bromination (Figure **3.10**). In addition, molecules

with degrees of substitution twenty-four or more reveal the addition of a water molecule to the structure. Since silanols are not detected by FTIR, it appears Si-O-Si bond opening occurs under the influence of the laser.

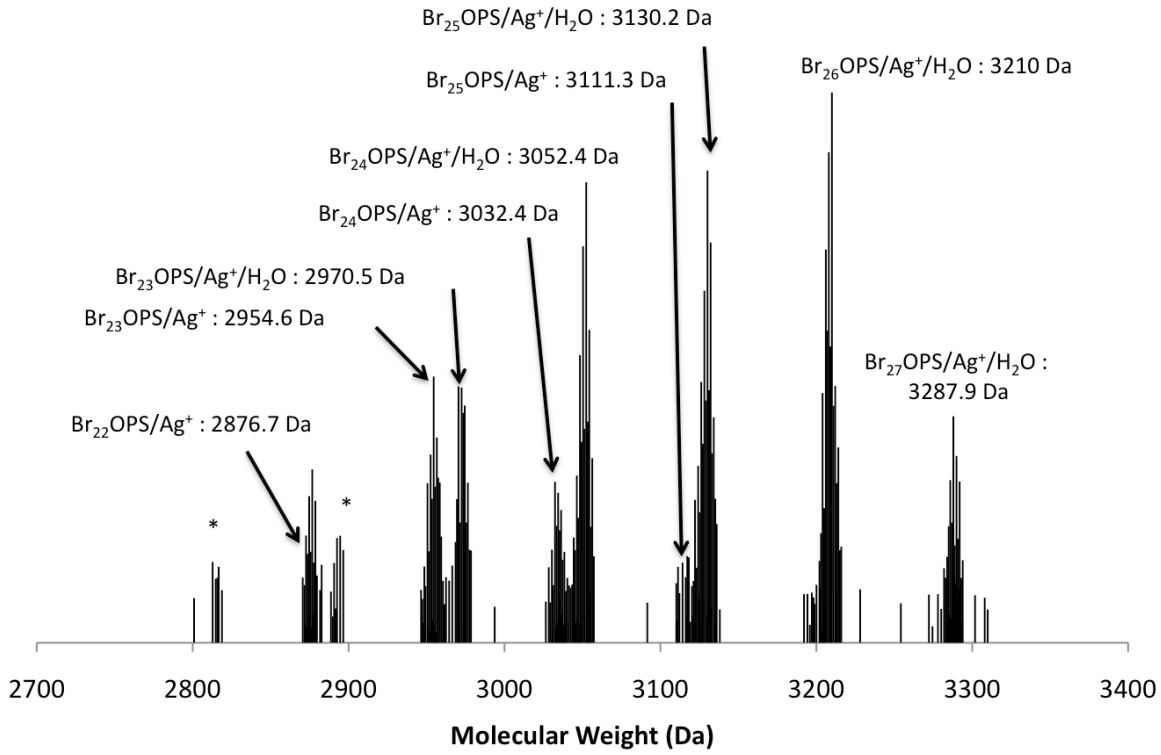

Figure 3.11 MALDI-TOF MS of tetraicosabrominated OPS (Ag^+/Dithranol).

The ^{1}H NMR in Figure **3.12** shows only two poorly resolved multiplets at 7.88 and 7.84 ppm, with a minor broad peak at 7.435 ppm. In contrast, the proton resonances for 1,2,5,-tribromo-3-trifluoromethyl-benzene are found at 8.14, 7.90 ppm.[40] The resonance from residual chloroform is seen at 7.222 ppm.

Single crystals suitable for X-ray diffraction were grown from dilute solutions of hot o-dichlorobenzene, and the refined crystal structure shows a solid solution, with multiple substitution patterns (Figure **3.13**). The partial filling factors indicate an average of 24 bromines. The crystal structure is relatively open, hosting disordered *o*-dichlorobenzene solvents, and having a lower density (2.0 g/cc) than the Br_{16}OPS.

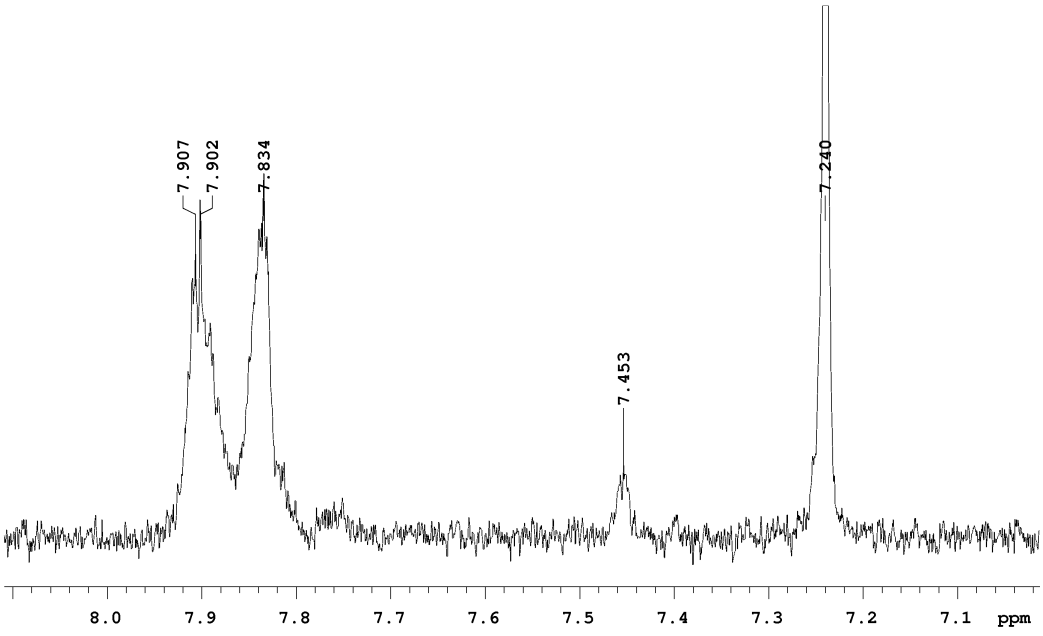

Figure 3.12 ^{1}H NMR spectrum of tetraicosabrominated OPS in $CS_2/CDCl_3$.

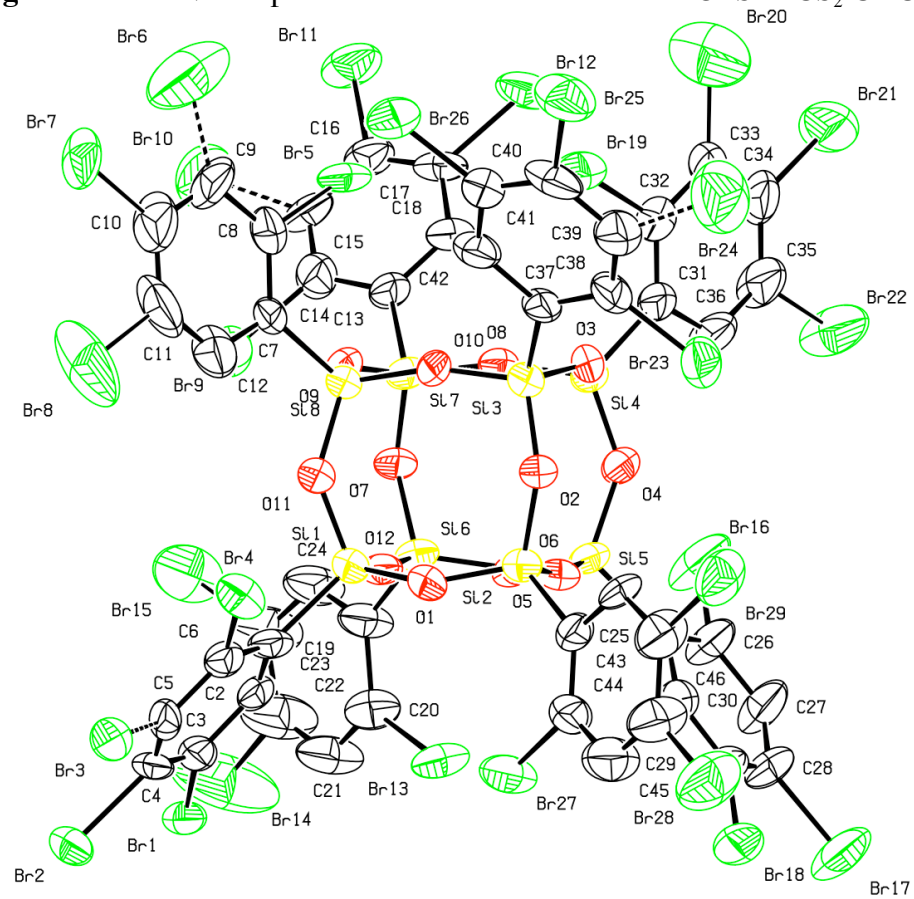

Figure 3.13 50 % thermal ellipsoid plots of tetraicosabrominated OPS • 5 *o*-dichlorobenzene (R-factor of 6.3 %). Hydrogen atoms and *o*-dichlorobenzene solvates are omitted for clarity. Dashed bonds indicate partially occupied bromines.
Full XRD data can be found in Appendix 7.

Table 3.3 Crystal Structure Data for tetraicosabrominated OPS • 5 *o*-dichlorobenzene

	Br_{24}OPS
Space Group	P-1, triclinic
Unit Cell Dimensions	a= 15.5726(10) Å b= 20.4685(13) Å c= 20.6449(13) Å
	a = 65.3990(10)° b= 74.6160(10)° g= 82.1720(10)°
Unit Cell Volume	5766.3(6)Å^3
Z	2
R-factor	6.3 % (12.7 %)*

* Before use of SQUEEZE to account for disordered solvent

These highly brominated materials may be valuable as high dielectric materials, or high refractive index materials, due to the high Z value of bromine. In addition, Pd catalyzed coupling should allow for the synthesis of highly stable materials with eight to twenty-four functional groups. The possibility of using multiple functional groups tethered to the same molecule should allow for the synthesis of nanocomposite materials with a variety of mechanical, optical, and electronic properties.

Comparison of the Bromo Derivatives

Table **3.4** details some of the differences between the three crystalline compounds. The found ceramic yields of these compounds are not dramatically different from that expected from theory, except for the Br_8OPS. This appears to be due to volatility of the *o*-Br_8OPS, which is found to volatilize ca. 410° C.

Table 3.4 Characterization data for the brominated OPS derivatives

Sample	**MW calculated (Ag^+ ion)**	**MW MALDI-TOF Found(% Intensity)**	**Ceramic Yield (Theor.)**	**Ceramic Yield (Found)**
Br_8OPS	1772.55	1772.1 (100%)	29 %	23 %
Br_{16}OPS	2403.72	2402.2 (100%)	21 %	19 %
Br_{24}OPS	3034.89	3032.3 (63%)	17%	16 %

The octabrominated compound shows a mass-loss onset at ca. 450˚C. The TGA traces of the hexadeca- and tetraicosa-brominated compounds show > 500˚C stability in air (see Figure **3.14**). The TGA trace of the Br_{16}OPS material conducted under nitrogen does not show evidence of sublimation.

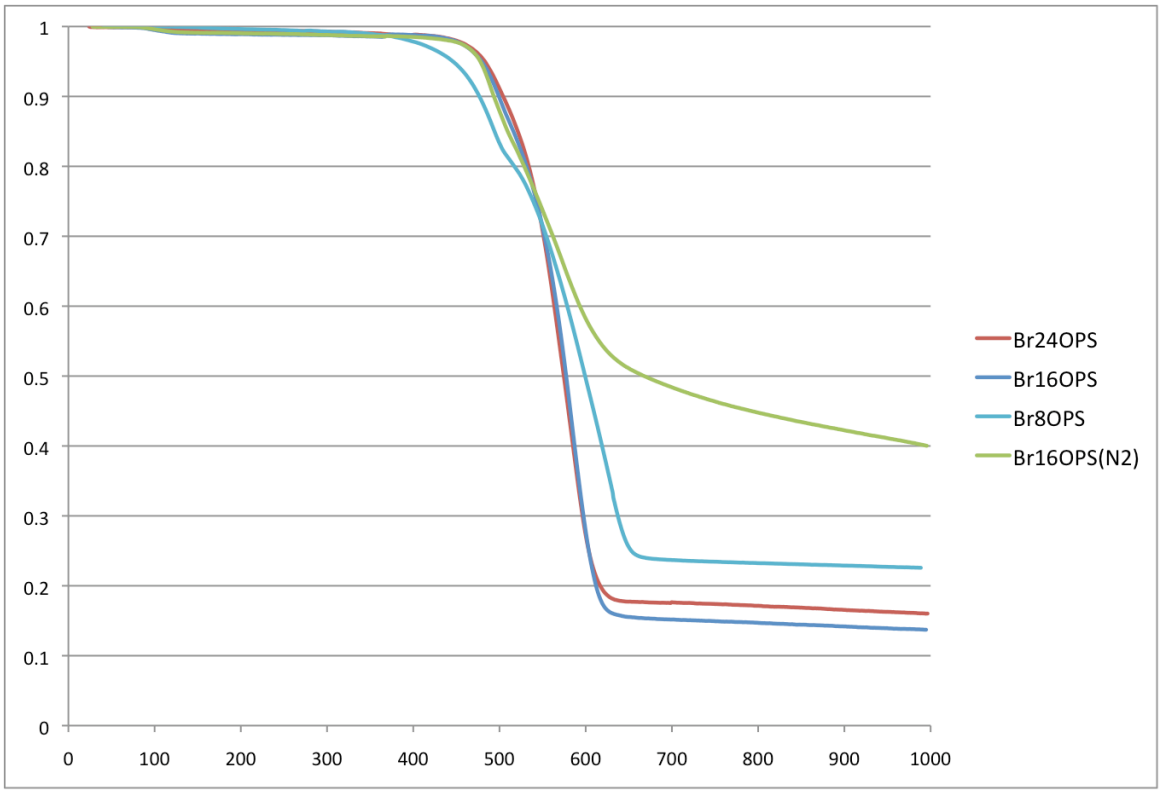

Figure 3.14. TGA traces of brominated OPS derivatives in air, ceramic yields in Table **3.1**.

DSC analysis is shown below in Figure **3.15**. Melting points range from 250-400+˚C. While the as-prepared Br_8OPS melts at ca. 260˚C, the crystalline octa-*ortho*-brominated OPS melts at ca. 360˚C, almost 100˚ higher. This is presumably due to the higher degree of crystallinity. The hexadecabrominated OPS melts at ca. 375˚C, but the tetraicosabrominated OPS has a melting point outside the instrument range. Together, these melting points are below or far below the mass losses found in the TGA analyses.

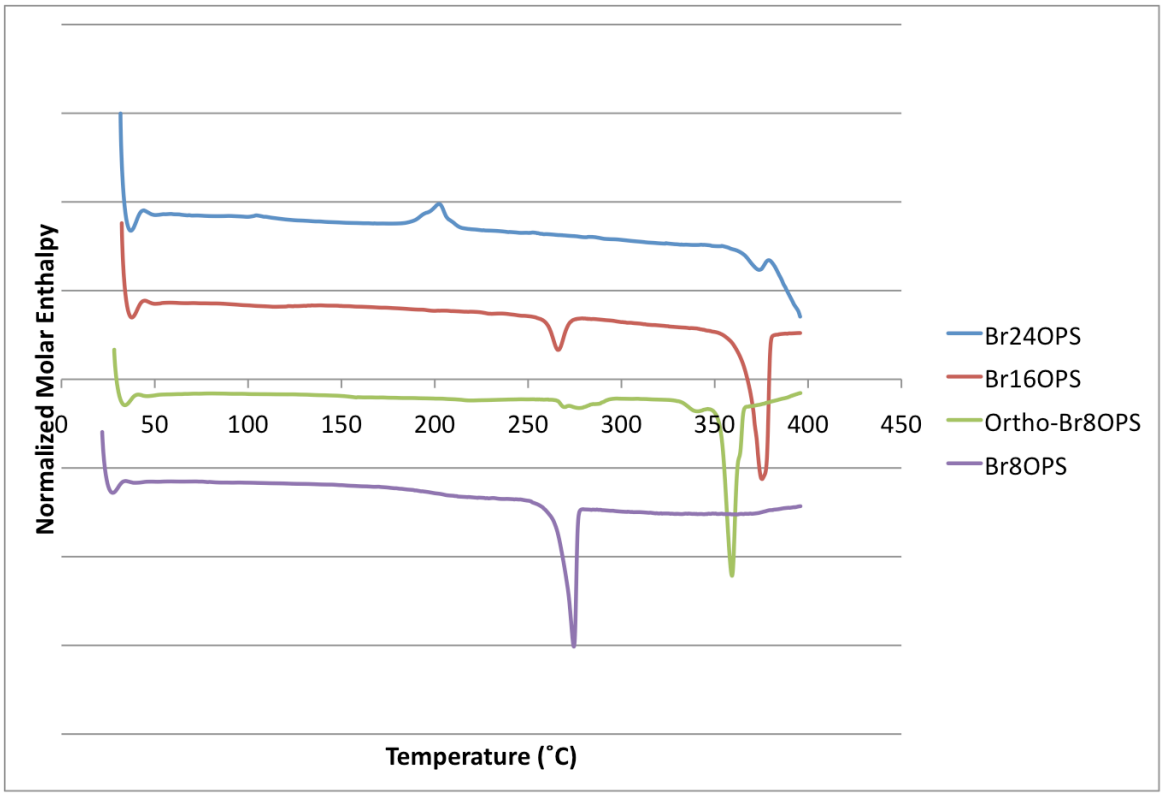

Figure 3.15. DSC traces of brominated OPS derivatives.

FTIR spectra of the compounds are shown in Figures **3.16** and **3.17**. The characteristic ν Si-O-Si bands are seen between 1200-1000 cm^{-1}. Equivalently scaled, the aromatic ν C-H region (3100-3000 cm^{-1}) shrinks as the degree of bromination increases. However, distinct differences are also seen in the aromatic regions 1500-1250 cm^{-1} and 850-700 cm^{-1}.

The FTIR spectra of octa(*o*-bromophenyl)silsesquioxane shows a striking feature at 755 cm^{-1}, in the aromatic δ C-H region (Figure **16**). This δ C-H resonance could be indicative of the dominant *ortho* substitution in the molecule. In each spectrum there are peaks from 1415-1428 cm^{-1} and 1580-1555 cm^{-1}, associated with aromatic ν C-C bands.[30]

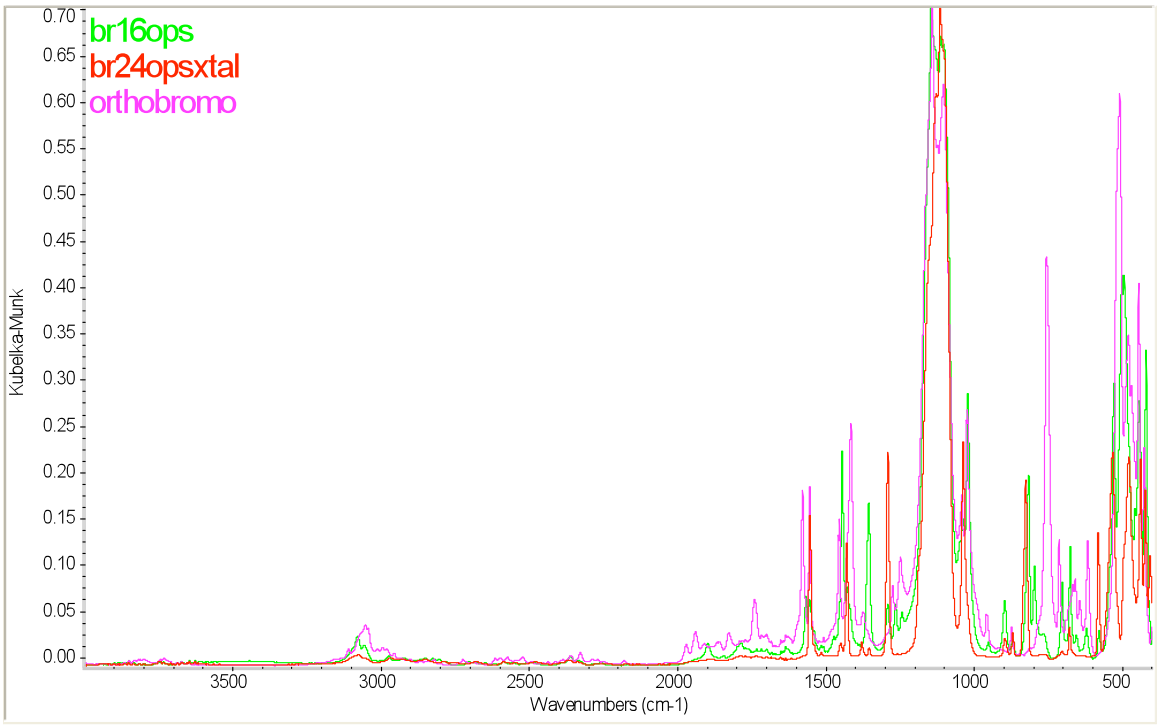

Figure 3.16. FTIR spectra of brominated OPS derivatives, 3200-400 cm^{-1}.

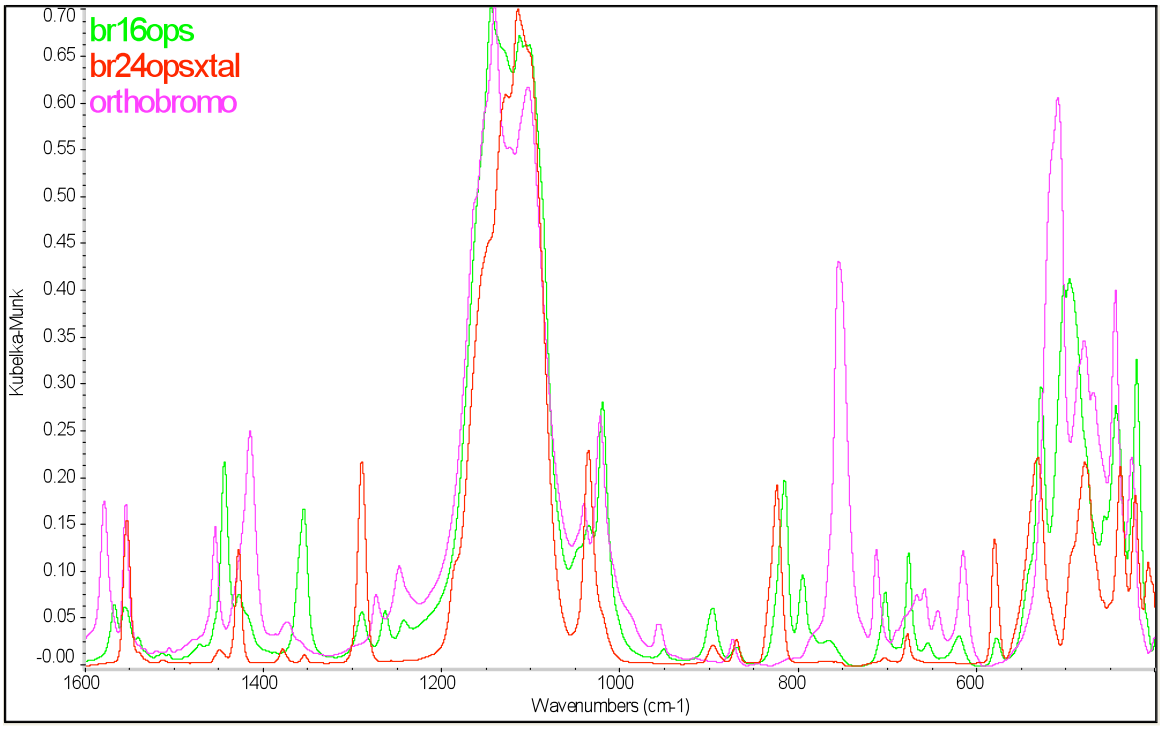

Figure 3.17. FTIR spectra of brominated OPS derivatives 1600-400 cm^{-1}.

Conclusions

This chapter has detailed the functionalization of OPS through selective bromination with or without the addition of an iron catalyst. We have shown there are multiple substitution routes with varying substitutional specificities. We can isolate crystalline derivatives with a high degree of substitutional specificity due to the purifying effect of recrystallization.

These derivatives include the octabromophenylsilsesquioxane in 80% yield, and a crystalline octa-*ortho*-brominated OPS derivative in low yield <5 %. The mechanism for the *ortho* substitution may be influenced or driven by interaction of bromine with the silsesquioxane cage face. It could be that the electron withdrawing nature of the cage drives this complexation by pulling electron density from halogen anions. If this is true, electrophilic aromatic substitution reactions with an OPS/halide anion complex might give different substitution patterns.

A Br_{16}OPS derivative has been isolated in 80% yield, and a crystalline octa(2,5,-dibromophenyl)silsesquioxane in 40% yield. A Br_{24}OPS derivative has been isolated in 10% yield, and a crystalline solid solution of substitutional isomers has been isolated, and its single crystal X-ray structure refined. Each of these derivatives could provide access to highly polyfunctional molecules, if suitable cross-coupling reactions may be found. The sterically confined geometry might allow the observation of intramolecular exciplexes or other photophysical phenomena.

These compounds have the potential to serve as high dielectrics due to their high electron density. They suggest the possibility of tunable high dielectric

characteristics by modifying the reaction chemistry. They may also serve as nano-building blocks with up to twenty-four functional groups.

We have shown that the degree of bromination in the OPS system may be increased from eight to sixteen to twenty-four bromines per OPS molecule, increasing the electron density and volume of the molecule. However, as this degree of substitution reaches twenty-four, Si-C cleavage reactions begin to dramatically reduce the yield of crystalline material. The crystal structure of tetraicosabrominated OPS has been refined, and it shows a solid solution of substitutional positions. The Br_{16}OPS and Br_{24}OPS show thermal stability in excess of 450˚C, and all three derivatives show melting behavior under DSC analysis.

Unique characteristics of these crystal structures will be detailed in Chapter 4. In particularly, the variation in densities from the *o*-Br_8OPS (1.67 g/cc) and the Br_{24}OPS (2.0 g/cc), to densely packed structures, in the case of the Br_{16}OPS (2.32 g/cc). At the heart of these effects will be the increasing number of bromines packed into the 1 nm diameter of the OPS molecule.

References Cited:

1. Detken, A.; Zimmermann, H.; Haeberlen, U.; Poupko, R.; Luz, Z. "Molecular Reorientation and Self-Diffusion in Solid Cubane by Deuterium and Proton NMR." J. Phys. Chem. 1996, 100, 9598–9604.
2. Hawker, C.J.; Wooley, K.L. "The Convergence of Synthetic Organic and Polymer Chemistry," *Science* **309**, 1200-5.
3. Feynman, R. "There's Plenty of Room at the Bottom." *Journal of Microelectromechanical Systems* **1**, 60-6 (1992).
4. Eaton, P.E.; Galoppini, E.; Gilardi, R. "Alkynylcubanes as Precursors of Rigid-Rod Molecules and Alkynylcyclooctatetraenes." *Journal of the American Chemical Society*, **116**, 7588-96 (1994).
5. Eaton, P.E.; Pramod, K.; Emrick, T.; Gilardi, R."Building with Cubane-1,4-diyl. Synthesis of Aryl-Substituted Cubanes, p-[n]Cubyls, and Cubane-Separated Bis(arenes)." *Journal of the American Chemical Society* **121**, 4111-23 (1999).
6. Reichert, V.R.; Mathias, L.J. "Expanded Tetrahedral Molecules from 1,3,5,7-Tetraphenyladamantane." *Macromolecules,* **27**, 7015-23 (1994).
7. Reichert, V.R.; Mathias, L.J. "Highly Cross-Linked Polymers Based on Acetylene Derivatives of Tetraphenyladamantane." *Macromolecules,* **27**, 7030-4 (1994).
8. Lee, M.W.; Farha, O.K. Hawthorne, M.F.; Hansch, C.H. "Alkoxy Derivatives of Dodecaborate : Discrete Nanomolecular Ions with Tunable Pseudometallic Properties." *Angewandte Chemie, International Edition in English* **46**, 3018 – 3022 (2007).
9. Farha, O. K.; Julius, R. L.; Lee, M. W.; Huertas, R. E.; Knobler, C. B.; Hawthorne, M. F. Synthesis of Stable Dodecaalkoxy Derivatives of hypercloso-$B_{12}H_{12}$. *Journal of the American Chemical Society* **127**, 18243–51 (2005).
10. Sanchez, C.; de A.A. Soler-Illia, G.J.; Ribot, F.; Lalot, T.; Mayer, C.R.; Cabuil, V. "Designed Hybrid Organic-Inorganic Nanocomposites from Functional Nanobuilding Blocks," *Chemistry of Materials*, **13**, 3061-8 (2001).
11. Mellot-Draznieks, C.; Girard, S.; Ferey, G. "Novel Inorganic Frameworks Constructed from Double-Four-Ring (D4R) Units: Computational Design, Structures, and Lattice Energies of Silicate, Aluminophosphate, and Gallophosphate Candidates." *Journal of the American Chemical Society* **124**, 15326-35 (2002).
12. Morris, R.E. "Modular materials from zeolite-like building blocks." *Journal of Materials Chemistry* **15**, 931-8 (2005).
13. Laine, R. M. "Nanobuilding blocks based on the $[OSiO_{1.5}]_x$ (x = 6, 8, 10) silsesquioxanes." *Journal of Materials Chemistry* **15**, 3725–44 (2005).

14. Brown, J.F. Jr.; Vogt, L.H.; Prescott, P.I. "Preparation and Characterization of the Lower Equilibrated Phenylsilsesquioxanes." *Journal of the American Chemical Society* **86**, 1120-5 (1964).

15. Sulaiman, Santy. unpublished results.

16. Rathore, R.; Burns, C.L. "Preparation of Hexakis(4-Bromophenyl)Benzene." *Organic Syntheses* **82**, 30 (2002).

17. Wu, J.; Watson, M.D.; Zhang, L.; Wang, Z.; Mullen, K. "Hexakis(4-iodophenyl)-peri-hexabenzocoronene- A Versatile Building Block for Highly Ordered Discotic Liquid Crystalline Materials." *Journal of the American Chemical Society* **126**, 177-86 (2004).

18. Guo, W.; Galoppini, E.; Gilardi, R.; Rydja, G.I.; Chen, Y.-H. "Weak Intermolecular Interactions in the Crystal Structures of Molecules with Tetrahedral Symmetry: Diamondoid Nets and Other Motifs." *Crystal Growth & Design* **1**, 231-7 (2001).

19. Reichert, V.R.; Mathias, L.J. "Expanded Tetrahedral Molecules from 1,3,5,7-Tetraphenyladamantane." *Macromolecules,* **27**, 7015-23 (1994).

20. Negishi, E.; Anastasia, L. "Palladium-Catalyzed Alkynylation." *Chemical Reviews* **103**, 1979–2017 (2003).

21. Miyaura, N.; Suzuki, A. "Palladium-Catalyzed Cross-Coupling Reactions of Organoboron Compounds." *Chemical Reviews* **95**, 2457-83 (1995).

22. Nicolaou, K.C.; Bulger, P.G.; Sarlah, D. "Palladium-Catalyzed Cross-Coupling Reactions in Total Synthesis." *Angewandte Chemie, International Edition in English* **44**, 4442-89 (2005).

23. Barrios-Landeros, F.; Carrow, B.P.; Hartwig, J.F. "Effect of Ligand Steric Properties and Halide Identity on the Mechanism for Oxidative Addition of Haloarenes to Trialkylphosphine Pd(0) Complexes." *Journal of the American Chemical Society* 131, 8141–54 (2009).

24. Hartwig, J.F.; Kawatsura, M.; Hauck, S. I.; Shaughnessy, K.H.; Alcazar-Roman, L.M. "Room-Temperature Palladium-Catalyzed Amination of Aryl Bromides and Chlorides and Extended Scope of Aromatic C-N Bond Formation with a Commercial Ligand." *Journal of Organic Chemistry* **64**, 5575-80 (1999).

25. Vorogushin, A.V; Huang, X.; Buchwald, S.L. "Use of Tunable Ligands Allows for Intermolecular Pd-Catalyzed C-O Bond Formation." *Journal of the American Chemical Society* 127, 8146-9 (2005).

26. Balthazor, T.M.; Grabiak, R.C. "Nickel-Catalyzed Arbuzov Reaction: Mechanistic Observations." *Journal of Organic Chemistry* **45**, 5425-6 (1980).

27. Fernandez-Rodriguez, M.A.; Hartwig, J.F. "A General, Efficient, and Functional-Group-Tolerant Catalyst System for the Palladium-Catalyzed Thioetherification of Aryl Bromides and Iodides." *Journal of Organic Chemistry* **74**, 1663-72 (2009).

28. Babudri, F.; Farinola, G.M.; Naso, F. "Synthesis of conjugated oligomers and polymers: the organometallic way." *Journal of Materials Chemistry* **14**, 11–34 (2004).

29. Wolfe, J.P.; Buchwald, S.L. "Room Temperature Catalytic Amination of Aryl Iodides." *Journal of Organic Chemistry*. **62**, 6066-8 (1997).

30. Morrison, R.T.; Boyd, R.N. *Organic Chemistry, 1966, 2nd ed*.

31. Galli, C. "Aromatic Iodination: Evidence of reaction Intermediate and of the *sigma*-Complex Character of the Transition State." *Journal of Organic Chemistry*, **56**,3238-45 (1991).

32. Brick, C.M. Tamaki, R.; Kim, S.-G.; Asuncion, M.Z.; Roll, M.; Nemoto, T.; Ouchi, Y.; Chujo Y.; Laine, R.M. "Spherical, Polyfunctional Molecules Using Poly(bromophenylsilsesquioxane)s as Nanoconstruction Sites." *Macromolecules* **38**, 4655-60 (2005).

33. He, C.B.; Xiao, Y.; Huang, J.C.; Lin, T.T.; Mya, K.Y.; Zhang, X.H. "Highly efficient luminescent organic clusters with quantum dot-like properties." *Journal of the American Chemical Society* **126**, 7792-3 (2004).

34. Erben, C.; Grade, H.; Goddard, G.D. "Bromination of octaphenylsilsesquioxane." *Silicon Chemistry* (2006). DOI: 10.1007/s11201-005-9000-5.

35. Takahashi, K. Unpublished results.

36. Feher, F.J.; Budzichowski, T.A. "Syntheses of highly-functionalized polyhedral oligosilsesquioxanes." *Journal of Organometallic Chemistry*, **379**, 33-40 (1989).

37. Park, S.S.; Xiao, C.; Hagelberg, F.; Hossain, D.; Pittman, C.U. Jr.; Saebo, S. "Endohedral and Exohedral Complexes of Polyhedral Double Four-Membered-Ring (D4R) Units with Atomic and Ionic Impurities." *Journal of Physical Chemistry A* **108**, 11260-72 (2004).

38. Spectral Database for Organic Compounds, SDBS. National Institute of Advanced Industrial Science and Technology (AIST), Japan. http://riodb01.ibase.aist.go.jp/sdbs/cgi-bin/cre_index.cgi?lang=eng

39. Iqbal, Z.; Lyubimtsev, A.; Hanack, M. "Synthesis of Phthalonitriles Using a Palladium Catalyst Synthesis of Phthalonitriles." Synlett 2009, 2287-90.

40. PLATON Reference : A.L.Spek (2008) PLATON, A Multipurpose Crystallographic Tool, Utrecht University, Utrecht, The Netherlands.

Chapter IV

Hexaarylbenzene and Graphene Nano-Building Blocks

Introduction

There is strong motivation to develop modular, synthetically flexible precursors, or nano-building blocks, for the production of nano-structured materials.[1-3] In principle this would allow the bulk properties of a material to be tailored through the judicious chemical modification of the constituent nano-building blocks.[2-4] Chapter 1 discusses possible candidates for this type of tool, and the merits of octaphenylsilsesquioxane (OPS) for such a role.[3-5]

We have previously discussed the significant body of work exploring the application of cubic silsesquioxane nano-building blocks for producing materials with tunable properties.[6-20] Chapters 2 and 3 describe the iodination and bromination of OPS in order to provide the necessary peripheral functionality. We will now discuss the synthesis of OPS-based nano-building blocks for potential applications in the area of organic opto-electronics.[21-23] We will briefly introduce conjugated organic molecules then describe our efforts to develop silsesquioxane (SQ) hybrid electronic materials can supplement or surpass the capabilities of their wholly organic counterparts.[24]

Organic electronics is a flourishing area of research built on the manipulation and delocalization of electron orbitals in small molecules, oligomers, and polymers to alter the electronic properties of the resulting materials.[25-31] In broad terms, this delocalization

is the extension of the π-orbital wavefunctions over multiple conjugated bonds.[25] The benzene ring is a primary element in organic semiconductors, including oligo- and poly-phenylenes,[27,28] phenylenevinylenes,[27,29] and phenyleneethynylenes (Figure **4.1**).[30] In addition, these π-orbitals allow for intermolecular charge transport through π-π stacking of adjacent molecules, oligomers or polymers.[31]

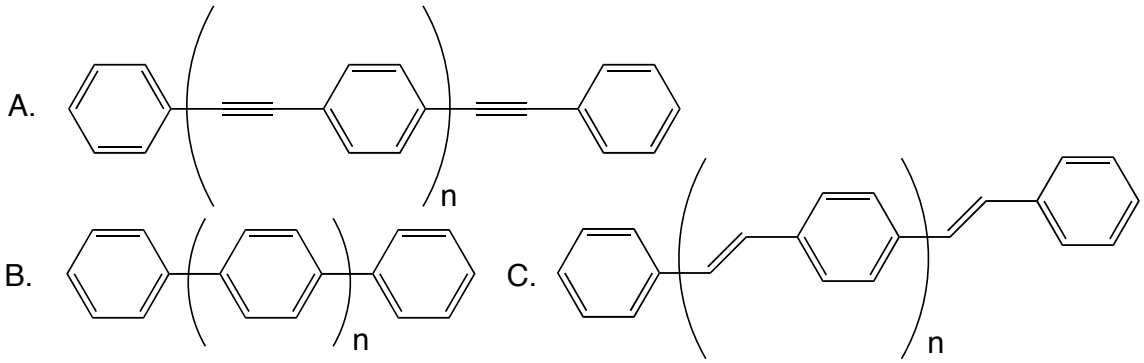

Figure 4.1. Conjugated polymers A. poly(*p*-phenyleneethynylene), B. poly(*p*-phenylene), C. poly(*p*-phenylenevinylene).

Polyphenylene systems have been explored extensively over the past fifty years, as demonstrated by the early review by Ried and Freitag[32] and the more recent review by Berresheim et al.[33] Early work conducted by Kovacic et al investigated the polymerization of benzene using aluminum trichloride as Lewis acid and cupric chloride as an oxidant.[34] These researchers also found that iron trichloride could be substituted as oxidant and Lewis acid catalyst.[35,36] Kovacic et al found that protons were stripped from the *para* position, and a new carbon-carbon bond was formed between two benzene molecules.[34]

The use of Diels-Alder condensation chemistry as a route for the synthesis of hexaaryl benzene systems was recognized by many,[32] and recently Pascal and Müllen have used this chemistry to access very large polyphenylene systems. Pascal explored

polyphenylenes consisting of nearly 300 carbon atoms and determined their crystal structures.[37-41] Müllen et al demonstrated the use of this chemistry to divergently synthesize polyphenylene dendrimers with molecular weights greater than 1 million Da.[42-45]

Hexa-arylbenzenes further serve as precursors for the synthesis of graphene-type or polynuclear aromatic hydrocarbon (PAH) compounds through an intramolecular dehydrogenative cyclization (Scholl reaction).[46] In the case of hexaphenylbenzene, Scholl cyclization gives the planar hexa-*peri*-benzocoronene and has been the subject of extensive research by Müllen et al (Scheme **1**).[45-48]

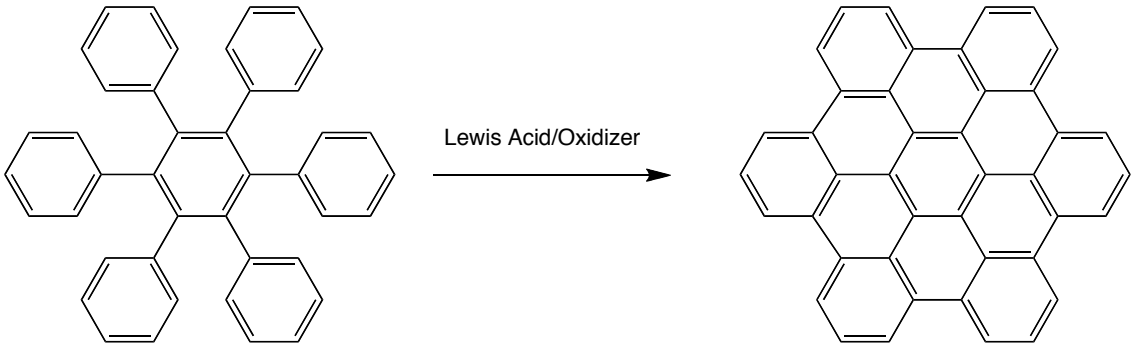

Scheme 4.1 Scholl cyclization of hexaphenylbenzene (HPB) to form hexa-*peri*-benzocoronene (HBC).

Carbon allotropes are of perennial interest, and the latest evolution in this trend is the synthesis and modification of graphenes.[21] The planar configuration allows for extensive π electron delocalization, giving rise to electronic[22] and magnetic[23] properties of great interest for advanced integrated circuits.[54-56]

The Scholl reaction has been studied extensively experimentally[28,34-36,46-48,56-63] and more recently, theoretically.[56,57] Computational analysis suggests that HPB reacts rapidly

in an *intra*-molecular fashion to yield hexa-*peri*-benzocoronene (HBC),[57,58] though Müllen has reported the successful isolation of partially cyclized hexaarylbenzenes.[46,57,58] A Lewis acid and oxidant drives the reaction and a multitude of reagents can be used including: $AlCl_3/CuCl_2$, $FeCl_3$, $MoCl_5$, $VOCl_3$, and DDQ/protic acid.[28,34-36,46-48,56-63]

We have pursued reaction Scheme **4.2** below to synthesize Octagraphene, a cubic silsesquioxane with a periphery of eight hexa-*peri*-benzocoronene moieties. The Sonogashira coupling of the aryl iodide with a terminal acetylene was previously reported by Asuncion et al.[64] This method has been modified to provide the crystalline, ethynyl functionalized OPS derivatives. Diels-Alder condensation of these derivatives with the commercially available tetraphenylcyclopentadienone, as well as the tetra-*p*-tolylcyclopentadienone, will be discussed. Finally the cyclization of these octa(hexaarylbenzene)silsesquioxanes by $FeCl_3/CH_3NO_2$ will be discussed.

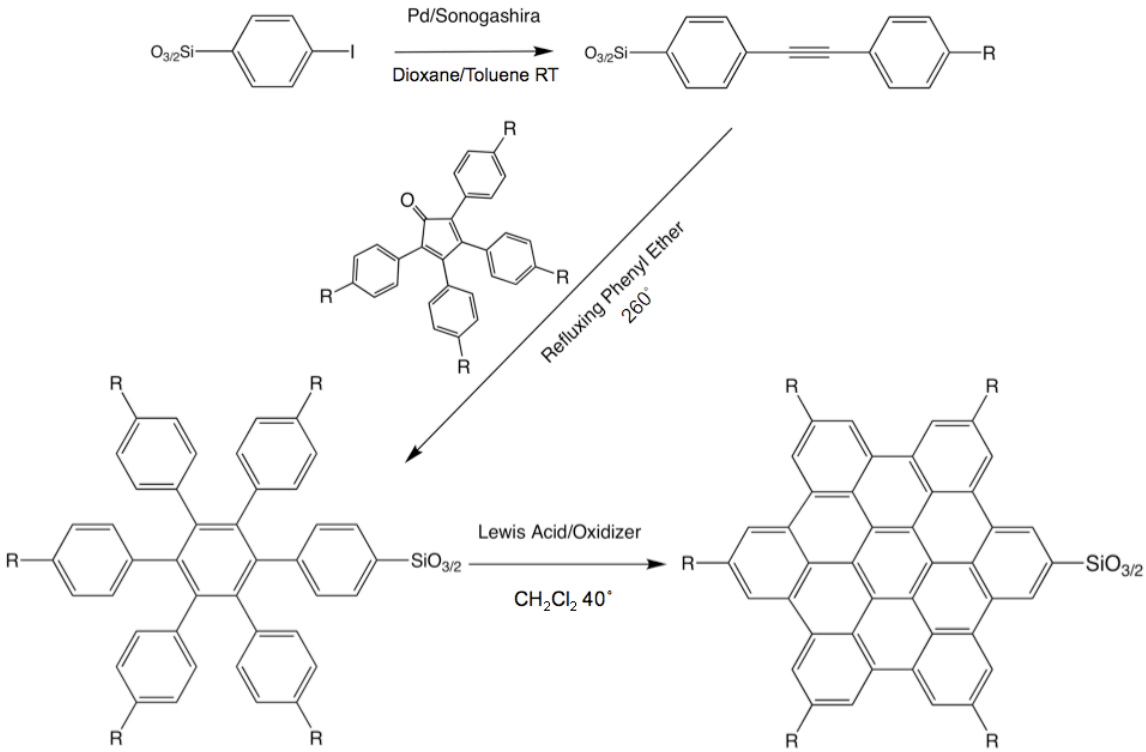

Scheme 4.2 Proposed synthesis for Octagraphene.

Results and Discussion

Sonogashira Coupling

The first required synthetic step is the Sonogashira coupling shown in Scheme **4.3** below. Pd(*t*-$Bu_3P)_2$/Pd_2DBA_3 is used as the palladium catalyst, following the Pd catalyzed functionalization of the bromophenylsilsesquioxanes by Brick et al.[65] $CuI(PPh_3)_3$ is used instead of CuI to reduce heterogeneity in the reaction.[66] The reaction is conducted preferably at RT, but low catalyst activity may require heating to 40-60°C. The reaction progress is readily monitored by MALDI-TOF analysis of aliquots precipitated into cold methanol.

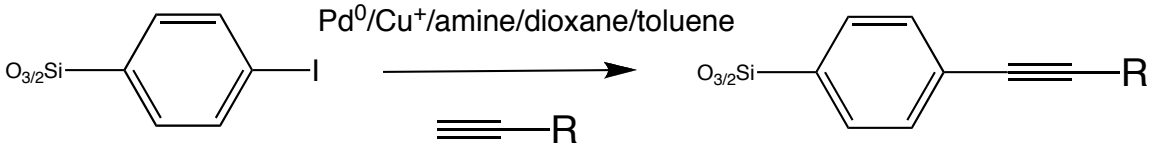

R=phenyl, *p*-tolyl, trimethylsilyl

Scheme 4.3 Sonogashira coupling of terminal acetylene and iodophenylsilsesquioxane.

Table 4.1. Characterization of ethynyl derivatives

Sample	Yield	MW calculated (Ag^+ ion)	MW MALDI-TOF Found (% Intensity)	Ceramic Yield (Theor.)	Ceramic Yield (Found)
Phenylacetylene (**1a**)	67%	1942.35	1941.7 (100%)	26 %	25 %
Tolylacetylene (**1b**)	91%	2054.57	2053.7 (100%)	23 %	23 %
TMSacetylene (**1c**)	85%	1911.08	1909.8 (100%)		

Once the reaction is complete, the reaction mixture is precipitated into cold methanol and filtered. The crude material is redissolved in toluene and treated with L-acetylcysteine dissolved in tetrahydrofuran to remove residual palladium.[67] After sitting

overnight at room temperature, the suspension is filtered and reprecipitated into cold methanol. Recrystallization for purification or the production of single crystals suitable for X-ray diffraction is effected by slow cooling of hot, saturated *m*-xylene or ethyl acetate solutions.

Figure **4.2** shows the ^{1}H NMR spectrum of the phenylacetylene derivative, **1a**. The nine aromatic protons are accounted for through the integration of the five overlapping multiplets, accounting for nine protons. The largest downfield shift is 7.71 ppm, which is between the predictions of 7.6 and 8.2 ppm for the CF_3 and NO_2 substituted diphenylacetylene derivatives calculated using the "ChemBioDraw Ultra" software package.[68] One interpretation of this data is that the silsequioxane cage is slightly more electron withdrawing than a CF_3 group.

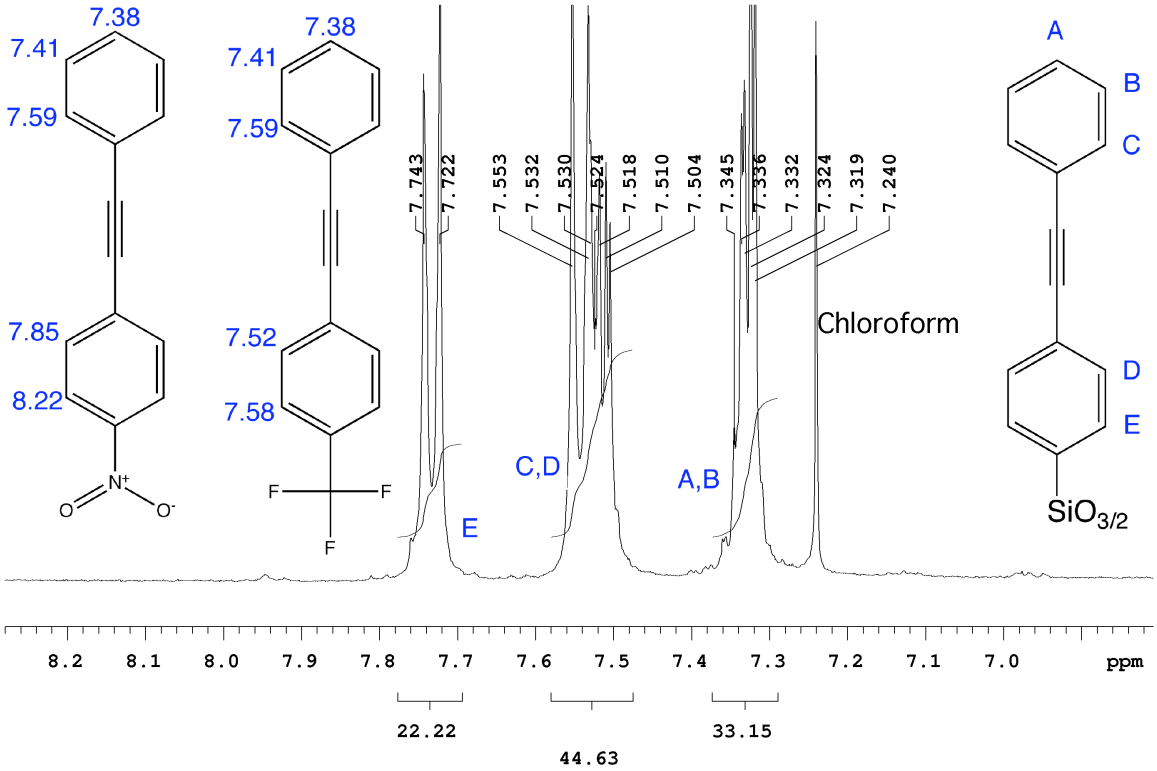

Figure 4.2. ^{1}H NMR spectrum of the phenylacetylene derivative, **1a** in $CDCl_3$.[68]

Figure **4.3** shows the ^{13}C NMR spectrum of **1a**. Eight peaks are detected in the aromatic region, representing the eight different carbon species. The larger four peaks correspond to carbons bonded to hydrogen, which are enhanced by proton decoupling. The largest downfield shift is 134 ppm, which is between the predictions of 133 and 148 ppm for the CF_3 and NO_2 substituted diphenylacetylene derivatives.[68] Again, one interpretation of this data is that the silsesquioxane cage is slightly more electron withdrawing than a CF_3 group.

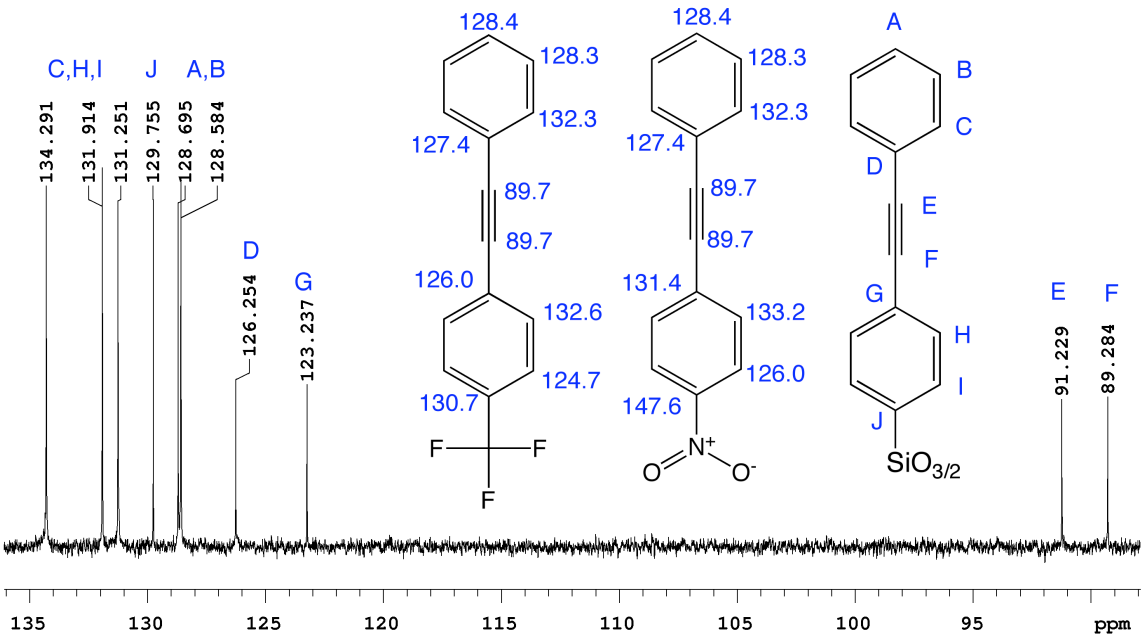

Figure 4.3. ^{13}C NMR spectrum of the phenylacetylene derivative, **1a** in $CDCl_3$.[68]

Figure **4.4** shows the MALDI-TOF spectrum of **1a**. The large peak corresponds to the single silver adduct of the octameric product. The small peak at 1832.8 Da corresponds to the octamer without a silver adduct and the small peak at 1840.7 Da represents the silsesquioxane cage compound with seven diphenylacetylene corners and one phenyl corner.

X-ray quality crystals of octa(diphenylacetylene)silsesquioxane, **1a**, were grown by slow cooling of hot, saturated *m*-xylene solutions, as described in the Experimental (Chapter 7). Single crystal X-ray diffraction analysis revealed that **1a** crystallizes in the triclinic space group P-1 (Figure **4.5)**. The structure was refined to an R-factor of 5.5 %. Additional crystallographic details are provided in Table **4.2**, below.

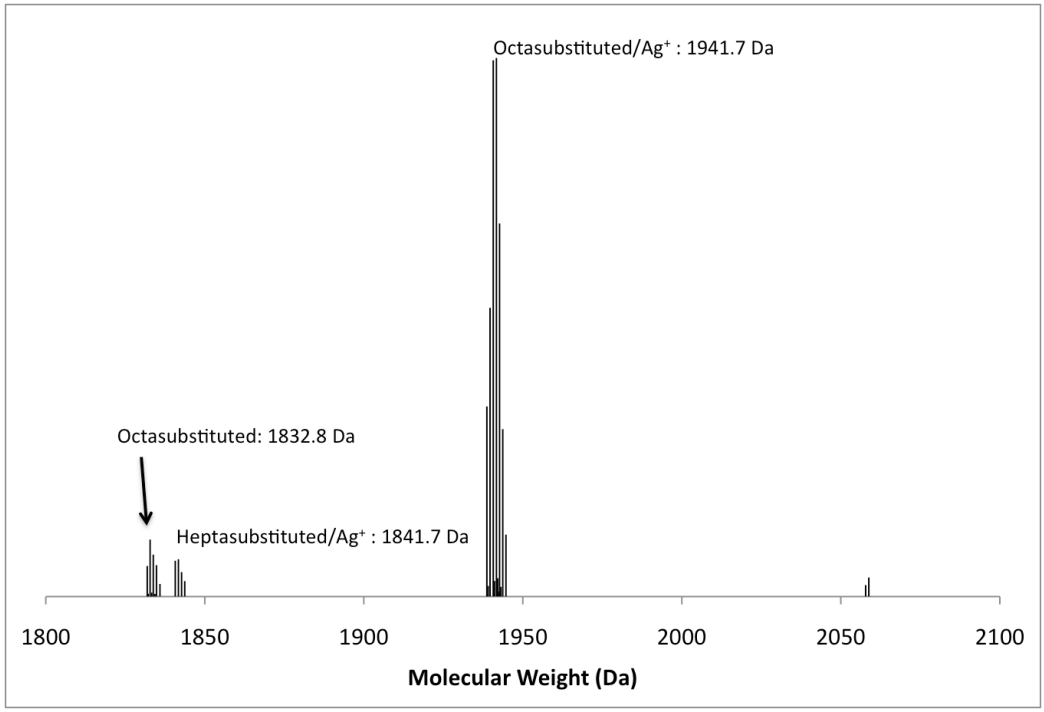

Figure 4.4. MALDI-TOF spectrum of the phenylacetylene derivative, **1a** (Ag^+/Dithranol).

Table 4.2. Crystal Structure Refinement Data for **1a** • 5 *m*-xylene

	1a • 5 *m*-xylene
Space Group	P-1, triclinic
Unit Cell Dimensions	a= 14.4668(9) Å b= 15.5858(10) Å c= 15.9361(10) Å
	α = 95.443(1)˚ β= 92.173(1)˚ γ= 115.487(1)˚
Unit Cell Volume	3216.5(4) $Å^3$
Z	1
R-factor	5.5 % (10.0 %)*

* Before use of SQUEEZE to account for disordered solvent

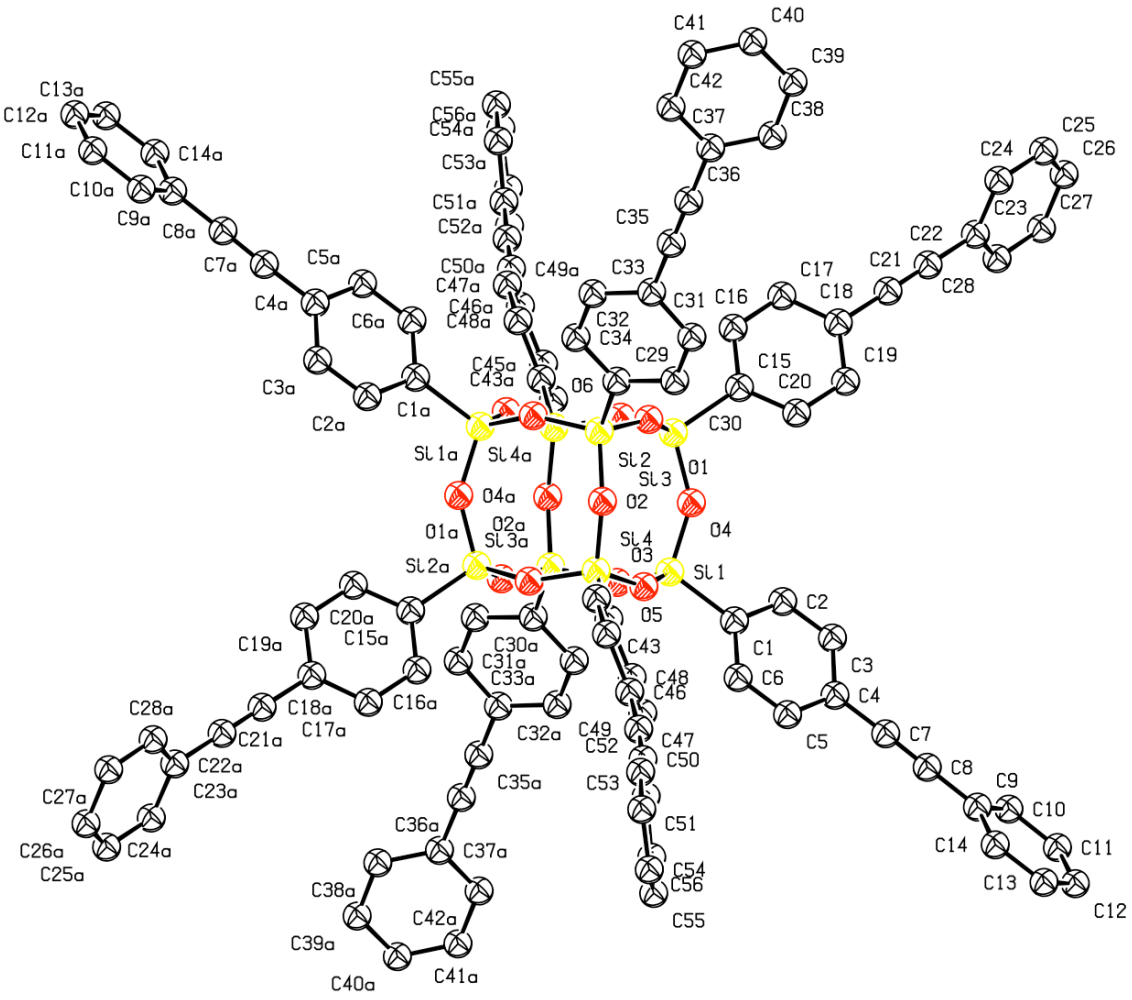

Figure 4.5. 50 % thermal ellipsoid plots of **1a** • 5 *m*-xylene. Hydrogen atoms and toluene solvates are omitted for clarity. Full XRD data can be found in Appendix 8.

Figure **4.6** shows the ^{1}H NMR spectra of the tolylacetylene derivative, **1b**. The eight aromatic protons are detected as four well separated multiplets. The methyl protons are found at 2.39 ppm. The integration of the methyl protons to the aromatic protons is 28%, close to the theoretical 27 % for the symmetric compound. Figure **4.7** shows the ^{13}C NMR spectrum of **1b**. Eight peaks are detected in the aromatic region, representing the eight different carbon species.

Figure **4.8** shows the MALDI-TOF spectrum of **1a**. The large peak corresponds to the single silver adduct of the octameric product. The small peak at 1944.9 Da corresponds to the octamer without a silver adduct. The small peak at 1938.7 Da corresponds to the silsesquioxane cage compound with seven tolylphenylacetylene corners and one phenyl corner with a silver adduct. The small peak at 2053.7 Da indicates the silsesquioxane cage compound with eight tolylphenylacetylene corners and one corner with an additional tolylacetylene unit with a silver adduct.

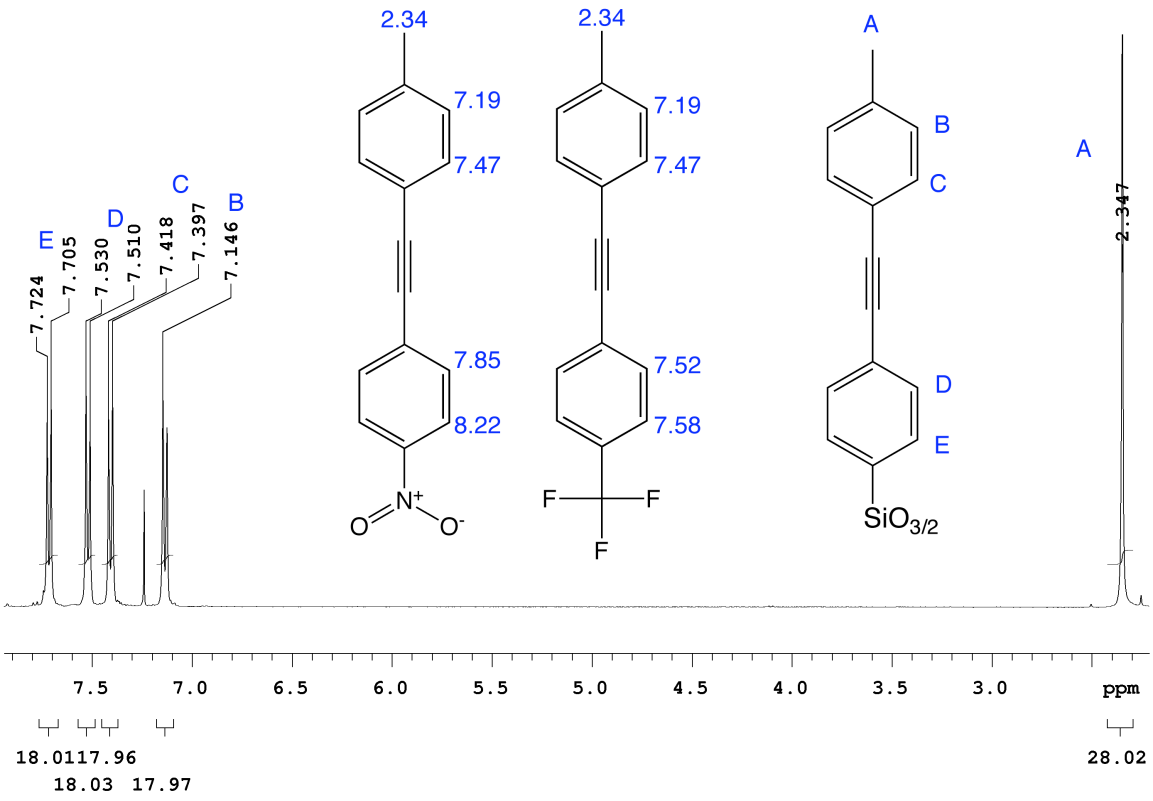

Figure 4.6. ^{1}H NMR spectrum of the tolylacetylene derivative, **1b** in $CDCl_3$.[68]

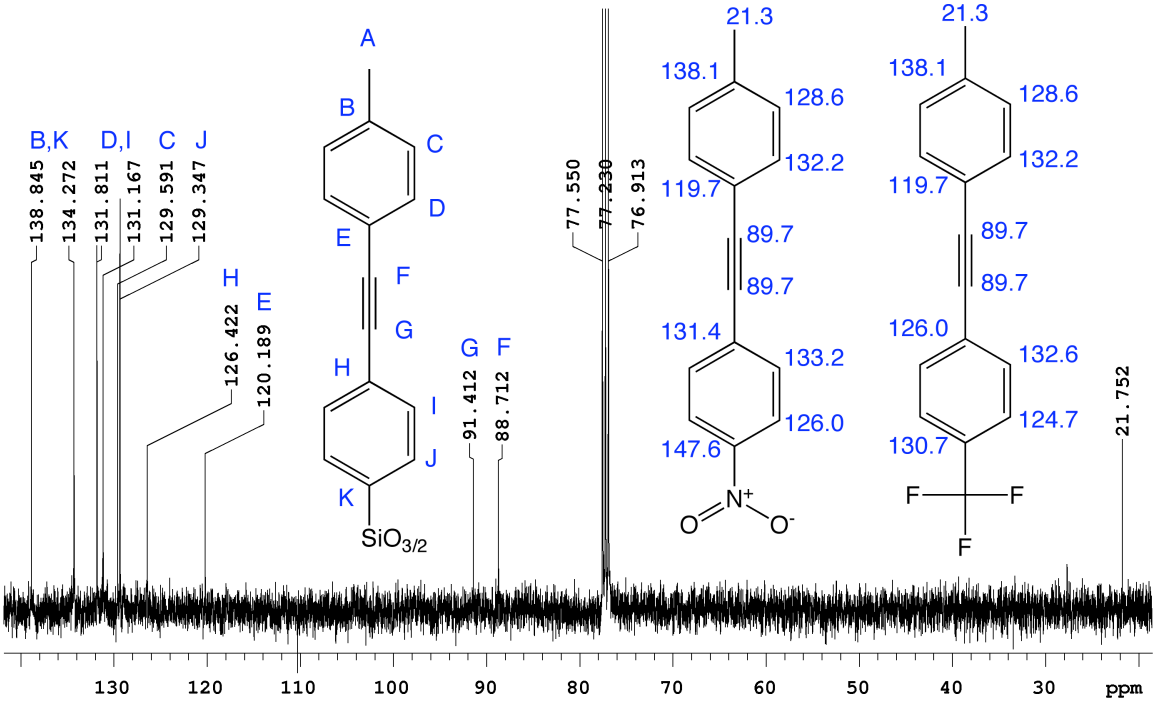

Figure 4.7. ^{13}C NMR spectrum of the tolylacetylene derivative, **1b** in $CDCl_3$.

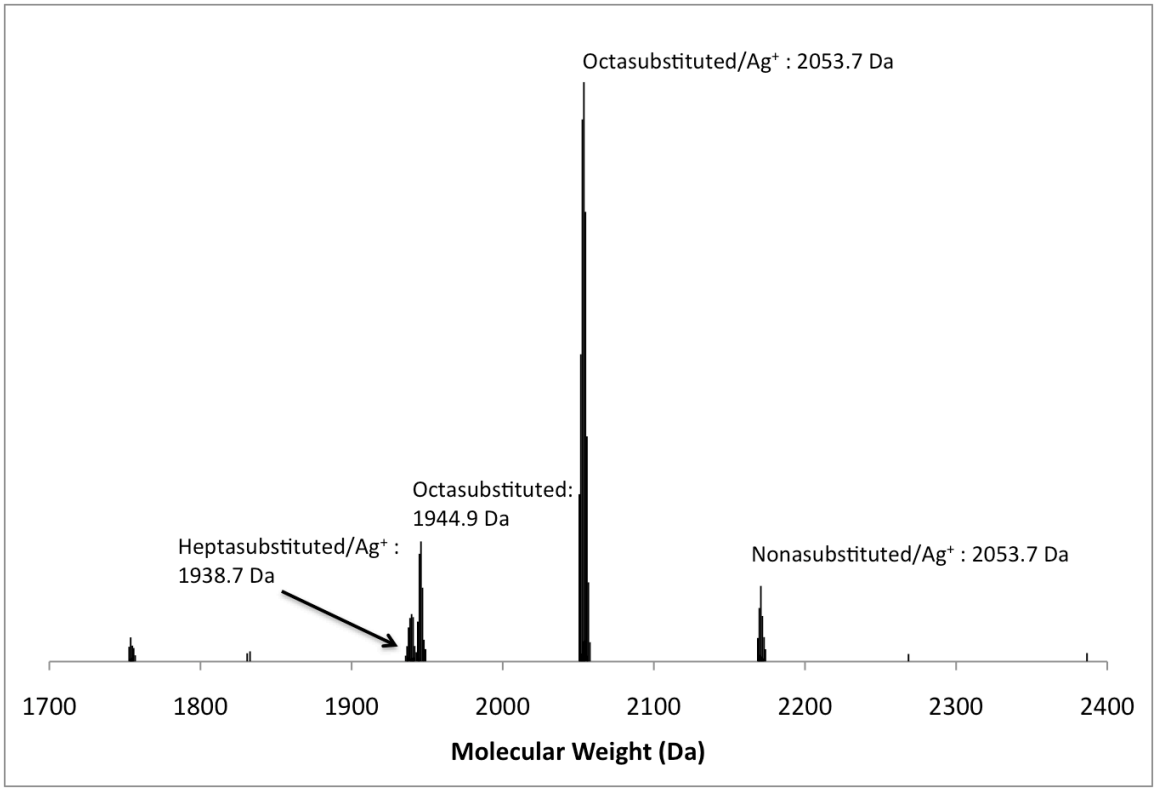

Figure 4.8. MALDI-TOF spectrum of the tolylacetylene derivative, **1b** (Ag^+/Dithranol).

Figure **4.9** shows the ^{1}H NMR spectra of the trimethylsilylacetylene derivative, **1c**. The four aromatic protons are detected as four well separated multiplets. The methyl protons are found at 0.4 ppm. The integration of the methyl protons to the aromatic protons is 69.2%, equal to the theoretical 69.2% for the symmetric compound.

Figure **4.10** shows the ^{13}C NMR spectrum of **1c**. As before, the visible peaks correspond to carbons bonded to hydrogen, which are enhanced by proton decoupling. The peak at 0.048 ppm corresponds the trimethylsilyl functional group. Figure **4.11** shows the MALDI-TOF spectrum of **1c**.

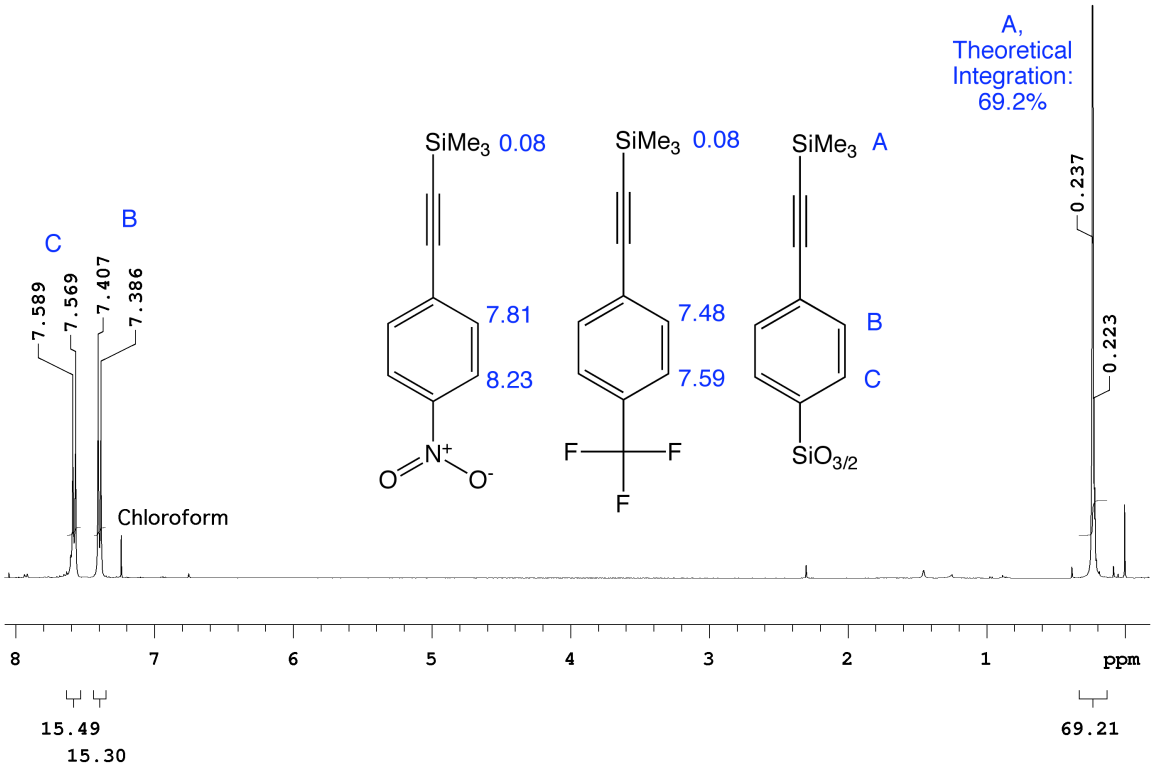

Figure 4.9 ^{1}H NMR spectrum of the trimethylsilylacetylene derivative, **1c** in $CS_2/CDCl_3$.[68]

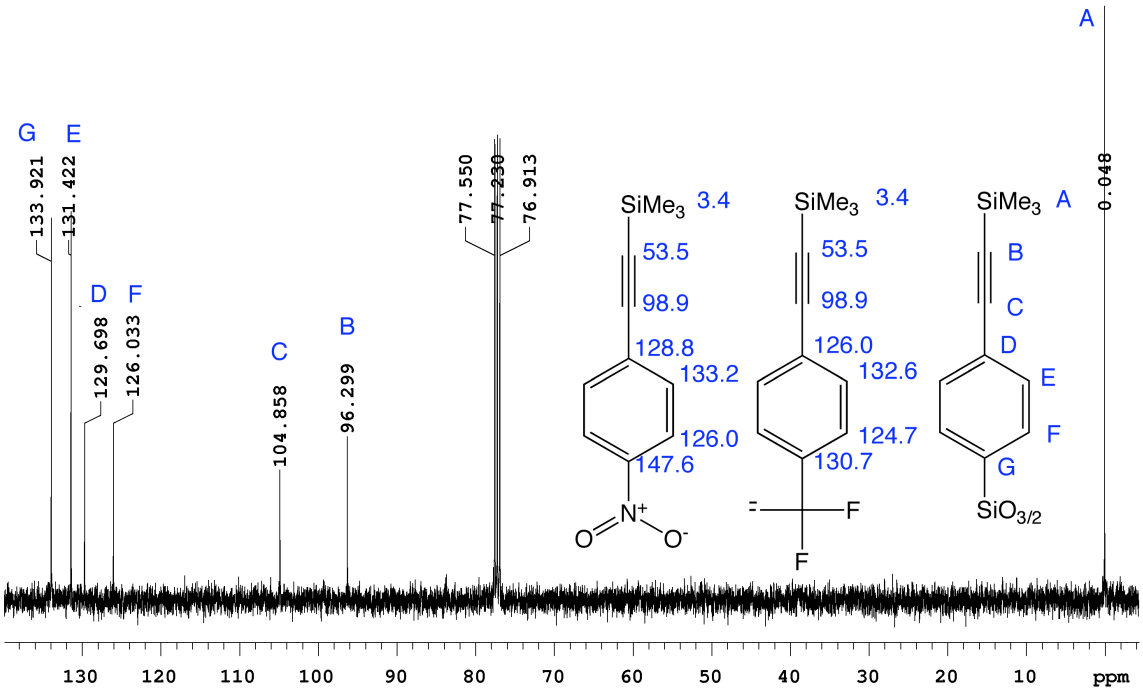

Figure 4.10. ^{13}C NMR spectrum of the trimethylsilylacetylene derivative, **1c** in $CS_2/CDCl_3$.

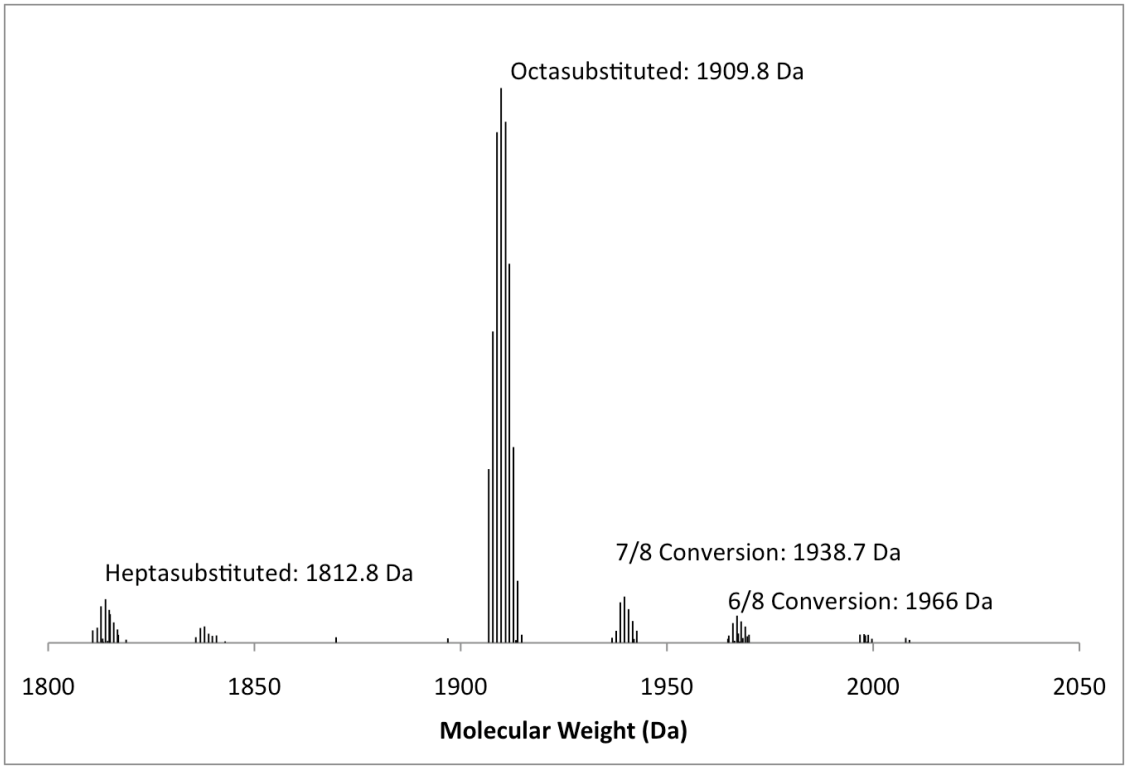

Figure 4.11. MALDI-TOF spectrum of the trimethylsilylacetylene derivative, **1c** (Ag^+/Dithranol).

Diels-Alder Condensation with Tetraarylcyclopentadienones

The Diels-Alder condensation of diphenylacetylene and tetraphenylcyclopentadienone (tetracyclone) to give hexaphenylbenzene (HPB) quantitatively is described in Williamson as a standard reaction for teaching Organic Chemistry.[69] The high reaction temperature required leads to the use of phenyl ether as solvent (B.P 260˚C).[32,33] Although tetraphenylcyclopentadienone is available commercially, to improve solubility in subsequent derivatives the permethylated 56 Aryl was synthesized via the condensation of the tolylacetylene derivative with the tetra(*p*-tolyl)cyclopentadienone. Tetra(*p*-tolyl)cyclopentadienone[70] was synthesized in two steps.

Scheme **4.4** shows the DMAP catalyzed condensation of p-tolylacetic acid by DCC was modified and used to synthesize the di-tolyl-acetone.[71] Initially reported by Bhandari and Ray, substituted phenylacetic acids may be condensed to form the diarylacetone derivative using dimethylaminopyridine (DMAP) and dicyclohexylcarboxydiimide (DCC).[69] Carboxylic acids are readily dehydrated by DCC in the absence of DMAP, producing dicyclohexyl urea and the corresponding carboxylic acid anhydride.[72] Therefore, the *p*-tolylacetic acid was mixed with DMAP catalyst prior to the addition of DCC. Additionally, the ratio of molar equivalents of DCC added to arylacetic acid was reduced from 1:1 to 1:2, to reflect the stoichiometry of the proposed reaction.

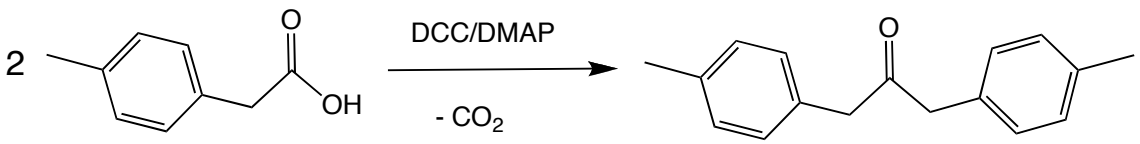

Scheme 4.4 Synthesis of di-*p*-tolylacetone.

With these modifications (see Experimental, Chapter 7), the reaction was conducted and ^{1}H NMR of the recrystallized product is shown in Figure **4.12.** The spectrum does not show evidence of solvent, DCC, DMAP or tolylacetic acid indicating the di(*p*-tolyl)acetone to be essentially free from precursor materials.

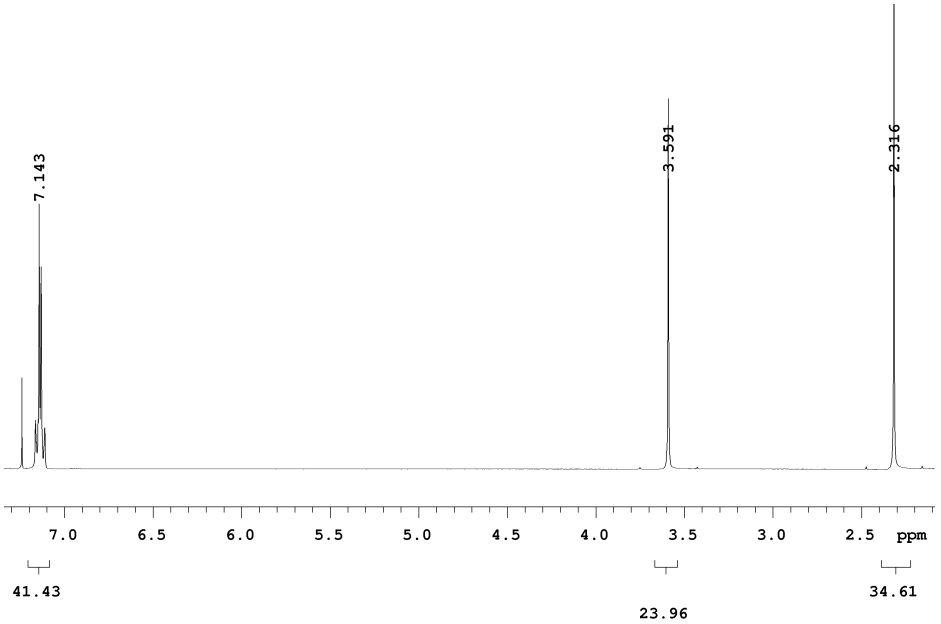

Figure 4.12 ^{1}H NMR of di(*p*-tolyl)acetone in $CDCl_3$.

Modifying the published preparation for tetraphenylcyclopentadieneone,[73] the recrystallized di(*p*-tolyl)acetone was condensed with the commercially available 4,4'-dimethylbenzil in refluxing ethanol with catalytic KOH (Scheme **4.5**). The product was recrystallized twice and washed repeatedly with methanol until all traces of base were eliminated.

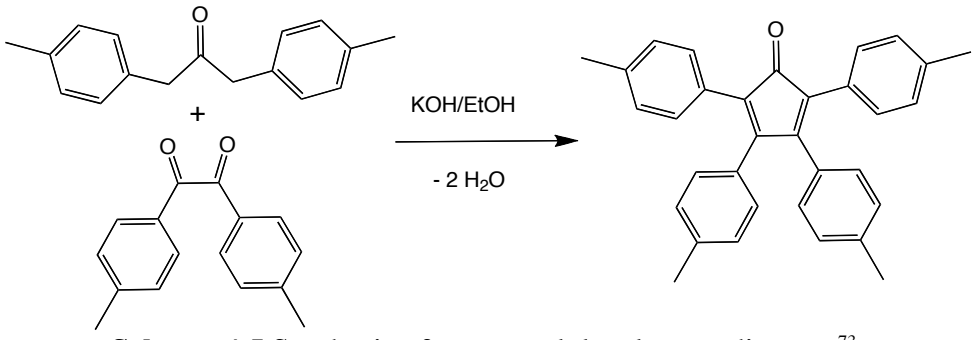

Scheme 4.5 Synthesis of tetra-*p*-tolylcyclopentadienone.[73]

The as-synthesized tetra(*p*-tolyl)cyclopentadienone is essentially pure by ^{1}H NMR, but may be recrystallized by the addition of an equivalent volume of methanol to a hot, saturated toluene solution of the tetracyclone. The ^{1}H NMR spectrum of the product is shown in Figure **4.13**.

The condensation of the aryl ethynyl substituted octaphenylsilsesquioxane with the respective tetraarylcyclopentadienone was conducted in refluxing phenyl ether, as shown in Scheme **4.1**. In each case, the reaction was found to be complete after 24 h. Condensation of **1a** with tetraphenylcyclopentadienone gives the unsubstituted octa(hexaphenylbenzene)silsesquioxane (or 56 Aryl). Following precipitation of the reaction mixture into cold methanol, recrystallization is readily effected by slow cooling of hot, saturated toluene or mesitylene solutions.

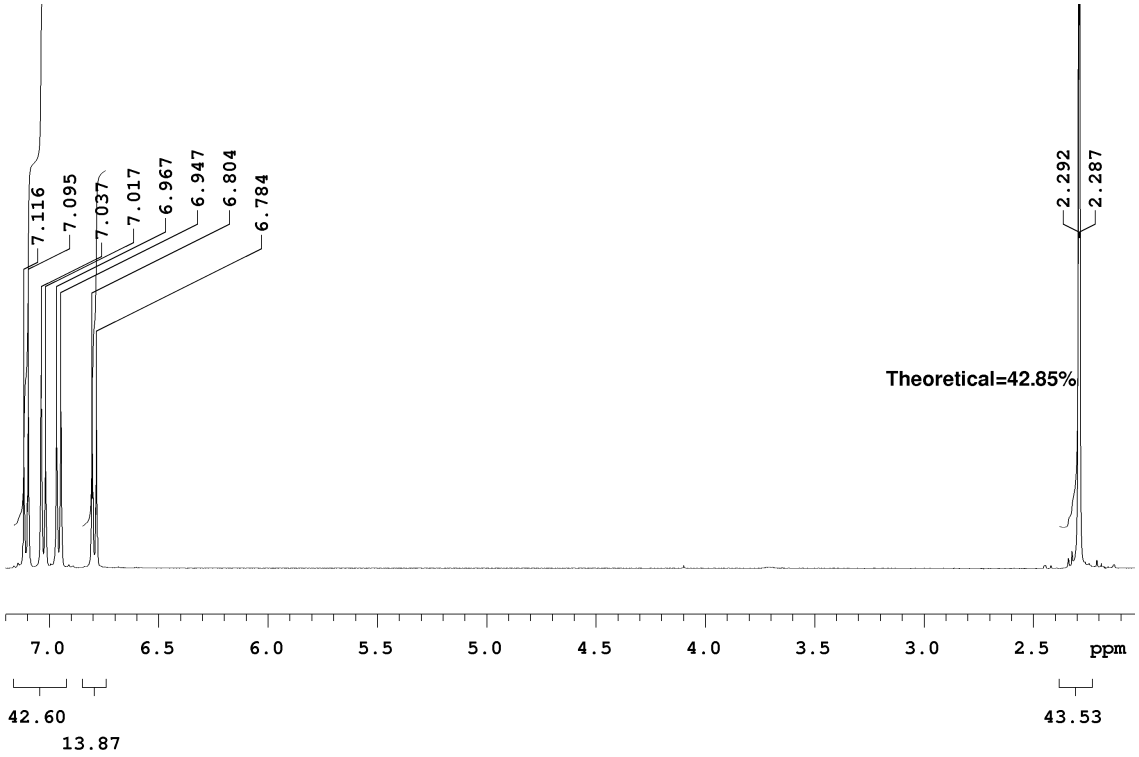

Figure 4.13 ^{1}H NMR of tetra(*p*-tolylcyclopentadienone in $CDCl_3$.

Figure **4.14** shows the ^{1}H spectrum of the 56 Aryl compound. The aromatic resonance are found between 6 and 7 ppm, consistent with the single proton resonance of hexaphenylbenzene at 6.8 ppm.[74] The breadth of the peaks is may be due to a reduced tumbling rate in solution, which leads to line broadening. The presence of two peaks indicates the presence of two distinct chemical environments. Presumably this is due to the interaction of the silsesquioxane cage with adjacent aromatic rings.

Figure **4.15** shows the ^{13}C spectrum of 56 Aryl, with thirteen resolved peaks, which correspond well to the reported shifts: "δ 140.5, 140.2 (s, quaternary), 131.3, 126.4, 125.0 ppm (s, C_6H_5)".[74] The relatively narrow peaks suggest that a reduced tumbling rate may not account for the breadth of the ^{1}H NMR peaks. Figure **4.16** shows the MALDI-TOF spectrum of 56 Aryl, the symmetric octamer and hepta(hexaphenylbenzene)-monophenyloctasilsesquioxane to the left.

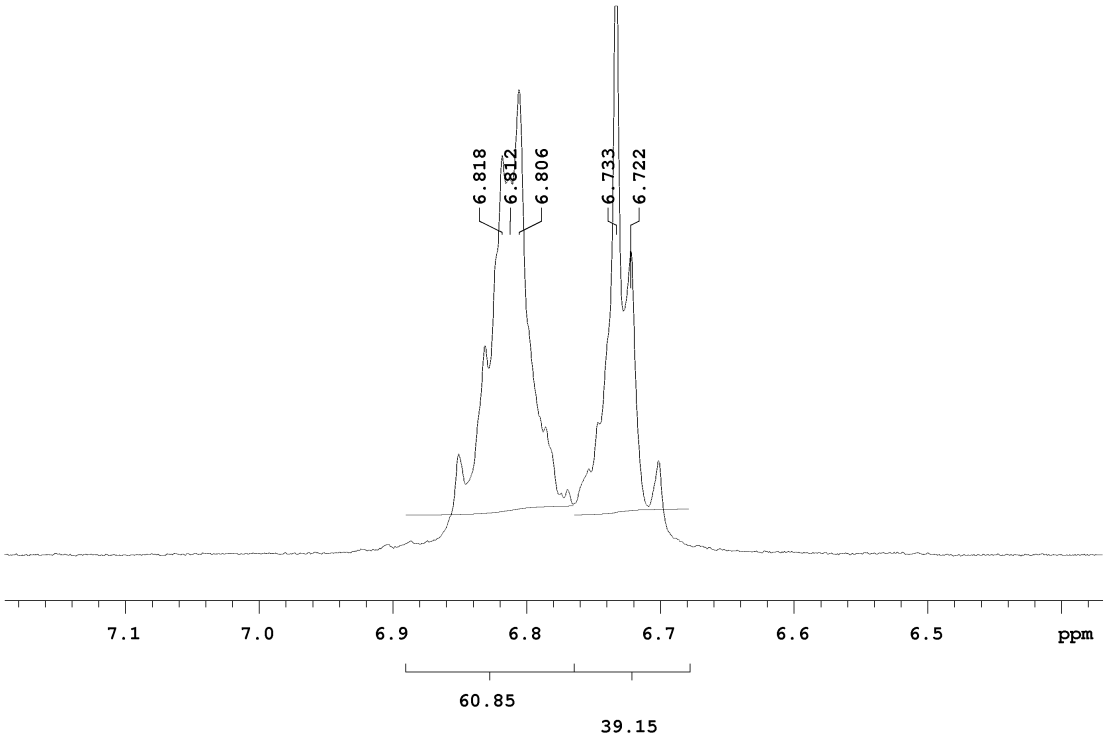

Figure 4.14 ^{1}H spectrum of 56 Aryl in $CDCl_3$.

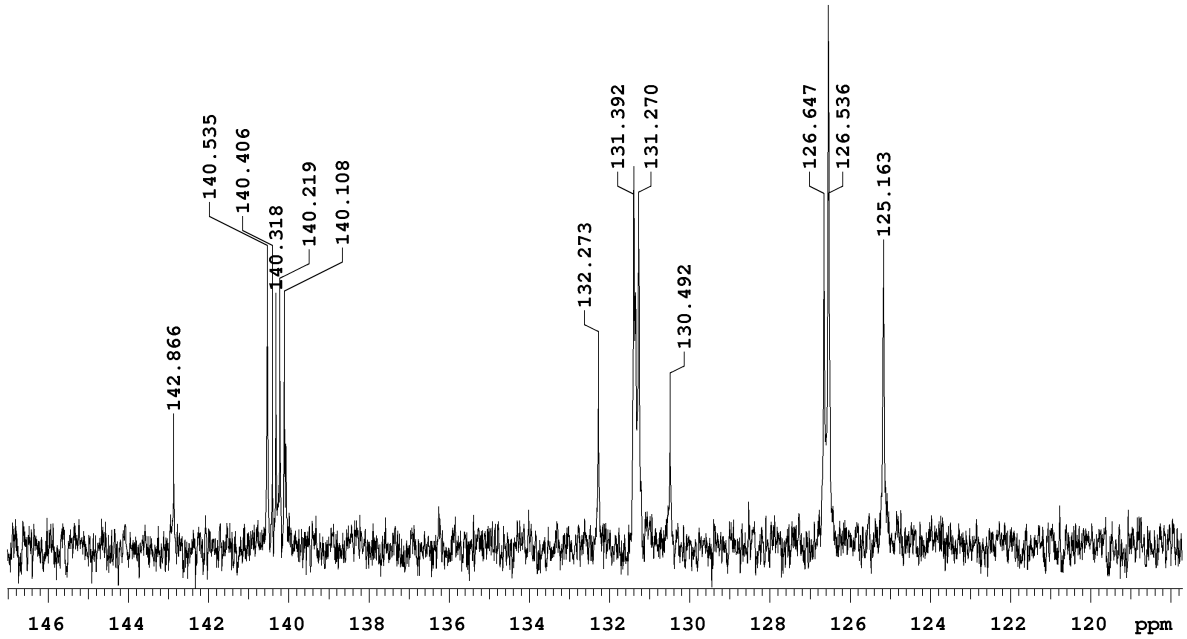

Figure 4.15 ^{13}C spectrum of the 56 Aryl in $CDCl_3$.

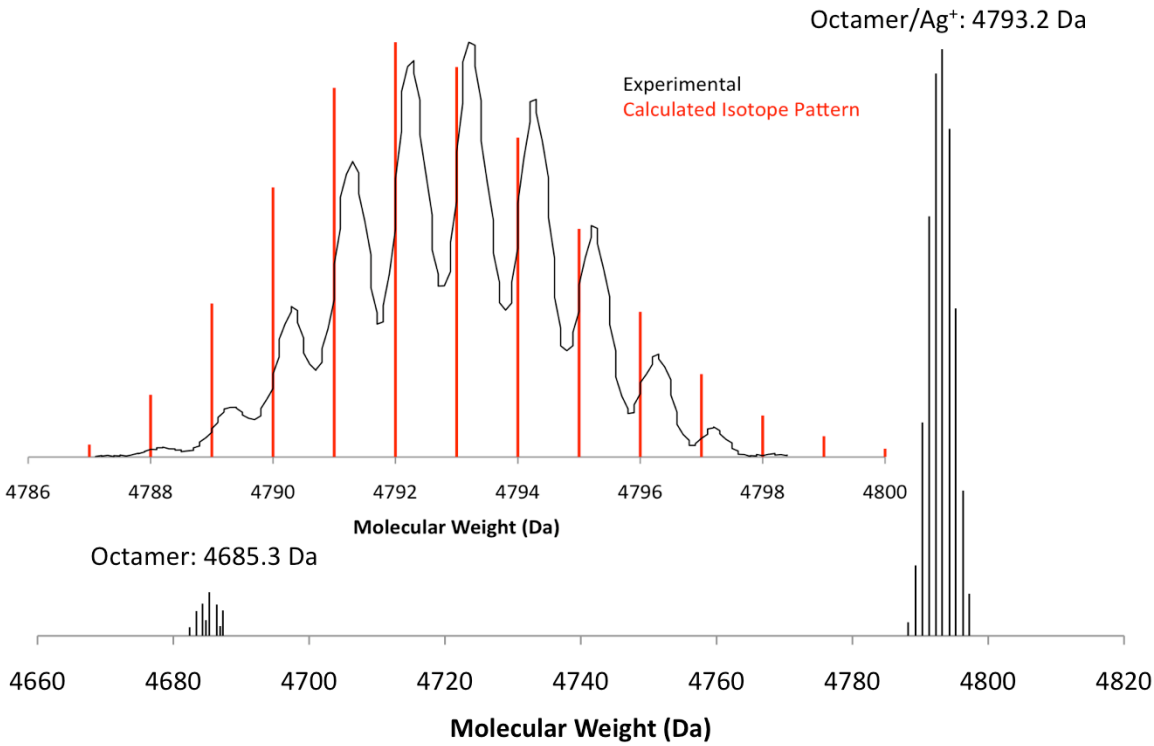

Figure 4.16 MALDI-TOF spectrum of the 56 Aryl(Ag^+/Dithranol).

Figure **4.17** shows the FTIR spectrum of 56 Aryl, with very pronounced aromatic signals at 3024-3060 cm^{-1} and 698 cm^{-1}. The ν Si-O-Si bands from 1200-1050 cm^{-1} are much lower in relative intensity than expected for a silsesquioxane compound due to the presence of 56 aromatic moieties per silsesquioxane cage.

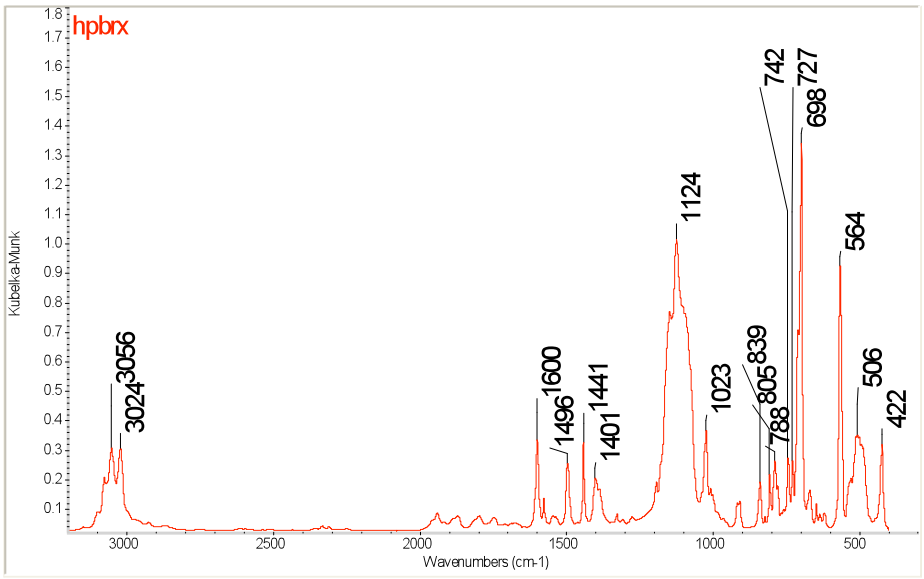

Figure 4.17. FTIR spectrum of the 56 Aryl.

This 56 Aryl crystallizes readily from hot toluene to yield crystals suitable for X-ray crystallography, see Figure **4.18**. The structure solution was refined to an R-factor of 5.7%. Large channels filled with eighteen disordered toluene solvates comprise 55% of the crystal volume. These were modeled using the PLATON software package.[75] Additional crystallographic details are found in Table **4.3** below.

The crystal structure shows open channels along the *a* and *b* crystallographic axes of 1 nm and 0.5 nm diameter, respectively, and these channels open into large voids between the molecules. The toluene quickly desorbs from the crystal, and powder diffraction indicates that this crystal structure collapses. The molecules are luminescent and the photophysical behavior will be discussed in greater detail in the future.

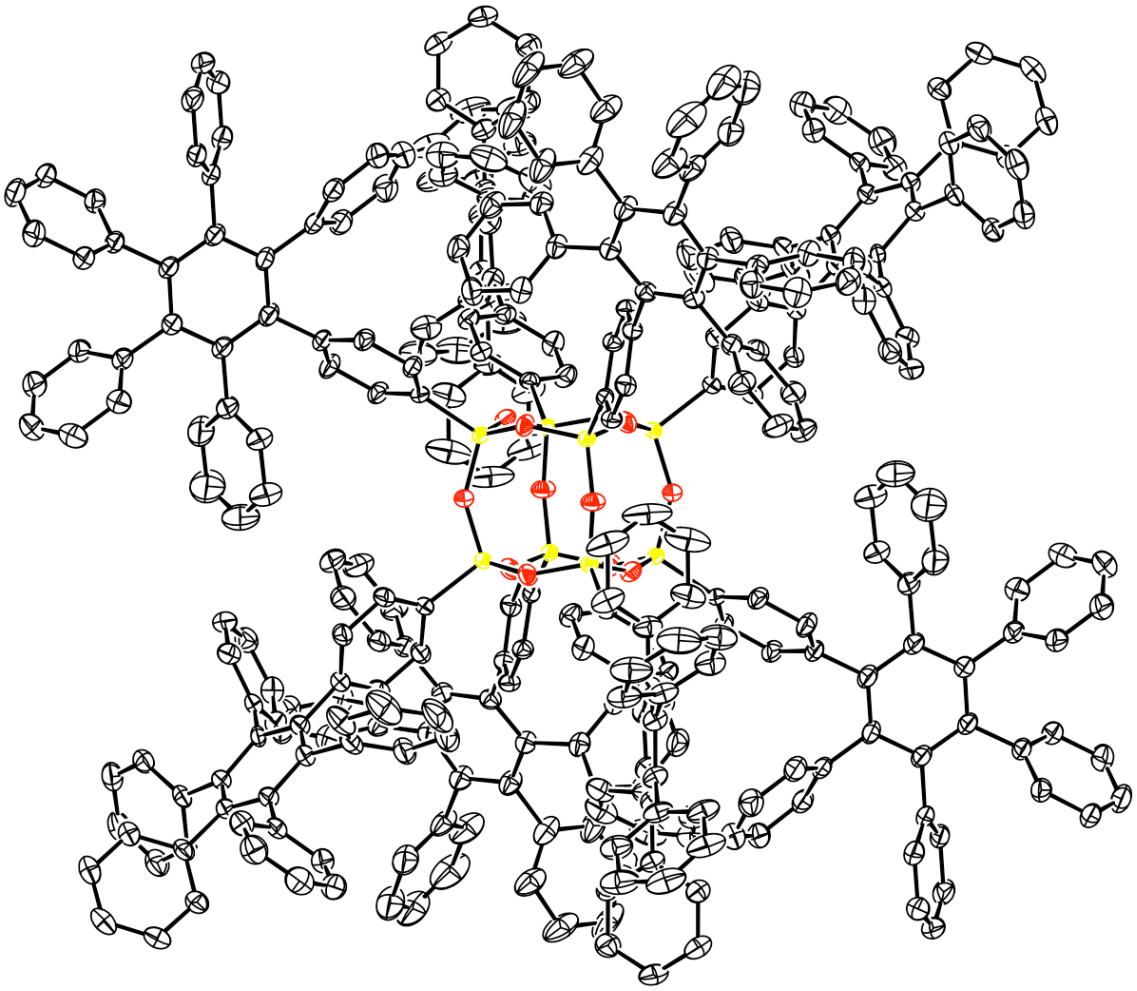

Figure 4.18. 50 % thermal ellipsoid plots of 56 Aryl • 18 toluene. Labels, hydrogen atoms and toluene solvates are omitted for clarity.
Full XRD data can be found in Appendix 9.

Table 4.3. Crystal Structure Refinement Data for 56 Aryl • 18 toluene.

	56 Aryl
Space Group	P-1, triclinic
Unit Cell Dimensions	a= 21.6705(18) Å b= 22.7273(19) Å c= 27.648(2) Å
	α = 70.874(1)˚ β= 88.818(1)˚ γ= 64.954(1)˚
Unit Cell Volume	11544.0(16) Å^3
Z	1
R-factor	5.7 % (28.7 %)*

* Before use of SQUEEZE to account for disordered solvent

The permethylated 56 Aryl was synthesized by condensing **1b** with recrystallized tetra(*p*-tolyl)cyclopentadienone. Figure **4.19** shows the ^{1}H spectrum of the permethylated 56 Aryl compound. In this case the aromatic resonances are again found again between 6-7 ppm. However, there are two different benzylic proton resonances seen.

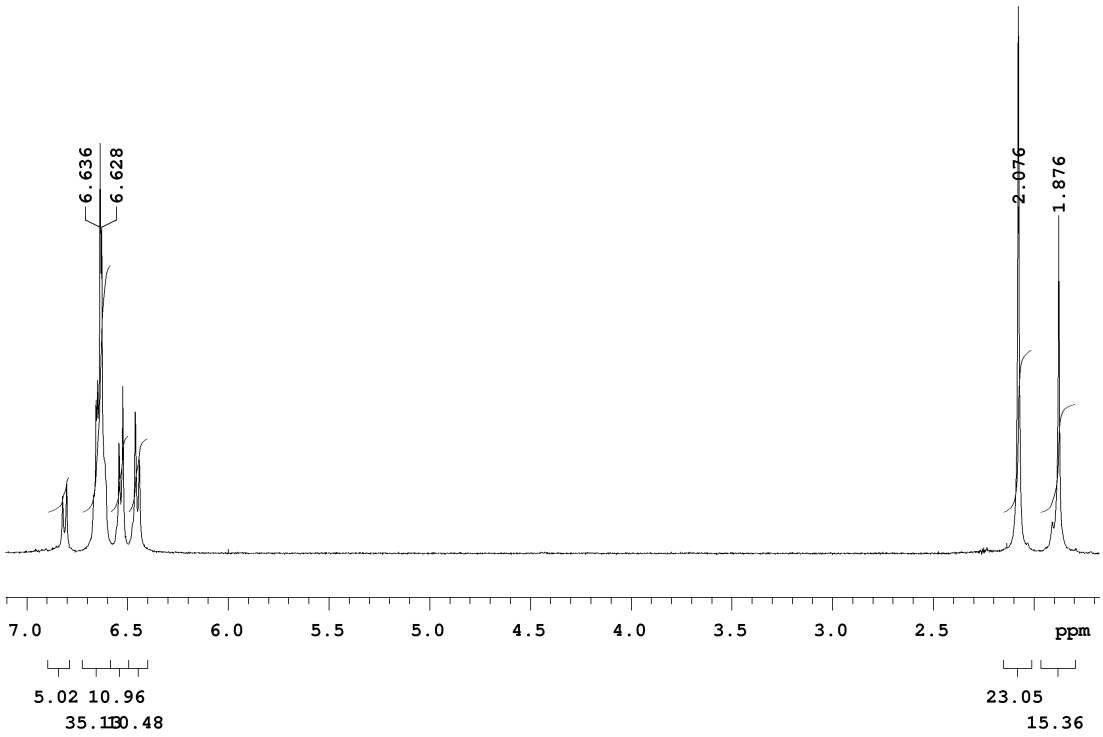

Figure 4.19. ^{1}H spectrum of the permethylated 56 Aryl in $CDCl_3$.

The integrations appear to correspond to the "inner" methyl groups, closer to the cage, and the "outer" methyl groups. Figure **4.20** schematically shows the chemical environments inhabited by the different methyl groups. There is potential for steric interference by the methyl groups on the "interior," adjacent to the silsesquioxane cage face. The aromatic resonance at 6.85 ppm would appear to correspond to the protons adjacent to the C-Si bond. The resonances at 6.55 and 6.45 ppm appear to correspond to the two inner aromatic rings. Figure **4.21** shows the MALDI-TOF spectrum of permethylated 56 Aryl, indicating the symmetric octamer.

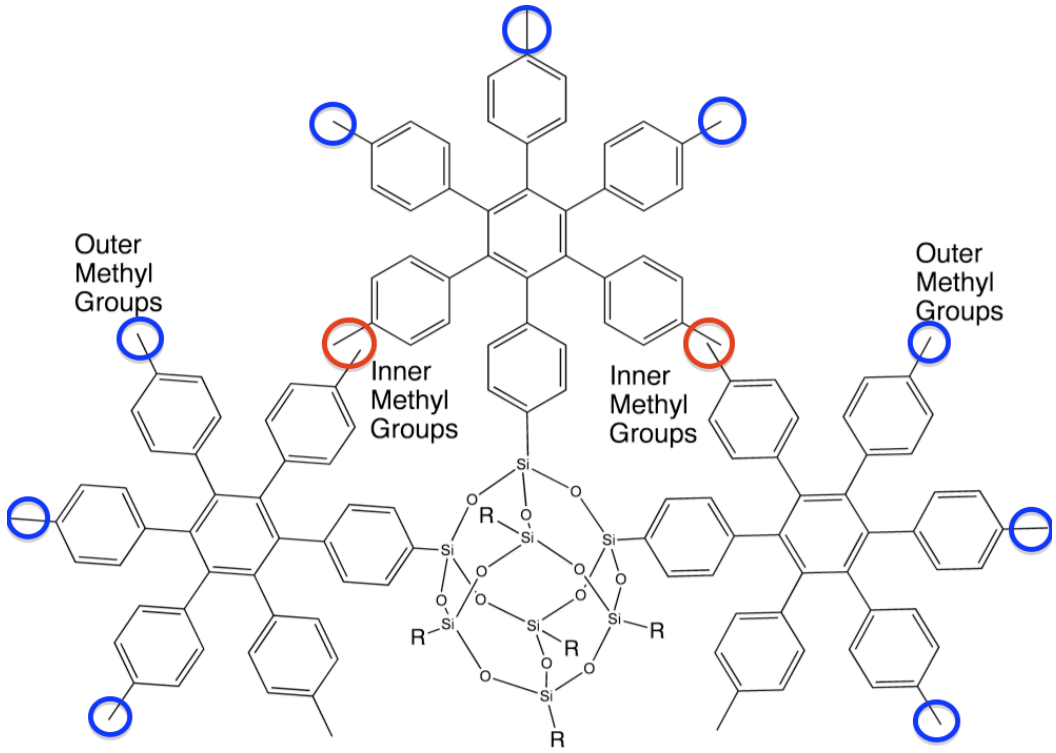

Figure 4.20. Depiction of methyl group environments in permethylated 56 Aryl.

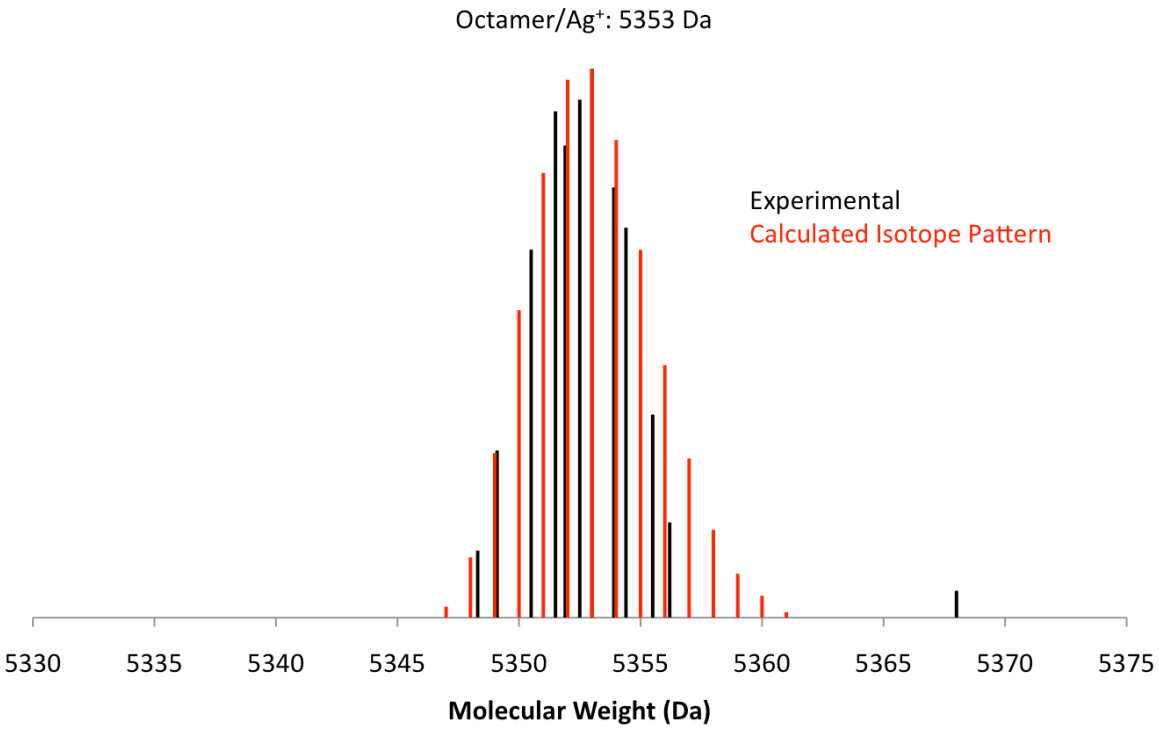

Figure 4.21 MALDI-TOF spectrum of the permethylated 56 Aryl (Ag^+/Dithranol).

Since alkylated hexaarylbenzenes are often used as the precursors for graphene systems, a third derivative was synthesized. Rathore reported the *t*-butylation of hexaphenylbenzene and its subsequent cyclization to form the hexa-*t*-butylated hexa-*peri*-benzocoronene, in dichloromethane with a nitromethane solution of $FeCl_3$.[76] The direct application of this protocol led to over-alkylated products as determined by ^1H NMR. Therefore, a milder catalyst, $SnCl_4$, was used to conduct the *t*-butylation of the 56 Aryl.

$SnCl_4$ is known to be a selective *t*-butylation catalyst, with a lower catalytic activity than $FeCl_3$ or $AlCl_3$.[77] The exhaustive alkylation of such a large macromolecule was difficult, and the proposed reaction required stoichiometric $SnCl_4$ and an excess of *t*-butyl chloride and a 4 d reaction time in refluxing methylene chloride (Scheme **4.6**).

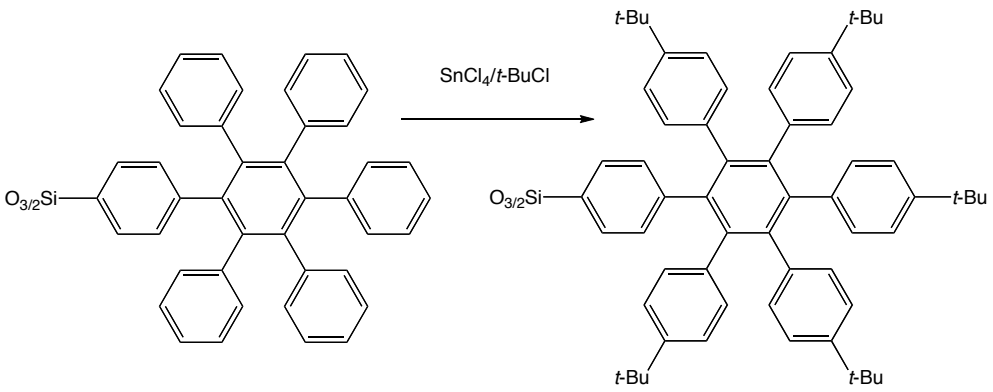

Scheme 4.6 *t*-Butylation of 56 Aryl.

Aliquots were taken to monitor reaction progress, and after 4 days, the reaction was stopped when the integration of the alkyl and aromatic proton resonances corresponded to a total of ~40 *t*-butyl groups per molecule (Figure **4.22**). The crude *t*-butylated compound was recrystallized twice from hot acetone, giving 30 % of the total yield as a white powder. Evaporation of the acetone allowed recovery of the less-

crystalline as a yellow, brittle, glassy solid. MALDI-TOF analysis of the compound in Figure **4.23** shows an average of 42 *t*-butyl groups per molecule.

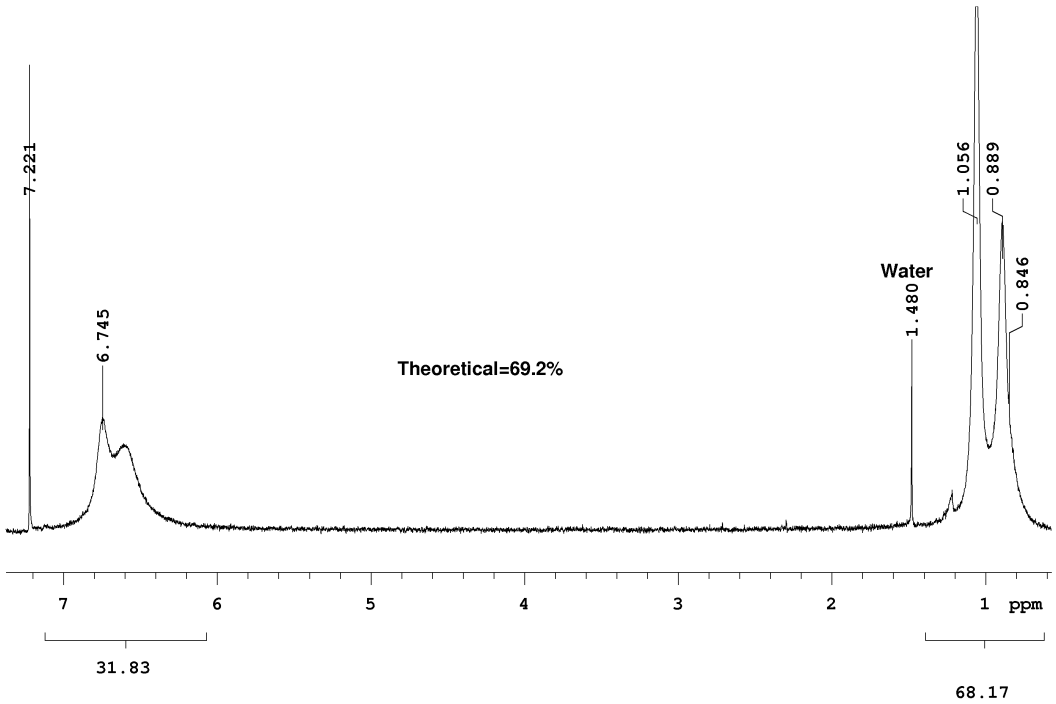

Figure 4.22. ^{1}H spectrum of the t-butylated 56 Aryl in $CDCl_3$.

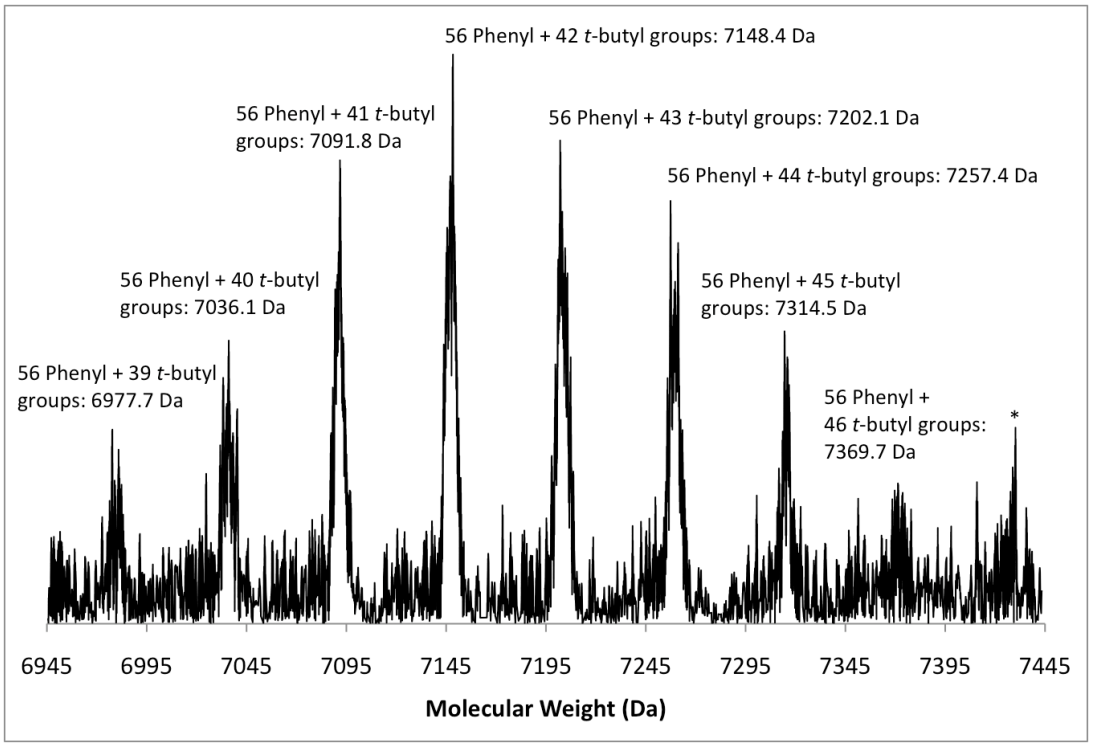

Figure 4.23. MALDI-TOF spectrum of the *t*-butylated 56 Aryl (Ag^{+}/Dithranol).

Scholl Reaction Studies

Initial studies targeting cyclization of the 56 Aryl (Scheme **4.7**) gave disappointing results, either producing intractable red or red-black solids or soluble materials with no detectable reaction. Concurrent cyclization/*t*-butylation studies were conducted to determine conditions for the efficient cyclization of these systems.[76] This ensured solubility of the products and allowed analysis by ^{1}H NMR, a valuable tool for monitoring these reactions. Previous work by Rathore shows that the aromatic resonances of HBC derivatives are in the range of 9-10 ppm.[76] This large downfield shift from the hexa-aryl benzene resonance at 6-7 ppm is due to increased ring currents in the delocalized π system.[78-80]

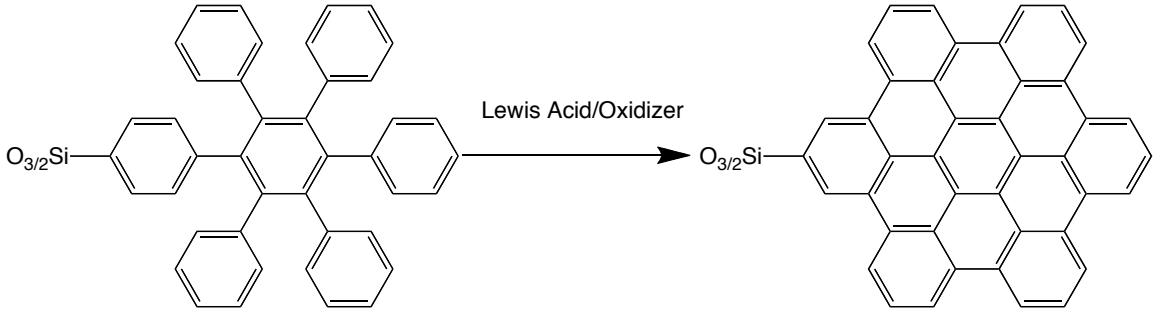

Scheme 4.7. Scholl-type dehydrogenative cyclization.

By using ^{1}H NMR to follow the progress of the Scholl reaction, it was determined that several modifications were necessary to the standard conditions used by Rathore.[76] First, the reaction needed to be heated to 40˚C. This presumably accelerates the reaction, but also increases the solubility of the silsesquioxane materials after the addition of the nitromethane/$FeCl_3$ solution.

Second, an additional Lewis Acid was necessary to scavenge the HCl produced during the reaction. This second improvement was suggested by the work of Kramer et

al, who found that certain Scholl reactions were significantly accelerated by the addition of an HCl scavenger.[64] This was accomplished by using of a 1.0 M solution of $SnCl_4$ in CH_2Cl_2.

With these modifications, the cyclization reaction was complete after 2 h, and was quenched by precipitation into cold methanol. The resulting precipitate was filtered, washed with an equal volume of 0.1 M methanolic HCl, and two more volumes of methanol. The resulting solid was then dried under vacuum and analyzed.

Using these modifications the cyclization reaction was performed on the *t*-butylated 56 Aryl compound, providing a soluble product with the expected downfield shift in the aromatic proton resonance (Figure **4.24**). The integration of the t-butyl protons is 77.5%, or roughly 95% conversion in comparison to theoretical, which indicates incomplete cyclization, on average.

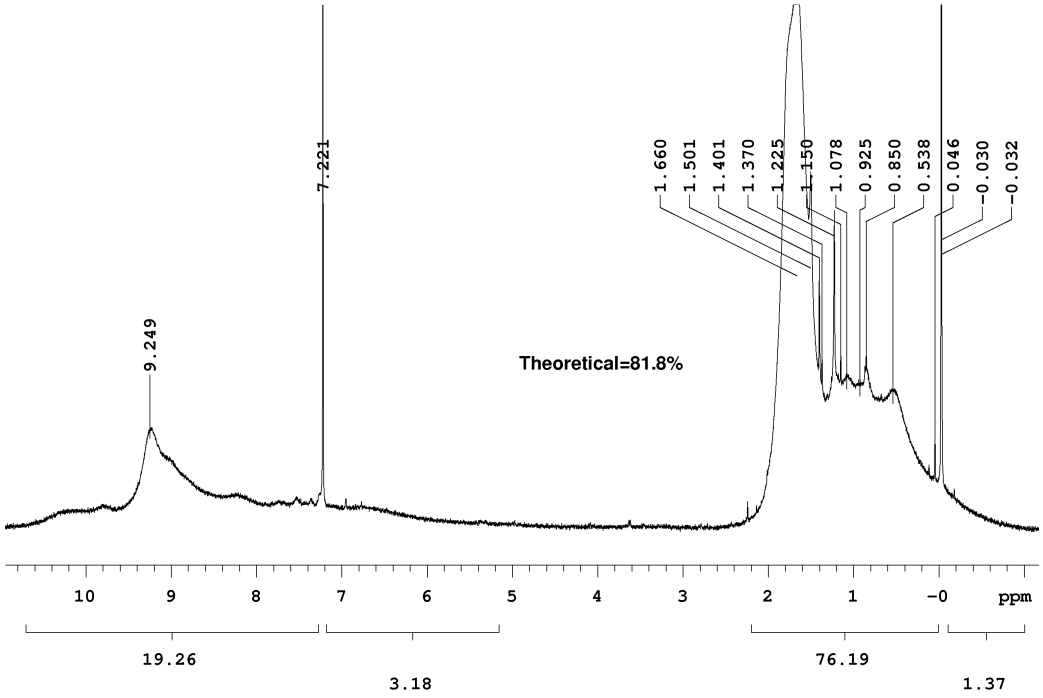

Figure 4.24 ^{1}H spectrum of the cyclized, *t*-butylated 56 Aryl in $CDCl_3$.

For the 56 Aryl system, the cyclization led to a dark orange-red precipitate upon quenching in methanol. The product was insoluble in all solvents, including hot *o*-dichlorobenzene and nitrobenzene. Using TCNQ as a matrix, the following MALDI-TOF spectrum was obtained (Figure **4.25**), and indicates incomplete cyclization of the 56 Aryl precursor.[49]

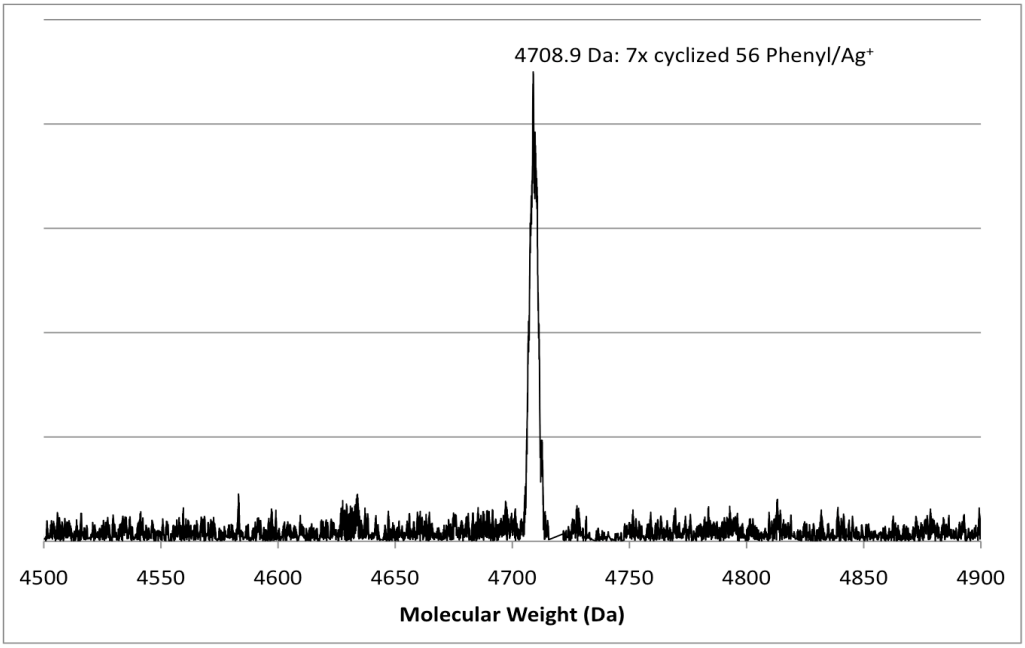

Figure 4.25 MALDI-TOF spectrum of the cyclized 56 Aryl.

The FTIR spectrum of this compound is shown in Figure **4.25**. The presence of the ν Si-O-Si bands of the silsesquioxane core are seen from 1200-1000 cm^{-1}, and the vibrational contributions of the aromatic rings can be seen at 3061 (ν ArC-H), 1575-1500 (ν/δ C-C), and 700 (δ C-H) cm^{-1}. Scaled to equivalent heights of the ν Si-O-Si bands, decreases in the ν ArC-H (3100-3000 cm^{-1}) bands suggest the loss of aromatic protons in the cyclization reaction. Additionally, peaks in the fingerprint region, (2000-1600 cm^{-1}) decrease, as well as a significant decrease in the intensity of the peak at 575 cm^{-1}.

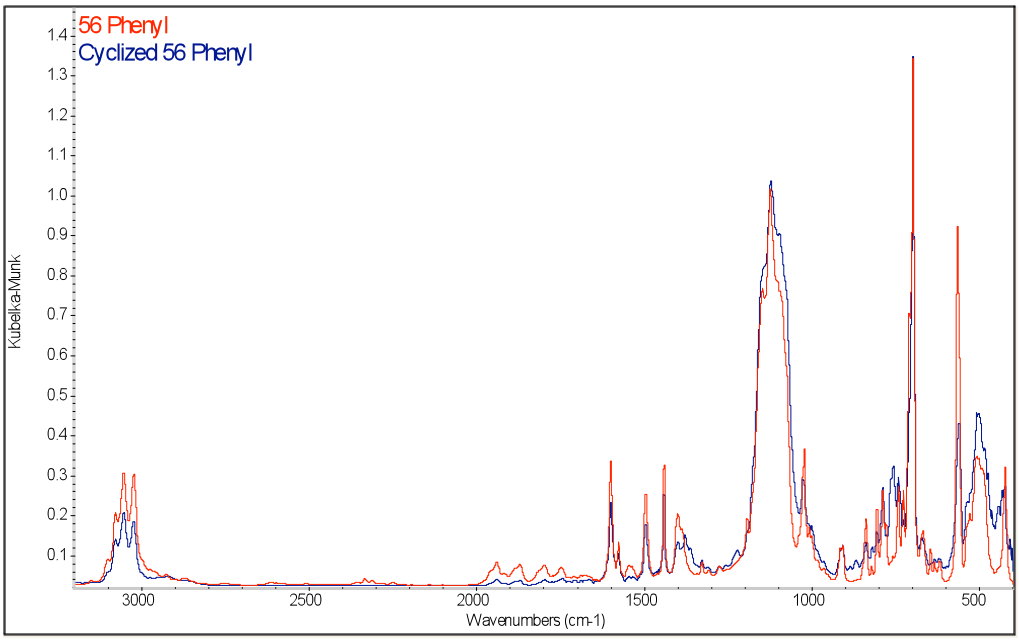

Figure 4.26 FTIR spectra of the 56 Aryl and its cyclization product, 3200-400cm^{-1}.

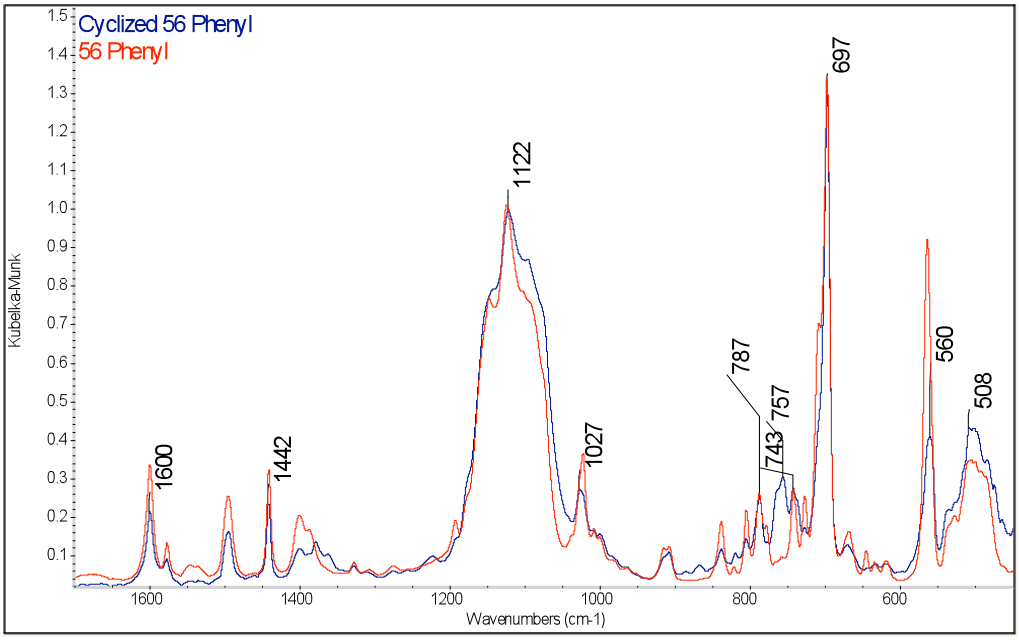

Figure 4.27 FTIR spectra of the 56 Aryl and its cyclization product, 1700-400 cm^{-1}.

In the case of the permethylated 56 Aryl compound, the cyclization gave a dark yellow precipitate upon quenching in methanol, which dried to a brittle green-black solid.

The product was again insoluble in all solvents, including hot *o*-dichlorobenzene and nitrobenzene. Grinding of the product by mortar and pestle provided a fine dark yellow powder for analysis by FTIR and powder X-ray diffraction.

The FTIR spectrum of this compound is shown in Figure **4.25**. The presence of the ν Si-O-Si bands of the silsesquioxane core are seen from 1200-1000 cm^{-1}, and the vibrational contributions of the aromatic rings can be seen at 3061 (ν ArC-H) and 2915 (ν Bz-H), 1575-1500 (ν/δ C-C), and 850-750 (δ C-H) cm^{-1}.

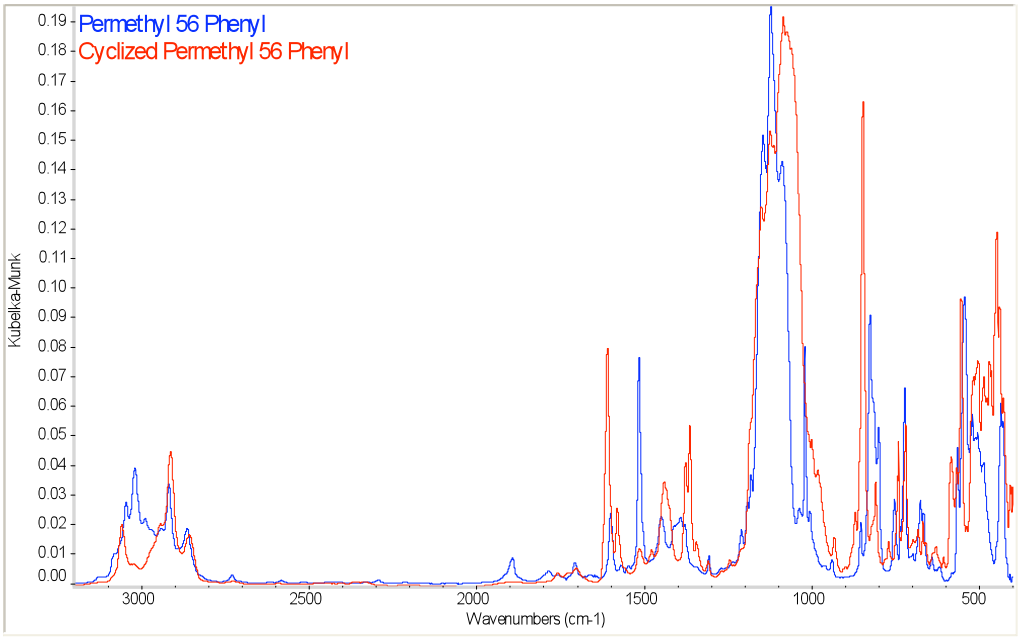

Figure 4.28 FTIR spectra of the permethyl 56 Aryl and its cyclization product, 3200-450 cm^{-1}.

Several pronounced differences are seen in this case. A dramatic decrease in the ν ArC-H bands (3100 tot 3000 cm^{-1}), which is consistent with a loss of aromatic protons. The absorbance at 1525 cm^{-1} decreases dramatically, and the intensity of the peak at 1600 cm^{-1} strongly increases. New peaks at 1350-1400 cm^{-1} arise, and peak shift from 840 to

850 cm^{-1} is seen. Finally the absorbance of the ν Si-O-Si bands broadens and shifts from 1075 to 1025 cm^{-1}.

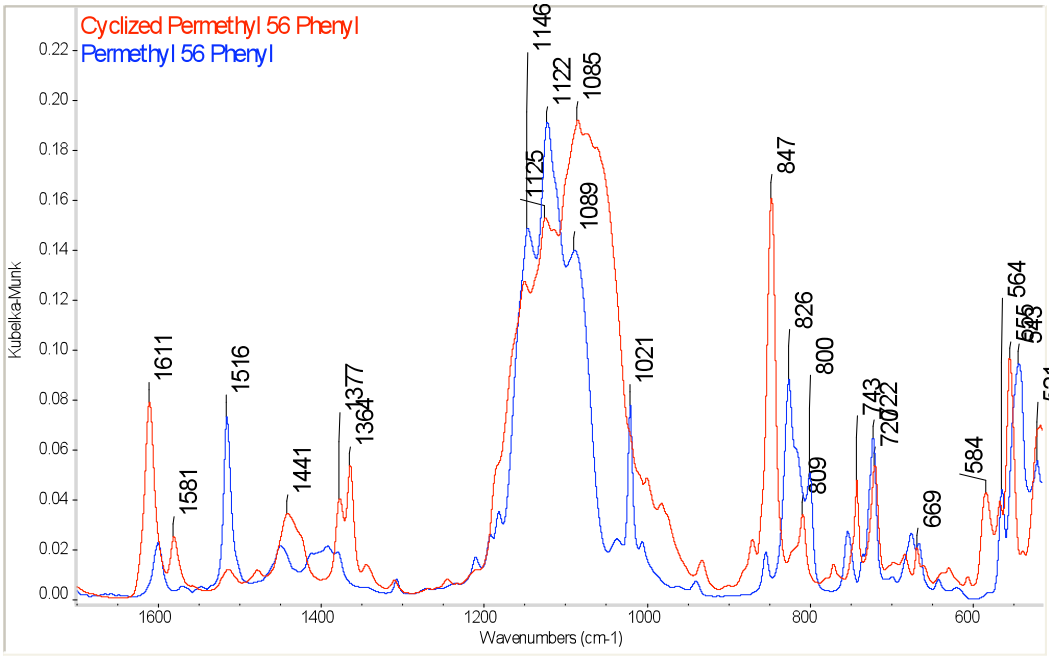

Figure 4.29 FTIR spectra of the permethyl 56 Aryl and its cyclization product, 1700-500 cm^{-1}.

The powder XRD pattern of the cyclized PMHPB material is shown in Figure **4.30**. Features are seen at *d*-spacings of 2.2, 3.6, 4.75, and 11-16 Å, respectively. The crystal structure of the 56 Aryl compound indicates face and edge distances of 16.4 and 11.5 Å, between the centroids of the hexaphenylbenzene moieties. Since π stacked PAH molecules stack nearly centroid-to-centroid, this should be a reasonable approximation of the probable spacing for the cyclized octahexaarylbenzenesilsesquioxane, if the spacing of the molecules is periodic. (Figure **4.31**). These values correspond well to the *d*-spacing feature from 11-16 Å. The silsesquioxane cage face and body diameters are 4.4 and 5.4 Å. In the hexa-*peri*-benzocoronene crystal structure, the π···π stacking distance between adjacent molecules is 3.4 Å,[81] which corresponds favorably to the feature at a *d*-spacing of 3.6 Å.

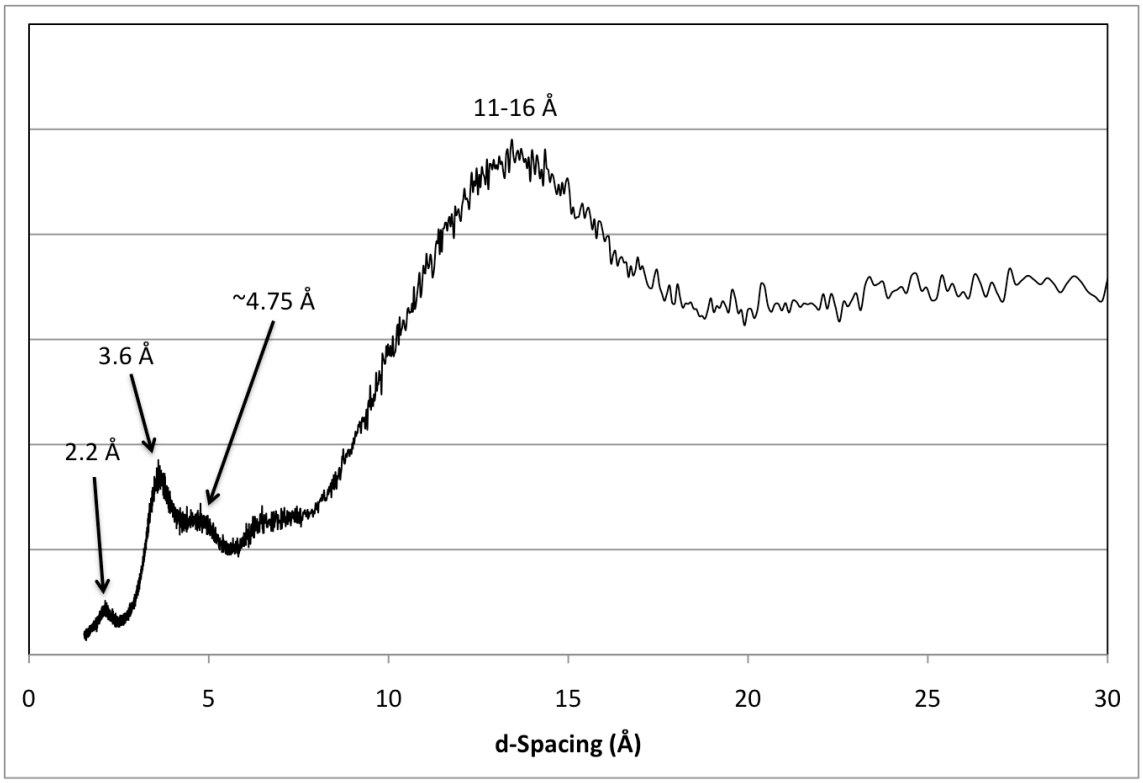

Figure 4.30 Powder XRD pattern of the cyclized permethylated 56 Aryl.

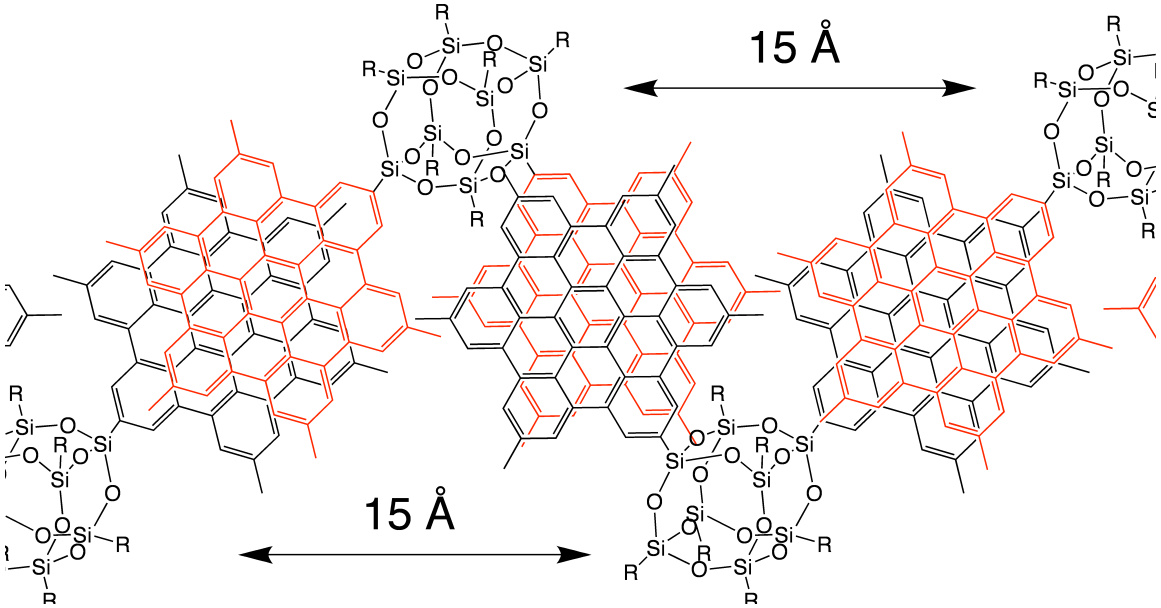

Figure 4.31 Diagram of possible *d*-spacings.

Conclusions

This chapter has detailed the synthesis and characterization of a unique set of highly conjugated silsesquioxanes derived from I_8OPS. The Sonogashira coupling of aryl acetylenes with I_8OPS provides access to a number of ethynyl functionalized OPS derivatives, including the octadiphenylacetyleneSQ, octa(4-methyldiphenylacetylene)SQ, and octa(trimethylsilylethynylphenyl)SQ. OctadiphenylacetyleneSQ has been further characterized by single-crystal X-ray diffraction, with a refinement consistent with the proposed structure.

The high temperature reaction of ethynyl functionalized OPS with tetraarylcyclopentadienones provides the octa(hexaarylbenzene)SQs in essentially quantitative yield. Recrystallization of the octa(hexaphenylbenzene)SQ, or 56 Aryl, gives single crystals suitable for X-ray diffraction, and allows for a structural determination. More than half of the unit cell of the 56 Aryl consists approximately eighteen disordered toluene solvates, and open channels are found along the *ab* plane.

Finally, dehydrogenative cyclization of the unsubstituted and methyl-substituted 56 Aryl systems hexaarylbenzene leads to highly insoluble products. The more disordered *t*-butylated 56 Aryl may be cyclized to provide a soluble product, which may be characterized by ^{1}H-NMR. In each case, some loss of aromatic protons may be ascertained by FTIR or ^{1}H-NMR, consistent with the proposed reaction.

These conjugated materials possess delocalized π-systems and may be suitable for use as active components in microelectronic systems. The octa-functionality could allow for intermolecular cooperative effects. The high thermal stability of the silsesquioxane cage should provide high stability at microelectronic operating temperatures.

References Cited:

1. Sanchez, C.; de A.A. Soler-Illia, G.J.; Ribot, F.; Lalot, T.; Mayer, C.R.; Cabuil, V. "Designed Hybrid Organic-Inorganic Nanocomposites from Functional Nanobuilding Blocks," *Chemistry of Materials*, **13**, 3061-8 (2001).
2. Hawker, C.J.; Wooley, K.L. "The Convergence of Synthetic Organic and Polymer Chemistry," *Science* **309**, 1200-5.
3. Tamaki, R., Tanaka, Y.; Asuncion, M.Z.; Choi, J.; Laine, R.M. "Octa(aminophenyl)silsesquioxane as a Nanoconstruction Site." *Journal of the American Chemical Society* **123**, 12416-7 (2001).
4. Roll, M.F.; Asuncion, M.Z.; Kampf, J.; Laine, R.M. "para-Octaiodophenylsilsesquioxane, $[p\text{-}IC_6H_4SiO_{1.5}]_8$, a Nearly Perfect Nano-Building Block." *ACS Nano* **2**, 320-6 (2008).
5. Brown, J.F. Jr.; Vogt, L.H.; Prescott, P.I. "Preparation and Characterization of the Lower Equilibrated Phenylsilsesquioxanes." *Journal of the American Chemical Society* **86**, 1120-5 (1964).
6. Brick, C.M. Tamaki, R.; Kim, S.-G.; Asuncion, M.Z.; Roll, M.; Nemoto, T.; Ouchi, Y.; Chujo Y.; Laine, R.M. "Spherical, Polyfunctional Molecules Using Poly(bromophenylsilsesquioxane)s as Nanoconstruction Sites." *Macromolecules* **38**, 4655-60 (2005).
7. Brick, C. M.; Ouchi, Y.; Chujo, Y.; Laine, R. M. Robust Polyaromatic Octasilsesquioxanes from Polybromophenylsilsesquioxanes, Br_xOPS, via Suzuki Coupling." *Macromolecules* **38**, 4661–5 (2005).
8. Sellinger, A.; Laine, R.M. "Silsesquioxanes as Synthetic Platforms. 3. Photocurable, Liquid Epoxides as Inorganic/Organic Hybrid Precursors." *Chemistry of Materials* **8**, 1592-3 (1996).
9. Sellinger, A.; Laine, R.M. "Silsesquioxanes as Synthetic Platforms. Thermally Curable and Photocurable Inorganic/Organic Hybrids." *Macromolecules* **29**, 2327-30 (1996).
10. Asuncion, M.Z.; Laine, R.M. "Silsesquioxane Barrier Materials." *Macromolecules* **40**, 555-62 (2007).
11. Choi, J.; Yee, A.F.; Laine, R.M. "Organic/Inorganic Hybrid Composites from Cubic Silsesquioxanes. Epoxy Resins of Octa(dimethylsiloxyethylcyclohexylepoxide) Silsesquioxane." *Macromolecules* **36**, 5666-82 (2003).
12. Choi, J.; Yee, A.F.; Laine, R.M. "Toughening of Cubic Silsesquioxane Epoxy Nanocomposites Using Core-Shell Rubber Particles: A Three-Component Hybrid System." *Macromolecules* **37**, 3267-76 (2004).
13. Choi, J.; Kim, S.G.; Laine, R.M. "Organic/Inorganic Hybrid Epoxy Nanocomposites from Aminophenylsilsesquioxanes." *Macromolecules* **37**, 99-109 (2004).

14. Tamaki, R.; Choi, J.; Laine, R.M. "A Polyimide Nanocomposite from Octa(aminophenyl)silsesquioxane." *Chemistry of Materials* **15**, 793-797 (2003).

15. Zhang, C.; Bunning, T.J.; Laine, R.M. "Synthesis and Characterization of Liquid Crystalline Silsesquioxanes." *Chemistry of Materials* **13**, 3653-62 (2001).

16. Choi, J.; Harcup, J.; Yee, A.F.; Zhu, Q.; Laine, R.M. "Organic/Inorganic Hybrid Composites from Cubic Silsesquioxanes." *Journal of the American Chemical Society* **123**, 11420-30 (2001).

17. Costa, R.O.R.; Vasconcelos, W.L.; Tamaki, R.; Laine, R.M. "Organic/Inorganic Nanocomposite Star Polymers via Atom Transfer Radical Polymerization of Methyl Methacrylate Using Octafunctional Silsesquioxane Cores." *Macromolecules* **34**, 5398-407 (2001).

18. Choi, J.; Tamaki, R.; Kim, S.G.; Laine, R.M. "Organic/Inorganic Imide Nanocomposites from Aminophenylsilsesquioxanes." *Chemistry of Materials* **15**, 3365-3375 (2003).

19. Zhang, C.; Babonneau, F.; Bonhomme, C.; Laine, R.M.; Soles, C.L.; Hristov, H.A.; Yee, A.F. "Highly Porous Polyhedral Silsesquioxane Polymers. Synthesis and Characterization." *Journal of the American Chemical Society* **120**, 8380-8391 (1998).

20. Sulaiman, S.; Brick, C.M. De Sana, C.M.; Katzenstein, J.M.; Laine, R.M.; Basheer, R.A. "Tailoring the Global Properties of Nanocomposites. Epoxy Resins with Very Low Coefficients of Thermal Expansion." *Macromolecules* **39**, 5167-9 (2006).

21. Samuel, I.D.W. Turnbull, G.A. "Organic Semiconductor Lasers." *Chemical Reviews* **107**, 1272–95 (2007).

22. Zaumseil, J.; Sirringhaus, H. "Electron and Ambipolar Transport in Organic Field-Effect Transistors." *Chemical Reviews* **107**, 1296–323 (2007).

23. Hagemann, O.; Jørgensen, M.; Krebs, F.C. "Synthesis of an All-in-One Molecule (for Organic Solar Cells)." *Journal of Organic Chemistry* **71**, 5546-59 (2006).

24. Sellinger review

25. Briseno, A.L.; Mannsfeld, S.C.B.; Ling, M.M; Liu, S.; Tseng, R.J.; Reese, C.; Roberts, M.E.; Yang, Y.; Wudl, F.; Bao, Z. "Patterning organic single-crystal transistor arrays." *Nature* **444**, 913-7 (2006).

26. Murphy, A.R.; Frechet, J.M.J. "Organic Semiconducting Oligomers for Use in Thin Film Transistors." *Chemical Reviews* **107**, 1066–96 (2007).

27. Scherf, U. "Oligo- and Polyarylenes, Oligo- and Polyarylenevinylenes." *Topics in Current Chemistry* **201**, 163-222 (1999).

28. Yamamoto, K.; Oyaizu, K.; Asada, T.; Nishide, H.; Tsuchida, E. "Preparation of Poly(1,4-phenylene) by oxidative polymerization of Benzene with 2,3,-Dichloro-5,6,-dicyano-p-benzoquinone." *Chemistry Letters* **1994**, 363-6.

29. Prins, P.; Grozema, F.C.; Siebbeles, L.D.A. "Efficient Charge Transport along Phenylene-Vinylene Molecular Wires." *Journal of Physical Chemisty B* **110**, 14659-66 (2006).

30. Aoki, T.; Kaneko, T.; Teraguchi, M. "Synthesis of functional p-conjugated polymers from aromatic acetylenes." *Polymer* **47**, 4867–92 (2006).

31. Warman, J.M.; de Haas, M.P.; Dicker, G.; Grozema, F.C.; Piris, J.; Debije, M.G. "Charge Mobilities in Organic Semiconducting Materials Determined by Pulse-Radiolysis Time-Resolved Microwave Conductivity: π-Bond-Conjugated Polymers versus π-π-Stacked Discotics." *Chemistry of Materials* **16**, 4600-9 (2004).

32. Ried, W.; Freitag, D. "Oligophenyls, Oligophenylenes, and Polyphenyls, a Class of Thermally Very Stable Compounds." *Angewandte Chemie, International Edition in English* **7**, 835-902 (1968).

33. Berresheim, A.J.; Muller, M.; Mullen, K. "Polyphenylene Nanostructures." *Chemical Reviews* **99**, 1747–1785 (1999).

34. Kovacic, P.; Kyriakis, A."Polymerization of Benzene to p-Polyphenyl by Aluminum Chloride-Cupric Chloride." *Journal of the American Chemical Society* **85**, 454-8 (1963).

35. Kovacic, P.; Koch, F.W. "Polymerization of Benzene to p-Polyphenyl by Ferric Chloride." *Journal of Organic Chemistry* **28**, 1864-7 (1963).

36. Kovacic, P.; Koch, F.W.; Stepitan, C.E. "Water Cocatalysis in the Polymerization of Benzene by Ferric Chloride." *Journal of Polymer Science, Part A* **2**, 1193-203 (1964).

37. Tong, L.; Ho, D.M.; Vogelaar, N.J.; Schutt, C.E.; Pascal, R.A. "The Albatrossenes: Large, Cleft-Containing, Polyphenyl Polycyclic Aromatic Hydrocarbons." *Journal of the American Chemical Society* **119**, 7291-302 (1997).

38. Lu, J.; Zhang, J.; Shen, X.; Ho, D.M.; Pascal, R.A. "Octaphenylbiphenylene and Dodecaphenyltriptycene." *Journal of the American Chemical Society* **124**, 8035-41 (2002).

39. Song, Q.; Lebeis, C. W.; Shen, X.; Ho, D.M.; Pascal, R.A. "Polyphenyl Macrocyclic Oligophenylenes." *Journal of the American Chemical Society* **127**, 13732-37 (2005).

40. Shen, X.; Ho, D.M.; Pascal, R.A. "Synthesis of Polyphenylene Dendrimers Related to 'Cubic Graphite'." *Journal of the American Chemical Society* **126**, 5798-805 (2004).

41. Tong, L.; Lau, H.; Ho, D.M.; Pascal, R.A. "Polyphenylbiphenyls and Polyphenylfluorenes." *Journal of the American Chemical Society* **120**, 6000-6 (1998).

42. Clark, C.G.; Wenzel, R.J.; Andreitchenko, E.V.; Steffen, W.; Zenobi, R.; Mullen, K. "Controlled MegaDalton Assembly with Locally Stiff but Globally Flexible

Polyphenylene Dendrimers." *Journal of the American Chemical Society* **129**, 3292-301 (2007).

43. Wasserfallen, D.; Mattersteig, G.; Enkelmann, V.; Mullen, K. "Synthesis and crystal structures of extremely crowded oligophenylenes as model precursors to 'cubic graphite'." *Tetrahedron* **62**, 5417–20 (2006).
44. Zhi, L.; Wu, J.; Li, J.; Stepputat, M.; Kolb, U.; Müllen, K. "Diels-Alder Reactions of Tetraphenylcyclopentadienones in Nanochannels: Fabrication of Nanotubes from Hyperbranched Polyphenylenes." *Advanced Materials* **17**, 1492-6 (2005).
45. Wu, J.; Grimsdale, A.C.; Mullen, K. "Combining one-, two- and three-dimensional polyphenylene nanostructures." *Journal of Materials Chemistry* **15**, 41–52 (2005).
46. Zhi, L.; Mullen, K."A bottom-up approach from molecular nanographenes to unconventional carbon materials." *Journal of Materials Chemistry* **18**, 1472–84 (2008).
47. Simpson, C.D.; Brand, J.D.; Berresheim, A.J.; Przybilla, L.; Rader, H.J.; Mullen, K. "Synthesis of a Giant 222 Carbon Graphite Sheet." *Chemistry: A European Journal* **8**, 1424-9 (2002).
48. Rouhanipour, A.; Roy, M.; Feng, X.; Räder, H.J; Müllen, K. "Subliming the Unsublimable : How to Deposit Nanographenes." *Angewandte Chemie, International Edition in English* **48**, 4602–4 (2009).
49. Simpson, C.D.; Mattersteig, G.; Martin, K.; Gherghel, L.; Bauer, R.E.; Rader, H.J.; Mullen, K. "Nanosized Molecular Propellers by Cyclodehydrogenation of Polyphenylene Dendrimers." *Journal of the American Chemical Society* **126**, 3139-47 (2004).
50. Matta, C.F.; Hernandez-Trujillo, J. "Bonding in Polycyclic Aromatic Hydrocarbons in Terms of the Electron Density and of Electron Delocalization." *Journal of Physical Chemistry A* **107**, 7496-504 (2003).
51. Randic, M. "Aromaticity of Polycyclic Conjugated Hydrocarbons." *Chemical Reviews* **103**, 3449–605 (2003).
52. Kokkin, D.L.; Schmidt, T.W. "On the Electronic Properties of Dehydrogenated Polycyclic Aromatic Hydrocarbons." *Journal of Physical Chemistry A* **110**, 6173-7 (2006).
53. Enoki, T.; Takai, K. "Unconventional electronic and magnetic functions of nanographene-based host–guest systems." *Dalton Transactions* **2008**, 3773–81.
54. Hwang, J.; Pototschnig, M.; Lettow, R.; Zumofen, G.; Renn,A.; Gotzinger, S.; Sandoghdar, V. "A single-molecule optical transistor." *Nature* **460**, 76-80 (2009).
55. Wang, X.; Zhi, L.; Tsao, N.; Tomovic, Z.; Li, J.; Müllen, K. "Transparent Carbon Films as Electrodes in Organic Solar Cells." *Angewandte Chemie, International Edition in English* **47**, 2990-2 (2008).

56. Wu, J.; Pisula, W.; Mullen, K. "Graphenes as Potential Materials for Electronics." *Chemical Reviews* **107**, 718–47 (2007).

57. King, B.T.; Kroulik, J.; Robertson, C.R.; Rempala, P.; Hilton, C.L.; Korinek, J.D.; Gortari, L.M." Controlling the Scholl Reaction." *Journal of Organic Chemistry* **72**, 2279-88 (2007).

58. Rempala, P.; Kroulik, J.; King, B.T. "Investigation of the Mechanism of the Intramolecular Scholl Reaction of Contiguous Phenylbenzenes." *Journal of Organic Chemistry* **71**, 5067-81 (2006).

59. Kovacic, P.; Hsu, L.-C. "Polymerization of Aromatic Nuclei. VIII. Molecular Weight Control in Benzene Polymerization." *Journal of Polymer Science: Part A* **4**, 5-28 (1966).

60. Kovacic, P.; Kyriakis, A. "Polymerization of Benzene to p-Polyphenyl." *Tetrahedron Letters* 467-9, (1962).

61. Kramer, B.; Fröhlich, R.; Waldvogel, S.R. "Oxidative Coupling Reactions Mediated by $MoCl_5$ Leading to 2,2'-Cyclolignans: The Specific Role of HCl." *European Journal of Organic Chemistry* **2003**, 3549-54.

62. Kumar, S.; Varshney, S.K. "Synthesis of Triphenylene and Dibenzopyrene Derivatives: Vanadium Oxytrichloride a Novel Reagent." *Synthesis* **2001**, 305–11.

63. Zhai, L.; Shukla, R.; Rathore, R. "Oxidative C-C Bond Formation (Scholl Reaction) with DDQ as an Efficient and Easily Recyclable Oxidant" *Organic Letters* **11**, 3474-7 (2009).

64. Asuncion M.Z.; Roll M.F.; Laine, R.M. "Octaalkynylsilsesquioxanes, Nano Sea Urchin Molecular Building Blocks for 3-D-Nanostructures." *Macromolecules* **41**, 8047-52 (2008).

65. Brick, C.M. Tamaki, R.; Kim, S.-G.; Asuncion, M.Z.; Roll, M.; Nemoto, T.; Ouchi, Y.; Chujo Y.; Laine, R.M. "Spherical, Polyfunctional Molecules Using Poly(bromophenylsilsesquioxane)s as Nanoconstruction Sites." *Macromolecules* **38**, 4655-60 (2005).

66. Fife, D.J.; Moore, W.M.; Morse, K.W. "Solution Equilibria of Tertiary Phosphine Complexes of Copper(I) Halides." *Inorganic Chemistry* **23**, 1684-91 (1984).

67. Konigsberger, K.; Chen, G.-P.; Wu, R.R.; Girgis, M.J.; Prasad, K.; Repic, O.; Blacklock, T.J. "A Practical Synthesis of 6-[2-(2,5-Dimethoxyphenyl)ethyl]-4-ethylquinazoline and the Art of Removing Palladium from the Products of Pd-Catalyzed Reactions." *Organic Process Research & Development* **7**, 733–742 (2003).

68. ChemOffice Ultra, CambridgeSoft.

69. Williamson, K.L. Macroscale and Microscale Organic Experiments, 2nd ed, D.C. Heath and company, Toronto, 1994.

70. Field, L.D.; Ho, K.M.; Lindall, C.M.;Masters, A.E.; Webb, A.G. "The Preparation and Characterization of Substituted Pentaphenylcyclo- pentadienyl Ligands, Their Precursors, and Complexes of Iron." *Austrailian Journal of Chemistry* **43**, 281-91 (1990).

71. Bhandari, S.; Suprabhat Ray, S. "A Novel Synthesis of Bisbenzyl Ketones by DCC Induced Condensation of Phenylacetic Acid." *Synthetic Communications* **28**, 765-71 (1998).

72. DeTar, D.F.; Silverstein, R. "Reactions of Carbodiimides. I. The Mechanisms of the Reactions of Acetic Acid with Dicyclohexylcarbodiimide." *Journal of the American Chemical Society* **88**, 1013-9 (1966).

73. Johnson, J.R.; Grummitt, O. "Tetraphenylcyclopentadienone." *Organic Syntheses* **23**, 92 (1943).

74. Carvalho, M.F.N.N.; Almeida, F.M.T.; Galvao, A.M.; Pombeiro, A.J.L. "Benzene ring assembly promoted by a camphor derived palladium complex." *Journal of Organometallic Chemistry* **679**, 143-7 (2003).

75. PLATON Reference : A.L.Spek (2008) PLATON, A Multipurpose Crystallographic Tool, Utrecht University, Utrecht, The Netherlands.

76. Rathore, R.; Burns, C.L. "A Practical One-Pot Synthesis of Soluble Hexa-peri-hexabenzocoronene and Isolation of Its Cation-Radical Salt." *Journal of Organic Chemistry* **68**, 4071-4 (2003).

77. Olah, G.A.; Flood, S.H.; Moffatt, M.F. "Aromatic Substitution. XVIII.' Friedel-Crafts *t*-Butylation of Benzene and Methylbenzenes with t-Butyl Bromide and Isobutylene." *Journal of the American Chemical Society* **86**, 1060-4 (1964).

78. Jonathan, N.; Gordon, S.; Dailey, B.P. "Chemical Shifts and Ring Currents in Condensed Ring Hydrocarbons." *Journal of Chemical Physics* **36**, 2443-8 (1962).

79. Abraham, R.J.; Canton, M.; Reid, M.; Griffiths, L. "Proton chemical shifts in NMR. Part 14. Proton chemical shifts, ring currents and pi-electron effects in condensed aromatic hydrocarbons and substituted benzenes." *Journal of the Chemical Society, Perkin Transactions 2* **2000**, 803–812.

80. Ochsenfeld, C. "An ab initio study of the relation between NMR chemical shifts and solid-state structures : hexabenzocoronene derivatives." *Physical Chemistry Chemical Physics* **2**, 2153-9 (2000).

81. Goddard, R.; Haenel, M.W.; Herndon, W.C.; Kruger, C.; Zander, M. "Crystallization of Large Planar Polycyclic Aromatic Hydrocarbons: The Molecular and Crystal Structures of Hexabenzo [bc,ef,hi,kZ,no,qr]coronene and Benzo[1,2,3-bc:4,5,6-b'c']dicoronene." *Journal of the American Chemical Society* **117**, 30-41 (1995).

Chapter V

Supermolecular Coordination of Halogenated OPS Derivatives

Introduction

This dissertation has presented routes to synthesize symmetric nano-building blocks[1-3] from octaphenylsilsesquioxane.[4] The goal is to develop nano-building blocks as tools for the production of materials with precisely tunable properties.[1-3] Such a nano-building block would possess three-dimensional symmetry and easily modifiable peripheral functionality to allow the assembly process to be subtly altered as needed.[1-3]

Chapter 1 discusses possible candidates for this type of tool, and the merits of octaphenylsilsesquioxane (OPS)[4] for such a role. Chapters 2 and 3 describe the iodination and bromination of OPS in order to provide access to the necessary peripheral functionality. Chapter 4 explores the synthesis of ethynyl, hexaarylbenzene and graphene modified silsesquioxanes. Examples of crystalline derivatives were presented in each chapter to demonstrate the ability to purify these compounds by recrystallization to provide well-ordered precursors for successive synthetic modifications. Now we turn our attention to an investigation of the crystalline ordering of these molecules.

Coordination crystals are a topic of great current interest.[5,6] Desiraju's review[5] of supermolecular coordination motifs, or synthons, now has >1900 citations. Some synthon examples include hydrogen bonding, halogen···halogen and iodine···nitro short contacts, and π···π stacking.[5-9] The topic of "halogen bonding" was the focus of a symposium at the

Fall 2009 National ACS Meeting in Washington D.C., and provides further impetus for studying the supermolecular coordination in halogenated polyhedral phenylsilsesquioxanes.[10]

In particular, the synthons of halogen substituted aromatic compounds, have been a subject of much investigation. There are three 2-D halogen···halogen synthons: Type I, Type II, and X_3, as seen in Figure **5.1**.[5,6,8,11,12] These different modes are characterized by geometries derived from crystal structure data. Type I contacts have a parallel "slipped-stack" orientation; Type II contacts have nearly perpendicular orientation, and I_3 contacts offer a trimeric, triangular motif.[5,6,8,11,12]

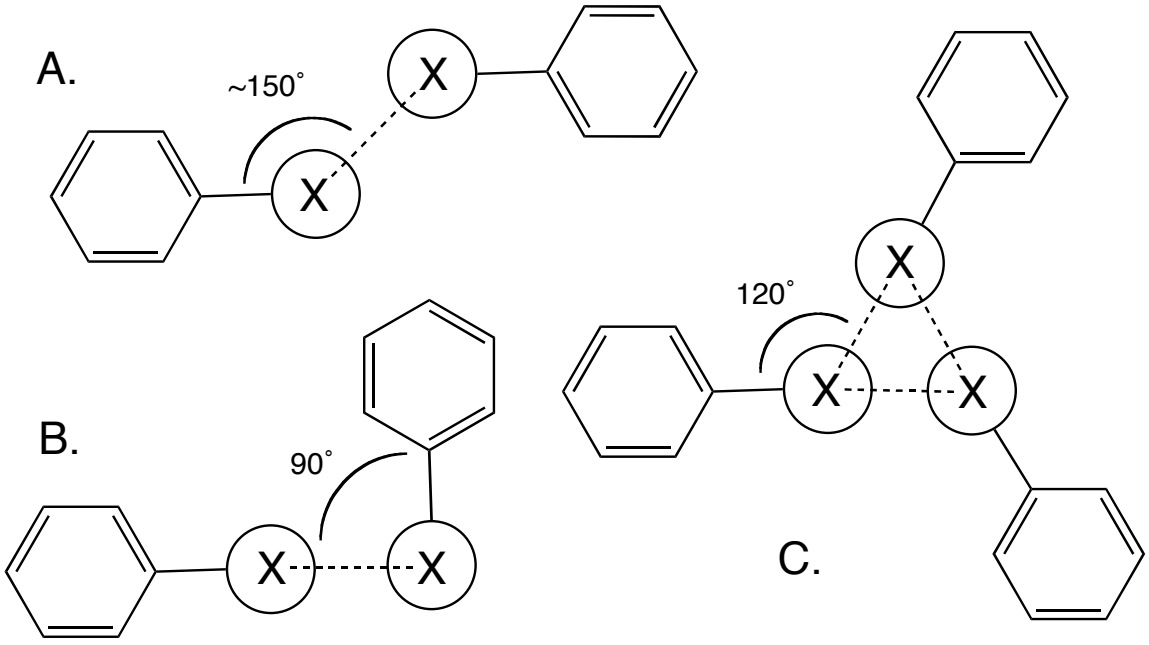

Figure 5.1 Type I (A.), Type II (B.), and X_3 (C.) halogen···halogen short contacts.[11]

Reports of halogen coordination have leveraged the extensive library of crystal data at the Cambridge Crystallographic Data Centre.[7,8,11-13] Systematic searches for specific geometries have allowed researchers to glean information regarding the synthon

geometry in halogenated organic crystal systems.[7,8,11-13] Many of the current experimental and theoretical studies use the availability of poly-halogenated aromatics to develop structure-property relationships.[7,8,11-13]

Recent theoretical analysis was done with respect to the underlying physical phenomena.[11,14] Calculations by Bosch, shown in Figure **5.2**, predict permanent polarization of iodobenzene.[14] Thus, the motifs seen in Figure **5.1** can be described as intermolecular, electrostatic interactions.

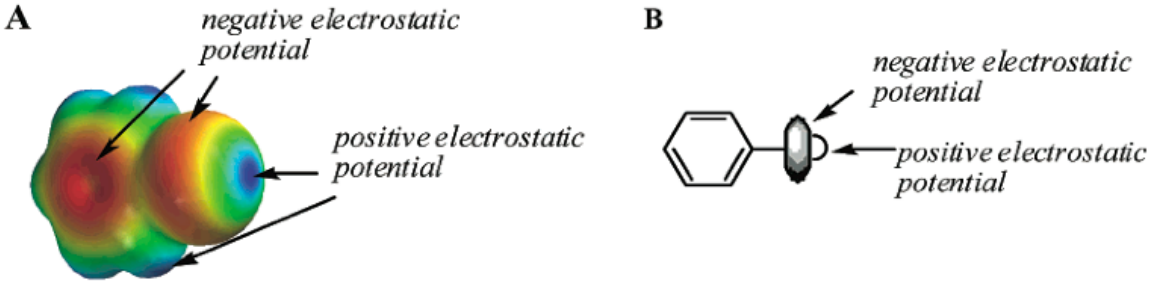

Figure 5.2 A. Calculated electrostatic potentials for iodobenzene. B General schematic model of halobenzene molecule.[14]

Each synthon has a characteristic set of short contacts, often defined as an interatomic distance less than the sum of the van der Waal radii. Desiraju has conducted extensive statistical studies of the CCDC in order to better understand the nature of these "halogen bonding" structures.[7,10,13] In a recent report, Ganguly and Desiraju tackle the ramifications of electrostatic coordination as the physical mechanism underpinning supermolecular synthons.[7]

Ganguly and Desiraju conclude that structure-determining electrostatic or "n-polar" interactions are capable of acting over larger distances than a simple sum of the standard van der Waal radii.[7,15] This is unsurprising considering vdW interactions are based on induced dipole or London forces, while the electrostatic forces are much

stronger.[16] In fact, the researchers calculate that the "n-polar" radii of the halogens is ~10 % larger than the standard vdW radii, and this calculation is done by modeling the electrostatic interaction of the atom with a pair of test charges.[7] In general terms, these halogen bonding forces are considered to be <10 kJ/mol, while hydrogen bonding forces may be significantly stronger, 20-40 kJ/mol.[5]

There are fewer examples of halogen···halogen coordination or "halogen bonding" in 3-D symmetric molecules.[12,16,17] Early examples include the tetrahedral X_4 synthons reported for tetrabromomethane and tetra(*p*-bromophenyl)methane.[16] Recently, examples of Br···C synthons in ethynyl and bromine functionalized adamantane derivatives have been reported, suggesting further opportunities to tailor crystal structures.[17] In addition, Desiraju has recently discussed C···I and I_4 synthons of mono- and tetra-iodinated tetraphenylmethane.[12]

Table **1** lists the numerical details for specific interactions that will be discussed in this chapter, and the sums of the vdW and "n-polar" radii are given in Å.

Table 5.1 Details of short contacts to be discussed in this chapter

Short Contact Type	Sum of vdW Radii (Å)	Sum of "n-polar" Radii (Å)
C···H	2.9	2.9
H···H	2.38	2.4
H···I	3.23	3.4
I···I	4.08	4.4
C···I	3.74	3.9
AromaticCentroid···I (ArC···I)	-	-
Br···Br	3.7	4.08
Tetrahedral Br_4	3.7	4.08

Desiraju defines crystal engineering as "the understanding of intermolecular interactions in the context of crystal packing and in the utilization of such understanding

in the design of new solids with desired physical and chemical properties."[6] This is fundamentally the same goal for nano-building blocks, so it is natural to explore them similarly. Desiraju describes three distinct phases of crystal engineering:

> 1.) the study of intermolecular interactions;
>
> 2.) the study of packing modes, in the context of these interactions and with the aim of defining a design strategy; and
>
> 3.) the study of crystal properties and their fine-tuning with deliberate variations in the packing.
>
> In effect these three stages represent the "what", "how", and "why" of crystal engineering.[6]

The study of the halogen···halogen intermolecular interactions has been well outlined and studied by several groups,[5-8,11-14,16,17] so our work begins at the second phase. Since the halogenated OPS derivatives possess a wealth of halogens, aromatic rings, and constrained polyhedral geometries, an effort to catalog coordination patterns, i.e. a "study of the packing modes,"[6] in these structures was undertaken. We initially expect that the "design strategy" (see above) will involve the unique 3-D structure of polyhedral silsesquioxanes in conjunction with halogen bonding to set the stage for the design of tailored materials.

From the perspective of materials chemistry, Metrangolo et al review reports of these halogen bonding forces used to direct solid-state organization and reactivity.[18] In particular, they highlight the ability of these forces to direct behavior in liquid crystals, organic semiconductors, magnetic materials, structured thin-films, non-linear optical materials and solid-state polymerization.[18,19] In the latter case, Caronna et al use halogen bonding between aromatic iodine and pyridyl groups to order molecules of *trans*-1,2,-

bis(4-pyridyl)ethylene (**bpe**) and subsequently photo-dimerize the **bpe** molecules using UV light.[19]

In the following sections, the two variables we will consider are chemical composition and geometry of the silsesquioxane core. We will begin by discussing the iodinated OPS, dPS and DPS. With these systems, we maintain the chemical composition, and alter core geometry to study the effects on the permitted coordination motifs and the degree of intermolecular interaction. Finally we will discuss the brominated OPS derivatives, examining the changes in coordination and intermolecular interaction as cubic core geometry is maintained and the chemical composition (and halogen substitution pattern) is changed.

With these structure-property relationships, open structures for infiltration, sequestration, or "guest-host" materials can be targeted. In addition, tighter intermolecular packing of electron rich molecules might be useful for the production of high dielectric materials.

Results and Discussion

Octa(p-iodophenyl)silsesquioxane

The crystal structures of the iodinated octaphenylsilsesquioxane show examples of I···I motifs, as well as C···I short contacts. The vdW radius of iodine is given by Bondi to be 2.04 Å, so an I···I short contact would be a less than 4.08 Å.[15] Ganguly and Desiraju calculate the "n-polar" radius for iodine as 2.2 Å,[8] where an I···I short contact would be a less than 4.4 Å. In contrast, both the "n-polar" and Bondi radii for carbon are 1.7 Å.

For reference, recently Desiraju described I···I short contacts in the I_3 motif of 3.75-3.79 Å (~8 % below VdW sum) as "particularly short."[20] The tetrahedral I_4 synthon in tetra(*p*-iodophenyl)methane described by Desiraju has I···I short contacts of 3.949 and 4.161 Å, an average of 4.05 Å.[12] Using the Bondi radii, C···I short contacts are less than 3.74 Å.[15] Using the "n-polar" radii, C···I short contacts are less than 3.9 Å.[7]

In I_8OPS there is a continuous network of channels comprising 39% of the unit cell occupied by disordered ethyl acetate solvates as calculated by PLATON.[25] If only close packing forces directed the formation of the crystal structure, the solvent would be expected to be trapped in one or two positions. However, the degree of solvate disorder suggests that these channels are held open by ArC···I (coordination of aromatic iodides and aromatic carbons) and I···I Type II short contacts.

The *para* substitution puts the iodine, known to be a strong halogen bonding species,[13] directed outwards on the edges of the molecule. Therefore, it might be expected that subsequent halogen bonding interactions of the iodine *must* be intermolecular. Furthermore, if I···I interactions dominate, there should be minimal interdigitation of the aromatic rings, leaving accessible voids close to the faces of the silsesquioxane cages. Lastly, such coordination could allow for "host" crystal structures, which could be infiltrated with a desired "guest."

Figure **5.3** shows two pairs of Type II contacts (3.8 Å) found in the I_8OPS structure. Though there are three coordinating iodines, the 90° coordination angles are best described by a Type II contact, not an I_3 motif. Each of these contacts is 4 % shorter than twice the vdW radius of iodine, or "particularly short."[20]

Figure **5.4** shows the recently reported crystal structure of cis-1,3,5-tris(iodomethyl)-1,3,5-triphenylcyclotriphosphazene. It possesses a double Type II coordination pattern analogous to the one seen in I_8OPS (Figure **5.3**).[21]

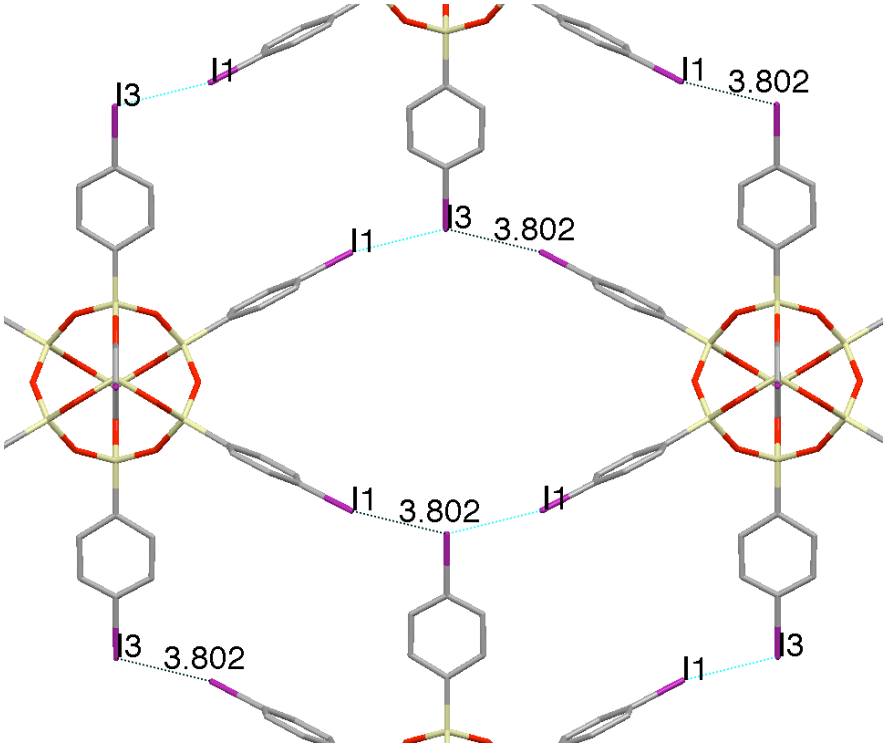

Figure 5.3 Four coplanar I_8OPS molecules coordinated via I···I Type II short contacts (distances in Å).

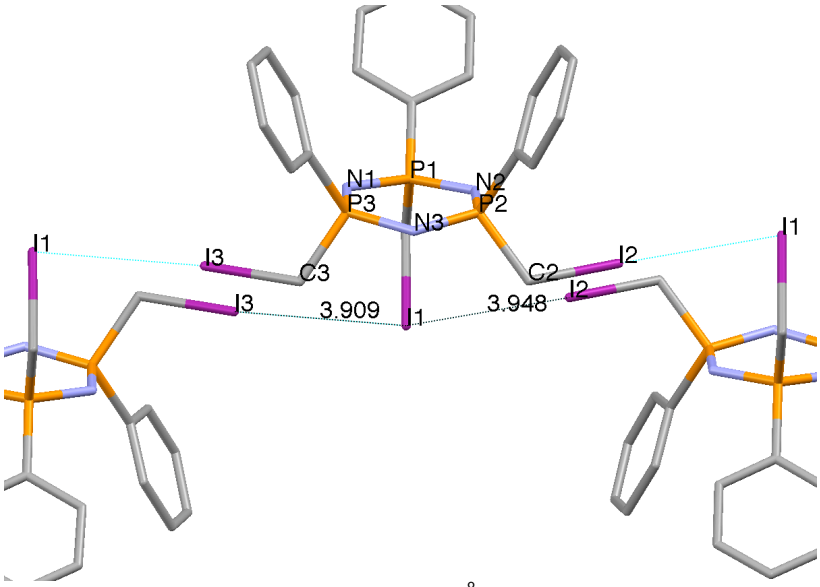

Figure 5.4 I···I Type II short contacts (Å) in cis-1,3,5-tris(Iodomethyl)-1,3,5-triphenylcyclotriphosphazene.[21]

Figures **5.5** and **5.6** allow for a comparison of AromaticCentroid···I (ArC···I) (Table **5.1**) short contacts in the I_8OPS structure and those found (4-iodophenyl)triphenylmethane. Desiraju's analysis of the motif shown in Figure **5.5**, also discussed the rarity of this type of contact.[12] The ArC···I distances is 3.746Å and the shortest C···I distance is 3.606 Å. In I_8OPS the analogous ArC···I distance is 3.395 Å and the shortest C···I distance is 3.349 Å, almost 10% shorter. In addition, the short ArC···I contact in I_8OPS is a result of three simultaneous short contacts of I3 with C14, C15, and C16. From their studies Metrangolo et al conclude that the shorter the halogen bonding distance, the stronger the bond.[18]

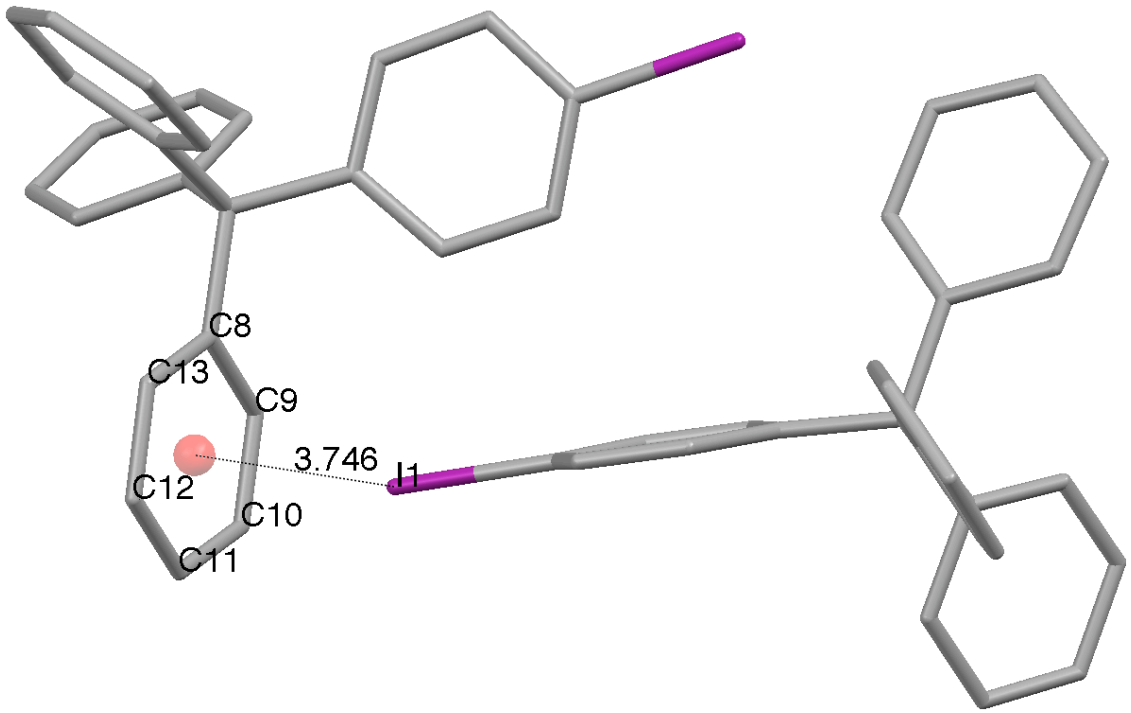

Figure 5.5 ArC···I interactions in (4-iodophenyl)triphenylmethane (Å).[12]

In Figure **5.7**, the combination of four one-dimensional ArC···I short contacts in I_8OPS forms a square pore between adjacent molecules. A similar coordination motif is found in the crystal structure of diiodoacetylene, with slightly larger coordination distances, as shown in Figure **5.8**.[22]

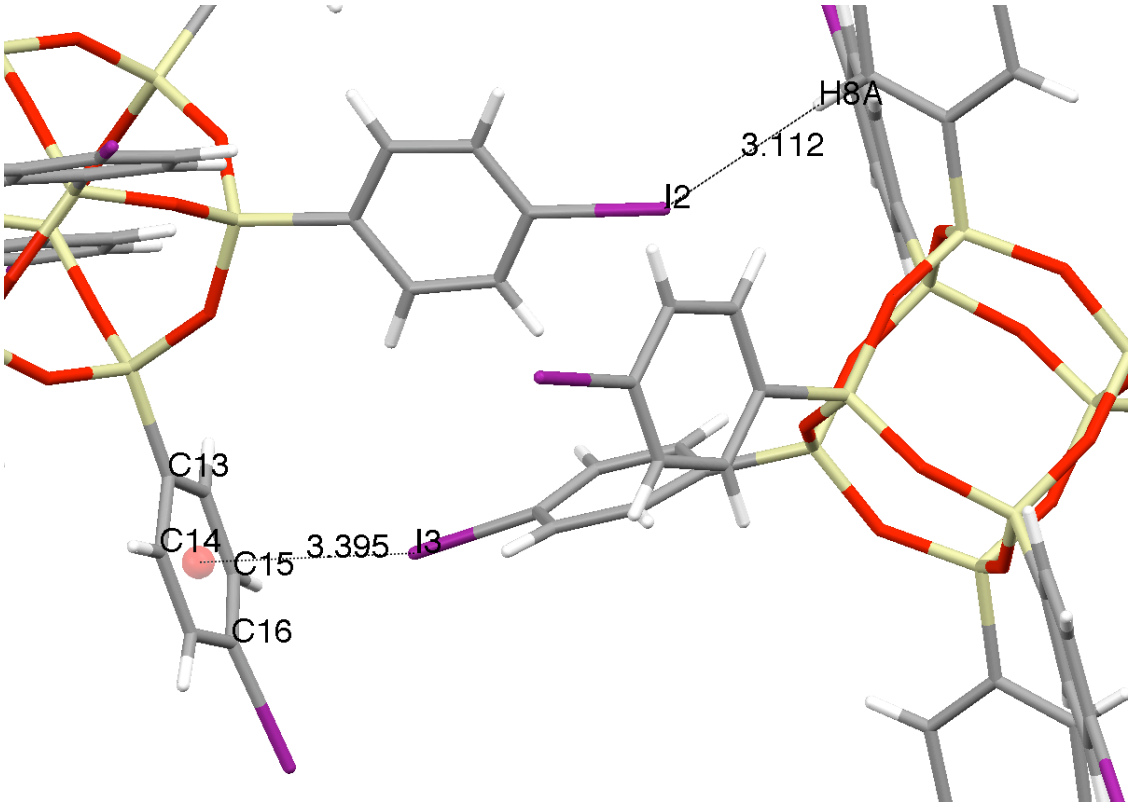

Figure 5.6 ArC···I interactions found in octa(*p*-iodophenyl)silsesquioxane (Å).

Table **5.2** lists the numerical details for the short contacts found in the I_8OPS structure. While there are a total of twenty-four contacts per molecule, these contacts are symmetrically related and are fully described by the five unique measurements listed. The short contacts range from 2 to 9 % less than the sum of the Van der Waal (vdW) radii of the two atoms.

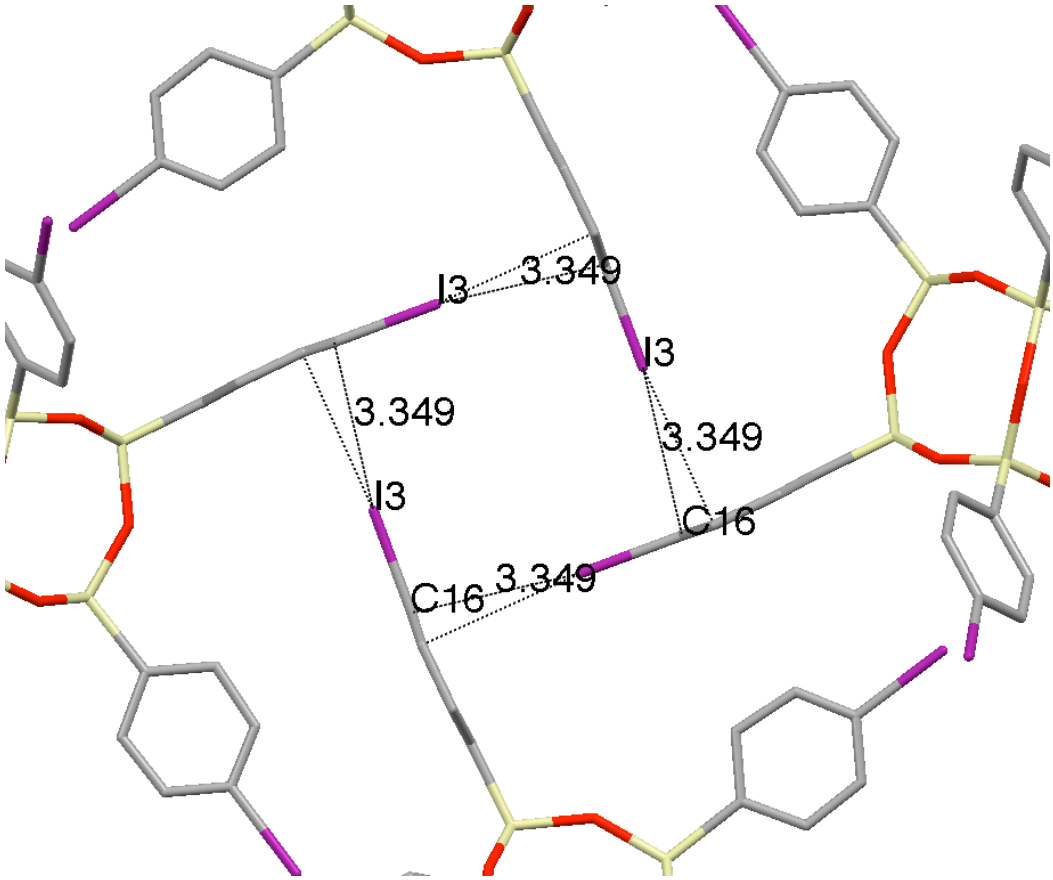

Figure 5.7 Square ArC···I coordination motif as seen in I_8OPS.

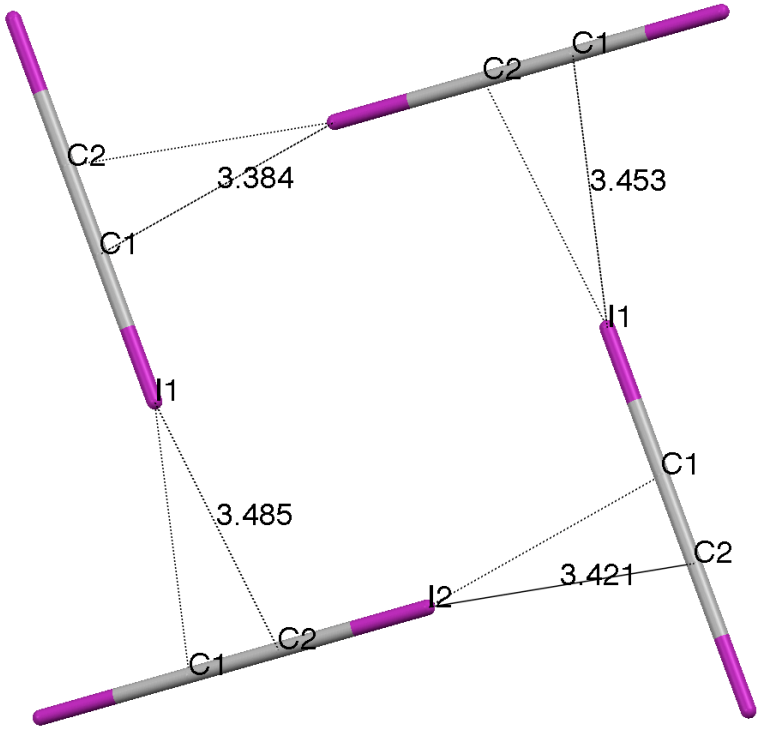

Figure 5.8 Square C···I coordination motif as seen in diiodoacetylene.[22]

Table 5.2 Listing of short contacts found in the crystal structure of octa(*p*-iodophenyl)silsesquioxane

Atom 1	Atom 2	Distance	vdW sum (Å)	Percent Under vdW sum	Number per molecule
I3	I1	3.802	4.08	-3.99%	8
H8A	I2	3.112	3.24	-2.14%	4
I3	C15	3.55	3.74	-3.53%	8
I3	C16	3.349	3.74	-8.99%	4

This initial discussion highlights one difference seen in the silsesquioxane structures, the presence of multiple, unique motifs along different crystallographic directions. Thus, I_8OPS exhibits supermolecular synthons analagous to published examples, with more significant short contacts, indicating stronger intermolecular interaction. Again, the stabilization energies are estimated to be of the order 10 kJ/mol.[3] The calculated density of the tetra(*p*-iodophenyl)methane is 2.2 g/cc, while the density of I_8OPS is 1.64 g/cc. In fact, the density of the (4-iodophenyl)triphenylmethane is 1.55 g/cc, even through it is primarily hydrocarbon. Finally, neither iodinated tetraphenylmethane structure possesses voids or channels with disordered solvates. The combination of 3-D symmetry and multifunctionality in I_8OPS multiplies the degree of supermolecular coordination, allowing for possible "guest/host" materials.

Deca(p-iodophenyl)silsesquioxane

In I_{10}dPS there are four voids comprising 23 % of the unit cell, as calculated by PLATON,[25] occupied by disordered ethyl acetate solvents. Again, if only close packing forces directed the formation of the crystal structure, solvates would be expected to be trapped in one or two positions. In this case, it appears the voids are held open by C···I, (coordination of aromatic iodides and aromatic carbons) I···O, (coordination of aromatic

iodides and cage oxygens) H···H, and C···H (edge-face interactions between aromatic moieties) short contacts.

Figure **5.9** shows the coordination of aromatic iodines to oxygens in the silsesquioxane cage. I1 and O3 are separated by a distance of 3.47 Å. The Bondi and "n-polar" radii for oxygen are 1.52 and 1.57 Å, respectively, so I···O short contacts are less than 3.56 Å using Bondi radii and 3.77 using "n-polar" radii. Short contacts have been reported in halogen bonding thyroid protein studies, and are consistent with the halogen bonding concept developed by Metrangolo et al.[18]

An additional coordination feature seen in I_{10}dPS is C···H, edge-face short contacts between adjacent aromatic rings (Figure **5.9**). A C···H short contact is less than 2.9 Å, and this coordination motif is seen in Phase I of benzene (Figure **5.10**), as recently discussed by Desiraju. [12]

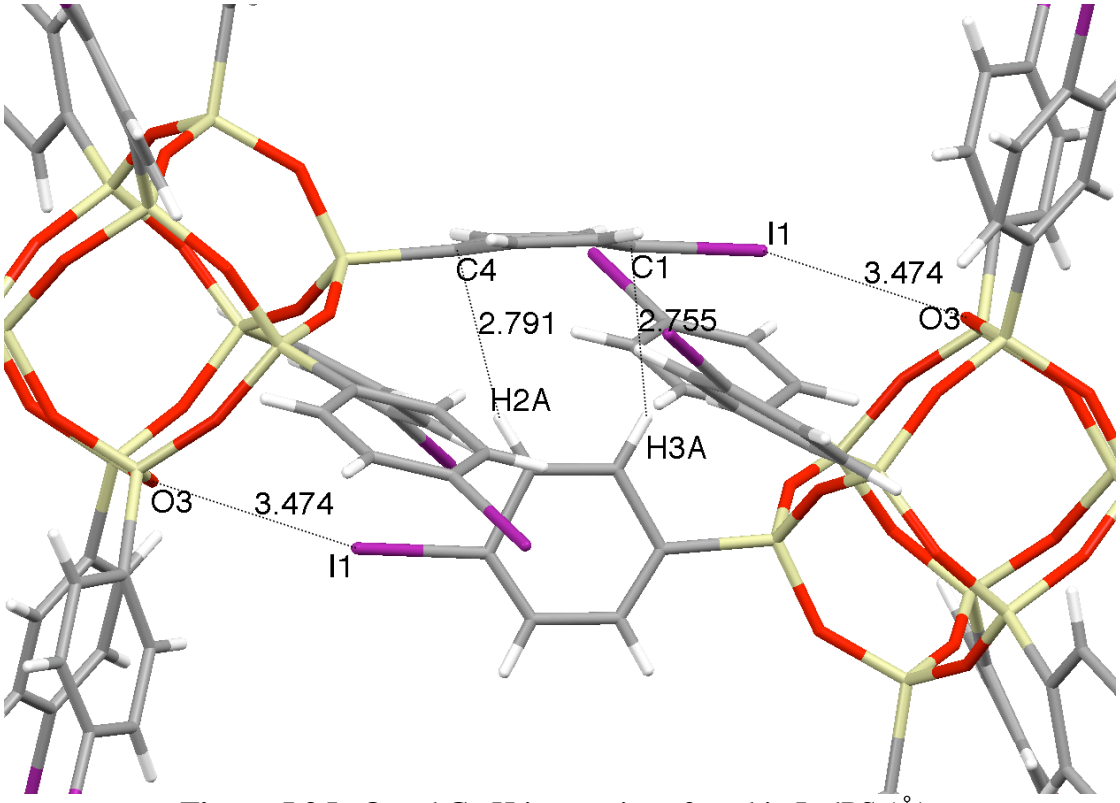

Figure 5.9 I···O and C···H interactions found in I_{10}dPS (Å).

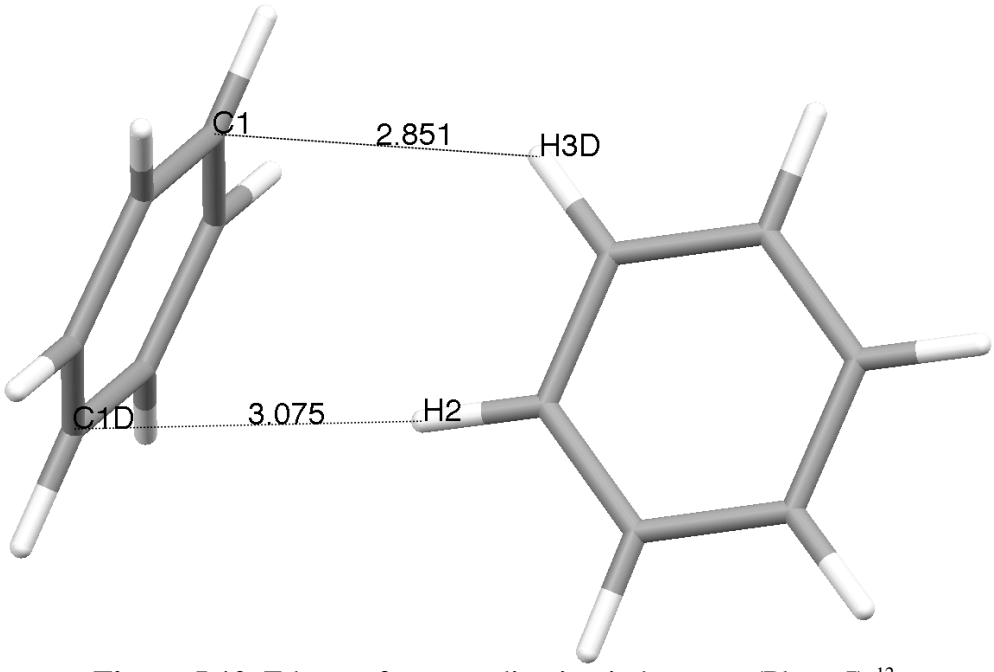

Figure 5.10 Edge-to-face coordination in benzene (Phase I).[12]

The crystal structure of I_{10}dPS also shows examples of H···I and H···H short contacts. The "n-polar" and Bondi radii of carbon are 1.2 and 1.19 Å, respectively, so an H···I short contact would be a less than 3.23 Å (Bondi) or 3.4 Å ("n-polar).[15] An H···H short contact would be a less than 2.38 Å (Bondi) or 2.4 Å ("n-polar).[15] Figure **5.11** shows significant H···I short contacts between H18A and I5, 6 % below the vdW sum and 11 % below the "n-polar" sum. The H···H short contacts are nominal, 2% below the vdW and "n-polar" sums.

Figure **5.12** shows C···C and C···I short contacts in I_{10}dPS. As with I_8OPS, using the Bondi radii, C···I short contacts are less than 3.74 Å.[15] Using the "n-polar" radii, C···I short contacts are less than 3.9 Å.[7] The four distinct C···I short contacts (C10-I4, C9-I4, C28-I3, C29-I3) are found, ranging from 3.4-3.6 Å, ~10 % below the sum of the radii.

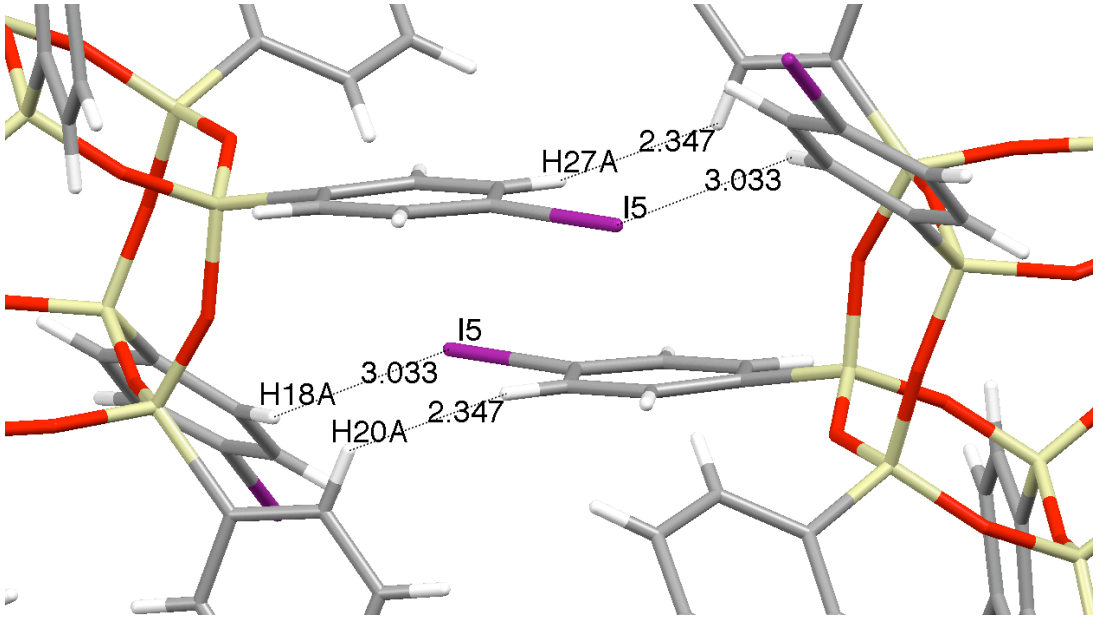

Figure 5.11 H···I and H···H short contacts found in I_{10}dPS (Å).

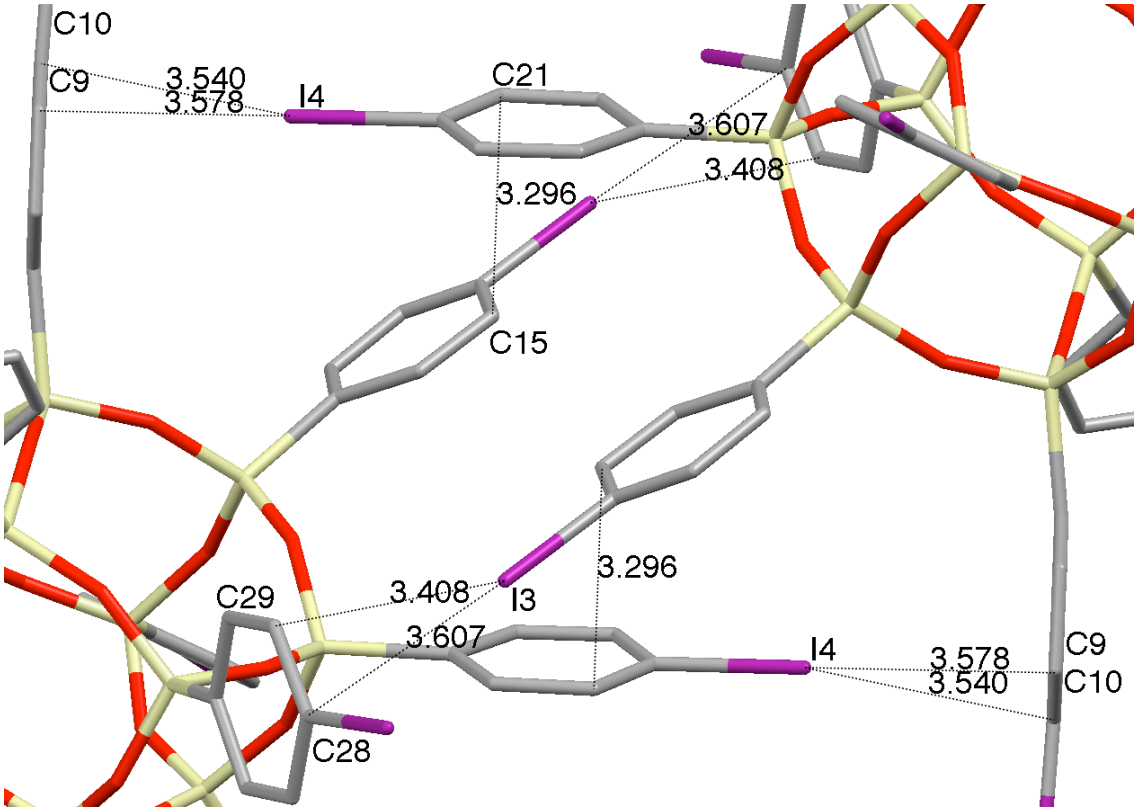

Figure 5.12 C···I and C···C short contacts found in I_{10}dPS (Å).

Figure **5.13** shows corresponding ArC···I distances 3.6 and 3.8 Å are similar to those seen in the (4-iodophenyl)triphenylmethane system, 3.75 Å. The C···C short contact between C15 and C21 is 3 % below the sum of the vdW or "n-polar" radii. Table **5.3** lists the numerical details for the forty-eight short contacts found in the I_{10}dPS structure.

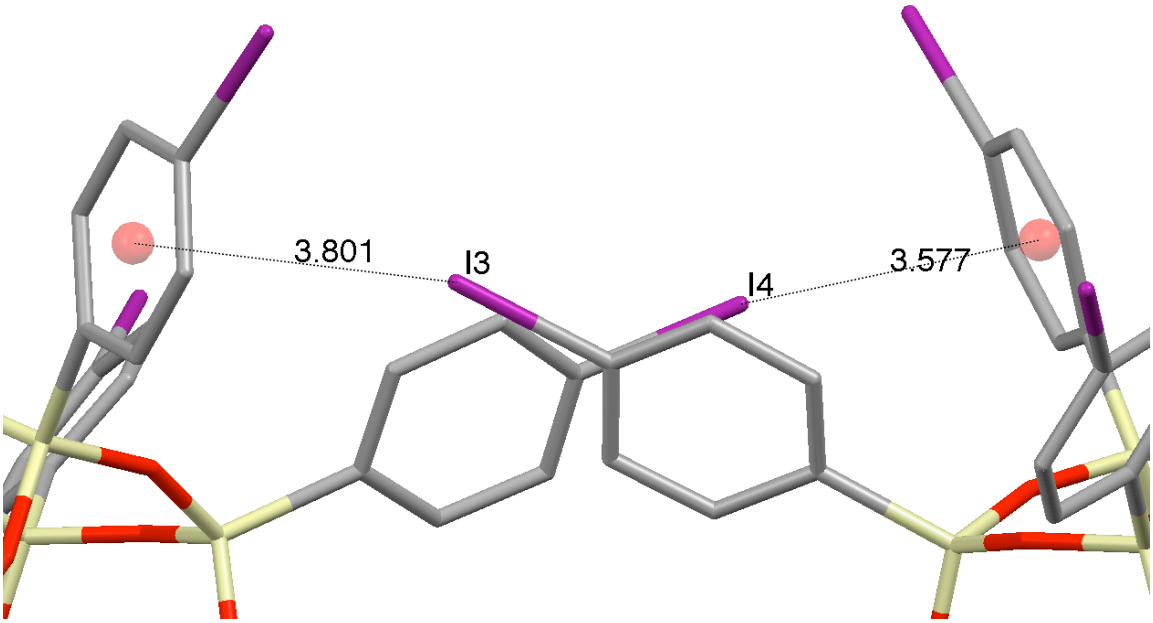

Figure 5.13 ArC···I interactions found in I_{10}dPS (Å).

Table 5.3 Listing of short contacts found in the crystal structure of deca(*p*-iodophenyl)silsesquioxane

Atom 1	Atom 2	Distance	vdW sum (Å)	Percent Under vdW sum	Number per molecule
C29	I3	3.408	3.74	-7.27%	4
H18A	I5	3.033	3.24	-4.54%	4
H3A	C1	2.755	2.9	-5.00%	2
C10	I4	3.54	3.74	-3.74%	4
H2A	C4	2.791	2.9	-3.76%	2
H17A	C11	2.793	2.9	-3.69%	4
C21	C15	3.296	3.4	-3.06%	4
C9	I4	3.578	3.74	-2.73%	4
C28	I3	3.607	3.74	-1.95%	4
C22	I2	3.621	3.74	-1.58%	4
H27A	H20A	2.347	2.4	-2.21%	4
O3	I1	3.474	3.56	-0.73%	4
C29	H9A	2.887	2.9	-0.45%	4

The crystal structure of I_{10}dPS demonstrates that the rigid silsesquioxane core effectively dictates which short contacts actively drive the intermolecular coordination in the crystal structure. While I_8OPS exhibits significant I···I coordination, I_{10}dPS shows none. Both structures exhibit C···I halogen bonding, with ArC···I distances similar or below those reported. Finally, C···C, C···H, and H···H short contacts are seen in the I_{10}dPS but I_8OPS shows none. By changing the geometry of the core, we see activation and deactivation of different coordination modes, or synthons.

Dodeca(p-iodophenyl)silsesquioxane

We now consider the dodecameric *p*-iodophenylsilsesquioxane. Based on the discussion of the I_8OPS and I_{10}dPS structures, we expect and find a combination of new coordination motifs in addition to the previously described examples.

Figure **5.14** shows a Type II I···I short contact (7% less than vdW sum), as found in the I_8OPS structure. However, a new type of short contact is also seen, a minimal (< 1 % less than the VdW sum) Si···I short contact. This is consistent with the previous work of Bosch et al regarding the electrostatic polarization of aromatic halides.[14] The electropositive cap of the iodine will have a relatively weak electrostatic attraction to the relatively electropositive Si atom.[14]

Analogous Si-F coordination is described in the perfluorinated alkyl silsesquioxanes studied by Mabry.[21] However, due to fluorine's high electronegativity and the strength of the Si-F bond, Mabry finds this short contact to be 16 % shorter than the sum of the VdW radii.[21]

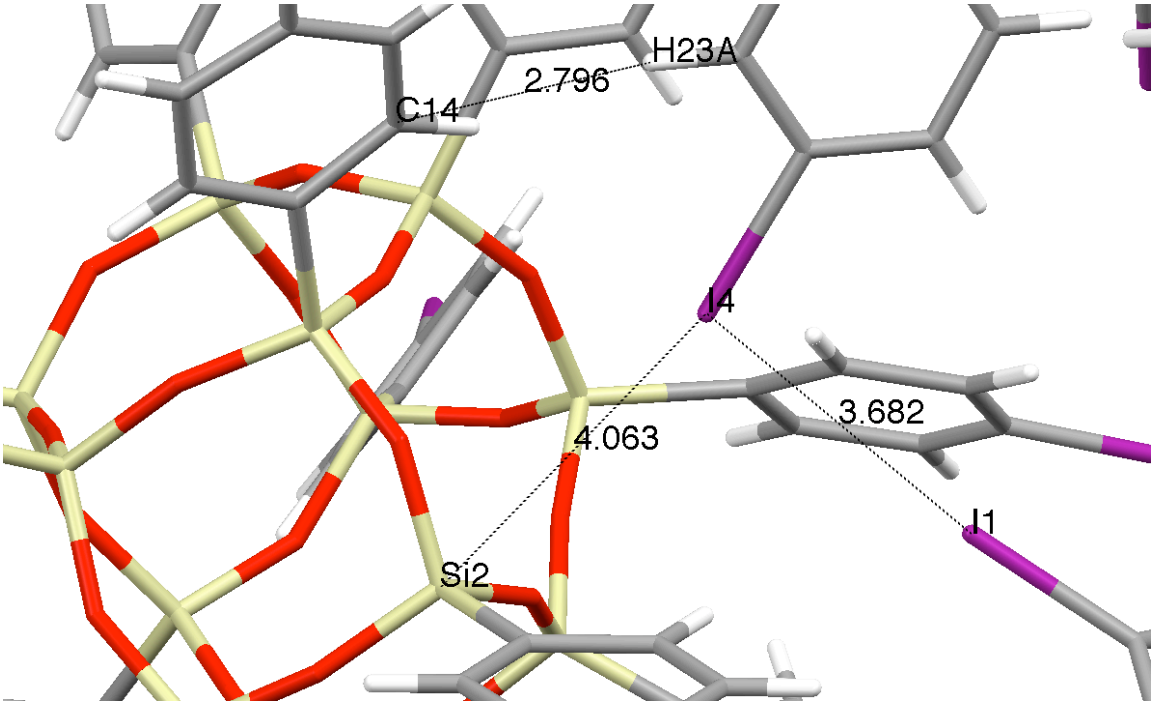

Figure 5.14 I_{12}DPS molecules coordinated via C···H, I···I, and Si···I short contacts.

Figure **5.15** shows ArC···I short contacts between the aromatic I6 and C18 on the adjacent aromatic ring in I_{12}DPS. In this case, the contact is found to be 12% below the sum of the vdW radii of the atoms. As expected from the fact that carbon and iodine atoms are the primary constituents of the organic periphery of these silsesquioxanes, we can see that the C···I short contacts are found in all three structures, I_8OPS, I_{10}dPS, and I_{12}DPS.

As found in the I_{10}dPS structure, there is edge-face coordination between adjacent aromatic rings. In this case, C-H short contacts are found between H12A/C18 (2.858 Å) and C11A/C26 (2.885 Å). Also in common, the iodine substituents of the coordinated aromatic rings are themselves involved in a short-contact coordination, in this case between I6 and C18 (Figure **5.15**). Figure **5.16** shows an additional C···I short contact

motif between C29 and I5, 2% under the sum of the vdW radii of the atoms 6% under the sum of the "n-polar" radii.[12]

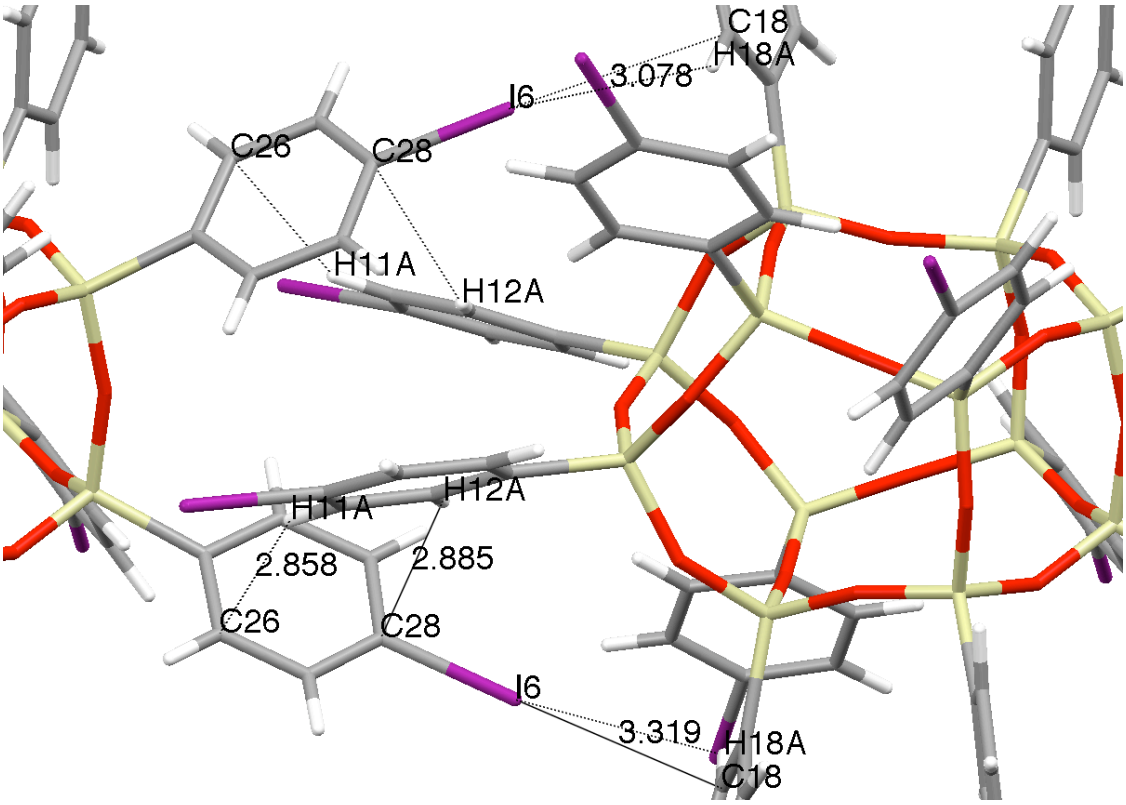

Figure 5.15 I_{12}DPS molecules coordinated via C···I and C···H short contacts.

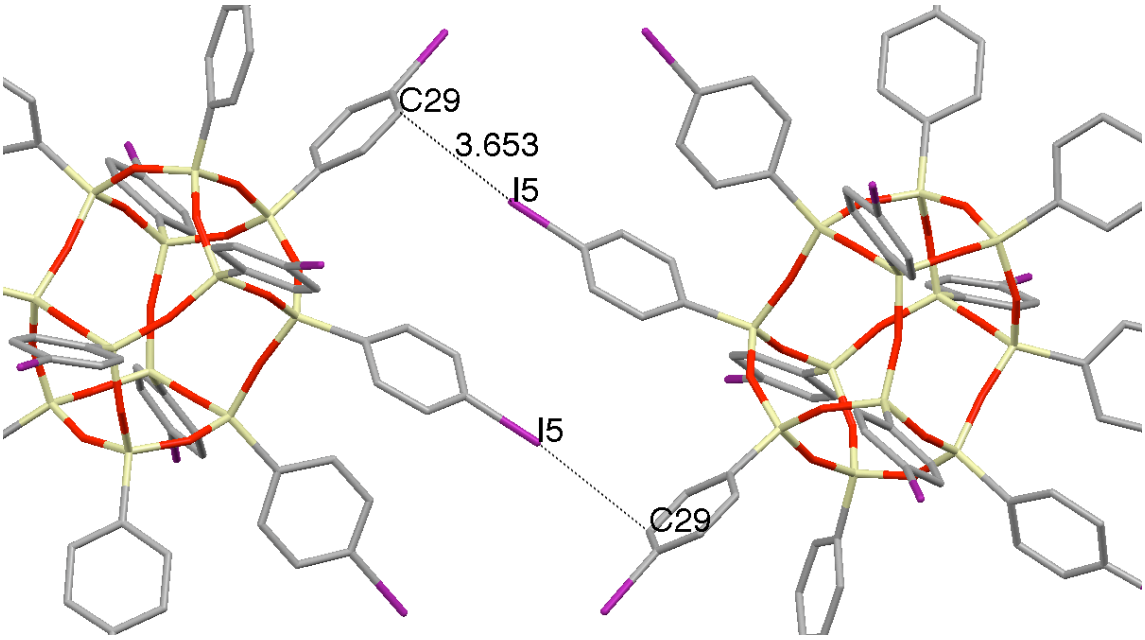

Figure 5.16 I_{12}DPS molecules coordinated via C···I short contacts.

In total, there are 36 contacts per I_{12}DPS molecule, which can be reduced by symmetry to the 9 measurements below in Table **5.4**. It may be worth noting that this are 25 % fewer contacts per molecule in the I_{12}DPS system versus the I_{10}dPS system. This may indicate that there exists a distribution of coordinating moieties on the periphery which maximizes the intermolecular interaction. The contact distances range from 1 to 13% below the sum of the van der Waal radii of the atoms.

Table 5.4 Listing of short contacts found in the crystal structure of dodeca(*p*-iodophenyl)silsesquioxane

Atom 1	Atom 2	Distance	vdW Sum	Percent Under vdW Sum	Number per molecule
I6	C18	3.319	3.74	-9.8%	4
I6	H18A	3.078	3.24	-3.2%	4
C26	H11A	2.858	2.9	-1.4%	4
C28	H12A	2.885	2.9	-0.5%	4
I1	I4	3.682	4.08	-7.0%	4
I4	Si2	4.063	4.14	-0.4%	4
H14A	H23A	2.082	2.4	-13.3%	4
C29	I5	3.653	3.74	-0.7%	4
C14	H23A	2.796	2.9	-3.6%	4

Thus far, we have seen that I_{12}OPS exhibits supermolecular synthons analogous to published examples, including the Si···I short contact not seen in I_8OPS or I_{10}dPS. Type II I···I are seen in both I_{12}DPS and I_8OPS. C···H short contacts are found in the edge-face coordination of adjacent aromatic rings, are seen in I_{12}DPS and I_{10}dPS. Finally, C···I short contacts are found in all three structures.

Even though the chemical compositions are the same, $(IC_6H_4SiO_{3/2})_n$, it can be seen that geometry of the silsesqioxane core dictates specific intermolecular short-contact motifs. Again, the combination of 3-D symmetry and multifunctionality in I_8OPS, I_{10}dPS, and I_{12}OPS multiplies the degree of supermolecular coordination.

We now shift our attention to the brominated OPS derivatives which have a different set of substitution patterns but all with the same cubic core.

Octa(o-bromophenyl)silsesquioxane

Figure **5.17** shows the octa(*o*-bromophenyl)silsesquioxane crystal structure, which has several unique *intra*-molecular coordination features, due to the *ortho* substitution pattern. Type I coordination is found in two pairs of bromophenyls on opposite sides of the molecule. One of these Br···Br interactions is a short-contact using Bondi vdW radii (3.7 Å), while the other is shorter than the sum of the "n-polar" radii (4.08 Å).[12]

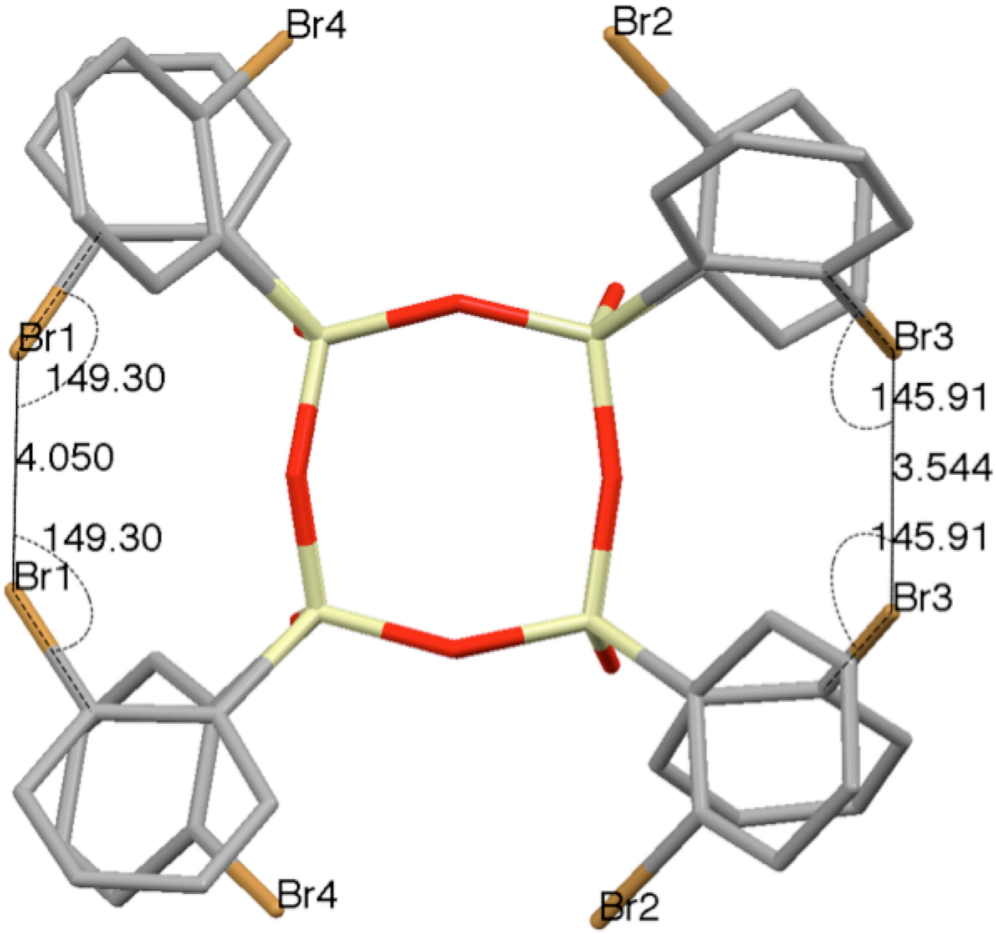

Figure 5.17 Intramolecular bromine short contacts in *o*-Br_8OPS.

Each molecule is paired with a second through a tetrahedral "Br_4" synthon, as shown in Figure **5.18**. Along the crystallographic *c*-axis two intramolecular Type I Br3-

Br3A contacts measure 3.54 Å, and four intermolecular Type I Br3-Br3A contacts measure 3.758 Å. A search of the Cambridge Crystallographic Database finds these distances to be the shortest reported for a Br_4 synthon.[22]

Thus, the four Br3, Br3A, Br3' and Br3A' atoms can be said to have a total of *six* simultaneous short contacts. Figure **5.18** shows tetrahedral coordination between four bromine atoms in tetra(*p*-bromophenyl)methane, with Br···Br distances of 3.9 Å, shorter than the sum of the "n-polar" radii, 4.08 Å. These coordination distances are 5-7% greater than those seen in the octa(*o*-bromophenyl)silsesquioxane structure.[16]

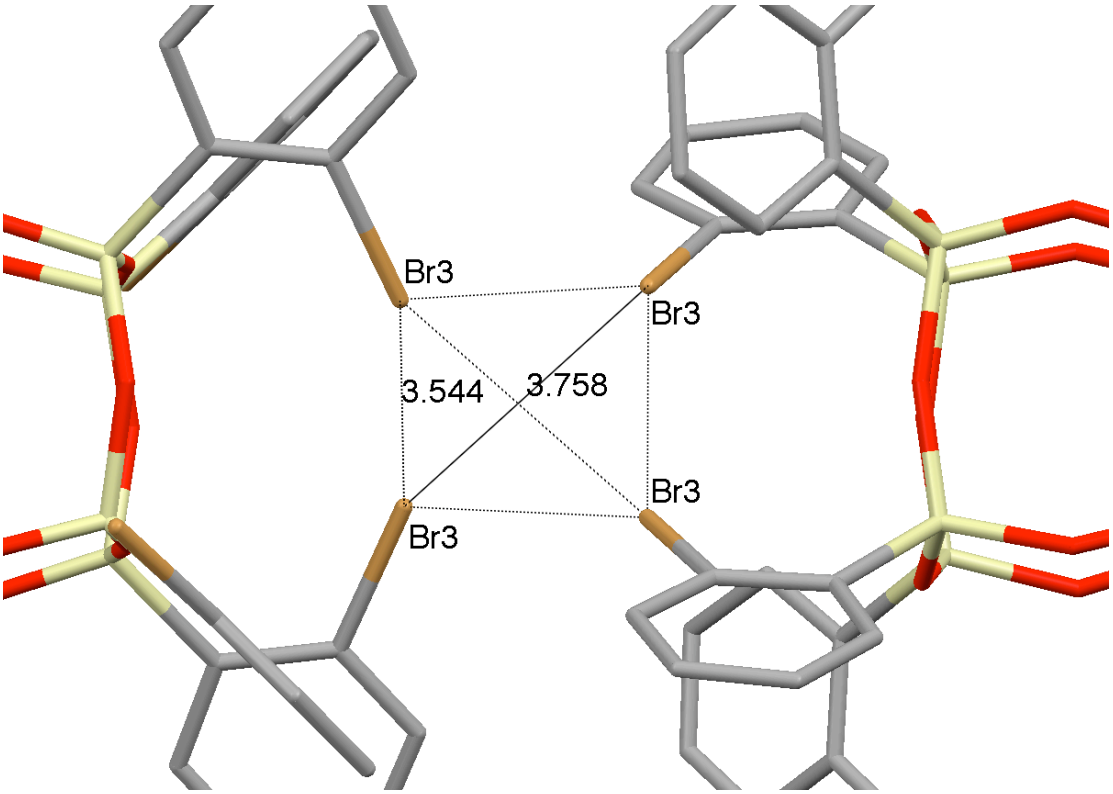

Figure 5.18 Tetrahedral bromine coordination in *o*-Br_8OPS.

Figure **5.20** shows that intermolecular coordination along the *a* and *b*-axes is dominated by C···H short contacts with the silica cage. Table **5.5** provides the full listing of short contacts found in the crystal structure of *o*-Br_8OPS. All contacts less than the

vdW sums are listed as well as Br···Br contacts under the sum of the "n-polar" radii (4.08 Å).[12] In total we find twenty-one contacts per *o*-Br_8OPS molecule. The calculated density of the crystal is 1.67 g/cc, slightly higher than I_8OPS, at 1.64 g/cc, despite the higher atomic weight of iodine.

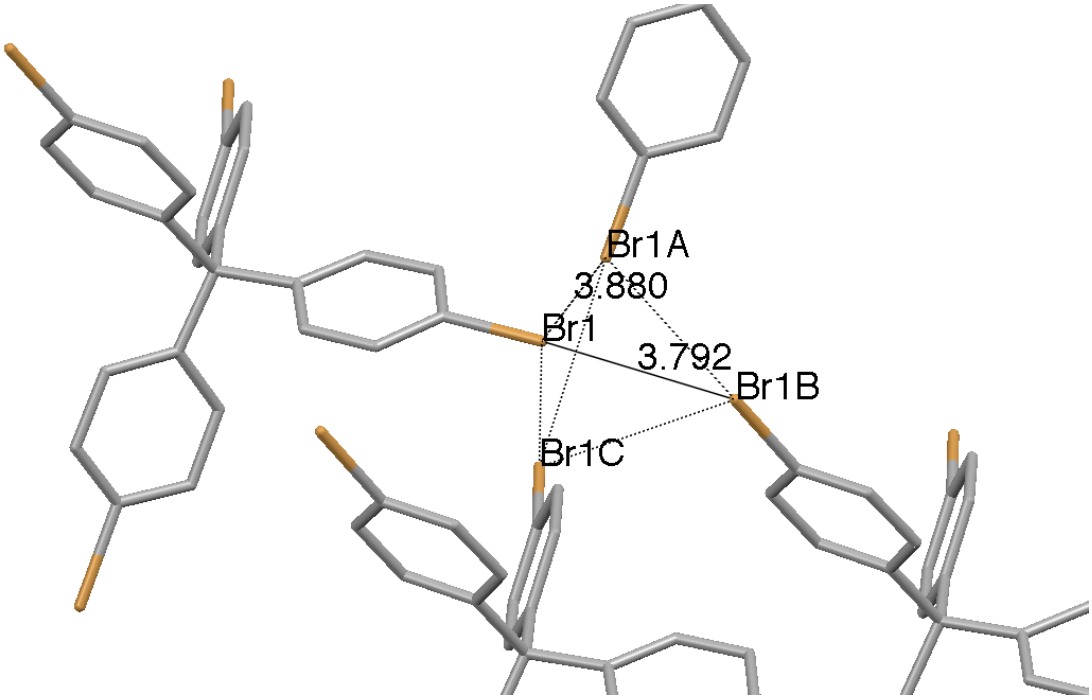

Figure 5.19 Tetrahedral coordination motif in tetrabromophenylmethane.[16]

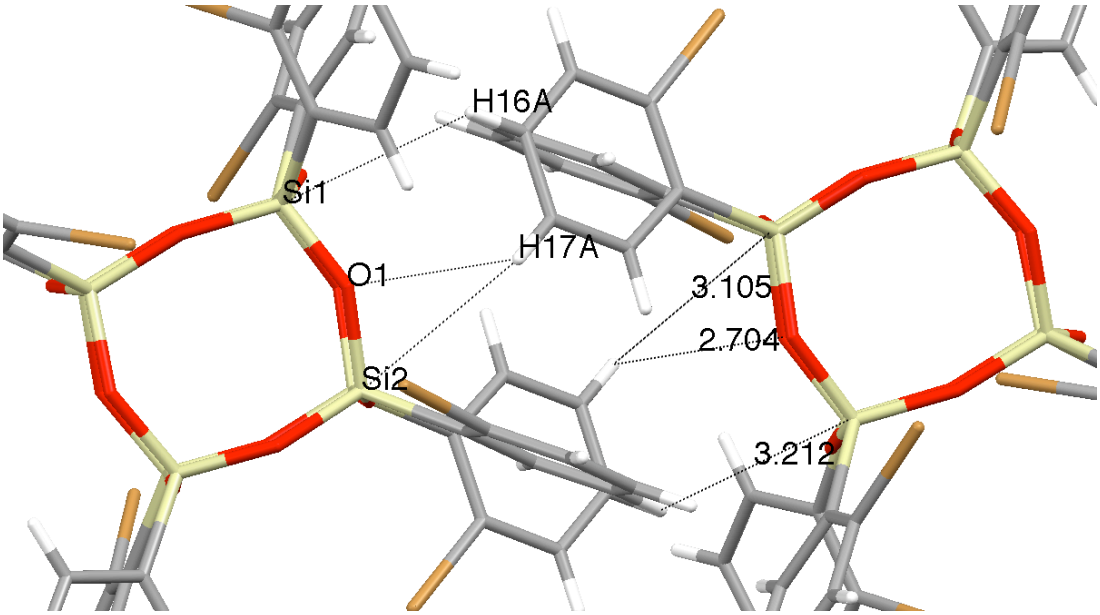

Figure 5.20 Cage and C-H Short Contacts along the *a* and *b*-axis in *o*-Br_8OPS.

Table 5.5 Listing of Short Contacts found in the crystal structure of *o*-Br_8OPS

Atom1	Atom2	Length (Å)	vdW sum (n-polar sum) (Å)	Percent under VdW sum (Percent under n-polar)	Number per molecule
Si1	H16A	3.212	3.3	-2.7%	4
Si2	H17A	3.105	3.3	-5.9%	4
O1	H17A	2.704	2.72	-0.6%	4
C10	H15A	2.819	2.9	-2.8%	4
Br3	Br3	3.544	3.7	-4.2%	1
Br3	Br3	3.758	3.7 (4.08)	1.57% (-7.9%)	4

The intermolecular Br_4 motif found in *o*-Br_8OPS has shorter contacts than any previously published. We also see *intra*-molecular coordination of bromines on adjacent phenyl rings via Type I short contacts. As the degree of bromination increases, while the molecular diameter remains constant, the number of short contacts is expected to increase.

Octa(2,5-dibromphenyl)silsesquioxane

In the crystal structures of all *para* I_8OPS and its derivatives, the substituted functionality is directed outwards. As a result we see that intermolecular coordination leads to a relatively open structure, with significant unit cell volume occupied by solvent molecules. In contrast, the intermolecular coordination in Br_{16}OPS is dominated by non-*para* substituted bromines, and the reverse is seen, very close-packed structures. Since halogen bonding can drive intermolecular coordination, we see that the geometry of the intermolecular packing may be strongly influenced by halogen substitution patterns.

The calculated density of octa(*o*-bromophenyl)silsesquioxane is 1.67 g/cc. In contrast, the density calculated for the octa(2,5-dibromphenyl)silsesquioxane crystal structure is 2.32 g/cc. Figure **5.21** shows short contacts between the cage silicon atoms (Si2) and the bromine in the 5 position (Br2) along the *b*-axis. Silicon is known to form

pentacoordinate complexes with electronegative atoms, and as stated earlier, Si-F short contacts (~16% below the vdW sum of the radii) were found in the crystal structures determined by Mabry of fluoroalkylsilsesquioxanes.[21]

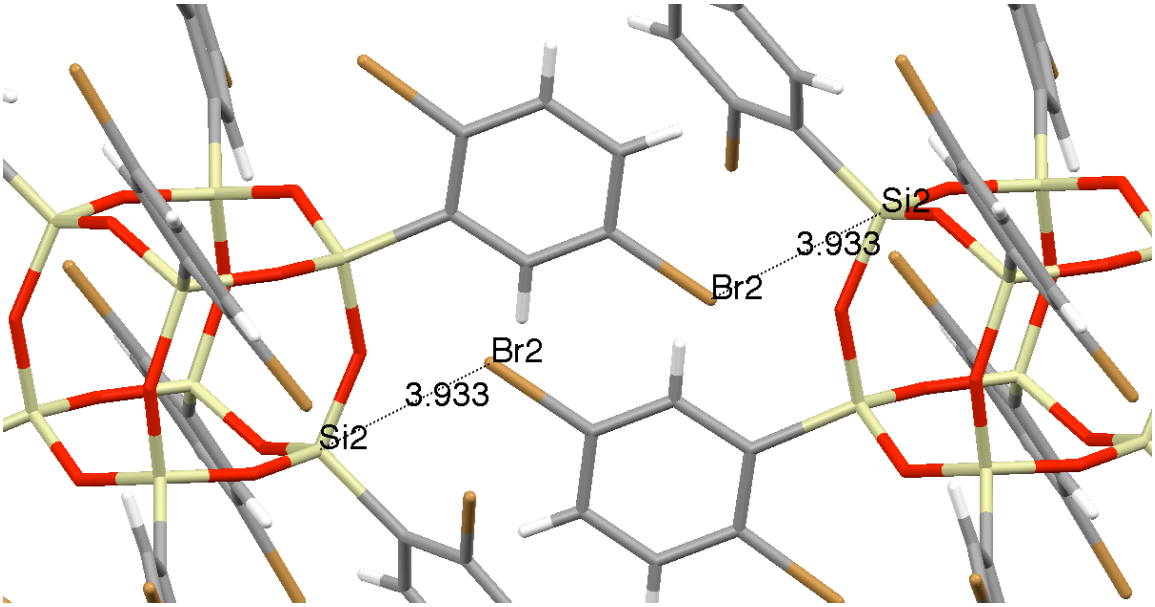

Figure 5.21 Si···Br short contact pair in Br_{16}OPS.

Along orthogonal axes, there are additional contacts. Figure **5.22** shows coplanar aromatic rings with multiple coordinating Br···Br short contacts. Though the Type II Br1···Br6 contacts are below the sum of the vdW radii; the Br5···Br6 contacts are only shorter than the sum of the "n-polar" radii. In this case, the negative "equatorial" sections of each bromine (Figure **5.2**) are in contact. Since like charges repel, the short contacts between these bromines are expected to be somewhat energetically unfavorable. Therefore, other short contacts with a higher energetic favorability must drive this geometry.

One unique feature of the OPS substrate is the constrained geometry and the octa-functionality. The 1 nm diameter of the molecule with sixteen bromines entails very short distances between bromines in the crystal structure, and Figure **5.23** demonstrates a 2-D

network of Br···Br contacts. For instance, two symmetric chains of Br1···Br4···Br5···Br8 short-contacts are found, joined by Br4···Br4'. The Type II Br5···Br8, Br1···Br4, and Br1···Br6 contacts are below the sum of the vdW radii. The Br4···Br4' contacts are shorter than the sum of the "n-polar" radii,[7] but again, the negative portions of each bromine are in contact, which is energetically unfavorable.

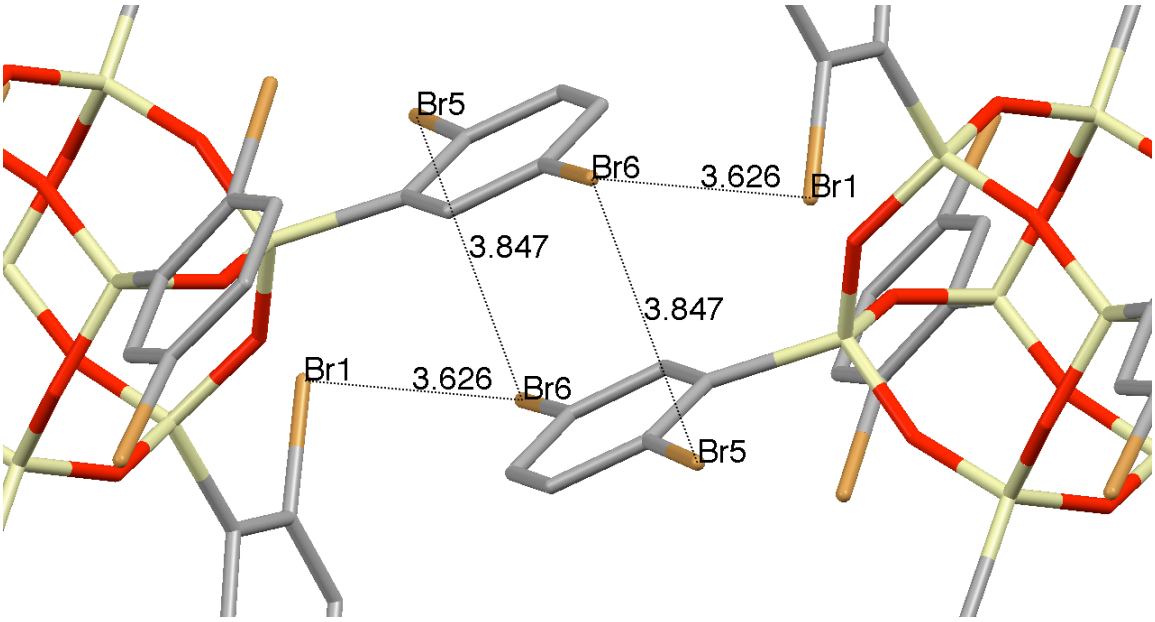

Figure 5.22 Br···Br short contact pairs in $Br_{16}OPS$.

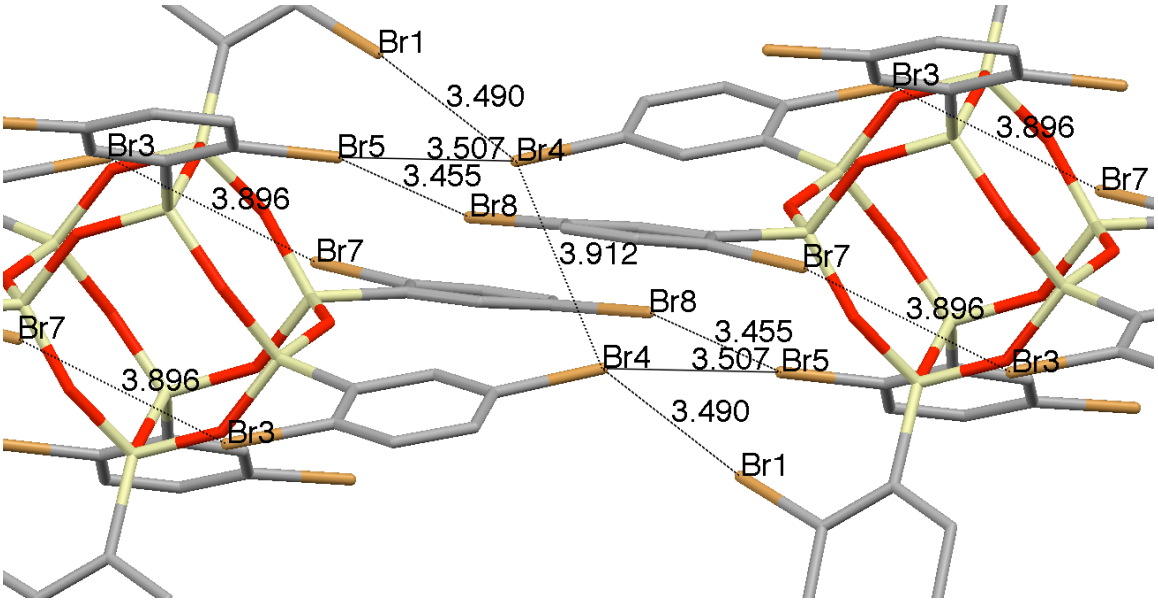

Figure 5.23 Si···Br short contact pairs in $Br_{16}OPS$.

Table **5.6** provides the full listing of short contacts found in the Br_{16}OPS crystal structure. All contacts less than the vdW sum are listed as well as Br···Br contacts under the sum of the "n-polar" radii (4.08 Å).[7] In total we find a total of forty-eight contacts per Br_{16}OPS molecule.

Table 5.6 Listing of Short Contacts found in the crystal structure of Br_{16}OPS

Atom1	Atom2	Length (Å)	vdW sum (n-polar sum) (Å)	Percent under VdW sum (Percent under n-polar)	Number per molecule
Br5	Br8	3.455	3.7	-6.6%	4
Br4	Br1	3.49	3.7	-5.7%	4
C22	Br7	3.349	3.55	-5.7%	4
Br5	Br4	3.507	3.7	-5.2%	4
H21A	Br1	2.921	3.05	-4.2%	4
H9A	Br7	2.976	3.05	-2.4%	4
Br6	Br1	3.626	3.7	-2.0%	4
Si2	Br2	3.933	3.95	-0.4%	4
Br8	Br3	3.806	3.7 (4.08)	2.9% (-4.9%)	4
Br6	Br5	3.847	3.7 (4.08)	3.97% (-3.8%)	4
Br3	Br7	3.896	3.7 (4.08)	5.3% (-2.6%)	2
Br4	Br4	3.912	3.7 (4.08)	5.7% (-2.2%)	2
Br8	Br7	3.94	3.7 (4.08)	6.5% (-1.5%)	4

In the Br_{16}OPS derivative we find examples of Si···Br short contacts, analogous to the Si···I contacts in the I_{12}DPS structure. We also see numerous Type II Br···Br short contacts and additional Br···Br short contacts. Finally, as the degree of bromination increases from eight to sixteen, the total number of short contacts per molecule rises from twenty-one to forty-eight.

In contrast to the iodinated systems where the substitution patterns are identical while the geometry of the cage changes, here we maintain the cubic geometry while changing the substitution number. In this case, doubling the degree of bromination more than doubles the number of intermolecular short contacts. This could give insight into the

production of thermally stable, high dielectric silsesquioxane materials, where tight intermolecular packing will increase the electron density of the crystal and the dielectric response.

Tetraicosabrominated Octa(phenyl)silsesquioxane

The Br_{24}OPS crystal system is unique in comparison to the previously discussed systems due to the significant disorder in the substitution pattern of the bromines. Despite this disorder, Br···Br, Si···Br, H···Br and C···Br drive the formation of a crystalline solid. The refinement of the structure using partially occupied sites gives an average of twenty-four bromines per molecule. In particular, *para* substituted bromines are found, unlike *o*-Br_8OPS and Br_{16}OPS.

As expected, the larger number of bromines in the Br_{24}OPS system yields a larger number of Si···Br contacts. As seen in Figure **5.24** along the *c*-axis, parallel aromatic rings symmetrically coordinate to silicon atoms on adjacent cages.

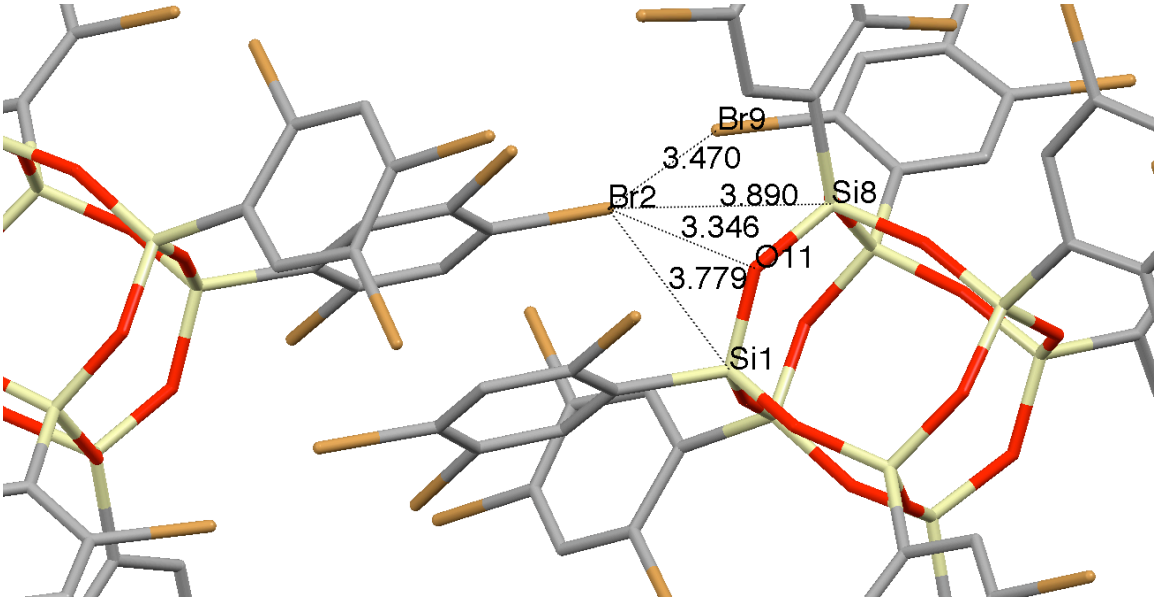

Figure 5.24. Si···Br short contacts along the *c* axis in Br_{24}OPS.

As seen in the iodinated compounds, there are several examples of Type II halogen-halogen short contacts. Figure **5.25** shows Type II short contacts between bromine atoms on adjacent molecules, as well as intramolecular examples of this coordination. Taken together, the net effect of these coordination patterns is to lower the density of the structure relative to that of the octa(2,5-dibromphenyl)silsesquioxane, 2.0 g/cc vs. 2.32 g/cc, despite the increase in the degree of bromine substitution.

As in I_8OPS, we see that halogen bonding can lower the density of crystalline solids due to coordination of *para* substituted halogens on the extreme corners. This drives intermolecular coordination at the extreme corners, preventing interdigitation of the phenyl rings, leaving void spaces near the faces of the silica cage.

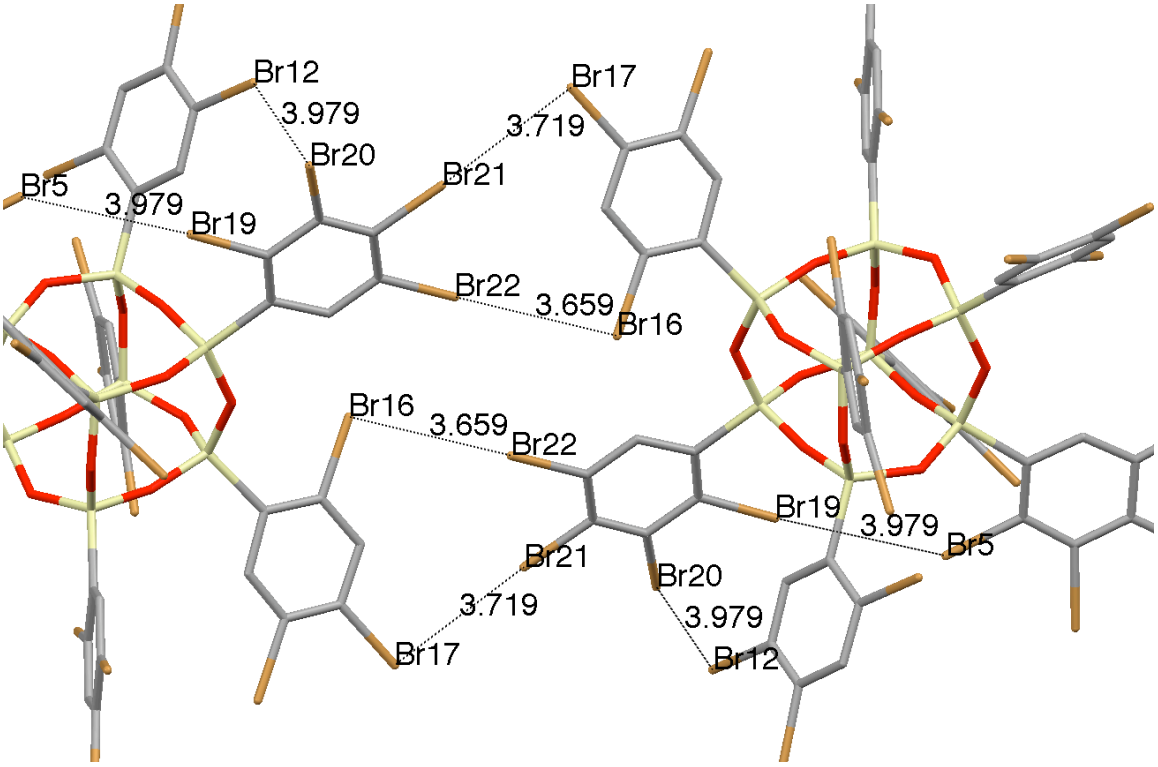

Figure 5.25 Br_{24}OPS Br···Br Type II short contacts in Br_{24}OPS.

Table **5.7** provides the full listing of short contacts found in the crystal structure of Br_{24}OPS. All contacts less than the vdW sum are listed as well as Br···Br contacts

under the sum of the "n-polar" radii (4.08 Å).[12] In total we find a total of eighty-nine contacts per Br_{24}OPS molecule.

Table 5.7 Listing of Short Contacts found in the crystal structure of tetraicosabrominated OPS

Atom1	Atom2	Length (Å)	vdW sum (n-polar sum) (Å)	Percent under VdW sum (Percent under n-polar)	Number per molecule
Br15	Br3	2.499	3.7	-32.5%	2
Br22	Br10	2.564	3.7	-30.7%	2
Br8	Br24	2.635	3.7	-28.8%	2
C23	Br3	2.523	3.55	-28.9%	2
C35	Br10	2.597	3.55	-26.8%	2
C11	Br24	2.785	3.55	-21.5%	2
Br10	H35	2.33	3.05	-23.6%	1
Br3	H23	2.348	3.05	-23.0%	1
Br3	C24	2.924	3.55	-17.6%	2
Br24	H11	2.426	3.05	-20.5%	1
C36	Br10	2.978	3.55	-16.1%	2
Br24	C12	3.206	3.55	-9.7%	2
Br4	Br25	3.427	3.7	-7.4%	2
Br11	Br16	3.438	3.7	-7.1%	2
Br9	Br2	3.47	3.7	-6.2%	2
C22	Br3	3.32	3.55	-6.5%	2
Br3	Br17	3.51	3.7	-5.1%	2
Br2	Si1	3.779	3.95	-4.3%	2
Br29	Br6	3.549	3.7	-4.1%	2
Br28	H21	2.927	3.05	-4.0%	2
Br18	Br27	3.602	3.7	-2.6%	2
Br26	Br29	3.605	3.7	-2.6%	2
C34	Br10	3.456	3.55	-2.6%	2
Br17	C5	3.462	3.55	-2.5%	2
Br11	Si7	3.877	3.95	-1.8%	2
Br15	Br20	3.631	3.7	-1.9%	2
Si8	Br2	3.89	3.95	-1.5%	2
Br7	Br29	3.657	3.7	-1.2%	2
Br16	Br22	3.659	3.7	-1.1%	2
Br25	Si3	3.91	3.95	-1.0%	2
Br2	O11	3.346	3.37	-0.7%	2
Br7	Br7	3.682	3.7	-0.5%	1
C4	Br17	3.54	3.55	-0.3%	2
Br2	H52	3.041	3.05	-0.3%	1
Br21	Br17	3.719	3.7 (4.08)	0.5% (-8.8%)	2
Br13	Br18	3.754	3.7 (4.08)	1.5% (-8.0%)	2
Br18	Br1	3.794	3.7 (4.08)	2.5% (-7.0%)	2
Br14	Br8	3.796	3.7 (4.08)	2.6% (-7.0%)	2

Br9	Br12	3.822	3.7 (4.08)	3.3% (-6.3%)	2
Br2	Br17	3.824	3.7 (4.08)	3.4% (-6.3%)	2
Br8	Br28	3.843	3.7 (4.08)	3.9% (-5.8%)	2
Br4	Br1	3.868	3.7 (4.08)	4.5% (-5.2%)	2
Br1	Br8	3.877	3.7 (4.08)	4.8% (-5.0%)	2
Br21	Br15	3.884	3.7 (4.08)	5.0% (-4.8%)	2
Br7	Br29	3.896	3.7 (4.08)	5.3% (-4.5%)	2
Br23	Br26	3.931	3.7 (4.08)	6.2% (-3.7%)	2
Br12	Br20	3.979	3.7 (4.08)	7.5% (-2.5%)	1
Br5	Br19	3.979	3.7 (4.08)	7.5% (-2.5%)	1

In this third brominated OPS derivative, we find more examples strong intermolecular coordination, including bromine short contacts with the entire Si-O-Si edge of a silsesquioxane cage (Figure **5.24**). We again see an increase in the number Type II Br···Br short contacts and additional Br···Br short contacts as the density of bromines increases. We see that as the cubic core geometry is maintained and the degree of bromination increased from eight to sixteen to twenty-four, the degree of intermolecular coordination continues to rise from twenty-one to forty-eight to eighty-nine.

Conclusions

There has been extensive study of coordination patterns in halogenated organic molecules,[5-8,11-14,16,17] but there have been few such examples of 3-D symmetric molecules.[12,16,17] The halogenated OPS derivatives possess not only unique coordination patterns, but often these structures possess different motifs along different crystallographic directions.

The traditional halogen bonding motifs described by Desiraju and others are reflected in the halogenated phenylsilsesquioxane systems. Examples of Type I, Type II,

and X_4 motifs are seen, while the X_3 motif is not seen. The short-contact distances determined are of the same order, or shorter, than previously documented examples.

The crystal structures of the I_8OPS and I_{10}dPS reveal short contacts which reduce the density of the crystal structure by holding open channels and cavities occupied by solvent molecules. The most striking case is the octamer, whose crystal structure is 39% solvent by volume. I_{12}DPS shows both Si···I contacts analogous to the Si···F contacts documented by Mabry.[21] C···H contacts consistent with the edge-face contacts seen in Phase I of benzene are also found in I_{12}DPS.[12]

The crystal structures of the brominated OPS derivatives show the ability for these short contacts to form open structures, in the case of the *o*-Br_8OPS (1.67 g/cc) and the Br_{24}OPS (2.0 g/cc), or densely packed structures, in the case of the Br_{16}OPS (2.32 g/cc). These compounds show a variety of Br···Br short contacts in addition to significant Si···Br short-contacts. In the case of the Br_{24}OPS compound, the robust supermolecular coordination compensates for the substitutional disorder of the system.

In summary, this chapter has detailed some observations in-line with previous work by Desiraju and others, and it is expected that as new crystalline OPS derivatives are synthesized, there will be more features unique to these systems. Based on the observations here, it would be expected that *para* halogenation would increase the probability of intermolecular coordination which leaves void space possibly accessible to guest species. Based on the *o*-Br_8OPS and Br_{16}OPS, *meta* halogenation may be a route towards tighter intermolecular packing. The structure of *o*-Br_8OPS appears to be dominated by a combination of inter- and intra-molecular interactions.

References Cited

1. Sanchez, C.; de A.A. Soler-Illia, G.J.; Ribot, F.; Lalot, T.; Mayer, C.R.; Cabuil, V. "Designed Hybrid Organic-Inorganic Nanocomposites from Functional Nanobuilding Blocks," *Chemistry of Materials*, **13**, 3061-8 (2001).
2. Hawker, C.J.; Wooley, K.L. "The Convergence of Synthetic Organic and Polymer Chemistry," *Science* **309**, 1200-5.
3. Tamaki, R., Tanaka, Y.; Asuncion, M.Z.; Choi, J.; Laine, R.M. "Octa(aminophenyl)silsesquioxane as a Nanoconstruction Site." *Journal of the American Chemical Society* **123**, 12416-7 (2001).
4. Brown, J.F. Jr.; Vogt, L.H.; Prescott, P.I. "Preparation and Characterization of the Lower Equilibrated Phenylsilsesquioxanes." *Journal of the American Chemical Society* **86**, 1120-5 (1964).
5. Desiraju, G.R. "Supramolecular Synthons in Crystal Engineering-A New Organic Synthesis." *Angewandte Chemie, International Edition in English* **34**, 2311-21 (1995).
6. Desiraju, G.R. "Crystal Engineering: A Holistic View." *Angewandte Chemie, International Edition in English* **46**, 8342-56 (2007).
7. Ganguly, P.; Desiraju, G.R. "Van der Waals and Polar Intermolecular Contact Distances: Quantifying Supramolecular Synthons." *Chemistry, an Asian Journal* **3**, 868-80 (2008).
8. Ghosh, S.; Reddy, C.M.; Desiraju, G.R. "Hexaiodobenzene: a redetermination at 100 K." *Acta Crystallographica* **E63**, o910–1 (2007).
9. Thalladi, V.R.; Goud, B.S.; Hoy, V.J.; Allen, F.H. Howard, J.A.K.; Desiraju, G.R. "Supramolecular synthons in crystal engineering. Structure simplification, synthon robustness and supramolecular retrosynthesis." *Chemical Communications* **1996**, 401-2.
10. Ritter, S.K. "Halogen Bonding Begins to Fly." *Chemical & Engineering News* September 21, 2009; pp. 39-42.
11. Awwadi, F.F.; Willett, R.D.; Peterson, K.A.; Twamley, B. "The Nature of Halogen··Halogen Synthons: Crystallographic and Theoretical Studies." *Chemistry: A European Journal* **12**, 8952–60 (2006).
12. Thaimattam, R.; Reddy, S.; Xue, F.; Mak, T.C.W.; Nangia, A.; Desiraju, G.R. "Molecular networks in the crystal structures of tetrakis(4-iodophenyl)methane and (4-iodophenyl)triphenylmethane." *New Journal of Chemistry* **1998**, 143-8.
13. Desiraju, G.R.; Parthasarathy, R. "The Nature of Halogen-Halogen Interactions: Are Short Halogen Contacts Due to Specific Attractive Forces or Due to Close Packing of Nonspherical Atoms?" *Journal of the American Chemical Society* 8725-6 (1989).

14. Bosch, E.; Barnes, C.L. “Triangular Halogen-Halogen-Halogen Interactions as a Cohesive Force in the Structures of Trihalomesitylenes.” *Crystal Growth & Design* **2**, 299-302 (2002).

15. Bondi, A. “van der Waals Volumes and Radii.” *Journal of Physical Chemistry* **68**, 441-51 (1964).

16. Reddy, D.S.; Craig, D.C.; Desiraju, G.R. “Supramolecular Synthons in Crystal Engineering. 4. Structure Simplification and Synthon Interchangeability in Some Organic Diamondoid Solids.” *Journal of the American Chemical Society* **118**, 4090-3 (1996).

17. Guo, W.; Galoppini, E.; Gilardi, R.; Rydja, G.I.; Chen, Y.-H. “Weak Intermolecular Interactions in the Crystal Structures of Molecules with Tetrahedral Symmetry: Diamondoid Nets and Other Motifs.” *Crystal Growth & Design* **1**, 231-237 (2001).

18. Metrangolo, P.; Meyer, F.; Pilati, T.; Resnati, G.; Terraneo, G. “Halogen Bonding in Supramolecular Chemistry.” *Angewandte Chemie, International Edition in English* **47**, 6114-27 (2008).

19. Caronna, T.; Liantonio, R.; Logothetis, T.A.; Metrangolo, P.; Pilati, T.; Resnati, G. “Halogen Bonding and π···π Stacking Control Reactivity in the Solid State.” *Journal of the American Chemical Society* **126**, 4500-1 (2004).

20. Reddy, C.M.; Kirchner, M.T.; Gundakaram, R.C.; Padmanabhan, K.A.; Desiraju, G.R. “Isostructurality, Polymorphism and Mechanical Properties of Some Hexahalogenated Benzenes: The Nature of Halogen···Halogen Interactions.” *Chemistry: A European Journal* **12**, 2222–34 (2006).

21. Jung, J.-H.; Potluri, S.K.; Zhang, H.; Wisian-Neilson, P. “Synthesis and Structure of Nongeminally Substituted Cyclic Phosphazenes with Haloalkyl and Thioester Functional Groups.” *Inorganic Chemistry* **43**, 7784-91 (2004).

22. Dunitz, J.D.; Gehrer, H.; Britton, D. “The Crystal Structure of Diiodoacetylene; an Example of Pseudosymmetry.” *Acta Crystallographica* **B28**, 1989-94 (1972).

23. Mabry, J.M.; Vij, A.; Iacono, S.T.; Viers, B.D. “Fluorinated Polyhedral Oligomeric Silsesquioxanes (F-POSS).” *Angewandte Chemie, International Edition in English* **47**, 4137-40 (2008).

24. Search of Cambridge Crystallographic Data Centre database via ConQuest.

25. PLATON Reference : A.L.Spek (2008) PLATON, A Multipurpose Crystallographic Tool, Utrecht University, Utrecht, The Netherlands.

Chapter VI

Future Work

This dissertation has presented synthetic routes for the synthesis of octaphenylsilsesquioxane (OPS) based nano-building blocks. In Chapter 2, iodination via ICl at ca. -40 ˚C was demonstrated to selectively *para* functionalize polyhedral phenylsilsesquioxanes giving I_8OPS, I_{10}dPS, and I_{12}DPS. Chapter 3 demonstrates the selective octa- and hexadeca-bromination of OPS to form Br_8OPS and Br_{16}OPS. The synthesis of a tetraicosabrominated OPS derivative, Br_{24}OPS, is accomplished by a two-stage bromination. The Sonogashira coupling was used in Chapter 4 as a route to incorporate ethynyl functionality onto the OPS core, allowing for the facile Diels-Alder condensation with tetraarylcyclopentadienones (tetracyclones). This condensation reaction extrudes CO and provides the reaction products in high yields and allows for additional new functionality to be incorporated. Chapter 5 details halogen-bonding motifs found in the halogenated phenylsilsesquioxanes.

We have demonstrated that the careful manipulation of synthetic conditions allows for the reaction of high-symmetry precursors, or tools, to synthesize high-symmetry nano-building blocks with a variety of conjugation and functionality. The incorporation of ethynyl functionality allows for the application of Diels-Alder tetracyclone condensation chemistry to dramatically increase the number of conjugated

moieties present and possibly generate complex 3-D networks. This type of manipulation should allow for production of materials with tunable optical and electronic properties.

Now we discuss some further avenues for study.

One area of immediate interest is the photophysics of these compounds due to the degree of conjugation of the organic periphery and the possibility of interactions with the silica core.[1] The octa(stilbene)silsesquioxanes have been a great interest in our research group, in particular, the differences in photophysical behavior from the small molecule analogs.[1] The conjugated compounds presented in this dissertation, the octa-(diarylacetylene)silsesquioxanes and the octa-hexaarylbenzene-silsesquioxanes could be analyzed by UV-Vis absorption and fluorescence spectroscopy. These studies would provide further data quantifying the extent of electronic influence by the silica core on peripheral conjugated moieties. Current electron paramagnetic resonance (EPR) studies are underway through collaboration with Dr. Schoenfeld at Berlin Free University.[2]

Isolation and further characterization of the octa(graphene)silsesquioxanes could be another area of future interest, as these compounds may be potentially be incorporated in advanced semiconductor devices.[3] Graphenes possess unique electronic properties due to their extended conjugation, which has been explored by Müllen et al.[4] Solid-state photophysical studies should provide insight in electronic interactions of the graphene periphery with the silica core, and the degree of $\pi\cdots\pi$ stacking. This is important because the π-π stacking can affect electron transport properties and fluorescence, crucial properties for electronic applications.[4]

Another area for future research is the use of the reactive ethynyl group for highly cross-linked and open framework solids. The use of a cobalt catalyst would, in principle,

allow for the cyclotrimerization[5] of adjacent nano-building blocks, creating a stable aromatic linker group. The goal of this work would be to create porous covalent organic frameworks (COFs) with high thermal stability and high surface areas. Polyphenylene aromatic groups have been modeled as effective hydrogen sorbents, and COFs with extensive aromatic functionality may be useful for hydrogen storage.[6]

One possible route for this is suggested in Scheme **1**.

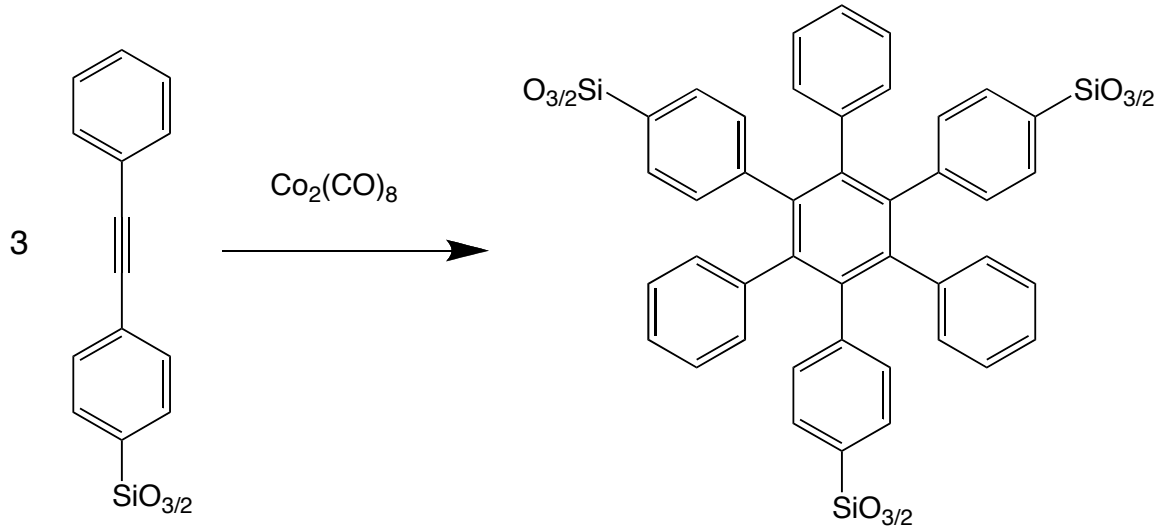

Scheme 6.1. Proposed cyclotrimerization of octa(Diphenylacetylene)silsesquioxane.

Another possible area of interest would be the incorporation of additional functionalities through the synthesis of functionalized tetraarylcyclopentadienones. This is schematically proposed in Scheme **6.2**. For instance, the synthesis of the di(*p*-bromophenyl)acetone from the corresponding *p*-bromophenylacetic acid should be available through the preparation described in this dissertation.[7] Condensation with commercially available 4,4'-dibromobenzil under the standard conditions should give the tetra(*p*-bromophenyl)tetracyclopentadienone in high yield.[8]

Finally, Diels-Alder condensation of this tetra-functional compound with an octaethynyl OPS derivative would provide a compound with thirty-two sites for

functionalization, shown in Scheme **6.3**. This type of highly functionalized octa-hexaarylbenzene silsesquioxane could be functionalized and cyclized to provide tunable organic semiconductor materials with high thermal stability. This functionality could be used to alter solid-state conformation through manipulation of the π···π stacking behavior. This functionality could also be used to extend conjugation even further beyond the 2 nm diameter of the 56 Phenyl.

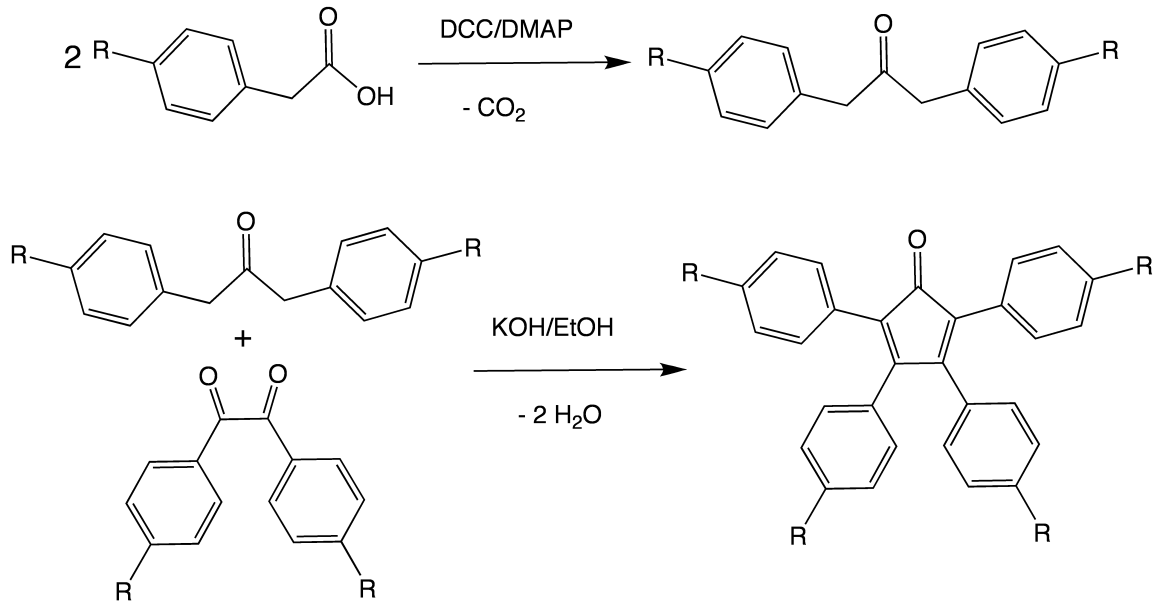

Scheme 6.2 Proposed synthesis of tetra(4-R-phenyl)tetracyclopentadieone.

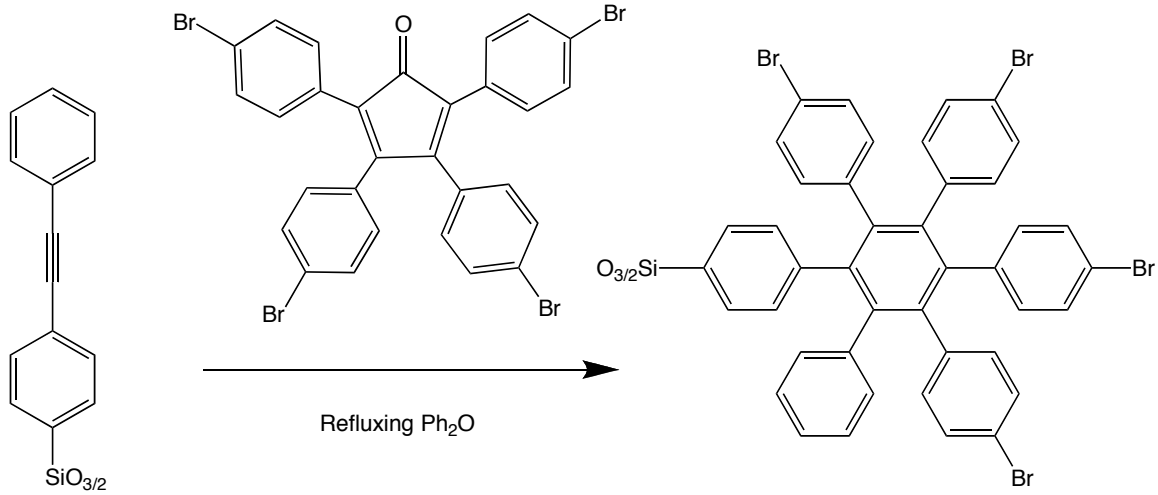

Scheme 6.3 Proposed Diels-Alder condensation of octa(diphenylacetylene)silsesquioxane with tetra(*p*-bromophenyl)tetracyclopentadienone.

Motivation for the investigation of halide complexation with the silsesquioxane cage was discussed in Chapter 3. Such halide complexes with silsesquioxane cages may provide insight into the fluoride catalyzed rearrangement of silsesquioxanes discussed by Liu et al,[9] Anderson et al,[10] Kozelj et al,[12] Marsmann et al,[12] and Ronchi et al.[13]

The octa(*o*-bromophenyl)silsesquioxane (*o*-Br_8OPS) could be a substrate for studying conjugated moieties under extremely sterically confined conditions. For instance, the octa(stilbene)silsesquioxane synthesized by the Heck coupling of styrene with *o*-Br_8OPS favors the *cis*- conformation.[14] This is yet another photophysical study that could yield information about the influence of the silsesquioxane core on the conjugation of the stilbene moieties. In addition, this steric stabilization could provide a valuable substrate to evaluate photophysical differences between the two stilbene conformations including absorption and emission characteristics, two-photon cross-sections, and quantum efficiencies.[14]

In addition, the deca- and dodeca-hedral analogs of these compounds may provide different behaviors due to changes in the angular distance between moieties or electronic character of the silsesquioxane core. For instance, intra-molecular exiplexes might form, if the distance between the conjugated moieties is decreased sufficiently.

To enable these studies, efficient syntheses of the decaphenylsilsesquioxane should be investigated through optimization of the scheme presented, as well other silsesquioxane rearrangement chemistries. Recent work by several groups indicates that fluoride may be used to rearrange silsesquioxanes very effectively.[9-12] Bassindale, et al[15] and Kawakami et al[16] have presented routes for the direct synthesis of other polyhedral

forms (e.g. T_6, T_{10}, T_{12}, T_{14}) by careful manipulation of the silane condensation chemistry.

The discussion of OPS bromination has introduced theoretical and experimental work suggesting the coordination of halide anions to silsequioxane cage faces. In our laboratory, we see some evidence for interactions between quaternary ammonium halides and OPS in recrystallization. This work should be extended to the decaphenylsilsesquioxane (dPS) system, since the insolubility and strong crystallization driving forces in OPS might kinetically overwhelm any halide complexation.

Finally, the presented evidence for thermolysis of the C-I bond in octa(*p*-iodophenyl)silsesquioxane suggests a study of the cross-linked materials resulting from radical recombination.[17,18] Materials produced via thermolysis could be compared to those generated by photolysis[19] or radical abstraction[20] mechanisms. Such materials may possess high surface areas and high thermal stability.

References Cited:

1. Laine, R.M.; Santy Sulaiman, S.; Brick, C.; Roll, M.; Tamaki, R.; Asuncion, M.Z.; Neurock, M.; Filhol, J.-S.; Lee, C.-Y.; Zhang, J.; Goodson III, T.; Curtis, J.; Ronchi, M.; Pizzoti, M. "Synthesis, and photophysical properties of Stilbeneoctasilsesquioxanes. Emission behavior coupled with theoretical modeling studies suggest a 3-D excited state involving the silica core." Manuscript in preparation.
2. Simon Schoenfeld, Freie Universitaet Berlin, Fachbereich Physik, AG Harneit
3. Rao, C.N.R.; Sood, A.K.; Subrahmanyam, K.S.; Govindaraj, A. "Graphene : The New Two-Dimensional Nanomaterial." *Angewandte Chemie, International Edition in English* **48**, 7752-78 (2009)
4. Wu, J.; Pisula, W.; Mullen, K. "Graphenes as Potential Materials for Electronics." *Chemical Reviews* **107**, 718–47 (2007).
5. Hahn, U.; Maisonhaute, E.; Amatore, C.; Nierengarten, J.-F. "Synthesis and Electrochemical Properties of Fullerene-Rich Nanoclusters Synthesized by Cobalt-Catalyzed Cyclotrimerization of Bis(aryl)alkyne Fullerodendrimers." *Angewandte Chemie, International Edition in English* **46**, 951-4 (2007).
6. Calabretta, A.; Negri, F. "Modelling Hydrogen Storage in 3D Polyphenylene Dendrimers." *CP633, Structural and Electronic Properties of Molecular Nanostructures*, edited by H. Kuzmany et al. American Institute of Physics (2002).
7. Bhandari, S.; Suprabhat Ray, S. "A Novel Synthesis of Bisbenzyl Ketones by DCC Induced Condensation of Phenylacetic Acid." *Synthetic Communications* **28**, 765-771 (1998).
8. Johnson, J.R.; Grummitt, O. "Tetraphenylcyclopentadienone." *Organic Syntheses* **23**, 92 (1943).
9. Liu, Z.-H.; Bassindale, A.R.; Taylor, P.G."Synthesis of Silsesqioxane Cages from Phenyl-cis-tetrol, 1,3-divinyltetraethoxydisiloxane, and Cyclopentyl Resins." *Chemical Research at Chinese Universities* **20**, 433-6 (2004).
10. Anderson, S.E.; Bodzin, D.J.; Haddad, T.S.; Boatz, J.A.; Mabry, J.M.; Mitchell, C.; Bowers, M.T. "Structural Investigation of Encapsulated Fluoride in Polyhedral Oligomeric Silsesquioxane Cages Using Ion Mobility Mass Spectrometry and Molecular Mechanics." *Chemistry of Materials* **20**, 4299-309 (2008).
11. Kozel, M.; Orel, B. "Synthesis of polyhedral phenylsilsesquioxanes with KF as the source of the fluoride ion." *Dalton Transactions* **2008**, 5072–5.

12. Rikowski, E.; Marsmann, H.C. "Cage-rearrangement of silsesquioxanes." *Polyhedron* **16**, 3357-61 (1997).

13. Ronchi, M.; Sulaiman, S.; Asuncion, M.Z., Laine, R.M. Unpublished results.

14. Petek, H.; Yoshihara, K.; Fujiwara, Y.; Lin, Z.; Penn, J.H.; Frederick, J.H. "Is the nonradiative decay of S1 cis-stilbene due to the dihydrophenanthrene isomerization channel? Suggestive evidence from photophysical measurements on 1,2-diphenylcycloalkenes." *Journal of Physical Chemistry* **94**, 7539-43 (1990).

15. Bassindale, A.R.; MacKinnon, I.A.; Maesano, M.G.; Taylor, P.G. "The preparation of hexasilsesquioxane (T6) cages by 'non aqueous' hydrolysis of trichlorosilanes." *Chemical Communications* **2003** 1382–3.

16. Kawakami, Y.; Yamaguchi, K.; Yokozawa, T.; Serizawa, T.; Hasegawa, M.; Kabe, Y. "Higher Polyhedral Silsesquioxane (POSS) Cage by Amine-catalyzed Condensation of Silanols and Related Siloxanes." *Chemistry Letters* **36**, 792-3 (2007).

17. Smith, D.W. Jr.; Shah, H.V.; Perera, K.P.U.; Perpall, M.W.; Babb, D.A.; Martin, S.J. "Polyarylene Networks via Bergman Cyclopolymerization of Bis-ortho-diynyl Arenes." *Advanced Functional Materials* **17**, 1237–46 (2007).

18. Johnson, J.P.; Bringley, D.A.; Wilson, E.E.; Lewis, K.D.; Beck, L.W.; Matzger, A.J. "Comparison of "Polynaphthalenes" Prepared by Two Mechanistically Distinct Routes." *Journal of the American Chemical Society* **125**, 14708-9 (2003).

19. Sharma, R.K.; Kharasch, N. "The Photolysis of Iodoaromatic Compounds." Angewandte Chemie, International Edition in English 7, 36-44 (1968).

20. Bunnett, J.F.; Wamser, C.C. "Radical Abstraction of Iodine from Aryl Iodides." *Journal of the American Chemical Society* **88**, 5534-7 (1966).

Chapter VII

Experimental

Materials

OPS was prepared using literature methods[51] or was a gift from Mayaterials. Cyanophenylboronic acid was prepared using the method of Li et al. ICl, 1.0 M in dichloromethane, N-methyldicylo-hexylamine, tri-*o*-tolyl phosphine, phenylboronic acid and other synthetic reagents were purchased from Sigma Aldrich and used as received. Silver oxide was purchased from F&M Scientific, ground and vacuum dried prior to use. Pd_2dba_3 was purchased from Strem Chemicals. Dichloromethane was purchased from Burdick-Jackson. Solvents were dried over 4Å molecular sieves. Dioxane and THF were distilled from sodium benzophenone ketyl under nitrogen.

Analytical Methods

Gel permeation chromatography (GPC). All GPC analyses were conducted on a Waters 440 system equipped with Waters Styragel columns (7.8x300, HT 0.5, 2, 3, 4) with RI detection using an Optilab DSP interferometric refractometer and THF as solvent. The system was calibrated using polystyrene standards and toluene as a reference.

Nuclear Magnetic Resonance (NMR). All ^1H NMR spectra were collected from samples dissolved in $CDCl_3$ and recorded on a Varian INOVA 400 MHz spectrometer. ^1H spectra were collected at 400 MHz using a 6000 Hz spectral width, a relaxation delay of 3.5 s, 30k data points, a pulse width of 38°, and $CHCl_3$ (7.24 ppm) as the internal

reference. ^{13}C spectra were collected at 100 MHz using 25141.4 Hz spectral width, a relaxation delay of 0.1 s, a 45 deg. pulse width with 256 repititions and $CHCl_3$ (77.23 ppm) as the internal reference.

Thermogravimetric analyses (TGA/DTA). All TGA/DTA analyses were run on a 2960 simultaneous DTA-TGA Instrument (TA Instruments, Inc. New Castle, DE). Samples (15-25 mg) were loaded in alumina pans and ramped at 10°C/min to 1000°C in dry air at a flow rate of 60 mL/min.

Matrix-Assisted Laser Desorption/Time-of-Flight Spectrometry (MALDI-TOF) was done on a Micromass TofSpec-2E equipped with a 337 nm nitrogen laser in positive-ion reflectron mode using poly(ethylene glycol) as a calibration standard, dithranol as the matrix and $AgNO_3$ as the ion source. Samples were prepared by mixing solutions of 5 parts matrix (10 mg/mL in THF), 5 parts sample (1 mg/mL in THF), and optionally 1 part $AgNO_3$ (2.5 mg/mL in water) or 1 part LiOTf (2.5 mg/mL in water) and blotting the mixture on the target plate.

The resulting chromatograms were averaged and smoothed once using the Savitzky-Golay algorithm. The baseline was subtracted using a 99^{th} order polynomial, and the spectra were centered using a channel width of half the full width at half-maximum.

Gas chromatography/mass spectroscopy GC/MS data were collected on a Thermo/electron TraceMS using splitless injection. This was accomplished by the reaction of 0.8 mL of $MeOH/H_2O/NH_4F$ solution with 10 mg of sample in 1.5 mL THF at 60°C/2 h. The resulting reaction mixture was separated into two phases by the addition of 5 mL of saturated brine. The THF layer was extracted, dried with sodium sulfate and subsequently injected into the instrument.

Synthetic methods

Synthesis of Octaiodophenylsilsesquioxane.

To an oven dried, single neck 1 L flask under flowing N_2 are added 292 mL of 1.0 M ICl/CH_2Cl_2 solution. The solution is cooled to –40°C using a dry ice/ethylene glycol/ethanol bath[2] and 26.7 g (25.8 mmol) of powdered OPS was added at an approximate rate of 5 g/min with stirring. HCl evolution began within 1 min of OPS addition. The flowing N_2 flushes the HCl from the reaction system. Residual OPS sticking to the sides of the flask is washed into the reaction solution with 40 mL of CH_2Cl_2. The reaction was stirred for 24 at temperature and allowed to warm to room temperature with stirring over another 24 h and quenched with 300 mL of ~1M sodium metabisulfite.

When all the ICl was consumed and quenched, the organic layer was extracted and washed 3x with water, filtered, and dried over anhydrous sodium sulfate. The volume was subsequently reduced by rotary evaporation to produce a white solid. This solid was further dried under vacuum, then redissolved in 400 mL of THF. This clear solution was then precipitated into 3 L of cold methanol providing a white powder that was then vacuum dried to give 47 g (23 mmol or 90% yield). The as precipitated material may then be recrystallized from hot ethyl acetate to give colorless crystals (~30-40% yield). Percent Conversion: 99%, GPC Mn: 1159, GPC PDI: 1.01, Ceramic Yield, Calculated: 23.5%, Found: 18.8%; MALDI Calculated: 2148.57 Da (Ag+), Found: 2148 Da (100%); ^{1}H NMR: 7.74 (m), 7.40 (m); ^{13}C NMR: 137.296, 135.430; FTIR (cm-1) νC-H 3100-

3000 (w), νC=C 1575 (s), 1550(s), 1490(s), νSi-O 1200-1050(vs), 1000 (s), δC-H 800(s), 750(s).

Peroxide Oxidation of Silica Core.

A, 2.5 g of KF, and 2.0 g of $NaHCO_3$ were added to a 250 mL round-bottom flask, then 25 mL of methanol and 20 mL of 30% H_2O_2 were added. The mixture was heated to reflux to induce dissolution using an oil bath. Then 3.0 g sample of phenylsilsesquioxane derivative dissolved in 25 mL of THF was added and the mixture was then refluxed for 4 h over which time the solution became clear yellow and later precipitated white silica. The solution was then filtered to remove the silica and extracted with ethyl acetate/brine three times in order to remove salts. The combined organic layers were dried over sodium sulfate and GC/MS samples were taken. To conduct ^1H NMR investigations, the organic layer was evaporated to remove the solvents, and the residual mixture was analyzed. Samples of commercial phenols were added at times, to spike different isomers, and better quantify their presence.

General Heck Reaction Conditions.

To an oven dried 50 mL Schlenk flask under N_2 was added 1.00 g (0.48 mmol, 3.9 mmol phenyl) of recrystallized I_8OPS followed by 108 mg (0.175 mmol) of Pd_2dba_3 and 288 mg (0.788 mmol) of tri-*o*-tolyl phosphine. Then 2.00 g (29.8 mmol) of granular copper metal. N-methyldicylohexylamine (3 mL, 14 mmol) followed by 4-methylstyrene (2.8 mL, 22 mmol) and 15 mL of dioxane were added by syringe. The reaction mixture was then heed at 95°C for 18 h with stirring under nitrogen. Thereafter the cooled mixture was filtered through a 1 cm celite column and precipitated into 75 mL of cold methanol.

The resulting solid was filtered off, redissolved in 7.5 mL of ethyl acetate, filtered through another 1 cm Celite column, and precipitated into 75 mL of cold methanol. The resulting white solid was vacuum dried for 4 h yielding 0.84 g (0.45 mmol, 87% yield) of white material. Yield:87%, Percent Conversion: 99%; GPC Mn: 1620, GPC PDI: 1.04, Ceramic Yield, Calculated: 24.4%, Found: 22%, MALDI Calculated: 2070.69 Da (Ag+), Found: 2071 Da (100%); ^{1}H NMR: 7.90 (s), 7.75 (s), 7.62 (s), 7.50 (s), 7.37 (s), 7.10-6.90 (m), 2.40-2.00 (s), 2.32 (s)* ^{13}C NMR: 134.59,134.30, 129.36, 127.33, 126.51, 125.83, 21.237 FTIR (cm-1) νC-H 3100-2900 (w), νC=C 1575 (s), 1550 (s), 1490 (s), νSi-O 1250 (s), 1200-1000 (vs), 1000 (s), 975 (s), δC-H 825 (s), 800 (s), 725 (s)

Stilbene: Yield: 91%, Percent Conversion: 99%, GPC Mn: 1609, PDI: 1.02; Ceramic Yield, Calculated: 26%, Found: 22%, MALDI Calculated: 1958.49 Da (Ag+), Found: 1958 Da (100%); ^{1}H NMR: 7.80 (s), 7.75 (s), 7.52 (m), 7.42 (m), 7.35 (m), 7.29 (s), 7.20-7.00 (m); ^{13}C NMR: 134.62, 128.66, 126.59, 125.94; FTIR (cm-1): νC-H 3100-3000, νC=C 1575, 1550, 1490, νSi-O 1250, 1200-1000, 1000, δC-H 825, 800, 725.

General Suzuki reaction conditions.

To an oven dried 50 mL Schlenk flask under N_2 was added 1.00 g (0.48 mmol, 3.9 mmol phenyl) of recrystallized I_8OPS followed by 70 mg (0.069 mmol) of Pd_2dba_3 and 168 mg (0.46 mmol) of tri-*o*-tolyl phosphine, phenylboronic acid (970 mg, 7.8 mmol), and silver (I) oxide (1.6 g, 6.9 mmol). Distilled THF (15 mL) was added by syringe and reaction was stirred under N_2 at ambient for 18 h. Thereafter, the mixture was filtered under vacuum to remove the Ag_2O particles and subsequently precipitated into 75 mL of

methanol. The resulting off-white solid was then recovered by filtration, redissolved in 7.5 mL of ethyl acetate, filtered through another 1 cm Celite column, reprecipitated in to 75 mL of cold methanol and vacuum dried for 4 h giving 0.67 g (0.4 mmol) of white powder with an 83% yield. Percent Conversion: 93%, GPC Mn: 1052, GPC PDI: 1.01; Ceramic Yield, Calculated: 25.4%, Found: 24%, MALDI Calculated: 1750.19 Da (Ag+), Found: 1749 Da (100%); ^{1}H NMR: 7.95-7.85 (m), 7.80-7.75 (m), 7.70-7.60 (m), 7.50-7.40 (d), 7.40-7.35 (m), ^{13}C NMR: 140.73, 134.77, 128.76, 127.60, 127.17, 126.65, 126.46; FTIR (cm-1): νC-H 3100-3000 (w), νC=C 1575 (w), 1550 (w), 1490 (w), νSi-O 1250 (s), 1200-1050 (vs), 1000 (s), δC-H 800-775 (s), 750 (s).

4-Cyanobiphenyl: Yield: 64%, Percent Conversion: 88%, GPC Mn: 1556, PDI:1.08; Ceramic Yield, Calculated: 26%, Found 26%; ^{1}H NMR: 7.00-8.00 (br), 7.90 (m), 7.80-7.60 (m); ^{13}C NMR: 144.81, 137.27, 134.91, 132.67, 127.73, 126.836, 118.625, 97.08; FTIR (cm-1): νC-H 3100-2900 (w), νCN 2200 (s), νC=C 1575 (s), 1550 w), 1490 (w), νSi-O 1250 (s), 1200-1050 (vs), 1000 (s), δC-H 775 (s), 750 (s).

General carbazole amination conditions.

To an oven-dried 50 mL Schlenk flask under N_2 was added 0.50 g (0.24 mmol, 1.95 mmol phenyl) of recrystallized I_8OPS followed by 360 mg (2.1 mmol) of carbazole, copper (I) oxide 420 mg (0.46 mmol) and 5 mL of N,N-dimethylacetimide was then added and the mixture heated with stirring at 150°C under N_2. After 6 h, an additional 360 mg of carbazole and 420 mg of Cu (I) oxide was added and stirring was continued for another 14 h followed by cooling to ambient. The reaction mixture was then filtered through a 1 cm Celite column and precipitated into 75 mL of cold methanol. The resulting solid was filtered off, redissolved in 7.5 mL of ethyl acetate, filtered a second

time through Celite and reprecipitated using 75 mL of cold methanol. After vacuum drying, 0.44 g (0.345 mmol) of powder was obtained consisting of a mixed substitution product. Percent Conversion: 92%, GPC Mn: 2516 GPC PDI: 1.2; Ceramic Yield, Calculated: 20.4%, Found: 23%, ^{1}H NMR: 8.20-6.20 (m), 8.00 (s), 7.18 (s); ^{13}C NMR: 128.33, 126.09, 123.53, 120.42, 122.40, 109.72; FTIR (cm-1): νC-H 3100-3000 (w), νC=C 1575 (s), 1550 (s), 1505 (s), 1495 (s), 1490 (vs), νC-N 1250 (s), νSi-O 1200-1000 (vs), 1000 (s), 975 (s) δC-H 850 (w), 800 (s), 775 (vs), 725 (s)

General vinyl pyridine reaction conditions.

To an oven dried 50 mL Schlenk flask under N_2 was added 1.00 g (0.48 mmol, 3.9 mmol phenyl) of recrystallized I_8OPS followed by 72 mg (0.156 mmol) of Pd_2dba_3 and 192 mg (0.627 mmol) of tri-*o*-tolyl phosphine and 300 mg (1.63 mmol) of copper/tin alloy (H_2CuSn). Thereafter, Et_3N (2.2 mL, 14.1 mmol), 2-vinylpyridine (2.5 mL, 22 mmol), and 30 mL of dioxane (60 mL for 4-vinylpyridine) were added by syringe.

The reaction mixture was then heated to 90°C under N_2 for 18 h and then allowed to cool to room temperature. The reaction mixture was filtered through 1 cm of Celite and precipitated into 75 mL of hexane/cyclohexane (50:50 v/v). The resulting solid was recovered by filtration and redissolved in 25 mL of THF/toluene, washed successively with 25 mL portions of saturated brine, 0.1 M $NaHSO_3$, and 0.1 M $NaHCO_3$, and then water. The organic layer was dried over sodium sulfate and solvent was removed by rotary evaporation. Thereafter the recovered solid was dissolved in 7.5 mL of ethyl acetate and precipitated into 75 mL of hexane/cyclohexane (50:50 v/v) providing 440 mg (0.236 mmol, 49% yield) of off-white powder. Percent Conversion: 91%; GPC Mn: 1513,

PDI: 1.02; Ceramic Yield, Calculated: 25.9%, Found: 20%, MALDI Calculated: 1858.5 Da (+), Found: 1858 Da (100%); 1H NMR: 8.55 (m), 7.80 (m), 7.60 (m), 7.35 (d), 7.18 (s), 7.15 (m); FTIR (cm-1): νC-H 3100-3000 (w), νC=C/uC=N 1625 (w), 1570 (s), 1560 (s), 1550 (s), 1450 (s), 1400 (s), 1375 (w), 1370 (w), νSi-O 1200-1000 (vs),1000 (s), 975 (s), δC-H 800 (s), 750 (s), 730 (s), 725 (s).

4-vinylpyridine: Yield: 48%, Percent Conversion: 90%, GPC Mn: 1454, PDI: 1.02; Ceramic Yield, Calculated: 25.9%, Found: 22%; MALDI Calculated: 1858.5 Da (+), Found: 1858 Da (100%); ^{1}H NMR: 8.56 (m), 7.76 (m), 7.54 (m), 7.40 (m) 7.37-7.10 (m), 7.28 (s), 7.20-7.00 (m); FTIR (cm-1): νC-H 3100-3000 (w), νC=C/νC=N 1625 (w), 1600 (s), 1550 (w), 1500 (w), 1380 (s), νSi-O 1200-1000 (vs),1000 (s), 975 (s), δC-H 800 (s), 700 (s).

Phosphonation of I_8OPS.

To an oven dried 50 mL Schlenk flask equipped with a reflux condenser under N_2 was added 1.00 g (0.48 mmol, 3.9 mmol phenyl) of recrystallized I_8OPS followed by 28 mg (0.039 mmol) of tetrakis(triethylphosphite)Ni(0), and 8 mL of m-xylene. Triethylphosphite (1.0 mL, 6.25 mmol) was then added by syringe. The mixture was then heated to reflux with stirring for 24 h. After cooling, the reaction mixture was added to 150 mL of cold hexane to precipitate the product. The precipitate was filtered off, redissolved in 7.5 toluene and reprecipitated into 100 mL of cold hexane. The precipitate was filtered to give 720 mg (0.33 mmol, 68%) of white product. Percent Conversion: --

%, GPC Mn: 1086; GPC PDI: 1.01; Ceramic Yield, Calculated: 49.4%, Found: 56%, MALDI Calculated: 2128.2 Da (Li+), Found: 2128 Da (100%); ^{1}H NMR: 7.90-7.70 (m), 4.20-4.00 (m), 2.35-2.25 (m); FTIR (cm^{-1}): νC-H 3100-3000, νC=C 2210, νC=C 1450, 1490, νSi-O 1250, 1200-1050, 1000, δC-H, 800, 725.

Br_8OPS

To a dry 100 mL schlenk flask under nitrogen was added 5.0 g OPS (4.85 mmol, 38.5 mmol phenyl) followed by 10 mL dichloromethane. A condenser was attached followed by an addition funnel. The flask was then heated to 60˚ C in an oil bath. To the addition funnel was added 3.3 mL of Bromine (64 mmol) and finally an additional 2 mL of dichloromethane, to wash the graduated cylinder. Following this, the nitrogen flow was stopped, and a vent to a bubbler containing aqueous base was added. At this point, the bromine solution was added dropwise, to the dispersion of OPS. The solution was stirred for 1 d. At this point, the flask was placed in an ice bath and a saturated 2:1 sodium metabisulfite:sodium carbonate was added to the top of the solution with vigorous stirring, until the color of the bromine disappeared (~10-20 mL) . The mixture was transferred to a separatory funnel, and the organic layer was extracted and washed sequentially with a 50 mL portion of water. The organic layer was removed, and charcoal and celite were added and stirred for 10 min. The black mixture was filtered then dried with sodium sulfate, and filtered again to give a clear, colorless liquid. The dichloromethane was removed by rotary evaporation, the resulting solid redissolved in ~ 10 mL of tetrahydrofuran, and subsequently precipitated into ~200 mL stirred, cold

methanol. The precipitate is filtered and dried under vacuum to yield 6.8g g (4.1 mmol) of white powder (84% yield).

o-Br_8OPS

To a dry 1 L round-bottom flask under nitrogen was added 60 g OPS (58 mmol, 464 mmol phenyl) followed by 600 mL dichloromethane. A condenser was attached followed by an addition funnel. The flask was then heated to 60 deg C in an oil bath. To the addition funnel was added 43 mL of Bromine (834 mmol) and finally an additional 2 mL of dichloromethane, to wash the graduated cylinder. Following this, the nitrogen flow was stopped, and a vent to a bubbler containing aqueous base was added. At this point, the bromine solution was added dropwise, to the dispersion of OPS. The solution was stirred for 7 d. At this point, the flask was removed from heat and allowed to settle over night. A saturated sodium metabisulfite was added to the top of the solution with vigorous stirring, until the color of the bromine disappeared (~15 mL) . The mixture was transferred to a separatory funnel, and the organic layer was extracted and washed sequentially with a 50 mL portion of water. The organic layer was removed, and charcoal and celite were added and stirred for 10 min. The black mixture was filtered then dried with sodium sulfate, and filtered again to give a clear, colorless liquid. Most of the dichloromethane was removed by rotary evaporation, leaving a viscous white oil. The flask was capped and placed in a freezer. The resulting solid triturated in ethyl acetate and filtered and dried under air, yielding 30 g white, microcrystalline powder. Oxidative cleavage of this material indicated that only 85% of the substitution was *ortho*- to the silicon. A 12 g portion of the material was recrystallized from twice from 100 mL of hot

m-xylene, and once from *o*-dichlorobenzene. The resulting large, colorless crystals were solvent exchanged with 2 portions of 15 mL of ethyl acetate, triturated, filtered and dried under vacuum, yielding 1.1 g of white microcrystalline powder (~2% of theoretical).

Br_{16}OPS

To a dry 100 mL schlenk flask under nitrogen was added 5.0 g OPS (4.85 mmol, 38.5 mmol phenyl) followed by .50 g $FeBr_3$ (1.7 mmol) and 10 mL dichloromethane. The red dispersion was stirred for 10 minutes at RT before placing the flask in an ice bath. A condenser was attached followed by an addition funnel. To the addition funnel was added 5.0 mL of Bromine (98 mmol) and finally an additional 2 mL of dichloromethane, to wash the graduated cylinder. Following this, the nitrogen flow was stopped, and a vent to a bubbler containing aqueous base was added. At this point, the bromine solution was added dropwise, to the dispersion of OPS. The solution was stirred for 1 d. At this point, the flask was placed in an ice bath and ~5 mL of a saturated solution of 2:1 sodium metabisulfite:potassium phosphate was added to the top of the solution with vigorous stirring, until the solution largely decolorized. The viscous dispersion was dissolved in ~100 mL of carbon disulfide and transferred to a separatory funnel. After the aqueous later was found to be neutral, the organic layer was extracted and charcoal and celite were added and stirred for 10 m. The black mixture was filtered to give a clear, colorless liquid, then dried with sodium sulfate, and filtered again. The carbon disulfide was diluted with ~50 mL of heptane and the solvent was removed by rotary evaporation. The resulting solid triturated in ~ 10 mL of ethyl acetate and filtered. The solid was washed with an additional ~5 mL of ethyl acetate. The filtrate was removed and the solid was

washed with methanol to yield 7.1 g (3.1 mmol, 64% yield) of a white microcrystalline solid. This microcrystalline solid may be further purified by stirring in tetrahydrofuran overnight at a concentration of 1 g/ 5 mL, and isolating the insoluble portion, in 25% overall yield. The filtrate was diluted to ~25 mL of solvent and precipitated into ~200 mL stirred, cold methanol. The precipitate is filtered and dried under vacuum to yield 1.9 g (0.82 mmol, 17% yield) of white powder. Total yield 81%

Br_{24}OPS

To a dry 100 mL schlenk flask under nitrogen was added 5.0 g OPS (4.85 mmol, 38.5 mmol phenyl) followed by 10 mL dichloromethane. The red dispersion was stirred for 10 minutes at RT before placing the flask in an ice bath. A condenser was attached followed by an addition funnel. To the addition funnel was added 8.5 mL of Bromine (165 mmol) and finally an additional 2 mL of dichloromethane, to wash the graduated cylinder. Following this, the nitrogen flow was stopped, and a vent to a bubbler containing aqueous base was added. At this point, the bromine solution was added dropwise, to the dispersion of OPS. The solution was stirred for ~5 h until the solid OPS entered solution. At this the mixture was cooled with an ice bath and the magnetic stirrer was turned off. At this point 0.50 g $FeBr_3$ (1.7 mmol) was quickly added and the vent reattached. 15 mL of dichloromethane was added via a pressure equalized addition funnel as the stirring was restarted leading to the vigorous generation of HBr. The reaction was stirred for an additional ~24 h. At this point, the viscous reaction solution was diluted with 100 mL of dichloromethane and quenched with 150 mL of water with a 10 g of sodium metabisulfite and 20 g of sodium carbonate was added to the top of the solution with vigorous stirring,

until the solution largely decolorized. The biphasic mixture was added to ~500 mL of carbon disulfide and transferred to a separatory funnel. After the aqueous later was found to be neutral, the organic layer was extracted and charcoal and celite were added and stirred for 10 min. The black mixture was filtered to give a clear, colorless liquid, which was subsequently dried with sodium sulfate, and filtered again. The carbon disulfide was diluted with ~50 mL of heptane and the solvent was removed by rotary evaporation, allowing the material to crystallize out of solution. The resulting solid was triturated in ~15 mL of tetrahydrofuran and filtered. The solid was then recrystallized 3x from hot *o*-dichlorobenzene. After the last recrystallization, the crystals are triturated in tetrahydrofuran and filtered. Single crystals for XRD analysis were grown from hot *o*-dichlorobenzene. The filtrate was removed and the solid was washed with tetrahydrofuran and methanol and dried to yield 1.2 g a white microcrystalline solid (8% yield).

General Sonogashira coupling reaction:

To a dry 50 mL Schlenk flask under N_2 and equipped with a magnetic stir bar under was added 4 g I_8OPS (16 mmol aryl iodide), Tris(triphenylphosphine) CuI, 10 mg (0.168 mmol, 7%), bis(tri-*t*-butylphosphine)palladium(0), 9 mg trisbenzylideneacetone-dipalladium(0). Subsequently 12 mL of toluene (previously distilled and degassed), 2 mL (2.6 mmol) phenylacetylene, 3.6 mL n-methyldicyclohexylamine, were added to the flask while stirring followed by 12 mL 1,4 dioxane (previously distilled and degassed). The solution was stirred at RT for 48 h. The solution turned yellow-brown. The mixture

precipitated into ~100 mL methanol to deactivate the catalyst. The resulting precipitate was collected by filtration. The dried precipitate was partially dissolved in ~10 mL of toluene and tetrahydrofuran was added until the solution was clear and homogeneous. A tetrahydrofuran solution of n-acetyl-l-cysteine was added along with 1g each of celite and activated carbon. The suspension was briefly stirred and allowed to sit over night. After 24 h the suspension was filtered and precipitated to yield a yellow powder, which could be recrystallized from hot m-xylene to yield 410 mg of off-white crystals (~10% of theoretical for complete conversion). The amorphous material was precipitated into cold methanol to give 2.25 g of yellow powder. Total yield: 67 % of theoretical for complete conversion.

Octa(4-methyldiphenylacetylene)silsesquioxane: Yield: 92% of theoretical for complete conversion. Recrystallization from *m*-xylene gave 270 mg as off-white crystals, 14% of theoretical for complete conversion.

Trimethylsilylacetylene Sonogashira coupling reaction:

To a dry 50 mL Schlenk flask under N_2 and equipped with a magnetic stir bar under was added 4 g I_8OPS (16 mmol aryl iodide), Tris(triphenylphosphine) CuI, 10 mg (0.03 mmol, 0.19 %), bis(tri-*t*-butylphosphine)palladium(0), 9 mg (0.02 mmol, 0.125%) trisbenzylideneacetonedipalladium(0) (0.02 mmol, 0.125%). Subsequently 6 mL of toluene (previously distilled and degassed), 2.6 mL (18 mmol) trimethylsilylacetylene, 3.4 mL n-methyldicyclohexylamine (16 mmol), were added to the flask while stirring followed by 6 mL 1,4-dioxane (previously distilled and degassed). The solution was

stirred at RT for 96 h. The solution turned yellow-brown. An additional 0.2 ml of n-methyldicyclohexylamine was added and the mixture was stirred for an additional 24 h. 10 ml of ethyl acetate was added to the flask and the suspension precipitated into ~100 mL methanol to deactivate the catalyst. The resulting precipitate was collected by filtration. The dried precipitate was suspended in ~10 mL of toluene and tetrahydrofuran was added until the solution was clear and homogeneous. A tetrahydrofuran solution of n-acetyl-l-cysteine was added along with 1g each of celite and activated carbon. The suspension was briefly stirred and allowed to sit over night. After 24 h the suspension was filtered and precipitated to yield a yellow powder, which was recrystallized from hot *m*-xylene to yield 3 g crystals (85% yield).

Tetra-p-tolylcyclopentadienone

In a 250 mL flask were put 13.5 g (90 mmol) tolylacetic acid and 3.3 g (27 mmol) of DMAP in 30 mL of dry methylene chloride. Stirring was started, and a solution of 10.7 g (52 mmol) of DCC in 55 mL in dry methylene chloride was added. Evolution of CO_2 was seen and the solution turned orange. Stirring was continued overnight. 150 mL of 50:50 hexane ethyl acetate was added and the organic layer was extracted over a pH 4 buffer potassium biphthalate buffer solution to remove DMAP and then a saturated sodium bicarbonate solution to remove residual tolylacetic acid, then finally with brine. The organic layer was filtered and rotovaped to an oil and placed in the freezer to crystallize. Crystals were isolated by filtration and washing with a small portion ~30 mL of hexane, and dried under vacuum, yielding 9.5 g (40 mmol, ~88% of theoretical). The crystals

were dissolved into ethanol with 9.5 g (40 mmol) of dimethyl benzil and heated in 75 mL of hot ethanol. The mixture is heated to boiling and 1.2 g of KOH in 10 mL of ethanol is added by pipet. The dark mixture is refluxed for 15 minutes, then cooled with ice. The dark blue/black crystalline tetracyclone is isolated by filtration and washed with methanol, methanol/water, and methanol. The crystals are dried, redispersed in methanol, filtered, washed with methanol, methanol/water, and methanol. The total yield of crystals was 12.4 g (70% of theoretical).

56 Phenyl

To a dry 20 mL round bottom flask was added was added 0.45 g (2 mmol) of recrystallized octadiphenylacetylene followed by the addition of tetraphenylcyclopentadienone (0.75 g, 2 mmol). Diphenyl ether, ~5 mL, was added by pipet and a condenser was attached. After introducing a slow nitrogen flow, the dark purple solution was heated to reflux by a variac controlled heating mantle and stirred for 2 d. At this time, the heating mantle was removed, the flask was loosely capped and allowed to cool to room temperature. During this cooling crystallization of the product began, and was allowed to continue undisturbed for 1 d. The mixture was diluted by addition of ~10 mL ethyl acetate and filtered to yield fine tan crystals. The filtrate was precipitated into ~100 mL cold methanol to yield a tan powder. While the total isolated yield is essentially quantitative, serial recrystallization yielded 0.4 g of highly crystalline octa(hexaphenylbenzene)octasilsesquioxane (35% of theoretical for complete conversion). Single crystals suitable for X-ray diffraction were grown from hot toluene.

Permethylated 56 Phenyl

To a dry 20 mL round bottom flask was added was added 200 mg recrystallized tolylethynylphenylsilsesquioxane followed by the addition of tetratolylcyclopentadienone (363 mg). Diphenyl ether, ~5 mL, was added by pipet and a condenser was attached. After introducing a slow nitrogen flow, the dark purple solution was heated to reflux by a variac controlled heating mantle and stirred for 1 d. After cooling to room temperature, 10 mL ethyl acetate was added and the solution was precipitated into ~100 mL cold methanol to yield a tan powder. This powder was redissolved into 10 ml of ethyl acetate and precipitated into 100 ml of cold methanol. The precipitate was collected by filtration, giving 408 mg of tan powder (75% of theoretical yield). The product was very soluble in toluene, ethyl acetate, xylenes, and tetrahydrofuran. Fractionation of the product could be accomplished by dissolution in a minimum of hot toluene, followed by the addition of 10 to 20 volumes of acetone, and placing the solution in a freezer for several days.

Semipermethyl56 Phenyl

To a dry 20 mL round bottom flask was added was added 200 mg recrystallized octadiphenylacetylenelsilsesquioxane followed by the addition of tetratolylcyclopentadienone (370 mg). Diphenyl ether, ~5 mL, was added by pipet and a condenser was attached. After introducing a slow nitrogen flow, the dark purple solution was heated to reflux by a variac controlled heating mantle and stirred for 1 d. After cooling to room temperature, 10 mL ethyl acetate was added and the solution was precipitated into ~100 mL cold methanol to yield a tan powder. This powder was

redissolved into 10 ml of ethyl acetate and precipitated into 100 ml of cold methanol. The precipitate was collected by filtration, giving 376 mg of tan powder (64% of theoretical yield). Recrystallization from nitrobenzene gave 60 mg of pale yellow crystals, and single crystals suitable for X-ray diffraction were grown from hot *m*-xylene/tetradecane.

Octa(4-methylbiphenyl)silsesquioxane

To a 250 mL round-bottom flask was added 5 g octaiodophenylsilsesquioxane, 9.9 g cesium carbonate and 4 g of p-tolyl boronic acid. 260 mg Pd and 720 mg tri-o-tolyl phosphine were added, followed by 120 mL of toluene. 2 mL of water and 1 mL of aliquat were added and the biphasic mixture was refluxed for 3 h. At this point the solution was cooled and the organic layer was extracted over 0.5 M HCl. The organic layer was reduced and precipitated into cold methanol. The resulting solid was recrystallized from hot toluene, yielding 1.34 g of white crystals (31%)

Dodecaiodophenylsilsesquioxane DDIPS

To an oven dried, single neck 500 mL flask under flowing N_2 are added 250 mL of 1.0 M ICl/CH_2Cl_2 solution. The solution is cooled to –60°C using a dry ice/ethylene glycol/ethanol bath[2] and 20.5 g (25.8 mmol) of powdered DPS was added at an approximate rate of 5 g/min with stirring. HCl evolution began within 1 min of DPS addition. The flowing N_2 flushes the HCl from the reaction system. Residual DPS sticking to the sides of the flask is washed into the reaction solution with 40 mL of

CH_2Cl_2. The reaction was stirred for 24 at temperature and allowed to warm to room temperature with stirring over another 24 h and quenched with 300 mL of ~1M sodium metabisulfite.

When all the ICl was consumed and quenched, the organic layer was extracted and washed 3x with water, filtered, and dried over anhydrous sodium sulfate. The volume was subsequently reduced by rotary evaporation to produce a white oil, which was placed in a freezer overnight. 250 mL of ethyl acetate was used to dissolve the non-crystalline material, followed by the vacuum filtration of the crystalline material and washing with additional 100 mL of ethyl acetate. The microcrystalline material was recrystallized from m-xylene with ~1% dodecane. The large crystals isolated were redissolved in 150 mL of hot tetrahydrofuran and precipitated into 750 mL of cold methanol. The precipitate was filtered washed with methanol and dried under vacuum to yield 5.6 g of white powder (14% of theoretical yield for complete conversion). The non-crystalline material was collected and precipitated into 1 L of cold methanol yielding 29 g of white powder. Total yield 34.6 g, 86 % of theoretical for complete conversion.

Decaphenylsilsesquioxane

To an oven dried 200 ml round bottom flask with a magnetic stir bar is added 3 g of dodecaphenylsilsesquioxane followed by 260 mg of 18-crown-6 and 160 mg of BaO. 100 ml of *m*-xylene is added to the flask, which is placed in a heating mantle on a magnetic stir plate. After stirring is commenced, a condenser is added and a nitrogen inlet is attached. A variac controlled heating mantle is used to bring the solution to reflux. After 1 d, the heating mantle is removed and the stirring halted. The solution is allowed to

settle and cool for ~1 h. At this time ~1 ml of concentrated aqueous HCl is added and stirring is restarted. After 30 min, the mixture is again allowed to settle and the organic layer is decanted from insoluble precipitates and water. 10 ml of toluene is added to the flask and the organic layer is again decanted. The combined organic layer is filtered and removed by distillation until only a few milliliters of yellow solution remain. The flask is again allowed to cool, and a white precipitate forms. 100 ml of tetrahydrofuran is added, and the resulting suspension is stirred overnight. The suspension is filtered, and the tetrahydrofuran is removed by rotary evaporation. The solid is triturated in a minimum volume of warm cyclohexane and filtered. The white, crystalline solid is washed with 1 ml of cyclohexane and dried, yielding 500 mg of decaphenylsilsesquioxane. Single crystals suitable for X-ray diffraction may be grown by the slow evaporation of CH_2Cl_2/toluene solutions.

Decaiodophenylsilsesquioxane DIPS

To an oven dried, single neck 50 mL Schlenk flask under flowing N_2 are added 13 mL of 1.0 M ICl/CH_2Cl_2 solution. The solution is cooled to –60°C using a dry ice/ethylene glycol/ethanol bath[2] and 1.1 g (0.63 mmol) of recrystallized decaphenylsilsesquioxane (dPS) was added at an approximate rate of 5 g/min with stirring. HCl evolution began within 1 min of dPS addition. The flowing N_2 flushes the HCl from the reaction system. Residual dPS sticking to the sides of the flask is washed into the reaction solution with 2 mL of CH_2Cl_2. The reaction was stirred for 24 h while being allowed to warm to room temperature quenched with 10 mL of ~1M sodium metabisulfite.

When all the ICl was consumed and quenched, the organic layer was extracted with 100 ml of ethyl acetate and 50 ml of brine and washed with saturated sodium bicarbonate and brine and filtered. The clear solution was allowed to evaporate until roughly 50 ml of solvent remained. The 380 mg of colorless crystals generated were separated by decanting the supernatant, which was subsequently rotovaped to an oil. A minimum amount of tetrahydrofuran was added (~5 ml) and the clear solution was precipitated into 100 mL of methanol. The flask was placed in the freezer overnight, and after 24 h 1.37 g of white powder was recovered by filtration, for a combined yield 1.75 g (80% of the theoretical).

Tert-butylation of hexaphenylbenzene

500 mg of recrystallized 56 Phenyl was added to an oven-dried 50 mL Schlenk flask flushed with nitrogen. Under nitrogen, 10 ml of tert-butyl chloride and 25 mL of 1.0M $SnCl_4$ in dichloromethane were added and the solution was heated to 40˚ C and stirred for 4 d. After two and four days, samples were taken, and the reaction was quenched after 4 d when 1H NMR indicated roughly one tert-butyl group per phenyl ring. The red solution was precipitated into 200 mL of cold methanol and filtered. The precipitate was washed with an additional 100 mL of methanol and dried under vacuum to yield 660 mg of off-white powder (90 % of theoretical for complete substitution of *para* positions).

General Cyclization Conditions

100 mg of recrystallized 56 Phenyl was added to an oven dried 50 mL Schlenk flask flushed with nitrogen. Under nitrogen, 5 mL of 1.0M $SnCl_4$ in dichloromethane was

added and a condenser, nitrogen inlet and outlet are attached. The solution was heated to 40˚ C in a silicone oil bath and stirred for 15 min to affect dissolution. At this time, 3 ml of anhydrous $FeCl_3$ in CH_3NO_2 (0.15 g/ ml) was added and the solution was stirred for an additional 2 h. At this time, the flask was removed from the oil bath, and the reaction solution is precipitated into 250 ml cold methanol. The red precipitate is recovered by filtration and washed with 200 ml methanolic HCl (0.1 M) until the filtrate is colorless. The precipitate is washed with an additional 100 ml of methanol and dried under vacuum, yielding 80 mg of orange-red solid (82 % of theoretical for complete conversion).

References Cited:

1. Li, W.; Nelson, D. P.; Jensen, M. S.; Hoerrner, R. S.; Cai, D.; Larsen, R. D.; Reider, P. J. "An Improved Protocol for the Preparation of 3-Pyridyl- and Some Arylboronic Acids. *Journal of Organic Chemistry* **67**, 5394–7 (2002).
2. Lee, D.W.; Jensen, C.M. "Dry-Ice Bath Based on Ethylene Glycol Mixtures." *Journal of Chemical Education* **77**, 629 (2000).

Appendix 1

Crystallographic data for Decaphenylsilsesquioxane

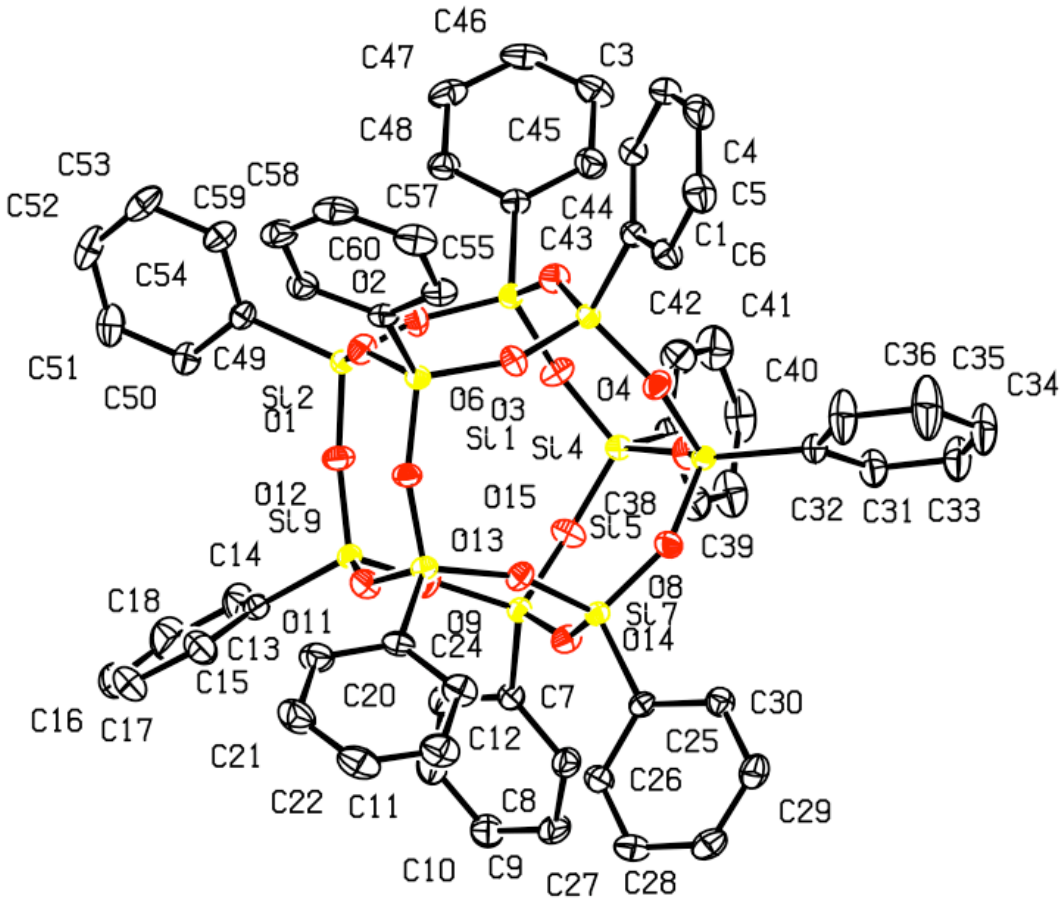

Figure A.1. 50 % thermal ellipsoid plots of decaphenylsilsesquioxane•toluene solvate. Hydrogen atoms and toluene solvates are omitted for clarity.

Structure Determination.

Colorless needles of **decap** were crystallized from a toluene solution at 23 deg. C. A crystal of dimensions 0.32 x 0.21 x 0.21 mm was mounted on a standard Bruker SMART-APEX CCD-based X-ray diffractometer equipped with a low temperature device and fine focus Mo-target X-ray tube (l = 0.71073 A) operated at 1500 W power (50 kV, 30 mA). The X-ray intensities were measured at 85(2) K; the detector was placed at a distance 5.055 cm from the crystal. A total of 2500 frames were collected with a scan width of 0.5° in w and 0.45° in f with an exposure time of 25 s/frame. The frames were integrated with the Bruker SAINT software package with a narrow frame algorithm. The integration of the data yielded a total of 228543 reflections to a maximum 2q value of 56.66° of which 50482 were independent and 40257 were greater than 2s(I). The final cell constants (Table 1) were based on the xyz centroids of 9252 reflections above 10s(I). Analysis of the data showed negligible decay during data collection; the data were processed with SADABS and corrected for absorption. The structure was solved and refined with the Bruker SHELXTL (version 2008/4) software package, using the space group P1bar with Z = 6 for the formula $C_{60}H_{50}O_{15}Si_{10},•C_7H_8$. There are three crystallographically independent clusters and lattice solvates. Two phenyl ligands and one toluene solvate are disordered. All non-hydrogen atoms were refined anisotropically with the hydrogen atoms placed in idealized positions. Full-matrix least-squares refinement based on F^2 converged at R1 = 0.0411 and wR2 = 0.1001 [based on I > 2sigma(I)], R1 = 0.0561 and wR2 = 0.1094 for all data. Additional details are presented in Table 1 and are given as Supporting Information in a CIF file.

Sheldrick, G.M. SHELXTL, v. 2008/4; Bruker Analytical X-ray, Madison, WI, 2008.

Saint Plus, v. 7.60A, Bruker Analytical X-ray, Madison, WI, 2009.

Sheldrick, G.M. SADABS, v. 2008/1. Program for Empirical Absorption Correction of Area Detector Data, University of Gottingen: Gottingen, Germany, 2008.

Table 1. Crystal data and structure refinement for decap.

Identification code	decap
Empirical formula	C67 H58 O15 Si10
Formula weight	1384.03
Temperature	85(2) K
Wavelength	0.71073 A
Crystal system, space group	Triclinic, P-1
Unit cell dimensions	a = 12.5377(9) A alpha = 72.706(1) deg. b = 24.6836(17) A beta = 80.434(1) deg. c = 35.061(2) A gamma = 81.395(1) deg.
Volume	10157.8(12) A^3
Z, Calculated density	6, 1.358 Mg/m^3
Absorption coefficient	0.260 mm^-1
F(000)	4320
Crystal size	0.21 x 0.21 x 0.32 mm
Theta range for data collection	1.67 to 28.33 deg.
Limiting indices	-16<=h<=16, -32<=k<=32, -46<=l<=46
Reflections collected / unique	228543 / 50482 [R(int) = 0.0516]
Completeness to theta = 28.33	99.7 %
Absorption correction	Semi-empirical from equivalents
Max. and min. transmission	0.9475 and 0.9215

Refinement method	Full-matrix least-squares on F^2
Data / restraints / parameters	50482 / 63 / 2636
Goodness-of-fit on F^2	1.014
Final R indices [I>2sigma(I)]	R1 = 0.0411, wR2 = 0.1001
R indices (all data)	R1 = 0.0561, wR2 = 0.1094
Largest diff. peak and hole	0.474 and -0.347 e.A^-3

Table 2. Atomic coordinates (x 10^4) and equivalent isotropic displacement parameters (A^2 x 10^3) for decap.

U(eq) is defined as one third of the trace of the orthogonalized Uij tensor.

	x	y	z	U(eq)
Si(1)	8550(1)	5428(1)	2638(1)	15(1)
Si(2)	10958(1)	5509(1)	2698(1)	15(1)
Si(3)	10306(1)	5595(1)	3582(1)	15(1)
Si(4)	10489(1)	4345(1)	4192(1)	16(1)
Si(5)	8036(1)	4280(1)	4182(1)	15(1)
Si(6)	7900(1)	5481(1)	3532(1)	15(1)
Si(7)	8690(1)	3462(1)	3629(1)	15(1)
Si(8)	9049(1)	4134(1)	2703(1)	16(1)
Si(9)	11452(1)	4188(1)	2763(1)	15(1)
Si(10)	11134(1)	3470(1)	3676(1)	15(1)
Si(11)	-221(1)	1261(1)	5893(1)	15(1)
Si(12)	222(1)	-60(1)	6031(1)	15(1)
Si(13)	2702(1)	-23(1)	6075(1)	16(1)
Si(14)	2236(1)	1295(1)	5987(1)	17(1)
Si(15)	1511(1)	1436(1)	6850(1)	16(1)
Si(16)	-871(1)	1302(1)	6769(1)	15(1)
Si(17)	-710(1)	119(1)	7391(1)	15(1)
Si(18)	-8(1)	-798(1)	6941(1)	15(1)
Si(19)	2423(1)	-722(1)	6986(1)	16(1)
Si(20)	1676(1)	210(1)	7460(1)	15(1)
Si(21)	2486(1)	6636(1)	-271(1)	18(1)
Si(22)	4961(1)	6582(1)	-289(1)	18(1)
Si(23)	4667(1)	6568(1)	625(1)	18(1)
Si(24)	4534(1)	7821(1)	657(1)	18(1)
Si(25)	4679(1)	8597(1)	-231(1)	15(1)
Si(26)	2139(1)	8691(1)	-191(1)	15(1)
Si(27)	2434(1)	7924(1)	-789(1)	15(1)
Si(28)	4924(1)	7867(1)	-843(1)	16(1)
Si(29)	1976(1)	7927(1)	696(1)	18(1)
Si(30)	2135(1)	6676(1)	627(1)	18(1)
O(1)	9744(1)	5642(1)	2569(1)	21(1)
O(2)	10908(1)	5613(1)	3135(1)	24(1)
O(3)	10593(1)	4970(1)	3882(1)	24(1)
O(4)	9209(1)	4258(1)	4326(1)	22(1)
O(5)	7726(1)	4888(1)	3874(1)	23(1)

O(6)	8017(1)	5354(1)	3100(1)	21(1)
O(7)	9000(1)	5714(1)	3577(1)	21(1)
O(8)	8094(1)	3794(1)	3953(1)	22(1)
O(9)	8644(1)	3890(1)	3179(1)	21(1)
O(10)	8643(1)	4809(1)	2555(1)	21(1)
O(11)	10371(1)	4059(1)	2622(1)	22(1)
O(12)	11394(1)	4856(1)	2726(1)	23(1)
O(13)	11521(1)	3848(1)	3228(1)	25(1)
O(14)	9952(1)	3268(1)	3698(1)	21(1)
O(15)	11054(1)	3859(1)	3979(1)	24(1)
O(16)	-306(1)	600(1)	5928(1)	19(1)
O(17)	1538(1)	-94(1)	5964(1)	20(1)
O(18)	2743(1)	637(1)	6056(1)	25(1)
O(19)	1042(1)	1364(1)	5849(1)	21(1)
O(20)	2148(1)	1461(1)	6405(1)	22(1)
O(21)	212(1)	1524(1)	6837(1)	21(1)
O(22)	-816(1)	619(1)	6973(1)	19(1)
O(23)	-605(1)	-480(1)	7278(1)	19(1)
O(24)	-169(1)	-376(1)	6499(1)	19(1)
O(25)	1267(1)	-945(1)	6994(1)	23(1)
O(26)	2234(1)	-269(1)	7244(1)	24(1)
O(27)	1874(1)	823(1)	7146(1)	26(1)
O(28)	375(1)	168(1)	7570(1)	21(1)
O(29)	2867(1)	-414(1)	6526(1)	26(1)
O(30)	-895(1)	1407(1)	6293(1)	18(1)
O(31)	3767(1)	6404(1)	-287(1)	27(1)
O(32)	5076(1)	6618(1)	154(1)	26(1)
O(33)	4884(1)	7145(1)	718(1)	21(1)
O(34)	4924(1)	8158(1)	196(1)	24(1)
O(35)	3393(1)	8805(1)	-223(1)	19(1)
O(36)	2037(1)	8266(1)	-452(1)	23(1)
O(37)	2338(1)	7256(1)	-585(1)	23(1)
O(38)	3694(1)	8015(1)	-962(1)	23(1)
O(39)	5077(1)	8259(1)	-566(1)	27(1)
O(40)	5107(1)	7200(1)	-603(1)	22(1)
O(41)	1714(1)	8396(1)	279(1)	20(1)
O(42)	1758(1)	7310(1)	677(1)	28(1)
O(43)	2024(1)	6702(1)	171(1)	31(1)
O(44)	3382(1)	6494(1)	714(1)	23(1)
O(45)	3228(1)	7932(1)	755(1)	22(1)
C(1)	6720(1)	6005(1)	3587(1)	19(1)
C(2)	6822(1)	6533(1)	3641(1)	25(1)
C(3)	5912(2)	6926(1)	3667(1)	33(1)
C(4)	4895(2)	6794(1)	3644(1)	34(1)
C(5)	4773(2)	6274(1)	3591(1)	32(1)
C(6)	5679(1)	5882(1)	3563(1)	24(1)
C(7)	12146(1)	2844(1)	3801(1)	19(1)
C(8)	11877(1)	2309(1)	4043(1)	24(1)

C(9)	12664(2)	1839(1)	4108(1)	29(1)
C(10)	13729(2)	1898(1)	3932(1)	30(1)
C(11)	14012(1)	2424(1)	3692(1)	29(1)
C(12)	13228(1)	2892(1)	3626(1)	24(1)
C(13)	12671(1)	3976(1)	2446(1)	21(1)
C(14)	13698(1)	3962(1)	2555(1)	33(1)
C(15)	14639(2)	3812(1)	2323(1)	46(1)
C(16)	14564(2)	3674(1)	1974(1)	47(1)
C(17)	13567(2)	3698(1)	1855(1)	48(1)
C(18)	12618(2)	3846(1)	2089(1)	35(1)
C(19)	8515(1)	3746(1)	2411(1)	21(1)
C(20)	8903(2)	3814(1)	2003(1)	28(1)
C(21)	8526(2)	3510(1)	1784(1)	36(1)
C(22)	7768(2)	3128(1)	1974(1)	36(1)
C(23)	7381(2)	3050(1)	2376(1)	33(1)
C(24)	7742(1)	3363(1)	2593(1)	27(1)
C(25)	7987(1)	2826(1)	3712(1)	17(1)
C(26)	8430(1)	2406(1)	3518(1)	24(1)
C(27)	7901(1)	1926(1)	3575(1)	28(1)
C(28)	6944(1)	1849(1)	3834(1)	28(1)
C(29)	6501(1)	2252(1)	4036(1)	27(1)
C(30)	7014(1)	2741(1)	3970(1)	22(1)
C(31)	6991(1)	4169(1)	4624(1)	21(1)
C(32)	7240(2)	3883(1)	5013(1)	30(1)
C(33)	6439(2)	3814(1)	5345(1)	39(1)
C(34)	5380(2)	4029(1)	5294(1)	45(1)
C(35)	5117(2)	4323(1)	4916(1)	58(1)
C(36)	5917(2)	4394(1)	4583(1)	44(1)
C(37)	11185(1)	4260(1)	4632(1)	21(1)
C(38)	11615(2)	3717(1)	4849(1)	29(1)
C(39)	12162(2)	3648(1)	5177(1)	39(1)
C(40)	12292(2)	4120(1)	5294(1)	40(1)
C(41)	11892(2)	4655(1)	5086(1)	41(1)
C(42)	11340(2)	4725(1)	4757(1)	32(1)
C(43)	10771(1)	6157(1)	3741(1)	18(1)
C(44)	10309(1)	6271(1)	4105(1)	28(1)
C(45)	10635(2)	6704(1)	4224(1)	35(1)
C(46)	11428(2)	7028(1)	3983(1)	34(1)
C(47)	11899(1)	6925(1)	3622(1)	30(1)
C(48)	11573(1)	6493(1)	3501(1)	24(1)
C(49)	11892(1)	5966(1)	2322(1)	19(1)
C(50)	12921(1)	5730(1)	2187(1)	24(1)
C(51)	13645(2)	6065(1)	1904(1)	32(1)
C(52)	13350(2)	6641(1)	1750(1)	34(1)
C(53)	12338(2)	6886(1)	1876(1)	33(1)
C(54)	11611(1)	6552(1)	2161(1)	25(1)
C(55)	7725(1)	5975(1)	2292(1)	19(1)
C(56)	6607(1)	6089(1)	2400(1)	24(1)

C(57)	5996(2)	6533(1)	2153(1)	31(1)
C(58)	6494(2)	6869(1)	1796(1)	32(1)
C(59)	7596(2)	6760(1)	1684(1)	29(1)
C(60)	8212(1)	6319(1)	1929(1)	24(1)
C(61)	2313(1)	93(1)	7919(1)	21(1)
C(62)	3285(1)	-267(1)	7972(1)	28(1)
C(63)	3782(2)	-376(1)	8317(1)	41(1)
C(64)	3317(2)	-128(1)	8615(1)	46(1)
C(65)	2360(2)	227(1)	8575(1)	42(1)
C(66)	1857(2)	338(1)	8228(1)	31(1)
C(67)	3404(1)	-1313(1)	7217(1)	21(1)
C(68)	3292(2)	-1532(1)	7638(1)	28(1)
C(69)	4056(2)	-1950(1)	7827(1)	35(1)
C(70)	4923(2)	-2167(1)	7600(1)	37(1)
C(71)	5040(2)	-1969(1)	7186(1)	37(1)
C(72)	4288(1)	-1540(1)	6995(1)	30(1)
C(73)	-560(1)	-1478(1)	7022(1)	17(1)
C(74)	-1382(1)	-1527(1)	6812(1)	23(1)
C(75)	-1811(2)	-2043(1)	6888(1)	30(1)
C(76)	-1424(2)	-2516(1)	7175(1)	32(1)
C(77)	-601(2)	-2484(1)	7383(1)	29(1)
C(78)	-166(1)	-1970(1)	7307(1)	23(1)
C(79)	-1886(1)	176(1)	7773(1)	18(1)
C(80)	-2939(1)	331(1)	7663(1)	23(1)
C(81)	-3838(1)	365(1)	7948(1)	29(1)
C(82)	-3701(2)	242(1)	8350(1)	33(1)
C(83)	-2673(2)	89(1)	8467(1)	35(1)
C(84)	-1770(2)	61(1)	8181(1)	28(1)
C(85)	-2078(1)	1679(1)	6992(1)	19(1)
C(86)	-3111(1)	1671(1)	6894(1)	23(1)
C(87)	-4027(2)	1952(1)	7065(1)	31(1)
C(88)	-3916(2)	2248(1)	7332(1)	40(1)
C(89)	-2906(2)	2255(1)	7439(1)	44(1)
C(90)	-1993(2)	1969(1)	7271(1)	31(1)
C(91)	1850(1)	1988(1)	7050(1)	20(1)
C(92)	1196(1)	2508(1)	7013(1)	25(1)
C(93)	1416(2)	2901(1)	7196(1)	32(1)
C(94)	2278(2)	2778(1)	7416(1)	37(1)
C(95)	2932(2)	2268(1)	7457(1)	34(1)
C(96)	2719(1)	1874(1)	7277(1)	27(1)
C(97)	3105(1)	1783(1)	5602(1)	22(1)
C(98)	3872(1)	2044(1)	5715(1)	29(1)
C(99)	4537(2)	2417(1)	5431(1)	34(1)
C(100)	4439(2)	2537(1)	5027(1)	35(1)
C(101)	3686(2)	2292(1)	4904(1)	35(1)
C(102)	3029(1)	1916(1)	5189(1)	28(1)
C(103)	3830(1)	-267(1)	5739(1)	22(1)
C(104)	4896(1)	-195(1)	5777(1)	29(1)

C(105)	5787(2)	-400(1)	5548(1)	39(1)
C(106)	5632(2)	-682(1)	5282(1)	41(1)
C(107)	4602(2)	-770(1)	5239(1)	40(1)
C(108)	3691(2)	-560(1)	5469(1)	30(1)
C(109)	-231(1)	-400(1)	5692(1)	18(1)
C(110)	-1023(1)	-124(1)	5440(1)	22(1)
C(111)	-1319(1)	-376(1)	5174(1)	25(1)
C(112)	-823(1)	-909(1)	5153(1)	27(1)
C(113)	-35(2)	-1191(1)	5397(1)	26(1)
C(114)	254(1)	-940(1)	5667(1)	23(1)
C(115)	-803(1)	1756(1)	5453(1)	19(1)
C(116)	-239(1)	2208(1)	5203(1)	23(1)
C(117)	-696(2)	2609(1)	4886(1)	29(1)
C(118)	-1724(2)	2566(1)	4815(1)	34(1)
C(119)	-2299(2)	2121(1)	5053(1)	36(1)
C(120)	-1842(1)	1720(1)	5371(1)	28(1)
C(121)	5933(1)	8026(1)	-1293(1)	21(1)
C(122)	6335(2)	7621(1)	-1500(1)	32(1)
C(123)	7101(2)	7741(1)	-1840(1)	36(1)
C(124)	7468(2)	8270(1)	-1984(1)	33(1)
C(125)	7088(2)	8682(1)	-1784(1)	34(1)
C(126)	6332(1)	8559(1)	-1441(1)	27(1)
C(127)	1566(1)	8165(1)	-1195(1)	18(1)
C(128)	1376(1)	8742(1)	-1400(1)	23(1)
C(129)	684(1)	8921(1)	-1696(1)	28(1)
C(130)	180(1)	8527(1)	-1794(1)	30(1)
C(131)	366(2)	7954(1)	-1598(1)	34(1)
C(132)	1051(1)	7772(1)	-1299(1)	27(1)
C(133)	1252(1)	6154(1)	969(1)	20(1)
C(134)	264(1)	6101(1)	857(1)	30(1)
C(135)	-421(2)	5708(1)	1104(1)	40(1)
C(136)	-115(2)	5356(1)	1463(1)	37(1)
C(137)	856(2)	5396(1)	1579(1)	38(1)
C(138)	1542(2)	5794(1)	1334(1)	30(1)
C(139)	1108(1)	8084(1)	1137(1)	23(1)
C(140)	1398(1)	8449(1)	1334(1)	26(1)
C(141)	792(2)	8528(1)	1686(1)	33(1)
C(142)	-130(2)	8243(1)	1848(1)	40(1)
C(143)	-440(2)	7890(1)	1658(1)	42(1)
C(144)	173(2)	7807(1)	1308(1)	32(1)
C(145)	1332(1)	9383(1)	-374(1)	19(1)
C(146)	487(1)	9454(1)	-609(1)	24(1)
C(147)	-95(1)	9989(1)	-742(1)	31(1)
C(148)	148(2)	10451(1)	-640(1)	34(1)
C(149)	979(2)	10392(1)	-412(1)	31(1)
C(150)	1568(1)	9863(1)	-283(1)	24(1)
C(151)	5427(1)	9225(1)	-340(1)	18(1)
C(152)	4930(1)	9783(1)	-475(1)	22(1)

C(153)	5511(2)	10253(1)	-556(1)	30(1)
C(154)	6594(2)	10170(1)	-500(1)	33(1)
C(155)	7107(2)	9623(1)	-365(1)	32(1)
C(156)	6527(1)	9154(1)	-286(1)	24(1)
C(157)	5179(1)	8084(1)	993(1)	24(1)
C(158)	4610(2)	8180(1)	1352(1)	30(1)
C(159)	5108(2)	8398(1)	1594(1)	41(1)
C(160)	6168(2)	8522(1)	1484(1)	50(1)
C(161)	6751(2)	8427(1)	1134(1)	55(1)
C(162)	6261(2)	8211(1)	888(1)	38(1)
C(163)	5391(1)	5951(1)	958(1)	23(1)
C(164)	6160(1)	6009(1)	1184(1)	22(1)
C(165)	6634(1)	5541(1)	1457(1)	28(1)
C(166)	6357(2)	5004(1)	1505(1)	51(1)
C(167)	5609(3)	4934(1)	1278(1)	76(1)
C(168)	5132(2)	5403(1)	1008(1)	56(1)
C(169)	5993(1)	6040(1)	-436(1)	27(1)
C(170)	6717(3)	5694(2)	-138(1)	30(1)
C(171)	7483(3)	5277(2)	-247(1)	38(1)
C(70A)	5886(3)	5482(1)	-328(1)	33(1)
C(72A)	6659(3)	5078(2)	-446(1)	44(1)
C(172)	7532(2)	5207(1)	-662(1)	52(1)
C(173)	6787(3)	5481(2)	-874(1)	40(1)
C(174)	6016(3)	5896(2)	-765(1)	32(1)
C(74A)	6947(3)	6222(2)	-732(1)	30(1)
C(73A)	7720(3)	5811(2)	-854(1)	42(1)
C(175)	1725(1)	6150(1)	-402(1)	29(1)
C(176)	2242(5)	5809(2)	-678(2)	25(1)
C(177)	1621(7)	5471(3)	-777(2)	42(2)
C(178)	582(9)	5454(4)	-642(4)	63(3)
C(179)	79(6)	5729(3)	-361(2)	40(2)
C(180)	677(6)	6101(3)	-267(2)	32(2)
C(76A)	2196(3)	5675(2)	-505(2)	45(1)
C(77A)	1589(4)	5312(2)	-602(2)	67(2)
C(78A)	466(5)	5420(3)	-570(3)	61(2)
C(79A)	-49(4)	5921(2)	-470(2)	58(2)
C(80A)	566(3)	6265(2)	-370(2)	39(1)
C(181)	4416(2)	4239(1)	3682(1)	42(1)
C(182)	3646(2)	4695(1)	3552(1)	45(1)
C(183)	3828(2)	5075(1)	3175(1)	44(1)
C(184)	4762(2)	5012(1)	2922(1)	46(1)
C(185)	5547(2)	4569(1)	3048(1)	49(1)
C(186)	5366(2)	4184(1)	3427(1)	45(1)
C(187)	4217(2)	3814(1)	4092(1)	66(1)
C(188)	5965(2)	-102(1)	6907(1)	31(1)
C(189)	5009(2)	266(1)	6862(1)	36(1)
C(190)	4947(2)	754(1)	6542(1)	37(1)
C(191)	5842(2)	882(1)	6254(1)	36(1)

C(192)	6798(2)	521(1)	6296(1)	40(1)
C(193)	6853(2)	36(1)	6618(1)	37(1)
C(194)	6032(2)	-630(1)	7257(1)	42(1)
C(195)	1551(3)	2104(2)	384(1)	36(1)
C(196)	893(4)	2095(2)	109(2)	54(2)
C(197)	941(4)	2464(2)	-268(2)	58(1)
C(198)	1682(4)	2855(2)	-391(2)	58(2)
C(199)	2405(4)	2845(3)	-113(2)	56(2)
C(200)	2292(3)	2515(2)	253(1)	50(1)
C(201)	1499(4)	1699(2)	792(1)	69(2)
C(15A)	1633(4)	2499(3)	321(1)	54(2)
C(16A)	880(5)	2156(3)	304(2)	63(2)
C(17A)	720(5)	2083(3)	-53(2)	71(2)
C(18A)	1322(5)	2337(3)	-402(2)	61(2)
C(19A)	2108(5)	2694(3)	-388(2)	62(2)
C(20A)	2132(5)	2813(3)	-49(2)	67(3)
C(21A)	1776(5)	2599(4)	705(2)	101(3)

Table 3. Bond lengths [A] and angles [deg] for decap.

Si(1)-O(6)	1.6131(11)
Si(1)-O(1)	1.6197(11)
Si(1)-O(10)	1.6205(11)
Si(1)-C(55)	1.8431(15)
Si(2)-O(12)	1.6018(11)
Si(2)-O(2)	1.6162(12)
Si(2)-O(1)	1.6181(11)
Si(2)-C(49)	1.8381(16)
Si(3)-O(2)	1.6149(12)
Si(3)-O(3)	1.6157(11)
Si(3)-O(7)	1.6207(11)
Si(3)-C(43)	1.8405(16)
Si(4)-O(3)	1.6106(11)
Si(4)-O(15)	1.6144(12)
Si(4)-O(4)	1.6223(11)
Si(4)-C(37)	1.8400(16)
Si(5)-O(5)	1.6045(11)
Si(5)-O(8)	1.6188(12)
Si(5)-O(4)	1.6193(12)
Si(5)-C(31)	1.8363(16)
Si(6)-O(5)	1.6090(11)
Si(6)-O(6)	1.6164(11)
Si(6)-O(7)	1.6182(11)
Si(6)-C(1)	1.8381(16)
Si(7)-O(8)	1.6136(12)
Si(7)-O(14)	1.6192(11)
Si(7)-O(9)	1.6229(11)
Si(7)-C(25)	1.8405(15)
Si(8)-O(9)	1.6172(11)
Si(8)-O(10)	1.6200(11)
Si(8)-O(11)	1.6257(12)
Si(8)-C(19)	1.8496(16)
Si(9)-O(12)	1.6063(11)
Si(9)-O(13)	1.6064(12)
Si(9)-O(11)	1.6220(12)
Si(9)-C(13)	1.8401(16)
Si(10)-O(13)	1.6072(11)
Si(10)-O(15)	1.6126(12)
Si(10)-O(14)	1.6174(11)
Si(10)-C(7)	1.8401(16)
Si(11)-O(19)	1.6161(11)
Si(11)-O(16)	1.6179(11)
Si(11)-O(30)	1.6183(11)

Si(11)-C(115)	1.8431(15)
Si(12)-O(24)	1.6213(11)
Si(12)-O(17)	1.6215(11)
Si(12)-O(16)	1.6220(11)
Si(12)-C(109)	1.8425(16)
Si(13)-O(29)	1.6159(12)
Si(13)-O(18)	1.6178(12)
Si(13)-O(17)	1.6199(11)
Si(13)-C(103)	1.8363(16)
Si(14)-O(18)	1.6144(12)
Si(14)-O(20)	1.6176(12)
Si(14)-O(19)	1.6180(12)
Si(14)-C(97)	1.8443(17)
Si(15)-O(27)	1.6102(12)
Si(15)-O(21)	1.6166(11)
Si(15)-O(20)	1.6178(12)
Si(15)-C(91)	1.8360(16)
Si(16)-O(21)	1.6152(12)
Si(16)-O(30)	1.6160(11)
Si(16)-O(22)	1.6206(11)
Si(16)-C(85)	1.8398(16)
Si(17)-O(22)	1.6195(11)
Si(17)-O(23)	1.6231(11)
Si(17)-O(28)	1.6241(11)
Si(17)-C(79)	1.8386(16)
Si(18)-O(25)	1.6147(11)
Si(18)-O(24)	1.6168(11)
Si(18)-O(23)	1.6265(11)
Si(18)-C(73)	1.8389(15)
Si(19)-O(26)	1.6058(12)
Si(19)-O(29)	1.6086(12)
Si(19)-O(25)	1.6178(12)
Si(19)-C(67)	1.8404(16)
Si(20)-O(26)	1.6020(12)
Si(20)-O(27)	1.6101(12)
Si(20)-O(28)	1.6246(11)
Si(20)-C(61)	1.8432(16)
Si(21)-O(37)	1.6030(11)
Si(21)-O(43)	1.6088(13)
Si(21)-O(31)	1.6189(12)
Si(21)-C(175)	1.8363(18)
Si(22)-O(40)	1.6094(12)
Si(22)-O(32)	1.6134(12)
Si(22)-O(31)	1.6217(12)
Si(22)-C(169)	1.8453(17)
Si(23)-O(44)	1.6166(12)
Si(23)-O(32)	1.6168(12)
Si(23)-O(33)	1.6207(12)

Si(23)-C(163)	1.8420(16)
Si(24)-O(34)	1.6132(12)
Si(24)-O(45)	1.6154(12)
Si(24)-O(33)	1.6203(11)
Si(24)-C(157)	1.8440(17)
Si(25)-O(39)	1.6105(12)
Si(25)-O(34)	1.6116(11)
Si(25)-O(35)	1.6151(11)
Si(25)-C(151)	1.8417(16)
Si(26)-O(36)	1.6150(12)
Si(26)-O(35)	1.6186(11)
Si(26)-O(41)	1.6245(11)
Si(26)-C(145)	1.8437(15)
Si(27)-O(37)	1.6060(11)
Si(27)-O(38)	1.6183(11)
Si(27)-O(36)	1.6195(12)
Si(27)-C(127)	1.8398(15)
Si(28)-O(39)	1.6093(12)
Si(28)-O(40)	1.6136(11)
Si(28)-O(38)	1.6233(12)
Si(28)-C(121)	1.8321(16)
Si(29)-O(42)	1.6105(12)
Si(29)-O(45)	1.6183(12)
Si(29)-O(41)	1.6216(11)
Si(29)-C(139)	1.8426(17)
Si(30)-O(43)	1.6089(13)
Si(30)-O(44)	1.6145(12)
Si(30)-O(42)	1.6171(13)
Si(30)-C(133)	1.8401(16)
C(1)-C(2)	1.398(2)
C(1)-C(6)	1.405(2)
C(2)-C(3)	1.392(2)
C(3)-C(4)	1.382(3)
C(4)-C(5)	1.383(3)
C(5)-C(6)	1.390(2)
C(7)-C(8)	1.398(2)
C(7)-C(12)	1.400(2)
C(8)-C(9)	1.394(2)
C(9)-C(10)	1.385(3)
C(10)-C(11)	1.382(3)
C(11)-C(12)	1.389(2)
C(13)-C(18)	1.394(3)
C(13)-C(14)	1.395(2)
C(14)-C(15)	1.386(3)
C(15)-C(16)	1.386(4)
C(16)-C(17)	1.370(3)
C(17)-C(18)	1.396(3)
C(19)-C(24)	1.398(2)

C(19)-C(20)	1.398(2)
C(20)-C(21)	1.397(3)
C(21)-C(22)	1.386(3)
C(22)-C(23)	1.377(3)
C(23)-C(24)	1.397(2)
C(25)-C(30)	1.396(2)
C(25)-C(26)	1.403(2)
C(26)-C(27)	1.389(2)
C(27)-C(28)	1.379(3)
C(28)-C(29)	1.388(3)
C(29)-C(30)	1.391(2)
C(31)-C(36)	1.391(2)
C(31)-C(32)	1.398(2)
C(32)-C(33)	1.392(2)
C(33)-C(34)	1.374(3)
C(34)-C(35)	1.376(3)
C(35)-C(36)	1.394(3)
C(37)-C(42)	1.393(2)
C(37)-C(38)	1.407(2)
C(38)-C(39)	1.392(3)
C(39)-C(40)	1.384(3)
C(40)-C(41)	1.370(3)
C(41)-C(42)	1.395(3)
C(43)-C(44)	1.399(2)
C(43)-C(48)	1.400(2)
C(44)-C(45)	1.392(2)
C(45)-C(46)	1.378(3)
C(46)-C(47)	1.385(3)
C(47)-C(48)	1.393(2)
C(49)-C(50)	1.401(2)
C(49)-C(54)	1.403(2)
C(50)-C(51)	1.390(2)
C(51)-C(52)	1.379(3)
C(52)-C(53)	1.384(3)
C(53)-C(54)	1.392(2)
C(55)-C(56)	1.399(2)
C(55)-C(60)	1.402(2)
C(56)-C(57)	1.393(2)
C(57)-C(58)	1.386(3)
C(58)-C(59)	1.381(3)
C(59)-C(60)	1.390(2)
C(61)-C(66)	1.395(2)
C(61)-C(62)	1.401(2)
C(62)-C(63)	1.389(3)
C(63)-C(64)	1.371(3)
C(64)-C(65)	1.377(3)
C(65)-C(66)	1.399(3)
C(67)-C(72)	1.390(2)

C(67)-C(68)	1.404(2)
C(68)-C(69)	1.390(2)
C(69)-C(70)	1.376(3)
C(70)-C(71)	1.376(3)
C(71)-C(72)	1.396(3)
C(73)-C(74)	1.401(2)
C(73)-C(78)	1.405(2)
C(74)-C(75)	1.393(2)
C(75)-C(76)	1.379(3)
C(76)-C(77)	1.384(3)
C(77)-C(78)	1.391(2)
C(79)-C(84)	1.400(2)
C(79)-C(80)	1.403(2)
C(80)-C(81)	1.387(2)
C(81)-C(82)	1.387(3)
C(82)-C(83)	1.381(3)
C(83)-C(84)	1.391(2)
C(85)-C(90)	1.398(2)
C(85)-C(86)	1.399(2)
C(86)-C(87)	1.393(2)
C(87)-C(88)	1.383(3)
C(88)-C(89)	1.382(3)
C(89)-C(90)	1.392(3)
C(91)-C(96)	1.399(2)
C(91)-C(92)	1.400(2)
C(92)-C(93)	1.394(2)
C(93)-C(94)	1.376(3)
C(94)-C(95)	1.378(3)
C(95)-C(96)	1.383(2)
C(97)-C(98)	1.400(2)
C(97)-C(102)	1.402(2)
C(98)-C(99)	1.394(2)
C(99)-C(100)	1.382(3)
C(100)-C(101)	1.380(3)
C(101)-C(102)	1.395(2)
C(103)-C(108)	1.395(2)
C(103)-C(104)	1.408(2)
C(104)-C(105)	1.385(3)
C(105)-C(106)	1.371(3)
C(106)-C(107)	1.380(3)
C(107)-C(108)	1.409(3)
C(109)-C(110)	1.400(2)
C(109)-C(114)	1.403(2)
C(110)-C(111)	1.390(2)
C(111)-C(112)	1.386(2)
C(112)-C(113)	1.383(2)
C(113)-C(114)	1.390(2)
C(115)-C(120)	1.400(2)

C(115)-C(116)	1.401(2)
C(116)-C(117)	1.389(2)
C(117)-C(118)	1.379(3)
C(118)-C(119)	1.383(3)
C(119)-C(120)	1.391(2)
C(121)-C(122)	1.392(2)
C(121)-C(126)	1.399(2)
C(122)-C(123)	1.389(2)
C(123)-C(124)	1.373(3)
C(124)-C(125)	1.386(3)
C(125)-C(126)	1.387(2)
C(127)-C(128)	1.396(2)
C(127)-C(132)	1.404(2)
C(128)-C(129)	1.390(2)
C(129)-C(130)	1.383(3)
C(130)-C(131)	1.381(3)
C(131)-C(132)	1.393(2)
C(133)-C(138)	1.394(2)
C(133)-C(134)	1.396(2)
C(134)-C(135)	1.390(3)
C(135)-C(136)	1.378(3)
C(136)-C(137)	1.370(3)
C(137)-C(138)	1.396(3)
C(139)-C(144)	1.401(2)
C(139)-C(140)	1.404(3)
C(140)-C(141)	1.388(2)
C(141)-C(142)	1.393(3)
C(142)-C(143)	1.374(3)
C(143)-C(144)	1.389(3)
C(145)-C(150)	1.400(2)
C(145)-C(146)	1.405(2)
C(146)-C(147)	1.397(2)
C(147)-C(148)	1.381(3)
C(148)-C(149)	1.382(3)
C(149)-C(150)	1.388(2)
C(151)-C(156)	1.400(2)
C(151)-C(152)	1.401(2)
C(152)-C(153)	1.394(2)
C(153)-C(154)	1.379(3)
C(154)-C(155)	1.387(3)
C(155)-C(156)	1.394(2)
C(157)-C(162)	1.402(2)
C(157)-C(158)	1.405(3)
C(158)-C(159)	1.396(3)
C(159)-C(160)	1.374(3)
C(160)-C(161)	1.383(4)
C(161)-C(162)	1.398(3)
C(163)-C(168)	1.391(3)

C(163)-C(164)	1.392(2)
C(164)-C(165)	1.392(2)
C(165)-C(166)	1.376(3)
C(166)-C(167)	1.386(3)
C(167)-C(168)	1.386(3)
C(169)-C(174)	1.299(4)
C(169)-C(70A)	1.338(4)
C(169)-C(74A)	1.475(4)
C(169)-C(170)	1.484(4)
C(170)-C(171)	1.395(5)
C(171)-C(172)	1.505(5)
C(70A)-C(72A)	1.387(5)
C(72A)-C(172)	1.248(5)
C(172)-C(173)	1.275(5)
C(172)-C(73A)	1.480(5)
C(173)-C(174)	1.394(5)
C(74A)-C(73A)	1.405(5)
C(175)-C(180)	1.330(7)
C(175)-C(76A)	1.353(4)
C(175)-C(80A)	1.430(5)
C(175)-C(176)	1.478(6)
C(176)-C(177)	1.370(10)
C(177)-C(178)	1.311(14)
C(178)-C(179)	1.375(14)
C(179)-C(180)	1.409(11)
C(76A)-C(77A)	1.403(7)
C(77A)-C(78A)	1.385(8)
C(78A)-C(79A)	1.418(9)
C(79A)-C(80A)	1.378(7)
C(181)-C(186)	1.382(3)
C(181)-C(182)	1.387(3)
C(181)-C(187)	1.513(3)
C(182)-C(183)	1.381(3)
C(183)-C(184)	1.367(3)
C(184)-C(185)	1.376(3)
C(185)-C(186)	1.390(3)
C(188)-C(193)	1.383(3)
C(188)-C(189)	1.392(3)
C(188)-C(194)	1.504(3)
C(189)-C(190)	1.383(3)
C(190)-C(191)	1.385(3)
C(191)-C(192)	1.383(3)
C(192)-C(193)	1.383(3)
C(195)-C(196)	1.376(5)
C(195)-C(200)	1.404(5)
C(195)-C(201)	1.479(5)
C(196)-C(197)	1.361(7)
C(197)-C(198)	1.366(7)

C(198)-C(199)	1.429(7)
C(199)-C(200)	1.297(7)
C(15A)-C(16A)	1.379(7)
C(15A)-C(20A)	1.399(7)
C(15A)-C(21A)	1.483(7)
C(16A)-C(17A)	1.365(8)
C(17A)-C(18A)	1.356(8)
C(18A)-C(19A)	1.432(8)
C(19A)-C(20A)	1.309(8)

O(6)-Si(1)-O(1)	109.79(6)
O(6)-Si(1)-O(10)	107.34(6)
O(1)-Si(1)-O(10)	110.23(6)
O(6)-Si(1)-C(55)	110.79(7)
O(1)-Si(1)-C(55)	106.89(7)
O(10)-Si(1)-C(55)	111.84(6)
O(12)-Si(2)-O(2)	109.19(6)
O(12)-Si(2)-O(1)	109.24(6)
O(2)-Si(2)-O(1)	108.78(6)
O(12)-Si(2)-C(49)	108.48(7)
O(2)-Si(2)-C(49)	110.49(7)
O(1)-Si(2)-C(49)	110.63(6)
O(2)-Si(3)-O(3)	109.00(6)
O(2)-Si(3)-O(7)	109.78(6)
O(3)-Si(3)-O(7)	109.06(6)
O(2)-Si(3)-C(43)	108.27(7)
O(3)-Si(3)-C(43)	111.43(7)
O(7)-Si(3)-C(43)	109.28(6)
O(3)-Si(4)-O(15)	110.33(6)
O(3)-Si(4)-O(4)	108.80(6)
O(15)-Si(4)-O(4)	108.41(6)
O(3)-Si(4)-C(37)	110.49(7)
O(15)-Si(4)-C(37)	107.47(7)
O(4)-Si(4)-C(37)	111.31(7)
O(5)-Si(5)-O(8)	108.08(6)
O(5)-Si(5)-O(4)	110.74(6)
O(8)-Si(5)-O(4)	108.98(6)
O(5)-Si(5)-C(31)	108.67(7)
O(8)-Si(5)-C(31)	111.08(7)
O(4)-Si(5)-C(31)	109.29(7)
O(5)-Si(6)-O(6)	107.41(6)
O(5)-Si(6)-O(7)	109.50(6)
O(6)-Si(6)-O(7)	109.74(6)
O(5)-Si(6)-C(1)	109.45(7)
O(6)-Si(6)-C(1)	110.40(6)
O(7)-Si(6)-C(1)	110.29(7)
O(8)-Si(7)-O(14)	109.99(6)
O(8)-Si(7)-O(9)	109.07(6)

O(14)-Si(7)-O(9)	108.63(6)
O(8)-Si(7)-C(25)	107.50(6)
O(14)-Si(7)-C(25)	109.42(6)
O(9)-Si(7)-C(25)	112.22(6)
O(9)-Si(8)-O(10)	109.40(6)
O(9)-Si(8)-O(11)	110.00(6)
O(10)-Si(8)-O(11)	107.88(6)
O(9)-Si(8)-C(19)	110.51(7)
O(10)-Si(8)-C(19)	110.18(6)
O(11)-Si(8)-C(19)	108.82(7)
O(12)-Si(9)-O(13)	107.13(7)
O(12)-Si(9)-O(11)	109.95(6)
O(13)-Si(9)-O(11)	110.16(6)
O(12)-Si(9)-C(13)	109.62(7)
O(13)-Si(9)-C(13)	110.08(7)
O(11)-Si(9)-C(13)	109.87(7)
O(13)-Si(10)-O(15)	108.20(7)
O(13)-Si(10)-O(14)	110.25(6)
O(15)-Si(10)-O(14)	109.19(6)
O(13)-Si(10)-C(7)	107.70(7)
O(15)-Si(10)-C(7)	111.51(7)
O(14)-Si(10)-C(7)	109.96(7)
O(19)-Si(11)-O(16)	109.49(6)
O(19)-Si(11)-O(30)	110.84(6)
O(16)-Si(11)-O(30)	108.58(6)
O(19)-Si(11)-C(115)	107.73(7)
O(16)-Si(11)-C(115)	112.40(7)
O(30)-Si(11)-C(115)	107.80(6)
O(24)-Si(12)-O(17)	108.46(6)
O(24)-Si(12)-O(16)	108.94(6)
O(17)-Si(12)-O(16)	110.36(6)
O(24)-Si(12)-C(109)	111.15(6)
O(17)-Si(12)-C(109)	109.56(6)
O(16)-Si(12)-C(109)	108.36(6)
O(29)-Si(13)-O(18)	108.50(7)
O(29)-Si(13)-O(17)	110.39(6)
O(18)-Si(13)-O(17)	109.31(6)
O(29)-Si(13)-C(103)	106.20(7)
O(18)-Si(13)-C(103)	111.26(7)
O(17)-Si(13)-C(103)	111.12(7)
O(18)-Si(14)-O(20)	108.79(6)
O(18)-Si(14)-O(19)	108.54(6)
O(20)-Si(14)-O(19)	110.25(6)
O(18)-Si(14)-C(97)	111.76(7)
O(20)-Si(14)-C(97)	107.72(7)
O(19)-Si(14)-C(97)	109.77(7)
O(27)-Si(15)-O(21)	110.98(6)
O(27)-Si(15)-O(20)	107.61(6)

O(21)-Si(15)-O(20)	109.88(6)
O(27)-Si(15)-C(91)	107.90(7)
O(21)-Si(15)-C(91)	107.89(7)
O(20)-Si(15)-C(91)	112.60(7)
O(21)-Si(16)-O(30)	109.62(6)
O(21)-Si(16)-O(22)	108.65(6)
O(30)-Si(16)-O(22)	106.75(6)
O(21)-Si(16)-C(85)	109.34(7)
O(30)-Si(16)-C(85)	111.03(6)
O(22)-Si(16)-C(85)	111.37(6)
O(22)-Si(17)-O(23)	106.13(6)
O(22)-Si(17)-O(28)	109.36(6)
O(23)-Si(17)-O(28)	110.21(6)
O(22)-Si(17)-C(79)	111.89(6)
O(23)-Si(17)-C(79)	111.27(6)
O(28)-Si(17)-C(79)	107.98(7)
O(25)-Si(18)-O(24)	110.59(6)
O(25)-Si(18)-O(23)	108.51(6)
O(24)-Si(18)-O(23)	108.79(6)
O(25)-Si(18)-C(73)	107.14(6)
O(24)-Si(18)-C(73)	111.14(6)
O(23)-Si(18)-C(73)	110.63(6)
O(26)-Si(19)-O(29)	109.44(7)
O(26)-Si(19)-O(25)	108.59(6)
O(29)-Si(19)-O(25)	108.35(6)
O(26)-Si(19)-C(67)	107.71(7)
O(29)-Si(19)-C(67)	111.49(7)
O(25)-Si(19)-C(67)	111.21(7)
O(26)-Si(20)-O(27)	107.71(7)
O(26)-Si(20)-O(28)	110.08(6)
O(27)-Si(20)-O(28)	108.67(6)
O(26)-Si(20)-C(61)	107.84(7)
O(27)-Si(20)-C(61)	111.74(7)
O(28)-Si(20)-C(61)	110.76(6)
O(37)-Si(21)-O(43)	107.53(7)
O(37)-Si(21)-O(31)	109.23(6)
O(43)-Si(21)-O(31)	109.56(7)
O(37)-Si(21)-C(175)	109.13(7)
O(43)-Si(21)-C(175)	110.79(8)
O(31)-Si(21)-C(175)	110.55(7)
O(40)-Si(22)-O(32)	108.45(6)
O(40)-Si(22)-O(31)	109.70(6)
O(32)-Si(22)-O(31)	109.33(7)
O(40)-Si(22)-C(169)	110.15(7)
O(32)-Si(22)-C(169)	110.85(7)
O(31)-Si(22)-C(169)	108.35(7)
O(44)-Si(23)-O(32)	108.72(6)
O(44)-Si(23)-O(33)	110.21(6)

O(32)-Si(23)-O(33)	108.71(6)
O(44)-Si(23)-C(163)	108.53(7)
O(32)-Si(23)-C(163)	111.90(7)
O(33)-Si(23)-C(163)	108.77(7)
O(34)-Si(24)-O(45)	110.03(6)
O(34)-Si(24)-O(33)	108.53(6)
O(45)-Si(24)-O(33)	109.24(6)
O(34)-Si(24)-C(157)	108.97(7)
O(45)-Si(24)-C(157)	109.19(7)
O(33)-Si(24)-C(157)	110.88(7)
O(39)-Si(25)-O(34)	106.71(7)
O(39)-Si(25)-O(35)	110.12(6)
O(34)-Si(25)-O(35)	110.29(6)
O(39)-Si(25)-C(151)	110.55(7)
O(34)-Si(25)-C(151)	110.15(7)
O(35)-Si(25)-C(151)	109.01(7)
O(36)-Si(26)-O(35)	110.73(6)
O(36)-Si(26)-O(41)	108.94(6)
O(35)-Si(26)-O(41)	108.13(6)
O(36)-Si(26)-C(145)	110.47(7)
O(35)-Si(26)-C(145)	108.35(7)
O(41)-Si(26)-C(145)	110.19(6)
O(37)-Si(27)-O(38)	108.94(6)
O(37)-Si(27)-O(36)	109.40(6)
O(38)-Si(27)-O(36)	108.76(6)
O(37)-Si(27)-C(127)	107.49(7)
O(38)-Si(27)-C(127)	111.38(6)
O(36)-Si(27)-C(127)	110.83(7)
O(39)-Si(28)-O(40)	110.66(7)
O(39)-Si(28)-O(38)	108.65(6)
O(40)-Si(28)-O(38)	108.88(6)
O(39)-Si(28)-C(121)	107.80(7)
O(40)-Si(28)-C(121)	109.58(7)
O(38)-Si(28)-C(121)	111.27(7)
O(42)-Si(29)-O(45)	111.11(6)
O(42)-Si(29)-O(41)	108.71(7)
O(45)-Si(29)-O(41)	109.10(6)
O(42)-Si(29)-C(139)	108.33(7)
O(45)-Si(29)-C(139)	107.61(7)
O(41)-Si(29)-C(139)	112.00(6)
O(43)-Si(30)-O(44)	110.54(7)
O(43)-Si(30)-O(42)	107.21(7)
O(44)-Si(30)-O(42)	108.97(6)
O(43)-Si(30)-C(133)	108.22(7)
O(44)-Si(30)-C(133)	110.44(7)
O(42)-Si(30)-C(133)	111.42(7)
Si(2)-O(1)-Si(1)	146.60(8)
Si(3)-O(2)-Si(2)	151.71(8)

Si(4)-O(3)-Si(3)	162.62(8)
Si(5)-O(4)-Si(4)	147.10(8)
Si(5)-O(5)-Si(6)	158.62(8)
Si(1)-O(6)-Si(6)	153.31(8)
Si(6)-O(7)-Si(3)	147.36(8)
Si(7)-O(8)-Si(5)	151.36(8)
Si(8)-O(9)-Si(7)	155.78(8)
Si(8)-O(10)-Si(1)	146.97(8)
Si(9)-O(11)-Si(8)	142.94(8)
Si(2)-O(12)-Si(9)	162.90(8)
Si(9)-O(13)-Si(10)	158.18(8)
Si(10)-O(14)-Si(7)	146.48(7)
Si(10)-O(15)-Si(4)	154.63(8)
Si(11)-O(16)-Si(12)	149.86(8)
Si(13)-O(17)-Si(12)	153.71(8)
Si(14)-O(18)-Si(13)	153.65(8)
Si(11)-O(19)-Si(14)	156.76(8)
Si(14)-O(20)-Si(15)	148.91(8)
Si(16)-O(21)-Si(15)	149.85(8)
Si(17)-O(22)-Si(16)	144.11(8)
Si(17)-O(23)-Si(18)	142.02(7)
Si(18)-O(24)-Si(12)	154.97(8)
Si(18)-O(25)-Si(19)	148.80(8)
Si(20)-O(26)-Si(19)	162.09(8)
Si(20)-O(27)-Si(15)	155.09(8)
Si(17)-O(28)-Si(20)	143.80(8)
Si(19)-O(29)-Si(13)	152.82(8)
Si(16)-O(30)-Si(11)	143.28(7)
Si(21)-O(31)-Si(22)	143.49(8)
Si(22)-O(32)-Si(23)	154.86(9)
Si(24)-O(33)-Si(23)	146.84(8)
Si(25)-O(34)-Si(24)	151.32(8)
Si(25)-O(35)-Si(26)	152.49(8)
Si(26)-O(36)-Si(27)	155.94(8)
Si(21)-O(37)-Si(27)	159.24(8)
Si(27)-O(38)-Si(28)	143.59(8)
Si(28)-O(39)-Si(25)	154.62(8)
Si(22)-O(40)-Si(28)	163.18(8)
Si(29)-O(41)-Si(26)	147.10(7)
Si(29)-O(42)-Si(30)	153.82(8)
Si(21)-O(43)-Si(30)	153.94(9)
Si(30)-O(44)-Si(23)	153.51(8)
Si(24)-O(45)-Si(29)	155.69(9)
C(2)-C(1)-C(6)	118.39(15)
C(2)-C(1)-Si(6)	122.27(12)
C(6)-C(1)-Si(6)	119.32(12)
C(3)-C(2)-C(1)	120.40(17)
C(4)-C(3)-C(2)	120.25(17)

C(3)-C(4)-C(5)	120.39(17)
C(4)-C(5)-C(6)	119.70(17)
C(5)-C(6)-C(1)	120.85(16)
C(8)-C(7)-C(12)	117.83(14)
C(8)-C(7)-Si(10)	123.14(12)
C(12)-C(7)-Si(10)	118.91(12)
C(9)-C(8)-C(7)	120.86(15)
C(10)-C(9)-C(8)	120.22(16)
C(11)-C(10)-C(9)	119.74(16)
C(10)-C(11)-C(12)	120.13(16)
C(11)-C(12)-C(7)	121.22(15)
C(18)-C(13)-C(14)	117.85(16)
C(18)-C(13)-Si(9)	122.60(14)
C(14)-C(13)-Si(9)	119.50(13)
C(15)-C(14)-C(13)	121.5(2)
C(16)-C(15)-C(14)	119.5(2)
C(17)-C(16)-C(15)	120.07(19)
C(16)-C(17)-C(18)	120.5(2)
C(13)-C(18)-C(17)	120.5(2)
C(24)-C(19)-C(20)	118.13(15)
C(24)-C(19)-Si(8)	121.07(13)
C(20)-C(19)-Si(8)	120.76(13)
C(21)-C(20)-C(19)	121.02(17)
C(22)-C(21)-C(20)	119.50(18)
C(23)-C(22)-C(21)	120.59(17)
C(22)-C(23)-C(24)	119.85(17)
C(23)-C(24)-C(19)	120.89(17)
C(30)-C(25)-C(26)	117.90(14)
C(30)-C(25)-Si(7)	121.73(12)
C(26)-C(25)-Si(7)	120.36(12)
C(27)-C(26)-C(25)	120.86(15)
C(28)-C(27)-C(26)	120.18(16)
C(27)-C(28)-C(29)	120.11(16)
C(28)-C(29)-C(30)	119.65(16)
C(29)-C(30)-C(25)	121.25(15)
C(36)-C(31)-C(32)	117.45(15)
C(36)-C(31)-Si(5)	120.28(13)
C(32)-C(31)-Si(5)	122.20(13)
C(33)-C(32)-C(31)	121.32(17)
C(34)-C(33)-C(32)	119.98(18)
C(33)-C(34)-C(35)	119.91(18)
C(34)-C(35)-C(36)	120.2(2)
C(31)-C(36)-C(35)	121.08(18)
C(42)-C(37)-C(38)	117.42(16)
C(42)-C(37)-Si(4)	122.03(13)
C(38)-C(37)-Si(4)	120.53(13)
C(39)-C(38)-C(37)	121.05(18)
C(40)-C(39)-C(38)	119.88(19)

C(41)-C(40)-C(39)	120.18(18)
C(40)-C(41)-C(42)	120.14(19)
C(37)-C(42)-C(41)	121.32(18)
C(44)-C(43)-C(48)	117.81(15)
C(44)-C(43)-Si(3)	120.59(12)
C(48)-C(43)-Si(3)	121.58(12)
C(45)-C(44)-C(43)	121.12(16)
C(46)-C(45)-C(44)	120.09(18)
C(45)-C(46)-C(47)	119.99(17)
C(46)-C(47)-C(48)	120.11(16)
C(47)-C(48)-C(43)	120.88(16)
C(50)-C(49)-C(54)	117.81(14)
C(50)-C(49)-Si(2)	120.08(12)
C(54)-C(49)-Si(2)	122.11(12)
C(51)-C(50)-C(49)	121.41(16)
C(52)-C(51)-C(50)	119.65(17)
C(51)-C(52)-C(53)	120.37(16)
C(52)-C(53)-C(54)	120.15(17)
C(53)-C(54)-C(49)	120.61(16)
C(56)-C(55)-C(60)	118.26(14)
C(56)-C(55)-Si(1)	120.51(12)
C(60)-C(55)-Si(1)	121.02(12)
C(57)-C(56)-C(55)	120.70(16)
C(58)-C(57)-C(56)	120.14(17)
C(59)-C(58)-C(57)	119.86(16)
C(58)-C(59)-C(60)	120.38(17)
C(59)-C(60)-C(55)	120.67(16)
C(66)-C(61)-C(62)	117.45(15)
C(66)-C(61)-Si(20)	122.92(13)
C(62)-C(61)-Si(20)	119.61(13)
C(63)-C(62)-C(61)	121.58(18)
C(64)-C(63)-C(62)	119.70(19)
C(63)-C(64)-C(65)	120.41(18)
C(64)-C(65)-C(66)	120.07(19)
C(61)-C(66)-C(65)	120.79(18)
C(72)-C(67)-C(68)	117.69(15)
C(72)-C(67)-Si(19)	123.18(13)
C(68)-C(67)-Si(19)	119.07(12)
C(69)-C(68)-C(67)	121.09(17)
C(70)-C(69)-C(68)	119.86(18)
C(71)-C(70)-C(69)	120.29(17)
C(70)-C(71)-C(72)	119.99(18)
C(67)-C(72)-C(71)	121.05(18)
C(74)-C(73)-C(78)	117.89(14)
C(74)-C(73)-Si(18)	122.17(12)
C(78)-C(73)-Si(18)	119.93(12)
C(75)-C(74)-C(73)	121.03(15)
C(76)-C(75)-C(74)	119.85(17)

C(75)-C(76)-C(77)	120.45(16)
C(76)-C(77)-C(78)	119.97(16)
C(77)-C(78)-C(73)	120.79(16)
C(84)-C(79)-C(80)	117.78(14)
C(84)-C(79)-Si(17)	121.79(12)
C(80)-C(79)-Si(17)	120.43(12)
C(81)-C(80)-C(79)	121.31(16)
C(82)-C(81)-C(80)	119.66(17)
C(83)-C(82)-C(81)	120.28(17)
C(82)-C(83)-C(84)	120.06(17)
C(83)-C(84)-C(79)	120.90(16)
C(90)-C(85)-C(86)	118.19(15)
C(90)-C(85)-Si(16)	121.06(13)
C(86)-C(85)-Si(16)	120.73(12)
C(87)-C(86)-C(85)	120.80(17)
C(88)-C(87)-C(86)	119.82(18)
C(89)-C(88)-C(87)	120.44(18)
C(88)-C(89)-C(90)	119.72(19)
C(89)-C(90)-C(85)	121.00(18)
C(96)-C(91)-C(92)	118.37(15)
C(96)-C(91)-Si(15)	120.14(12)
C(92)-C(91)-Si(15)	121.23(13)
C(93)-C(92)-C(91)	120.27(17)
C(94)-C(93)-C(92)	119.99(17)
C(93)-C(94)-C(95)	120.64(17)
C(94)-C(95)-C(96)	119.81(18)
C(95)-C(96)-C(91)	120.91(17)
C(98)-C(97)-C(102)	117.16(15)
C(98)-C(97)-Si(14)	120.36(13)
C(102)-C(97)-Si(14)	122.48(13)
C(99)-C(98)-C(97)	121.66(17)
C(100)-C(99)-C(98)	119.62(18)
C(101)-C(100)-C(99)	120.31(17)
C(100)-C(101)-C(102)	119.85(18)
C(101)-C(102)-C(97)	121.39(17)
C(108)-C(103)-C(104)	118.28(16)
C(108)-C(103)-Si(13)	123.26(14)
C(104)-C(103)-Si(13)	118.28(13)
C(105)-C(104)-C(103)	121.14(19)
C(106)-C(105)-C(104)	119.7(2)
C(105)-C(106)-C(107)	121.15(18)
C(106)-C(107)-C(108)	119.56(19)
C(103)-C(108)-C(107)	120.19(19)
C(110)-C(109)-C(114)	117.83(14)
C(110)-C(109)-Si(12)	121.95(12)
C(114)-C(109)-Si(12)	120.16(12)
C(111)-C(110)-C(109)	121.17(15)
C(112)-C(111)-C(110)	119.85(15)

C(113)-C(112)-C(111)	120.18(16)
C(112)-C(113)-C(114)	119.96(16)
C(113)-C(114)-C(109)	121.01(15)
C(120)-C(115)-C(116)	117.74(14)
C(120)-C(115)-Si(11)	121.90(12)
C(116)-C(115)-Si(11)	120.22(12)
C(117)-C(116)-C(115)	121.14(16)
C(118)-C(117)-C(116)	119.86(16)
C(117)-C(118)-C(119)	120.40(16)
C(118)-C(119)-C(120)	119.74(18)
C(119)-C(120)-C(115)	121.11(16)
C(122)-C(121)-C(126)	117.37(15)
C(122)-C(121)-Si(28)	121.45(13)
C(126)-C(121)-Si(28)	121.18(13)
C(123)-C(122)-C(121)	121.41(17)
C(124)-C(123)-C(122)	120.23(18)
C(123)-C(124)-C(125)	119.75(17)
C(124)-C(125)-C(126)	119.93(17)
C(125)-C(126)-C(121)	121.29(17)
C(128)-C(127)-C(132)	118.12(14)
C(128)-C(127)-Si(27)	121.33(12)
C(132)-C(127)-Si(27)	120.53(12)
C(129)-C(128)-C(127)	120.68(16)
C(130)-C(129)-C(128)	120.43(16)
C(131)-C(130)-C(129)	119.90(16)
C(130)-C(131)-C(132)	120.02(17)
C(131)-C(132)-C(127)	120.85(16)
C(138)-C(133)-C(134)	117.90(15)
C(138)-C(133)-Si(30)	122.68(13)
C(134)-C(133)-Si(30)	119.39(12)
C(135)-C(134)-C(133)	121.20(17)
C(136)-C(135)-C(134)	119.76(19)
C(137)-C(136)-C(135)	120.22(17)
C(136)-C(137)-C(138)	120.33(18)
C(133)-C(138)-C(137)	120.57(18)
C(144)-C(139)-C(140)	117.41(16)
C(144)-C(139)-Si(29)	120.81(14)
C(140)-C(139)-Si(29)	121.60(12)
C(141)-C(140)-C(139)	121.44(17)
C(140)-C(141)-C(142)	119.58(19)
C(143)-C(142)-C(141)	120.05(18)
C(142)-C(143)-C(144)	120.35(19)
C(143)-C(144)-C(139)	121.16(19)
C(150)-C(145)-C(146)	117.83(14)
C(150)-C(145)-Si(26)	119.36(12)
C(146)-C(145)-Si(26)	122.80(13)
C(147)-C(146)-C(145)	120.50(17)
C(148)-C(147)-C(146)	120.12(17)

C(147)-C(148)-C(149)	120.36(16)
C(148)-C(149)-C(150)	119.74(18)
C(149)-C(150)-C(145)	121.43(16)
C(156)-C(151)-C(152)	117.89(14)
C(156)-C(151)-Si(25)	120.01(12)
C(152)-C(151)-Si(25)	122.09(12)
C(153)-C(152)-C(151)	121.15(16)
C(154)-C(153)-C(152)	119.82(16)
C(153)-C(154)-C(155)	120.31(16)
C(154)-C(155)-C(156)	119.90(17)
C(155)-C(156)-C(151)	120.91(16)
C(162)-C(157)-C(158)	117.98(17)
C(162)-C(157)-Si(24)	119.95(14)
C(158)-C(157)-Si(24)	122.04(13)
C(159)-C(158)-C(157)	120.79(18)
C(160)-C(159)-C(158)	120.2(2)
C(159)-C(160)-C(161)	120.2(2)
C(160)-C(161)-C(162)	120.2(2)
C(161)-C(162)-C(157)	120.6(2)
C(168)-C(163)-C(164)	117.56(15)
C(168)-C(163)-Si(23)	119.87(14)
C(164)-C(163)-Si(23)	122.48(12)
C(165)-C(164)-C(163)	121.51(15)
C(166)-C(165)-C(164)	119.83(17)
C(165)-C(166)-C(167)	119.67(18)
C(166)-C(167)-C(168)	120.2(2)
C(167)-C(168)-C(163)	121.3(2)
C(174)-C(169)-C(70A)	72.9(3)
C(174)-C(169)-C(74A)	67.6(2)
C(70A)-C(169)-C(74A)	115.7(2)
C(174)-C(169)-C(170)	118.4(3)
C(70A)-C(169)-C(170)	66.5(2)
C(74A)-C(169)-C(170)	90.5(2)
C(174)-C(169)-Si(22)	122.8(2)
C(70A)-C(169)-Si(22)	124.2(2)
C(74A)-C(169)-Si(22)	119.67(17)
C(170)-C(169)-Si(22)	118.10(19)
C(171)-C(170)-C(169)	118.0(3)
C(170)-C(171)-C(172)	118.1(3)
C(169)-C(70A)-C(72A)	123.8(4)
C(172)-C(72A)-C(70A)	122.5(4)
C(72A)-C(172)-C(173)	74.7(3)
C(72A)-C(172)-C(73A)	120.8(3)
C(173)-C(172)-C(73A)	67.8(3)
C(72A)-C(172)-C(171)	67.6(3)
C(173)-C(172)-C(171)	118.1(3)
C(73A)-C(172)-C(171)	91.8(2)
C(172)-C(173)-C(174)	123.5(4)

C(169)-C(174)-C(173)	122.8(4)
C(73A)-C(74A)-C(169)	120.0(3)
C(74A)-C(73A)-C(172)	116.4(3)
C(180)-C(175)-C(76A)	109.9(4)
C(180)-C(175)-C(80A)	19.4(3)
C(76A)-C(175)-C(80A)	118.4(3)
C(180)-C(175)-C(176)	116.4(4)
C(76A)-C(175)-C(176)	23.8(2)
C(80A)-C(175)-C(176)	116.4(3)
C(180)-C(175)-Si(21)	122.4(4)
C(76A)-C(175)-Si(21)	123.5(2)
C(80A)-C(175)-Si(21)	118.0(2)
C(176)-C(175)-Si(21)	121.2(3)
C(177)-C(176)-C(175)	118.5(5)
C(178)-C(177)-C(176)	122.0(8)
C(177)-C(178)-C(179)	121.8(11)
C(178)-C(179)-C(180)	117.3(7)
C(175)-C(180)-C(179)	123.3(6)
C(175)-C(76A)-C(77A)	122.1(4)
C(78A)-C(77A)-C(76A)	119.6(5)
C(77A)-C(78A)-C(79A)	119.5(6)
C(80A)-C(79A)-C(78A)	119.3(5)
C(79A)-C(80A)-C(175)	120.7(4)
C(186)-C(181)-C(182)	118.1(2)
C(186)-C(181)-C(187)	121.1(2)
C(182)-C(181)-C(187)	120.8(2)
C(183)-C(182)-C(181)	120.2(2)
C(184)-C(183)-C(182)	121.3(2)
C(183)-C(184)-C(185)	119.4(2)
C(184)-C(185)-C(186)	119.6(2)
C(181)-C(186)-C(185)	121.3(2)
C(193)-C(188)-C(189)	117.59(17)
C(193)-C(188)-C(194)	121.17(18)
C(189)-C(188)-C(194)	121.24(18)
C(190)-C(189)-C(188)	121.42(18)
C(189)-C(190)-C(191)	120.06(18)
C(192)-C(191)-C(190)	119.10(18)
C(193)-C(192)-C(191)	120.29(18)
C(192)-C(193)-C(188)	121.53(18)
C(196)-C(195)-C(200)	115.9(4)
C(196)-C(195)-C(201)	122.4(4)
C(200)-C(195)-C(201)	121.6(4)
C(197)-C(196)-C(195)	122.7(4)
C(196)-C(197)-C(198)	120.2(4)
C(197)-C(198)-C(199)	117.2(5)
C(200)-C(199)-C(198)	121.0(5)
C(199)-C(200)-C(195)	122.5(4)
C(16A)-C(15A)-C(20A)	116.0(5)

C(16A)-C(15A)-C(21A)	121.8(5)
C(20A)-C(15A)-C(21A)	121.6(6)
C(17A)-C(16A)-C(15A)	121.6(5)
C(18A)-C(17A)-C(16A)	120.5(5)
C(17A)-C(18A)-C(19A)	118.4(5)
C(20A)-C(19A)-C(18A)	118.7(5)
C(19A)-C(20A)-C(15A)	122.7(6)

Symmetry transformations used to generate equivalent atoms:

Table 4. Anisotropic displacement parameters (A^2 x 10^3) for decap.

The anisotropic displacement factor exponent takes the form: -2 pi^2 [h^2 a*^2 U11 + ... + 2 h k a* b* U12]

	U11	U22	U33	U23	U13	U12
Si(1)	15(1)	15(1)	16(1)	-4(1)	-3(1)	0(1)
Si(2)	15(1)	14(1)	16(1)	-4(1)	-1(1)	-2(1)
Si(3)	16(1)	16(1)	16(1)	-4(1)	-2(1)	-3(1)
Si(4)	15(1)	16(1)	17(1)	-5(1)	-4(1)	-2(1)
Si(5)	14(1)	15(1)	16(1)	-4(1)	-1(1)	-2(1)
Si(6)	14(1)	15(1)	16(1)	-4(1)	-2(1)	-1(1)
Si(7)	15(1)	14(1)	16(1)	-4(1)	-2(1)	-2(1)
Si(8)	18(1)	14(1)	17(1)	-4(1)	-5(1)	-1(1)
Si(9)	15(1)	13(1)	16(1)	-3(1)	-1(1)	-1(1)
Si(10)	14(1)	15(1)	16(1)	-3(1)	-2(1)	-1(1)
Si(11)	17(1)	14(1)	15(1)	-4(1)	-2(1)	-1(1)
Si(12)	17(1)	14(1)	14(1)	-4(1)	-2(1)	-2(1)
Si(13)	14(1)	16(1)	17(1)	-5(1)	0(1)	-2(1)
Si(14)	15(1)	17(1)	19(1)	-8(1)	0(1)	-2(1)
Si(15)	17(1)	15(1)	17(1)	-5(1)	-3(1)	-3(1)
Si(16)	15(1)	15(1)	15(1)	-4(1)	-2(1)	0(1)
Si(17)	14(1)	15(1)	14(1)	-4(1)	-2(1)	-1(1)
Si(18)	15(1)	14(1)	15(1)	-4(1)	-2(1)	-2(1)
Si(19)	14(1)	17(1)	17(1)	-6(1)	-2(1)	0(1)
Si(20)	16(1)	16(1)	15(1)	-4(1)	-4(1)	-1(1)
Si(21)	16(1)	15(1)	21(1)	-3(1)	-5(1)	-3(1)
Si(22)	15(1)	15(1)	24(1)	-7(1)	-4(1)	0(1)
Si(23)	16(1)	17(1)	19(1)	-2(1)	-5(1)	-1(1)
Si(24)	15(1)	14(1)	21(1)	1(1)	-5(1)	-2(1)
Si(25)	14(1)	14(1)	16(1)	-4(1)	-2(1)	-2(1)
Si(26)	14(1)	16(1)	15(1)	-4(1)	-3(1)	1(1)
Si(27)	15(1)	16(1)	15(1)	-4(1)	-3(1)	-1(1)
Si(28)	14(1)	16(1)	18(1)	-6(1)	-1(1)	-2(1)
Si(29)	15(1)	15(1)	20(1)	0(1)	-2(1)	-1(1)
Si(30)	15(1)	19(1)	18(1)	-2(1)	-3(1)	-4(1)
O(1)	16(1)	22(1)	24(1)	-3(1)	-3(1)	-2(1)
O(2)	25(1)	31(1)	19(1)	-11(1)	3(1)	-10(1)
O(3)	26(1)	17(1)	26(1)	-1(1)	-8(1)	-5(1)
O(4)	16(1)	30(1)	22(1)	-8(1)	-3(1)	-4(1)
O(5)	21(1)	18(1)	23(1)	0(1)	0(1)	1(1)
O(6)	19(1)	26(1)	18(1)	-9(1)	-2(1)	-1(1)

O(7)	17(1)	23(1)	26(1)	-8(1)	-5(1)	-3(1)
O(8)	23(1)	21(1)	24(1)	-10(1)	1(1)	-6(1)
O(9)	23(1)	19(1)	18(1)	-1(1)	-4(1)	-5(1)
O(10)	30(1)	14(1)	18(1)	-4(1)	-6(1)	1(1)
O(11)	18(1)	25(1)	26(1)	-11(1)	-3(1)	-3(1)
O(12)	21(1)	15(1)	32(1)	-7(1)	-2(1)	-2(1)
O(13)	21(1)	28(1)	18(1)	4(1)	-2(1)	-1(1)
O(14)	16(1)	20(1)	26(1)	-4(1)	-5(1)	-3(1)
O(15)	23(1)	24(1)	29(1)	-14(1)	-7(1)	3(1)
O(16)	24(1)	16(1)	18(1)	-5(1)	-5(1)	-1(1)
O(17)	18(1)	21(1)	22(1)	-6(1)	-3(1)	-3(1)
O(18)	18(1)	20(1)	41(1)	-14(1)	-3(1)	-1(1)
O(19)	18(1)	23(1)	22(1)	-7(1)	-3(1)	-3(1)
O(20)	22(1)	25(1)	20(1)	-10(1)	0(1)	-4(1)
O(21)	18(1)	23(1)	24(1)	-9(1)	-2(1)	-4(1)
O(22)	21(1)	16(1)	18(1)	-2(1)	-2(1)	-1(1)
O(23)	25(1)	16(1)	16(1)	-5(1)	1(1)	-2(1)
O(24)	24(1)	18(1)	15(1)	-3(1)	-1(1)	-4(1)
O(25)	17(1)	20(1)	32(1)	-9(1)	-7(1)	-2(1)
O(26)	22(1)	25(1)	28(1)	-14(1)	-6(1)	1(1)
O(27)	28(1)	18(1)	29(1)	1(1)	-10(1)	-5(1)
O(28)	16(1)	27(1)	19(1)	-6(1)	-4(1)	-2(1)
O(29)	20(1)	36(1)	19(1)	-3(1)	-2(1)	1(1)
O(30)	21(1)	18(1)	16(1)	-6(1)	-2(1)	2(1)
O(31)	17(1)	20(1)	48(1)	-13(1)	-8(1)	0(1)
O(32)	25(1)	29(1)	21(1)	-6(1)	-3(1)	2(1)
O(33)	20(1)	16(1)	25(1)	-2(1)	-6(1)	0(1)
O(34)	19(1)	22(1)	24(1)	5(1)	-5(1)	-3(1)
O(35)	16(1)	20(1)	22(1)	-4(1)	-4(1)	-1(1)
O(36)	21(1)	27(1)	24(1)	-14(1)	-5(1)	2(1)
O(37)	28(1)	18(1)	24(1)	-1(1)	-10(1)	-4(1)
O(38)	15(1)	30(1)	20(1)	-2(1)	-1(1)	-2(1)
O(39)	23(1)	32(1)	33(1)	-22(1)	4(1)	-8(1)
O(40)	22(1)	19(1)	22(1)	-4(1)	0(1)	1(1)
O(41)	19(1)	20(1)	18(1)	-3(1)	-1(1)	1(1)
O(42)	23(1)	18(1)	42(1)	-4(1)	-5(1)	-4(1)
O(43)	24(1)	51(1)	19(1)	-5(1)	-2(1)	-12(1)
O(44)	16(1)	27(1)	25(1)	-5(1)	-5(1)	-3(1)
O(45)	17(1)	22(1)	26(1)	-3(1)	-4(1)	-1(1)
C(1)	21(1)	18(1)	16(1)	-4(1)	-3(1)	1(1)
C(2)	27(1)	21(1)	25(1)	-7(1)	2(1)	-4(1)
C(3)	42(1)	18(1)	32(1)	-7(1)	6(1)	2(1)
C(4)	32(1)	30(1)	29(1)	-3(1)	4(1)	12(1)
C(5)	21(1)	40(1)	31(1)	-9(1)	-4(1)	5(1)
C(6)	20(1)	25(1)	26(1)	-8(1)	-4(1)	2(1)
C(7)	19(1)	19(1)	18(1)	-4(1)	-4(1)	-1(1)
C(8)	21(1)	22(1)	25(1)	-3(1)	1(1)	-1(1)
C(9)	31(1)	18(1)	30(1)	1(1)	-2(1)	2(1)

C(10)	27(1)	27(1)	30(1)	-3(1)	-3(1)	8(1)
C(11)	18(1)	34(1)	30(1)	-4(1)	-1(1)	2(1)
C(12)	21(1)	24(1)	26(1)	-2(1)	-3(1)	-2(1)
C(13)	21(1)	16(1)	24(1)	-3(1)	3(1)	-2(1)
C(14)	22(1)	37(1)	33(1)	-6(1)	1(1)	0(1)
C(15)	23(1)	47(1)	55(1)	-6(1)	7(1)	4(1)
C(16)	39(1)	31(1)	56(1)	-7(1)	25(1)	3(1)
C(17)	62(2)	38(1)	41(1)	-22(1)	18(1)	-6(1)
C(18)	37(1)	36(1)	36(1)	-19(1)	5(1)	-5(1)
C(19)	20(1)	18(1)	26(1)	-9(1)	-8(1)	2(1)
C(20)	35(1)	24(1)	28(1)	-10(1)	-7(1)	-2(1)
C(21)	45(1)	37(1)	31(1)	-19(1)	-8(1)	-1(1)
C(22)	35(1)	38(1)	47(1)	-27(1)	-12(1)	-4(1)
C(23)	26(1)	34(1)	46(1)	-19(1)	-6(1)	-7(1)
C(24)	23(1)	29(1)	32(1)	-12(1)	-7(1)	-2(1)
C(25)	18(1)	16(1)	18(1)	-3(1)	-4(1)	-3(1)
C(26)	23(1)	22(1)	26(1)	-10(1)	0(1)	-2(1)
C(27)	31(1)	21(1)	35(1)	-13(1)	-6(1)	-2(1)
C(28)	31(1)	23(1)	33(1)	-4(1)	-8(1)	-11(1)
C(29)	22(1)	31(1)	29(1)	-6(1)	0(1)	-11(1)
C(30)	20(1)	24(1)	24(1)	-7(1)	-2(1)	-2(1)
C(31)	20(1)	23(1)	20(1)	-6(1)	2(1)	-4(1)
C(32)	26(1)	35(1)	23(1)	-3(1)	1(1)	4(1)
C(33)	34(1)	48(1)	22(1)	0(1)	4(1)	3(1)
C(34)	31(1)	65(1)	28(1)	-2(1)	10(1)	-3(1)
C(35)	20(1)	103(2)	34(1)	-1(1)	3(1)	3(1)
C(36)	22(1)	74(2)	24(1)	0(1)	0(1)	0(1)
C(37)	16(1)	27(1)	19(1)	-7(1)	-2(1)	-2(1)
C(38)	30(1)	32(1)	23(1)	-5(1)	-7(1)	3(1)
C(39)	28(1)	56(1)	26(1)	-6(1)	-8(1)	7(1)
C(40)	24(1)	75(2)	22(1)	-12(1)	-6(1)	-10(1)
C(41)	43(1)	58(1)	31(1)	-20(1)	-7(1)	-20(1)
C(42)	37(1)	33(1)	29(1)	-11(1)	-8(1)	-8(1)
C(43)	15(1)	18(1)	24(1)	-6(1)	-5(1)	0(1)
C(44)	28(1)	28(1)	30(1)	-13(1)	1(1)	-6(1)
C(45)	40(1)	34(1)	37(1)	-22(1)	-4(1)	-2(1)
C(46)	34(1)	22(1)	54(1)	-20(1)	-17(1)	0(1)
C(47)	24(1)	20(1)	45(1)	-6(1)	-6(1)	-5(1)
C(48)	22(1)	21(1)	30(1)	-8(1)	-3(1)	-1(1)
C(49)	19(1)	20(1)	17(1)	-2(1)	-4(1)	-4(1)
C(50)	21(1)	26(1)	22(1)	-3(1)	-2(1)	-3(1)
C(51)	22(1)	46(1)	25(1)	-5(1)	0(1)	-8(1)
C(52)	33(1)	43(1)	22(1)	5(1)	-4(1)	-21(1)
C(53)	42(1)	24(1)	29(1)	7(1)	-13(1)	-12(1)
C(54)	26(1)	21(1)	27(1)	0(1)	-6(1)	-4(1)
C(55)	23(1)	15(1)	22(1)	-6(1)	-8(1)	0(1)
C(56)	23(1)	21(1)	31(1)	-9(1)	-10(1)	-2(1)
C(57)	25(1)	28(1)	44(1)	-15(1)	-17(1)	5(1)

C(58)	45(1)	21(1)	36(1)	-9(1)	-25(1)	8(1)
C(59)	45(1)	19(1)	25(1)	-4(1)	-13(1)	0(1)
C(60)	29(1)	21(1)	22(1)	-6(1)	-7(1)	0(1)
C(61)	20(1)	26(1)	17(1)	-4(1)	-2(1)	-8(1)
C(62)	23(1)	35(1)	27(1)	-3(1)	-7(1)	-6(1)
C(63)	27(1)	55(1)	35(1)	3(1)	-14(1)	-10(1)
C(64)	40(1)	75(2)	25(1)	-3(1)	-11(1)	-29(1)
C(65)	45(1)	65(1)	23(1)	-20(1)	4(1)	-27(1)
C(66)	28(1)	42(1)	26(1)	-16(1)	1(1)	-11(1)
C(67)	18(1)	20(1)	28(1)	-8(1)	-7(1)	-1(1)
C(68)	29(1)	24(1)	28(1)	-4(1)	-6(1)	-2(1)
C(69)	43(1)	26(1)	36(1)	-1(1)	-18(1)	-2(1)
C(70)	35(1)	22(1)	56(1)	-7(1)	-24(1)	4(1)
C(71)	26(1)	36(1)	53(1)	-21(1)	-10(1)	8(1)
C(72)	23(1)	34(1)	35(1)	-15(1)	-7(1)	5(1)
C(73)	18(1)	17(1)	17(1)	-6(1)	2(1)	-3(1)
C(74)	22(1)	22(1)	25(1)	-8(1)	-4(1)	-2(1)
C(75)	26(1)	32(1)	37(1)	-17(1)	2(1)	-10(1)
C(76)	36(1)	22(1)	37(1)	-15(1)	13(1)	-13(1)
C(77)	35(1)	16(1)	27(1)	-2(1)	9(1)	0(1)
C(78)	25(1)	21(1)	20(1)	-5(1)	-1(1)	1(1)
C(79)	18(1)	17(1)	20(1)	-7(1)	1(1)	-3(1)
C(80)	22(1)	23(1)	23(1)	-5(1)	0(1)	-3(1)
C(81)	20(1)	30(1)	34(1)	-8(1)	2(1)	-1(1)
C(82)	30(1)	37(1)	30(1)	-12(1)	9(1)	-2(1)
C(83)	36(1)	48(1)	20(1)	-14(1)	3(1)	-3(1)
C(84)	26(1)	37(1)	22(1)	-12(1)	-2(1)	-1(1)
C(85)	19(1)	18(1)	17(1)	-4(1)	0(1)	1(1)
C(86)	20(1)	21(1)	26(1)	-4(1)	-1(1)	-1(1)
C(87)	21(1)	31(1)	36(1)	-4(1)	0(1)	3(1)
C(88)	33(1)	42(1)	43(1)	-19(1)	6(1)	9(1)
C(89)	44(1)	54(1)	40(1)	-33(1)	0(1)	6(1)
C(90)	30(1)	40(1)	28(1)	-20(1)	-4(1)	3(1)
C(91)	23(1)	20(1)	18(1)	-7(1)	1(1)	-6(1)
C(92)	27(1)	22(1)	25(1)	-7(1)	1(1)	-4(1)
C(93)	43(1)	22(1)	32(1)	-12(1)	6(1)	-6(1)
C(94)	54(1)	35(1)	29(1)	-18(1)	5(1)	-22(1)
C(95)	37(1)	44(1)	30(1)	-15(1)	-7(1)	-16(1)
C(96)	26(1)	31(1)	27(1)	-11(1)	-5(1)	-5(1)
C(97)	21(1)	22(1)	23(1)	-8(1)	1(1)	-3(1)
C(98)	31(1)	29(1)	26(1)	-4(1)	-6(1)	-10(1)
C(99)	32(1)	34(1)	36(1)	-4(1)	-5(1)	-15(1)
C(100)	31(1)	35(1)	33(1)	-1(1)	4(1)	-10(1)
C(101)	36(1)	43(1)	23(1)	-8(1)	4(1)	-8(1)
C(102)	27(1)	34(1)	25(1)	-11(1)	0(1)	-8(1)
C(103)	25(1)	16(1)	19(1)	-1(1)	2(1)	2(1)
C(104)	22(1)	27(1)	29(1)	0(1)	4(1)	-1(1)
C(105)	28(1)	35(1)	40(1)	1(1)	7(1)	5(1)

C(106)	43(1)	31(1)	31(1)	2(1)	11(1)	16(1)
C(107)	66(1)	22(1)	22(1)	-5(1)	4(1)	8(1)
C(108)	42(1)	23(1)	21(1)	-4(1)	0(1)	1(1)
C(109)	18(1)	19(1)	16(1)	-6(1)	0(1)	-5(1)
C(110)	18(1)	26(1)	22(1)	-9(1)	-1(1)	-2(1)
C(111)	19(1)	37(1)	20(1)	-9(1)	-3(1)	-7(1)
C(112)	27(1)	37(1)	22(1)	-15(1)	2(1)	-15(1)
C(113)	33(1)	24(1)	25(1)	-13(1)	1(1)	-6(1)
C(114)	26(1)	21(1)	23(1)	-7(1)	-4(1)	-4(1)
C(115)	24(1)	17(1)	16(1)	-5(1)	-3(1)	0(1)
C(116)	30(1)	20(1)	21(1)	-6(1)	-5(1)	-4(1)
C(117)	47(1)	19(1)	22(1)	-2(1)	-6(1)	-6(1)
C(118)	47(1)	27(1)	24(1)	-1(1)	-14(1)	4(1)
C(119)	33(1)	37(1)	35(1)	0(1)	-17(1)	-1(1)
C(120)	27(1)	29(1)	24(1)	1(1)	-7(1)	-5(1)
C(121)	16(1)	23(1)	21(1)	-6(1)	-1(1)	-1(1)
C(122)	32(1)	31(1)	33(1)	-14(1)	8(1)	-10(1)
C(123)	33(1)	41(1)	33(1)	-18(1)	10(1)	-5(1)
C(124)	22(1)	44(1)	26(1)	-3(1)	4(1)	-4(1)
C(125)	28(1)	28(1)	36(1)	1(1)	2(1)	-6(1)
C(126)	25(1)	22(1)	32(1)	-6(1)	-1(1)	0(1)
C(127)	15(1)	23(1)	16(1)	-5(1)	-2(1)	0(1)
C(128)	22(1)	25(1)	21(1)	-2(1)	-4(1)	-4(1)
C(129)	25(1)	29(1)	23(1)	2(1)	-6(1)	0(1)
C(130)	26(1)	42(1)	21(1)	-4(1)	-9(1)	-1(1)
C(131)	36(1)	38(1)	33(1)	-11(1)	-14(1)	-7(1)
C(132)	31(1)	25(1)	26(1)	-7(1)	-10(1)	-1(1)
C(133)	22(1)	17(1)	20(1)	-8(1)	1(1)	-3(1)
C(134)	26(1)	38(1)	27(1)	-7(1)	-2(1)	-13(1)
C(135)	36(1)	47(1)	41(1)	-16(1)	5(1)	-24(1)
C(136)	46(1)	25(1)	39(1)	-10(1)	14(1)	-18(1)
C(137)	55(1)	24(1)	28(1)	1(1)	2(1)	-6(1)
C(138)	35(1)	25(1)	27(1)	-2(1)	-5(1)	-6(1)
C(139)	19(1)	23(1)	19(1)	3(1)	-4(1)	2(1)
C(140)	24(1)	23(1)	24(1)	0(1)	-3(1)	1(1)
C(141)	36(1)	32(1)	26(1)	-7(1)	-3(1)	6(1)
C(142)	36(1)	52(1)	22(1)	-5(1)	6(1)	3(1)
C(143)	28(1)	58(1)	30(1)	-2(1)	8(1)	-11(1)
C(144)	25(1)	43(1)	24(1)	-2(1)	-1(1)	-8(1)
C(145)	18(1)	21(1)	15(1)	-3(1)	-1(1)	2(1)
C(146)	18(1)	28(1)	22(1)	-3(1)	-2(1)	-1(1)
C(147)	21(1)	36(1)	27(1)	2(1)	-5(1)	6(1)
C(148)	34(1)	25(1)	29(1)	3(1)	-1(1)	13(1)
C(149)	42(1)	21(1)	26(1)	-6(1)	-1(1)	5(1)
C(150)	29(1)	21(1)	19(1)	-5(1)	-4(1)	3(1)
C(151)	23(1)	19(1)	15(1)	-6(1)	-1(1)	-6(1)
C(152)	31(1)	20(1)	17(1)	-5(1)	-4(1)	-3(1)
C(153)	51(1)	20(1)	20(1)	-5(1)	-3(1)	-10(1)

C(154)	49(1)	33(1)	21(1)	-8(1)	4(1)	-25(1)
C(155)	32(1)	41(1)	28(1)	-11(1)	-1(1)	-19(1)
C(156)	23(1)	25(1)	24(1)	-6(1)	-2(1)	-7(1)
C(157)	27(1)	15(1)	27(1)	0(1)	-11(1)	-3(1)
C(158)	34(1)	20(1)	35(1)	-7(1)	-11(1)	3(1)
C(159)	64(1)	23(1)	40(1)	-10(1)	-23(1)	3(1)
C(160)	79(2)	34(1)	45(1)	3(1)	-34(1)	-26(1)
C(161)	56(1)	64(1)	45(1)	9(1)	-26(1)	-40(1)
C(162)	34(1)	49(1)	29(1)	3(1)	-12(1)	-19(1)
C(163)	23(1)	17(1)	26(1)	-1(1)	-8(1)	-1(1)
C(164)	20(1)	21(1)	23(1)	-6(1)	-3(1)	-1(1)
C(165)	24(1)	33(1)	27(1)	-6(1)	-10(1)	4(1)
C(166)	63(1)	23(1)	61(1)	6(1)	-35(1)	3(1)
C(167)	111(2)	20(1)	102(2)	10(1)	-72(2)	-15(1)
C(168)	74(1)	24(1)	76(2)	3(1)	-53(1)	-13(1)
C(169)	20(1)	22(1)	45(1)	-17(1)	-10(1)	3(1)
C(170)	31(2)	23(2)	36(2)	-6(2)	-11(2)	4(1)
C(171)	27(2)	23(2)	62(3)	-9(2)	-12(2)	8(2)
C(70A)	31(2)	21(2)	50(2)	-12(2)	-12(2)	1(1)
C(72A)	40(2)	26(2)	77(3)	-28(2)	-25(2)	11(2)
C(172)	33(1)	41(1)	97(2)	-46(1)	-20(1)	16(1)
C(173)	35(2)	37(2)	56(2)	-33(2)	-1(2)	1(2)
C(174)	26(2)	32(2)	41(2)	-20(2)	-8(2)	7(2)
C(74A)	23(2)	32(2)	35(2)	-14(1)	-2(1)	4(1)
C(73A)	32(2)	54(2)	46(2)	-29(2)	-3(2)	12(2)
C(175)	26(1)	22(1)	41(1)	-9(1)	-11(1)	-6(1)
C(176)	34(3)	23(2)	22(2)	-9(2)	-2(2)	-9(2)
C(177)	52(4)	34(3)	49(4)	-21(3)	-2(3)	-14(3)
C(178)	59(5)	70(4)	87(5)	-59(4)	17(4)	-40(4)
C(179)	25(3)	51(4)	51(4)	-20(3)	-7(3)	-14(3)
C(180)	31(3)	38(3)	31(3)	-16(2)	-8(2)	-3(3)
C(76A)	33(2)	34(2)	77(3)	-24(2)	-19(2)	-2(2)
C(77A)	51(3)	34(2)	135(5)	-42(3)	-32(3)	-1(2)
C(78A)	38(3)	51(3)	109(5)	-30(3)	-22(3)	-19(2)
C(79A)	28(2)	48(3)	110(5)	-34(3)	-23(2)	-7(2)
C(80A)	22(2)	37(2)	64(3)	-19(2)	-15(2)	-4(2)
C(181)	39(1)	44(1)	42(1)	-7(1)	-6(1)	-14(1)
C(182)	33(1)	52(1)	54(1)	-19(1)	-6(1)	-6(1)
C(183)	40(1)	37(1)	58(1)	-8(1)	-22(1)	-6(1)
C(184)	40(1)	42(1)	54(1)	5(1)	-21(1)	-18(1)
C(185)	31(1)	59(1)	50(1)	-5(1)	-3(1)	-10(1)
C(186)	40(1)	38(1)	52(1)	-2(1)	-15(1)	3(1)
C(187)	74(2)	71(2)	46(1)	1(1)	-3(1)	-26(2)
C(188)	32(1)	31(1)	32(1)	-10(1)	-8(1)	-7(1)
C(189)	24(1)	47(1)	34(1)	-9(1)	-1(1)	-6(1)
C(190)	24(1)	43(1)	41(1)	-10(1)	-7(1)	2(1)
C(191)	36(1)	34(1)	34(1)	-2(1)	-6(1)	-6(1)
C(192)	31(1)	38(1)	44(1)	-10(1)	8(1)	-5(1)

C(193)	27(1)	32(1)	49(1)	-10(1)	-2(1)	1(1)
C(194)	47(1)	37(1)	40(1)	-4(1)	-12(1)	-4(1)
C(195)	26(2)	37(2)	46(2)	-14(2)	-3(2)	2(2)
C(196)	48(3)	51(3)	72(3)	-20(3)	-34(3)	4(2)
C(197)	46(3)	78(3)	63(3)	-39(3)	-18(2)	4(3)
C(198)	36(3)	65(3)	52(3)	0(2)	5(2)	16(2)
C(199)	9(2)	85(4)	81(4)	-37(3)	10(2)	-10(2)
C(200)	27(2)	64(3)	66(3)	-24(2)	-16(2)	-3(2)
C(201)	48(3)	88(4)	53(3)	-8(3)	4(2)	19(3)
C(15A)	26(3)	83(4)	51(3)	-15(3)	-9(2)	1(3)
C(16A)	43(3)	74(4)	66(4)	-10(4)	11(3)	-24(3)
C(17A)	33(3)	85(5)	91(6)	-19(5)	15(4)	-32(3)
C(18A)	53(4)	86(5)	48(3)	-24(3)	-12(3)	-1(3)
C(19A)	49(4)	69(5)	55(4)	3(3)	6(3)	-20(3)
C(20A)	20(3)	70(5)	103(6)	-30(4)	17(4)	-2(3)
C(21A)	47(4)	184(9)	68(4)	-28(5)	-13(3)	-7(5)

Table 5. Hydrogen coordinates (x 10^4) and isotropic displacement parameters (A^2 x 10^3) for decap.

	x	y	z	U(eq)
H(2A)	7518	6624	3661	30
H(3A)	5990	7285	3700	39
H(4A)	4276	7063	3665	41
H(5A)	4073	6187	3574	38
H(6A)	5594	5525	3527	29
H(8A)	11148	2264	4166	29
H(9A)	12469	1478	4275	34
H(10A)	14264	1577	3975	36
H(11A)	14744	2466	3573	35
H(12A)	13431	3252	3460	29
H(14A)	13753	4059	2793	39
H(15A)	15331	3804	2403	55
H(16A)	15205	3562	1816	57
H(17A)	13520	3614	1611	57
H(18A)	11930	3859	2005	42
H(20A)	9432	4071	1874	34
H(21A)	8788	3564	1506	43
H(22A)	7514	2919	1826	43
H(23A)	6869	2783	2505	39
H(24A)	7457	3315	2868	32
H(26A)	9100	2449	3346	28
H(27A)	8200	1651	3436	33
H(28A)	6587	1520	3873	34
H(29A)	5852	2195	4220	33
H(30A)	6695	3021	4102	27
H(32A)	7969	3732	5051	36
H(33A)	6625	3619	5606	47
H(34A)	4830	3975	5520	55
H(35A)	4387	4478	4882	70
H(36A)	5726	4600	4324	52
H(38A)	11529	3391	4769	35
H(39A)	12446	3279	5320	47
H(40A)	12660	4073	5520	48
H(41A)	11990	4978	5165	49
H(42A)	11065	5098	4615	38
H(44A)	9764	6049	4273	33
H(45A)	10309	6777	4471	42
H(46A)	11652	7323	4066	40

H(47A)	12446	7148	3456	36
H(48A)	11899	6425	3253	29
H(50A)	13128	5334	2291	29
H(51A)	14340	5898	1816	38
H(52A)	13845	6871	1557	41
H(53A)	12139	7283	1769	39
H(54A)	10918	6724	2247	31
H(56A)	6261	5862	2645	29
H(57A)	5237	6605	2230	37
H(58A)	6077	7173	1629	39
H(59A)	7935	6989	1438	35
H(60A)	8970	6250	1849	29
H(62A)	3613	-441	7767	34
H(63A)	4442	-622	8346	49
H(64A)	3657	-201	8851	55
H(65A)	2042	398	8783	50
H(66A)	1196	583	8203	37
H(68A)	2685	-1392	7796	33
H(69A)	3980	-2086	8113	42
H(70A)	5442	-2455	7729	45
H(71A)	5634	-2124	7030	44
H(72A)	4382	-1401	6710	36
H(74A)	-1651	-1203	6614	27
H(75A)	-2369	-2070	6744	36
H(76A)	-1724	-2867	7229	38
H(77A)	-333	-2812	7578	35
H(78A)	404	-1951	7449	27
H(80A)	-3038	415	7388	28
H(81A)	-4545	471	7868	35
H(82A)	-4315	262	8546	40
H(83A)	-2583	4	8743	42
H(84A)	-1065	-38	8263	33
H(86A)	-3189	1471	6708	28
H(87A)	-4725	1940	6998	37
H(88A)	-4538	2448	7444	48
H(89A)	-2836	2454	7626	52
H(90A)	-1301	1970	7347	38
H(92A)	600	2593	6861	30
H(93A)	971	3254	7170	39
H(94A)	2424	3046	7542	44
H(95A)	3527	2187	7608	41
H(96A)	3168	1522	7307	32
H(98A)	3940	1965	5993	34
H(99A)	5054	2587	5515	41
H(10B)	4892	2790	4832	42
H(10C)	3616	2379	4626	42
H(10D)	2518	1745	5102	33
H(10E)	5007	-2	5962	34

H(10F)	6501	-345	5576	47
H(10G)	6244	-820	5125	49
H(10H)	4508	-971	5056	47
H(10I)	2980	-617	5439	36
H(11B)	-1364	242	5452	26
H(11C)	-1861	-184	5006	30
H(11D)	-1024	-1082	4971	32
H(11E)	308	-1555	5381	31
H(11F)	788	-1139	5836	27
H(11G)	469	2241	5252	28
H(11H)	-302	2913	4720	35
H(11I)	-2040	2843	4600	40
H(11J)	-3003	2090	5001	43
H(12B)	-2241	1417	5535	34
H(12C)	6081	7254	-1406	38
H(12D)	7373	7456	-1974	43
H(12E)	7979	8355	-2221	39
H(12F)	7346	9047	-1880	40
H(12G)	6079	8843	-1304	33
H(12H)	1723	9016	-1338	28
H(12I)	556	9315	-1831	33
H(13A)	-292	8652	-1996	36
H(13B)	27	7683	-1667	40
H(13C)	1170	7377	-1164	32
H(13D)	55	6337	607	36
H(13E)	-1097	5682	1026	47
H(13F)	-578	5084	1632	44
H(13G)	1063	5151	1826	46
H(13H)	2212	5819	1417	36
H(14B)	2023	8646	1224	31
H(14C)	1004	8775	1816	39
H(14D)	-545	8293	2090	48
H(14E)	-1077	7702	1766	50
H(14F)	-46	7558	1181	39
H(14G)	311	9136	-677	29
H(14H)	-658	10034	-903	37
H(14I)	-260	10813	-727	41
H(14J)	1147	10712	-345	38
H(15B)	2143	9826	-128	28
H(15C)	4184	9843	-513	27
H(15D)	5163	10628	-648	36
H(15E)	6989	10490	-554	39
H(15F)	7852	9568	-327	39
H(15G)	6883	8780	-195	29
H(15H)	3877	8096	1430	36
H(15I)	4714	8461	1836	49
H(16B)	6501	8673	1649	61
H(16C)	7486	8509	1061	66

H(16D)	6665	8149	648	46
H(16E)	6366	6377	1149	26
H(16F)	7148	5591	1611	34
H(16G)	6676	4683	1692	61
H(16H)	5424	4563	1306	91
H(16I)	4618	5350	856	67
H(17B)	6661	5755	120	36
H(17C)	7960	5044	-65	46
H(70B)	5243	5354	-160	40
H(72B)	6519	4690	-360	53
H(172)	8083	4914	-704	63
H(17D)	6755	5397	-1119	47
H(17E)	5485	6081	-939	38
H(74B)	7038	6616	-839	36
H(73A)	8332	5917	-1049	51
H(17F)	2988	5823	-785	31
H(17G)	1952	5241	-948	51
H(17H)	166	5247	-742	76
H(17I)	-642	5669	-235	48
H(18B)	314	6329	-99	38
H(76B)	2961	5585	-513	54
H(77B)	1946	4994	-689	80
H(78B)	44	5160	-614	73
H(79A)	-811	6019	-473	69
H(80B)	216	6581	-280	46
H(18C)	2990	4747	3724	54
H(18D)	3295	5386	3090	53
H(18E)	4869	5271	2660	56
H(18F)	6208	4527	2877	58
H(18G)	5906	3876	3511	55
H(18H)	4915	3649	4190	99
H(18I)	3830	3510	4070	99
H(18J)	3776	4008	4281	99
H(18K)	4387	181	7056	43
H(19A)	4289	1002	6520	44
H(19B)	5800	1213	6031	43
H(19C)	7421	607	6102	47
H(19D)	7516	-207	6643	44
H(19E)	6753	-842	7231	63
H(19F)	5475	-871	7259	63
H(19G)	5910	-522	7509	63
H(19H)	385	1820	185	65
H(19I)	458	2450	-446	69
H(19J)	1714	3123	-650	70
H(19K)	2979	3083	-198	68
H(20B)	2726	2554	439	60
H(20C)	751	1604	886	104
H(20D)	1730	1874	978	104

H(20E)	1982	1350	784	104
H(16J)	462	1966	546	76
H(17J)	183	1851	-56	85
H(18L)	1225	2280	-649	73
H(19L)	2602	2843	-620	75
H(20F)	2503	3125	-56	80
H(21B)	1097	2787	813	152
H(21C)	2360	2844	657	152
H(21D)	1966	2234	900	152

Appendix 2

Crystallographic data for I_8OPS

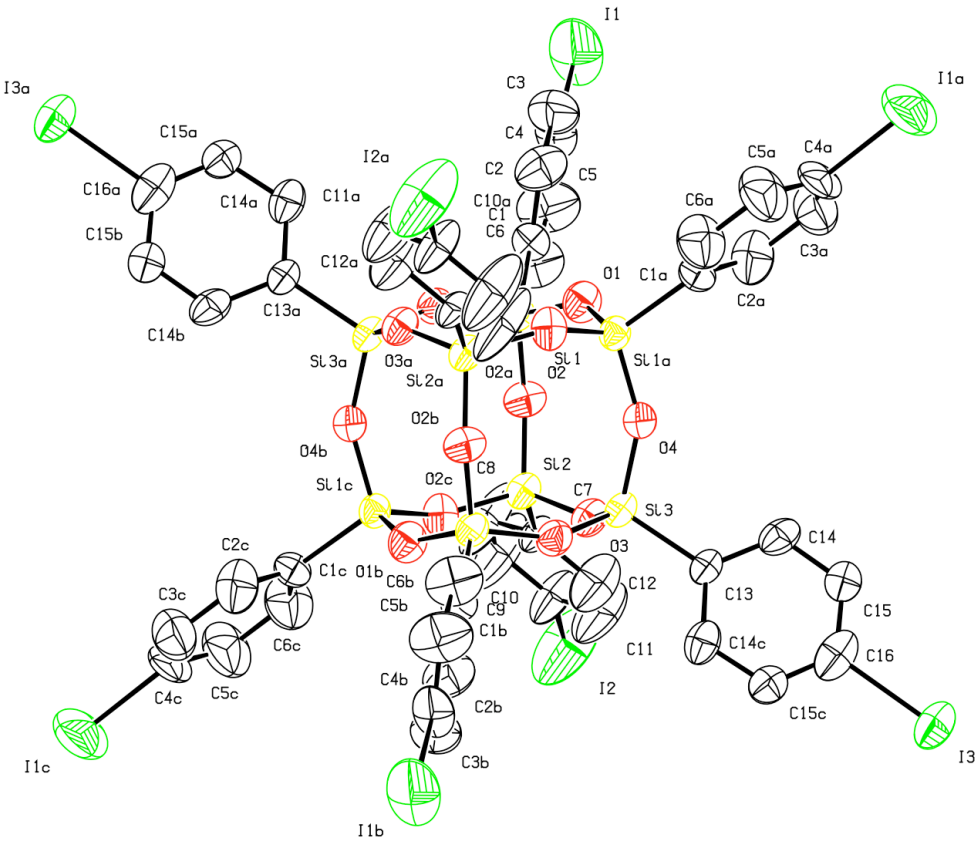

Figure A.2. 50 % thermal ellipsoid plots of octa(p-iodophenyl)silsesquioxane. Hydrogen atoms are omitted for clarity.

Structure Determination.

Colorless needles of **8i3** were crystallized from an ethyl acetate solution at room temperature. A crystal of dimensions 0.52 x 0.08 x 0.08 mm was mounted on a standard Bruker SMART CCD-based X-ray diffractometer equipped with a normal focus Mo-target X-ray tube (λ = 0.71073 A) operated at 2000 W power (50 kV, 40 mA). The X-ray intensities were measured at 123(2) K; the detector was placed at a distance of 4.980 cm from the crystal. A total of 2583 frames were collected with a scan width of 0.3° in ω and phi with an exposure time of 45 s/frame. The frames were integrated with the Bruker SAINT software package with a narrow frame algorithm. The integration of the data yielded a total of 28258 reflections to a maximum 2θ value of 42.24° of which 2399 were independent and 1861 were greater than $2\sigma(I)$. The final cell constants (Table 1) were based on the xyz centroids of 6910 reflections above $10\sigma(I)$. Analysis of the data showed negligible decay during data collection; the data were processed with SADABS and corrected for absorption. The structure was solved and refined with the Bruker SHELXTL (version 6.12) software package, using the space group I4/m with Z = 4 for the formula $C_{48}H_{32}O_{12}Si_8I_8 \bullet C_4H_8O_2$. The crystals afforded only limited high angle diffraction data even with extended collection time. The complex lies on the intersection of a mirror place and 2-fold axis (2/m) in the crystal lattice. All non-hydrogen atoms were refined anisotropically with the hydrogen atoms placed in idealized positions. Full matrix least-squares refinement based on F^2 converged at R1 = 0.0740 and wR2 = 0.2186 [based on I > 2sigma(I)], R1 = 0.0915 and wR2 = 0.2302 for all data. The structure also contains a molecule of ethyl acetate solvate that lies on a 4-fold axis and is disordered.

Additional details are presented in Table 1 and are given as Supporting Information in a CIF file.

Sheldrick, G.M. SHELXTL, v. 6.12; Bruker Analytical X-ray, Madison, WI, 2001.

Sheldrick, G.M. SADABS, v. 2.10. Program for Empirical Absorption Correction of Area Detector Data, University of Gottingen: Gottingen, Germany, 2003.

Saint Plus, v. 7.01, Bruker Analytical X-ray, Madison, WI, 2004.

Table 1. Crystal data and structure refinement for 8i3.

Identification code	8i3
Empirical formula	C52 H40 I8 O14 Si8
Formula weight	2128.76
Temperature	123(2) K
Wavelength	0.71073 A
Crystal system, space group	Tetragonal, I4/m
Unit cell dimensions	a = 20.0403(11) A alpha = 90 deg. b = 20.0403(11) A beta = 90 deg. c = 21.4606(12) A gamma = 90 deg.
Volume	8618.9(8) A^3
Z, Calculated density	4, 1.641 Mg/m^3
Absorption coefficient	3.035 mm^-1
F(000)	4000
Crystal size	0.52 x 0.08 x 0.08 mm

Theta range for data collection	2.87 to 21.12 deg.
Limiting indices	-13<=h<=14, -20<=k<=20, -21<=l<=21
Reflections collected / unique	28258 / 2399 [R(int) = 0.0747]
Completeness to theta = 21.12	98.5 %
Absorption correction	Semi-empirical from equivalents
Max. and min. transmission	0.7933 and 0.3013
Refinement method	Full-matrix least-squares on F^2
Data / restraints / parameters	2399 / 0 / 193
Goodness-of-fit on F^2	1.134
Final R indices [I>2sigma(I)]	R1 = 0.0740, wR2 = 0.2186
R indices (all data)	R1 = 0.0915, wR2 = 0.2302
Extinction coefficient	0.00012(3)
Largest diff. peak and hole	2.118 and -1.303 e.A^-3

Table 2. Atomic coordinates (x 10^4) and equivalent isotropic displacement parameters (A^2 x 10^3) for 8i3.

U(eq) is defined as one third of the trace of the orthogonalized Uij tensor.

	x	y	z	U(eq)
I(1)	2565(1)	5801(1)	3554(1)	117(1)
I(2)	3953(1)	2483(1)	0	134(1)
I(3)	-1367(1)	551(1)	0	66(1)
Si(1)	727(1)	5243(1)	1024(1)	34(1)
Si(2)	1083(1)	4204(1)	0	36(1)
Si(3)	-370(1)	3717(1)	0	35(1)
O(1)	0	5000	1251(3)	48(2)
O(2)	1076(2)	4674(2)	604(2)	44(1)
O(3)	431(2)	3729(3)	0	41(2)
O(4)	-636(2)	4102(2)	613(2)	43(1)
C(1)	1238(3)	5418(3)	1710(3)	39(2)
C(2)	1004(4)	5779(4)	2179(4)	72(2)
C(3)	1399(4)	5896(4)	2723(4)	81(3)
C(4)	2008(3)	5644(4)	2769(3)	64(2)
C(5)	2249(4)	5260(5)	2309(4)	91(3)
C(6)	1873(4)	5140(4)	1769(4)	78(3)
C(7)	1861(4)	3721(4)	0	42(2)
C(8)	2462(6)	4021(5)	0	118(6)
C(9)	3037(6)	3661(6)	0	125(7)
C(10)	3051(4)	3022(4)	0	64(3)
C(11)	2497(6)	2725(5)	0	100(5)
C(12)	1880(5)	3043(5)	0	81(4)
C(13)	-676(4)	2871(4)	0	37(2)
C(14)	-816(3)	2532(3)	551(3)	46(2)
C(15)	-1041(3)	1889(3)	538(3)	49(2)
C(16)	-1108(4)	1570(4)	0	59(3)

Table 3. Bond lengths [A] and angles [deg] for 8i3.

I(1)-C(4)	2.046(6)
I(2)-C(10)	2.107(8)
I(3)-C(16)	2.107(9)
Si(1)-O(4)#1	1.590(4)
Si(1)-O(1)	1.613(2)
Si(1)-O(2)	1.613(4)
Si(1)-C(1)	1.829(6)
Si(2)-O(2)	1.603(4)
Si(2)-O(2)#2	1.603(4)
Si(2)-O(3)	1.616(5)
Si(2)-C(7)	1.834(8)
Si(3)-O(3)	1.605(5)
Si(3)-O(4)	1.616(4)
Si(3)-O(4)#2	1.616(4)
Si(3)-C(13)	1.803(8)
O(1)-Si(1)#1	1.613(2)
O(4)-Si(1)#1	1.590(4)
C(1)-C(2)	1.326(9)
C(1)-C(6)	1.394(9)
C(2)-C(3)	1.430(11)
C(3)-C(4)	1.323(11)
C(4)-C(5)	1.342(11)
C(5)-C(6)	1.403(11)
C(7)-C(8)	1.346(14)
C(7)-C(12)	1.360(13)
C(8)-C(9)	1.359(16)
C(9)-C(10)	1.282(14)
C(10)-C(11)	1.259(15)
C(11)-C(12)	1.391(16)
C(13)-C(14)#2	1.393(8)
C(13)-C(14)	1.393(8)
C(14)-C(15)	1.366(8)
C(15)-C(16)	1.327(8)
C(16)-C(15)#2	1.327(8)
O(4)#1-Si(1)-O(1)	108.25(19)
O(4)#1-Si(1)-O(2)	108.9(2)
O(1)-Si(1)-O(2)	110.31(18)
O(4)#1-Si(1)-C(1)	110.7(2)
O(1)-Si(1)-C(1)	108.7(3)
O(2)-Si(1)-C(1)	110.0(2)
O(2)-Si(2)-O(2)#2	108.0(3)
O(2)-Si(2)-O(3)	109.83(18)
O(2)#2-Si(2)-O(3)	109.83(18)

O(2)-Si(2)-C(7)	108.5(2)
O(2)#2-Si(2)-C(7)	108.5(2)
O(3)-Si(2)-C(7)	112.2(3)
O(3)-Si(3)-O(4)	108.80(18)
O(3)-Si(3)-O(4)#2	108.80(18)
O(4)-Si(3)-O(4)#2	109.1(3)
O(3)-Si(3)-C(13)	110.8(3)
O(4)-Si(3)-C(13)	109.7(2)
O(4)#2-Si(3)-C(13)	109.7(2)
Si(1)#1-O(1)-Si(1)	144.7(4)
Si(2)-O(2)-Si(1)	150.5(3)
Si(3)-O(3)-Si(2)	144.8(4)
Si(1)#1-O(4)-Si(3)	152.0(3)
C(2)-C(1)-C(6)	118.2(6)
C(2)-C(1)-Si(1)	121.2(5)
C(6)-C(1)-Si(1)	120.5(5)
C(1)-C(2)-C(3)	120.8(7)
C(4)-C(3)-C(2)	120.6(7)
C(3)-C(4)-C(5)	119.8(7)
C(3)-C(4)-I(1)	120.4(5)
C(5)-C(4)-I(1)	119.8(6)
C(4)-C(5)-C(6)	120.8(8)
C(1)-C(6)-C(5)	119.8(7)
C(8)-C(7)-C(12)	114.8(9)
C(8)-C(7)-Si(2)	121.7(7)
C(12)-C(7)-Si(2)	123.4(7)
C(7)-C(8)-C(9)	121.5(10)
C(10)-C(9)-C(8)	123.3(10)
C(11)-C(10)-C(9)	116.9(10)
C(11)-C(10)-I(2)	121.0(7)
C(9)-C(10)-I(2)	122.1(7)
C(10)-C(11)-C(12)	124.6(10)
C(7)-C(12)-C(11)	118.8(9)
C(14)#2-C(13)-C(14)	116.3(7)
C(14)#2-C(13)-Si(3)	121.8(4)
C(14)-C(13)-Si(3)	121.8(4)
C(15)-C(14)-C(13)	120.7(6)
C(16)-C(15)-C(14)	120.3(6)
C(15)-C(16)-C(15)#2	121.1(9)
C(15)-C(16)-I(3)	119.4(4)
C(15)#2-C(16)-I(3)	119.4(4)

Symmetry transformations used to generate equivalent atoms:

#1 -x,-y+1,z #2 x,y,-z

Table 4. Anisotropic displacement parameters (A^2 x 10^3) for 8i3.

The anisotropic displacement factor exponent takes the form: -2 pi^2 [h^2 a*^2 U11 + ... + 2 h k a* b* U12]

	U11	U22	U33	U23	U13	U12
I(1)	128(1)	148(1)	76(1)	24(1)	-50(1)	-61(1)
I(2)	54(1)	70(1)	279(2)	0	0	22(1)
I(3)	67(1)	43(1)	88(1)	0	0	-13(1)
Si(1)	30(1)	33(1)	40(1)	-1(1)	-3(1)	-3(1)
Si(2)	26(1)	31(1)	50(1)	0	0	3(1)
Si(3)	31(1)	26(1)	48(1)	0	0	-1(1)
O(1)	37(3)	50(3)	57(3)	0	0	-7(3)
O(2)	32(2)	47(2)	53(2)	-10(2)	-1(2)	2(2)
O(3)	34(3)	34(3)	55(3)	0	0	3(2)
O(4)	48(2)	39(2)	41(2)	1(2)	6(2)	-5(2)
C(1)	32(3)	47(3)	39(3)	2(3)	-7(3)	3(3)
C(2)	62(4)	65(4)	90(5)	-15(4)	-5(4)	-2(4)
C(3)	97(6)	85(5)	61(5)	-12(4)	-1(4)	-13(5)
C(4)	62(4)	88(5)	44(4)	16(3)	-31(3)	-27(4)
C(5)	87(5)	100(6)	87(5)	-14(5)	-41(4)	15(5)
C(6)	59(4)	86(5)	89(5)	-10(4)	-18(4)	10(4)
C(7)	48(5)	23(4)	56(5)	0	0	7(4)
C(8)	61(7)	38(6)	255(18)	0	0	-13(5)
C(9)	44(6)	57(7)	270(20)	0	0	-15(5)
C(10)	28(4)	31(5)	132(9)	0	0	6(4)
C(11)	82(8)	39(6)	178(13)	0	0	19(6)
C(12)	48(6)	57(6)	139(10)	0	0	-1(5)
C(13)	39(4)	28(4)	46(5)	0	0	-2(4)
C(14)	40(3)	35(3)	65(4)	-9(3)	3(3)	7(3)
C(15)	51(3)	44(3)	52(4)	3(3)	1(3)	-3(3)
C(16)	28(4)	43(5)	105(8)	0	0	0(4)

Table 5. Hydrogen coordinates (x 10^4) and isotropic displacement parameters (A^2 x 10^3) for 8i3.

	x	y	z	U(eq)
H(2A)	567	5962	2154	87
H(3A)	1224	6158	3054	97
H(5A)	2680	5066	2350	110
H(6A)	2050	4871	1445	93
H(8A)	2485	4494	0	141
H(9A)	3449	3896	0	150
H(11A)	2501	2251	0	119
H(12A)	1478	2790	0	98
H(14A)	-753	2749	940	56
H(15A)	-1151	1668	917	59

Appendix 3

Crystallographic data for I_{10}dPS

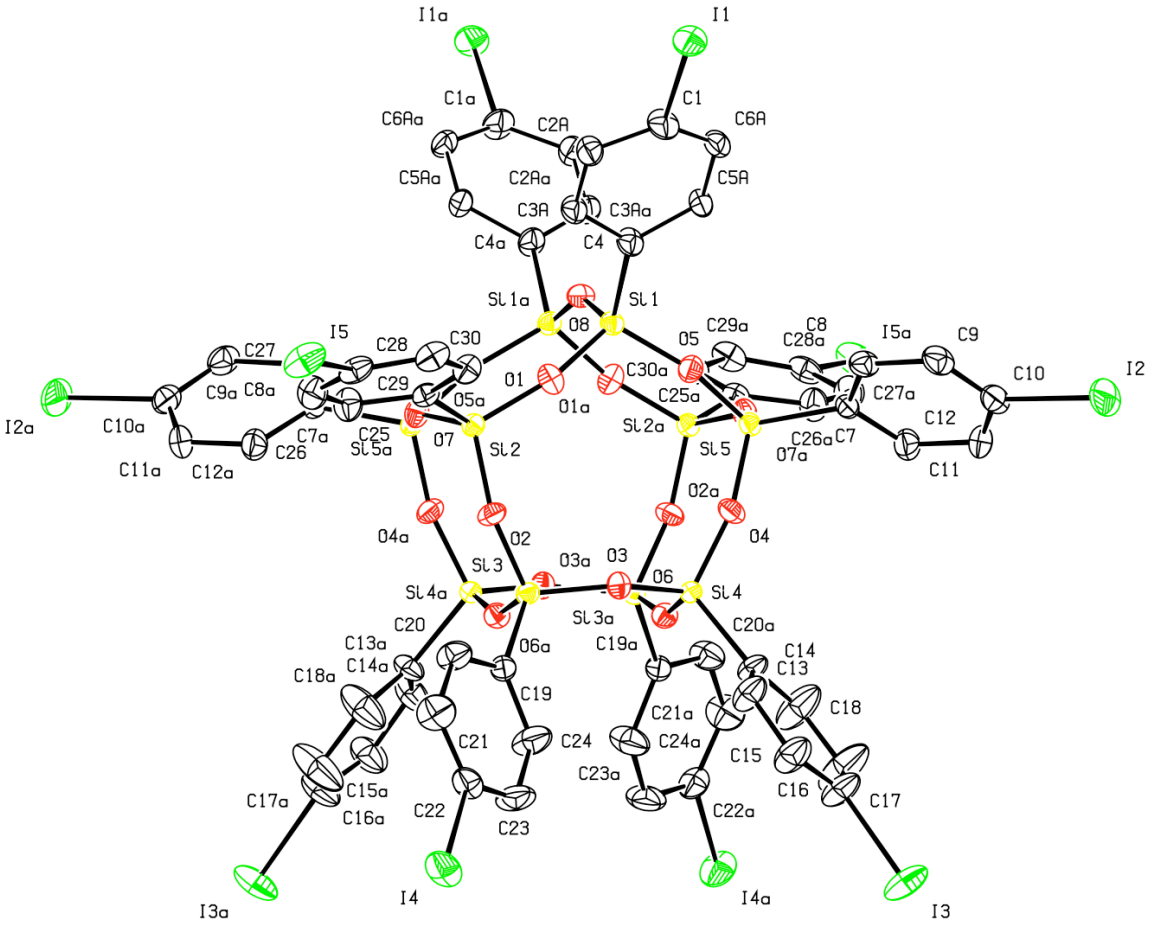

Figure A.3. 50 % thermal ellipsoid plots of deca(p-iodophenyl)silsesquioxane. Hydrogen atoms are omitted for clarity. Hydrogen atoms are omitted for clarity.

Structure Determination.

Colorless blocks of **10i1** were grown from an ethyl acetate solution at 25 deg. C. A crystal of dimensions 0.48 x 0.39 x 0.35 mm was mounted on a Bruker SMART APEX CCD-based X-ray diffractometer equipped with a low temperature device and fine focus Mo-target X-ray tube (l = 0.71073 A) operated at 1500 W power (50 kV, 30 mA). The X-ray intensities were measured at 85(1) K; the detector was placed at a distance 5.055 cm from the crystal. A total of 4460 frames were collected with a scan width of 0.5° in w and 0.45° in phi with an exposure time of 15 s/frame. The integration of the data yielded a total of 192719 reflections to a maximum 2q value of 60.14° of which 13019 were independent and 12075 were greater than 2s(I). The final cell constants (Table 1) were based on the xyz centroids of 9383 reflections above 10s(I). Analysis of the data showed negligible decay during data collection; the data were processed with SADABS and corrected for absorption. The structure was solved and refined with the Bruker SHELXTL (version 2008/4) software package, using the space group C2/c with Z = 4 for the formula $C_{60}H_{40}O_{15}Si_{10}I_{10}$. All non-hydrogen atoms were refined anisotropically with the hydrogen atoms placed in idealized positions. The cluster lies on a two-fold axis of the crystal lattice. Ethyl acetate solvate molecules were disordered in large voids in the lattice and were treated as diffuse scattering by use of the SQUEEZE subroutine of the PLATON program suite. Full matrix least-squares refinement based on F^2 converged at R1 = 0.0461 and wR2 = 0.1152 [based on I > 2sigma(I)], R1 = 0.0492 and wR2 = 0.1170 for all data. Additional details are presented in Table 1 and are given as Supporting Information in a CIF file.

Sheldrick, G.M. SHELXTL, v. 2008/4; Bruker Analytical X-ray, Madison, WI, 2008.

Sheldrick, G.M. SADABS, v. 2008/1. Program for Empirical Absorption Correction of Area Detector Data, University of Gottingen: Gottingen, Germany, 2008.

Saint Plus, v. 7.60a, Bruker Analytical X-ray, Madison, WI, 2009.

A.L. Spek. (2008) PLATON, v. 180108, A Multi-purpose Crystallographic Tool, Utrecht University, Utrecht, The Netherlands.

Table 1. Crystal data and structure refinement for 10i1.

Identification code	10i1
Empirical formula	C60 H40 I10 O15 Si10
Formula weight	2550.82
Temperature	85(2) K
Wavelength	0.71073 A
Crystal system, space group	Monoclinic, C2/c
Unit cell dimensions	a = 28.054(2) Å alpha = 90 deg. b = 15.6168(11) Å beta=108.859(1)deg. c = 22.3246(16) Å gamma = 90 deg.
Volume	9255.7(11) A^3
Z, Calculated density	4, 1.831 Mg/m^3
Absorption coefficient	3.527 mm^-1
F(000)	4760
Crystal size	0.48 x 0.39 x 0.35 mm
Theta range for data collection	1.51 to 29.62 deg.
Limiting indices	-38<=h<=38, -21<=k<=21, -30<=l<=30
Reflections collected / unique	192719 / 13019 [R(int) = 0.0331]
Completeness to theta = 29.62	99.8 %
Absorption correction	Semi-empirical from equivalents
Max. and min. transmission	0.3716 and 0.2823

Refinement method	Full-matrix least-squares on F^2
Data / restraints / parameters	13019 / 0 / 465
Goodness-of-fit on F^2	1.058
Final R indices [I>2sigma(I)]	R1 = 0.0461, wR2 = 0.1152
R indices (all data)	R1 = 0.0492, wR2 = 0.1170
Largest diff. peak and hole	3.864 and -3.301 e.A^-3

Table 2. Atomic coordinates (x 10^4) and equivalent isotropic displacement parameters (A^2 x 10^3) for 10i1.
U(eq) is defined as one third of the trace of the orthogonalized Uij tensor.

	x	y	z	U(eq)
I(1)	5013(1)	-2549(1)	10224(1)	33(1)
I(2)	2052(1)	1489(1)	8881(1)	52(1)
I(3)	3320(1)	6984(1)	8932(1)	51(1)
I(4)	6646(1)	6828(1)	10537(1)	42(1)
I(5)	7742(1)	1065(1)	11400(1)	40(1)
Si(1)	4978(1)	649(1)	8182(1)	18(1)
Si(2)	5963(1)	1802(1)	8606(1)	16(1)
Si(3)	5580(1)	3709(1)	8455(1)	17(1)
Si(4)	4421(1)	3693(1)	7948(1)	16(1)
Si(5)	3998(1)	1793(1)	7753(1)	17(1)
O(1)	5446(1)	1282(2)	8500(1)	24(1)
O(2)	5864(1)	2810(2)	8679(1)	23(1)
O(3)	4996(1)	3617(2)	8415(1)	21(1)
O(4)	4159(1)	2776(2)	7921(1)	23(1)
O(5)	4462(1)	1166(2)	8096(1)	23(1)
O(6)	4404(1)	3958(2)	7240(1)	21(1)
O(7)	6165(1)	1667(2)	8010(1)	21(1)
O(8)	5000	339(2)	7500	21(1)
C(1)	5008(2)	-1604(3)	9551(2)	31(1)
C(2)	5004(4)	-704(6)	9779(4)	36(2)
C(3)	5001(5)	-56(6)	9352(4)	39(2)
C(2A)	5461(3)	-1303(6)	9514(4)	27(2)
C(3A)	5451(3)	-638(5)	9090(4)	26(2)
C(4)	5000(2)	-272(3)	8708(2)	24(1)
C(5)	5017(4)	-1075(6)	8567(5)	36(2)
C(6)	5019(5)	-1733(6)	8992(5)	39(2)
C(5A)	4549(3)	-712(5)	8687(4)	22(1)
C(6A)	4553(3)	-1383(5)	9102(4)	26(2)
C(7)	3458(1)	1592(2)	8032(2)	20(1)
C(8)	3491(2)	1110(3)	8571(2)	26(1)
C(9)	3083(2)	1070(3)	8802(2)	31(1)
C(10)	2648(2)	1510(3)	8500(2)	33(1)
C(11)	2601(2)	1990(3)	7969(3)	34(1)
C(12)	3004(2)	2022(3)	7736(2)	29(1)
C(13)	4108(2)	4551(3)	8244(2)	26(1)
C(14)	4288(2)	4843(3)	8869(2)	37(1)
C(15)	4069(2)	5538(4)	9072(3)	44(1)

C(16)	3656(2)	5929(3)	8644(3)	41(1)
C(17)	3479(3)	5679(5)	8025(3)	71(2)
C(18)	3713(2)	4996(5)	7829(3)	59(2)
C(19)	5881(1)	4556(3)	9025(2)	22(1)
C(20)	6319(2)	4413(3)	9530(2)	33(1)
C(21)	6544(2)	5056(4)	9962(2)	41(1)
C(22)	6326(2)	5856(3)	9885(2)	31(1)
C(23)	5897(2)	6026(3)	9390(3)	43(1)
C(24)	5682(2)	5376(3)	8955(3)	42(1)
C(25)	6451(1)	1461(2)	9339(2)	20(1)
C(26)	6959(2)	1570(3)	9413(2)	30(1)
C(27)	7331(2)	1433(3)	9992(2)	32(1)
C(28)	7190(2)	1178(3)	10506(2)	28(1)
C(29)	6692(2)	1026(3)	10446(2)	29(1)
C(30)	6326(2)	1170(3)	9865(2)	26(1)

Table 3. Bond lengths [A] and angles [deg] for 10i1.

I(1)-C(1)	2.102(4)
I(2)-C(10)	2.105(4)
I(3)-C(16)	2.101(5)
I(4)-C(22)	2.094(4)
I(5)-C(28)	2.101(4)
Si(1)-O(1)	1.612(3)
Si(1)-O(5)	1.615(3)
Si(1)-O(8)	1.6179(15)
Si(1)-C(4)	1.846(4)
Si(2)-O(1)	1.611(3)
Si(2)-O(2)	1.616(3)
Si(2)-O(7)	1.621(3)
Si(2)-C(25)	1.840(4)
Si(3)-O(2)	1.612(3)
Si(3)-O(6)#1	1.615(3)
Si(3)-O(3)	1.620(3)
Si(3)-C(19)	1.840(4)
Si(4)-O(4)	1.604(3)
Si(4)-O(3)	1.616(3)
Si(4)-O(6)	1.618(3)
Si(4)-C(13)	1.838(4)
Si(5)-O(4)	1.609(3)
Si(5)-O(5)	1.610(3)
Si(5)-O(7)#1	1.625(3)
Si(5)-C(7)	1.843(4)
O(6)-Si(3)#1	1.615(3)
O(7)-Si(5)#1	1.625(3)
O(8)-Si(1)#1	1.6179(15)
C(1)-C(6)	1.274(11)
C(1)-C(2A)	1.381(9)
C(1)-C(6A)	1.388(9)
C(1)-C(2)	1.495(11)
C(2)-C(3)	1.389(13)
C(3)-C(4)	1.476(10)
C(2A)-C(3A)	1.399(11)
C(3A)-C(4)	1.399(9)
C(4)-C(5)	1.297(10)
C(4)-C(5A)	1.426(8)
C(5)-C(6)	1.399(13)
C(5A)-C(6A)	1.397(11)
C(7)-C(8)	1.398(5)
C(7)-C(12)	1.400(6)
C(8)-C(9)	1.399(6)

C(9)-C(10)	1.374(7)
C(10)-C(11)	1.373(7)
C(11)-C(12)	1.390(6)
C(13)-C(18)	1.382(7)
C(13)-C(14)	1.396(6)
C(14)-C(15)	1.394(7)
C(15)-C(16)	1.382(7)
C(16)-C(17)	1.366(8)
C(17)-C(18)	1.395(8)
C(19)-C(24)	1.386(6)
C(19)-C(20)	1.390(6)
C(20)-C(21)	1.394(6)
C(21)-C(22)	1.378(7)
C(22)-C(23)	1.371(7)
C(23)-C(24)	1.400(7)
C(25)-C(26)	1.393(6)
C(25)-C(30)	1.404(5)
C(26)-C(27)	1.390(6)
C(27)-C(28)	1.388(7)
C(28)-C(29)	1.379(7)
C(29)-C(30)	1.388(6)

O(1)-Si(1)-O(5)	108.52(16)
O(1)-Si(1)-O(8)	108.92(14)
O(5)-Si(1)-O(8)	110.07(13)
O(1)-Si(1)-C(4)	110.08(17)
O(5)-Si(1)-C(4)	107.99(17)
O(8)-Si(1)-C(4)	111.21(19)
O(1)-Si(2)-O(2)	109.30(16)
O(1)-Si(2)-O(7)	110.51(15)
O(2)-Si(2)-O(7)	109.03(16)
O(1)-Si(2)-C(25)	111.16(17)
O(2)-Si(2)-C(25)	107.14(16)
O(7)-Si(2)-C(25)	109.63(16)
O(2)-Si(3)-O(6)#1	110.14(15)
O(2)-Si(3)-O(3)	109.26(16)
O(6)#1-Si(3)-O(3)	108.00(15)
O(2)-Si(3)-C(19)	109.96(17)
O(6)#1-Si(3)-C(19)	110.06(17)
O(3)-Si(3)-C(19)	109.39(16)
O(4)-Si(4)-O(3)	107.97(16)
O(4)-Si(4)-O(6)	108.92(15)
O(3)-Si(4)-O(6)	110.92(15)
O(4)-Si(4)-C(13)	113.41(18)
O(3)-Si(4)-C(13)	108.26(17)
O(6)-Si(4)-C(13)	107.37(17)
O(4)-Si(5)-O(5)	110.28(16)
O(4)-Si(5)-O(7)#1	108.80(16)

O(5)-Si(5)-O(7)#1	109.64(15)
O(4)-Si(5)-C(7)	106.37(16)
O(5)-Si(5)-C(7)	111.20(17)
O(7)#1-Si(5)-C(7)	110.48(16)
Si(2)-O(1)-Si(1)	160.0(2)
Si(3)-O(2)-Si(2)	154.3(2)
Si(4)-O(3)-Si(3)	144.06(19)
Si(4)-O(4)-Si(5)	162.1(2)
Si(5)-O(5)-Si(1)	156.3(2)
Si(3)#1-O(6)-Si(4)	151.05(19)
Si(2)-O(7)-Si(5)#1	142.19(19)
Si(1)-O(8)-Si(1)#1	145.2(3)
C(6)-C(1)-C(2A)	71.4(7)
C(6)-C(1)-C(6A)	68.9(7)
C(2A)-C(1)-C(6A)	121.4(6)
C(6)-C(1)-C(2)	119.2(6)
C(2A)-C(1)-C(2)	79.0(6)
C(6A)-C(1)-C(2)	84.6(6)
C(6)-C(1)-I(1)	126.3(5)
C(2A)-C(1)-I(1)	119.2(4)
C(6A)-C(1)-I(1)	118.8(4)
C(2)-C(1)-I(1)	114.5(4)
C(3)-C(2)-C(1)	116.8(7)
C(2)-C(3)-C(4)	119.9(8)
C(1)-C(2A)-C(3A)	118.4(7)
C(2A)-C(3A)-C(4)	122.0(7)
C(5)-C(4)-C(3A)	69.9(6)
C(5)-C(4)-C(5A)	68.3(6)
C(3A)-C(4)-C(5A)	116.2(5)
C(5)-C(4)-C(3)	118.1(6)
C(3A)-C(4)-C(3)	77.5(6)
C(5A)-C(4)-C(3)	82.2(6)
C(5)-C(4)-Si(1)	126.5(5)
C(3A)-C(4)-Si(1)	122.9(4)
C(5A)-C(4)-Si(1)	120.5(4)
C(3)-C(4)-Si(1)	115.5(5)
C(4)-C(5)-C(6)	122.5(8)
C(1)-C(6)-C(5)	123.5(8)
C(6A)-C(5A)-C(4)	121.5(7)
C(1)-C(6A)-C(5A)	118.2(7)
C(8)-C(7)-C(12)	117.5(4)
C(8)-C(7)-Si(5)	123.4(3)
C(12)-C(7)-Si(5)	118.7(3)
C(7)-C(8)-C(9)	120.5(4)
C(10)-C(9)-C(8)	120.0(4)
C(11)-C(10)-C(9)	121.2(4)
C(11)-C(10)-I(2)	119.5(4)
C(9)-C(10)-I(2)	119.3(3)

C(10)-C(11)-C(12)	118.8(4)
C(11)-C(12)-C(7)	122.1(4)
C(18)-C(13)-C(14)	117.3(4)
C(18)-C(13)-Si(4)	119.9(4)
C(14)-C(13)-Si(4)	122.5(3)
C(15)-C(14)-C(13)	121.6(5)
C(16)-C(15)-C(14)	118.6(5)
C(17)-C(16)-C(15)	121.5(5)
C(17)-C(16)-I(3)	118.8(4)
C(15)-C(16)-I(3)	119.5(4)
C(16)-C(17)-C(18)	118.7(5)
C(13)-C(18)-C(17)	122.1(5)
C(24)-C(19)-C(20)	117.3(4)
C(24)-C(19)-Si(3)	120.5(3)
C(20)-C(19)-Si(3)	122.2(3)
C(19)-C(20)-C(21)	122.0(4)
C(22)-C(21)-C(20)	118.9(4)
C(23)-C(22)-C(21)	121.0(4)
C(23)-C(22)-I(4)	119.2(4)
C(21)-C(22)-I(4)	119.8(4)
C(22)-C(23)-C(24)	119.2(5)
C(19)-C(24)-C(23)	121.6(5)
C(26)-C(25)-C(30)	117.6(4)
C(26)-C(25)-Si(2)	120.6(3)
C(30)-C(25)-Si(2)	121.4(3)
C(27)-C(26)-C(25)	121.6(4)
C(28)-C(27)-C(26)	118.9(4)
C(29)-C(28)-C(27)	121.3(4)
C(29)-C(28)-I(5)	119.4(3)
C(27)-C(28)-I(5)	119.3(3)
C(28)-C(29)-C(30)	119.0(4)
C(29)-C(30)-C(25)	121.6(4)

Symmetry transformations used to generate equivalent atoms:
#1 -x+1,y,-z+3/2

Table 4. Anisotropic displacement parameters (A^2 x 10^3) for 10i1.

The anisotropic displacement factor exponent takes the form: -2 pi^2 [h^2 a*^2 U11 + ... + 2 h k a* b* U12]

	U11	U22	U33	U23	U13	U12
I(1)	41(1)	30(1)	32(1)	15(1)	16(1)	4(1)
I(2)	54(1)	46(1)	80(1)	-14(1)	54(1)	-10(1)
I(3)	63(1)	39(1)	53(1)	-9(1)	21(1)	25(1)
I(4)	48(1)	41(1)	41(1)	-24(1)	21(1)	-18(1)
I(5)	44(1)	40(1)	25(1)	-4(1)	-6(1)	15(1)
Si(1)	18(1)	18(1)	18(1)	3(1)	6(1)	0(1)
Si(2)	17(1)	17(1)	16(1)	1(1)	5(1)	1(1)
Si(3)	17(1)	16(1)	18(1)	-2(1)	5(1)	1(1)
Si(4)	16(1)	15(1)	18(1)	-1(1)	6(1)	0(1)
Si(5)	17(1)	17(1)	17(1)	0(1)	7(1)	-2(1)
O(1)	22(1)	30(1)	20(1)	-1(1)	7(1)	-6(1)
O(2)	24(1)	17(1)	25(1)	0(1)	5(1)	5(1)
O(3)	17(1)	24(1)	20(1)	0(1)	5(1)	-1(1)
O(4)	26(1)	20(1)	27(1)	-2(1)	13(1)	-7(1)
O(5)	21(1)	24(1)	25(1)	4(1)	10(1)	3(1)
O(6)	22(1)	21(1)	19(1)	2(1)	7(1)	1(1)
O(7)	20(1)	27(1)	18(1)	2(1)	8(1)	3(1)
O(8)	27(2)	17(2)	20(2)	0	10(2)	0
C(1)	34(2)	30(2)	31(2)	14(2)	12(2)	-1(2)
C(2)	57(6)	31(4)	22(4)	3(3)	18(4)	-1(4)
C(3)	71(7)	22(4)	28(4)	-5(3)	21(5)	-8(4)
C(2A)	20(3)	29(4)	28(4)	10(3)	4(3)	2(3)
C(3A)	22(3)	26(4)	29(4)	9(3)	9(3)	1(3)
C(4)	24(2)	26(2)	24(2)	7(2)	10(1)	0(2)
C(5)	62(6)	21(4)	30(4)	2(3)	21(4)	9(4)
C(6)	63(7)	19(4)	40(5)	0(4)	22(5)	3(4)
C(5A)	17(3)	25(4)	22(3)	5(3)	5(3)	-2(3)
C(6A)	24(4)	24(4)	31(4)	6(3)	11(3)	-3(3)
C(7)	19(2)	18(2)	23(2)	-2(1)	9(1)	-3(1)
C(8)	33(2)	22(2)	26(2)	2(1)	14(2)	-1(2)
C(9)	41(2)	28(2)	32(2)	-2(2)	22(2)	-7(2)
C(10)	38(2)	27(2)	43(2)	-13(2)	28(2)	-9(2)
C(11)	24(2)	35(2)	48(3)	-1(2)	20(2)	2(2)
C(12)	24(2)	32(2)	34(2)	5(2)	13(2)	0(2)
C(13)	27(2)	22(2)	25(2)	-6(1)	5(2)	7(2)
C(14)	34(2)	41(3)	33(2)	-10(2)	7(2)	12(2)

C(15)	38(3)	43(3)	44(3)	-19(2)	4(2)	10(2)
C(16)	45(3)	37(3)	37(2)	-12(2)	8(2)	17(2)
C(17)	58(4)	74(5)	58(4)	-28(3)	-15(3)	40(4)
C(18)	46(3)	66(4)	45(3)	-25(3)	-12(2)	28(3)
C(19)	22(2)	21(2)	24(2)	-4(1)	8(1)	-1(1)
C(20)	33(2)	28(2)	31(2)	-6(2)	0(2)	3(2)
C(21)	40(3)	42(3)	31(2)	-11(2)	-2(2)	-1(2)
C(22)	35(2)	32(2)	30(2)	-14(2)	16(2)	-11(2)
C(23)	45(3)	21(2)	56(3)	-13(2)	6(2)	2(2)
C(24)	37(2)	28(2)	48(3)	-11(2)	-7(2)	8(2)
C(25)	22(2)	18(2)	20(2)	1(1)	5(1)	4(1)
C(26)	24(2)	37(2)	25(2)	6(2)	5(2)	2(2)
C(27)	24(2)	37(2)	30(2)	3(2)	0(2)	1(2)
C(28)	31(2)	25(2)	21(2)	-1(1)	-1(2)	9(2)
C(29)	37(2)	29(2)	20(2)	2(2)	8(2)	8(2)
C(30)	26(2)	28(2)	23(2)	2(2)	9(2)	4(2)

Table 5. Hydrogen coordinates (x 10^4) and isotropic displacement parameters (A^2 x 10^3) for 10i1.

	x	y	z	U(eq)
H(2A)	5005	-583	10196	43
H(3A)	4998	527	9474	47
H(2B)	5771	-1542	9770	32
H(3B)	5761	-428	9061	31
H(5A)	5029	-1221	8159	44
H(6A)	5029	-2308	8857	47
H(5B)	4239	-543	8385	26
H(6B)	4252	-1681	9078	31
H(8B)	3792	807	8782	31
H(9A)	3108	738	9167	37
H(11A)	2299	2295	7764	40
H(12A)	2971	2346	7365	35
H(14A)	4567	4561	9162	45
H(15A)	4200	5739	9495	53
H(17A)	3201	5965	7733	86
H(18A)	3596	4831	7396	70
H(20A)	6468	3860	9582	40
H(21A)	6844	4944	10303	49
H(23A)	5748	6579	9342	52
H(24A)	5393	5500	8602	51
H(26A)	7054	1740	9059	35
H(27A)	7676	1513	10035	39
H(29A)	6602	825	10796	35
H(30A)	5982	1070	9822	31

Appendix 4

Crystallographic data for I_{12}DPS

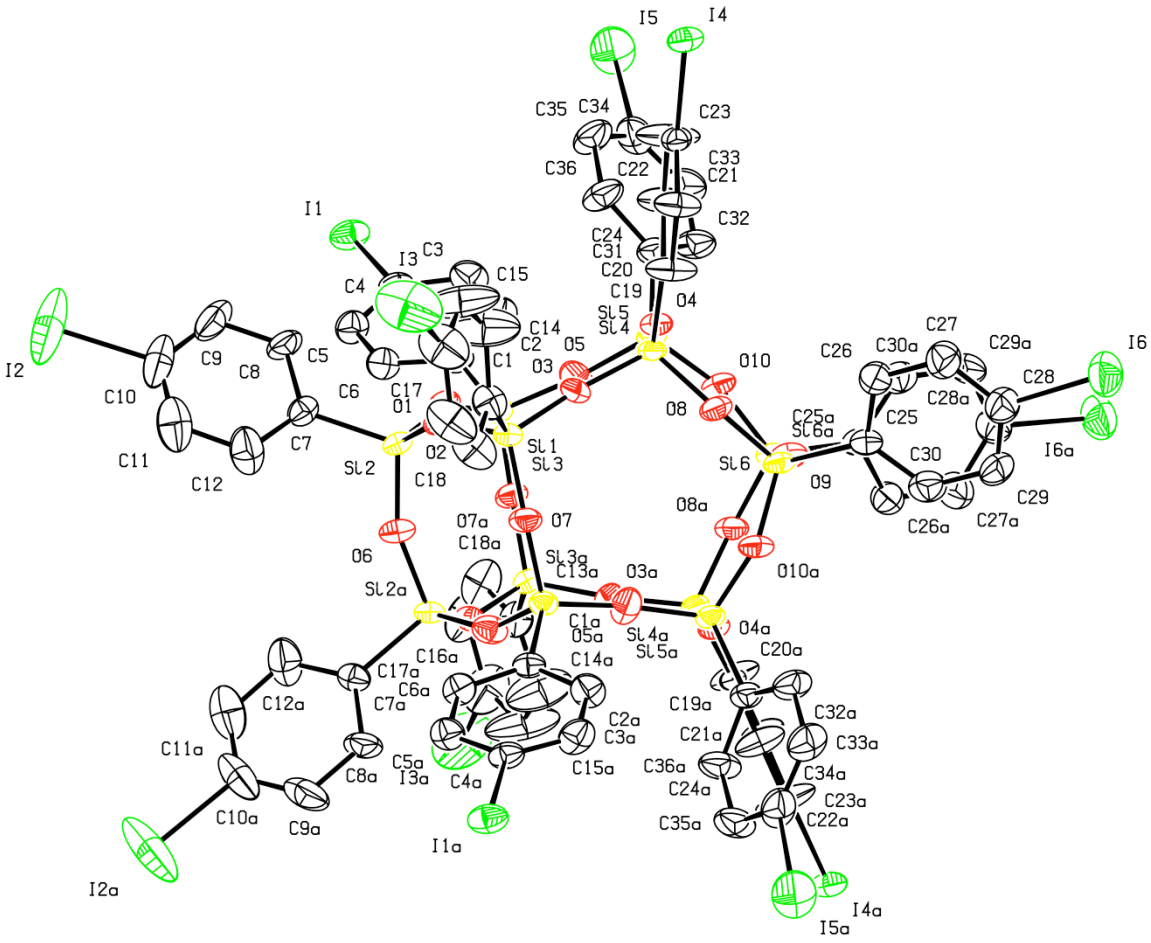

Figure A.4. 50 % thermal ellipsoid plots of dodeca(p-iodophenyl)silsesquioxane. Hydrogen atoms and m-xylene solvates are omitted for clarity.

Structure Determination.

Colorless blocks of **12i5a** were grown from a m-xylene/dodecane solution at 25 deg. C. A crystal of dimensions 0.44 x 0.44 x 0.30 mm was mounted on a Bruker SMART APEX CCD-based X-ray diffractometer equipped with a low temperature device and fine focus Mo-target X-ray tube (l = 0.71073 A) operated at 1500 W power (50 kV, 30 mA). The X-ray intensities were measured at 85(1) K; the detector was placed at a distance 5.055 cm from the crystal. A total of 3250 frames were collected with a scan width of 0.5° in w and 0.45° in phi with an exposure time of 15 s/frame. The integration of the data yielded a total of 173661 reflections to a maximum 2q value of 59.34° of which 16839 were independent and 13867 were greater than 2s(I). The final cell constants (Table 1) were based on the xyz centroids of 9454 reflections above 10s(I). Analysis of the data showed negligible decay during data collection; the data were processed with SADABS and corrected for absorption. The structure was solved and refined with the Bruker SHELXTL (version 2008/3) software package, using the space group C2/c with Z = 4 for the formula $C_{72}H_{48}O_{12}I_{12}$•2(C_8H_{10}). All non-hydrogen atoms were refined anisotropically with the hydrogen atoms placed in idealized positions. The cluster lies on a two-fold axis of the crystal lattice. Full matrix least-squares refinement based on F^2 converged at R1 = 0.0919 and wR2 = 0.2732 [based on I > 2sigma(I)], R1 = 0.1064 and wR2 = 0.2885 for all data. Additional details are presented in Table 1 and are given as Supporting Information in a CIF file.

Sheldrick, G.M. SHELXTL, v. 2008/3; Bruker Analytical X-ray, Madison, WI, 2008.

Sheldrick, G.M. SADABS, v. 2008/1. Program for Empirical Absorption Correction of Area Detector Data, University of Gottingen: Gottingen, Germany, 2008.

Saint Plus, v. 7.53a, Bruker Analytical X-ray, Madison, WI, 2008.

Table 1. Crystal data and structure refinement for 12i5a.

Identification code	12i5a
Empirical formula	C104 H88 I12 O18 Si12
Formula weight	3485.62
Temperature	85(2) K
Wavelength	0.71073 A
Crystal system, space group	Monoclinic, C2/c
Unit cell dimensions	a = 32.082(9) A alpha = 90 deg. b = 14.704(4) A beta =118.438(4)deg. c = 28.755(8) A gamma = 90 deg.
Volume	11928(5) A^3
Z, Calculated density	4, 1.941 Mg/m^3
Absorption coefficient	3.297 mm^-1
F(000)	6640
Crystal size	0.44 x 0.44 x 0.30 mm
Theta range for data collection	1.44 to 29.67 deg.
Limiting indices	-44<=h<=44, -20<=k<=20, -39<=l<=40
Reflections collected / unique	173661 / 16839 [R(int) = 0.0422]
Completeness to theta = 29.67	99.7 %
Absorption correction	Semi-empirical from equivalents
Max. and min. transmission	0.4379 and 0.3248

Refinement method	Full-matrix least-squares on F^2
Data / restraints / parameters	16839 / 0 / 663
Goodness-of-fit on F^2	1.093
Final R indices [I>2sigma(I)]	R1 = 0.0919, wR2 = 0.2732
R indices (all data)	R1 = 0.1064, wR2 = 0.2885
Largest diff. peak and hole	4.370 and -4.306 e.A^-3

Table 2. Atomic coordinates (x 10^4) and equivalent isotropic displacement parameters (A^2 x 10^3) for 12i5a.

U(eq) is defined as one third of the trace of the orthogonalized Uij tensor.

	x	y	z	U(eq)
I(1)	8236(1)	2718(1)	4826(1)	40(1)
I(2)	5816(1)	6763(1)	4429(1)	120(1)
I(3)	2869(1)	2503(1)	3894(1)	101(1)
I(4)	4487(1)	-1569(1)	5481(1)	34(1)
I(5)	7967(1)	-888(1)	5735(1)	76(1)
I(6)	3658(1)	-5941(1)	2555(1)	63(1)
O(1)	5639(1)	2111(3)	3347(2)	35(1)
O(2)	4772(1)	2271(3)	3188(1)	28(1)
O(3)	4663(1)	525(3)	3212(1)	31(1)
O(4)	5365(1)	-658(3)	3610(1)	29(1)
O(5)	5888(2)	407(3)	3380(2)	41(1)
O(6)	5000	2990(5)	2500	33(1)
O(7)	4124(1)	1454(3)	2348(2)	33(1)
O(8)	4506(1)	-1147(3)	2892(1)	31(1)
O(9)	5000	-1969(5)	2500	34(1)
O(10)	5838(1)	-1319(3)	3139(1)	32(1)
Si(1)	5986(1)	1420(1)	3260(1)	25(1)
Si(2)	5186(1)	2783(1)	3118(1)	24(1)
Si(3)	4387(1)	1466(1)	2979(1)	24(1)
Si(4)	4808(1)	-510(1)	3398(1)	24(1)
Si(5)	5848(1)	-603(1)	3565(1)	26(1)
Si(6)	4477(1)	-1802(1)	2429(1)	27(1)
C(1)	6604(2)	1771(4)	3710(2)	28(1)
C(2)	6959(2)	1128(5)	3987(3)	39(2)
C(3)	7427(2)	1400(5)	4321(3)	43(2)
C(4)	7532(2)	2306(4)	4365(2)	33(1)
C(5)	7187(2)	2957(5)	4115(2)	37(1)
C(6)	6723(2)	2685(5)	3791(2)	35(1)
C(7)	5357(2)	3862(4)	3478(2)	30(1)
C(8)	5750(3)	3921(5)	3986(2)	45(2)
C(9)	5881(3)	4732(6)	4258(3)	62(2)
C(10)	5621(3)	5505(6)	4030(4)	64(2)

C(11)	5233(3)	5475(6)	3547(4)	67(2)
C(12)	5097(3)	4653(6)	3262(4)	60(3)
C(13)	3939(2)	1652(5)	3197(3)	38(1)
C(14)	4055(3)	1533(11)	3726(4)	89(4)
C(15)	3746(3)	1792(12)	3917(3)	97(5)
C(16)	3329(3)	2131(8)	3602(4)	69(2)
C(17)	3166(3)	2207(7)	3059(4)	66(2)
C(18)	3491(3)	1971(6)	2872(4)	58(2)
C(19)	4695(2)	-822(3)	3951(2)	24(1)
C(20)	4243(2)	-884(6)	3895(2)	47(2)
C(21)	4174(2)	-1096(6)	4329(2)	44(2)
C(22)	4561(2)	-1250(4)	4809(2)	28(1)
C(23)	5009(2)	-1183(8)	4875(2)	64(3)
C(24)	5074(2)	-994(6)	4440(2)	49(2)
C(25)	4212(2)	-2898(4)	2440(2)	30(1)
C(26)	4140(2)	-3145(5)	2865(3)	43(2)
C(27)	3975(3)	-4007(5)	2891(3)	50(2)
C(28)	3883(2)	-4624(5)	2491(3)	45(2)
C(29)	3956(3)	-4421(5)	2065(3)	47(2)
C(30)	4120(3)	-3546(5)	2046(3)	45(2)
C(31)	6385(2)	-842(4)	4191(2)	32(1)
C(32)	6745(2)	-1400(5)	4204(2)	42(2)
C(33)	7195(2)	-1429(6)	4650(3)	50(2)
C(34)	7281(3)	-929(5)	5072(3)	49(2)
C(35)	6946(3)	-386(6)	5094(3)	52(2)
C(36)	6490(2)	-357(6)	4648(3)	49(2)
C(37)	3086(3)	9098(9)	2472(4)	71(3)
C(38)	3151(4)	8140(10)	2520(5)	82(3)
C(39)	3073(4)	7727(11)	2909(5)	95(4)
C(40)	2925(4)	8219(10)	3195(4)	80(4)
C(41)	2868(3)	9129(10)	3140(4)	75(3)
C(42)	2942(3)	9550(9)	2767(4)	72(3)
C(43)	3162(3)	9547(11)	2036(4)	84(4)
C(44)	2707(5)	9703(12)	3479(5)	115(4)
C(45)	4395(3)	4647(6)	4222(4)	64(2)
C(46)	3913(4)	4625(9)	4021(4)	82(3)
C(47)	3654(4)	5450(10)	3977(6)	93(4)
C(48)	3896(4)	6272(9)	4127(5)	86(3)
C(49)	4365(4)	6283(8)	4314(4)	74(3)
C(50)	4618(4)	5497(8)	4374(4)	69(3)
C(51)	4665(4)	3802(7)	4263(4)	73(3)
C(52)	3090(5)	5288(19)	3719(8)	163(9)

Table 3. Bond lengths [A] and angles [deg] for 12i5a.

I(1)-C(4)	2.093(5)
I(2)-C(10)	2.110(8)
I(3)-C(16)	2.088(11)
I(4)-C(22)	2.107(6)
I(5)-C(34)	2.117(7)
I(6)-C(28)	2.105(8)
O(1)-Si(1)	1.613(5)
O(1)-Si(2)	1.616(4)
O(2)-Si(3)	1.606(4)
O(2)-Si(2)	1.621(4)
O(3)-Si(4)	1.606(4)
O(3)-Si(3)	1.608(4)
O(4)-Si(4)	1.606(4)
O(4)-Si(5)	1.616(5)
O(5)-Si(1)	1.593(5)
O(5)-Si(5)	1.603(5)
O(6)-Si(2)#1	1.6102(19)
O(6)-Si(2)	1.6102(19)
O(7)-Si(3)	1.597(4)
O(7)-Si(1)#1	1.612(4)
O(8)-Si(4)	1.608(4)
O(8)-Si(6)	1.611(5)
O(9)-Si(6)#1	1.6090(19)
O(9)-Si(6)	1.6090(19)
O(10)-Si(5)	1.604(5)
O(10)-Si(6)#1	1.618(4)
Si(1)-O(7)#1	1.612(4)
Si(1)-C(1)	1.852(5)
Si(2)-C(7)	1.830(6)
Si(3)-C(13)	1.842(7)
Si(4)-C(19)	1.851(6)
Si(5)-C(31)	1.839(5)
Si(6)-O(10)#1	1.618(4)
Si(6)-C(25)	1.830(6)
C(1)-C(6)	1.387(9)
C(1)-C(2)	1.400(8)
C(2)-C(3)	1.400(8)
C(3)-C(4)	1.365(10)
C(4)-C(5)	1.379(9)
C(5)-C(6)	1.385(8)
C(7)-C(12)	1.393(10)
C(7)-C(8)	1.407(7)
C(8)-C(9)	1.377(10)

C(9)-C(10)	1.377(13)
C(10)-C(11)	1.353(13)
C(11)-C(12)	1.407(13)
C(13)-C(18)	1.372(9)
C(13)-C(14)	1.393(12)
C(14)-C(15)	1.393(15)
C(15)-C(16)	1.306(13)
C(16)-C(17)	1.396(14)
C(17)-C(18)	1.424(14)
C(19)-C(24)	1.376(7)
C(19)-C(20)	1.381(8)
C(20)-C(21)	1.404(9)
C(21)-C(22)	1.366(7)
C(22)-C(23)	1.359(9)
C(23)-C(24)	1.393(10)
C(25)-C(26)	1.395(10)
C(25)-C(30)	1.400(10)
C(26)-C(27)	1.389(11)
C(27)-C(28)	1.383(11)
C(28)-C(29)	1.384(12)
C(29)-C(30)	1.400(11)
C(31)-C(36)	1.387(9)
C(31)-C(32)	1.404(9)
C(32)-C(33)	1.403(8)
C(33)-C(34)	1.330(12)
C(34)-C(35)	1.367(12)
C(35)-C(36)	1.414(9)
C(37)-C(42)	1.322(17)
C(37)-C(38)	1.421(19)
C(37)-C(43)	1.538(17)
C(38)-C(39)	1.40(2)
C(39)-C(40)	1.34(2)
C(40)-C(41)	1.349(19)
C(41)-C(42)	1.355(16)
C(41)-C(44)	1.551(18)
C(45)-C(46)	1.370(14)
C(45)-C(50)	1.402(14)
C(45)-C(51)	1.487(14)
C(46)-C(47)	1.441(18)
C(47)-C(48)	1.388(19)
C(47)-C(52)	1.615(18)
C(48)-C(49)	1.337(17)
C(49)-C(50)	1.374(16)

Si(1)-O(1)-Si(2)	151.1(3)
Si(3)-O(2)-Si(2)	145.7(3)
Si(4)-O(3)-Si(3)	165.6(3)
Si(4)-O(4)-Si(5)	153.9(3)

Si(1)-O(5)-Si(5)	173.2(3)
Si(2)#1-O(6)-Si(2)	158.3(5)
Si(3)-O(7)-Si(1)#1	163.3(3)
Si(4)-O(8)-Si(6)	150.3(3)
Si(6)#1-O(9)-Si(6)	162.5(5)
Si(5)-O(10)-Si(6)#1	146.6(3)
O(5)-Si(1)-O(7)#1	107.4(3)
O(5)-Si(1)-O(1)	109.5(3)
O(7)#1-Si(1)-O(1)	109.8(2)
O(5)-Si(1)-C(1)	111.4(2)
O(7)#1-Si(1)-C(1)	110.9(3)
O(1)-Si(1)-C(1)	107.8(2)
O(6)-Si(2)-O(1)	110.7(2)
O(6)-Si(2)-O(2)	109.29(18)
O(1)-Si(2)-O(2)	107.2(2)
O(6)-Si(2)-C(7)	108.4(3)
O(1)-Si(2)-C(7)	109.3(2)
O(2)-Si(2)-C(7)	112.0(3)
O(7)-Si(3)-O(2)	109.2(2)
O(7)-Si(3)-O(3)	110.6(2)
O(2)-Si(3)-O(3)	107.8(2)
O(7)-Si(3)-C(13)	108.3(3)
O(2)-Si(3)-C(13)	110.5(3)
O(3)-Si(3)-C(13)	110.5(3)
O(3)-Si(4)-O(4)	110.3(2)
O(3)-Si(4)-O(8)	107.3(2)
O(4)-Si(4)-O(8)	110.3(2)
O(3)-Si(4)-C(19)	112.1(2)
O(4)-Si(4)-C(19)	106.1(2)
O(8)-Si(4)-C(19)	110.7(2)
O(5)-Si(5)-O(10)	109.3(3)
O(5)-Si(5)-O(4)	107.8(3)
O(10)-Si(5)-O(4)	110.9(2)
O(5)-Si(5)-C(31)	108.4(3)
O(10)-Si(5)-C(31)	106.9(3)
O(4)-Si(5)-C(31)	113.5(3)
O(9)-Si(6)-O(8)	109.9(2)
O(9)-Si(6)-O(10)#1	107.9(2)
O(8)-Si(6)-O(10)#1	109.5(2)
O(9)-Si(6)-C(25)	109.2(3)
O(8)-Si(6)-C(25)	110.9(3)
O(10)#1-Si(6)-C(25)	109.4(2)
C(6)-C(1)-C(2)	118.3(5)
C(6)-C(1)-Si(1)	120.3(4)
C(2)-C(1)-Si(1)	121.3(5)
C(3)-C(2)-C(1)	120.9(6)
C(4)-C(3)-C(2)	118.6(6)
C(3)-C(4)-C(5)	121.9(5)

C(3)-C(4)-I(1)	119.0(4)
C(5)-C(4)-I(1)	119.1(5)
C(4)-C(5)-C(6)	119.3(6)
C(5)-C(6)-C(1)	120.9(6)
C(12)-C(7)-C(8)	117.5(6)
C(12)-C(7)-Si(2)	121.1(5)
C(8)-C(7)-Si(2)	121.4(5)
C(9)-C(8)-C(7)	121.6(7)
C(8)-C(9)-C(10)	119.4(7)
C(11)-C(10)-C(9)	121.0(8)
C(11)-C(10)-I(2)	118.4(6)
C(9)-C(10)-I(2)	120.6(6)
C(10)-C(11)-C(12)	120.2(8)
C(7)-C(12)-C(11)	120.3(8)
C(18)-C(13)-C(14)	115.8(8)
C(18)-C(13)-Si(3)	123.5(6)
C(14)-C(13)-Si(3)	120.5(5)
C(15)-C(14)-C(13)	121.7(9)
C(16)-C(15)-C(14)	121.1(9)
C(15)-C(16)-C(17)	121.4(10)
C(15)-C(16)-I(3)	120.5(8)
C(17)-C(16)-I(3)	117.9(6)
C(16)-C(17)-C(18)	116.8(8)
C(13)-C(18)-C(17)	122.9(9)
C(24)-C(19)-C(20)	118.5(5)
C(24)-C(19)-Si(4)	118.9(5)
C(20)-C(19)-Si(4)	122.6(4)
C(19)-C(20)-C(21)	120.7(5)
C(22)-C(21)-C(20)	119.0(6)
C(23)-C(22)-C(21)	121.3(6)
C(23)-C(22)-I(4)	117.4(4)
C(21)-C(22)-I(4)	121.2(5)
C(22)-C(23)-C(24)	119.4(5)
C(19)-C(24)-C(23)	121.0(6)
C(26)-C(25)-C(30)	118.1(6)
C(26)-C(25)-Si(6)	121.2(5)
C(30)-C(25)-Si(6)	120.4(5)
C(27)-C(26)-C(25)	120.8(7)
C(28)-C(27)-C(26)	119.3(8)
C(27)-C(28)-C(29)	122.4(7)
C(27)-C(28)-I(6)	118.5(6)
C(29)-C(28)-I(6)	119.1(6)
C(28)-C(29)-C(30)	117.2(7)
C(29)-C(30)-C(25)	122.2(7)
C(36)-C(31)-C(32)	116.8(5)
C(36)-C(31)-Si(5)	121.3(5)
C(32)-C(31)-Si(5)	120.9(5)
C(33)-C(32)-C(31)	121.1(7)

C(34)-C(33)-C(32)	119.7(7)
C(33)-C(34)-C(35)	122.6(6)
C(33)-C(34)-I(5)	120.9(6)
C(35)-C(34)-I(5)	116.4(6)
C(34)-C(35)-C(36)	118.2(7)
C(31)-C(36)-C(35)	121.6(7)
C(42)-C(37)-C(38)	121.2(12)
C(42)-C(37)-C(43)	123.1(12)
C(38)-C(37)-C(43)	115.6(12)
C(39)-C(38)-C(37)	115.7(13)
C(40)-C(39)-C(38)	120.5(14)
C(39)-C(40)-C(41)	122.2(13)
C(40)-C(41)-C(42)	118.7(12)
C(40)-C(41)-C(44)	122.3(12)
C(42)-C(41)-C(44)	119.0(13)
C(37)-C(42)-C(41)	121.6(13)
C(46)-C(45)-C(50)	117.3(10)
C(46)-C(45)-C(51)	120.8(10)
C(50)-C(45)-C(51)	121.9(9)
C(45)-C(46)-C(47)	120.2(11)
C(48)-C(47)-C(46)	119.6(10)
C(48)-C(47)-C(52)	127.5(14)
C(46)-C(47)-C(52)	112.8(14)
C(49)-C(48)-C(47)	119.3(11)
C(48)-C(49)-C(50)	121.7(11)
C(49)-C(50)-C(45)	121.8(10)

Symmetry transformations used to generate equivalent atoms:

#1 -x+1,y,-z+1/2

Table 4. Anisotropic displacement parameters (A^2 x 10^3) for 12i5a.

The anisotropic displacement factor exponent takes the form: -2 pi^2 [h^2 a*^2 U11 + ... + 2 h k a* b* U12]

	U11	U22	U33	U23	U13	U12
I(1)	29(1)	58(1)	29(1)	-3(1)	10(1)	-12(1)
I(2)	171(1)	72(1)	187(1)	-80(1)	142(1)	-65(1)
I(3)	91(1)	144(1)	106(1)	31(1)	77(1)	40(1)
I(4)	32(1)	48(1)	21(1)	-1(1)	11(1)	-9(1)
I(5)	38(1)	69(1)	72(1)	1(1)	-14(1)	-2(1)
I(6)	69(1)	42(1)	71(1)	-4(1)	28(1)	-11(1)
O(1)	28(2)	43(2)	29(2)	-6(2)	8(1)	3(2)
O(2)	30(1)	30(2)	22(1)	-5(1)	13(1)	-3(1)
O(3)	41(2)	28(2)	24(1)	7(1)	16(1)	3(2)
O(4)	29(2)	36(2)	18(1)	2(1)	8(1)	3(1)
O(5)	28(2)	36(2)	42(2)	9(2)	2(2)	-7(2)
O(6)	32(2)	47(3)	19(2)	0	12(2)	0
O(7)	33(2)	38(2)	19(2)	2(1)	5(1)	-4(2)
O(8)	33(2)	39(2)	18(1)	-4(1)	10(1)	-7(2)
O(9)	26(2)	50(3)	23(2)	0	9(2)	0
O(10)	29(2)	44(2)	17(1)	-5(1)	5(1)	0(2)
Si(1)	20(1)	29(1)	20(1)	-2(1)	4(1)	-1(1)
Si(2)	23(1)	32(1)	16(1)	-3(1)	8(1)	-1(1)
Si(3)	24(1)	29(1)	19(1)	3(1)	9(1)	1(1)
Si(4)	26(1)	28(1)	14(1)	2(1)	8(1)	0(1)
Si(5)	22(1)	32(1)	16(1)	0(1)	3(1)	1(1)
Si(6)	23(1)	36(1)	15(1)	0(1)	4(1)	-3(1)
C(1)	22(2)	37(3)	22(2)	-3(2)	9(1)	-4(2)
C(2)	27(2)	41(3)	41(3)	-4(2)	10(2)	0(2)
C(3)	26(2)	50(4)	40(3)	7(3)	6(2)	-1(2)
C(4)	25(2)	45(3)	24(2)	-1(2)	8(2)	-9(2)
C(5)	31(2)	40(3)	37(2)	-3(2)	14(2)	-8(2)
C(6)	31(2)	39(3)	35(2)	1(2)	15(2)	-4(2)
C(7)	29(2)	36(3)	29(2)	-6(2)	16(2)	-8(2)
C(8)	51(3)	49(3)	25(2)	-11(2)	10(2)	-21(3)
C(9)	85(4)	61(4)	49(3)	-29(3)	38(3)	-39(3)
C(10)	86(3)	44(3)	92(4)	-33(3)	67(3)	-28(3)

C(11)	67(4)	42(4)	108(6)	-4(4)	55(4)	1(3)
C(12)	46(3)	39(4)	80(5)	0(4)	18(4)	2(3)
C(13)	37(2)	40(3)	45(3)	3(2)	25(2)	-3(2)
C(14)	63(4)	166(12)	55(4)	21(5)	41(3)	31(6)
C(15)	59(4)	207(15)	35(3)	6(5)	30(3)	23(7)
C(16)	64(3)	81(6)	81(4)	20(4)	49(3)	17(4)
C(17)	52(3)	75(5)	81(5)	30(4)	40(3)	19(4)
C(18)	41(3)	62(5)	72(4)	20(4)	27(3)	4(3)
C(19)	28(2)	25(2)	15(2)	1(2)	8(1)	-2(2)
C(20)	25(2)	90(5)	22(2)	16(3)	9(2)	-3(3)
C(21)	29(2)	75(4)	25(2)	14(3)	10(2)	-6(3)
C(22)	33(2)	32(2)	20(2)	0(2)	14(2)	-4(2)
C(23)	30(2)	139(8)	24(2)	27(3)	13(2)	6(4)
C(24)	28(2)	93(6)	25(2)	16(3)	13(2)	5(3)
C(25)	27(2)	37(3)	23(2)	2(2)	8(2)	2(2)
C(26)	57(3)	38(3)	39(3)	-2(2)	28(2)	-8(3)
C(27)	64(3)	44(4)	50(3)	-4(3)	33(3)	-9(3)
C(28)	44(3)	43(3)	44(3)	-4(3)	17(2)	-4(3)
C(29)	46(3)	45(3)	33(3)	-9(3)	4(2)	-5(3)
C(30)	42(3)	50(4)	33(3)	2(3)	10(2)	-2(3)
C(31)	29(2)	37(3)	22(2)	-1(2)	6(2)	1(2)
C(32)	33(2)	57(4)	28(2)	4(2)	7(2)	15(3)
C(33)	35(3)	60(4)	45(3)	10(3)	11(2)	15(3)
C(34)	35(3)	44(4)	50(4)	7(3)	4(3)	2(3)
C(35)	42(3)	57(4)	33(3)	-13(3)	-3(3)	8(3)
C(36)	40(3)	62(4)	28(3)	-11(3)	2(2)	18(3)
C(37)	36(3)	101(8)	62(5)	-6(5)	14(3)	-2(4)
C(38)	60(5)	109(9)	74(6)	19(6)	31(4)	18(5)
C(39)	78(6)	115(9)	70(6)	17(6)	18(5)	42(6)
C(40)	66(5)	109(9)	51(4)	24(5)	16(4)	4(6)
C(41)	50(4)	120(9)	49(4)	-25(5)	18(3)	-13(5)
C(42)	62(4)	101(8)	60(4)	-3(5)	36(3)	-13(5)
C(43)	57(4)	133(11)	71(5)	11(6)	38(4)	-1(6)
C(44)	133(7)	162(12)	83(5)	-62(6)	79(4)	-52(8)
C(45)	89(4)	49(4)	81(4)	-11(3)	61(3)	2(4)
C(46)	100(4)	77(7)	108(5)	8(5)	81(4)	8(5)
C(47)	70(4)	99(9)	136(8)	-9(7)	70(4)	8(5)
C(48)	121(6)	75(6)	90(5)	-20(5)	73(4)	2(6)
C(49)	96(6)	63(5)	65(5)	-21(4)	39(4)	-1(5)
C(50)	84(5)	69(6)	58(4)	-5(4)	37(4)	-5(5)
C(51)	96(5)	58(5)	82(5)	3(4)	57(4)	12(5)
C(52)	87(6)	260(20)	171(12)	39(15)	85(7)	66(11)

Table 5. Hydrogen coordinates (x 10^4) and isotropic displacement parameters (A^2 x 10^3) for 12i5a.

	x	y	z	U(eq)
H(2A)	6882	499	3948	47
H(3A)	7666	963	4512	51
H(5A)	7266	3585	4163	44
H(6B)	6483	3132	3622	42
H(8A)	5929	3389	4146	54
H(9B)	6149	4758	4600	75
H(11A)	5051	6010	3400	80
H(12A)	4828	4639	2921	72
H(14A)	4351	1269	3962	107
H(15A)	3841	1721	4282	117
H(17A)	2853	2406	2825	79
H(18A)	3393	2037	2506	70
H(20A)	3976	-782	3558	56
H(21A)	3864	-1133	4290	53
H(23A)	5274	-1265	5215	77
H(24A)	5386	-984	4481	58
H(26A)	4204	-2719	3139	51
H(27A)	3926	-4170	3181	60
H(29A)	3898	-4857	1797	56
H(30A)	4170	-3387	1756	54
H(32A)	6684	-1764	3905	51
H(33A)	7437	-1804	4651	60
H(35A)	7017	-36	5401	63
H(36A)	6250	3	4661	59
H(38A)	3243	7802	2302	98
H(39A)	3124	7092	2972	114
H(40A)	2859	7917	3444	96
H(42A)	2890	10187	2717	86
H(43A)	2970	9233	1699	126
H(43B)	3498	9508	2128	126
H(43C)	3067	10188	2001	126
H(44A)	2951	9675	3851	172
H(44B)	2409	9459	3442	172
H(44C)	2661	10336	3358	172
H(46A)	3748	4063	3910	99
H(48A)	3729	6822	4097	103

H(49A)	4528	6848	4408	89
H(50A)	4953	5530	4523	83
H(51A)	4793	3553	4622	109
H(51B)	4926	3942	4189	109
H(51C)	4454	3355	4007	109
H(52A)	2933	5865	3709	244
H(52B)	3026	4848	3934	244
H(52C)	2968	5052	3359	244

Appendix 5

Crystallographic data for *o*-Br_8OPS

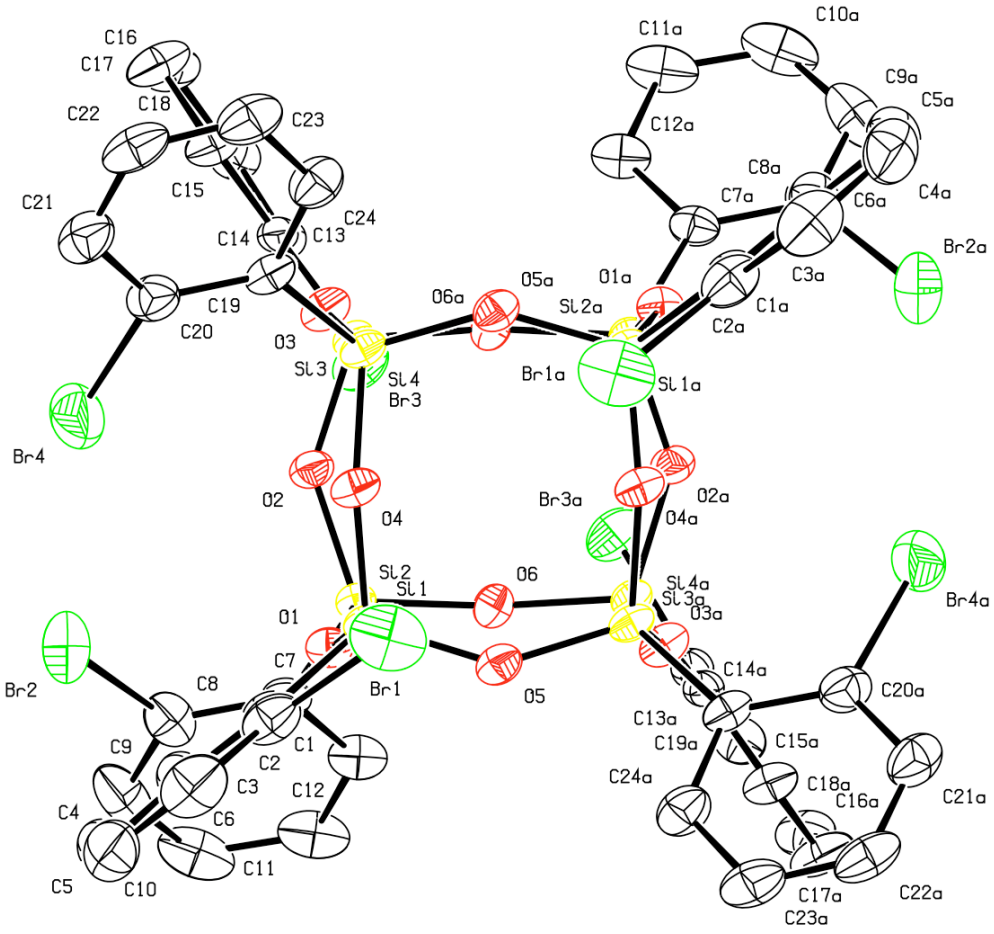

Figure A.5. 50 % thermal ellipsoid plots of octa(*o*-bromophenyl)silsesquioxane • *m*-xylene solvate. Hydrogen atoms and *m*-xylene solvates are omitted for clarity.

Structure Determination.

Colorless octahedral crystals of **obr8a** were grown from a meta-xylene solution at 20 deg. C. A crystal of dimensions 0.33 x 0.28 x 0.23 mm was mounted on a Bruker SMART APEX CCD-based X-ray diffractometer equipped with a low temperature device and fine focus Mo-target X-ray tube (l = 0.71073 A) operated at 1500 W power (50 kV, 30 mA). The X-ray intensities were measured at 85(1) K; the detector was placed at a distance 5.055 cm from the crystal. A total of 5280 frames were collected with a scan width of 0.5° in w and 0.45° in phi with an exposure time of 30 s/frame. The integration of the data yielded a total of 333383 reflections to a maximum 2q value of 56.68° of which 9574 were independent and 8392 were greater than 2s(I). The final cell constants (Table 1) were based on the xyz centroids of 9816 reflections above 10s(I). Analysis of the data showed negligible decay during data collection; the data were processed with SADABS and corrected for absorption. The structure was solved and refined with the Bruker SHELXTL (version 2008/3) software package, using the space group I4(1)/a with Z = 8 for the formula $C_{48}H_{32}O_{12}Si_8Br_8 \bullet 2.5(C_8H_{10})$. All non-hydrogen atoms were refined anisotropically with the hydrogen atoms placed in idealized positions. The cluster lies on a two-fold axis of the crystal lattice. Two of the meta-xylene solvate molecules are disordered and were modeled by use of partial occupancy atoms. The remaining solvate molecules are disordered in four voids in th elattice and were treated as diffuse scattering by use of the SQUEEZE subroutine of the PLATON program suite. Full matrix least-squares refinement based on F^2 converged at R1 = 0.0526 and wR2 = 0.1460 [based on I > 2sigma(I)], R1 = 0.0626 and wR2 = 0.1530 for

all data. Additional details are presented in Table 1 and are given as Supporting Information in a CIF file.

Sheldrick, G.M. SHELXTL, v. 2008/3; Bruker Analytical X-ray, Madison, WI, 2008.

Sheldrick, G.M. SADABS, v. 2008/1. Program for Empirical Absorption Correction of Area Detector Data, University of Gottingen: Gottingen, Germany, 2008.

Saint Plus, v. 7.53a, Bruker Analytical X-ray, Madison, WI, 2008.

A.L. Spek. (2008) PLATON, v. 180108, A Multi-purpose Crystallographic Tool, Utrecht University, Utrecht, The Netherlands.

Table 1. Crystal data and structure refinement for obr8a.

Identification code	obr8a
Empirical formula	C68 H57 Br8 O12 Si8
Formula weight	1930.14
Temperature	85(2) K
Wavelength	0.71073 A
Crystal system, space group	Tetragonal, I4(1)/a
Unit cell dimensions	a = 20.5738(10) A alpha = 90 deg. b = 20.5738(10) A beta = 90 deg. c = 36.261(4) A gamma = 90 deg.
Volume	15348.5(19) A^3
Z, Calculated density	8, 1.671 Mg/m^3
Absorption coefficient	4.362 mm^-1
F(000)	7624
Crystal size	0.33 x 0.28 x 0.23 mm
Theta range for data collection	1.79 to 28.34 deg.
Limiting indices	-27<=h<=27, -27<=k<=27, -48<=l<=48
Reflections collected / unique	333383 / 9574 [R(int) = 0.0477]
Completeness to theta = 28.34	99.8 %
Absorption correction	Semi-empirical from equivalents

Max. and min. transmission	0.3686 and 0.2779
Refinement method	Full-matrix least-squares on F^2
Data / restraints / parameters	9574 / 262 / 490
Goodness-of-fit on F^2	1.089
Final R indices [I>2sigma(I)]	R1 = 0.0526, wR2 = 0.1460
R indices (all data)	R1 = 0.0626, wR2 = 0.1530
Largest diff. peak and hole	0.994 and -1.329 e.A^-3

Table 2. Atomic coordinates (x 10^4) and equivalent isotropic displacement parameters (A^2 x 10^3) for obr8a.

U(eq) is defined as one third of the trace of the orthogonalized Uij tensor.

	x	y	z	U(eq)
Br(1)	838(1)	1983(1)	-1834(1)	57(1)
Br(2)	2590(1)	2259(1)	-19(1)	53(1)
Br(3)	536(1)	3174(1)	864(1)	37(1)
Br(4)	2135(1)	3605(1)	-1019(1)	68(1)
Si(1)	935(1)	1983(1)	-901(1)	23(1)
Si(2)	958(1)	2018(1)	-59(1)	20(1)
Si(3)	526(1)	3433(1)	-57(1)	20(1)
Si(4)	488(1)	3464(1)	-898(1)	22(1)
O(1)	1177(1)	1867(1)	-480(1)	24(1)
O(2)	972(1)	2794(1)	5(1)	25(1)
O(3)	624(1)	3689(1)	-476(1)	26(1)
O(4)	763(1)	2739(1)	-959(1)	26(1)
O(5)	292(1)	1547(1)	-972(1)	27(1)
O(6)	228(1)	1752(1)	1(1)	25(1)
C(1)	1613(1)	1712(1)	-1200(1)	30(1)
C(2)	1602(2)	1713(1)	-1586(1)	38(1)
C(3)	2130(2)	1512(2)	-1797(1)	52(1)
C(4)	2683(2)	1284(2)	-1620(1)	55(1)
C(5)	2719(2)	1262(2)	-1240(1)	50(1)
C(6)	2187(1)	1484(1)	-1034(1)	38(1)
C(7)	1494(1)	1580(1)	268(1)	26(1)
C(8)	2160(1)	1658(2)	293(1)	37(1)
C(9)	2543(2)	1297(2)	537(1)	50(1)
C(10)	2248(2)	836(2)	759(1)	49(1)
C(11)	1585(2)	740(2)	744(1)	42(1)
C(12)	1216(2)	1109(1)	503(1)	34(1)
C(13)	758(1)	4081(1)	270(1)	22(1)
C(14)	728(1)	4003(1)	654(1)	25(1)
C(15)	860(1)	4498(1)	899(1)	32(1)
C(16)	1056(2)	5092(1)	759(1)	39(1)
C(17)	1111(2)	5189(1)	386(1)	43(1)
C(18)	956(1)	4689(1)	143(1)	32(1)
C(19)	856(1)	4064(1)	-1216(1)	26(1)
C(20)	1525(1)	4140(1)	-1274(1)	35(1)
C(21)	1779(2)	4609(1)	-1511(1)	41(1)
C(22)	1361(2)	5027(1)	-1691(1)	42(1)

C(23)	702(2)	4981(1)	-1635(1)	44(1)
C(24)	453(2)	4501(1)	-1404(1)	37(1)
C(25)	2861(3)	3530(2)	7872(2)	87(2)
C(26)	2201(3)	3368(3)	7798(1)	72(1)
C(27)	1789(3)	3819(3)	7633(1)	94(2)
C(28)	2046(4)	4414(3)	7537(2)	120(2)
C(29)	2648(4)	4590(4)	7603(2)	136(2)
C(30)	3072(4)	4130(3)	7775(2)	112(2)
C(31)	3302(3)	3016(3)	8038(2)	111(2)
C(32)	1087(3)	3614(4)	7577(2)	129(3)
C(25A)	2324(5)	3723(5)	7767(7)	103(4)
C(26A)	1653(6)	3565(10)	7745(6)	105(4)
C(27A)	1246(5)	3890(6)	7500(5)	101(4)
C(29A)	1469(8)	4472(8)	7365(7)	122(4)
C(28A)	2041(8)	4734(9)	7441(6)	120(4)
C(30A)	2474(10)	4334(7)	7661(8)	120(4)
C(31A)	2768(8)	3172(8)	7888(8)	120(6)
C(32A)	676(8)	3488(11)	7362(9)	135(9)

Table 3. Bond lengths [A] and angles [deg] for obr8a.

Br(1)-C(2)	1.897(3)
Br(2)-C(8)	1.895(3)
Br(3)-C(14)	1.910(2)
Br(4)-C(20)	1.908(3)
Si(1)-O(4)	1.6086(17)
Si(1)-O(5)	1.6184(18)
Si(1)-O(1)	1.6225(17)
Si(1)-C(1)	1.854(3)
Si(2)-O(6)	1.6124(17)
Si(2)-O(2)	1.6145(17)
Si(2)-O(1)	1.6224(17)
Si(2)-C(7)	1.853(2)
Si(3)-O(6)#1	1.6111(17)
Si(3)-O(2)	1.6181(17)
Si(3)-O(3)	1.6208(17)
Si(3)-C(13)	1.846(2)
Si(4)-O(4)	1.6116(17)
Si(4)-O(3)	1.6244(17)
Si(4)-O(5)#1	1.6268(19)
Si(4)-C(19)	1.850(2)
O(5)-Si(4)#1	1.6268(19)
O(6)-Si(3)#1	1.6111(17)
C(1)-C(2)	1.398(4)
C(1)-C(6)	1.406(4)
C(2)-C(3)	1.392(4)
C(3)-C(4)	1.387(5)
C(4)-C(5)	1.380(5)
C(5)-C(6)	1.402(4)
C(7)-C(8)	1.383(4)
C(7)-C(12)	1.412(4)
C(8)-C(9)	1.399(4)
C(9)-C(10)	1.382(5)
C(10)-C(11)	1.380(5)
C(11)-C(12)	1.383(4)
C(13)-C(18)	1.394(3)
C(13)-C(14)	1.403(3)
C(14)-C(15)	1.378(3)
C(15)-C(16)	1.383(4)
C(16)-C(17)	1.373(4)
C(17)-C(18)	1.391(4)
C(19)-C(24)	1.400(4)
C(19)-C(20)	1.401(4)
C(20)-C(21)	1.393(4)

C(21)-C(22)	1.379(4)
C(22)-C(23)	1.373(5)
C(23)-C(24)	1.394(4)
C(25)-C(30)	1.354(8)
C(25)-C(26)	1.424(8)
C(25)-C(31)	1.518(7)
C(26)-C(27)	1.391(8)
C(27)-C(28)	1.377(8)
C(27)-C(32)	1.519(7)
C(28)-C(29)	1.313(11)
C(29)-C(30)	1.432(11)
C(25A)-C(30A)	1.350(15)
C(25A)-C(26A)	1.420(14)
C(25A)-C(31A)	1.520(9)
C(26A)-C(27A)	1.390(16)
C(27A)-C(29A)	1.373(16)
C(27A)-C(32A)	1.522(9)
C(29A)-C(28A)	1.323(18)
C(28A)-C(30A)	1.453(19)

O(4)-Si(1)-O(5)	109.62(10)
O(4)-Si(1)-O(1)	109.41(9)
O(5)-Si(1)-O(1)	108.53(9)
O(4)-Si(1)-C(1)	112.37(10)
O(5)-Si(1)-C(1)	110.80(10)
O(1)-Si(1)-C(1)	105.98(11)
O(6)-Si(2)-O(2)	109.47(9)
O(6)-Si(2)-O(1)	108.70(9)
O(2)-Si(2)-O(1)	108.55(9)
O(6)-Si(2)-C(7)	107.64(10)
O(2)-Si(2)-C(7)	112.28(10)
O(1)-Si(2)-C(7)	110.14(10)
O(6)#1-Si(3)-O(2)	109.71(9)
O(6)#1-Si(3)-O(3)	108.66(9)
O(2)-Si(3)-O(3)	108.82(9)
O(6)#1-Si(3)-C(13)	109.61(10)
O(2)-Si(3)-C(13)	110.55(9)
O(3)-Si(3)-C(13)	109.45(9)
O(4)-Si(4)-O(3)	109.35(9)
O(4)-Si(4)-O(5)#1	108.13(9)
O(3)-Si(4)-O(5)#1	109.19(9)
O(4)-Si(4)-C(19)	112.84(10)
O(3)-Si(4)-C(19)	109.08(10)
O(5)#1-Si(4)-C(19)	108.19(10)
Si(2)-O(1)-Si(1)	140.56(11)
Si(2)-O(2)-Si(3)	140.64(12)

Si(3)-O(3)-Si(4)	140.29(11)
Si(1)-O(4)-Si(4)	162.73(12)
Si(1)-O(5)-Si(4)#1	142.01(11)
Si(3)#1-O(6)-Si(2)	163.49(12)
C(2)-C(1)-C(6)	116.3(2)
C(2)-C(1)-Si(1)	124.9(2)
C(6)-C(1)-Si(1)	118.8(2)
C(3)-C(2)-C(1)	122.5(3)
C(3)-C(2)-Br(1)	118.2(2)
C(1)-C(2)-Br(1)	119.3(2)
C(4)-C(3)-C(2)	119.1(3)
C(5)-C(4)-C(3)	121.1(3)
C(4)-C(5)-C(6)	118.6(3)
C(5)-C(6)-C(1)	122.4(3)
C(8)-C(7)-C(12)	116.2(2)
C(8)-C(7)-Si(2)	125.1(2)
C(12)-C(7)-Si(2)	118.62(19)
C(7)-C(8)-C(9)	122.5(3)
C(7)-C(8)-Br(2)	120.0(2)
C(9)-C(8)-Br(2)	117.5(2)
C(10)-C(9)-C(8)	119.1(3)
C(11)-C(10)-C(9)	120.6(3)
C(10)-C(11)-C(12)	119.3(3)
C(11)-C(12)-C(7)	122.4(3)
C(18)-C(13)-C(14)	116.2(2)
C(18)-C(13)-Si(3)	120.90(18)
C(14)-C(13)-Si(3)	122.87(17)
C(15)-C(14)-C(13)	123.2(2)
C(15)-C(14)-Br(3)	116.32(18)
C(13)-C(14)-Br(3)	120.47(17)
C(14)-C(15)-C(16)	118.4(2)
C(17)-C(16)-C(15)	120.8(2)
C(16)-C(17)-C(18)	119.8(3)
C(17)-C(18)-C(13)	121.5(2)
C(24)-C(19)-C(20)	115.8(2)
C(24)-C(19)-Si(4)	119.2(2)
C(20)-C(19)-Si(4)	124.84(19)
C(21)-C(20)-C(19)	122.6(3)
C(21)-C(20)-Br(4)	116.9(2)
C(19)-C(20)-Br(4)	120.54(19)
C(22)-C(21)-C(20)	119.3(3)
C(23)-C(22)-C(21)	120.2(3)
C(22)-C(23)-C(24)	120.0(3)
C(23)-C(24)-C(19)	122.1(3)
C(30)-C(25)-C(26)	118.1(6)
C(30)-C(25)-C(31)	123.0(6)
C(26)-C(25)-C(31)	118.8(5)
C(27)-C(26)-C(25)	120.4(5)

C(28)-C(27)-C(26)	117.9(6)
C(28)-C(27)-C(32)	125.3(6)
C(26)-C(27)-C(32)	116.8(5)
C(29)-C(28)-C(27)	124.1(7)
C(28)-C(29)-C(30)	118.2(7)
C(25)-C(30)-C(29)	121.3(7)
C(30A)-C(25A)-C(26A)	114.8(13)
C(30A)-C(25A)-C(31A)	129.6(13)
C(26A)-C(25A)-C(31A)	115.5(12)
C(27A)-C(26A)-C(25A)	120.7(14)
C(29A)-C(27A)-C(26A)	116.5(12)
C(29A)-C(27A)-C(32A)	127.9(17)
C(26A)-C(27A)-C(32A)	114.4(15)
C(28A)-C(29A)-C(27A)	125.3(16)
C(29A)-C(28A)-C(30A)	115.4(16)
C(25A)-C(30A)-C(28A)	122.8(16)

Symmetry transformations used to generate equivalent atoms:

#1 -x+0,-y+1/2,z+0

Table 4. Anisotropic displacement parameters (A^2 x 10^3) for obr8a.

The anisotropic displacement factor exponent takes the form: -2 pi^2 [h^2 a*^2 U11 + ... + 2 h k a* b* U12]

	U11	U22	U33	U23	U13	U12
Br(1)	77(1)	67(1)	28(1)	-2(1)	-2(1)	11(1)
Br(2)	35(1)	69(1)	56(1)	2(1)	0(1)	-12(1)
Br(3)	50(1)	34(1)	27(1)	4(1)	3(1)	-9(1)
Br(4)	39(1)	58(1)	107(1)	33(1)	4(1)	0(1)
Si(1)	31(1)	19(1)	19(1)	-1(1)	3(1)	-1(1)
Si(2)	23(1)	18(1)	20(1)	-1(1)	0(1)	0(1)
Si(3)	26(1)	17(1)	18(1)	-2(1)	1(1)	-2(1)
Si(4)	32(1)	17(1)	18(1)	1(1)	2(1)	-3(1)
O(1)	31(1)	23(1)	19(1)	-1(1)	3(1)	2(1)
O(2)	29(1)	19(1)	28(1)	-3(1)	-1(1)	-1(1)
O(3)	38(1)	23(1)	18(1)	-1(1)	3(1)	-5(1)
O(4)	36(1)	19(1)	24(1)	1(1)	2(1)	-1(1)
O(5)	32(1)	22(1)	27(1)	-4(1)	1(1)	-2(1)
O(6)	25(1)	25(1)	24(1)	1(1)	1(1)	-4(1)
C(1)	39(1)	23(1)	27(1)	-6(1)	9(1)	-4(1)
C(2)	53(2)	32(1)	29(1)	-7(1)	10(1)	-7(1)
C(3)	70(2)	51(2)	35(1)	-13(1)	22(1)	-11(2)
C(4)	47(2)	53(2)	64(2)	-20(2)	25(2)	-8(1)
C(5)	40(2)	53(2)	57(2)	-14(2)	14(1)	1(1)
C(6)	35(1)	41(1)	38(1)	-9(1)	8(1)	0(1)
C(7)	33(1)	24(1)	22(1)	-6(1)	-2(1)	5(1)
C(8)	34(1)	46(2)	30(1)	-6(1)	-3(1)	5(1)
C(9)	36(1)	73(2)	42(2)	-16(2)	-8(1)	19(1)
C(10)	68(2)	55(2)	25(1)	-1(1)	-6(1)	28(2)
C(11)	66(2)	39(1)	21(1)	1(1)	-2(1)	17(1)
C(12)	46(1)	31(1)	23(1)	0(1)	-2(1)	7(1)
C(13)	24(1)	18(1)	23(1)	-2(1)	-1(1)	1(1)
C(14)	25(1)	24(1)	25(1)	-1(1)	-2(1)	1(1)
C(15)	36(1)	33(1)	27(1)	-6(1)	-4(1)	4(1)
C(16)	51(2)	28(1)	39(1)	-12(1)	-12(1)	2(1)
C(17)	65(2)	20(1)	43(2)	1(1)	-8(1)	-8(1)
C(18)	45(1)	21(1)	29(1)	2(1)	-2(1)	-2(1)
C(19)	39(1)	19(1)	20(1)	-1(1)	4(1)	-4(1)

C(20)	41(1)	28(1)	36(1)	3(1)	8(1)	-1(1)
C(21)	49(2)	34(1)	41(1)	-1(1)	17(1)	-8(1)
C(22)	72(2)	27(1)	26(1)	1(1)	13(1)	-10(1)
C(23)	66(2)	30(1)	36(1)	10(1)	-7(1)	-3(1)
C(24)	46(1)	32(1)	32(1)	9(1)	-1(1)	-6(1)
C(25)	109(3)	85(3)	68(3)	-30(2)	40(2)	-31(3)
C(26)	100(3)	62(3)	55(2)	-8(2)	23(2)	-7(2)
C(27)	158(4)	72(3)	51(2)	0(2)	33(3)	30(3)
C(28)	229(4)	75(3)	54(3)	-2(2)	59(3)	40(3)
C(29)	237(5)	95(4)	75(3)	-14(3)	100(3)	-15(4)
C(30)	169(4)	91(3)	76(3)	-33(3)	68(3)	-50(3)
C(31)	89(4)	115(5)	129(6)	-17(4)	17(4)	-11(4)
C(32)	152(4)	129(5)	107(6)	-8(5)	-12(5)	68(4)
C(25A)	150(6)	94(6)	67(10)	-14(7)	32(8)	4(6)
C(26A)	148(5)	95(8)	70(9)	-21(7)	30(7)	8(6)
C(27A)	136(7)	90(7)	76(10)	-19(7)	55(7)	29(5)
C(29A)	189(7)	101(8)	75(11)	-11(7)	70(8)	27(6)
C(28A)	211(8)	89(8)	60(10)	-4(7)	79(8)	-3(6)
C(30A)	193(8)	96(6)	70(10)	-20(8)	58(8)	-10(6)
C(31A)	153(9)	114(9)	92(16)	-32(11)	63(12)	43(10)
C(32A)	156(11)	116(14)	130(20)	-10(20)	-4(11)	31(10)

Table 5. Hydrogen coordinates (x 10^4) and isotropic displacement parameters (A^2 x 10^3) for obr8a.

	x	y	z	U(eq)
H(3A)	2112	1530	-2058	62
H(4A)	3042	1140	-1763	66
H(5B)	3097	1100	-1121	60
H(6B)	2216	1481	-773	46
H(9A)	2999	1367	551	60
H(10A)	2505	583	923	59
H(11A)	1384	424	897	50
H(12A)	760	1044	496	40
H(15A)	817	4433	1157	38
H(16A)	1154	5438	924	47
H(17A)	1254	5597	293	51
H(18A)	985	4764	-115	38
H(21A)	2235	4641	-1548	50
H(22A)	1529	5347	-1853	50
H(23A)	416	5276	-1755	52
H(24A)	-4	4469	-1373	44
H(26)	2041	2949	7860	87
H(28)	1769	4715	7415	144
H(29)	2798	5011	7538	163
H(30)	3511	4247	7823	134
H(31A)	3756	3121	7982	166
H(31B)	3193	2590	7935	166
H(31C)	3242	3006	8306	166
H(32A)	1074	3213	7431	194
H(32B)	852	3958	7447	194
H(32C)	883	3536	7817	194
H(26A)	1480	3234	7899	125
H(29A)	1191	4705	7203	146
H(28A)	2160	5155	7357	144
H(30A)	2881	4510	7735	144
H(31D)	3036	3032	7679	179
H(31E)	2504	2806	7975	179
H(31F)	3049	3323	8089	179
H(32D)	272	3735	7393	203
H(32E)	649	3083	7503	203
H(32F)	739	3387	7100	203

Appendix 6

Crystallographic data for $Br_{16}OPS$

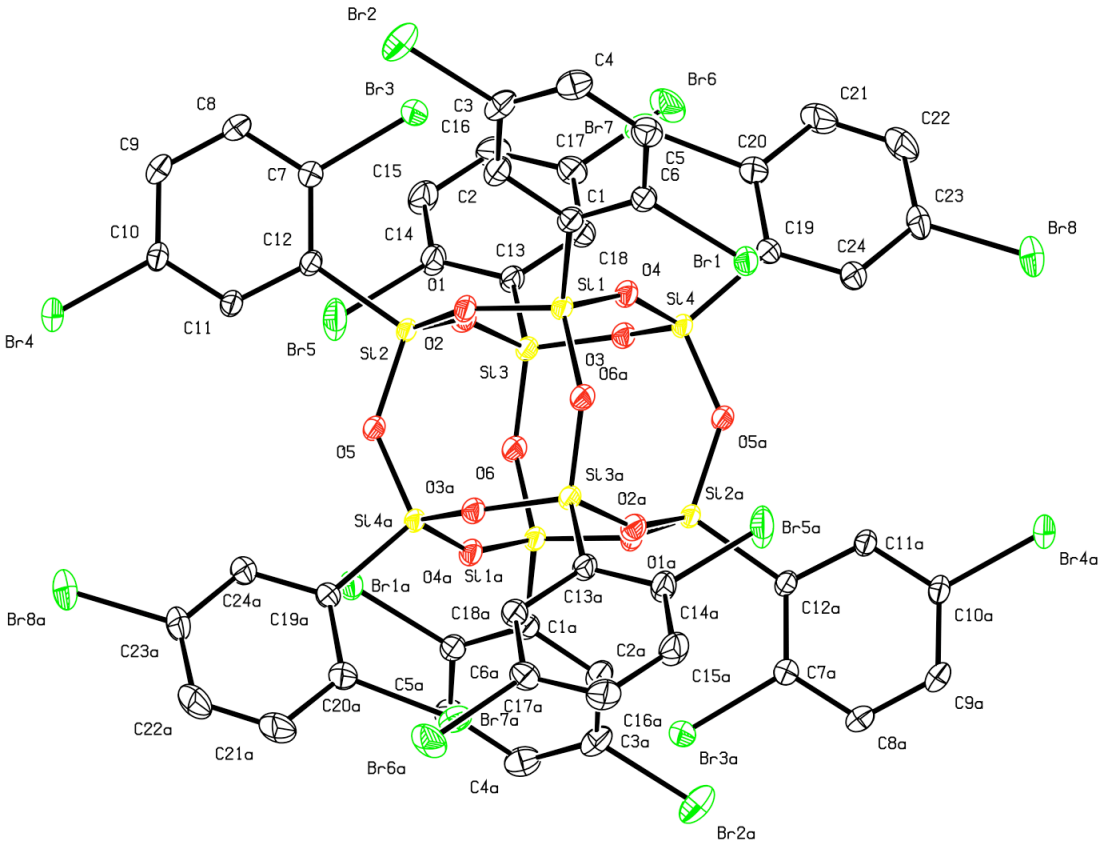

Figure A.6. 50 % thermal ellipsoid plots of Octa(2,5-dibromophenyl)silsesquioxane carbon disulfide solvate. Hydrogen atoms and carbon disulfide solvates are omitted for clarity.

Structure Determination.

Colorless plates of **brops** were grown from a carbon disulfide/dodecane solution at 25 deg. C. A crystal of dimensions 0.25 x 0.15 x 0.10 mm was mounted on a Bruker SMART APEX CCD-based X-ray diffractometer equipped with a low temperature device and fine focus Mo-target X-ray tube (l = 0.71073 A) operated at 1500 W power (50 kV, 30 mA). The X-ray intensities were measured at 85(1) K; the detector was placed at a distance 5.055 cm from the crystal. A total of 4095 frames were collected with a scan width of 0.5° in w and 0.45° in phi with an exposure time of 30 s/frame. The integration of the data yielded a total of 66787 reflections to a maximum 2q value of 60.30° of which 9554 were independent and 8581 were greater than 2s(I). The final cell constants (Table 1) were based on the xyz centroids of 9644 reflections above 10s(I). Analysis of the data showed negligible decay during data collection; the data were processed with SADABS and corrected for absorption. The structure was solved and refined with the Bruker SHELXTL (version 2008/3) software package, using the space group P1bar with Z = 1 for the formula $C_{48}H_{24}O_{12}Si_8Br_{16}•CS_2$. The cluster lies on an inversion center in the crystal lattice. The carbon disulfide does as well and is disordered. All non-hydrogen atoms were refined anisotropically with the hydrogen atoms placed in idealized positions. Full matrix least-squares refinement based on F^2 converged at R1 = 0.0270 and wR2 = 0.0742 [based on I > 2sigma(I)], R1 = 0.0313 and wR2 = 0.0765 for all data. Additional details are presented in Table 1 and are given as Supporting Information in a CIF file.

Sheldrick, G.M. SHELXTL, v. 2008/3; Bruker Analytical X-ray, Madison, WI, 2008.

Sheldrick, G.M. SADABS, v. 2008/1. Program for Empirical Absorption Correction of Area Detector Data, University of Gottingen: Gottingen, Germany, 2008.

Saint Plus, v. 7.53a, Bruker Analytical X-ray, Madison, WI, 2008.

Table 1. Crystal data and structure refinement for brops.

Identification code	brops
Empirical formula	C49 H24 Br16 O12 S2 Si8
Formula weight	2372.08
Temperature	85(2) K
Wavelength	0.71073 A
Crystal system, space group	Triclinic, P-1
Unit cell dimensions	a = 12.7172(9) A alpha=97.592(1)deg. b = 12.7392(9) A beta=109.075(1)deg. c = 13.0890(9) A gamma=116.231(1)deg
Volume	1699.3(2) A^3
Z, Calculated density	1, 2.318 Mg/m^3
Absorption coefficient	9.681 mm^-1
F(000)	1118
Crystal size	0.25 x 0.15 x 0.10 mm
Theta range for data collection	1.74 to 29.65 deg.
Limiting indices	-17<=h<=17, -17<=k<=17, -18<=l<=18
Reflections collected / unique	66787 / 9554 [R(int) = 0.0319]
Completeness to theta = 29.65	99.7 %
Absorption correction	Semi-empirical from equivalents
Max. and min. transmission	0.3812 and 0.1677

Refinement method	Full-matrix least-squares on F^2
Data / restraints / parameters	9554 / 17 / 410
Goodness-of-fit on F^2	1.045
Final R indices [I>2sigma(I)]	R1 = 0.0270, wR2 = 0.0742
R indices (all data)	R1 = 0.0313, wR2 = 0.0765
Largest diff. peak and hole	1.429 and -1.258 e.A^-3

Table 2. Atomic coordinates (x 10^4) and equivalent isotropic displacement parameters (A^2 x 10^3) for brops.
U(eq) is defined as one third of the trace of the orthogonalized Uij tensor.

	x	y	z	U(eq)
Br(1)	8325(1)	5235(1)	3982(1)	21(1)
Br(2)	4965(1)	-797(1)	1706(1)	32(1)
Br(3)	2039(1)	779(1)	528(1)	25(1)
Br(4)	-15(1)	-1538(1)	-4977(1)	26(1)
Br(5)	-184(1)	2309(1)	-2446(1)	37(1)
Br(6)	-57(1)	4565(1)	2395(1)	31(1)
Br(7)	2912(1)	3749(1)	2732(1)	30(1)
Br(8)	7426(1)	9207(1)	6434(1)	41(1)
Si(1)	5864(1)	3821(1)	1282(1)	16(1)
Si(2)	3358(1)	2555(1)	-974(1)	15(1)
Si(3)	2661(1)	4506(1)	-187(1)	16(1)
Si(4)	5160(1)	5768(1)	2067(1)	15(1)
O(1)	4656(2)	2819(2)	71(2)	18(1)
O(2)	2806(2)	3326(2)	-498(2)	19(1)
O(3)	3768(2)	5404(2)	1092(2)	17(1)
O(4)	5419(2)	4641(2)	1872(2)	18(1)
O(5)	3721(2)	3024(2)	-1977(2)	18(1)
O(6)	2916(2)	5286(2)	-1051(2)	18(1)
C(1)	6316(3)	2948(2)	2185(2)	18(1)
C(2)	5618(3)	1647(2)	1728(2)	21(1)
C(3)	5925(3)	956(2)	2367(3)	24(1)
C(4)	6914(3)	1507(3)	3465(3)	26(1)
C(5)	7621(3)	2787(3)	3931(2)	24(1)
C(6)	7315(3)	3481(2)	3288(2)	19(1)
C(7)	1504(3)	139(2)	-1068(2)	19(1)
C(8)	521(3)	-1088(3)	-1621(3)	26(1)
C(9)	75(3)	-1604(2)	-2791(3)	26(1)
C(10)	621(3)	-869(2)	-3374(2)	19(1)
C(11)	1614(2)	355(2)	-2819(2)	18(1)
C(12)	2091(2)	896(2)	-1636(2)	16(1)
C(13)	1061(3)	3977(2)	-167(2)	19(1)
C(14)	-117(3)	3007(3)	-1037(2)	24(1)
C(15)	-1273(3)	2510(3)	-919(3)	28(1)
C(16)	-1261(3)	2985(3)	103(3)	28(1)
C(17)	-107(3)	3955(3)	973(2)	23(1)
C(18)	1036(3)	4458(2)	844(2)	20(1)
C(19)	5159(3)	6170(2)	3472(2)	19(1)
C(20)	4170(3)	5391(3)	3736(2)	24(1)
C(21)	4094(3)	5758(3)	4743(3)	33(1)
C(22)	5036(4)	6904(3)	5531(3)	36(1)

C(23)	6061(3)	7671(3)	5318(3)	29(1)
C(24)	6116(3)	7324(3)	4297(2)	23(1)
S(1)	5440(4)	395(4)	5404(3)	72(1)
S(2)	3241(3)	-2183(3)	3689(2)	67(1)
C(25)	4333(9)	-957(6)	4493(9)	58(2)

Table 3. Bond lengths [A] and angles [deg] for brops.

Br(1)-C(6)	1.906(3)
Br(2)-C(3)	1.902(3)
Br(3)-C(7)	1.903(3)
Br(4)-C(10)	1.896(3)
Br(5)-C(14)	1.898(3)
Br(6)-C(17)	1.890(3)
Br(7)-C(20)	1.898(3)
Br(8)-C(23)	1.887(3)
Si(1)-O(4)	1.6139(19)
Si(1)-O(6)#1	1.6212(19)
Si(1)-O(1)	1.6251(19)
Si(1)-C(1)	1.852(3)
Si(2)-O(2)	1.607(2)
Si(2)-O(1)	1.619(2)
Si(2)-O(5)	1.6285(19)
Si(2)-C(12)	1.846(2)
Si(3)-O(2)	1.609(2)
Si(3)-O(6)	1.619(2)
Si(3)-O(3)	1.6195(19)
Si(3)-C(13)	1.850(3)
Si(4)-O(4)	1.6157(19)
Si(4)-O(3)	1.618(2)
Si(4)-O(5)#1	1.6213(19)
Si(4)-C(19)	1.843(3)
O(5)-Si(4)#1	1.6213(19)
O(6)-Si(1)#1	1.6212(19)
C(1)-C(6)	1.393(4)
C(1)-C(2)	1.408(3)
C(2)-C(3)	1.383(4)
C(3)-C(4)	1.382(4)
C(4)-C(5)	1.387(4)
C(5)-C(6)	1.388(4)
C(7)-C(8)	1.383(4)
C(7)-C(12)	1.397(3)
C(8)-C(9)	1.391(4)

C(9)-C(10)	1.379(4)
C(10)-C(11)	1.384(3)
C(11)-C(12)	1.406(3)
C(13)-C(14)	1.394(4)
C(13)-C(18)	1.399(4)
C(14)-C(15)	1.391(4)
C(15)-C(16)	1.386(4)
C(16)-C(17)	1.382(4)
C(17)-C(18)	1.384(4)
C(19)-C(24)	1.396(4)
C(19)-C(20)	1.400(4)
C(20)-C(21)	1.388(4)
C(21)-C(22)	1.371(5)
C(22)-C(23)	1.384(5)
C(23)-C(24)	1.385(4)
S(1)-C(25)	1.608(7)
S(2)-C(25)	1.473(7)

O(4)-Si(1)-O(6)#1	109.56(10)
O(4)-Si(1)-O(1)	109.00(10)
O(6)#1-Si(1)-O(1)	109.27(10)
O(4)-Si(1)-C(1)	111.46(11)
O(6)#1-Si(1)-C(1)	109.91(11)
O(1)-Si(1)-C(1)	107.59(11)
O(2)-Si(2)-O(1)	108.27(10)
O(2)-Si(2)-O(5)	108.82(10)
O(1)-Si(2)-O(5)	109.60(10)
O(2)-Si(2)-C(12)	110.23(11)
O(1)-Si(2)-C(12)	112.98(11)
O(5)-Si(2)-C(12)	106.88(10)
O(2)-Si(3)-O(6)	110.16(10)
O(2)-Si(3)-O(3)	108.28(11)
O(6)-Si(3)-O(3)	107.51(10)
O(2)-Si(3)-C(13)	109.02(11)
O(6)-Si(3)-C(13)	114.23(11)
O(3)-Si(3)-C(13)	107.44(11)
O(4)-Si(4)-O(3)	110.50(10)
O(4)-Si(4)-O(5)#1	109.43(10)
O(3)-Si(4)-O(5)#1	107.96(10)
O(4)-Si(4)-C(19)	111.90(11)
O(3)-Si(4)-C(19)	107.97(11)
O(5)#1-Si(4)-C(19)	108.98(11)
Si(2)-O(1)-Si(1)	144.10(13)
Si(2)-O(2)-Si(3)	155.88(13)
Si(4)-O(3)-Si(3)	144.18(13)
Si(1)-O(4)-Si(4)	153.96(13)
Si(4)#1-O(5)-Si(2)	137.47(12)
Si(3)-O(6)-Si(1)#1	137.83(13)

C(6)-C(1)-C(2)	116.8(2)
C(6)-C(1)-Si(1)	124.93(19)
C(2)-C(1)-Si(1)	118.3(2)
C(3)-C(2)-C(1)	120.4(3)
C(4)-C(3)-C(2)	121.8(3)
C(4)-C(3)-Br(2)	119.5(2)
C(2)-C(3)-Br(2)	118.8(2)
C(3)-C(4)-C(5)	118.9(3)
C(4)-C(5)-C(6)	119.3(3)
C(5)-C(6)-C(1)	122.9(2)
C(5)-C(6)-Br(1)	117.1(2)
C(1)-C(6)-Br(1)	120.1(2)
C(8)-C(7)-C(12)	122.6(2)
C(8)-C(7)-Br(3)	116.9(2)
C(12)-C(7)-Br(3)	120.44(19)
C(7)-C(8)-C(9)	119.6(3)
C(10)-C(9)-C(8)	118.8(2)
C(9)-C(10)-C(11)	121.6(2)
C(9)-C(10)-Br(4)	119.5(2)
C(11)-C(10)-Br(4)	118.9(2)
C(10)-C(11)-C(12)	120.7(2)
C(7)-C(12)-C(11)	116.6(2)
C(7)-C(12)-Si(2)	125.28(19)
C(11)-C(12)-Si(2)	118.00(18)
C(14)-C(13)-C(18)	116.9(2)
C(14)-C(13)-Si(3)	124.3(2)
C(18)-C(13)-Si(3)	118.2(2)
C(15)-C(14)-C(13)	122.6(3)
C(15)-C(14)-Br(5)	117.4(2)
C(13)-C(14)-Br(5)	119.9(2)
C(16)-C(15)-C(14)	119.1(3)
C(17)-C(16)-C(15)	119.2(3)
C(16)-C(17)-C(18)	121.4(3)
C(16)-C(17)-Br(6)	119.7(2)
C(18)-C(17)-Br(6)	118.8(2)
C(17)-C(18)-C(13)	120.7(2)
C(24)-C(19)-C(20)	116.9(2)
C(24)-C(19)-Si(4)	120.4(2)
C(20)-C(19)-Si(4)	122.5(2)
C(21)-C(20)-C(19)	122.2(3)
C(21)-C(20)-Br(7)	117.6(2)
C(19)-C(20)-Br(7)	120.1(2)
C(22)-C(21)-C(20)	119.6(3)
C(21)-C(22)-C(23)	119.5(3)
C(22)-C(23)-C(24)	121.0(3)
C(22)-C(23)-Br(8)	120.1(2)
C(24)-C(23)-Br(8)	118.9(2)
C(23)-C(24)-C(19)	120.7(3)

S(2)-C(25)-S(1) 175.2(8)

Symmetry transformations used to generate equivalent atoms:

#1 -x+1,-y+1,-z

Table 4. Anisotropic displacement parameters (A^2 x 10^3) for brops.

The anisotropic displacement factor exponent takes the form: -2 pi^2 [h^2 a*^2 U11 + ... + 2 h k a* b* U12]

	U11	U22	U33	U23	U13	U12
Br(1)	21(1)	18(1)	19(1)	1(1)	10(1)	6(1)
Br(2)	26(1)	16(1)	48(1)	8(1)	12(1)	10(1)
Br(3)	26(1)	21(1)	18(1)	4(1)	12(1)	5(1)
Br(4)	28(1)	19(1)	17(1)	-2(1)	5(1)	7(1)
Br(5)	28(1)	30(1)	30(1)	-12(1)	15(1)	1(1)
Br(6)	35(1)	41(1)	28(1)	10(1)	23(1)	21(1)
Br(7)	26(1)	23(1)	29(1)	10(1)	12(1)	2(1)
Br(8)	52(1)	29(1)	24(1)	-5(1)	16(1)	11(1)
Si(1)	16(1)	11(1)	16(1)	2(1)	9(1)	5(1)
Si(2)	16(1)	10(1)	16(1)	1(1)	9(1)	3(1)
Si(3)	16(1)	12(1)	18(1)	2(1)	10(1)	4(1)
Si(4)	16(1)	11(1)	15(1)	1(1)	9(1)	4(1)
O(1)	17(1)	12(1)	18(1)	1(1)	8(1)	4(1)
O(2)	22(1)	15(1)	22(1)	3(1)	14(1)	8(1)
O(3)	18(1)	14(1)	18(1)	2(1)	10(1)	6(1)
O(4)	19(1)	13(1)	19(1)	2(1)	10(1)	7(1)
O(5)	18(1)	12(1)	18(1)	1(1)	10(1)	3(1)
O(6)	17(1)	15(1)	19(1)	3(1)	9(1)	5(1)
C(1)	19(1)	15(1)	22(1)	5(1)	12(1)	8(1)
C(2)	19(1)	16(1)	26(1)	3(1)	12(1)	7(1)
C(3)	22(1)	15(1)	36(2)	8(1)	15(1)	9(1)
C(4)	26(1)	25(1)	34(2)	14(1)	16(1)	15(1)
C(5)	23(1)	26(1)	23(1)	9(1)	11(1)	12(1)
C(6)	19(1)	16(1)	21(1)	4(1)	13(1)	7(1)
C(7)	20(1)	16(1)	18(1)	4(1)	8(1)	6(1)
C(8)	25(1)	17(1)	24(1)	6(1)	10(1)	2(1)
C(9)	24(1)	14(1)	25(1)	2(1)	8(1)	1(1)
C(10)	20(1)	14(1)	17(1)	0(1)	6(1)	6(1)
C(11)	18(1)	13(1)	18(1)	2(1)	9(1)	5(1)
C(12)	15(1)	12(1)	18(1)	2(1)	8(1)	4(1)

C(13)	20(1)	15(1)	21(1)	2(1)	12(1)	6(1)
C(14)	21(1)	19(1)	25(1)	0(1)	13(1)	4(1)
C(15)	19(1)	24(1)	32(2)	2(1)	13(1)	3(1)
C(16)	21(1)	29(1)	34(2)	10(1)	18(1)	9(1)
C(17)	26(1)	24(1)	24(1)	7(1)	17(1)	13(1)
C(18)	20(1)	18(1)	21(1)	4(1)	11(1)	8(1)
C(19)	22(1)	17(1)	17(1)	4(1)	12(1)	8(1)
C(20)	24(1)	23(1)	22(1)	6(1)	12(1)	7(1)
C(21)	33(2)	40(2)	31(2)	13(1)	24(1)	15(1)
C(22)	43(2)	42(2)	26(2)	7(1)	25(1)	19(2)
C(23)	35(2)	24(1)	20(1)	-1(1)	13(1)	10(1)
C(24)	26(1)	20(1)	21(1)	4(1)	13(1)	9(1)
S(1)	64(2)	106(3)	80(2)	61(2)	39(1)	58(2)
S(2)	88(2)	104(2)	62(2)	50(2)	48(1)	74(2)
C(25)	64(5)	90(5)	104(6)	87(5)	63(4)	70(4)

Table 5. Hydrogen coordinates (x 10^4) and isotropic displacement parameters (A^2 x 10^3) for brops.

	x	y	z	U(eq)
H(2A)	4932	1241	976	26
H(4A)	7105	1016	3894	32
H(5B)	8309	3186	4682	28
H(8A)	153	-1576	-1205	31
H(9A)	-595	-2447	-3181	31
H(11A)	1978	835	-3243	21
H(15A)	-2061	1854	-1532	34
H(16A)	-2037	2647	205	34
H(18A)	1812	5138	1449	24
H(21A)	3393	5218	4886	40
H(22A)	4985	7170	6217	43
H(24A)	6813	7876	4158	27

Appendix 7

Crystallographic data for $Br_{24}OPS$

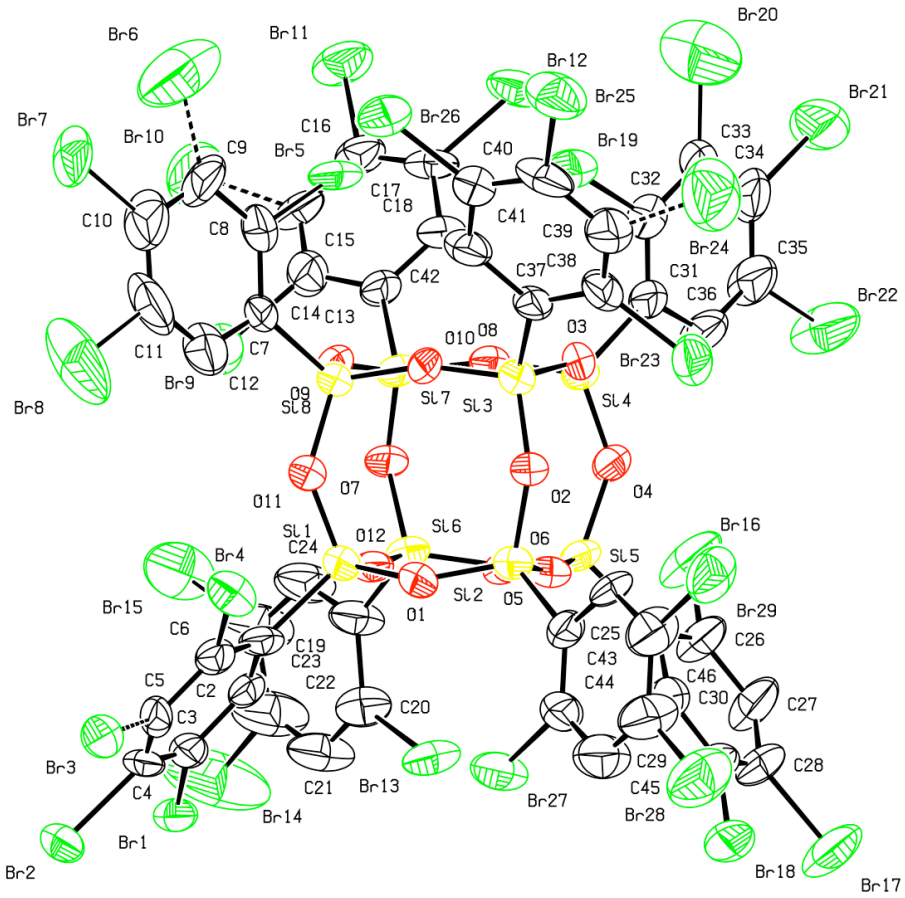

Figure A.7. 50 % thermal ellipsoid plots of tetraicosabrominated OPS *o*-dichlorobenzene solvate (R-factor of 6.3 %). Hydrogen atoms and *o*-dichlorobenzene solvates are omitted for clarity. Dashed bonds indicate partially occupied bromines.

Structure Determination.

Colorless plates of **br3ops** were grown from a o-dichlorobenzene solution at 25 deg. C. A crystal of dimensions 0.20 x 0.15 x 0.14 mm was mounted on a Bruker SMART APEX CCD-based X-ray diffractometer equipped with a low temperature device and fine focus Mo-target X-ray tube (l = 0.71073 A) operated at 1500 W power (50 kV, 30 mA). The X-ray intensities were measured at 85(1) K; the detector was placed at a distance 5.055 cm from the crystal. A total of 4095 frames were collected with a scan width of 0.5° in w and 0.45° in phi with an exposure time of 30 s/frame. The integration of the data yielded a total of 136685 reflections to a maximum 2q value of 42.80° of which 13049 were independent and 10155 were greater than 2s(I). The final cell constants (Table 1) were based on the xyz centroids of 9953 reflections above 10s(I). Analysis of the data showed negligible decay during data collection; the data were processed with SADABS and corrected for absorption. The structure was solved and refined with the Bruker SHELXTL (version 2008/3) software package, using the space group P1bar with Z = 2 for the formula $C_{48}H_{16}O_{12}Si_8Br_{24}•5(C_6H_4Cl_2)$. All non-hydrogen atoms were refined anisotropically with the hydrogen atoms placed in idealized positions. A number of the bromine sites exhibit substitution disorder and are at partial occupancy. One of the dichlorobenzene solvate molecules is disordered and was modeled by use of partial occupancy atoms. The remaining solvate molecules are disordered a large solvent accessible void in the lattice and were treated as diffuse scattering by use of the SQUEEZE subroutine of the PLATON program suite. Full matrix least-squares refinement based on F^2 converged at R1 = 0.0629 and wR2 = 0.1935

[based on I > 2sigma(I)], R1 = 0.0757 and wR2 = 0.2024 for all data. Additional details are presented in Table 1 and are given as Supporting Information in a CIF file.

Sheldrick, G.M. SHELXTL, v. 2008/3; Bruker Analytical X-ray, Madison, WI, 2008.

Sheldrick, G.M. SADABS, v. 2008/1. Program for Empirical Absorption Correction of Area Detector Data, University of Gottingen: Gottingen, Germany, 2008.

Saint Plus, v. 7.53a, Bruker Analytical X-ray, Madison, WI, 2008.

A.L. Spek. (2008) PLATON, v. 180108, A Multi-purpose Crystallographic Tool, Utrecht University, Utrecht, The Netherlands.

Table 1. Crystal data and structure refinement for br3ops.

Identification code	br3ops
Empirical formula	C78 H36 Br24 Cl5 O12 Si8
Formula weight	3484.88
Temperature	85(2) K
Wavelength	0.71073 A
Crystal system, space group	Triclinic, P-1
Unit cell dimensions	a = 15.5726(10) Å alpha = 65.399(1)° b = 20.4685(13) Å beta = 74.616(1)° c = 20.6449(13) Å gamma = 82.172(1)°
Volume	5766.3(6) A^3
Z, Calculated density	2, 2.007 Mg/m^3
Absorption coefficient	8.573 mm^-1
F(000)	3274
Crystal size	0.20 x 0.15 x 0.14 mm
Theta range for data collection	1.09 to 21.40 deg.
Limiting indices	-15<=h<=15, -20<=k<=21, -21<=l<=21
Reflections collected / unique	136685 / 13049 [R(int) = 0.0540]
Completeness to theta = 21.40	99.9 %
Absorption correction	Semi-empirical from equivalents
Max. and min. transmission	0.3799 and 0.2789

Refinement method	Full-matrix least-squares on F^2
Data / restraints / parameters	13049 / 296 / 967
Goodness-of-fit on F^2	1.089
Final R indices [I>2sigma(I)]	R1 = 0.0629, wR2 = 0.1935
R indices (all data)	R1 = 0.0757, wR2 = 0.2024
Largest diff. peak and hole	2.258 and -1.409 e.A^-3

Table 2. Atomic coordinates (x 10^4) and equivalent isotropic displacement parameters (A^2 x 10^3) for br3ops.

U(eq) is defined as one third of the trace of the orthogonalized Uij tensor.

	x	y	z	U(eq)
Br(1)	1616(1)	5226(1)	-1317(1)	60(1)
Br(2)	756(1)	3564(1)	-358(1)	72(1)
Br(3)	250(3)	2957(3)	1393(3)	70(1)
Br(4)	341(1)	3912(1)	2253(1)	62(1)
Br(5)	-1602(2)	7392(2)	2878(2)	73(1)
Br(6)	-3684(6)	6836(7)	3681(5)	172(5)
Br(7)	-4082(2)	5172(3)	4180(2)	89(1)
Br(8)	-2609(4)	4165(3)	3404(3)	166(3)
Br(9)	-1191(1)	8256(1)	-56(1)	83(1)
Br(10)	-2575(5)	9608(4)	7(6)	126(3)
Br(11)	-2094(1)	10753(1)	464(1)	85(1)
Br(12)	-505(1)	10338(1)	1430(1)	80(1)
Br(13)	3392(1)	6370(1)	-863(1)	72(1)
Br(14)	1876(3)	7639(2)	-3292(1)	199(2)
Br(15)	98(2)	8307(1)	-2278(1)	116(1)
Br(16)	4255(1)	8699(1)	-348(1)	102(1)
Br(17)	7434(1)	7133(1)	-731(1)	106(1)
Br(18)	6395(1)	5598(1)	483(1)	75(1)
Br(19)	373(1)	8400(1)	2932(1)	76(1)
Br(20)	700(4)	9843(4)	3058(4)	200(3)
Br(21)	2295(1)	10906(1)	1842(1)	130(1)
Br(22)	3789(3)	10309(3)	657(4)	151(3)
Br(23)	2584(1)	6069(1)	4141(1)	82(1)
Br(24)	1522(6)	6025(6)	5744(4)	134(3)
Br(25)	-519(1)	5608(1)	6383(1)	89(1)
Br(26)	-1756(1)	5891(1)	5164(1)	76(1)
Br(27)	3910(1)	4663(1)	1062(1)	74(1)
Br(28)	5481(1)	3132(1)	3443(1)	110(1)
Br(29)	4158(1)	4041(1)	4380(1)	86(1)
Si(1)	1160(2)	5605(2)	1271(2)	43(1)
Si(2)	2565(2)	5588(2)	2041(2)	44(1)
Si(3)	1295(2)	6355(2)	2926(2)	48(1)
Si(4)	1903(2)	7799(2)	1762(2)	49(1)
Si(5)	3189(2)	7128(2)	818(2)	46(1)
Si(6)	1753(2)	7164(2)	57(2)	45(1)

Si(7)	385(2)	7824(2)	960(2)	49(1)
Si(8)	-184(2)	6351(2)	2115(2)	45(1)
O(1)	1888(4)	5284(3)	1782(4)	45(2)
O(2)	2027(4)	5791(4)	2740(4)	47(2)
O(3)	1745(4)	7134(4)	2543(4)	51(2)
O(4)	2810(4)	7650(4)	1246(4)	55(2)
O(5)	2993(4)	6309(4)	1377(4)	46(2)
O(6)	2674(4)	7342(4)	178(4)	52(2)
O(7)	950(4)	7707(3)	224(4)	49(2)
O(8)	1075(4)	7860(3)	1404(4)	47(2)
O(9)	-238(4)	7126(4)	1459(4)	50(2)
O(10)	455(4)	6394(4)	2590(4)	46(2)
O(11)	228(4)	5759(3)	1770(4)	44(2)
O(12)	1498(4)	6349(3)	611(4)	44(2)
C(1)	1025(6)	4998(6)	846(6)	45(3)
C(2)	1284(6)	5240(6)	92(6)	48(3)
C(3)	1218(6)	4836(6)	-284(3)	51(3)
C(4)	888(7)	4157(6)	106(7)	52(3)
C(5)	627(6)	3909(4)	828(6)	53(3)
C(6)	700(6)	4303(5)	1219(3)	45(3)
C(7)	-1306(6)	6050(6)	2699(6)	53(3)
C(8)	-1912(7)	6466(4)	3025(7)	75(4)
C(9)	-2743(6)	6214(7)	3463(8)	112(6)
C(10)	-2975(6)	5547(8)	3548(8)	111(6)
C(11)	-2357(9)	5097(5)	3279(8)	110(6)
C(12)	-1555(8)	5400(7)	2801(6)	80(4)
C(13)	-295(6)	8671(5)	756(6)	50(3)
C(14)	-990(7)	8843(5)	393(6)	61(3)
C(15)	-1478(5)	9470(6)	282(6)	65(3)
C(16)	-1342(6)	9927(4)	571(7)	60(3)
C(17)	-701(7)	9753(5)	978(6)	58(3)
C(18)	-170(7)	9131(5)	1052(6)	51(3)
C(19)	1823(8)	7294(6)	-885(6)	63(3)
C(20)	2508(6)	6977(5)	-1325(6)	65(3)
C(21)	2498(10)	7075(8)	-2017(8)	88(4)
C(22)	1830(13)	7485(9)	-2313(5)	108(5)
C(23)	1114(9)	7801(9)	-1933(9)	111(5)
C(24)	1175(9)	7717(7)	-1231(7)	78(4)
C(25)	4403(6)	7173(6)	418(6)	52(3)
C(26)	4855(6)	7788(4)	-79(7)	67(3)
C(27)	5761(7)	7783(7)	-425(9)	82(4)
C(28)	6210(4)	7120(7)	-261(7)	69(4)
C(29)	5787(7)	6501(4)	229(7)	57(3)
C(30)	4916(7)	6523(6)	558(6)	51(3)
C(31)	1987(7)	8671(6)	1821(7)	64(3)
C(32)	1392(6)	8926(6)	2296(6)	69(3)
C(33)	1477(7)	9620(7)	2295(6)	78(3)
C(34)	2178(9)	9996(5)	1844(11)	102(4)

C(35)	2793(7)	9766(7)	1323(8)	103(5)
C(36)	2715(8)	9094(7)	1342(9)	89(4)
C(37)	857(7)	6101(6)	3921(6)	52(3)
C(38)	1328(4)	6005(7)	4438(6)	59(3)
C(39)	931(8)	5878(7)	5128(7)	76(4)
C(40)	9(9)	5822(6)	5383(4)	70(4)
C(41)	-499(4)	5934(6)	4884(7)	58(3)
C(42)	-85(8)	6062(6)	4174(6)	55(3)
C(43)	3432(6)	4897(6)	2382(6)	48(3)
C(44)	3971(8)	4517(6)	2018(4)	60(3)
C(45)	4591(9)	3996(8)	2325(8)	83(4)
C(46)	4666(8)	3861(6)	3021(7)	84(4)
C(47)	4105(8)	4240(8)	3411(4)	74(4)
C(48)	3496(6)	4753(6)	3089(7)	54(3)
C(49)	5245(8)	6846(8)	2051(8)	89(3)
C(50)	5806(9)	6255(8)	2102(9)	103(4)
C(51)	6704(9)	6329(9)	1762(9)	106(4)
C(52)	7046(10)	6999(10)	1396(11)	135(6)
C(53)	6497(9)	7612(9)	1323(12)	136(6)
C(54)	5593(8)	7508(9)	1625(10)	114(5)
Cl(1)	4131(2)	6750(3)	2444(3)	109(1)
Cl(2)	4967(5)	8301(4)	1372(5)	132(3)
Cl(2A)	5610(9)	5418(8)	2385(8)	119(5)

Table 3. Bond lengths [A] and angles [deg] for br3ops.

Br(1)-C(3)	1.894(5)
Br(2)-C(4)	1.891(5)
Br(3)-C(5)	1.886(5)
Br(4)-C(6)	1.892(5)
Br(5)-C(8)	1.900(5)
Br(6)-C(9)	1.896(5)
Br(7)-C(10)	1.896(5)
Br(8)-C(11)	1.899(5)
Br(9)-C(14)	1.892(5)
Br(10)-C(15)	1.888(5)
Br(11)-C(16)	1.889(5)
Br(12)-C(17)	1.891(5)
Br(13)-C(20)	1.896(5)
Br(14)-C(22)	1.893(5)
Br(15)-C(23)	1.902(5)
Br(16)-C(26)	1.896(5)
Br(17)-C(28)	1.894(5)
Br(18)-C(29)	1.887(5)
Br(19)-C(32)	1.894(5)
Br(20)-C(33)	1.894(5)
Br(21)-C(34)	1.894(5)
Br(22)-C(35)	1.897(5)
Br(23)-C(38)	1.895(5)
Br(24)-C(39)	1.891(5)
Br(25)-C(40)	1.892(5)
Br(26)-C(41)	1.891(5)
Br(27)-C(44)	1.895(5)
Br(28)-C(46)	1.895(5)
Br(29)-C(47)	1.892(5)
Si(1)-O(12)	1.600(7)
Si(1)-O(11)	1.619(7)
Si(1)-O(1)	1.640(7)
Si(1)-C(1)	1.854(10)
Si(2)-O(1)	1.593(7)
Si(2)-O(5)	1.612(7)
Si(2)-O(2)	1.649(7)
Si(2)-C(43)	1.863(10)
Si(3)-O(2)	1.600(7)
Si(3)-O(10)	1.615(7)
Si(3)-O(3)	1.619(8)
Si(3)-C(37)	1.850(10)
Si(4)-O(3)	1.603(8)
Si(4)-O(4)	1.604(7)

Si(4)-O(8)	1.615(7)
Si(4)-C(31)	1.862(11)
Si(5)-O(6)	1.602(8)
Si(5)-O(5)	1.605(7)
Si(5)-O(4)	1.616(7)
Si(5)-C(25)	1.849(10)
Si(6)-O(12)	1.612(7)
Si(6)-O(7)	1.622(7)
Si(6)-O(6)	1.632(7)
Si(6)-C(19)	1.824(12)
Si(7)-O(8)	1.613(7)
Si(7)-O(9)	1.633(8)
Si(7)-O(7)	1.636(7)
Si(7)-C(13)	1.853(9)
Si(8)-O(10)	1.603(7)
Si(8)-O(9)	1.610(8)
Si(8)-O(11)	1.627(7)
Si(8)-C(7)	1.856(10)
C(1)-C(2)	1.382(15)
C(1)-C(6)	1.397(14)
C(2)-C(3)	1.376(14)
C(3)-C(4)	1.374(14)
C(4)-C(5)	1.321(14)
C(5)-C(6)	1.389(14)
C(7)-C(12)	1.351(13)
C(7)-C(8)	1.411(11)
C(8)-C(9)	1.389(12)
C(9)-C(10)	1.389(15)
C(10)-C(11)	1.406(13)
C(11)-C(12)	1.402(13)
C(13)-C(18)	1.374(12)
C(13)-C(14)	1.402(11)
C(14)-C(15)	1.363(11)
C(15)-C(16)	1.365(13)
C(16)-C(17)	1.389(11)
C(17)-C(18)	1.394(11)
C(19)-C(24)	1.382(16)
C(19)-C(20)	1.474(15)
C(20)-C(21)	1.361(17)
C(21)-C(22)	1.354(19)
C(22)-C(23)	1.429(19)
C(23)-C(24)	1.414(18)
C(25)-C(26)	1.385(15)
C(25)-C(30)	1.415(15)
C(26)-C(27)	1.402(16)
C(27)-C(28)	1.390(17)
C(28)-C(29)	1.367(15)
C(29)-C(30)	1.351(15)

C(31)-C(32)	1.380(15)
C(31)-C(36)	1.404(17)
C(32)-C(33)	1.444(16)
C(33)-C(34)	1.321(18)
C(34)-C(35)	1.430(19)
C(35)-C(36)	1.382(17)
C(37)-C(38)	1.383(15)
C(37)-C(42)	1.421(15)
C(38)-C(39)	1.323(15)
C(39)-C(40)	1.394(17)
C(40)-C(41)	1.386(16)
C(41)-C(42)	1.364(15)
C(43)-C(44)	1.360(14)
C(43)-C(48)	1.391(15)
C(44)-C(45)	1.398(17)
C(45)-C(46)	1.379(18)
C(46)-C(47)	1.406(17)
C(47)-C(48)	1.388(15)
C(49)-C(54)	1.363(15)
C(49)-C(50)	1.376(13)
C(49)-Cl(1)	1.709(13)
C(50)-C(51)	1.385(14)
C(50)-Cl(2A)	1.61(2)
C(51)-C(52)	1.362(16)
C(52)-C(53)	1.396(14)
C(53)-C(54)	1.386(14)
C(54)-Cl(2)	1.729(17)

O(12)-Si(1)-O(11)	108.5(3)
O(12)-Si(1)-O(1)	109.4(4)
O(11)-Si(1)-O(1)	108.1(4)
O(12)-Si(1)-C(1)	106.4(4)
O(11)-Si(1)-C(1)	112.0(4)
O(1)-Si(1)-C(1)	112.2(4)
O(1)-Si(2)-O(5)	109.0(4)
O(1)-Si(2)-O(2)	109.7(4)
O(5)-Si(2)-O(2)	108.5(4)
O(1)-Si(2)-C(43)	111.5(4)
O(5)-Si(2)-C(43)	112.2(4)
O(2)-Si(2)-C(43)	105.7(4)
O(2)-Si(3)-O(10)	109.3(4)
O(2)-Si(3)-O(3)	107.7(4)
O(10)-Si(3)-O(3)	109.2(4)
O(2)-Si(3)-C(37)	113.0(5)
O(10)-Si(3)-C(37)	106.7(4)
O(3)-Si(3)-C(37)	110.9(4)
O(3)-Si(4)-O(4)	108.8(4)
O(3)-Si(4)-O(8)	108.2(4)

O(4)-Si(4)-O(8)	109.6(4)
O(3)-Si(4)-C(31)	113.1(5)
O(4)-Si(4)-C(31)	108.5(4)
O(8)-Si(4)-C(31)	108.6(5)
O(6)-Si(5)-O(5)	109.4(4)
O(6)-Si(5)-O(4)	107.6(4)
O(5)-Si(5)-O(4)	109.4(4)
O(6)-Si(5)-C(25)	109.1(4)
O(5)-Si(5)-C(25)	106.8(4)
O(4)-Si(5)-C(25)	114.5(4)
O(12)-Si(6)-O(7)	109.3(4)
O(12)-Si(6)-O(6)	108.4(4)
O(7)-Si(6)-O(6)	110.5(4)
O(12)-Si(6)-C(19)	110.7(5)
O(7)-Si(6)-C(19)	104.6(4)
O(6)-Si(6)-C(19)	113.3(5)
O(8)-Si(7)-O(9)	109.4(4)
O(8)-Si(7)-O(7)	108.8(4)
O(9)-Si(7)-O(7)	107.1(4)
O(8)-Si(7)-C(13)	107.2(4)
O(9)-Si(7)-C(13)	111.2(4)
O(7)-Si(7)-C(13)	113.1(4)
O(10)-Si(8)-O(9)	109.0(4)
O(10)-Si(8)-O(11)	109.3(4)
O(9)-Si(8)-O(11)	109.2(4)
O(10)-Si(8)-C(7)	110.8(4)
O(9)-Si(8)-C(7)	111.4(4)
O(11)-Si(8)-C(7)	107.1(4)
Si(2)-O(1)-Si(1)	137.9(4)
Si(3)-O(2)-Si(2)	140.4(5)
Si(4)-O(3)-Si(3)	138.1(4)
Si(4)-O(4)-Si(5)	139.0(4)
Si(5)-O(5)-Si(2)	164.3(4)
Si(5)-O(6)-Si(6)	139.5(5)
Si(6)-O(7)-Si(7)	134.8(5)
Si(7)-O(8)-Si(4)	167.9(4)
Si(8)-O(9)-Si(7)	138.3(4)
Si(8)-O(10)-Si(3)	164.5(5)
Si(1)-O(11)-Si(8)	137.6(4)
Si(1)-O(12)-Si(6)	169.2(4)
C(2)-C(1)-C(6)	116.0(9)
C(2)-C(1)-Si(1)	117.9(8)
C(6)-C(1)-Si(1)	126.0(7)
C(3)-C(2)-C(1)	123.1(10)
C(4)-C(3)-C(2)	118.8(7)
C(4)-C(3)-Br(1)	122.4(7)
C(2)-C(3)-Br(1)	118.8(8)
C(5)-C(4)-C(3)	119.9(5)

C(5)-C(4)-Br(2)	118.0(8)
C(3)-C(4)-Br(2)	122.1(8)
C(4)-C(5)-C(6)	122.3(6)
C(4)-C(5)-Br(3)	121.5(8)
C(6)-C(5)-Br(3)	115.8(7)
C(5)-C(6)-C(1)	119.8(6)
C(5)-C(6)-Br(4)	120.6(6)
C(1)-C(6)-Br(4)	119.6(7)
C(12)-C(7)-C(8)	118.8(9)
C(12)-C(7)-Si(8)	117.5(7)
C(8)-C(7)-Si(8)	123.7(7)
C(9)-C(8)-C(7)	121.5(7)
C(9)-C(8)-Br(5)	118.1(8)
C(7)-C(8)-Br(5)	120.3(7)
C(8)-C(9)-C(10)	117.8(7)
C(8)-C(9)-Br(6)	122.2(9)
C(10)-C(9)-Br(6)	117.0(9)
C(9)-C(10)-C(11)	121.6(6)
C(9)-C(10)-Br(7)	118.4(9)
C(11)-C(10)-Br(7)	119.2(10)
C(12)-C(11)-C(10)	117.2(8)
C(12)-C(11)-Br(8)	117.9(9)
C(10)-C(11)-Br(8)	124.1(9)
C(7)-C(12)-C(11)	122.1(10)
C(18)-C(13)-C(14)	117.3(8)
C(18)-C(13)-Si(7)	117.2(7)
C(14)-C(13)-Si(7)	125.1(7)
C(15)-C(14)-C(13)	121.7(6)
C(15)-C(14)-Br(9)	117.6(7)
C(13)-C(14)-Br(9)	120.3(6)
C(14)-C(15)-C(16)	120.2(7)
C(14)-C(15)-Br(10)	121.7(7)
C(16)-C(15)-Br(10)	115.3(7)
C(15)-C(16)-C(17)	119.9(5)
C(15)-C(16)-Br(11)	118.7(7)
C(17)-C(16)-Br(11)	121.3(7)
C(16)-C(17)-C(18)	119.3(6)
C(16)-C(17)-Br(12)	122.4(6)
C(18)-C(17)-Br(12)	118.3(7)
C(13)-C(18)-C(17)	121.3(9)
C(24)-C(19)-C(20)	115.2(10)
C(24)-C(19)-Si(6)	118.6(9)
C(20)-C(19)-Si(6)	126.2(8)
C(21)-C(20)-C(19)	123.0(8)
C(21)-C(20)-Br(13)	120.2(9)
C(19)-C(20)-Br(13)	116.7(8)
C(22)-C(21)-C(20)	118.3(11)
C(21)-C(22)-C(23)	123.9(8)

C(21)-C(22)-Br(14)	116.6(10)
C(23)-C(22)-Br(14)	119.5(9)
C(24)-C(23)-C(22)	115.8(7)
C(24)-C(23)-Br(15)	118.0(9)
C(22)-C(23)-Br(15)	126.2(9)
C(19)-C(24)-C(23)	123.5(11)
C(26)-C(25)-C(30)	115.5(9)
C(26)-C(25)-Si(5)	125.5(7)
C(30)-C(25)-Si(5)	118.6(9)
C(25)-C(26)-C(27)	123.4(8)
C(25)-C(26)-Br(16)	120.7(7)
C(27)-C(26)-Br(16)	115.9(8)
C(28)-C(27)-C(26)	117.2(10)
C(29)-C(28)-C(27)	121.1(7)
C(29)-C(28)-Br(17)	122.6(8)
C(27)-C(28)-Br(17)	116.2(9)
C(30)-C(29)-C(28)	120.2(7)
C(30)-C(29)-Br(18)	118.0(8)
C(28)-C(29)-Br(18)	121.8(8)
C(29)-C(30)-C(25)	122.6(10)
C(32)-C(31)-C(36)	118.4(10)
C(32)-C(31)-Si(4)	125.0(8)
C(36)-C(31)-Si(4)	116.7(9)
C(31)-C(32)-C(33)	122.2(7)
C(31)-C(32)-Br(19)	120.6(8)
C(33)-C(32)-Br(19)	117.0(7)
C(34)-C(33)-C(32)	117.4(7)
C(34)-C(33)-Br(20)	124.4(9)
C(32)-C(33)-Br(20)	117.2(8)
C(33)-C(34)-C(35)	122.2(6)
C(33)-C(34)-Br(21)	117.7(10)
C(35)-C(34)-Br(21)	119.9(10)
C(36)-C(35)-C(34)	119.4(8)
C(36)-C(35)-Br(22)	117.6(9)
C(34)-C(35)-Br(22)	122.8(8)
C(35)-C(36)-C(31)	120.0(11)
C(38)-C(37)-C(42)	116.1(9)
C(38)-C(37)-Si(3)	127.7(7)
C(42)-C(37)-Si(3)	115.9(8)
C(39)-C(38)-C(37)	122.3(7)
C(39)-C(38)-Br(23)	118.9(8)
C(37)-C(38)-Br(23)	118.7(7)
C(38)-C(39)-C(40)	121.8(8)
C(38)-C(39)-Br(24)	121.0(9)
C(40)-C(39)-Br(24)	114.9(8)
C(41)-C(40)-C(39)	118.3(6)
C(41)-C(40)-Br(25)	121.7(9)
C(39)-C(40)-Br(25)	120.0(9)

C(42)-C(41)-C(40)	119.5(7)
C(42)-C(41)-Br(26)	118.6(8)
C(40)-C(41)-Br(26)	121.9(8)
C(41)-C(42)-C(37)	121.9(10)
C(44)-C(43)-C(48)	118.5(9)
C(44)-C(43)-Si(2)	126.3(8)
C(48)-C(43)-Si(2)	115.1(7)
C(43)-C(44)-C(45)	122.3(8)
C(43)-C(44)-Br(27)	121.3(8)
C(45)-C(44)-Br(27)	116.3(8)
C(46)-C(45)-C(44)	119.2(11)
C(45)-C(46)-C(47)	119.3(7)
C(45)-C(46)-Br(28)	118.8(9)
C(47)-C(46)-Br(28)	121.7(9)
C(48)-C(47)-C(46)	119.8(7)
C(48)-C(47)-Br(29)	119.7(9)
C(46)-C(47)-Br(29)	120.4(8)
C(47)-C(48)-C(43)	120.8(9)
C(54)-C(49)-C(50)	117.7(12)
C(54)-C(49)-Cl(1)	121.1(10)
C(50)-C(49)-Cl(1)	120.9(11)
C(49)-C(50)-C(51)	121.2(13)
C(49)-C(50)-Cl(2A)	131.7(12)
C(51)-C(50)-Cl(2A)	106.1(12)
C(52)-C(51)-C(50)	119.5(13)
C(51)-C(52)-C(53)	121.0(13)
C(54)-C(53)-C(52)	117.1(14)
C(49)-C(54)-C(53)	122.9(13)
C(49)-C(54)-Cl(2)	124.5(10)
C(53)-C(54)-Cl(2)	112.5(12)

Symmetry transformations used to generate equivalent atoms:

Table 4. Anisotropic displacement parameters (A^2 x 10^3) for br3ops.

The anisotropic displacement factor exponent takes the form: -2 pi^2 [h^2 a*^2 U11 + ... + 2 h k a* b* U12]

	U11	U22	U33	U23	U13	U12
Br(1)	46(1)	91(1)	66(1)	-56(1)	-16(1)	18(1)
Br(2)	65(1)	86(1)	104(1)	-74(1)	-34(1)	20(1)
Br(3)	54(3)	68(3)	103(4)	-55(3)	-9(3)	-8(2)
Br(4)	80(1)	53(1)	61(1)	-29(1)	-20(1)	0(1)
Br(5)	55(1)	80(2)	99(2)	-66(2)	-1(1)	18(1)
Br(6)	95(5)	298(14)	103(6)	-77(7)	-30(5)	62(7)
Br(7)	55(2)	153(5)	65(2)	-48(3)	14(2)	-58(3)
Br(8)	231(5)	175(5)	106(3)	-67(3)	33(3)	-160(5)
Br(9)	64(1)	69(1)	146(1)	-65(1)	-49(1)	20(1)
Br(10)	98(5)	104(5)	203(9)	-77(6)	-75(6)	38(4)
Br(11)	64(1)	63(1)	118(1)	-40(1)	-11(1)	22(1)
Br(12)	101(1)	67(1)	90(1)	-56(1)	-24(1)	30(1)
Br(13)	56(1)	79(1)	76(1)	-42(1)	-1(1)	22(1)
Br(14)	344(4)	180(2)	97(2)	-87(2)	-97(2)	116(3)
Br(15)	149(2)	119(2)	107(2)	-60(2)	-83(2)	67(2)
Br(16)	38(1)	53(1)	177(2)	-28(1)	5(1)	2(1)
Br(17)	38(1)	122(1)	146(2)	-58(1)	-6(1)	18(1)
Br(18)	57(1)	82(1)	105(1)	-56(1)	-37(1)	36(1)
Br(19)	60(1)	93(1)	83(1)	-57(1)	7(1)	-4(1)
Br(20)	194(6)	220(6)	254(7)	-171(6)	-56(5)	36(5)
Br(21)	92(1)	112(1)	224(2)	-122(2)	-3(1)	-10(1)
Br(22)	69(2)	94(3)	288(7)	-121(4)	53(3)	-40(2)
Br(23)	59(1)	135(1)	78(1)	-66(1)	-11(1)	-19(1)
Br(24)	125(6)	189(9)	109(6)	-68(6)	-38(5)	-22(6)
Br(25)	106(1)	100(1)	64(1)	-48(1)	4(1)	-14(1)
Br(26)	58(1)	99(1)	73(1)	-49(1)	9(1)	-5(1)
Br(27)	88(1)	80(1)	68(1)	-50(1)	-27(1)	31(1)
Br(28)	81(1)	131(2)	109(1)	-42(1)	-34(1)	30(1)
Br(29)	60(1)	138(1)	66(1)	-40(1)	-28(1)	7(1)
Si(1)	41(2)	46(2)	53(2)	-30(2)	-13(1)	4(1)
Si(2)	40(2)	49(2)	48(2)	-28(2)	-9(1)	6(1)
Si(3)	40(2)	62(2)	56(2)	-39(2)	-7(1)	-2(1)
Si(4)	32(2)	52(2)	75(2)	-41(2)	-4(1)	0(1)
Si(5)	30(2)	50(2)	60(2)	-32(2)	-1(1)	5(1)
Si(6)	39(2)	44(2)	53(2)	-25(1)	-7(1)	12(1)

Si(7)	35(2)	48(2)	70(2)	-36(2)	-7(1)	10(1)
Si(8)	37(2)	52(2)	59(2)	-38(2)	-8(1)	1(1)
O(1)	48(4)	43(4)	52(4)	-28(3)	-12(3)	2(3)
O(2)	36(4)	61(4)	53(4)	-37(4)	-4(3)	0(3)
O(3)	38(4)	64(5)	72(5)	-47(4)	-14(4)	-2(3)
O(4)	32(4)	56(4)	88(6)	-45(4)	-6(4)	0(3)
O(5)	44(4)	55(4)	47(4)	-33(4)	-2(3)	3(3)
O(6)	36(4)	52(4)	64(5)	-27(4)	-1(3)	5(3)
O(7)	44(4)	45(4)	69(5)	-37(4)	-11(4)	12(3)
O(8)	38(4)	47(4)	66(5)	-37(4)	-4(3)	3(3)
O(9)	32(4)	51(4)	77(5)	-34(4)	-15(3)	7(3)
O(10)	28(3)	66(5)	50(4)	-34(4)	2(3)	-10(3)
O(11)	40(4)	45(4)	55(4)	-29(3)	-10(3)	1(3)
O(12)	41(4)	48(4)	51(4)	-30(4)	-10(3)	13(3)
C(1)	43(6)	53(7)	45(7)	-29(6)	-14(5)	22(5)
C(2)	27(5)	49(6)	76(9)	-36(6)	-13(5)	9(5)
C(3)	41(6)	67(8)	67(8)	-45(7)	-26(6)	20(6)
C(4)	45(6)	69(8)	69(9)	-56(7)	-19(6)	22(6)
C(5)	40(6)	41(6)	99(10)	-43(7)	-32(6)	10(5)
C(6)	37(6)	40(6)	59(7)	-23(6)	-12(5)	7(5)
C(7)	40(6)	85(8)	54(7)	-50(7)	-4(5)	-11(6)
C(8)	56(8)	94(10)	106(11)	-69(9)	-7(7)	-24(7)
C(9)	30(7)	220(20)	117(13)	-110(14)	11(8)	-21(10)
C(10)	65(9)	191(16)	96(11)	-83(11)	18(8)	-58(10)
C(11)	120(12)	139(13)	111(11)	-86(10)	2(10)	-68(10)
C(12)	74(9)	122(12)	54(8)	-50(8)	14(7)	-46(9)
C(13)	37(6)	47(6)	73(8)	-33(6)	-13(6)	10(5)
C(14)	54(7)	49(7)	91(9)	-35(7)	-21(7)	-1(6)
C(15)	32(6)	73(9)	80(9)	-32(7)	-2(6)	13(6)
C(16)	49(7)	42(7)	82(9)	-26(6)	-7(6)	10(5)
C(17)	60(7)	48(7)	60(8)	-32(6)	5(6)	11(6)
C(18)	50(6)	53(7)	50(7)	-28(6)	-4(5)	12(5)
C(19)	78(7)	64(7)	58(7)	-39(6)	-21(5)	28(5)
C(20)	66(7)	55(7)	65(7)	-25(6)	-6(5)	12(5)
C(21)	109(10)	93(10)	68(7)	-52(7)	-12(6)	29(7)
C(22)	147(12)	115(11)	65(8)	-50(8)	-33(8)	53(9)
C(23)	143(10)	115(10)	89(8)	-56(8)	-63(7)	74(9)
C(24)	98(9)	76(8)	74(7)	-46(7)	-40(7)	46(7)
C(25)	31(6)	66(8)	64(7)	-37(6)	-8(5)	11(6)
C(26)	33(6)	53(7)	97(10)	-22(7)	-2(6)	3(6)
C(27)	34(7)	73(9)	123(12)	-30(8)	-6(7)	-3(6)
C(28)	35(6)	80(10)	95(10)	-42(8)	-18(7)	24(7)
C(29)	44(7)	67(8)	79(9)	-49(7)	-31(6)	29(6)
C(30)	49(7)	65(7)	45(7)	-27(6)	-21(5)	9(6)
C(31)	37(6)	65(7)	108(9)	-59(7)	-7(5)	-3(5)
C(32)	44(6)	81(7)	98(9)	-53(7)	-14(5)	-2(5)
C(33)	55(7)	78(7)	141(10)	-77(8)	-37(5)	12(5)
C(34)	51(7)	94(8)	209(13)	-101(9)	-38(6)	1(6)

C(35)	47(7)	77(8)	198(14)	-84(9)	7(7)	-21(6)
C(36)	36(6)	76(7)	166(13)	-75(8)	9(6)	-10(5)
C(37)	42(6)	75(8)	48(7)	-43(6)	17(5)	-23(5)
C(38)	61(7)	81(8)	51(8)	-43(6)	-7(6)	-11(6)
C(39)	64(9)	92(10)	83(10)	-53(8)	1(8)	-15(7)
C(40)	102(11)	60(8)	50(8)	-37(6)	11(8)	-16(7)
C(41)	53(7)	62(7)	68(9)	-38(6)	-12(6)	1(6)
C(42)	65(8)	60(7)	48(7)	-34(6)	-2(6)	-3(6)
C(43)	34(6)	68(7)	49(7)	-30(6)	-13(5)	6(5)
C(44)	57(7)	80(8)	65(8)	-48(7)	-25(6)	14(6)
C(45)	84(10)	103(11)	80(10)	-55(9)	-34(8)	34(8)
C(46)	69(9)	99(11)	76(10)	-39(9)	-4(8)	13(8)
C(47)	60(8)	108(11)	52(8)	-29(7)	-17(6)	11(8)
C(48)	26(5)	63(7)	77(9)	-37(6)	-13(5)	19(5)
C(49)	58(6)	133(7)	108(11)	-73(8)	-29(6)	-1(5)
C(50)	86(7)	132(8)	122(12)	-70(9)	-52(8)	17(6)
C(51)	89(8)	142(10)	111(12)	-79(10)	-30(8)	28(7)
C(52)	72(9)	169(12)	143(15)	-59(13)	-7(10)	24(7)
C(53)	73(7)	139(11)	167(16)	-48(12)	-3(10)	-1(6)
C(54)	61(6)	131(8)	150(15)	-65(10)	-11(8)	4(6)
Cl(1)	62(2)	167(4)	109(3)	-67(3)	-10(2)	-16(2)
Cl(2)	86(4)	118(5)	201(9)	-90(5)	-4(5)	4(4)
Cl(2A)	98(9)	135(8)	131(12)	-58(9)	-31(8)	-6(7)

Table 5. Hydrogen coordinates (x 10^4) and isotropic displacement parameters (A^2 x 10^3) for br3ops.

	x	y	z	U(eq)
H(2)	1519	5707	-180	58
H(5)	381	3445	1088	63
H(8)	-1748	6929	2943	91
H(9)	-3138	6489	3697	135
H(10)	-3566	5390	3793	133
H(11)	-2479	4609	3416	132
H(12)	-1175	5141	2542	96
H(15)	-1915	9590	2	78
H(18)	286	9024	1311	61
H(21)	2949	6862	-2286	106
H(23)	627	8053	-2139	133
H(24)	747	7965	-984	94
H(27)	6055	8216	-758	99
H(30)	4636	6086	897	61
H(33)	1045	9800	2608	94
H(35)	3251	10074	968	123
H(36)	3154	8918	1030	107
H(39)	1284	5823	5460	91
H(42)	-436	6127	3838	66
H(45)	4956	3737	2058	100
H(48)	3117	5008	3354	65
H(50A)	5574	5787	2375	123
H(51)	7078	5917	1784	127
H(52)	7668	7049	1187	162
H(53)	6732	8080	1078	163
H(54A)	5198	7916	1531	137

Appendix 8

Crystallographic data for

Octa(diphenylacetylene)silsesquioxane

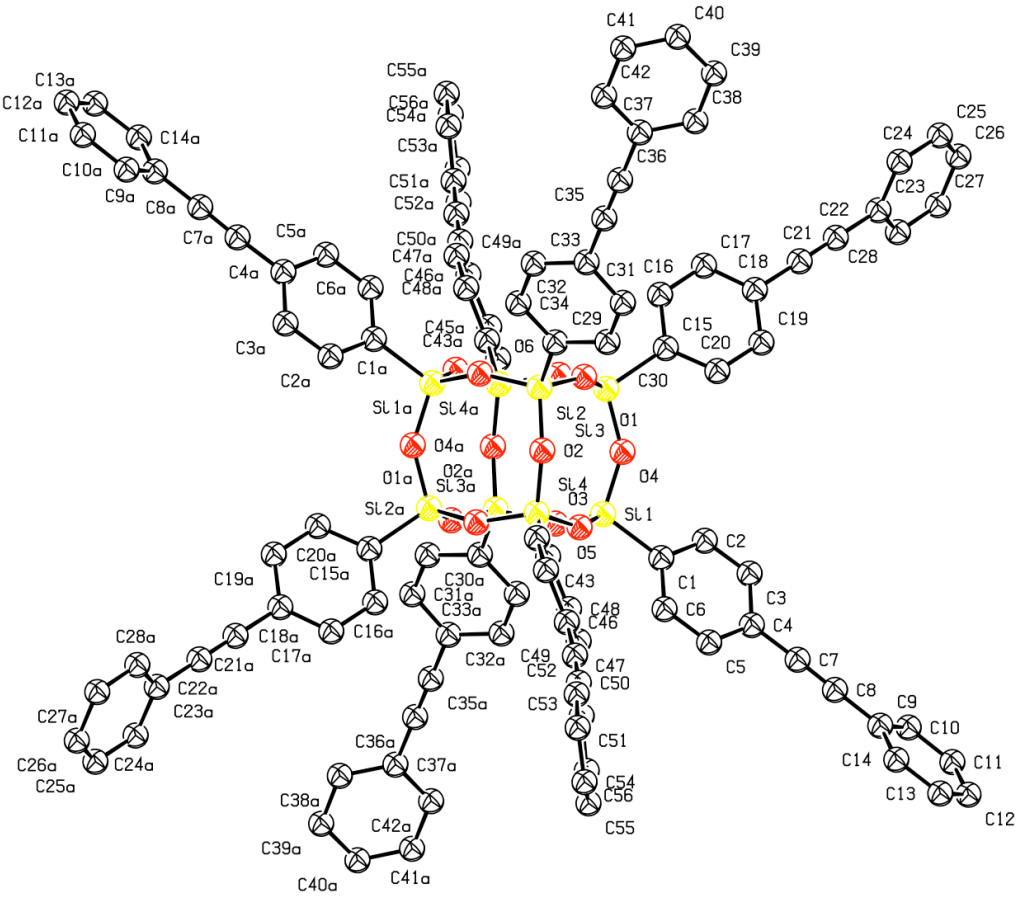

Figure A.8. 50 % thermal ellipsoid plots of octa(diphenylacetylene)silsesquioxane•*m*-xylene solvate. Hydrogen atoms and *m*-xylene solvates are omitted for clarity.

Structure Determination.

Yellow blocks of **diph2** were grown from a m-xylene solution at 25 deg. C. A crystal of dimensions 0.48 x 0.40 x 0.39 mm was mounted on a Bruker SMART APEX CCD-based X-ray diffractometer equipped with a low temperature device and fine focus Mo-target X-ray tube (l = 0.71073 A) operated at 1500 W power (50 kV, 30 mA). The X-ray intensities were measured at 85(1) K; the detector was placed at a distance 5.055 cm from the crystal. A total of 5190 frames were collected with a scan width of 0.5° in w and 0.45° in phi with an exposure time of 10 s/frame. The integration of the data yielded a total of 146378 reflections to a maximum 2q value of 56.58° of which 15959 were independent and 13937 were greater than 2s(I). The final cell constants (Table 1) were based on the xyz centroids of 9406 reflections above 10s(I). Analysis of the data showed negligible decay during data collection; the data were processed with SADABS and corrected for absorption. The structure was solved and refined with the Bruker SHELXTL (version 2008/3) software package, using the space group P1bar with Z = 1 for the formula $C_{112}H_{72}O_{12}Si_8 \bullet 5(C_8H_{10})$. All non-hydrogen atoms were refined anisotropically with the hydrogen atoms placed in idealized positions. One m-xylene solvate molecule is disordered and was modeled as diffuse scattering by use of the SQUEEZE subroutine of the PLATON program suite. Full matrix least-squares refinement based on F^2 converged at R1 = 0.0553 and wR2 = 0.1698 [based on I > 2sigma(I)], R1 = 0.0602 and wR2 = 0.1759 for all data. Additional details are presented in Table 1 and are given as Supporting Information in a CIF file.

Sheldrick, G.M. SHELXTL, v. 2008/3; Bruker Analytical X-ray, Madison, WI, 2008.

Sheldrick, G.M. SADABS, v. 2008/1. Program for Empirical Absorption Correction of Area Detector Data, University of Gottingen: Gottingen, Germany, 2008.

Saint Plus, v. 7.53a, Bruker Analytical X-ray, Madison, WI, 2008.

A.L. Spek. (2008) PLATON, v. 180108, A Multi-purpose Crystallographic Tool, Utrecht University, Utrecht, The Netherlands.

Table 1. Crystal data and structure refinement for diph2.

Identification code	diph2
Empirical formula	C152 H122 O12 Si8
Formula weight	2365.22
Temperature	85(2) K
Wavelength	0.71073 A
Crystal system, space group	Triclinic, P-1
Unit cell dimensions	a = 14.4668(9) Å alpha = 95.443(1)° b = 15.5858(10) Å beta = 92.173(1)° c = 15.9361(10) Å gamma = 115.487(1)°
Volume	3216.5(4) A^3
Z, Calculated density	1, 1.221 Mg/m^3
Absorption coefficient	0.146 mm^-1
F(000)	1242
Crystal size	0.48 x 0.40 x 0.39 mm
Theta range for data collection	1.29 to 28.29 deg.
Limiting indices	-19<=h<=19, -20<=k<=20, -21<=l<=21
Reflections collected / unique	146378 / 15959 [R(int) = 0.0214]
Completeness to theta = 28.29	99.9 %
Absorption correction	Semi-empirical from equivalents
Max. and min. transmission	0.9453 and 0.9332

Refinement method	Full-matrix least-squares on F^2
Data / restraints / parameters	15959 / 48 / 743
Goodness-of-fit on F^2	1.091
Final R indices [I>2sigma(I)]	R1 = 0.0553, wR2 = 0.1698
R indices (all data)	R1 = 0.0603, wR2 = 0.1759
Largest diff. peak and hole	1.156 and -0.620 e.A^-3

Table 2. Atomic coordinates (x 10^4) and equivalent isotropic displacement parameters (A^2 x 10^3) for diph2.
U(eq) is defined as one third of the trace of the orthogonalized Uij tensor.

	x	y	z	U(eq)
Si(1)	8256(1)	9553(1)	4000(1)	19(1)
Si(2)	8680(1)	8160(1)	5043(1)	18(1)
Si(3)	9533(1)	9730(1)	6600(1)	18(1)
Si(4)	9105(1)	11124(1)	5555(1)	18(1)
O(1)	8921(1)	8740(1)	5979(1)	27(1)
O(2)	9178(1)	10515(1)	6304(1)	25(1)
O(3)	8426(1)	10421(1)	4727(1)	25(1)
O(4)	8153(1)	8622(1)	4430(1)	26(1)
O(5)	9244(1)	9890(1)	3451(1)	26(1)
O(6)	9747(1)	8242(1)	4700(1)	26(1)
C(1)	7068(1)	9245(1)	3332(1)	23(1)
C(2)	6453(1)	8302(1)	2955(1)	32(1)
C(3)	5535(1)	8069(1)	2476(1)	36(1)
C(4)	5212(1)	8784(1)	2359(1)	31(1)
C(5)	5816(1)	9713(1)	2727(1)	36(1)
C(6)	6730(1)	9936(1)	3208(1)	32(1)
C(7)	4268(1)	8563(1)	1870(1)	35(1)
C(8)	3489(1)	8407(1)	1462(1)	35(1)
C(9)	2545(1)	8215(1)	982(1)	32(1)
C(10)	2188(1)	7540(1)	271(1)	40(1)
C(11)	1276(2)	7356(2)	-190(1)	48(1)
C(12)	707(1)	7841(1)	68(1)	42(1)
C(13)	1059(1)	8522(1)	772(1)	35(1)
C(14)	1972(1)	8718(1)	1228(1)	33(1)
C(15)	7808(1)	6882(1)	5018(1)	22(1)
C(16)	8181(1)	6235(1)	5239(1)	31(1)
C(17)	7559(1)	5254(1)	5126(1)	34(1)
C(18)	6546(1)	4895(1)	4771(1)	28(1)
C(19)	6156(1)	5535(1)	4574(1)	30(1)
C(20)	6780(1)	6518(1)	4705(1)	27(1)
C(21)	5920(1)	3878(1)	4599(1)	33(1)
C(22)	5426(1)	3033(1)	4428(1)	35(1)
C(23)	4854(1)	2017(1)	4186(1)	35(1)
C(24)	4588(2)	1380(1)	4792(2)	47(1)
C(25)	4057(2)	400(1)	4533(2)	57(1)
C(26)	3802(2)	53(1)	3692(2)	53(1)
C(27)	4054(1)	679(1)	3082(2)	47(1)
C(28)	4581(1)	1661(1)	3324(1)	42(1)

C(29)	9222(1)	9476(1)	7683(1)	22(1)
C(30)	8193(1)	9027(1)	7867(1)	27(1)
C(31)	7934(1)	8696(1)	8643(1)	29(1)
C(32)	8701(1)	8794(1)	9254(1)	27(1)
C(33)	9733(1)	9278(1)	9091(1)	28(1)
C(34)	9989(1)	9617(1)	8317(1)	26(1)
C(35)	8430(1)	8358(1)	10020(1)	31(1)
C(36)	8204(1)	7942(1)	10629(1)	32(1)
C(37)	7935(1)	7391(1)	11330(1)	31(1)
C(38)	6958(2)	6624(1)	11319(1)	41(1)
C(39)	6723(2)	6055(1)	11975(1)	47(1)
C(40)	7452(2)	6250(1)	12645(1)	47(1)
C(41)	8404(2)	7019(1)	12672(1)	43(1)
C(42)	8647(1)	7592(1)	12022(1)	36(1)
C(43)	8520(1)	11908(1)	5948(1)	24(1)
C(44)	8615(1)	12225(1)	6806(1)	33(1)
C(45)	8169(2)	12807(1)	7117(1)	41(1)
C(46)	7607(1)	13085(1)	6565(1)	41(1)
C(47)	7496(1)	12768(1)	5705(2)	44(1)
C(48)	7954(1)	12191(1)	5397(1)	37(1)
C(49)	7166(2)	13707(1)	6890(2)	50(1)
C(50)	6853(2)	14254(1)	7175(2)	50(1)
C(51)	6505(2)	14942(1)	7520(1)	42(1)
C(52)	6504(3)	15144(3)	8381(2)	97(1)
C(53)	6199(3)	15836(3)	8695(2)	106(1)
C(54)	5881(2)	16310(2)	8168(2)	65(1)
C(55)	5898(2)	16127(2)	7337(2)	67(1)
C(56)	6215(2)	15451(2)	7009(1)	56(1)
C(57)	5988(2)	9013(2)	10032(2)	61(1)
C(58)	5580(2)	8052(2)	10156(2)	65(1)
C(59)	4711(2)	7360(2)	9689(2)	73(1)
C(60)	4264(3)	7655(3)	9038(2)	88(1)
C(61)	4637(3)	8559(3)	8903(2)	94(1)
C(62)	5509(3)	9264(2)	9409(2)	82(1)
C(63)	6934(3)	9751(2)	10571(2)	80(1)
C(64)	4218(3)	6355(3)	9833(4)	115(2)
C(65)	694(2)	5684(2)	6576(2)	68(1)
C(66)	-77(2)	5903(2)	6893(2)	59(1)
C(67)	117(3)	6817(2)	7269(2)	68(1)
C(68)	1164(3)	7532(2)	7343(2)	82(1)
C(69)	1967(3)	7322(2)	7066(2)	88(1)
C(70)	1730(3)	6406(2)	6689(2)	81(1)
C(71)	423(2)	4690(2)	6160(2)	82(1)
C(72)	-715(3)	7028(2)	7588(2)	87(1)

Table 3. Bond lengths [A] and angles [deg] for diph2.

Si(1)-O(4)	1.6146(11)
Si(1)-O(5)	1.6182(11)
Si(1)-O(3)	1.6206(11)
Si(1)-C(1)	1.8370(14)
Si(2)-O(1)	1.6116(11)
Si(2)-O(4)	1.6140(11)
Si(2)-O(6)	1.6144(11)
Si(2)-C(15)	1.8380(13)
Si(3)-O(5)#1	1.6142(10)
Si(3)-O(1)	1.6165(11)
Si(3)-O(2)	1.6171(11)
Si(3)-C(29)	1.8355(14)
Si(4)-O(3)	1.6147(11)
Si(4)-O(6)#1	1.6163(10)
Si(4)-O(2)	1.6214(11)
Si(4)-C(43)	1.8396(15)
O(5)-Si(3)#1	1.6142(10)
O(6)-Si(4)#1	1.6163(10)
C(1)-C(6)	1.387(2)
C(1)-C(2)	1.407(2)
C(2)-C(3)	1.391(2)
C(3)-C(4)	1.404(2)
C(4)-C(5)	1.384(2)
C(4)-C(7)	1.433(2)
C(5)-C(6)	1.391(2)
C(7)-C(8)	1.197(2)
C(8)-C(9)	1.437(2)
C(9)-C(10)	1.385(2)
C(9)-C(14)	1.406(2)
C(10)-C(11)	1.388(3)
C(11)-C(12)	1.385(3)
C(12)-C(13)	1.383(3)
C(13)-C(14)	1.380(2)
C(15)-C(20)	1.3950(19)
C(15)-C(16)	1.397(2)
C(16)-C(17)	1.389(2)
C(17)-C(18)	1.398(2)
C(18)-C(19)	1.394(2)
C(18)-C(21)	1.439(2)
C(19)-C(20)	1.393(2)
C(21)-C(22)	1.195(2)
C(22)-C(23)	1.440(2)
C(23)-C(24)	1.395(3)

C(23)-C(28)	1.405(3)
C(24)-C(25)	1.394(3)
C(25)-C(26)	1.370(4)
C(26)-C(27)	1.389(3)
C(27)-C(28)	1.390(3)
C(29)-C(34)	1.4014(19)
C(29)-C(30)	1.4026(19)
C(30)-C(31)	1.388(2)
C(31)-C(32)	1.395(2)
C(32)-C(33)	1.400(2)
C(32)-C(35)	1.438(2)
C(33)-C(34)	1.388(2)
C(35)-C(36)	1.196(2)
C(36)-C(37)	1.437(2)
C(37)-C(42)	1.395(2)
C(37)-C(38)	1.403(2)
C(38)-C(39)	1.393(3)
C(39)-C(40)	1.386(3)
C(40)-C(41)	1.378(3)
C(41)-C(42)	1.387(2)
C(43)-C(44)	1.391(2)
C(43)-C(48)	1.403(2)
C(44)-C(45)	1.388(2)
C(45)-C(46)	1.394(3)
C(46)-C(47)	1.391(3)
C(46)-C(49)	1.442(3)
C(47)-C(48)	1.394(3)
C(49)-C(50)	1.189(3)
C(50)-C(51)	1.442(3)
C(51)-C(56)	1.361(3)
C(51)-C(52)	1.378(3)
C(52)-C(53)	1.389(5)
C(53)-C(54)	1.358(5)
C(54)-C(55)	1.332(4)
C(55)-C(56)	1.386(3)
C(57)-C(62)	1.369(4)
C(57)-C(58)	1.390(4)
C(57)-C(63)	1.517(4)
C(58)-C(59)	1.381(4)
C(59)-C(60)	1.415(5)
C(59)-C(64)	1.460(5)
C(60)-C(61)	1.317(5)
C(61)-C(62)	1.418(5)
C(65)-C(66)	1.396(4)
C(65)-C(70)	1.426(4)
C(65)-C(71)	1.503(4)
C(66)-C(67)	1.396(3)
C(67)-C(68)	1.435(5)

C(67)-C(72)	1.473(5)
C(68)-C(69)	1.411(5)
C(69)-C(70)	1.384(5)
O(4)-Si(1)-O(5)	108.81(6)
O(4)-Si(1)-O(3)	110.01(6)
O(5)-Si(1)-O(3)	108.72(6)
O(4)-Si(1)-C(1)	108.83(6)
O(5)-Si(1)-C(1)	111.25(6)
O(3)-Si(1)-C(1)	109.21(6)
O(1)-Si(2)-O(4)	109.02(6)
O(1)-Si(2)-O(6)	108.65(6)
O(4)-Si(2)-O(6)	110.07(6)
O(1)-Si(2)-C(15)	112.93(6)
O(4)-Si(2)-C(15)	108.19(6)
O(6)-Si(2)-C(15)	107.97(6)
O(5)#1-Si(3)-O(1)	109.99(6)
O(5)#1-Si(3)-O(2)	109.70(6)
O(1)-Si(3)-O(2)	108.50(6)
O(5)#1-Si(3)-C(29)	109.16(6)
O(1)-Si(3)-C(29)	107.46(6)
O(2)-Si(3)-C(29)	111.99(6)
O(3)-Si(4)-O(6)#1	108.50(6)
O(3)-Si(4)-O(2)	110.86(6)
O(6)#1-Si(4)-O(2)	108.59(6)
O(3)-Si(4)-C(43)	110.04(6)
O(6)#1-Si(4)-C(43)	110.30(6)
O(2)-Si(4)-C(43)	108.54(6)
Si(2)-O(1)-Si(3)	149.20(7)
Si(3)-O(2)-Si(4)	147.09(7)
Si(4)-O(3)-Si(1)	147.99(7)
Si(2)-O(4)-Si(1)	147.49(7)
Si(3)#1-O(5)-Si(1)	150.02(7)
Si(2)-O(6)-Si(4)#1	150.88(7)
C(6)-C(1)-C(2)	117.79(13)
C(6)-C(1)-Si(1)	120.61(11)
C(2)-C(1)-Si(1)	121.56(11)
C(3)-C(2)-C(1)	121.13(15)
C(2)-C(3)-C(4)	119.88(15)
C(5)-C(4)-C(3)	119.22(14)
C(5)-C(4)-C(7)	119.76(16)
C(3)-C(4)-C(7)	121.02(15)
C(4)-C(5)-C(6)	120.36(16)
C(1)-C(6)-C(5)	121.63(15)
C(8)-C(7)-C(4)	178.0(2)
C(7)-C(8)-C(9)	179.2(2)
C(10)-C(9)-C(14)	119.09(15)
C(10)-C(9)-C(8)	120.80(16)

C(14)-C(9)-C(8)	120.10(15)
C(9)-C(10)-C(11)	120.54(17)
C(12)-C(11)-C(10)	119.93(18)
C(13)-C(12)-C(11)	120.04(16)
C(14)-C(13)-C(12)	120.40(17)
C(13)-C(14)-C(9)	119.97(16)
C(20)-C(15)-C(16)	118.10(13)
C(20)-C(15)-Si(2)	120.98(11)
C(16)-C(15)-Si(2)	120.66(10)
C(17)-C(16)-C(15)	121.26(14)
C(16)-C(17)-C(18)	120.14(15)
C(19)-C(18)-C(17)	119.03(13)
C(19)-C(18)-C(21)	120.56(14)
C(17)-C(18)-C(21)	120.40(15)
C(20)-C(19)-C(18)	120.33(14)
C(19)-C(20)-C(15)	121.02(14)
C(22)-C(21)-C(18)	177.12(19)
C(21)-C(22)-C(23)	177.3(2)
C(24)-C(23)-C(28)	119.64(16)
C(24)-C(23)-C(22)	120.96(18)
C(28)-C(23)-C(22)	119.38(17)
C(25)-C(24)-C(23)	119.4(2)
C(26)-C(25)-C(24)	120.9(2)
C(25)-C(26)-C(27)	120.25(18)
C(26)-C(27)-C(28)	120.0(2)
C(27)-C(28)-C(23)	119.8(2)
C(34)-C(29)-C(30)	118.12(13)
C(34)-C(29)-Si(3)	121.33(11)
C(30)-C(29)-Si(3)	120.11(10)
C(31)-C(30)-C(29)	121.22(14)
C(30)-C(31)-C(32)	120.17(14)
C(31)-C(32)-C(33)	119.07(14)
C(31)-C(32)-C(35)	120.16(14)
C(33)-C(32)-C(35)	120.68(14)
C(34)-C(33)-C(32)	120.48(14)
C(33)-C(34)-C(29)	120.80(13)
C(36)-C(35)-C(32)	175.68(18)
C(35)-C(36)-C(37)	176.37(19)
C(42)-C(37)-C(38)	118.89(15)
C(42)-C(37)-C(36)	120.74(15)
C(38)-C(37)-C(36)	120.35(16)
C(39)-C(38)-C(37)	120.10(18)
C(40)-C(39)-C(38)	120.07(18)
C(41)-C(40)-C(39)	120.07(17)
C(40)-C(41)-C(42)	120.41(18)
C(41)-C(42)-C(37)	120.40(17)
C(44)-C(43)-C(48)	118.05(14)
C(44)-C(43)-Si(4)	120.67(11)

C(48)-C(43)-Si(4)	121.27(12)
C(45)-C(44)-C(43)	121.55(16)
C(44)-C(45)-C(46)	120.05(18)
C(47)-C(46)-C(45)	119.25(16)
C(47)-C(46)-C(49)	121.01(19)
C(45)-C(46)-C(49)	119.7(2)
C(46)-C(47)-C(48)	120.38(18)
C(47)-C(48)-C(43)	120.70(18)
C(50)-C(49)-C(46)	176.5(2)
C(49)-C(50)-C(51)	178.2(2)
C(56)-C(51)-C(52)	117.5(2)
C(56)-C(51)-C(50)	121.1(2)
C(52)-C(51)-C(50)	121.3(2)
C(51)-C(52)-C(53)	119.9(3)
C(54)-C(53)-C(52)	121.3(3)
C(55)-C(54)-C(53)	118.9(2)
C(54)-C(55)-C(56)	120.9(3)
C(51)-C(56)-C(55)	121.5(2)
C(62)-C(57)-C(58)	117.8(3)
C(62)-C(57)-C(63)	121.6(3)
C(58)-C(57)-C(63)	120.7(3)
C(59)-C(58)-C(57)	122.6(3)
C(58)-C(59)-C(60)	117.2(3)
C(58)-C(59)-C(64)	124.5(4)
C(60)-C(59)-C(64)	118.3(4)
C(61)-C(60)-C(59)	121.5(4)
C(60)-C(61)-C(62)	120.4(4)
C(57)-C(62)-C(61)	120.5(3)
C(66)-C(65)-C(70)	118.8(3)
C(66)-C(65)-C(71)	119.6(3)
C(70)-C(65)-C(71)	121.6(3)
C(67)-C(66)-C(65)	122.6(3)
C(66)-C(67)-C(68)	116.8(3)
C(66)-C(67)-C(72)	121.3(3)
C(68)-C(67)-C(72)	121.9(3)
C(69)-C(68)-C(67)	121.9(3)
C(70)-C(69)-C(68)	118.8(3)
C(69)-C(70)-C(65)	120.9(3)

Symmetry transformations used to generate equivalent atoms:

#1 -x+2,-y+2,-z+1

Table 4. Anisotropic displacement parameters (A^2 x 10^3) for diph2.

The anisotropic displacement factor exponent takes the form: -2 pi^2 [h^2 a*^2 U11 + ... + 2 h k a* b* U12]

	U11	U22	U33	U23	U13	U12
Si(1)	17(1)	19(1)	21(1)	5(1)	0(1)	8(1)
Si(2)	17(1)	16(1)	21(1)	4(1)	1(1)	6(1)
Si(3)	19(1)	18(1)	18(1)	5(1)	2(1)	8(1)
Si(4)	18(1)	17(1)	22(1)	4(1)	2(1)	9(1)
O(1)	32(1)	21(1)	23(1)	3(1)	3(1)	7(1)
O(2)	33(1)	27(1)	24(1)	8(1)	6(1)	19(1)
O(3)	23(1)	25(1)	27(1)	-1(1)	-3(1)	12(1)
O(4)	24(1)	22(1)	31(1)	9(1)	-4(1)	8(1)
O(5)	20(1)	34(1)	24(1)	8(1)	3(1)	11(1)
O(6)	21(1)	22(1)	35(1)	6(1)	7(1)	8(1)
C(1)	19(1)	27(1)	23(1)	5(1)	1(1)	11(1)
C(2)	31(1)	29(1)	36(1)	4(1)	-7(1)	14(1)
C(3)	30(1)	34(1)	38(1)	2(1)	-9(1)	11(1)
C(4)	23(1)	43(1)	29(1)	5(1)	-1(1)	17(1)
C(5)	32(1)	39(1)	42(1)	6(1)	-4(1)	22(1)
C(6)	29(1)	30(1)	39(1)	3(1)	-5(1)	14(1)
C(7)	29(1)	45(1)	34(1)	5(1)	-1(1)	18(1)
C(8)	31(1)	42(1)	34(1)	3(1)	-2(1)	18(1)
C(9)	26(1)	39(1)	33(1)	7(1)	-2(1)	14(1)
C(10)	37(1)	42(1)	43(1)	-2(1)	-6(1)	23(1)
C(11)	48(1)	45(1)	48(1)	-12(1)	-18(1)	24(1)
C(12)	32(1)	44(1)	48(1)	1(1)	-13(1)	18(1)
C(13)	30(1)	40(1)	37(1)	8(1)	1(1)	18(1)
C(14)	30(1)	39(1)	30(1)	3(1)	-2(1)	16(1)
C(15)	22(1)	18(1)	24(1)	4(1)	4(1)	8(1)
C(16)	24(1)	23(1)	44(1)	8(1)	0(1)	10(1)
C(17)	30(1)	22(1)	51(1)	9(1)	4(1)	12(1)
C(18)	27(1)	20(1)	35(1)	3(1)	7(1)	7(1)
C(19)	22(1)	23(1)	41(1)	3(1)	3(1)	6(1)
C(20)	23(1)	22(1)	37(1)	6(1)	3(1)	9(1)
C(21)	28(1)	24(1)	44(1)	3(1)	6(1)	9(1)
C(22)	28(1)	26(1)	48(1)	4(1)	6(1)	10(1)
C(23)	25(1)	21(1)	56(1)	1(1)	5(1)	9(1)
C(24)	48(1)	28(1)	59(1)	3(1)	23(1)	9(1)
C(25)	59(1)	27(1)	78(2)	8(1)	35(1)	10(1)

C(26)	35(1)	24(1)	88(2)	-8(1)	24(1)	3(1)
C(27)	31(1)	36(1)	69(1)	-11(1)	-4(1)	14(1)
C(28)	33(1)	31(1)	60(1)	-1(1)	-6(1)	15(1)
C(29)	23(1)	22(1)	21(1)	5(1)	3(1)	10(1)
C(30)	23(1)	31(1)	25(1)	7(1)	2(1)	10(1)
C(31)	24(1)	33(1)	28(1)	7(1)	6(1)	8(1)
C(32)	31(1)	29(1)	23(1)	7(1)	5(1)	13(1)
C(33)	29(1)	35(1)	22(1)	7(1)	0(1)	14(1)
C(34)	24(1)	29(1)	24(1)	6(1)	3(1)	11(1)
C(35)	33(1)	33(1)	28(1)	6(1)	4(1)	13(1)
C(36)	34(1)	34(1)	27(1)	6(1)	6(1)	12(1)
C(37)	39(1)	31(1)	24(1)	7(1)	9(1)	14(1)
C(38)	43(1)	38(1)	34(1)	7(1)	6(1)	10(1)
C(39)	52(1)	35(1)	43(1)	10(1)	16(1)	6(1)
C(40)	75(1)	36(1)	29(1)	13(1)	18(1)	21(1)
C(41)	62(1)	41(1)	26(1)	7(1)	3(1)	22(1)
C(42)	43(1)	33(1)	28(1)	6(1)	4(1)	14(1)
C(43)	22(1)	19(1)	33(1)	6(1)	5(1)	10(1)
C(44)	40(1)	33(1)	35(1)	9(1)	12(1)	24(1)
C(45)	54(1)	36(1)	44(1)	10(1)	22(1)	28(1)
C(46)	38(1)	28(1)	67(1)	12(1)	20(1)	21(1)
C(47)	39(1)	33(1)	67(1)	4(1)	-4(1)	24(1)
C(48)	40(1)	30(1)	46(1)	0(1)	-7(1)	22(1)
C(49)	48(1)	36(1)	77(1)	16(1)	25(1)	26(1)
C(50)	49(1)	39(1)	72(1)	16(1)	23(1)	27(1)
C(51)	48(1)	42(1)	48(1)	6(1)	13(1)	30(1)
C(52)	133(2)	182(2)	44(1)	23(1)	20(1)	130(2)
C(53)	122(2)	190(3)	45(1)	-32(1)	-5(1)	115(2)
C(54)	53(1)	52(1)	89(2)	-24(1)	13(1)	27(1)
C(55)	83(1)	71(1)	80(1)	21(1)	27(1)	62(1)
C(56)	74(1)	81(1)	41(1)	0(1)	4(1)	62(1)
C(57)	73(1)	62(1)	63(1)	19(1)	38(1)	38(1)
C(58)	77(1)	65(1)	72(2)	24(1)	34(1)	42(1)
C(59)	65(1)	67(2)	97(2)	17(1)	38(1)	35(1)
C(60)	70(2)	112(3)	91(2)	20(2)	26(2)	47(2)
C(61)	80(2)	125(3)	90(2)	51(2)	30(2)	48(2)
C(62)	91(2)	80(2)	95(2)	44(2)	42(2)	47(2)
C(63)	104(2)	62(2)	76(2)	12(1)	39(2)	35(2)
C(64)	79(2)	72(2)	197(5)	24(3)	46(3)	32(2)
C(65)	88(2)	45(1)	73(2)	22(1)	29(1)	26(1)
C(66)	77(2)	49(1)	58(1)	4(1)	-5(1)	35(1)
C(67)	110(2)	54(1)	49(1)	4(1)	-10(1)	45(1)
C(68)	91(2)	54(1)	84(2)	8(1)	-10(2)	17(1)
C(69)	74(2)	68(2)	103(3)	23(2)	-5(2)	12(2)
C(70)	69(2)	71(2)	106(2)	36(2)	19(2)	27(1)
C(71)	87(2)	45(1)	117(2)	18(1)	54(2)	28(1)
C(72)	113(2)	72(2)	89(2)	-18(2)	-12(2)	60(2)

Table 5. Hydrogen coordinates (x 10^4) and isotropic displacement parameters (A^2 x 10^3) for diph2.

	x	y	z	U(eq)
H(2A)	6668	7816	3030	39
H(3A)	5127	7428	2228	43
H(5B)	5604	10201	2651	43
H(6A)	7133	10577	3457	39
H(10A)	2572	7199	98	47
H(11A)	1042	6899	-681	57
H(12A)	74	7705	-240	50
H(13A)	670	8858	943	42
H(14A)	2214	9191	1708	39
H(16A)	8872	6470	5470	37
H(17A)	7823	4827	5290	41
H(19A)	5462	5300	4348	36
H(20A)	6501	6948	4580	33
H(24A)	4767	1613	5376	57
H(25A)	3869	-35	4945	68
H(26A)	3452	-618	3525	64
H(27A)	3866	437	2500	56
H(28A)	4757	2090	2908	50
H(30A)	7664	8947	7452	32
H(31A)	7233	8401	8758	35
H(33A)	10262	9375	9514	34
H(34A)	10692	9948	8217	31
H(38A)	6455	6493	10863	49
H(39A)	6063	5533	11963	57
H(40A)	7295	5854	13086	56
H(41A)	8896	7158	13138	51
H(42A)	9303	8124	12049	43
H(44A)	8994	12038	7190	39
H(45A)	8247	13016	7706	49
H(47A)	7107	12947	5325	53
H(48A)	7881	11987	4807	44
H(52A)	6712	14811	8759	116
H(53A)	6213	15979	9290	127
H(54A)	5651	16765	8389	78
H(55A)	5689	16463	6963	80
H(56A)	6229	15341	6414	67
H(58A)	5911	7865	10579	78
H(60A)	3682	7191	8691	105
H(61A)	4319	8739	8465	113

H(62A)	5764	9916	9314	98
H(63A)	7544	9879	10263	120
H(63B)	7008	9505	11101	120
H(63C)	6860	10345	10698	120
H(64A)	4671	6226	10222	172
H(64B)	4086	5946	9294	172
H(64C)	3567	6219	10080	172
H(66A)	-760	5410	6850	71
H(68A)	1321	8164	7586	98
H(69A)	2658	7800	7137	105
H(70A)	2266	6256	6502	97
H(71A)	-222	4239	6354	122
H(71B)	973	4509	6309	122
H(71C)	342	4674	5544	122
H(72A)	-1240	6893	7123	130
H(72B)	-434	7704	7820	130
H(72C)	-1024	6626	8032	130

Appendix 9

Crystallographic data for

Octa(hexaphenylbenzene)silsesquioxane

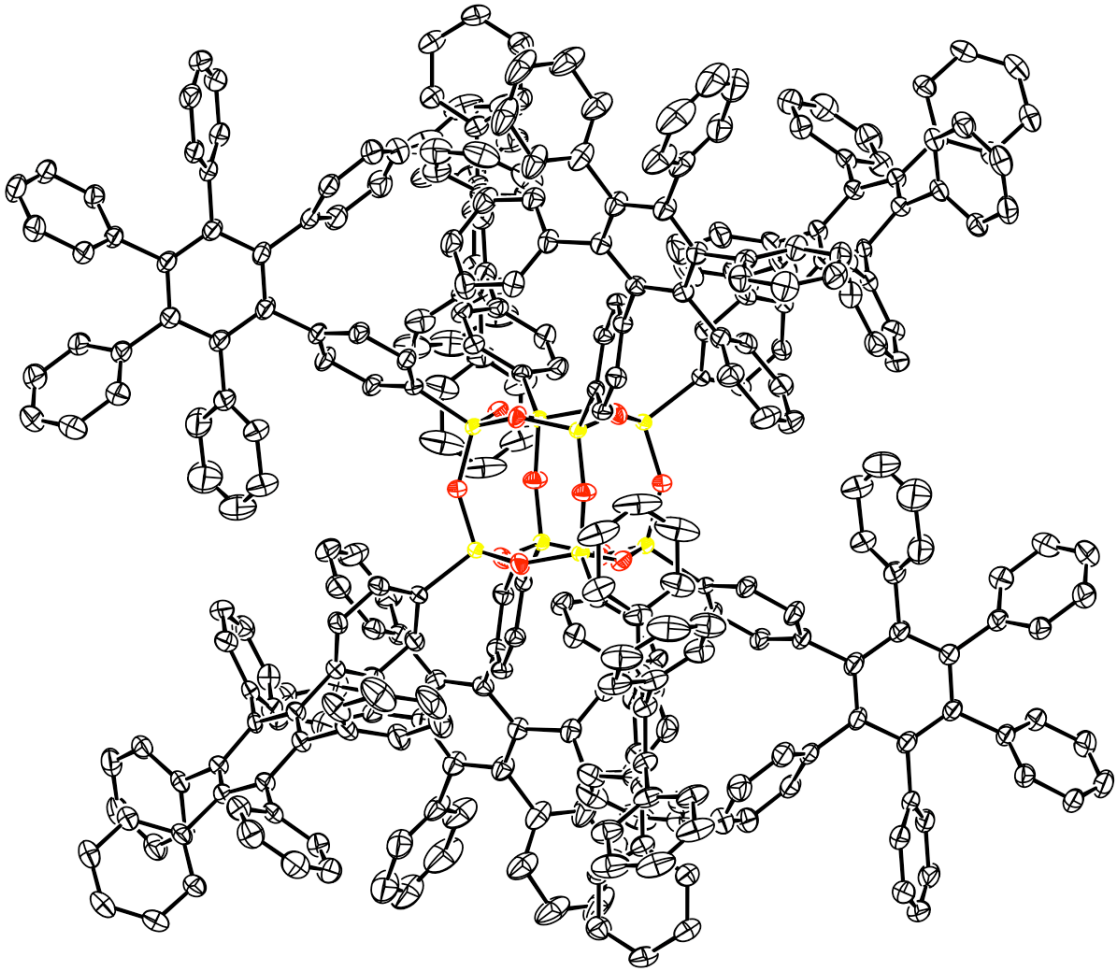

Figure A.9. 50 % thermal ellipsoid plots of octa(hexaphenylbenzene)silsesquioxane • octadeca toluene solvate. Labels, hydrogen atoms and toluene solvates are omitted for clarity.

Structure Determination.

Colorless prisms of **hpb** were grown from a toluene solution at 25 deg. C. A crystal of dimensions 0.36 x 0.35 x 0.17 mm mounted on a Bruker SMART APEX CCD-based X-ray diffractometer equipped with a low temperature device and fine focus Mo-target X-ray tube (l = 0.71073 A) operated at 1500 W power (50 kV, 30 mA). The X-ray intensities were measured at 85(2) K; the detector was placed at a distance 5.055 cm from the crystal. A total of 4095 frames were collected with a scan width of 0.5° in w and 0.45° in phi with an exposure time of 50 s/frame. The integration of the data yielded a total of 350341 reflections to a maximum 2q value of 54.30° of which 51117 were independent and 36764 were greater than 2s(I). The final cell constants (Table 1) were based on the xyz centroids of 9619 reflections above 10s(I). Analysis of the data showed negligible decay during data collection; the data were processed with SADABS and corrected for absorption. The structure was solved and refined with the Bruker SHELXTL software package, using the space group P1bar with Z = 1 for the formula $C_{336}H_{232}O_{12}Si_8 \bullet 18(C_7H_8)$. All non-hydrogen atoms were refined anisotropically with the hydrogen atoms placed in idealized positions. The structure contains a large solvent filled cavity centered about the crystallographic origin. The toluene solvates are show significant disorder and were modeled as diffuse solvent scattering by use of the SQUEEZE subroutine of the PLATON program suite. Full matrix least-squares refinement based on F^2 converged at R1 = 0.0566 and wR2 = 0.1577 [based on I > 2sigma(I)], R1 = 0.0775 and wR2 = 0.1655 for all data. Additional details are presented in Table 1 and are given as Supporting Information in a CIF file.

Sheldrick, G.M. SHELXTL, v. 2008/3; Bruker Analytical X-ray, Madison, WI, 2008.

Sheldrick, G.M. SADABS, v. 2008/1. Program for Empirical Absorption Correction of Area Detector Data, University of Gottingen: Gottingen, Germany, 2008.

Saint Plus, v. 7.53, Bruker Analytical X-ray, Madison, WI, 2008.

A.L. Spek. (2008) PLATON, v. 180108, A Multi-purpose Crystallographic Tool, Utrecht University, Utrecht, The Netherlands.

Table 1. Crystal data and structure refinement for hpb.

Identification code	hpb
Empirical formula	C462 H376 O12 Si8
Formula weight	6344.35
Temperature	85(2) K
Wavelength	0.71073 A
Crystal system, space group	Triclinic, P-1
Unit cell dimensions	a = 21.6705(18) Å alpha = 70.874(1)° b = 22.7273(19) Å beta = 88.818(1)° c = 27.648(2) Å gamma = 64.954(1)°
Volume	11544.0(16) A^3
Z, Calculated density	1, 0.913 Mg/m^3
Absorption coefficient	0.073 mm^-1
F(000)	3356
Crystal size	0.36 x 0.35 x 0.17 mm
Theta range for data collection	1.05 to 27.15 deg.
Limiting indices	-27<=h<=27, -29<=k<=29, -35<=l<=35
Reflections collected / unique	350341 / 51117 [R(int) = 0.0521]
Completeness to theta = 27.15	99.8 %
Absorption correction	Semi-empirical from equivalents

Max. and min. transmission	0.9877 and 0.9743
Refinement method	Full-matrix least-squares on F^2
Data / restraints / parameters	51117 / 0 / 1603
Goodness-of-fit on F^2	1.040
Final R indices [I>2sigma(I)]	R1 = 0.0566, wR2 = 0.1577
R indices (all data)	R1 = 0.0755, wR2 = 0.1655
Largest diff. peak and hole	0.478 and -0.284 e.A^-3

Table 2. Atomic coordinates (x 10^4) and equivalent isotropic displacement parameters (A^2 x 10^3) for hpb.

U(eq) is defined as one third of the trace of the orthogonalized Uij tensor.

	x	y	z	U(eq)
Si(1)	9402(1)	188(1)	5833(1)	20(1)
Si(2)	9031(1)	1311(1)	4720(1)	20(1)
Si(3)	10580(1)	872(1)	4637(1)	20(1)
Si(4)	9053(1)	247(1)	4251(1)	21(1)
O(1)	10205(1)	-24(1)	5952(1)	29(1)
O(2)	9060(1)	857(1)	5312(1)	27(1)
O(3)	9765(1)	1314(1)	4621(1)	28(1)
O(4)	10695(1)	439(1)	4255(1)	27(1)
O(5)	10904(1)	353(1)	5221(1)	27(1)
O(6)	8853(1)	963(1)	4353(1)	28(1)
C(1)	8956(1)	397(1)	6366(1)	23(1)
C(2)	8236(1)	736(1)	6283(1)	25(1)
C(3)	7868(1)	905(1)	6672(1)	26(1)
C(4)	8209(1)	741(1)	7154(1)	25(1)
C(5)	8921(1)	420(1)	7236(1)	27(1)
C(6)	9293(1)	247(1)	6846(1)	27(1)
C(7)	7783(1)	922(1)	7564(1)	26(1)
C(8)	7317(1)	638(1)	7718(1)	27(1)
C(9)	6850(1)	875(1)	8045(1)	34(1)
C(10)	6876(1)	1361(1)	8240(1)	34(1)
C(11)	7380(1)	1593(1)	8125(1)	29(1)
C(12)	7836(1)	1381(1)	7776(1)	26(1)
C(13)	7328(1)	92(1)	7525(1)	30(1)
C(14)	7933(1)	-513(1)	7623(1)	38(1)
C(15)	7980(1)	-1016(1)	7424(1)	45(1)
C(16)	7415(1)	-918(1)	7126(1)	43(1)
C(17)	6812(1)	-329(1)	7035(1)	39(1)
C(18)	6765(1)	173(1)	7234(1)	33(1)
C(19)	6323(1)	606(1)	8203(1)	43(1)
C(20)	6508(1)	-56(1)	8550(1)	55(1)
C(21)	6000(2)	-273(1)	8720(1)	69(1)
C(22)	5328(2)	159(2)	8545(1)	74(1)
C(23)	5132(1)	828(1)	8189(1)	67(1)
C(24)	5632(1)	1045(1)	8024(1)	53(1)
C(25)	6348(1)	1640(1)	8569(1)	42(1)
C(26)	6392(1)	1246(1)	9081(1)	59(1)

C(27)	5884(2)	1519(2)	9371(1)	77(1)
C(28)	5336(2)	2153(2)	9157(1)	83(1)
C(29)	5289(1)	2538(1)	8652(1)	84(1)
C(30)	5800(1)	2283(1)	8359(1)	60(1)
C(31)	7444(1)	2056(1)	8380(1)	29(1)
C(32)	7772(1)	1768(1)	8883(1)	38(1)
C(33)	7851(1)	2182(1)	9128(1)	46(1)
C(34)	7606(1)	2882(1)	8873(1)	43(1)
C(35)	7265(1)	3174(1)	8375(1)	42(1)
C(36)	7184(1)	2766(1)	8127(1)	36(1)
C(37)	8339(1)	1678(1)	7624(1)	28(1)
C(38)	8861(1)	1536(1)	7987(1)	40(1)
C(39)	9328(1)	1818(1)	7851(1)	50(1)
C(40)	9268(1)	2246(1)	7341(1)	51(1)
C(41)	8757(1)	2380(1)	6979(1)	46(1)
C(42)	8292(1)	2098(1)	7116(1)	35(1)
C(43)	8363(1)	2199(1)	4576(1)	24(1)
C(44)	7826(1)	2337(1)	4876(1)	30(1)
C(45)	7293(1)	2995(1)	4749(1)	32(1)
C(46)	7269(1)	3534(1)	4314(1)	28(1)
C(47)	7809(1)	3411(1)	4027(1)	31(1)
C(48)	8355(1)	2748(1)	4160(1)	31(1)
C(49)	6644(1)	4216(1)	4146(1)	29(1)
C(50)	6501(1)	4646(1)	4443(1)	27(1)
C(51)	5882(1)	5288(1)	4278(1)	28(1)
C(52)	5455(1)	5487(1)	3822(1)	28(1)
C(53)	5607(1)	5036(1)	3537(1)	29(1)
C(54)	6202(1)	4402(1)	3703(1)	31(1)
C(55)	6971(1)	4436(1)	4903(1)	31(1)
C(56)	7563(1)	4534(1)	4855(1)	35(1)
C(57)	8022(1)	4330(1)	5286(1)	40(1)
C(58)	7905(1)	4012(1)	5764(1)	38(1)
C(59)	7323(1)	3896(1)	5821(1)	38(1)
C(60)	6858(1)	4109(1)	5396(1)	34(1)
C(61)	5684(1)	5696(1)	4631(1)	30(1)
C(62)	6096(1)	5955(1)	4777(1)	35(1)
C(63)	5925(1)	6260(1)	5150(1)	42(1)
C(64)	5351(1)	6304(1)	5388(1)	44(1)
C(65)	4924(1)	6059(1)	5239(1)	40(1)
C(66)	5085(1)	5769(1)	4858(1)	33(1)
C(67)	4853(1)	6185(1)	3623(1)	29(1)
C(68)	4197(1)	6278(1)	3497(1)	33(1)
C(69)	3662(1)	6939(1)	3271(1)	37(1)
C(70)	3782(1)	7516(1)	3172(1)	39(1)
C(71)	4425(1)	7433(1)	3306(1)	38(1)
C(72)	4966(1)	6776(1)	3530(1)	33(1)
C(73)	5154(1)	5206(1)	3068(1)	31(1)
C(74)	5091(1)	5721(1)	2607(1)	40(1)

C(75)	4707(1)	5817(1)	2167(1)	47(1)
C(76)	4379(1)	5416(1)	2183(1)	49(1)
C(77)	4427(1)	4910(1)	2643(1)	44(1)
C(78)	4809(1)	4804(1)	3082(1)	37(1)
C(79)	6373(1)	3916(1)	3410(1)	36(1)
C(80)	6376(1)	3274(1)	3631(1)	45(1)
C(81)	6569(1)	2812(1)	3368(1)	60(1)
C(82)	6736(1)	2985(1)	2885(1)	70(1)
C(83)	6725(1)	3636(1)	2645(1)	71(1)
C(84)	6551(1)	4095(1)	2919(1)	50(1)
C(85)	10972(1)	1469(1)	4420(1)	24(1)
C(86)	11229(1)	1586(1)	3949(1)	28(1)
C(87)	11474(1)	2083(1)	3780(1)	31(1)
C(88)	11461(1)	2478(1)	4074(1)	32(1)
C(89)	11228(1)	2350(1)	4552(1)	35(1)
C(90)	10986(1)	1850(1)	4722(1)	30(1)
C(91)	11679(1)	3044(1)	3874(1)	33(1)
C(92)	11189(1)	3736(1)	3766(1)	36(1)
C(93)	11384(1)	4277(1)	3577(1)	33(1)
C(94)	12073(1)	4117(1)	3491(1)	31(1)
C(95)	12557(1)	3430(1)	3600(1)	31(1)
C(96)	12356(1)	2892(1)	3796(1)	30(1)
C(97)	10466(1)	3882(1)	3867(1)	50(1)
C(98)	10069(1)	3721(1)	3596(1)	57(1)
C(99)	9406(1)	3834(1)	3708(1)	88(1)
C(100)	9150(1)	4097(2)	4083(2)	112(1)
C(101)	9537(2)	4275(2)	4349(2)	103(1)
C(102)	10198(1)	4165(1)	4247(1)	72(1)
C(103)	10869(1)	5006(1)	3486(1)	37(1)
C(104)	10277(1)	5315(1)	3138(1)	47(1)
C(105)	9782(1)	5990(1)	3079(1)	58(1)
C(106)	9884(1)	6343(1)	3364(1)	57(1)
C(107)	10474(1)	6042(1)	3705(1)	49(1)
C(108)	10962(1)	5377(1)	3772(1)	41(1)
C(109)	12286(1)	4693(1)	3300(1)	32(1)
C(110)	11972(1)	5242(1)	2843(1)	37(1)
C(111)	12186(1)	5766(1)	2674(1)	43(1)
C(112)	12718(1)	5735(1)	2958(1)	46(1)
C(113)	13046(1)	5183(1)	3420(1)	40(1)
C(114)	12821(1)	4670(1)	3587(1)	35(1)
C(115)	13285(1)	3268(1)	3499(1)	31(1)
C(116)	13431(1)	3504(1)	3004(1)	36(1)
C(117)	14106(1)	3358(1)	2915(1)	46(1)
C(118)	14637(1)	2976(1)	3321(1)	51(1)
C(119)	14498(1)	2730(1)	3817(1)	48(1)
C(120)	13824(1)	2876(1)	3907(1)	39(1)
C(121)	12888(1)	2150(1)	3936(1)	30(1)
C(122)	13268(1)	1906(1)	3576(1)	35(1)

C(123)	13778(1)	1228(1)	3716(1)	43(1)
C(124)	13905(1)	782(1)	4223(1)	48(1)
C(125)	13524(1)	1009(1)	4582(1)	47(1)
C(126)	13018(1)	1691(1)	4442(1)	38(1)
C(127)	8411(1)	383(1)	3753(1)	23(1)
C(128)	8230(1)	945(1)	3296(1)	33(1)
C(129)	7775(1)	1052(1)	2893(1)	33(1)
C(130)	7484(1)	595(1)	2949(1)	28(1)
C(131)	7663(1)	32(1)	3405(1)	30(1)
C(132)	8120(1)	-72(1)	3803(1)	27(1)
C(133)	6991(1)	729(1)	2511(1)	32(1)
C(134)	6300(1)	898(1)	2567(1)	30(1)
C(135)	5826(1)	1096(1)	2139(1)	29(1)
C(136)	6051(1)	1102(1)	1660(1)	32(1)
C(137)	6757(1)	893(1)	1611(1)	33(1)
C(138)	7218(1)	717(1)	2033(1)	32(1)
C(139)	6081(1)	844(1)	3093(1)	34(1)
C(140)	6094(1)	1284(1)	3335(1)	42(1)
C(141)	5930(1)	1201(1)	3828(1)	51(1)
C(142)	5752(1)	681(1)	4090(1)	55(1)
C(143)	5728(1)	244(1)	3851(1)	50(1)
C(144)	5890(1)	320(1)	3358(1)	40(1)
C(145)	5084(1)	1303(1)	2199(1)	30(1)
C(146)	4702(1)	1884(1)	2330(1)	34(1)
C(147)	4007(1)	2094(1)	2360(1)	39(1)
C(148)	3687(1)	1715(1)	2272(1)	40(1)
C(149)	4066(1)	1134(1)	2155(1)	39(1)
C(150)	4758(1)	926(1)	2113(1)	33(1)
C(151)	5541(1)	1345(1)	1198(1)	35(1)
C(152)	5018(1)	2009(1)	1027(1)	47(1)
C(153)	4520(1)	2230(1)	608(1)	60(1)
C(154)	4554(1)	1774(1)	364(1)	58(1)
C(155)	5076(1)	1128(1)	523(1)	54(1)
C(156)	5568(1)	906(1)	935(1)	43(1)
C(157)	7016(1)	846(1)	1113(1)	39(1)
C(158)	6852(1)	1431(1)	684(1)	48(1)
C(159)	7118(1)	1383(1)	225(1)	65(1)
C(160)	7542(1)	731(1)	205(1)	68(1)
C(161)	7706(1)	142(1)	634(1)	57(1)
C(162)	7447(1)	201(1)	1088(1)	45(1)
C(163)	7969(1)	505(1)	1987(1)	39(1)
C(164)	8453(1)	-164(1)	2275(1)	51(1)
C(165)	9151(1)	-369(2)	2239(1)	73(1)
C(166)	9360(1)	90(2)	1915(1)	80(1)
C(167)	8895(1)	739(2)	1636(1)	71(1)
C(168)	8194(1)	951(1)	1665(1)	52(1)

Table 3. Bond lengths [A] and angles [deg] for hpb

Si(1)-O(1)	1.6060(10)
Si(1)-O(2)	1.6096(10)
Si(1)-O(4)#1	1.6161(10)
Si(1)-C(1)	1.8275(13)
Si(2)-O(2)	1.6092(10)
Si(2)-O(6)	1.6117(10)
Si(2)-O(3)	1.6120(10)
Si(2)-C(43)	1.8307(13)
Si(3)-O(5)	1.6096(10)
Si(3)-O(3)	1.6134(9)
Si(3)-O(4)	1.6140(10)
Si(3)-C(85)	1.8289(14)
Si(4)-O(5)#1	1.6108(10)
Si(4)-O(1)#1	1.6174(9)
Si(4)-O(6)	1.6178(10)
Si(4)-C(127)	1.8316(14)
O(1)-Si(4)#1	1.6174(10)
O(4)-Si(1)#1	1.6161(10)
O(5)-Si(4)#1	1.6108(10)
C(1)-C(6)	1.395(2)
C(1)-C(2)	1.4011(18)
C(2)-C(3)	1.3829(18)
C(3)-C(4)	1.392(2)
C(4)-C(5)	1.3845(19)
C(4)-C(7)	1.4986(18)
C(5)-C(6)	1.3928(19)
C(7)-C(12)	1.3966(19)
C(7)-C(8)	1.4052(19)
C(8)-C(9)	1.3986(19)
C(8)-C(13)	1.4933(19)
C(9)-C(10)	1.399(2)
C(9)-C(19)	1.504(2)
C(10)-C(11)	1.392(2)
C(10)-C(25)	1.504(2)
C(11)-C(12)	1.4138(18)
C(11)-C(31)	1.495(2)
C(12)-C(37)	1.4971(19)
C(13)-C(18)	1.387(2)
C(13)-C(14)	1.388(2)
C(14)-C(15)	1.389(2)
C(15)-C(16)	1.385(3)
C(16)-C(17)	1.369(2)
C(17)-C(18)	1.390(2)

C(19)-C(20)	1.379(3)
C(19)-C(24)	1.388(3)
C(20)-C(21)	1.401(3)
C(21)-C(22)	1.352(4)
C(22)-C(23)	1.396(4)
C(23)-C(24)	1.382(3)
C(25)-C(30)	1.374(3)
C(25)-C(26)	1.384(3)
C(26)-C(27)	1.396(3)
C(27)-C(28)	1.364(4)
C(28)-C(29)	1.363(4)
C(29)-C(30)	1.395(3)
C(31)-C(36)	1.386(2)
C(31)-C(32)	1.386(2)
C(32)-C(33)	1.389(2)
C(33)-C(34)	1.368(3)
C(34)-C(35)	1.381(3)
C(35)-C(36)	1.384(2)
C(37)-C(38)	1.385(2)
C(37)-C(42)	1.392(2)
C(38)-C(39)	1.397(2)
C(39)-C(40)	1.397(3)
C(40)-C(41)	1.372(3)
C(41)-C(42)	1.393(2)
C(43)-C(48)	1.386(2)
C(43)-C(44)	1.4009(18)
C(44)-C(45)	1.3816(19)
C(45)-C(46)	1.391(2)
C(46)-C(47)	1.380(2)
C(46)-C(49)	1.4935(19)
C(47)-C(48)	1.3979(19)
C(49)-C(54)	1.402(2)
C(49)-C(50)	1.4077(19)
C(50)-C(51)	1.4373(18)
C(50)-C(55)	1.459(2)
C(51)-C(52)	1.404(2)
C(51)-C(61)	1.496(2)
C(52)-C(53)	1.4182(19)
C(52)-C(67)	1.4908(19)
C(53)-C(54)	1.4021(19)
C(53)-C(73)	1.483(2)
C(54)-C(79)	1.499(2)
C(55)-C(56)	1.388(2)
C(55)-C(60)	1.395(2)
C(56)-C(57)	1.384(2)
C(57)-C(58)	1.361(2)

C(58)-C(59)	1.390(2)
C(59)-C(60)	1.377(2)
C(61)-C(62)	1.387(2)
C(61)-C(66)	1.399(2)
C(62)-C(63)	1.384(2)
C(63)-C(64)	1.377(3)
C(64)-C(65)	1.393(3)
C(65)-C(66)	1.382(2)
C(67)-C(68)	1.380(2)
C(67)-C(72)	1.406(2)
C(68)-C(69)	1.390(2)
C(69)-C(70)	1.385(2)
C(70)-C(71)	1.366(2)
C(71)-C(72)	1.390(2)
C(73)-C(74)	1.383(2)
C(73)-C(78)	1.396(2)
C(74)-C(75)	1.390(2)
C(75)-C(76)	1.363(3)
C(76)-C(77)	1.377(3)
C(77)-C(78)	1.376(2)
C(79)-C(80)	1.381(2)
C(79)-C(84)	1.381(2)
C(80)-C(81)	1.386(2)
C(81)-C(82)	1.352(3)
C(82)-C(83)	1.399(4)
C(83)-C(84)	1.407(3)
C(85)-C(86)	1.3936(19)
C(85)-C(90)	1.3953(19)
C(86)-C(87)	1.3866(19)
C(87)-C(88)	1.389(2)
C(88)-C(89)	1.389(2)
C(88)-C(91)	1.4896(19)
C(89)-C(90)	1.388(2)
C(91)-C(96)	1.388(2)
C(91)-C(92)	1.407(2)
C(92)-C(93)	1.405(2)
C(92)-C(97)	1.498(2)
C(93)-C(94)	1.414(2)
C(93)-C(103)	1.492(2)
C(94)-C(95)	1.395(2)
C(94)-C(109)	1.5011(19)
C(95)-C(96)	1.4090(19)
C(95)-C(115)	1.5026(19)
C(96)-C(121)	1.506(2)
C(97)-C(98)	1.382(3)
C(97)-C(102)	1.397(3)
C(98)-C(99)	1.397(3)
C(99)-C(100)	1.358(4)

C(100)-C(101)	1.384(5)
C(101)-C(102)	1.386(3)
C(103)-C(104)	1.383(2)
C(103)-C(108)	1.402(2)
C(104)-C(105)	1.407(2)
C(105)-C(106)	1.373(3)
C(106)-C(107)	1.371(3)
C(107)-C(108)	1.381(2)
C(109)-C(110)	1.379(2)
C(109)-C(114)	1.391(2)
C(110)-C(111)	1.395(2)
C(111)-C(112)	1.372(3)
C(112)-C(113)	1.393(3)
C(113)-C(114)	1.390(2)
C(115)-C(116)	1.380(2)
C(115)-C(120)	1.394(2)
C(116)-C(117)	1.392(2)
C(117)-C(118)	1.380(3)
C(118)-C(119)	1.381(3)
C(119)-C(120)	1.391(2)
C(121)-C(122)	1.384(2)
C(121)-C(126)	1.392(2)
C(122)-C(123)	1.389(2)
C(123)-C(124)	1.384(3)
C(124)-C(125)	1.370(3)
C(125)-C(126)	1.393(2)

C(127)-C(128)	1.386(2)
C(127)-C(132)	1.3946(19)
C(128)-C(129)	1.393(2)
C(129)-C(130)	1.394(2)
C(130)-C(131)	1.385(2)
C(130)-C(133)	1.496(2)
C(131)-C(132)	1.388(2)
C(133)-C(134)	1.400(2)
C(133)-C(138)	1.404(2)
C(134)-C(135)	1.403(2)
C(134)-C(139)	1.502(2)
C(135)-C(136)	1.398(2)
C(135)-C(145)	1.4946(19)
C(136)-C(137)	1.417(2)
C(136)-C(151)	1.497(2)
C(137)-C(138)	1.388(2)
C(137)-C(157)	1.496(2)
C(138)-C(163)	1.504(2)
C(139)-C(140)	1.384(2)
C(139)-C(144)	1.401(2)

C(140)-C(141)	1.375(3)
C(141)-C(142)	1.372(3)
C(142)-C(143)	1.377(3)
C(143)-C(144)	1.376(2)
C(145)-C(146)	1.391(2)
C(145)-C(150)	1.393(2)
C(146)-C(147)	1.383(2)
C(147)-C(148)	1.391(2)
C(148)-C(149)	1.367(2)
C(149)-C(150)	1.384(2)
C(151)-C(152)	1.375(3)
C(151)-C(156)	1.396(2)
C(152)-C(153)	1.403(3)
C(153)-C(154)	1.390(3)
C(154)-C(155)	1.349(3)
C(155)-C(156)	1.381(2)
C(157)-C(158)	1.373(2)
C(157)-C(162)	1.389(3)
C(158)-C(159)	1.400(3)
C(159)-C(160)	1.393(3)
C(160)-C(161)	1.378(3)
C(161)-C(162)	1.388(2)
C(163)-C(168)	1.366(3)
C(163)-C(164)	1.392(3)
C(164)-C(165)	1.393(3)
C(165)-C(166)	1.366(4)
C(166)-C(167)	1.347(4)
C(167)-C(168)	1.396(3)

O(1)-Si(1)-O(2)	110.08(5)
O(1)-Si(1)-O(4)#1	110.06(5)
O(2)-Si(1)-O(4)#1	107.72(5)
O(1)-Si(1)-C(1)	110.17(6)
O(2)-Si(1)-C(1)	108.55(5)
O(4)#1-Si(1)-C(1)	110.20(5)
O(2)-Si(2)-O(6)	108.47(5)
O(2)-Si(2)-O(3)	110.25(5)
O(6)-Si(2)-O(3)	108.79(5)
O(2)-Si(2)-C(43)	109.24(6)
O(6)-Si(2)-C(43)	110.06(6)
O(3)-Si(2)-C(43)	110.02(6)
O(5)-Si(3)-O(3)	108.49(5)
O(5)-Si(3)-O(4)	110.47(5)
O(3)-Si(3)-O(4)	108.70(5)
O(5)-Si(3)-C(85)	110.38(6)
O(3)-Si(3)-C(85)	108.96(5)
O(4)-Si(3)-C(85)	109.79(6)
O(5)#1-Si(4)-O(1)#1	109.45(5)

O(5)#1-Si(4)-O(6)	110.05(5)
O(1)#1-Si(4)-O(6)	107.99(5)
O(5)#1-Si(4)-C(127)	110.42(6)
O(1)#1-Si(4)-C(127)	109.18(6)
O(6)-Si(4)-C(127)	109.71(6)
Si(1)-O(1)-Si(4)#1	147.22(7)
Si(2)-O(2)-Si(1)	154.24(6)
Si(2)-O(3)-Si(3)	147.87(7)
Si(3)-O(4)-Si(1)#1	144.19(7)
Si(3)-O(5)-Si(4)#1	153.52(7)
Si(2)-O(6)-Si(4)	144.89(7)
C(6)-C(1)-C(2)	118.21(12)
C(6)-C(1)-Si(1)	123.77(10)
C(2)-C(1)-Si(1)	118.01(10)
C(3)-C(2)-C(1)	120.88(13)
C(2)-C(3)-C(4)	120.44(12)
C(5)-C(4)-C(3)	119.28(12)
C(5)-C(4)-C(7)	122.61(13)
C(3)-C(4)-C(7)	118.11(12)
C(4)-C(5)-C(6)	120.41(13)
C(5)-C(6)-C(1)	120.76(12)
C(12)-C(7)-C(8)	120.82(12)
C(12)-C(7)-C(4)	120.54(12)
C(8)-C(7)-C(4)	118.61(12)
C(9)-C(8)-C(7)	119.33(13)
C(9)-C(8)-C(13)	121.40(13)
C(7)-C(8)-C(13)	119.27(12)
C(8)-C(9)-C(10)	119.96(13)
C(8)-C(9)-C(19)	121.24(13)
C(10)-C(9)-C(19)	118.79(13)
C(11)-C(10)-C(9)	120.45(13)
C(11)-C(10)-C(25)	120.05(13)
C(9)-C(10)-C(25)	119.49(13)
C(10)-C(11)-C(12)	120.02(13)
C(10)-C(11)-C(31)	119.51(12)
C(12)-C(11)-C(31)	120.46(12)
C(7)-C(12)-C(11)	118.99(12)
C(7)-C(12)-C(37)	121.48(12)
C(11)-C(12)-C(37)	119.46(12)
C(18)-C(13)-C(14)	118.17(14)
C(18)-C(13)-C(8)	122.78(13)
C(14)-C(13)-C(8)	119.01(14)
C(13)-C(14)-C(15)	121.08(16)
C(16)-C(15)-C(14)	119.80(16)
C(17)-C(16)-C(15)	119.69(15)
C(16)-C(17)-C(18)	120.48(16)
C(13)-C(18)-C(17)	120.75(15)
C(20)-C(19)-C(24)	119.02(17)

C(20)-C(19)-C(9)	121.31(18)
C(24)-C(19)-C(9)	119.55(17)
C(19)-C(20)-C(21)	120.0(2)
C(22)-C(21)-C(20)	120.6(2)
C(21)-C(22)-C(23)	120.14(19)
C(24)-C(23)-C(22)	119.3(2)
C(23)-C(24)-C(19)	120.9(2)
C(30)-C(25)-C(26)	119.08(17)
C(30)-C(25)-C(10)	120.09(16)
C(26)-C(25)-C(10)	120.80(18)
C(25)-C(26)-C(27)	119.0(2)
C(28)-C(27)-C(26)	121.6(2)
C(29)-C(28)-C(27)	119.3(2)
C(28)-C(29)-C(30)	120.0(3)
C(25)-C(30)-C(29)	120.9(2)
C(36)-C(31)-C(32)	118.84(14)
C(36)-C(31)-C(11)	121.83(13)
C(32)-C(31)-C(11)	119.32(13)
C(31)-C(32)-C(33)	120.69(15)
C(34)-C(33)-C(32)	120.19(16)
C(33)-C(34)-C(35)	119.42(15)
C(34)-C(35)-C(36)	120.89(16)
C(35)-C(36)-C(31)	119.94(15)
C(38)-C(37)-C(42)	118.94(14)
C(38)-C(37)-C(12)	120.40(13)
C(42)-C(37)-C(12)	120.67(13)
C(37)-C(38)-C(39)	120.92(16)
C(38)-C(39)-C(40)	119.35(17)
C(41)-C(40)-C(39)	119.91(16)
C(40)-C(41)-C(42)	120.53(17)
C(37)-C(42)-C(41)	120.34(16)
C(48)-C(43)-C(44)	118.00(12)
C(48)-C(43)-Si(2)	121.72(10)
C(44)-C(43)-Si(2)	120.23(10)
C(45)-C(44)-C(43)	120.85(13)
C(44)-C(45)-C(46)	120.67(13)
C(47)-C(46)-C(45)	118.94(12)
C(47)-C(46)-C(49)	121.35(13)
C(45)-C(46)-C(49)	119.59(12)
C(46)-C(47)-C(48)	120.38(13)
C(43)-C(48)-C(47)	121.00(13)
C(54)-C(49)-C(50)	121.63(12)
C(54)-C(49)-C(46)	118.70(13)
C(50)-C(49)-C(46)	119.64(13)
C(49)-C(50)-C(51)	117.80(13)
C(49)-C(50)-C(55)	120.23(12)
C(51)-C(50)-C(55)	121.97(12)
C(52)-C(51)-C(50)	120.56(13)

C(52)-C(51)-C(61)	121.66(12)
C(50)-C(51)-C(61)	117.56(13)
C(51)-C(52)-C(53)	120.08(12)
C(51)-C(52)-C(67)	120.32(12)
C(53)-C(52)-C(67)	119.56(13)
C(54)-C(53)-C(52)	119.56(14)
C(54)-C(53)-C(73)	118.15(13)
C(52)-C(53)-C(73)	122.29(12)
C(49)-C(54)-C(53)	120.26(13)
C(49)-C(54)-C(79)	119.22(12)
C(53)-C(54)-C(79)	120.51(14)
C(56)-C(55)-C(60)	118.38(14)
C(56)-C(55)-C(50)	119.99(14)
C(60)-C(55)-C(50)	121.57(13)
C(57)-C(56)-C(55)	121.04(15)
C(58)-C(57)-C(56)	120.05(15)
C(57)-C(58)-C(59)	119.93(15)
C(60)-C(59)-C(58)	120.38(15)
C(59)-C(60)-C(55)	120.18(14)
C(62)-C(61)-C(66)	118.36(14)
C(62)-C(61)-C(51)	122.89(13)
C(66)-C(61)-C(51)	118.52(13)
C(63)-C(62)-C(61)	120.42(15)
C(64)-C(63)-C(62)	120.97(16)
C(63)-C(64)-C(65)	119.38(16)
C(66)-C(65)-C(64)	119.67(16)
C(65)-C(66)-C(61)	121.12(15)
C(68)-C(67)-C(72)	118.51(13)
C(68)-C(67)-C(52)	122.80(13)
C(72)-C(67)-C(52)	118.58(13)
C(67)-C(68)-C(69)	120.96(15)
C(70)-C(69)-C(68)	120.00(15)
C(71)-C(70)-C(69)	119.71(14)
C(70)-C(71)-C(72)	120.95(15)
C(71)-C(72)-C(67)	119.83(15)
C(74)-C(73)-C(78)	118.40(15)
C(74)-C(73)-C(53)	122.44(14)
C(78)-C(73)-C(53)	119.03(14)
C(73)-C(74)-C(75)	119.98(16)
C(76)-C(75)-C(74)	121.10(17)
C(75)-C(76)-C(77)	119.41(17)
C(78)-C(77)-C(76)	120.36(17)
C(77)-C(78)-C(73)	120.74(16)
C(80)-C(79)-C(84)	118.96(16)
C(80)-C(79)-C(54)	120.78(15)
C(84)-C(79)-C(54)	120.23(15)
C(79)-C(80)-C(81)	120.48(19)
C(82)-C(81)-C(80)	121.1(2)

C(81)-C(82)-C(83)	119.97(19)
C(82)-C(83)-C(84)	118.8(2)
C(79)-C(84)-C(83)	120.6(2)
C(86)-C(85)-C(90)	118.16(12)
C(86)-C(85)-Si(3)	122.52(10)
C(90)-C(85)-Si(3)	119.25(10)
C(87)-C(86)-C(85)	120.80(13)
C(86)-C(87)-C(88)	120.60(13)
C(89)-C(88)-C(87)	119.05(13)
C(89)-C(88)-C(91)	120.51(13)
C(87)-C(88)-C(91)	120.43(13)
C(90)-C(89)-C(88)	120.24(13)
C(89)-C(90)-C(85)	121.07(13)
C(96)-C(91)-C(92)	120.38(13)
C(96)-C(91)-C(88)	120.47(13)
C(92)-C(91)-C(88)	119.15(13)
C(93)-C(92)-C(91)	119.99(13)
C(93)-C(92)-C(97)	120.90(13)
C(91)-C(92)-C(97)	119.10(13)
C(92)-C(93)-C(94)	119.20(13)
C(92)-C(93)-C(103)	119.63(13)
C(94)-C(93)-C(103)	121.14(13)
C(95)-C(94)-C(93)	120.57(13)
C(95)-C(94)-C(109)	120.14(13)
C(93)-C(94)-C(109)	119.25(13)
C(94)-C(95)-C(96)	119.64(13)
C(94)-C(95)-C(115)	120.02(12)
C(96)-C(95)-C(115)	120.33(13)
C(91)-C(96)-C(95)	120.21(13)
C(91)-C(96)-C(121)	120.41(12)
C(95)-C(96)-C(121)	119.35(12)
C(98)-C(97)-C(102)	119.82(18)
C(98)-C(97)-C(92)	120.27(17)
C(102)-C(97)-C(92)	119.89(18)
C(97)-C(98)-C(99)	119.7(2)
C(100)-C(99)-C(98)	120.5(3)
C(99)-C(100)-C(101)	120.2(2)
C(100)-C(101)-C(102)	120.4(3)
C(101)-C(102)-C(97)	119.3(3)
C(104)-C(103)-C(108)	118.74(15)
C(104)-C(103)-C(93)	120.75(15)
C(108)-C(103)-C(93)	120.44(15)
C(103)-C(104)-C(105)	119.75(17)
C(106)-C(105)-C(104)	120.38(19)
C(107)-C(106)-C(105)	120.22(17)
C(106)-C(107)-C(108)	120.12(18)
C(107)-C(108)-C(103)	120.78(17)
C(110)-C(109)-C(114)	118.80(14)

C(110)-C(109)-C(94)	121.82(14)
C(114)-C(109)-C(94)	119.37(14)
C(109)-C(110)-C(111)	120.37(16)
C(112)-C(111)-C(110)	120.33(17)
C(111)-C(112)-C(113)	120.34(15)
C(114)-C(113)-C(112)	118.75(16)
C(113)-C(114)-C(109)	121.41(16)
C(116)-C(115)-C(120)	118.96(14)
C(116)-C(115)-C(95)	120.84(14)
C(120)-C(115)-C(95)	120.21(14)
C(115)-C(116)-C(117)	120.41(17)
C(118)-C(117)-C(116)	120.38(17)
C(117)-C(118)-C(119)	119.79(16)
C(118)-C(119)-C(120)	119.88(18)
C(119)-C(120)-C(115)	120.58(17)
C(122)-C(121)-C(126)	118.19(14)
C(122)-C(121)-C(96)	121.98(14)
C(126)-C(121)-C(96)	119.82(13)
C(121)-C(122)-C(123)	121.22(16)
C(124)-C(123)-C(122)	119.71(16)
C(125)-C(124)-C(123)	119.96(16)
C(124)-C(125)-C(126)	120.21(17)
C(121)-C(126)-C(125)	120.68(16)
C(128)-C(127)-C(132)	118.31(13)
C(128)-C(127)-Si(4)	118.70(10)
C(132)-C(127)-Si(4)	122.91(11)
C(127)-C(128)-C(129)	121.09(14)
C(128)-C(129)-C(130)	120.03(14)
C(131)-C(130)-C(129)	119.16(13)
C(131)-C(130)-C(133)	122.30(13)
C(129)-C(130)-C(133)	118.53(13)
C(130)-C(131)-C(132)	120.42(13)
C(131)-C(132)-C(127)	120.98(13)
C(134)-C(133)-C(138)	119.98(13)
C(134)-C(133)-C(130)	120.39(13)
C(138)-C(133)-C(130)	119.57(13)
C(133)-C(134)-C(135)	119.96(13)
C(133)-C(134)-C(139)	119.04(13)
C(135)-C(134)-C(139)	120.98(13)
C(136)-C(135)-C(134)	119.83(13)
C(136)-C(135)-C(145)	120.69(12)
C(134)-C(135)-C(145)	119.47(13)
C(135)-C(136)-C(137)	120.06(13)
C(135)-C(136)-C(151)	119.80(13)
C(137)-C(136)-C(151)	120.13(13)
C(138)-C(137)-C(136)	119.60(14)
C(138)-C(137)-C(157)	119.52(13)
C(136)-C(137)-C(157)	120.87(13)

C(137)-C(138)-C(133)	120.42(13)
C(137)-C(138)-C(163)	120.41(13)
C(133)-C(138)-C(163)	119.17(13)
C(140)-C(139)-C(144)	118.68(15)
C(140)-C(139)-C(134)	121.25(15)
C(144)-C(139)-C(134)	119.99(14)
C(141)-C(140)-C(139)	120.39(18)
C(142)-C(141)-C(140)	120.80(18)
C(141)-C(142)-C(143)	119.53(17)
C(144)-C(143)-C(142)	120.52(19)
C(143)-C(144)-C(139)	120.07(17)
C(146)-C(145)-C(150)	118.68(13)
C(146)-C(145)-C(135)	120.78(13)
C(150)-C(145)-C(135)	120.53(13)
C(147)-C(146)-C(145)	120.61(14)
C(146)-C(147)-C(148)	120.10(15)
C(149)-C(148)-C(147)	119.36(15)
C(148)-C(149)-C(150)	121.12(15)
C(149)-C(150)-C(145)	120.09(14)
C(152)-C(151)-C(156)	118.09(15)
C(152)-C(151)-C(136)	120.29(15)
C(156)-C(151)-C(136)	121.61(15)
C(151)-C(152)-C(153)	120.6(2)
C(154)-C(153)-C(152)	119.7(2)
C(155)-C(154)-C(153)	119.61(18)
C(154)-C(155)-C(156)	121.0(2)
C(155)-C(156)-C(151)	120.88(19)
C(158)-C(157)-C(162)	119.44(16)
C(158)-C(157)-C(137)	121.11(16)
C(162)-C(157)-C(137)	119.41(15)
C(157)-C(158)-C(159)	120.64(19)
C(160)-C(159)-C(158)	119.2(2)
C(161)-C(160)-C(159)	120.33(18)
C(160)-C(161)-C(162)	119.7(2)
C(161)-C(162)-C(157)	120.70(18)
C(168)-C(163)-C(164)	118.42(17)
C(168)-C(163)-C(138)	121.83(16)
C(164)-C(163)-C(138)	119.75(16)
C(163)-C(164)-C(165)	120.5(2)
C(166)-C(165)-C(164)	119.7(2)
C(167)-C(166)-C(165)	120.2(2)
C(166)-C(167)-C(168)	120.9(2)
C(163)-C(168)-C(167)	120.3(2)

Symmetry transformations used to generate equivalent atoms:

#1 -x+2,-y,-z+1

Table 4. Anisotropic displacement parameters (A^2 x 10^3) for hpb.

The anisotropic displacement factor exponent takes the form: -2 pi^2 [h^2 a*^2 U11 + ... + 2 h k a* b* U12

	U11	U22	U33	U23	U13	U12
Si(1)	18(1)	21(1)	25(1)	-12(1)	8(1)	-10(1)
Si(2)	17(1)	19(1)	26(1)	-11(1)	7(1)	-8(1)
Si(3)	18(1)	20(1)	26(1)	-12(1)	8(1)	-11(1)
Si(4)	18(1)	22(1)	26(1)	-12(1)	6(1)	-10(1)
O(1)	22(1)	39(1)	32(1)	-19(1)	9(1)	-14(1)
O(2)	28(1)	24(1)	27(1)	-11(1)	10(1)	-8(1)
O(3)	21(1)	25(1)	42(1)	-14(1)	10(1)	-11(1)
O(4)	33(1)	28(1)	34(1)	-19(1)	15(1)	-20(1)
O(5)	26(1)	30(1)	30(1)	-9(1)	3(1)	-16(1)
O(6)	26(1)	24(1)	35(1)	-15(1)	2(1)	-9(1)
C(1)	23(1)	23(1)	28(1)	-14(1)	11(1)	-13(1)
C(2)	25(1)	28(1)	26(1)	-11(1)	7(1)	-13(1)
C(3)	21(1)	28(1)	30(1)	-10(1)	7(1)	-11(1)
C(4)	28(1)	26(1)	27(1)	-13(1)	13(1)	-14(1)
C(5)	28(1)	29(1)	26(1)	-14(1)	5(1)	-12(1)
C(6)	22(1)	28(1)	33(1)	-14(1)	8(1)	-11(1)
C(7)	25(1)	28(1)	24(1)	-10(1)	8(1)	-11(1)
C(8)	33(1)	30(1)	23(1)	-11(1)	8(1)	-17(1)
C(9)	44(1)	42(1)	31(1)	-19(1)	17(1)	-29(1)
C(10)	42(1)	42(1)	31(1)	-21(1)	20(1)	-27(1)
C(11)	35(1)	31(1)	25(1)	-12(1)	12(1)	-18(1)
C(12)	27(1)	28(1)	23(1)	-9(1)	9(1)	-14(1)
C(13)	40(1)	32(1)	24(1)	-12(1)	14(1)	-22(1)
C(14)	44(1)	33(1)	39(1)	-12(1)	4(1)	-21(1)
C(15)	50(1)	31(1)	59(1)	-21(1)	15(1)	-18(1)
C(16)	52(1)	43(1)	54(1)	-30(1)	19(1)	-30(1)
C(17)	49(1)	51(1)	38(1)	-25(1)	17(1)	-34(1)
C(18)	38(1)	38(1)	33(1)	-16(1)	16(1)	-22(1)
C(19)	61(1)	63(1)	42(1)	-38(1)	34(1)	-47(1)

C(20)	87(2)	67(1)	52(1)	-38(1)	42(1)	-60(1)
C(21)	112(2)	83(2)	73(1)	-55(1)	66(1)	-80(2)
C(22)	105(2)	112(2)	92(2)	-82(2)	78(2)	-94(2)
C(23)	70(1)	114(2)	78(2)	-70(2)	51(1)	-71(1)
C(24)	60(1)	83(1)	55(1)	-47(1)	34(1)	-52(1)
C(25)	54(1)	64(1)	47(1)	-39(1)	34(1)	-45(1)
C(26)	75(1)	100(2)	47(1)	-45(1)	38(1)	-64(1)
C(27)	102(2)	136(2)	59(1)	-66(2)	59(1)	-91(2)
C(28)	100(2)	115(2)	112(2)	-91(2)	86(2)	-83(2)
C(29)	92(2)	78(2)	134(2)	-72(2)	88(2)	-61(1)
C(30)	68(1)	58(1)	85(2)	-44(1)	54(1)	-43(1)
C(31)	31(1)	36(1)	29(1)	-16(1)	14(1)	-20(1)
C(32)	46(1)	37(1)	34(1)	-15(1)	9(1)	-19(1)
C(33)	57(1)	55(1)	33(1)	-22(1)	5(1)	-26(1)
C(34)	51(1)	50(1)	47(1)	-33(1)	18(1)	-30(1)
C(35)	50(1)	36(1)	47(1)	-19(1)	11(1)	-23(1)
C(36)	42(1)	36(1)	35(1)	-13(1)	6(1)	-20(1)
C(37)	29(1)	29(1)	34(1)	-16(1)	12(1)	-15(1)
C(38)	39(1)	52(1)	40(1)	-24(1)	15(1)	-25(1)
C(39)	40(1)	71(1)	62(1)	-37(1)	19(1)	-35(1)
C(40)	41(1)	49(1)	77(1)	-25(1)	28(1)	-30(1)
C(41)	38(1)	35(1)	60(1)	-10(1)	22(1)	-17(1)
C(42)	29(1)	29(1)	42(1)	-9(1)	11(1)	-10(1)
C(43)	19(1)	21(1)	33(1)	-13(1)	6(1)	-8(1)
C(44)	28(1)	22(1)	35(1)	-10(1)	11(1)	-10(1)
C(45)	25(1)	28(1)	43(1)	-15(1)	14(1)	-9(1)
C(46)	23(1)	23(1)	39(1)	-13(1)	5(1)	-9(1)
C(47)	31(1)	22(1)	36(1)	-8(1)	10(1)	-11(1)
C(48)	24(1)	27(1)	39(1)	-13(1)	12(1)	-9(1)
C(49)	26(1)	23(1)	37(1)	-11(1)	10(1)	-10(1)
C(50)	29(1)	16(1)	38(1)	-12(1)	16(1)	-11(1)
C(51)	23(1)	22(1)	36(1)	-11(1)	6(1)	-9(1)
C(52)	26(1)	22(1)	37(1)	-12(1)	9(1)	-10(1)
C(53)	26(1)	25(1)	37(1)	-13(1)	9(1)	-10(1)
C(54)	28(1)	23(1)	41(1)	-14(1)	9(1)	-9(1)
C(55)	26(1)	19(1)	46(1)	-15(1)	8(1)	-7(1)
C(56)	28(1)	31(1)	42(1)	-12(1)	8(1)	-10(1)
C(57)	27(1)	40(1)	56(1)	-22(1)	6(1)	-16(1)
C(58)	36(1)	32(1)	42(1)	-15(1)	-4(1)	-10(1)
C(59)	44(1)	33(1)	38(1)	-12(1)	5(1)	-18(1)
C(60)	32(1)	31(1)	42(1)	-13(1)	9(1)	-16(1)
C(61)	28(1)	18(1)	37(1)	-9(1)	2(1)	-4(1)
C(62)	32(1)	25(1)	41(1)	-10(1)	-1(1)	-8(1)
C(63)	47(1)	28(1)	48(1)	-14(1)	-6(1)	-13(1)
C(64)	56(1)	32(1)	40(1)	-18(1)	4(1)	-13(1)
C(65)	44(1)	34(1)	41(1)	-16(1)	12(1)	-13(1)
C(66)	32(1)	23(1)	42(1)	-13(1)	4(1)	-9(1)
C(67)	27(1)	24(1)	32(1)	-12(1)	8(1)	-6(1)

C(68)	31(1)	31(1)	34(1)	-13(1)	7(1)	-10(1)
C(69)	28(1)	38(1)	36(1)	-15(1)	5(1)	-6(1)
C(70)	39(1)	29(1)	33(1)	-10(1)	2(1)	-1(1)
C(71)	47(1)	27(1)	36(1)	-13(1)	8(1)	-11(1)
C(72)	35(1)	28(1)	33(1)	-12(1)	5(1)	-11(1)
C(73)	27(1)	24(1)	39(1)	-16(1)	9(1)	-7(1)
C(74)	37(1)	34(1)	42(1)	-10(1)	3(1)	-13(1)
C(75)	50(1)	43(1)	41(1)	-12(1)	1(1)	-16(1)
C(76)	45(1)	51(1)	49(1)	-24(1)	0(1)	-15(1)
C(77)	40(1)	44(1)	53(1)	-24(1)	6(1)	-19(1)
C(78)	37(1)	33(1)	44(1)	-16(1)	8(1)	-16(1)
C(79)	29(1)	29(1)	43(1)	-18(1)	1(1)	-3(1)
C(80)	40(1)	33(1)	61(1)	-23(1)	-1(1)	-10(1)
C(81)	53(1)	42(1)	88(2)	-38(1)	-6(1)	-12(1)
C(82)	62(1)	55(1)	88(2)	-51(1)	0(1)	-2(1)
C(83)	69(1)	70(2)	63(1)	-44(1)	10(1)	-6(1)
C(84)	49(1)	42(1)	48(1)	-25(1)	7(1)	-3(1)
C(85)	19(1)	24(1)	34(1)	-13(1)	9(1)	-11(1)
C(86)	31(1)	29(1)	35(1)	-17(1)	12(1)	-19(1)
C(87)	33(1)	33(1)	37(1)	-16(1)	17(1)	-21(1)
C(88)	31(1)	29(1)	47(1)	-18(1)	16(1)	-20(1)
C(89)	43(1)	41(1)	45(1)	-28(1)	22(1)	-31(1)
C(90)	33(1)	34(1)	36(1)	-19(1)	16(1)	-22(1)
C(91)	38(1)	35(1)	43(1)	-21(1)	19(1)	-25(1)
C(92)	33(1)	35(1)	54(1)	-22(1)	20(1)	-22(1)
C(93)	30(1)	30(1)	47(1)	-18(1)	12(1)	-16(1)
C(94)	32(1)	31(1)	39(1)	-14(1)	12(1)	-21(1)
C(95)	33(1)	33(1)	37(1)	-16(1)	12(1)	-22(1)
C(96)	36(1)	29(1)	36(1)	-16(1)	13(1)	-22(1)
C(97)	39(1)	36(1)	85(1)	-26(1)	32(1)	-24(1)
C(98)	35(1)	45(1)	95(2)	-21(1)	18(1)	-23(1)
C(99)	41(1)	70(2)	157(3)	-38(2)	31(2)	-32(1)
C(100)	58(2)	101(2)	203(4)	-73(2)	74(2)	-45(2)
C(101)	88(2)	97(2)	164(3)	-77(2)	89(2)	-57(2)
C(102)	72(1)	61(1)	115(2)	-53(1)	65(1)	-44(1)
C(103)	34(1)	32(1)	53(1)	-19(1)	19(1)	-20(1)
C(104)	36(1)	42(1)	70(1)	-27(1)	12(1)	-18(1)
C(105)	35(1)	50(1)	85(2)	-32(1)	8(1)	-11(1)
C(106)	44(1)	38(1)	88(2)	-29(1)	21(1)	-14(1)
C(107)	46(1)	43(1)	71(1)	-32(1)	21(1)	-23(1)
C(108)	36(1)	38(1)	61(1)	-27(1)	20(1)	-21(1)
C(109)	33(1)	29(1)	44(1)	-18(1)	16(1)	-19(1)
C(110)	34(1)	32(1)	51(1)	-16(1)	13(1)	-18(1)
C(111)	47(1)	32(1)	51(1)	-10(1)	12(1)	-21(1)
C(112)	55(1)	39(1)	62(1)	-23(1)	20(1)	-33(1)
C(113)	40(1)	37(1)	56(1)	-24(1)	16(1)	-25(1)
C(114)	38(1)	31(1)	43(1)	-19(1)	14(1)	-19(1)
C(115)	29(1)	26(1)	48(1)	-17(1)	11(1)	-17(1)

C(116)	38(1)	30(1)	50(1)	-19(1)	19(1)	-21(1)
C(117)	48(1)	40(1)	69(1)	-28(1)	32(1)	-30(1)
C(118)	35(1)	44(1)	92(2)	-37(1)	28(1)	-24(1)
C(119)	32(1)	39(1)	80(1)	-31(1)	7(1)	-16(1)
C(120)	39(1)	34(1)	54(1)	-22(1)	11(1)	-21(1)
C(121)	32(1)	31(1)	40(1)	-17(1)	12(1)	-21(1)
C(122)	37(1)	36(1)	43(1)	-19(1)	11(1)	-24(1)
C(123)	40(1)	39(1)	61(1)	-29(1)	15(1)	-20(1)
C(124)	41(1)	35(1)	65(1)	-16(1)	4(1)	-14(1)
C(125)	47(1)	37(1)	51(1)	-6(1)	1(1)	-21(1)
C(126)	42(1)	39(1)	44(1)	-17(1)	10(1)	-24(1)
C(127)	19(1)	28(1)	28(1)	-15(1)	6(1)	-10(1)
C(128)	33(1)	36(1)	35(1)	-13(1)	1(1)	-20(1)
C(129)	40(1)	33(1)	31(1)	-9(1)	2(1)	-20(1)
C(130)	24(1)	34(1)	30(1)	-15(1)	3(1)	-13(1)
C(131)	28(1)	33(1)	36(1)	-14(1)	4(1)	-18(1)
C(132)	23(1)	29(1)	31(1)	-10(1)	5(1)	-14(1)
C(133)	32(1)	31(1)	34(1)	-11(1)	4(1)	-15(1)
C(134)	32(1)	34(1)	28(1)	-12(1)	2(1)	-17(1)
C(135)	27(1)	33(1)	30(1)	-12(1)	2(1)	-16(1)
C(136)	30(1)	40(1)	30(1)	-12(1)	3(1)	-19(1)
C(137)	31(1)	39(1)	33(1)	-13(1)	6(1)	-19(1)
C(138)	30(1)	38(1)	34(1)	-13(1)	7(1)	-19(1)
C(139)	26(1)	43(1)	31(1)	-15(1)	0(1)	-12(1)
C(140)	32(1)	45(1)	44(1)	-23(1)	1(1)	-8(1)
C(141)	41(1)	58(1)	46(1)	-30(1)	-4(1)	-5(1)
C(142)	41(1)	72(1)	36(1)	-22(1)	7(1)	-8(1)
C(143)	43(1)	62(1)	37(1)	-9(1)	6(1)	-21(1)
C(144)	36(1)	49(1)	34(1)	-12(1)	4(1)	-19(1)
C(145)	29(1)	39(1)	25(1)	-11(1)	4(1)	-19(1)
C(146)	33(1)	38(1)	37(1)	-16(1)	5(1)	-19(1)
C(147)	37(1)	44(1)	42(1)	-24(1)	12(1)	-18(1)
C(148)	30(1)	57(1)	40(1)	-21(1)	12(1)	-24(1)
C(149)	38(1)	56(1)	38(1)	-21(1)	12(1)	-32(1)
C(150)	34(1)	40(1)	31(1)	-18(1)	10(1)	-20(1)
C(151)	30(1)	55(1)	24(1)	-9(1)	5(1)	-25(1)
C(152)	38(1)	61(1)	37(1)	-8(1)	5(1)	-25(1)
C(153)	38(1)	81(2)	39(1)	4(1)	0(1)	-25(1)
C(154)	48(1)	102(2)	31(1)	-18(1)	8(1)	-46(1)
C(155)	44(1)	104(2)	36(1)	-31(1)	14(1)	-47(1)
C(156)	40(1)	74(1)	33(1)	-25(1)	12(1)	-36(1)
C(157)	30(1)	59(1)	34(1)	-16(1)	5(1)	-26(1)
C(158)	33(1)	67(1)	37(1)	-11(1)	8(1)	-22(1)
C(159)	44(1)	98(2)	37(1)	-10(1)	12(1)	-27(1)
C(160)	46(1)	110(2)	37(1)	-24(1)	16(1)	-26(1)
C(161)	40(1)	85(2)	48(1)	-33(1)	11(1)	-20(1)
C(162)	39(1)	61(1)	40(1)	-24(1)	9(1)	-24(1)
C(163)	30(1)	56(1)	38(1)	-22(1)	5(1)	-20(1)

C(164)	36(1)	67(1)	44(1)	-25(1)	6(1)	-11(1)
C(165)	34(1)	113(2)	54(1)	-39(1)	3(1)	-9(1)
C(166)	33(1)	154(3)	62(1)	-51(2)	12(1)	-40(1)
C(167)	51(1)	125(2)	62(1)	-39(2)	20(1)	-57(2)
C(168)	43(1)	74(1)	49(1)	-20(1)	8(1)	-36(1)

Table 5. Hydrogen coordinates (x 10^4) and isotropic displacement parameters (A^2 x 10^3) for hpb.

	x	y	z	U(eq)
H(2A)	7997	851	5957	31
H(3A)	7380	1134	6610	32
H(5B)	9157	317	7561	32
H(6A)	9781	25	6908	32
H(14D)	8321	-584	7829	45
H(15A)	8398	-1426	7493	55
H(16A)	7446	-1258	6986	52
H(17A)	6423	-264	6833	47
H(18A)	6342	577	7170	40
H(20A)	6979	-364	8672	66
H(21A)	6130	-729	8960	83
H(22A)	4988	7	8665	89
H(23A)	4660	1130	8062	80
H(24A)	5500	1501	7785	63
H(26A)	6763	797	9233	71
H(27A)	5922	1257	9725	92
H(28A)	4990	2325	9358	100
H(29A)	4909	2981	8499	101
H(30A)	5768	2557	8008	72
H(32A)	7946	1283	9063	45
H(33A)	8076	1980	9473	55
H(34A)	7669	3164	9036	51
H(35A)	7085	3661	8200	50
H(36A)	6950	2973	7784	43
H(38A)	8903	1244	8333	48
H(39A)	9683	1720	8103	60
H(40A)	9580	2444	7245	61
H(41A)	8719	2668	6632	56
H(42A)	7941	2193	6862	42
H(44A)	7829	1972	5170	36
H(45A)	6938	3081	4962	39
H(47A)	7809	3780	3738	37

H(48A)	8727	2672	3962	37
H(56A)	7654	4745	4522	42
H(57A)	8418	4411	5247	48
H(58A)	8221	3870	6060	46
H(59A)	7246	3668	6155	46
H(60A)	6458	4033	5438	40
H(62A)	6497	5923	4620	42
H(63A)	6208	6441	5243	50
H(64A)	5247	6500	5652	52
H(65A)	4523	6092	5398	49
H(66A)	4785	5616	4749	39
H(68A)	4110	5884	3566	39
H(69A)	3214	6994	3184	44
H(70A)	3419	7968	3012	47
H(71A)	4503	7831	3245	46
H(72A)	5410	6725	3621	39
H(74A)	5311	6009	2590	48
H(75A)	4671	6168	1851	57
H(76A)	4121	5484	1880	59
H(77A)	4195	4632	2658	52
H(78A)	4838	4454	3397	45
H(80A)	6244	3149	3965	54
H(81A)	6585	2366	3531	72
H(82A)	6861	2665	2708	84
H(83A)	6833	3766	2303	85
H(84A)	6557	4533	2765	60
H(86A)	11237	1323	3742	34
H(87A)	11652	2152	3460	37
H(89A)	11234	2604	4763	42
H(90A)	10828	1767	5049	36
H(98A)	10247	3535	3334	69
H(99A)	9131	3726	3520	105
H(10G)	8703	4159	4164	135
H(10H)	9349	4474	4602	124
H(10F)	10467	4280	4433	86
H(10A)	10204	5073	2939	57
H(10E)	9374	6203	2841	70
H(10B)	9546	6796	3324	68
H(10C)	10548	6292	3896	59
H(10D)	11365	5170	4014	49
H(11D)	11608	5264	2642	45
H(11I)	11963	6146	2361	52
H(11H)	12864	6092	2839	56
H(11E)	13416	5159	3617	47
H(11C)	13038	4295	3904	42
H(11A)	13069	3766	2722	43
H(11F)	14202	3522	2573	56
H(11G)	15096	2883	3259	62

H(11B)	14863	2462	4097	57
H(12C)	13730	2708	4248	46
H(12D)	13177	2208	3226	42
H(12A)	14038	1071	3465	51
H(12G)	14256	320	4322	58
H(12H)	13604	699	4928	56
H(12F)	12760	1845	4695	46
H(12E)	8421	1263	3257	39
H(12B)	7662	1436	2581	40
H(13A)	7470	-284	3445	36
H(13B)	8238	-460	4113	32
H(14F)	6218	1646	3160	50
H(14I)	5940	1507	3990	61
H(14J)	5646	623	4432	66
H(14G)	5598	-112	4029	60
H(14H)	5872	15	3197	48
H(14A)	4920	2138	2399	41
H(14C)	3748	2499	2441	47
H(14E)	3211	1857	2293	48
H(14B)	3850	870	2102	46
H(15B)	5011	526	2027	39
H(15G)	4994	2321	1195	56
H(15H)	4162	2690	492	72
H(15F)	4212	1916	86	69
H(15E)	5105	821	349	65
H(15C)	5930	448	1042	52
H(15D)	6555	1873	698	57
H(15I)	7010	1789	-69	78
H(16I)	7720	692	-106	81
H(16F)	7994	-302	619	69
H(16B)	7567	-205	1386	53
H(16D)	8307	-484	2498	62
H(16E)	9479	-825	2438	88
H(16G)	9835	-49	1887	96
H(16H)	9046	1057	1417	86
H(16C)	7871	1407	1460	62